Environmental Science

Thomas M. Missimer
Burton Jones
Robert G. Maliva *Editors*

Intakes and Outfalls for Seawater Reverse-Osmosis Desalination Facilities

Innovations and Environmental Impacts

Springer

Environmental Science and Engineering

Environmental Science

More information about this series at http://www.springer.com/series/3234

Thomas M. Missimer · Burton Jones
Robert G. Maliva
Editors

Intakes and Outfalls for Seawater Reverse-Osmosis Desalination Facilities

Innovations and Environmental Impacts

Springer

Editors
Thomas M. Missimer
U.A. Whitaker College of Engineering
Florida Gulf Coast University
Fort Myers, FL
USA

Robert G. Maliva
Schlumberger Water Services
Fort Myers, FL
USA

Burton Jones
King Abdullah University of Science
and Technology
Thuwal
Saudi Arabia

ISSN 1863-5520 ISSN 1863-5539 (electronic)
Environmental Science and Engineering
ISSN 1431-6250
Environmental Science
ISBN 978-3-319-13202-0 ISBN 978-3-319-13203-7 (eBook)
DOI 10.1007/978-3-319-13203-7

Library of Congress Control Number: 2015932845

Springer Cham Heidelberg New York Dordrecht London

Printed on acid-free paper

Springer International Publishing AG Switzerland is part of Springer Science+Business Media (www.springer.com)

Foreword

The *Greening* of Seawater Reverse Osmosis (SWRO) Systems: Focus on Intakes and Outfalls

Seawater reverse osmosis (SWRO) has emerged as the conventional seawater desalination technology, globally. While SWRO is less energy intensive than thermal processes' such as multi-stage flash (MSF) and multi-effect distillation (MED), it is still an energy intensive process (3–4 kWh/m^3). Moreover, with increasing emphasis on green technologies, the present practice of SWRO is characterized by a number of significant environmental impacts, including energy consumption, greenhouse gas (GHG) emissions, entrainment and impingement of marine organisms through intakes, and marine pollution during concentrate discharge via outfalls. SWRO is also a chemical-intensive and material-intensive process with a sizable footprint. Besides salts, SWRO brines can also contain chemicals used in pretreatment (e.g., coagulants and antiscalants) and RO cleaning agents. Periodic replacement of RO modules results in a significant solid waste problem. Thus, a challenge is realization of the *greening* of SWRO systems.

It has been estimated that further optimization of the SWRO process and its various components could potentially provide a 20 % reduction in specific energy consumption, with a concomitant reduction in GHG emissions. However, beyond this perceived limit, only emerging technologies such as forward osmosis (FO) offer the possibility of further energy reduction. SWRO pretreatment by ultrafiltration (UF), as an alternative to granular media filtration (GMF), provides an opportunity for reduced amounts of chemical coagulant (e.g., UF with in-line coagulation). New fouling resistant RO membranes can provide an opportunity for reduced use of chemical cleaning agents. Improvements in membrane fabrication have resulted in extended material life and less frequent replacement of RO modules. However, beyond these improvements, potentially major contributions to the greening of SWRO can be realized through advancements in the design and operation of SWRO intakes and outfalls, the focus of this book.

While intake choice is generally perceived as being between surface (open) and subsurface intakes, there are many subcategory options. Surface intakes can be single purpose or colocated with a power plant as well as offshore submerged, nearshore submerged, or nearshore surface intakes. Subsurface intakes can be onshore (vertical wells), including vertical beach wells or deep aquifer wells, horizontal wells, radial or collector wells, and beach infiltration galleries; or offshore wells, including horizontal drains (wells), and seabed infiltration galleries.

The use of surface, colocated, nearshore intakes is typical for water and power cogeneration plants (e.g., many in the GCC region), but these are also used by some SWRO plants (e.g., Tampa Bay USA). The use of surface, single purpose intakes is common for many larger SWRO systems. Subsurface, onshore intakes are used by small to medium capacity SWRO plants; however, subsurface, offshore intakes are under consideration for larger SWRO systems. An under-recognized attribute of subsurface intakes is that they also function as an SWRO pretreatment process, simulating a slow sand filter as a physical and biological process, without chemicals. Of particular importance is the ability of subsurface intakes to remove bacteria, algae, and biopolymers (e.g., proteins and polysaccharides), reducing both organic and biofouling of RO membranes; moreover, subsurface intakes inherently eliminate impingement and entrainment. A notable example is the Fukuoka (Japan) seabed infiltration gallery which operates before a UF pretreatment step, alone reducing the silt density index (SDI) to below three and allowing the subsequent UF to operate for long periods without backwashing. Improvements in open intake design and operation have largely focused on minimizing impingement and entrainment.

In summary, open surface intakes are generally characterized by high intake volumes (i.e., larger SWRO systems), offer a potential for colocation, are unaffected by (but also do not beneficially affect) feed water quality, and are vulnerable to impingement and entrainment. Subsurface intakes are generally used for smaller capacity SWRO systems (but seabed galleries are increasingly being considered for larger systems), are unaffected by (but can beneficially affect) water quality, and can mitigate impingement and entrainment. To drive home the importance of intakes and outfalls, it has been estimated that they account for up to 35 % of the costs of SWRO systems.

The two general categories of SWRO outfalls are surface and subsurface outfalls. The former can take the form of nearshore and offshore, with further delineation into an outfall channel, a single pipe, or a multiport diffuser. Less common are offshore and inland subsurface outfalls, taking the form of a percolation gallery, deep well injection, evaporation ponds, sewer discharge, and zero liquid discharge (ZLD), most of the latter (except for percolation galleries) being the domain of inland brackish water RO (BWRO) systems. Nearshore outfall channels are more typical for cogeneration (distillation and power) plants or colocation (SWRO plant next to power) plants. Single offshore pipes are more common for smaller SWRO plants. Multiport diffusers are more common for larger SWRO plants and are increasingly becoming the norm for such new plants. There are several types of multiport diffusers, including pipeline diffusers (nozzles arranged along a pipe) and

rosette-style diffusers (several outlet risers above the seafloor with a small number of nozzles). Advancements in modeling of multi-diffuser systems allow prediction of a regulatory mixing zone. In subsurface offshore outfalls, the concentrate is slowly dissipated into the surf zone (e.g., perforated laterals placed under the ocean floor).

The *greening* of SWRO can be promoted by the use of subsurface intakes (no impingement/entrainment of organisms, pretreatment without chemicals and associated residuals); the minimization of chemical use (e.g., UF with lower or no coagulant addition); no antiscalants (scaling control by acid addition and/or limiting recovery); brine disposal through a multiport-diffuser outfall (i.e., minimize extent of mixing zone); and integration of renewable energy (e.g., solar, wind, and/or or geothermal) in design and operation (direct use or (indirect) energy compensation, reduced GHG emissions (95 % of which are associate with direct energy use)). This book will highlight the important role of two of these SWRO system components, *intakes and outfalls*.

Gary Amy
Sabine Lattemann

Preface

Freshwater supplies are dwindling as global population growth, industrialization, and agricultural expansion occur worldwide. Desalination of seawater is rapidly becoming a key aspect of global water management to balance the needs of numerous coastal countries, particularly in arid lands and industrialized counties. Seawater desalination is an energy-intensive process that has some real and perceived environmental impacts. Therefore, it is important to reduce the energy consumption of desalination, the carbon footprint, the environmental impacts, and the overall cost. Currently, the most energy efficient desalination large-scale commercial process is seawater reverse osmosis (SWRO).

It is the purpose of this book to address two important aspects of the SWRO process, design of intakes and outfalls and assessment and reduction of environmental impacts. Most of the book content is based on technical presentations made at an international workshop on desalination system intakes and outfalls sponsored and held during October 7–8, 2013 at the King Abdullah University of Science and Technology (KAUST) in Thuwal, Saudi Arabia. Additional chapters were solicited by the editors to cover various aspects of intakes and outfalls not occurring during the workshop.

The Water Desalination and Reuse Center and the Red Sea Research Center at KAUST jointly organized the workshop with generous support from KAUST's Office of Research Support. The presence of KAUST on the Red Sea, where increasing urbanization and industrialization along the coast demands additional freshwater supply, provided much of the impetus for the workshop. Saudi Arabia currently produces about 18 % of the global production of desalinated water with an expected capacity of nearly 6 million cubic meters per day in 2015. Over the long term the dependence on desalinated water in the region and much of the world will only increase. A long-term goal of this workshop and similar efforts is to reduce the energy intensity and increase water-use efficiency throughout the life cycle of desalination plants, minimizing environmental impacts to the greatest extent possible. In other words, the goal is to develop desalination plant design that promotes sustainable interaction of the human environment within our natural environment.

This book covers a considerable number of subjects that have not been published extensively in the peer-reviewed literature. The book is divided into two major sections; intakes and outfalls with some overlapping subject matter involving environmental impact assessment and reduction. The intakes section is further subdivided into surface or "open-ocean" intakes and subsurface intakes.

The overall design philosophy of intakes for SWRO plants is covered in Chap. 1. Design concepts for velocity-cap, and tunnel intake systems are covered in Chaps. 2–3. The very important issue of impingement and entrainment is covered in Chap. 4, which includes a summary of the latest U.S. environmental regulations and a summary of research. Design and impacts of passive screen intake systems are discussed in detail in Chap. 5. In recent years it has been suggested that deep intake systems could be used to obtain higher quality feed water for SWRO systems. In Chap. 6, the use of deep intakes along the Red Sea coastline of Saudi Arabia is assessed. This comprehensive study shows the variation in algae, bacteria, and various types of natural organic matter with depth in the Red Sea and how the bathymetric features of the Red Sea impact deep intake system feasibility.

Discussion of subsurface intake systems begins with Chap. 7, which provides a comprehensive planning methodology that is used to analyze the Red Sea coastal areas of Saudi Arabia and the coasts of Florida to assess technical feasibility of using various subsurface intake systems. Use of wells as intakes, the most mature subsurface intake technology, is covered in Chap. 8 with an assessment of the improvement in raw water quality that occurs between the raw seawater and after traveling through an aquifer to a production well occurring in Chap. 9. Beach and seabed gallery intake system design and innovations in their use are covered in Chaps. 10–12. Applications of seabed gallery feasibility for the Red Sea and Arabian Gulf coasts and nearshore areas of Saudi Arabia are discussed in detail in Chaps. 11 and 12. The generally new concept of using slant wells as intakes is discussed in Chap. 13. The application of coastal modeling to assess the technical feasibility of developing gallery intake systems, with an emphasis on southern California, is covered in Chap. 14. The innovations in design and operation of SWRO intake system are summarized in Chap. 15.

The second part of the book covers assessment and mitigation of environmental impacts associated with discharge of concentrate from SWRO plants and subsequent wastewater discharge. Overall, this group of papers progresses from modeling approaches for coastal discharges.

Chapter 16 provides an overall of coastal discharges and how they are managed. Chapter 17 discusses the results of laboratory modeling of various configurations of concentrate diffusers, their performance and design criteria, and applications. Chapter 18 builds from the nearfield modeling toward a tiered approach of nearfield and farfield modeling, observation, and analysis for design, placement, and implementation of new facilities. Additional evaluations and design criteria for dense brine discharges are provided in Chap. 19. Chapter 20 presents a modeling evaluation of the dispersion of heat and salt from a discharge in the Gulf of Arabia and the response of the dispersion to variations in the coastal currents. Because the

Red Sea is an enclosed basin, discharges within that basin may have impacts that can spread either along the coast or even across the axis of the basin. The model results described in Chap. 21 demonstrates the potential for that very farfield dispersion. Chapter 22 discusses the use of AUV's for farfield mapping and long-term deployments building a statistical database that can be used for comparison against numerical models where the resolution is now approaching the scale of the near-field. Chapter 23 discusses the innovations in management of coastal discharges and evaluation of environmental impacts.

The purpose of this book is to provide the latest summary of pertinent research on intake and outfall design concepts for SWRO facilities. It should be used by design engineers, geologists, project owners, and facility operators for use as a reference and to obtain new ideas that could produce innovative designs that will reduce the energy consumption and operational costs of SWRO facilities. Also, we have provided summaries of where additional scientific and engineering research should be conducted to make improvements to intake and outfall performance.

Fort Myers, Florida, January 2015 — Thomas M. Missimer
Thuwal, Saudi Arabia — Burton Jones
Fort Myers, Florida — Robert G. Maliva

Contents

Contributors

Samir Al-Mashharawi Water Desalination and Reuse Center, King Abdullah University of Science and Technology, Thuwal, Saudi Arabia

Sami Al-Sanea Mechanical Engineering Department, King Saud University, Riyadh, Saudi Arabia

Raed Bashitialshaaer Department of Water Resources Engineering, Lund University, Lund, Sweden

Zenon Batang Coastal and Marine Resources Core Lab, King Abdullah University of Science and Technology, Thuwal, Saudi Arabia

Peter Baudish Jacobs, Sydney, Australia

Tobias Bleninger Dpto. de Engenharia Ambiental (DEA), Universidade Federal do Paraná (UFPR), Curitiba, Brazil

Keith Craig Veolia Water Australia, NSW, Australia

Abdullah H.A. Dehwah Water Desalination and Reuse Center, King Abdullah University of Science and Technology, Thuwal, Saudi Arabia

Ganesh Gopalakrishnan Scripps Institution of Oceanography, University of California San Diego, San Diego, California

Timothy W. Hogan Alden Research Laboratory, Holden, MA, USA

Ibrahim Hoteit Division of Physical Sciences and Engineering, King Abdullah University of Science and Technology, Thuwal, Saudi Arabia

Scott A. Jenkins Scripps Institution of Oceanography, University of California San Diego, San Diego, CA, USA

Burton Jones Red Sea Research Center, King Abdullah University of Science and Technology, Thuwal, Saudi Arabia; Department of Biological Sciences, University of Southern California, Los Angeles, CA, USA

Aditya R. Kartadikaria Division of Physical Sciences and Engineering, King Abdullah University of Science and Technology, Thuwal, Saudi Arabia

Magnus Larson Department of Water Resources Engineering, Lund University, Lund, Sweden

Sheng Li Water Desalination and Reuse Center, King Abdullah University of Science and Technology, Thuwal, Saudi Arabia

Luis Lujan Water Desalination and Reuse Center, King Abdullah University of Science and Technology, Thuwal, Saudi Arabia

Robert G. Maliva Schlumberger Water Services, Fort Myers, FL, USA

Francis L. Mallon Coastal and Marine Resources Core Lab, King Abdullah University of Science and Technology, Thuwal, Saudi Arabia

David Mantilla Water Desalination and Reuse Center, King Abdullah University of Science and Technology, Thuwal, Saudi Arabia

Thomas M. Missimer U.A. Whitaker College of Engineering, Florida Gulf Coast University, Fort Myers, FL, USA

Robin Morelissen Hydraulic Engineering, Deltares, Delft, The Netherlands

Jamel Orfi Mechanical Engineering Department, King Saud University, Riyadh, Saudi Arabia

Thomas Pankratz Water Desalination Report, Houston, TX, USA

Kenneth M. Persson Department of Water Resources Engineering, Lund University, Lund, Sweden

Rinaldi Rachman Water Desalination and Reuse Center, King Abdullah University of Science and Technology, Thuwal, Saudi Arabia

Matthew Ragan Department of Biological Sciences, University of Southern California, Los Angeles, CA, USA

Philip J.W. Roberts Georgia Institute of Tecnology, Atlanta, USA

Bridget Seegers Department of Biological Sciences, University of Southern California, Los Angeles, CA, USA

Elizabeth Teel Department of Biological Sciences, University of Southern California, Los Angeles, CA, USA

Yesubabu Viswanadhapalli Division of Physical Sciences and Engineering, King Abdullah University of Science and Technology, Thuwal, Saudi Arabia

Dennis E. Williams Geoscience Support Services, Inc., Claremont, CA, USA

Harvey Winters Fairleigh Dickinson University, Teaneck, USA

Fengchao Yao Division of Physical Sciences and Engineering, King Abdullah University of Science and Technology, Thuwal, Saudi Arabia

Peng Zhan Division of Physical Sciences and Engineering, King Abdullah University of Science and Technology, Thuwal, Saudi Arabia

Part I
Intakes

Chapter 1
Overview of Intake Systems for Seawater Reverse Osmosis Facilities

Thomas Pankratz

Abstract The intake is a critical component of every seawater reverse osmosis facility and controls to a great degree the design and operational cost of downstream treatment processes. Two general classes of intake types occur; surface or open-ocean intakes and subsurface intakes. Globally, most large-capacity SWRO plants use open-ocean intake systems with the actual intake located either onshore (commonly shared with a power plant) or offshore. The most common offshore intake type uses a velocity cap at the top of the invert pipe. Inshore or offshore passive screen intakes are used to reduce the impacts of impingement and entrainment. Subsurface intake systems, either wells or galleries, are being used in hundreds of small to medium capacity SWRO facilities. Because of the greater attention being given to the environmental impacts of impingement and entrainment of marine organisms, subsurface intake systems are being specified for a greater number of facilities with higher capacity.

1.1 Introduction

Seawater desalination facilities require an intake that is capable of providing a reliable quantity and relatively consistent quality of seawater to ensure that the plant production targets can be met. While this fundamental objective may appear obvious, it is complicated by the fact that the ocean is a dynamic entity with constantly changing conditions.

Powerful waves and changing currents can damage structures, affect water depths, and dramatically alter water quality and temperature. And, as one moves

T. Pankratz (✉)
Water Desalination Report, P. O. Box 75064, Houston, TX 77234, USA
e-mail: PankratzTM@gmail.com

T.M. Missimer et al. (eds.), *Intakes and Outfalls for Seawater Reverse-Osmosis Desalination Facilities*, Environmental Science and Engineering,
DOI 10.1007/978-3-319-13203-7_1

closer to shore, these changes often become more dramatic and occur with increasing frequency. Operational problems are compounded by the corrosiveness of seawater and the marine organisms that can attack and foul equipment and systems.

To meet the design objectives, it is essential that a thorough assessment of the intake site conditions be conducted. Physical characteristics, meteorological and oceanographic data, marine biology and the potential effects of fouling, pollution and navigation must be evaluated. Only then can an appropriate intake design be selected.

As reverse osmosis (RO) has grown to become the predominant seawater desalination process, so have the number and production capacities of the resulting facilities. More and larger capacity plants are being built in locations where none had previously existed, raising concerns over the possible environmental impacts of withdrawing large volumes of seawater. For many seawater desalination projects, the potential for intake-related marine life mortality may represent the most significant direct adverse environmental impact of a project.

Because intake designs are highly site specific—perhaps more so then any other aspect of the desalination plant—the design, modeling, monitoring and permitting activities that surround them may represent a significant portion of a project capital costs. Whereas, seawater intakes formerly represented 4–12 % of an entire facility capital cost, some intake arrangements may now cost 35 % or more of a project capital cost, and it is possible that intake-related issues may ultimately determine the feasibility of the desalination plant itself.

This chapter will consider the seawater intake technology options available for seawater RO plants, including intakes shared with electric power plants, and will review the technologies employed to minimize environmental impacts, while meeting the intake objective of providing a reliable quantity of seawater at the best quality available. A comparison of the intake types is given in Table 1.1. Greater descriptive detail on intakes and diagrams and photographs of various types are contained in Missimer (2009) and in various chapters in this book.

1.2 Water Quality and Quantity

Historically, most large seawater desalination plants have employed the multistage flash evaporation (MSF) or multiple effect distillation (MED) desalination processes and have been co-located at an electric power generating plant with which they share a common shoreline, or nearshore seawater intake. Because a power plant condenser and a MSF or MED facility utilize similar size condenser tubes, both require only a nominal level of treatment, and usually that can be provided by a traveling water screen or rotating drum screen with 6–9.5 mm wire mesh openings.

Table 1.1 Assessment of intake options for SWRO plants

	Intake options summary				
	Vertical wells	Infiltration gallery	Open ocean, with offshore passive screens	Open ocean with velocity cap, onshore mechanical screens	Conventional shoreline, with mechanical screens
Feasibility	Limited by local geology	Limited by local hydrogeology, offshore sea conditions	Moderate-high	High	High
Feedwater quality produced	High	High	Moderate-high	Moderate	Low
Environmental implications	No impingement, entrainment	No impingement, entrainment, but construction impacts	No impingement, low entrainment	Low impingement, moderate entrainment	Impingement and entrainment
Flexibility	Low, space limitations may limit well addition	Low	Production limitations can be overcome by adding screens	Moderate	Moderate
Reliability	Wells can be rehabilitated and/or new ones added	Difficult to predict, cleaning may be marginally effective	Plugging can be monitored and cleaning is effective	Plugging can be monitored and cleaning is effective	Plugging can be monitored and cleaning is effective
Susceptibility to operational anomalies	Low	Low	Moderately vulnerable to jellyfish runs, algal blooms	Moderately vulnerable to algal blooms	Moderate to highly vulnerable to jellyfish runs, algal blooms
Maintenance	Low	When/if required, could be substantial	Pig pipeline 2X per year, clean/inspect screens quarterly	Pig pipeline 2X per year, maintain screens as required	Maintain screens as required
Construction risk	Moderate	High	Low-moderate	Low-moderate	Low
Relative capital cost, typical	Low-moderate	High	Moderate-high	Moderate-high	Moderate

Conversely, the performance of a seawater reverse osmosis (SWRO) plant may benefit greatly from a more consistent quality of water and a finer level of screening. Since most seawater RO plants are standalone facilities with a purpose-built intake, there is a much greater focus on selecting a design/location that will provide a consistent seawater quality possible and the lowest practical suspended solids. As the first step in the SWRO pretreatment process, the intake effectiveness can have far-reaching effects on overall plant operation and performance.

Like most process systems, desalination plants operate most efficiently and predictably when feedwater characteristics remain relatively constant and are not subject to rapid or dramatic water quality fluctuations. Therefore, the water quality review should consider both seasonal and diurnal fluctuations. The assessment should consider all constituents that may impact plant operation and process performance including a thorough review of historical water quality data including seawater temperature, total dissolved solids (TDS), total suspended solids (TSS), and total organic carbon (TOC) is crucial.

Most seawater RO facilities convert 40 to 50 % of the intake water to product water, while the remaining water, which includes the salt removed by the RO system, is pumped back to the sea for controlled discharge. It is therefore beneficial to locate the desalination plant as close to the seashore as possible to minimize intake/discharge pumping requirements.

1.3 Environmental Considerations

Potential environmental impacts associated with concentrate discharge are often considered the greatest single ecological impediment when siting a seawater desalination facility. However, it has now been widely demonstrated that a properly modeled, designed and strategically located outfall can effectively mitigate discharge impacts, while marine life impingement and entrainment resulting from intake operation is often a greater, harder-to-quantify concern.

Impingement occurs when marine organisms are trapped against intake screens by the velocity and force of water flowing through them (Chap. 4). The fate of impinged organisms differs between intake designs and among marine life species, age, and water conditions. Some ‘hardy’ species may be able to survive impingement and be returned to the sea, but the 24-h survival rate of less robust species and/or juvenile fish may be less than 15 %.

Entrainment occurs when smaller organisms pass through an intake screen and into the process equipment (Chap. 4). Entrained organisms are generally considered to have a mortality rate of 100 %.

The number of affected organisms will, of course, vary considerably with the volume and velocity of feedwater and the use of mitigation measures employed to minimize their impact. If intake velocities are sufficiently low, usually less than 0.15 m/s, fish may be able swim away to avoid impingement or entrainment. The swimming performance for different species of fish can predict the types and ages

that are most vulnerable, however, even large fish are frequently caught on intake screens, indicating that swimming ability is not the only factor in impingement. Cold temperatures or seasonal variations in age-selective migrations or growth are also factors.

Since the early 1970s, seawater intakes for electric power plant cooling water intakes have been required to employ the best technology available to minimize adverse environmental impact under §316(b) of the US. Environmental Protection Agency (USEPA) Clean Water Act (CWA). The section of the CWA has been updated three times and applies to all intakes that withdraw greater than 7570 m^3/d of seawater and use 25 % or more of the water for cooling purposes. Some state regulatory agencies have indicated that the siting of a new or existing seawater intake for a desalination facility will require a §316(b)-type assessment of impingement and entrainment impacts as part of the environmental review and permitting process.

1.4 Intake Categories

Seawater intakes can be broadly categorized as *surface intakes* where water is collected from the open ocean above the seabed, and *subsurface intakes* where water is collected via vertical wells, infiltration galleries or other locations beneath the seabed. The most appropriate type of seawater intake can only be determined after a thorough site assessment and careful environmental evaluation.

1.5 Surface Water Intakes

Large seawater desalination plants have traditionally employed open-ocean, surface water intakes that are equipped with mechanically cleaned screens and virtually identical to those installed electric power generating plants use to obtain condenser cooling water.

In most arrangements, a pump station and screening chamber is located onshore and directly connected to the open ocean by means of a concrete channel or jetty, or an intake pipe that may extend out hundreds of meters into the sea.

1.5.1 Traveling Water Screens

Traveling water screens, also referred to as band screens, have been employed on seawater intakes since the 1890s (Fig. 1.1). The screens are equipped with revolving panels fitted with wire mesh panels that usually have 6–9.5 mm openings.

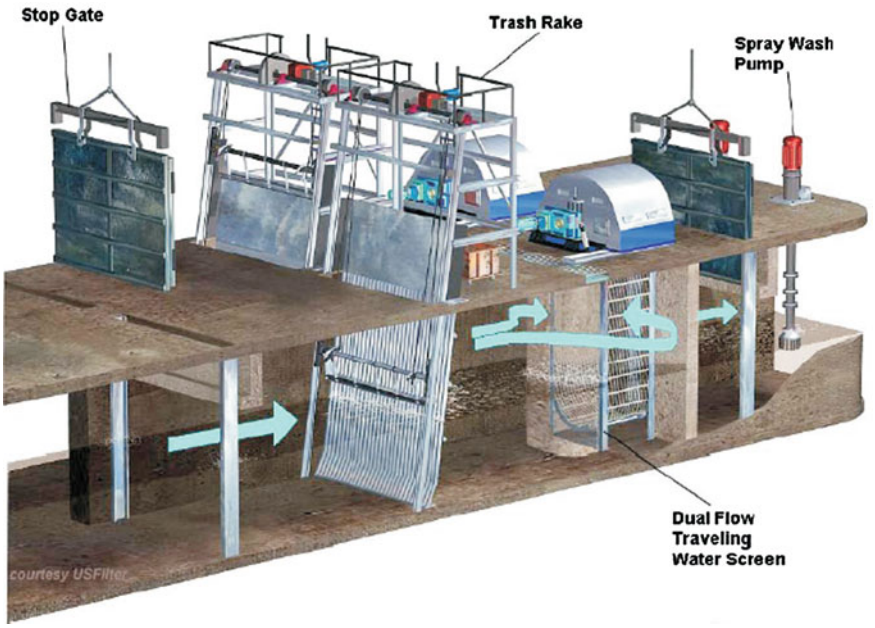

Fig. 1.1 Dual-flow traveling water screen (From Pankratz 2007)

As the wire mesh panels revolve out of the flow, a high-pressure water spray is used to remove accumulated debris, washing it into a trough where it is sluiced away for further disposal.

The screens are almost always located onshore in concrete channels, either at the far end of a forebay or a longer channel that extends out beyond the surf zone. The screens may also be installed in a wet well or pump station that is connected to the sea by a pipe that extends out into the sea and terminates in a coarse-screened inlet or a velocity cap.

The screens are usually designed so that the maximum water velocity through the screen is less than 0.15 m/s.

1.5.1.1 Rotating Drum Screens

Rotating drum screens are an alternative to traveling water screens, and consist of wire mesh panels mounted on the periphery of a large cylinder that slowly rotates on a horizontal axis (Fig. 1.2). They are cleaned with a spray wash system similar to traveling water screens. Drum screens may range up to 15 m in width and 4 m in diameter.

Fig. 1.2 Drum screen (From Pankratz 2007)

1.5.1.2 Fine Mesh Traveling Screens

Fine mesh traveling screens have been used to successfully reduce entrainment of eggs, larvae and juvenile fish at some intake locations where traveling water screens have been outfitted with wire mesh panels having openings ranging from 0.5 to 5 mm, and which may reduce entrainment by up to 80 %.

However, fine mesh screens may result in operational problems due to the increased amount of debris removed along with the marine life, and in some locations, the fine mesh is only utilized seasonally, during periods of egg and larval abundance.

1.5.1.3 Ristroph Screens

Ristroph screens are a modification of a conventional traveling water screen in which screen panels are fitted with watertight fish buckets that collect fish and lift them out of the water where they are gently washed from the screen with a low-pressure spray, prior to debris removal with a high-pressure spray wash (Fig. 1.3).

Studies at a New York power plant seawater intake, showed the 24-h survival of marine life impinged on conventional screens averaged 15 % compared with 80–90 % survival rates for Ristroph-type traveling water screens. A review of 10

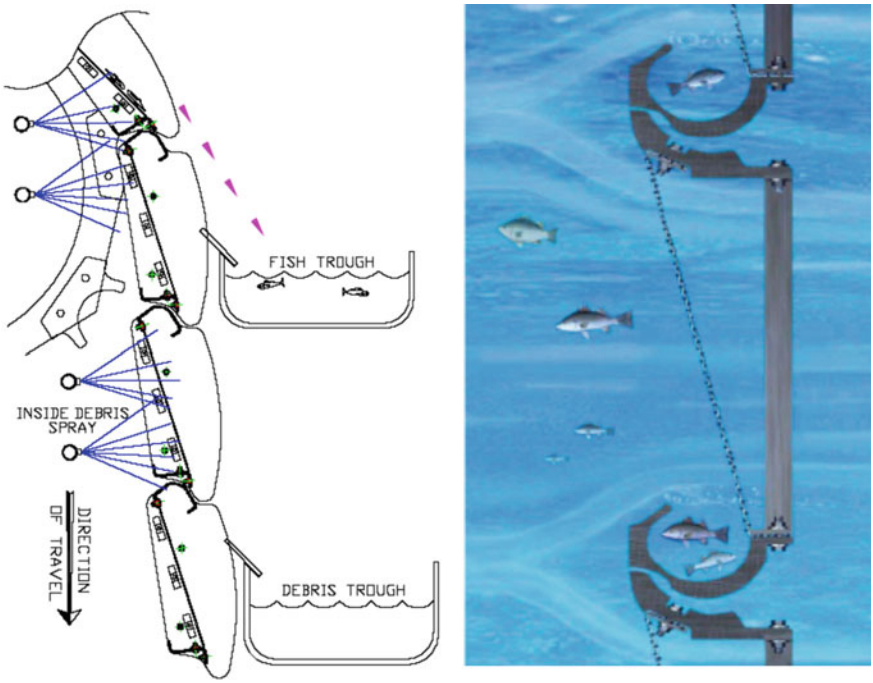

Fig. 1.3 Ristroph screen apparatus

similar sites reported that Ristroph modifications improved impingement survival 70–80 % among various species.

Although Ristroph screens may be effective at improving the survival of impinged marine life, they do not affect entrained organisms.

1.6 Offshore Intakes

Submerged, offshore intakes have long been a preferred seawater intake arrangement, particularly for shallow coastlines. Power plants and desalination plants often employ them in a desire to obtain a 'better', more consistent quality of water that is less susceptible to operational upsets from storm events, algal blooms and jellyfish. An offshore intake may also mitigate environmental impacts if it is designed and located in an area so as to reduce marine life impingement and entrainment.

In most offshore intake arrangements, the intake structure is usually located well beyond the surf zone, so it is less vulnerable to wave action. In some locations, this may be as little as 200 m offshore, but for larger plants, or locations with gently sloping sea bottoms, the intake could be located more than 1000 m offshore.

The offshore intake terminal is usually equipped with a coarse screen having 50–225 mm openings, or a velocity cap (see Sect. 1.7). Water enters the intake structure and is conveyed to an onshore pump station through a connecting pipe or tunnel (see Chaps. 2 and 3).

For most SWRO applications, especially those locations with a sandy seabed, a high-density polyethylene (HDPE) pipe can be fitted with concrete collars/anchors and laid directly on the seabed, although the portion of the pipeline that extends through the surf zone and onshore to the pump station is usually laid in a dredged trench and backfilled (Chap. 5).

Where intake lines must pass through environmentally sensitive areas or extend far offshore to reach deeper water, trenchless installation methods including tunneling, pipe jacking (microtunnelling) or horizontal directional drilling (HDD) may be used for all, or a portion of the line (Chaps. 2 and 3).

Unless the intake terminal of an offshore intake is fitted with a passive screen system, the onshore pump station must be equipped with traveling water screens or rotating drum screens to protect downstream pumps and pretreatment equipment.

1.7 Velocity Caps

The vertical riser of an offshore intake pipe may be fitted with a velocity cap that acts as a behavioral barrier to guide aquatic organisms away from the intake structure. The velocity cap is a horizontal, flat cover located slightly above the terminus of the vertical riser to convert a vertical flow into a horizontal flow at the intake's entrance (Fig. 1.4).

The cover converts vertical flow into horizontal flow at the intake entrance, and works on the premise that fish will avoid rapid changes in horizontal flow. Fish do not exhibit this same avoidance behavior to the vertical flow that occurs without the use of such a device. Velocity caps have been implemented at many offshore intakes and have been successful in decreasing the marine life impingement.

The design is based on the premise that a change in flow pattern created by a velocity cap, and operating at an entrance velocity of about 0.30 m/s, and as high as 0.9 m/s, triggers an avoidance response mechanism in fish, which aids in escaping impingement. This avoidance behavior was not exhibited in response to a vertical flow that would occur with an uncapped riser. It was also found that extending the cap and riser lip by 1.5 times the height of the opening would result in a more uniform entrance velocity, increasing the reaction time of a fish.

In recent years, the definition of a velocity cap has strayed well beyond its original definition, and many now incorrectly refer to any offshore covered intake head—regardless of its entrance velocity and the height of its opening—as a velocity cap.

This was noted in a 2012 USEPA review of proposed rule changes for the Section 316(b) of the Clean Water Act:

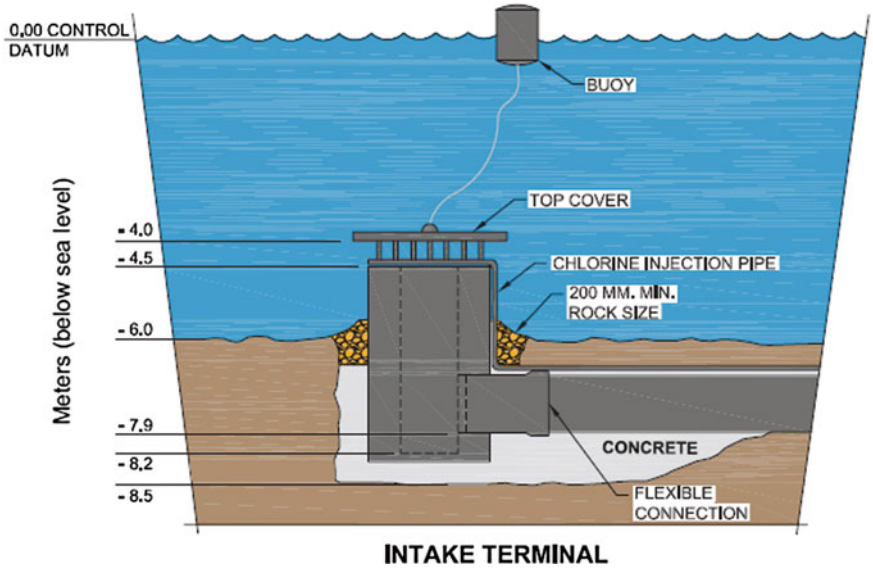

Fig. 1.4 Velocity cap intake structure (From Missimer 2009)

> "EPA is aware that low intake velocity is sometimes confused with velocity cap technologies, and EPA would like to clarify that these concepts are not the same. Most velocity caps do not operate as a fish diversion technology at low velocities, and in fact are often designed for an intake velocity exceeding one foot per second."

In its final rule on cooling water intake structures issued on 15 August 2014, the USEPA noted that it had reviewed studies documenting performance from 11 offshore intakes equipped with a velocity cap. The data shows that by solely locating an intake over 240 m offshore, even without a velocity cap, it is possible to achieve a 60–73 % impingement reduction. Similarly, it also shows that the use of an EPA-defined velocity cap alone can achieve a 50–97 % reduction in impingement.

Based on this record of performance, the final rule designated offshore intakes fitted with a properly designed velocity cap as one of the "pre-approved" best technologies available for impingement.

To qualify as a pathway for impingement compliance, a velocity cap must usually be located more than 240 m offshore.

Virtually all velocity cap intakes require some on-shore screening system, usually a traveling water screen or rotating drum screen to protect downstream pumps and pretreatment equipment. The screens may be equipped with a Ristroph-type marine life handling system to further reduce impingement mortality and/or fine screens to reduce entrainment of entrapped organisms.

1.8 Passive Screens

Another intake arrangement utilizes fixed cylindrical screens constructed of trapezoidal- or triangular-shaped "wedgewire" bars arranged to provide 0.5–3.0 mm wide slotted openings (Chap. 5). The screens are usually oriented on a horizontal axis with the total screening area sized to maintain a velocity of less than 0.15 m/s to minimize debris and marine life impingement.

Passive screens are best suited for areas with an ambient cross-flow current that acts to 'self-clean' the screen face. Systems may also be equipped with an air backwash system to clear screens if debris accumulations do occur. As with all submerged equipment, material selections should reflect the corrosion and biofouling potential of seawater.

Passive screens have a proven ability to reduce impingement—due to their low through-flow velocities—and entrainment—through exclusion resulting from the narrow slot openings. Tests have shown that 1 mm openings are highly effective for larval exclusion and may reduce entrainment by 80 % or more.

1.9 Subsurface Intakes

Subsurface intakes are those in which seawater is withdrawn below the surface of the seabed and may consist of horizontal or vertical beach wells, infiltration galleries, or seabed filtration systems. In each of these designs, the open seawater is separated from the point of intake by a geologic unit (Missimer 2009; Missimer et al. 2013). A subsurface intake can be used where geologic conditions beneath the seabed can support water extraction while providing some level of natural filtration.

The use of subsurface intakes offers a distinct environmental advantage because the ecological impact associated with impingement and entrainment of marine life is virtually eliminated. However, subsurface designs must consider their potential impact on nearby fresh groundwater aquifers.

1.9.1 Vertical Wells

Vertical onshore wells that are hydraulically connected to the sea, or draw water from saline aquifers or deep regional aquifer systems that contain seawater may be used to feed seawater desalination plants (see Chap. 8). The site geology must be adequate to allow individual well yields to be high enough so that the number of production wells needed to meet an RO plants raw water supply is reasonable or cost-competitive with other supply options.

Often, the term 'beach well' is used to describe any vertical well, but this is incorrect if it applies to wells that are not directly recharged by seawater and located on or very near to the beach.

Many vertical wells make use of beach sand, coral or other geologic structures as a filter medium, and are often economical alternative to open sea intakes for desalination plants, especially those with production capacities less than 20,000 m^3/d, although one 80,200 m^3/d seawater RO plant has successfully employed vertical wells.

A vertical beach well usually consists a non-metallic well casing, well screen, and a vertical turbine or submersible pump. Site suitability is determined by drilling test wells and conducting a detailed hydrogeologic investigation to determine the formation transmissivity and substrate characteristics. It is preferred to locate beach wells as close to the coastline as possible, and the maximum yield from individual wells may range up to 4000 m^3/day or more.

1.9.2 Horizontal Directional Drilling

Horizontal directional drilling (HDD) techniques can be used to position a horizontal well within porous strata 2–4 m under the seabed. Drilling can be accomplished by sonic, rotary, percussion, or jetting techniques. The advantages offered by HDD technology versus conventional trench installation techniques include minimized surface disturbance/impacts, reduction in the quantity of excavated material, accuracy of conduit placement, and backfill and compaction of open trenches is eliminated.

One HDD wellfield system uses a relatively new type of porous polyethylene well pipe that acts as both a well screen and packing in one, and does not require additional external media packing for long-term operation. Pre-packed well screens and filter mesh well screens that can be pulled over a slotted pipe are other options offered by several manufacturers.

When designing a seabed filtration system the well screen and packing system should be sized so that the entrance velocity through the packing and screen does not exceed the prescribed maximum flow velocity for the adjacent formation materials.

Multiple horizontal wells can be installed from the same origin within a caisson in a similar manner to collector wells to supply higher production requirements.

1.9.3 Slant (Angled) Well

A slant well or angled well is similar to both vertical and horizontal directionally drilled (HDD) wells. This is because a slant well is nearly horizontal, yet constructed like a vertical well. The shallow-entry drill rig is angled approximately

15–25° from the horizontal, and then drilled straight, unlike a HDD drill rig that gradually turns as it drills to achieve a horizontal well (see Chap. 13).

1.9.4 Radial Collector Wells

Radial collector wells are a variation of the beach well in which multiple horizontal collector wells are connected to a central caisson that acts a wet well or pumping station from which water is pumped to the desalination plant. The use of multiple horizontal wells means that the production of each radial well can be significantly greater than a single vertical well.

Individual horizontal wells can be drilled or well screens can be hydraulically jacked out from the bottom of the caisson using a direct-jack or pull-back process. Caissons may be 2.75–6 m in diameter and 9–45 m deep, with 200–300 mm diameter radial arms. The caisson can be completed with a flush-grade top slab or in a buried concrete vault and backfilled with beach sand to reduce visual impact. The laterals can extend up to 150 m away from the central caisson.

1.9.5 Infiltration Galleries

An infiltration gallery type intake is a variation of the slow sand granular media filter that has been used in the water treatment industry for two centuries. The systems rely on the slow movement of seawater through the sand to remove particulate matter and biologically degrade bacteria and other organic compounds.

Galleries are designed similarly, whether located close to shore and beneath a beach, or hundreds of meters offshore (see Chaps. 10–12). A typical system consists of a header/lateral underdrain system buried in trenches 2–4 m below the seabed and backfilled with graded sand and/or gravel. The underdrain is used to collect seawater that filters through the seabed at a rate that usually ranges from 2–8 m/day, and conveys it to shore via a pipeline.

Large-scale galleries can be difficult to construct and may require expensive and time-consuming construction methods for their installation. However, they generally produce higher quality water than surface intakes, and their use may reduce the cost and chemical requirements of RO pretreatment systems.

1.9.6 Onshore Karst Pit

In some locations the onshore geology may be hydraulically connected to the sea by underground fissures typical of karst topography formed by the dissolution of soluble limestone or dolomite rocks. These underground networks may serve to

Fig. 1.5 Onshore karst pit intake in Curaçao

feed a below grade basin constructed onshore, and from which seawater may be pumped to a desalination plant.

One such intake was employed for a 26,000 m^3/d SWRO plant in Curaçao, in which a 6 m deep intake basin was located 100 m inland from the shoreline (Fig. 1.5). The basin walls were constructed of prefabricated, perforated concrete slabs and large, limestone rocks were installed around the basin's periphery to ensure a continuous infiltration of seawater.

1.10 Conclusions

The intake system is a critical component of all SWRO plants. The production of feed water to a SWRO plant must be reliable and consistently meet the operational capacity of the plant and should be of a consistent quality.

The intake water quality is critical to the downstream process operations within a SWRO plant. Pretreatment processes must be used to remove debris, suspended solids and organic compounds that adversely impact the primary membrane process. Therefore, the design and location of the intake play an important role in the full plant design and in the overall operational cost of a facility.

A key issue impacting the choice of which intake type to use is the operational reliability of the intake under all operating conditions that could occur at a site. While lower environmental impacts and reduced cost of operation are very important issues, reliability of a facility allows it to be financed and built. Therefore, there is a general bias toward the use of existing and proven intake types, particularly for large capacity SWRO facilities.

References

Missimer, T. M. (2009). *Water supply development, aquifer storage, and concentrate disposal for membrane water treatment facilities* (2nd ed.). Methods in Water Resources Evaluation Series No. 1. Sugar Land, TX: Schlumberger Water Services.

Missimer, T. M., Ghaffour, N., Dehwah, A. H. A., Rachman, R., Maliva, R. G., & Amy, G. (2013). Subsurface intakes for seawater reverse osmosis facilities: Capacity limitation, water quality improvement, and economics. *Desalination, 322*, 37–51. doi:10.1016/j.desal.2013.04.021.

Pankratz, T. (2007). Desalination: Intake and pretreatment options. In *Presentation at Conference on Middle East Electricity, Dubai, UAE*, February 12, 2007.

Chapter 2
Design Considerations for Tunnelled Seawater Intakes

Peter Baudish

Abstract As a result of prolonged drought conditions and declining raw water storages, six large capacity seawater reverse osmosis (SWRO) desalination plants were constructed to secure the water supplies of the five major Australian state capital cities. For a variety of reasons including capacity, local geology, site topography, environmental concerns as well as the construction programme and construction risk mitigation considerations associated with hostile marine conditions, tunnels were adopted for five of the SWRO plants, connecting the desalination plants with their open intakes and brine concentrate outfall systems. The tunnel system is a relatively new concept for SWRO intake and outfall design. The design of marine intake and outfall works is very complex because of the wide range of constraints that must be accommodated as well as the hydraulic interactions among the intake system, pre-treatment facilities, desalination plant, and outfall system over a wide range of possible climatic, physical, and operational conditions. The challenges posed in the design and construction of tunnel and marine structures in high-energy open ocean environments are presented. These challenges include those associated with waves and currents, short- and long-term hydraulic considerations, durability and corrosion, biofouling control, and ongoing operation and maintenance. Different intake design approaches at two of the Australian SWRO plants are discussed.

2.1 Introduction

Between 2004 and 2012 six major seawater reverse osmosis (SWRO) desalination plants were constructed to serve Australia's largest coastal cities—two for Perth and one each for Brisbane-Gold Coast, Sydney, Melbourne and Adelaide (Fig. 2.1). The plants range in production capacity from 45 to 150 GL/a, with their intakes and brine return outfalls designed for flows as high as 18.5 m^3/s. Five of the plants have

P. Baudish (✉)
Jacobs, Sydney, Australia
e-mail: Peter.Baudish@Jacobs.com

T.M. Missimer et al. (eds.), *Intakes and Outfalls for Seawater Reverse-Osmosis Desalination Facilities*, Environmental Science and Engineering,
DOI 10.1007/978-3-319-13203-7_2

Fig. 2.1 Location of major Australian SWRO desalination plants

had tunnelled intakes and outfalls. The marine works are located in relatively hostile wave climate environments in the South Pacific, Southern and Indian Oceans.

The intake and outfall tunnels are up to 65 m below sea level, 2500 m in length, 4 m in internal diameter and of both incline and decline configurations. As well as the tunnels, there are marine intake structures, brine return diffusers, connective risers through the seabed floor, shore based seawater pump stations and fine screens. The tunnel and associated marine works are major engineering undertakings in their own right, forming a significant proportion of the project capital cost, and may also be the area of greatest project risk.

This chapter presents technical challenges associated with the design and construction of seawater tunnels and marine works in hostile marine climates with a focus on intakes. As many of these issues and challenges also apply to brine concentrate return systems only a few considerations specifically related to brine concentrate return tunnel and marine works are discussed. This chapter covers:

- Site-specific onshore and offshore topographic, geotechnical and geological conditions
- Marine wave climate and oceanography

- Risk, environmental and cost drivers for tunnelled intake and brine concentrate return conduits
- General hydraulic and environmental performance requirements
- Hydraulic considerations
- Operability, fouling, sedimentation, maintenance, and durability considerations
- Tunnel profile issues
- Intake pumping station and screen configurations.

2.2 Background

Australia is a highly urbanized country and though equal to mainland USA in land area, it is relatively sparsely populated. Over 80 % of the 22 million people live near the coast, with some 65 % in the major state capital cities. Increasing population accompanied by the longest recorded drought and limited alternative water resources led to the construction of major desalination plants around Australia to provide strategic diversification of water sources and drought security (Alspach et al. 2009). Most of the desalination plants were delivered through fast-track design-build contracts combined with an operational and maintenance contract (DBOM).

One of the disadvantages of a high coastal population density is the lack of available sites for large desalination plants with sufficient land area and/or suitable zoning classification. In the Australian context of rapid implementation of these desalination projects (as a drought response measure), this was a significant issue.

Consequently, the sites chosen may not have been ideal due to some or all of the following reasons:

1. Sites not located immediately adjacent to the ocean
2. Intakes and outfall in oceans with hostile wave climates with marine construction potentially at risk from large swells, rogue waves, or seasonally unfavourable climatic conditions
3. Unfavourable geotechnical conditions
4. Not close to the center of demand and thus having high connective product water infrastructure costs
5. Potential impacts on coastal and marine environments

The first three factors in conjunction with the large plant capacities, specific environmental constraints, cost effectiveness as well as the assessment of construction risk and delivery time frame, led to the use of tunnelled intakes and outfalls as the selected solution in Australia for the seawater intakes and brine concentrate returns for all but the first major desalination plant (Table 2.1).

Table 2.1 Seawater intake and outfall configuration

SWRO plant location (city served)	Conduit details[a]	Marine conditions	Launch[b] depth	Seabed depth
Kwinana (Perth)	1 × 2.4 m, 1 × 1.6 m dia. GRP ~350 m	Quiescent—Cockburn Sound	NA	8 m
Tugun (Brisbane—Gold Coast)	2 × 2.8 m dia. Tunnels ~2200 m long	Hostile (8 m Hsig[c]) and cyclone risk	70 m	22 m
Kurnell (Sydney)	2 × 2500 m long 3.4 m dia. tunnels	Hostile (7 m Hsig) and wave reflection	18 m	25 m
Binningup (Perth)	3 × ~960 m, 2.4/2.0 m dia. tunnel and bored	Moderate (4 m Hsig), protected reef	NA	10 m
Port Stanvac (Adelaide)	2 × ~1250 m long 2.8 m dia. tunnels	Moderate (4 m Hsig)	50 m	30 m
Wonthaggi, Melbourne	2 × 1200 m, 4.0 m dia. tunnels	Hostile (8 m) + Bass Strait	18 m	20 m

For descriptions of site geotechnical, environmental and oceanographic at each location refer Baudish et al. (2011)
[a]Lengths of intakes and brine outfalls are indicative
[b]Tunnel depth below ground level at launch shaft
[c]*Hsig* significant wave height

2.3 Intake Design and Construction Considerations

Open sea water inlet conduits are prone to marine organism ingress and colonization as well as sediment accumulation from sand and shell matter. Long, large diameter conduits, such as tunnels, amplify these issues as they cannot be readily taken out of service. They are difficult to inspect because of their depth and length. They are also likely to have internal conduits for maintenance purposes or biofouling control and therefore, are not suitable for pigging. They have a number of specific design considerations and issues that are not common with open shore based intakes.

2.3.1 Marine and Geomorphological Information Requirements

General marine issues and information requirements for the design of seabed structures and conduits include:

- Seabed geomorphology and bathymetric profile information is required for construction and siting seabed assets ideally being on relatively flat terrain clear of reefs and large boulders so as to minimise underwater preparation works

Fig. 2.2 Surge and wave conditions—Sydney desalination plant inlet

- Seabed surface sediment particle size distribution data is required for the consideration of scour as well as height of sediment suspended by currents, particularly by storm-wave induced orbital currents in the water column
- Extreme sea levels driven by tide and climatic conditions are of particular importance for pump stations, outlet shafts and gravity brine drains and overflow systems. These conditions include potential long-term sea level rise and drive hydraulic performance criteria as well as onshore ground and structure levels
- Currents induce loading on both permanent seabed structures and temporary marine construction equipment, such as jack-up barges and associated construction plant and equipment. Prevailing currents may be used to advantage in the design of brine diffusers to maximize dispersion and dilution as well as to optimize the relative positioning of intake and brine return systems to each other
- Long term wave climate data is unlikely to be available specific to the selected site. Regional data may have to be calibrated, modelled and interpreted taking into account the specific bathymetry, shore features and wave reflectance issues (Fig. 2.2)
- Site-specific wave climate data is necessary to derive wave-induced currents and loads on seabed structures—this data can be used to optimize positioning of structures in water deep enough to minimize loading on marine structures, but at the same time shallow enough to minimize length of tunnels for economic (cost) and construction timing reasons

- Environmental conditions need to be well understood. These include salinity and temperature, the range of marine flora, fauna and biofouling organisms. Their considerations may impact the design of intake screens, antifouling measures and operation as well as maintenance of offshore works.

2.3.2 Marine and Tunnel Construction and Operation

The detailed design of the tunnel and marine structures must take into account the construction methodology and type of equipment likely to be employed. Tunnel boring machines (TBMs) and jack-up barges for marine works and drilling risers are highly specialized equipment and both are likely to be long lead items. Jack-up barges in particular must be selected and potentially modified to suit the site-specific marine works, depths and oceanographic conditions.

Construction and operational issues to be addressed during the design include the following:

- In a fast track environment, TBM and jack-up barges will be on the critical path for construction, requiring early decisions on intake riser style and diameter, tunnel diameter and profile.
- Seabed structures should be deep enough to avoid being a navigation hazard, to avoid the effects of extreme waves and at a depth where good seawater quality is expected. They also need to be shallow enough to be constructed from jack-up barges. Intakes also should be positioned high enough off the seabed to minimize sediment entrainment.
- Jack-up barges must be able to be raised during storms to provide clearance for maximum swells caused by inclement weather. Weather causes wave intensity variations and storm surges which can limit marine construction activities. The occurrence of intense storms dictates the need for accurate forecasts and early warning systems.
- Stable and accurate positioning requirements for drilling, for the installation of riser liners, riser caps and screen and diffuser structures as well as accurate intersection with tunnels.
- Timing of marine (riser construction) and tunnelling construction operations also impacts the marine structures design. Tunnel risers may be constructed before or after the tunnelling and this needs to be considered, as risers may be connected to the tunnel through the crown or offset and connected via a lateral.
- Pressure differential limits for segmented liner construction impact on bolting and grouting design.

For large remote intakes that use HDPE pipelines on the seabed, a duplicate intake line may be installed to allow one intake to be taken out of service, while the other is pigged or its screen maintained. This “luxury” does not apply to large tunnel intakes. It is only a marginal cost difference to construct tunnels and marine

works to suit an ultimate capacity. Due to the size and cost of tunnels, and in particular their construction risk, a single intake tunnel (and outfall) is typical. Thus future operation and maintenance requirements associated with a single intake in deep water needs to be addressed in the design development. Consideration needs to be made for the:

- inspection (and maintenance) provisions for the tunnels which are typically 20 m below sea bed and 40 m below sea level
- potential dewatering and safely carrying out inspection and maintenance
- limitations on diver access and ROV technology.

Of note is that since the long seawater intake tunnels in Australia have entered into service (i.e. from 2008 onwards) there have been advances in monitoring technology. ROV video cameras are now employed for regular monitoring of tunnel condition, in particular, for signs of sediment ingress and marine growth.

2.3.3 Intake Design

Intakes need to operate in a way that minimizes marine impacts, particularly impingement and entrainment of marine life. Key environmental performance criteria for intakes include limitations on maximum intake screen aperture and associated screen velocities. Similarly, outfall systems are now required to achieve stringent environmental performance objectives even when running at reduced capacity.

The upper limit to velocity through the intake screen bars is typically specified as an average of 0.10 or 0.15 m/s. While this limit on velocity may have the objective of protecting marine life or to avoid the intake of sediment, it is a major factor impacting on the size and weight of the seabed intake structure.

Typical screen bar/aperture spacings are in the range of 50–300 mm and, in combination with an allowance for marine growth on the bars, can have a significant impact on the overall size of the intake structure. Thus design needs to balance the size, constructability (in hostile marine environments) and cost factors versus long-term operation and maintenance. Considerations include:

- providing an allowance for marine growth, and interpreting any flow-on effects in the context of meeting project performance specifications, ambient ocean currents, the specified bar spacing and determining resultant impacts on the structure size
- use of anti-fouling copper-nickel alloys to suppress marine growth
- planning in situ maintenance regimes and/or design of removable screens
- the prevention or control of marine growth inside the riser and tunnels.

2.3.4 Hydraulic Design

Typically the tunnelled intakes and outfalls in Australia have been designed and constructed as segmented precast concrete lined tunnels. Minimum practical diameters for tunneling by TBM are about 2.8 m internal diameter. Diameters larger than 2.8 m are only constructed if required to suit the hydraulic requirements of an intake.

Large diameter HDPE pipeline style intakes are typically installed by floating, sinking and anchoring on the ocean floor. These HDPE pipelines are often designed to be cleaned by pigging, so that their internal condition can be restored. Piping provided for biofouling control or for other types of maintenance can be located external to the pipe. For tunnels small diameter piping is usually installed internal to the tunnel. Thus, the tunnel is not suited to mechanical cleaning or pigging. Due to their length and depth and internal fixings, tunnels are likely to be difficult to clean once in service.

Whilst there is published information on friction co-efficients for segmented tunnels, these co-efficients are not reflective of long-term friction over the 50 or 100 year tunnel design life of a seawater intake. Even if seawater tunnels have been designed to enable their dewatering and cleaning, the intention is not to do so. Thus, the designer must take a view as to the potential long-term changes in hydraulic characteristics due to marine growth and related performance alteration including:

- potential long term loss of diameter in some or all of the intake conduit components
- long term roughness factors to be adopted.

These are significant issues as they affect the choice of tunnel diameter, long term pumping heads, intake pump selection and screen design. Long-term data on marine growth in long conduits where biocide control is practiced is lacking, but it is clear that some growth will still occur. The highest rates of growth will occur at the intake screen, riser and tunnel entry, and then decreasing along the tunnel length where there is less light.

Intake screens require particular attention for the design of cleaning provisions. Ideally screens should be removable so that they can be mechanically cleaned above water. Biocides cannot be used for biofouling control on the screen proper due to risk of escape into the marine environment. They should be applied at the entry to the intake riser, with particular attention given to achieving effective mixing.

Other factors that need to be considered in design include:

- effect of tidal variations, swells and storm surges, as well as the potential long term impacts of climate change
- hydraulic limitations caused by fixed brine nozzles which are quite sensitive to flow rate and with some flow combinations potentially resulting in overflows of seawater within the site proper. This may require design mitigation measures such as spill provision from the brine outlet to the seawater intake
- temperature and salinity.

Dynamic surge impacts associated with sudden stoppage of the seawater pumps must also be considered, as this can lead to significant surges of over 5 m at intakes and potentially overflow onto the site. These effects can be mitigated by reducing momentum by increasing tunnel diameter or providing a large volume in the intake wet well to absorb the surge. Surge is a factor to be taken into account in deciding on the internal diameter of the tunnel.

2.3.5 Durability Aspects

Durability issues for tunnelled infrastructure and associated connective works should not be underestimated. Tunnel and marine works may be specified to have design lives of 50 or even 100 years. Achieving such design lives needs careful control through design, fabrication, construction and operational stages. The use of fibre reinforced concrete for tunnel segments has greatly extended the expected design life of the tunnel lining compared to conventional reinforcement.

When estimating expected design life of tunnel segments, it is also important to consider the accelerated ingress and corrosion rates expected to result from the occasional exposure of the concrete segments to air during tunnel dewatering. This requires chloride ingress modelling.

Coarse intake bar screens and metal fittings are typically composed of a super-duplex or copper nickel alloy. The latter is preferred due to its natural inhibition properties against marine growth. Coated steel with anodic protection may be appropriate for accessible shore-based equipment, such as screens.

Within intake tunnels there are additional considerations, such as when chlorine is used for control of marine growth, injected at the mouth of the intake risers. While this requires transport of diluted chlorine solution in piping within the tunnel, consideration of the impact of chlorine needs to be taken into account in materials selection of tunnel fixings and chlorine piping. Metals may not be appropriate, while plastics must also be selected for permanent installation to meet the 100-year design life of each component. Chlorine is typically delivered to the injection point as diluted sodium hypochlorite or gaseous chlorine in solution. Scaling risk needs to be addressed with the former, and the more aggressive nature of chlorine in the latter.

2.4 Integration of Design

The intake tunnel is inextricably linked to the design of the intake pump station and intake screens. Almost invariably site-specific solutions are required. Traditionally, fine 3 mm screens are placed upstream of the pumps. These screens capture any material that may pass through the coarse ocean intake screens, including filamentous algae and non-motile marine life such as jellyfish, and also protect the

pumps from damage. This following section outlines alternative design solutions developed for the Sydney and Gold Coast desalination intakes (and outfalls), largely due to geotechnical conditions, tunnel drive method, and specific site limitations.

2.4.1 Gold Coast SWRO Desalination Plant

The GCD site is located about 700 m inland on a former municipal waste landfill site adjacent to the north west corner of the Gold Coast airport at Tugun (Fig. 2.3).

The on-site geotechnical conditions show deep consolidated sand both onshore and offshore overlaying sedimentary bedrock. Sound rock is found at depths around −55 to −60 m AHD. The plant site is approximately RL +7 m AHD grading gently seawards down to developed coastal dunes at about RL +5 to 6 m.

Marine climate issues include a summer cyclone season with ocean maximum currents up to 0.5 m/s. During high wave storm events (8 m height at ARI 1000 years) seabed orbital currents can reach 3 m/s or greater. The 6-month summer cyclone season precluded marine construction in this period. There is littoral sediment drift of some 500,000 m^3 per annum northward. The required siting of the intake to achieve stability required seabed depths below 18 m of depth to minimize sand and sediment entry into the intake. This also allows it to be located clear of the

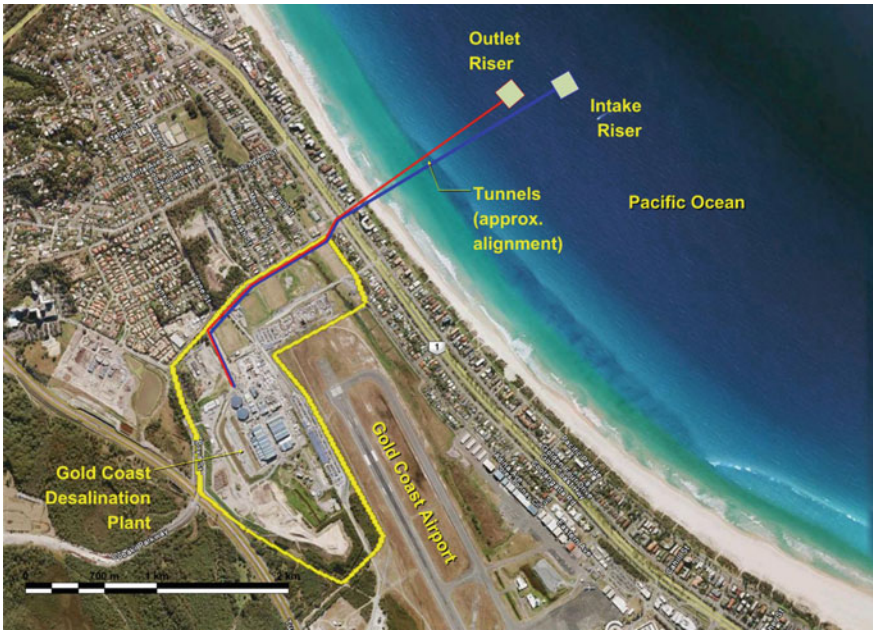

Fig. 2.3 Gold Coast desalination plant—tunnel and marine structures locations

Fig. 2.4 Tunnel access shaft and TBM components/TBM segment being lowered for assembly below ground

more active near-coastal zone which could have otherwise resulted in undermining or covering the intake or outfall structures.

As outlined in Chap. 3, although there is little marine vegetation on the sandy seabed, the area is regarded as having a high environmental value. Tunnels were selected on the basis of program, environmental factors and visual impact during construction, as well as to minimize marine construction risk. Tunnelling also eliminated the need for an intake pump station remote from the plant site. This simplified the design and greatly reduced local impacts, as a suitable site for such a pump station was not readily available.

Specific features of the Gold Coast intake and outfall tunnel, and the seawater intake pumping arrangement were:

- Deep intake and outfall shafts. Tunnel boring machines (TBMs) work most effectively in rock or hard ground conditions. At the Gold Coast site, this meant that 70 m deep launch shafts were required to locate the TBM's in suitable rock (Fig. 2.4). This necessitated that the shafts be used for all construction activities including lowering and raising of TBM components, shift personnel, tunnel segments and also for removal of tunnel spoil.
- The depth at which sound rock was located was very consistent and did not favour an incline or decline arrangement. Both the intake and brine concentrate return tunnels were therefore graded upwards from land to sea in a slight incline (Fig. 2.5). This ensured any water entering the tunnels during construction drained back to the shaft by gravity, where it was easy to manage. This also resulted in the tunnel being slightly higher and closer to the seabed at the distal end, reducing the time to construct the riser connecting the tunnel to the sea floor.
- The single intake screen is approximately 4.4 m high, 5.8 m in diameter and with 2 m high copper nickel screens with a bar spacing of 140 mm (Fig. 2.6).
- The four 1.33 m^3/s vertical turbine seawater intake pumps were located within the 9.6 m dia. tunnel intake shaft (Fig. 2.7). This simplified the intake arrangement and reduced both costs and construction time for this element of the project, which was on the critical path for the overall project. However, this also

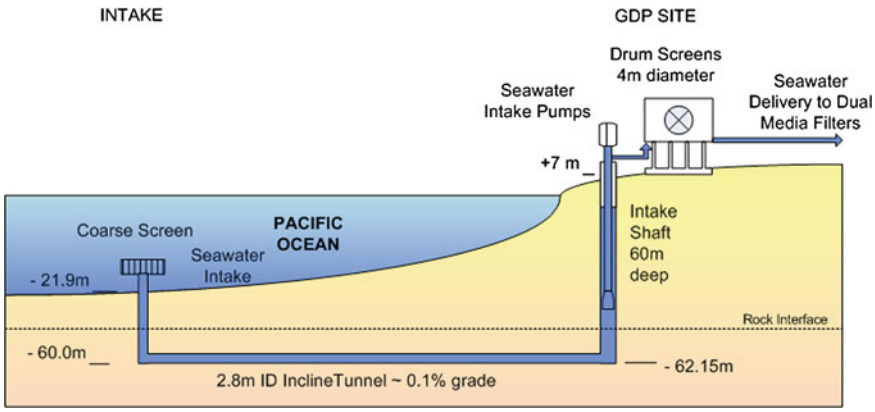

Fig. 2.5 Schematic of the GCD seawater intake arrangement

Fig. 2.6 Intake coarse screen being installed from the jack-up barge

meant that it was not feasible to locate fine screens upstream of the pumps, introducing a potential risk of pump fouling under very poor water quality conditions. Given the good intake conditions afforded by locating the intake far enough offshore in deeper water, and through the use of high clearance pumps, this risk was considered acceptable. Both numerical and physical modelling of the intake/pump suction were carried out to optimize pump inlet design to avoid the development of unfavourable pumping conditions (unbalanced flows/vortexes) for these large capacity pumps (Mould and Sprengel 2010).

- Seawater is delivered from the intake pumps to the two (duty/standby) 4 m diameter, 3 mm mesh dual entry drum screens (Fig. 2.8). The screens are housed in an above ground structure enabling gravity flow to the pre-treatment filters. During operation of the plant to date, there has been very little trash collected by the fine screens, demonstrating the advantages of careful location of the intake structure to ensure good intake water quality.

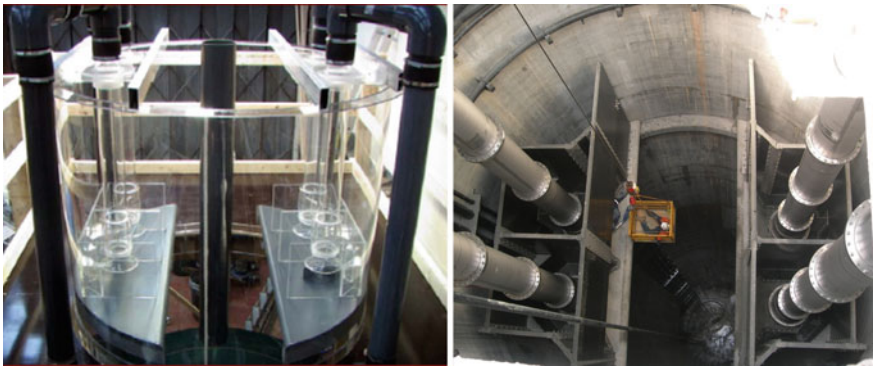

Fig. 2.7 Intake physical model and as-installed seawater pumps

Fig. 2.8 Intake pumps and elevated screen structure 4 m diameter drum screen

2.4.2 Sydney SWRO Desalination Plant

The Sydney desalination plant (SDP) is located at Kurnell, to the south of the Sydney airport (Fig. 2.9). Site constraints included a conservation area to the north and a freshwater ecosystem that leads to the Towra Point wetlands adjoining Botany Bay. The plant site geotechnical conditions included shallow loose sands with a high water table interspersed with peaty lenses, underlain by firm sandstone that ranges from −6 to −30 m AHD and undulates underground across the site. This relief is caused by the buried remnants of former drowned river valleys.

Though closer to the sheltered waters of Botany Bay, the intake and brine outfall are located eastwards to the Tasman Sea (Pacific Ocean).

The desalination plant site itself is located at a relatively low elevation (5–6 m ASL finished level), but the ground and rock profile rises seawards to nearly 35 m before sloping down to the 20–25 m high sandstone cliffs at the edge of the Tasman Sea. The sea floor below the cliffs is rocky, and descends to 25 m below sea level

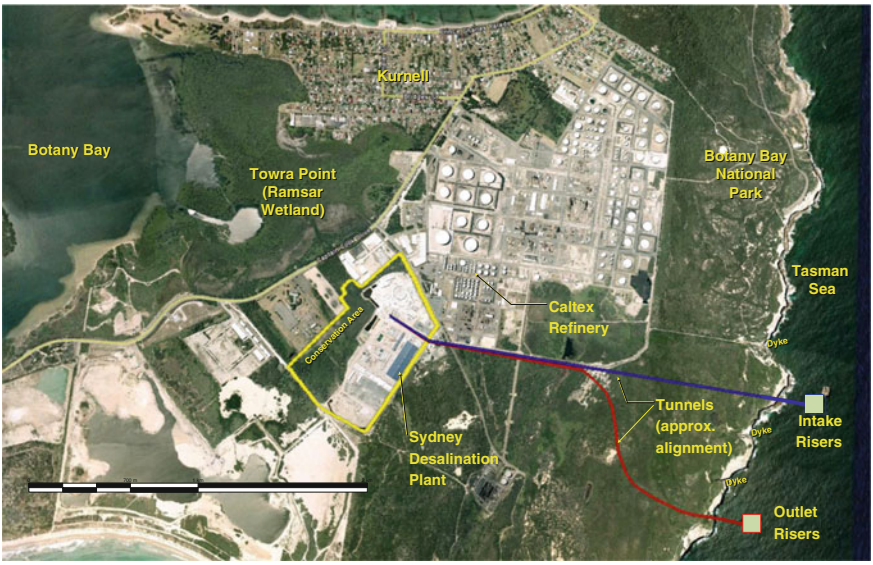

Fig. 2.9 Tunnel and marine structures location—Sydney desalination plant

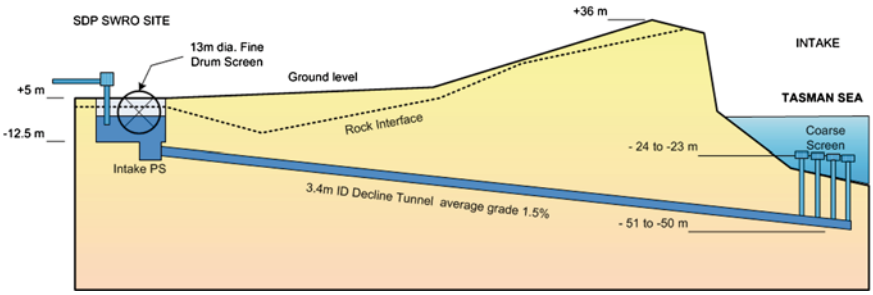

Fig. 2.10 Schematic of the SDP seawater intake arrangement

within a few hundred metres of the cliffs, a depth at which both the intake and concentrate return structures are located (Fig. 2.10).

The coastline bordering the Tasman Ocean is within Botany Bay National Park. There is a wide range of marine flora and fauna associated with reefs and rocky seabed. Migrating whales are frequently observed in the area between April and December. Restrictions to riser construction activity were required when whales were in close proximity.

Specific marine conditions at the intake and outlet site included continuous high energy incident and reflected waves with 1:10 year Hsig of 7.3 m and estimated extreme waves heights of approximately 12 m. Currents typically range between 0.1 and 0.4 m/s. Modelling of the specific local wave climate (as distinct from regional data) was required to assess the influences of the steeply rising floor and

Table 2.2 Key design issues for incline and decline tunnels

Issue	Incline tunnel	Decline tunnel
Tunnel dewatering	At the landside shaft	Sea side (or landside by progressive movement of pump)
Sediments	May be transported towards seawater pump station	Likely to accumulate at intake end of tunnel
Floating matter	Likely to be remain near the intake marine riser	Likely to be transported towards the seawater pump station
Air entrainment (brine return)	Air will flow along the tunnel crown to the brine outlet	Air must be released before entering the tunnel

cliff face on extreme wave heights as well as frequencies and influences of reflected waves.

Trenched pipelines were never considered for the intake and outlet because of the cliff profile, marine conditions and sandstone geology (both onshore and seabed). Tunnels were adopted. Though primarily in hard sandstone, the tunnel routes crossed near vertical fault lines (weathered dykes). Due to location within the national park, extensive exploratory drilling was not possible. Thus, geotechnical information related to dyke strike and dip and expected condition at the dyke-tunnel route intersections was limited. Igneous dykes had measured widths of 1.3–2.7 m. A limited joint swarm was present at mid length of the route for both tunnels.

The shallow sound rock available at one end of the desalination plant site opened up the possibility of a decline tunnel. This approach was adopted after careful consideration of the technical and operational advantages and disadvantages of a decline arrangement (Table 2.2).

In terms of construction, the decline tunnel offered significant advantages in construction efficiency, including ease of assembly/disassembly of the TBM within a "box-cut", and transport of tunnel segments and removal of tunnel spoil which did not have to be lowered or raised via a shaft (Fig. 2.11).

A decline tunnel was adopted for both the intake and brine return tunnels, connected directly to an intake pump station. Compared to the Gold Coast plant this resulted in a more conventional arrangement of the fine screens upstream of the sea water inlet pumps (Fig. 2.12).

There are two 12.7 m diameter (2 × 100 %) capacity drum screens for the 250 ML/d Sydney plant (Fig. 2.13). When the plant is augmented to 500 ML/d, two additional screens will be added, resulting in four 33 % capacity screens. The large screen diameter was required to accommodate the tidal range as well as ultimate friction effects through the long intake tunnel. There are five 2 m^3/s seawater intake pumps, two for each 125 ML/d SWRO module and a common standby. An additional five pumps will be installed when the plant is augmented. As for the Gold Coast plant, modelling of the inlets to the pump suction was required to ensure optimum flow and performance of the pumps.

Marine construction was extremely difficult due the prevalent swells and the reflected wave waves from the nearby cliff face. Originally, the risers to tunnel were

Fig. 2.11 TBM assembly within the "box-cut" leading to the tunnel portals/haulage railway and spoil conveyors leading out of the "box-cut"

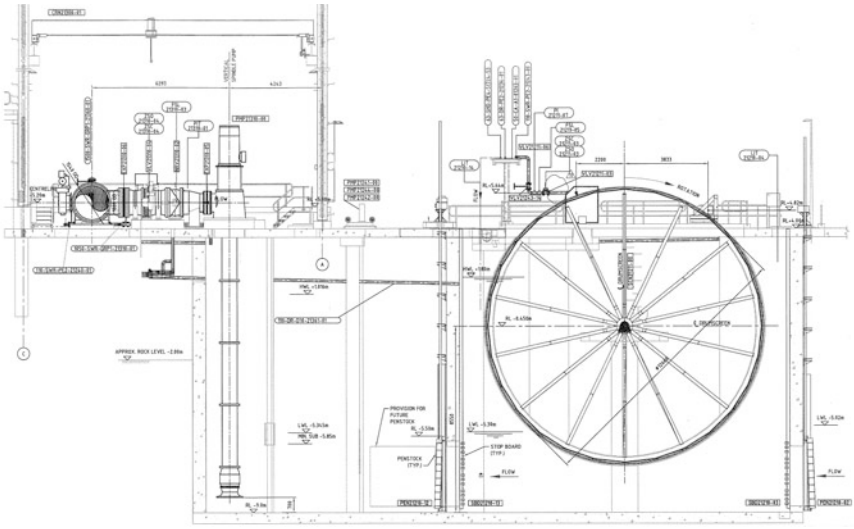

Fig. 2.12 SDP Intake pumps and fine screen general arrangement

planned to be connected through the tunnel crown. A change of design to a lateral connection arrangement was adopted early during the construction phase to enable more independent construction of the tunnel and riser/marine works. The risers are connected to the tunnel via stub laterals. Some further details of the construction methodology for the marine works are provided in Chap. 3.

The risers were of ribbed GRP construction, and grouted into bored holes. The lateral also has a GRP liner. The main elements of the seabed marine intake and brine return structures were precast concrete sections to which copper-nickel alloy screens/super duplex nozzles were attached respectively.

Fig. 2.13 SDP intake pump/fine screen during installation

2.4.3 Construction Scale

A few details from the Sydney desalination project give some idea of the magnitude of the tunnel and marine works. The intake and outlet structures were positioned within a contract prescribed area. The areas are located approximately 300–350 m offshore from the headland at Cape Solander and approximately 700 m apart as shown in Fig. 2.9.

The intake system comprises:

- Four cylindrical, precast concrete intake structures 8.5 m in diameter and 5.2 m high (Fig. 2.14)
- 32 screens (8 per intake structure) 1.9 m high × 3.0 m long with copper-nickel alloy bars at 340 mm spacing
- Four fibreglass lined 'risers' each with a 1.5 m ID, located approximately 20 m apart and extending from the seabed down to tunnel level; fibreglass lined connective stub cross tunnels with a 1.4 m ID approximately 6.0 m in length, connecting the risers to the tunnel

Fig. 2.14 Pre-cast intake coarse screen structure/screen base being lowered

- A 3.4 m ID tunnel approximately 2.5 km in length, sloping downwards at up to a 2.5 % decline from on-shore and lined with fibre reinforced precast concrete segments
- Eight chlorine solution pipes mounted within the tunnel (one duty and one standby pipe per intake riser)
- A reinforced concrete pumping station structure approximately 35 m^2 and 20 m deep with a distribution channel and bays for four drum screens
- Two drum screens 12.7 m in diameter
- Five 2 m^3/s vertical pumps.

The brine concentrate return outlet system comprises:

- Two cylindrical, precast concrete outlet structures 6.8 m in diameter and 3.7 m high located on the seabed in more than 20 m of water
- Eight tapered super duplex UNS32750 brine nozzles, (four per outlet structure) with an exit ID of 370 mm for a plant capacity of 250 ML/d. The nozzles will be changed when the plant is expanded to 500 ML/d
- Two fibreglass lined risers each with a 1.4 m ID extending up from tunnel level to the seabed
- Two 1.8 m diameter stub cross tunnels approximately 6.0 m long connecting the risers to the main tunnel
- A 3.4 m ID decline tunnel approximately 2.5 km long
- A reinforced concrete deaeration—air release structure approximately 40 m × 5 m wide and 12 m deep
- A 900 mm diameter raw seawater pump discharge cross-connection and control valve to supplement flows and achieve specified brine dispersion requirements over the full operating range of SWRO plant flows.

Major construction equipment included:

- A jack-up barge (self elevating marine construction platform) from which the riser shafts were drilled and constructed. When elevated the barge was 10 m above the mean sea surface level. The barge had a displacement of 2820 t and had 66 m long legs

- Two double shielded hard rock tunnelling machines, one each for the inlet tunnel and one for the outlet tunnel. The cutting face was 4165 mm in diameter and the TBM body 4100 mm in diameter. The TBM cutting face weighed 33 t, and there were 16 trailers with a total length 123 m
- The tunnel lining erected behind the TBM was a six segment configuration. A total of 22,800 segments were required for the 5.0 km combined length of tunnels. Each segment is 225 mm thick and weighs 1.5 t.

2.5 Conclusions

Where desalination plants are constructed on coastlines exposed to hostile open ocean conditions, and tunnels are adopted as intake and brine concentrate return conduits, the tunnel and marine infrastructure become a significant proportion of the overall capital cost of the project. The marine works are an area of the project where a large part of the overall project risk lies, usually being on the critical path and potentially subject to extremes of weather and ocean conditions.

The design of the marine intake and outfall works is very complex because of the wide range of constraints that must be accommodated as well as the hydraulic interactions between the intake system, pre-treatment, desalination plant and outfall system over a wide range of possible climatic, physical and operational conditions.

As each desalination site has a unique combination of physical, environmental and social constraints, the solutions developed for the seawater intake and brine return systems may well be quite different even if they have similar performance requirements.

Acknowledgments The information presented in this chapter has largely been derived from experiences gained by Jacobs staff during siting and environmental studies and tender and detail designs related to the six major Australian SWRO plants, in particular the Gold Coast and Sydney SWRO plants. I would like to acknowledge the valuable contributions and insights of Daryll Pain, Phil Banks, Ralph Burch and Doug Franklin.

The Gold Coast Desalination Plant was designed and constructed by the Gold Coast Desalination Alliance comprising alliance partners SureSmart Water, John Holland, Veolia Water; Jacobs (SKM), Halcrow and Cardno.

The plant is operated by Veolia Water for SureSmart Water. The Sydney Desalination Plant was designed and constructed by John Holland and Veolia Water (the Bluewater construction JV) and the Jacobs (SKM)–Mansell design JV. The plant is operated by Veolia Water.

References

Alspach, B., Burch, R., & Baudish, P. (2009). Seawater desalination in Australia: Water supply solutions without environmental cost. In *IDA World Congress*, *Dubai*, November 2009.

Baudish, P., Lavery, N., Burch, R., Pain, D., Franklin, D., & Banks, P. (2011). Design considerations and interactions for tunnelled seawater intake and brine outfall systems. In *IDA World Congress*, *Perth*, November 2011.

Mould, R. J., & Sprengel, J. (2010). Innovative design for a large seawater intake pump station. In *AWA National Conference, Brisbane*.

Chapter 3
Sydney and Gold Coast Desalination Plant Intake Design, Construction and Operating Experience

Keith Craig

Abstract Australia has embarked on the development of several large capacity seawater reverse osmosis (SWRO) facilities to meet future water demands and to provide water security during severe drought conditions. Two of these SWRO facilities, Sydney and Gold Coast, have installed permeate capacities of 266,000 and 133,000 m^3/day respectively. The coastal areas of Sydney and Gold Coast contain sensitive marine environments that necessitated the development of intake systems that connect tunnels from the SWRO plant to offshore capacity cap intake structures. The design of these tunnel intake systems is quite unique and has been successfully designed and constructed. The design of the tunnels and intake structures are herein documented with an initial operational assessment.

3.1 Introduction

The Sydney and Gold Coast seawater reverse osmosis (SWRO) desalination plants are among the largest desalination plants in Australia and provide water to major urban centres of Sydney, Gold Coast and Brisbane. The plants were designed and are operated by Veolia.

A key aspect of the design was the selection of the intake type and design for these large plants to provide suitable seawater quality and quantity to the plants and minimise any environmental impacts from the intake (Craig 2013).

K. Craig (✉)
Veolia Water Australia, NSW, Australia
e-mail: keith.craig@veolia.com

T.M. Missimer et al. (eds.), *Intakes and Outfalls for Seawater Reverse-Osmosis Desalination Facilities*, Environmental Science and Engineering,
DOI 10.1007/978-3-319-13203-7_3

3.2 Sydney Plant Overview

The Sydney Desalination plant has a capacity of 266,000 m^3/day and is located in the southern part of Sydney at Kurnell (Figs. 3.1 and 3.2). The plant can supply up to 15 % of Sydney's water supply and was built following a prolonged drought period.

The Sydney plant is a seawater reverse osmosis process and is divided into two 133,000 m^3/day modules. The treatment includes:

- Open intake with screening
- Sulphuric acid
- Ferric chloride and polydadmaac coagulants
- Dual media filtration pre-treatment
- Cartridge filtration
- Two pass RO
- Remineralisation with lime, carbon dioxide and
- Chlorination, fluoridation then chloramination

The plant was placed into full operation in June 2010. The plant is owned by the Sydney Desalination Company and operated by Veolia.

Fig. 3.1 Sydney SWRO plant

Fig. 3.2 Sydney SWRO water treatment plant intake location at Kurnell, Australia

3.3 Sydney Plant Intake

The size of the Sydney plant together with the nature of the coastline at the intake site had a major influence on the selection of an open intake system for the delivery of sufficient seawater to the desalination plant.

The coast consists of 25 m sandstone cliffs with a rocky seabed that drops within a few hundred metres of the shoreline to a 25 m depth. The coastline is within Botany Bay National Park in an area frequented by migrating whales with a wide range of marine flora and fauna associated with the rocky seabed. Modelling of specific local wave climate was required to assess the influence of the steeply rising

floor and cliff face on the extreme wave height which includes the high energy incidents and reflected waves (extreme height 7.5 m) experienced in the area.

Inputs to the coastline and oceanic waters off Sydney include stormwater and sewer overflows during major storms emerging from Botany Bay, and sewage effluent discharges from the deep ocean outfalls. There is significant influence of the flood and ebb tides from Botany Bay on the northern end of the headland of the Kurnell peninsula, however, modelling of storm flows from Botany Bay indicate that these are likely to bypass the intake site.

Trenched pipelines were never considered for the intake because of the cliff profile, sandstone geology and marine conditions. The construction of a tunnel was considered the best solution for the intake based on the geology and environmental sensitivity of the marine environment (Evans 2011).

The tunnel design was for a shallow shaft via a box cut at the plant where the tunnel boring machine (TBM) was launched, then a downward slopping tunnel to the intake location in the ocean. This allowed a reduced time period for the tunnel construction. The ultimate capacity of any future plant upgrade on the site was used in sizing the intake tunnel allowing for a 500,000 m^3/day output capacity at the site. The tunnel excavated diameter was 4.15 m with a finished internal diameter of 3.4 m and an overall length tunnel of 2.5 km (Fig. 3.3). Pre-fabricated concrete tunnel liners (1200 sections) were employed with each liner being 225 mm thick and weighing 1.5 metric tons.

The intake is located 300 m offshore in 25 m of water and consists of four intake risers (Fig. 3.4). The multiple risers provided security for the operations around blockage and other issues.

There was a major challenge to design and undertake ocean floor construction within a coastal surf zone on a turbulent, shallow rock platform within a marine national park. Day to day marine work was constrained with the work site only 250 m away from the coastline and subject to wave refraction and turbulence greatly limiting operating times. The site was also subject to extremely strong currents severely limiting suitable work days. Divers worked in water depths of 25–28 m from a crane barge anchored in position above the riser locations. The divers cleared loose rock off the seabed and placed grout between large grout filled geofabric socks pinned to the rock. This formed level bases on which to accurately position the riser structures. The riser structures were precast on-shore at Port Botany and delivered to site by an A-Frame barge towed by a tug.

Riser construction and drilling was carried out from the Seafox 6, a self elevating platform (SEP) or jack-up barge (Fig. 3.5). The methodology for drilling of risers required the SEP to be relocated for the drilling of every riser. To minimise the weather-dependent relocation of the SEP, methods and techniques such as the use of airbags, frame structures and underwater lifting techniques were developed, which allowed the team to install riser structures for an adjacent hole already drilled, whilst positioned over another hole. This gave the optimum program outcome.

Fig. 3.3 Sydney SWRO plant intake tunnel

A recirculation method for offshore drilling work was adopted which involved the use of a drill casing assembled on the SEP and lowered to a steel ring located within each riser structure on the seabed. Drilling was undertaken in a completely contained operational environment, by reverse circulation of seawater. Spoil collected via recirculation was brought up through the drill sleeve, deposited and separated from the water in different skips on the SEP. This greatly minimised the environmental and visual impacts of the operation.

Extensive monitoring of seawater quality over approximately two years confirmed the best location for the intake and quality of the seawater for the design of the desalination processes stages and in particular the pre-treatment stage (Sydney Water Interim Report 2006). Pre-treatment pilot plant studies were undertaken using a temporary test intake near the location of the proposed full scale plant intake which enabled detailed long term monitoring of seawater quality in the region and optimisation of the pre-treatment process design. The seawater quality in the defined intake zone was generally of high quality with low turbidity, total dissolved solids (TSS) concentrations, silt density index (SDI), organics concentrations, little or no algae and no hydrocarbons (Table 3.1).

The requirements of the seabed intake structure performance included:

- Upper limit on the velocity between screen bars
- A minimum spacing between screen bars
- Minimum height above the seabed
- A minimum depth below the sea surface
- Non-corrosive or antifouling bar materials
- In-built redundancy (for security or over capacity for future augmentations)

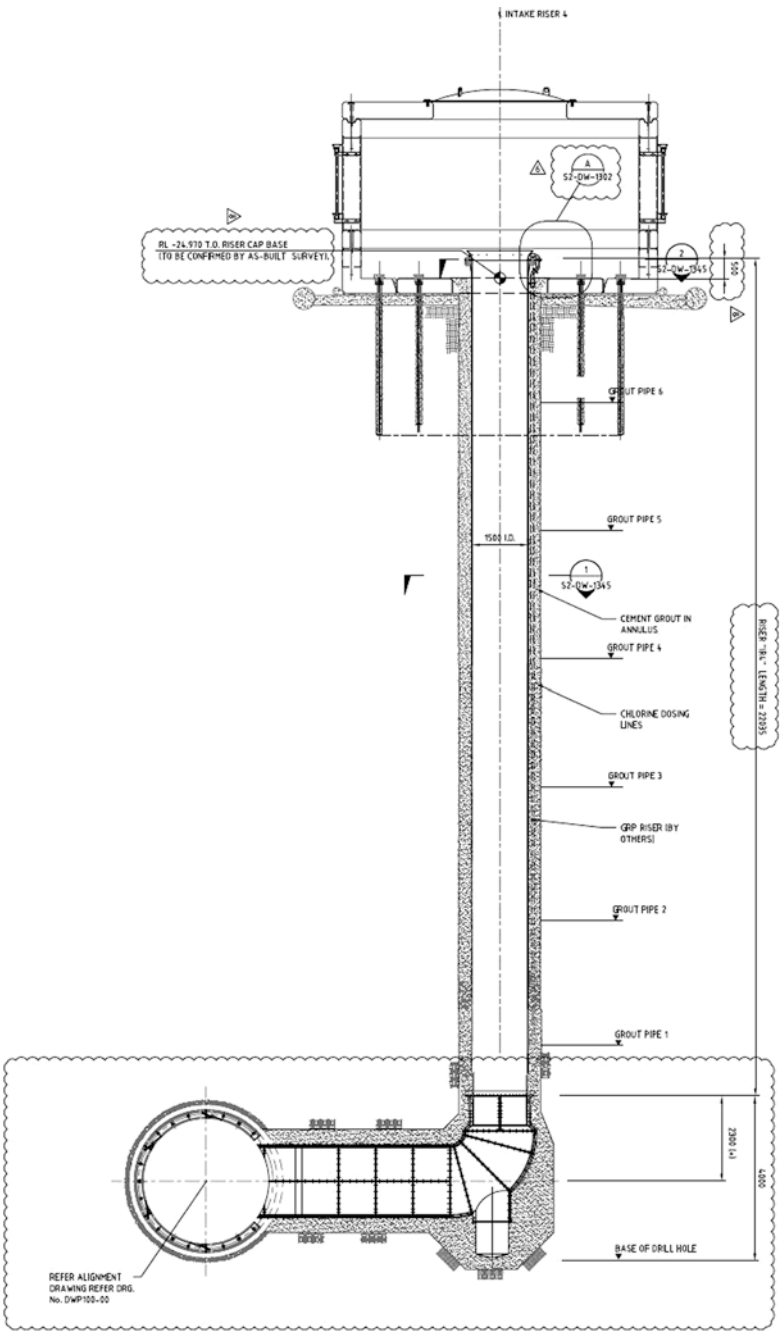

Fig. 3.4 Sydney SWRO plant intake riser and screen from the tunnel to the seabed

Fig. 3.5 Sydney coastline showing the intake riser site with a jack-up drilling and grouting barge

Table 3.1 Seawater quality at the Sydney site

Parameter	Mean	Range
Turbidity (NTU)	0.59	0.22–1.22
TSS (mg/L)	<2	<2–6
SDI	12.5	7.1–25.1
DOC (mg/L)	0.85	0.5–2.1

The velocity cap placed over the intake riser converts the vertical flow of seawater into a horizontal flow entering the intake riser (Fig. 3.6). It has been noted in full scale operations that fish would avoid rapid changes to the horizontal flow and velocity cap intakes have been shown to provide significant reduction in fish impingement (see Chap. 4).

The inflow velocity for the Sydney plant is designed for <0.1 m/s to reduce entrainment and impingement of marine organisms. Shock chlorination capability was provided to control biofouling in the intake and tunnel. The intake screen had an aperture spacing of 300 mm and was made of cupronickel to reduce marine growth and minimise the requirement for screen cleaning by divers.

Onshore two 3 mm drums screens were constructed to remove any entrained marine debris (Fig. 3.7). Each screen is capable of treating the maximum flow rate, but normally both operate together in parallel before the pumping station.

To confirm there were negligible impacts on the marine environment from both the intake and outfall a Marine Monitoring Program (MMP) was developed. The program included three phases of design, baselines studies pre-commissioning and post commissioning or verification studies. The impact monitoring included

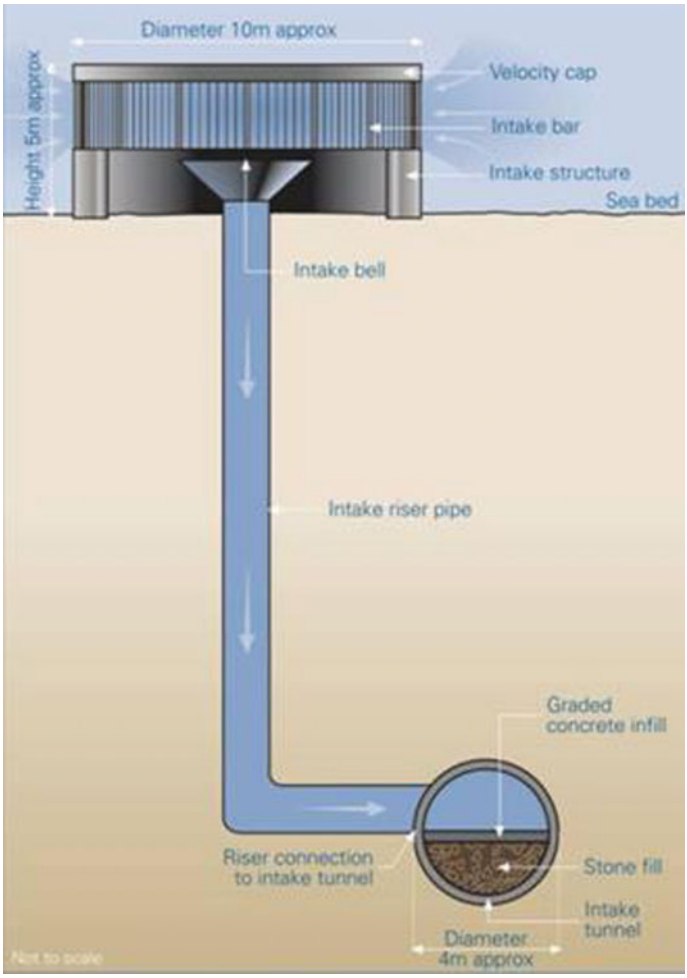

Fig. 3.6 Sydney intake structure from the velocity cap on the seabed to the water tunnel

measurements of water quality, surveys of reef habitat and recruitment of sessile organisms. A fish census surveys was undertaken at three locations over four calendar seasons both prior to commissioning and post commissioning to determine if the operation of plant affected fish populations in the area (Fig. 3.8).

The intake performance has shown minimal effect on the marine ecology and there has been only a small quantity of solids collected on the onshore drum screens. A remote operating vehicle (ROV) inspection is used periodically to monitor the tunnel condition during operation and the effectiveness of the shock chlorination to control biofouling in the intake system. The result of successive

Fig. 3.7 Sydney SWRO plant intake drum screens

ROV inspections has shown the absence of significant marine growth in the tunnel. After two years of operation a growth of approximately 1 cm (thickness) located at the distal end of the tunnel near the riser was measured. This is likely enhanced by the presence of light which was measured during the ROV inspection. The growth was not significant along the remainder of the tunnel length.

Inspection of the intake within the velocity cap shows that abundant marine life is present (Fig. 3.9). Fish were observed swimming freely inside of the intake structure.

3.4 Gold Coast Plant Overview

The Gold Coast Desalination plant has a permeate capacity of 133,000 m^3/day and is located at Tugun on the Gold Coast of Queensland (Figs. 3.10 and 3.11). The plant can supply the Gold Coast as well as supplementing the water supply of Brisbane during drought periods. It is an SWRO plant and the pretreatment, treatment, and post-treatment stages include:

- Open intake with screening
- Sulphuric acid feed
- Ferric sulphate and polydadmaac coagulants feed

Fig. 3.8 Sydney SWRO plant intake marine fisheries evaluation area showing the intake and reference sampling locations

- Dual media filtration pre-treatment
- Cartridge filtration
- Two pass RO
- Remineralisation with lime, carbon dioxide and
- Chlorination, fluoridation then chlorination

The Gold Coast plant is a key part Seqwater Grid and Regional Drought Strategy Contingency Supply Plan developed to secure the future water supply to the region. The plant was in full operation in March 2009 and is owned by Seqwater and operated by Veolia.

Fig. 3.9 Interior view of the velocity cap intake during operation of the Sydney SWRO plant

Fig. 3.10 Aerial view of the Gold Coast SWRO plant

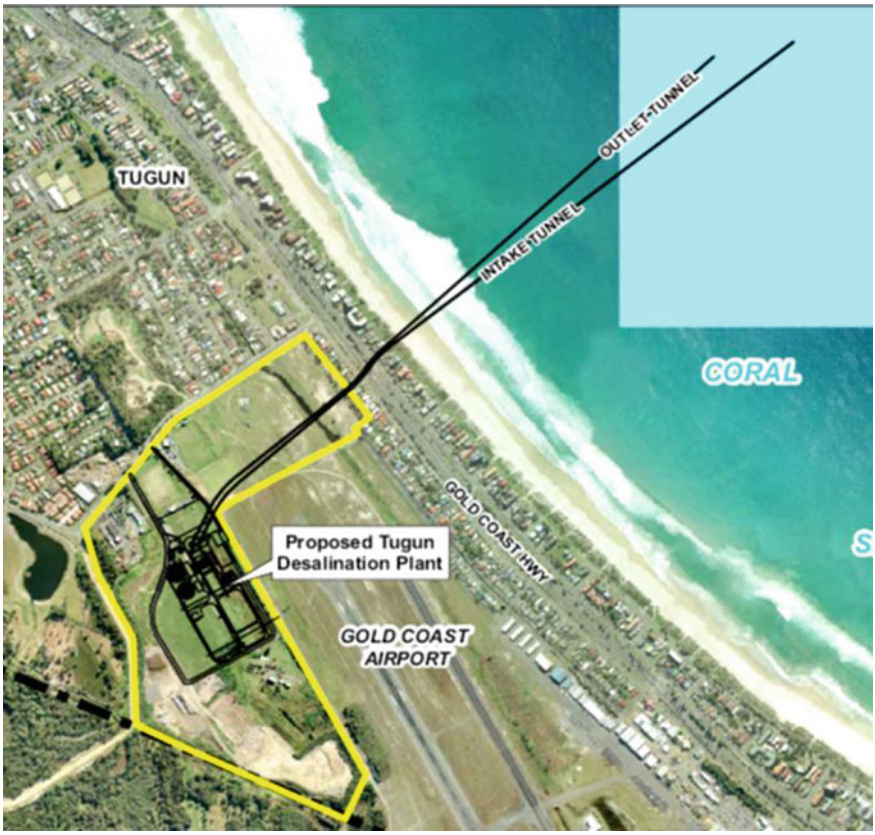

Fig. 3.11 Gold Coast SWRO plant location and schematic of intake and outfall tunnels

3.5 Gold Coast Plant Intake

The Gold Coast is a renowned tourist destination with pristine white sandy beaches. The coast is densely populated with a high real estate value and no ocean front industrial land is available. This offered significant challenges in terms of design, construction and operation. The site selected, 500 m inland at the southern end of the Gold Coast, is located on a former uncontrolled landfill site and is also directly adjacent to a busy international airport. Furthermore, residents are located only 300 m away from the site and sports fields are located next to the plant fence. In line with the goals of the project, it was essential to minimise any direct impacts to the neighbouring community, as well as the environment. This encompasses power sourcing, impacts to the environment at and around the site, and impact to the marine environment at the points of intake and discharge.

The requirements for this location hence included no marine infrastructure to be visible on the coast and construction could not be allowed to disrupt any community and tourist activities. Given these conditions and the large capacity of the plant, an open intake was evaluated as the most viable intake option.

Trench options for installation of the intake conveyance pipeline were considered and compared to bored tunnels and infiltration systems during the site assessment. The tunnel option to an open intake was selected based on the program, environmental and visual impacts during construction, minimisation of marine construction risk and an intake pump station located at the plant.

The plant intake location is in an open embayment with water circulation in the embayment driven primarily by wind drift and the East Australian Current which flows in a south-easterly direction. The most significant potential land-based influences on the receiving environment are discharges from Currumbin Creek, located 3.4 km to the north of the project location, and the Tweed River, 5 km to the south. The embayment has a gently sloping, uniform bottom of primarily fine to medium grain quartz sand, with some shell and small amounts of silt and clay.

Marine issues at the intake site included:

- Summer cyclone occurrence
- Ocean currents typically to a maximum velocity of 0.5 m/s
- High storm event waves (up to 8 m in height)

The siting of the intake in a stable seabed at depths below 18 m was determined to minimize sand and sediment entry into the intake, and maintain the intake works clear of the active coastal zone. The intake seabed contains little marine vegetation. However, it still has high environmental value, containing a variety of marine life. The seabed is primarily bare sand, with some widely scattered tube anemones, sipunculid worms, sea stars, and burrowing sponges. Bottom fishes, including shovelnose rays, flathead, flounder, and skates, have been observed. Epibenthic fauna and flora in the diffuser location are not abundant. Video surveys indicate that no seagrass or macroalgal (seaweed) beds occur in the area, although drift algae are sometimes observed (Viskovich et al. 2013).

A pre-treatment pilot plant study was undertaken with an intake system in the general area of the full-scale plant intake which enabled ongoing monitoring of seawater quality and measurement of variation over the seasons. The data collected allowed the optimization of the pre-treatment design of the plant.

The tunnel construction for the full scale plant was via a 70 m deep shaft at the plant site with a 2.8 m diameter 2.2 km tunnel (Fig. 3.12). A tunnel boring machine (TBM) was used to construct the tunnel and pre-fabricated fibre reinforced concrete tunnel liners were used as liners to give longer design life. The intake tunnel runs 1.5 km offshore and 40 m under the seabed. The intake velocity-cap structure is located in 22 m of water and 6 m above the seabed.

Fig. 3.12 Lowering of tunnel boring machine into the riser shaft connecting the SWRO plant to the tunnel

Entrainment and impingement of adult marine organisms can be avoided by minimizing the water velocity at the mouth of the intake structure with the California Coastal Commission recommending in the past that intake velocities below 0.15 m/s constituting "Best Technology Available" to minimize impingement (see Chap. 5). The intake was designed as a velocity cap over the intake pipe with the intake velocity kept below 0.15 m/s. The actual velocity generally is around 0.05 m/s as modeled at 100 % flow (Fig. 3.13). In addition to velocity considerations, the spacing of the screen bars (140 mm) on the intake was selected to avoid impingement, allowing fish to swim freely across the structure (Fig. 3.14). The edges of the bars were also rounded to eliminate the presence of any sharp angles or surfaces that could potentially injure fish or other free-swimming animals (Cannesson et al. 2009).

The seawater at the intake zone was generally of high quality with low turbidity, TSS, SDI, organics with little algae and no hydrocarbons (Table 3.2).

The seawater passes through fine screening (3 mm) via rotating drum screens located onshore to remove any entrained marine debris. The intake is also intermittently chlorinated typically once per day to control biofouling in the intake tunnel and structure.

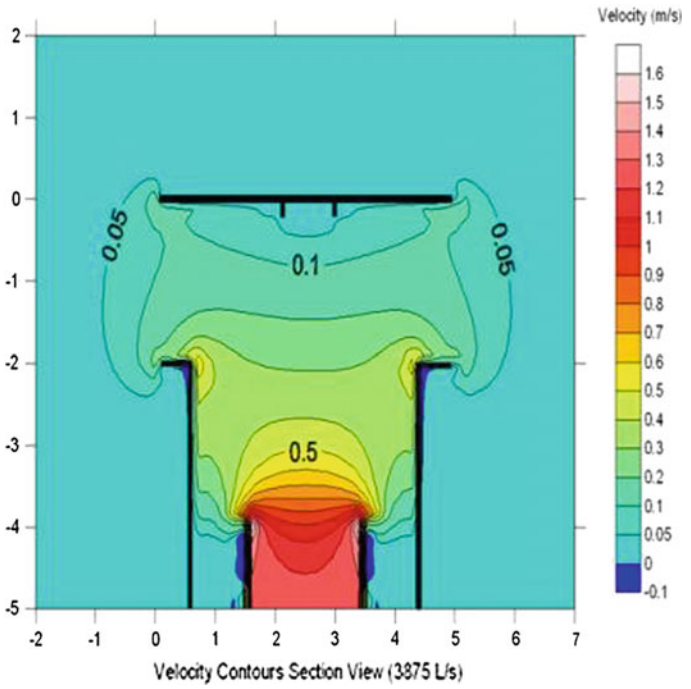

Fig. 3.13 Velocities within the cross-section of the velocity-cap intake structure at the Gold Coast SWRO plant

The suitability of the intake structure design has been confirmed by a diver's inspection upon start-up of the plant. Fish were observed to be swimming unhindered across the intake mushroom (Fig. 3.15). After the first 10 months of plant intake operation, only 20 kg of organisms were collected from the onshore rotating drum screens. This consisted mainly of small fish 20 cm in length and is thought to be due to the growth of fish in the intake shaft during a 4-week plant shutdown. Since plant inception the entrainment of only around 160 kg marine life has been collected from the 3 mm onshore drum screens and consisted of predominantly cornflake seaweed and a few blue blubber jellyfish. Ongoing marine monitoring is being undertaken to evaluate environmental performance of the intake over time.

ROV inspections are carried out annually to monitor the tunnel condition during operation and the effectiveness of the shock chlorination to control biofouling in the intake system. The results of successive ROV inspections have shown limited marine growth and good condition of the intake system (Fig. 3.16).

Fig. 3.14 Very large velocity-cap intake structure used at the Gold Coast SWRP plant

Table 3.2 Seawater quality at the Gold Coast site

Parameter	Mean	Range
Turbidity (NTU)	0.63	0.2–1.2
TSS (mg/L)	2.2	1–8
SDI	19.9	10.3–31.2
TOC (mg/L)	1.2	0.9–2.5

Fig. 3.15 View of the Gold Coast SWRO plant velocity-cap intake interior during operation

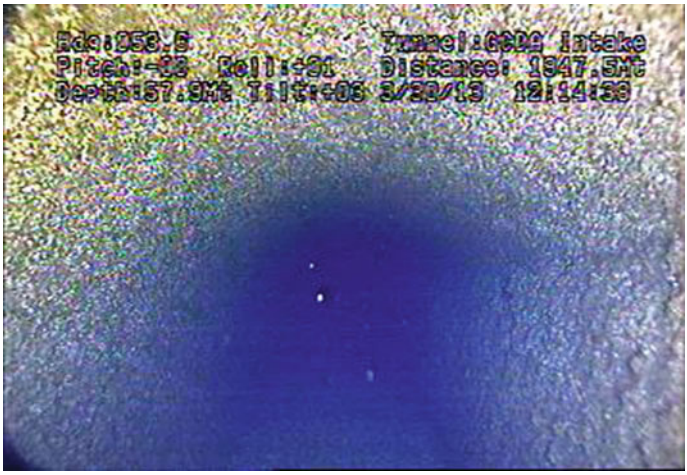

Fig. 3.16 ROV inspection of the Gold Coast SWRO plant intake tunnel

3.6 Conclusions

The use of bored tunnels with open intakes for two Australian SWRO plants at Sydney and the Gold Coast has allowed the plants to be built to program standards, to provide water capacity and quality to meet the plant feed water requirements, and to minimize environmental impacts.

Different coastal conditions at the two plant sites resulted in differences in siting of the intake structures in terms of distance offshore and water depth. The sites were chosen based on pre-design environmental investigations to ensure good seawater quality, minimization of sediment entrainment, and minimization of environmental impacts.

The velocity caps and screen design have been effective and the low inlet velocities have minimised any entrainment and impingement of marine organisms. The use of shock chlorination has been effective in controlling biofouling in the tunnels as evidenced by the regular ROV inspections.

Ongoing environmental monitoring has shown minimal impacts on the marine ecology.

References

Craig, K. (2013). *Sydney and the Gold Coast Intakes*. Thuwal, Saudi Arabia: KAUST Intakes and Outfall Seminar Presentation.

Evans, R. (2011). Sydney Desalination Plant. ACCA Technical Paper.

Cannesson, N., Johnstone, P. M., Mitchell, M. A., & Boerlage, S. E. E. (2009). Community, environmental and marine impact minimisation at the Gold Coast desalination plant. In

Proceedings of the International Desalination Association World Congress on Desalination and Water Reuse. Dubai UAE.

Sydney Water Corporation (2006). Desalination planning study ocean sampling water quality 2005–2006 interim report.

Viskovich, P. G., Gordon, H. F., & Walker, S. J. (2013). Light at the end of the tunnel—a benthic community perspective. In *Proceeding of the International Desalination Association* (*IDA*) *World Congress on Desalination and Water Reuse World Congress on Desalination and Water Reuse*. Tianjin, China.

Chapter 4
Impingement and Entrainment at SWRO Desalination Facility Intakes

Timothy W. Hogan

Abstract Seawater desalination intakes have potential to negatively impact marine life. The principal impacts of concern are broadly categorized into impingement and entrainment (I&E). Each represents an interaction between the marine organisms in the source water body and the intake screening technology used at the desalination facility. Impingement is the entrapment of larger organisms against the screen mesh by the flow of the withdrawn water. Entrainment is the passage of smaller organisms through the screening mesh. Concern over the impacts of I&E has formed the basis of a major portion of the environmental regulation of seawater intakes in the U.S. for power generation and other industrial uses. In addition, the impacts of I&E at seawater desalination intakes is growing as a global environmental concern. The withdrawal of seawater for desalination has impacts that cannot be eliminated; however, they can be minimized. There are well-recognized approaches for predicting the potential for I&E, for documenting the magnitude of I&E, and for assessing the impacts of I&E on natural populations. More importantly, the body of knowledge surrounding I&E and the means for minimizing its impacts is extensive. Although some impacts are unavoidable, various technological and operational methods, many of which have undergone extensive laboratory and field evaluation, are available and proven to improve the protection of marine life at desalination facility intakes. This chapter reviews the biology of I&E at seawater intakes, the sampling approaches for assessing and quantifying I&E, the methods for predicting the potential for I&E, the methods for assessing the impact of I&E on natural populations, and the common approaches and technologies available for minimizing I&E at seawater intakes.

T.W. Hogan (✉)
Alden Research Laboratory, Holden, MA, USA
e-mail: thogan@aldenlab.com

T.M. Missimer et al. (eds.), *Intakes and Outfalls for Seawater Reverse-Osmosis Desalination Facilities*, Environmental Science and Engineering,
DOI 10.1007/978-3-319-13203-7_4

4.1 Introduction

The operation of intakes at seawater reverse osmosis (SWRO) desalination plants has potential to negatively impact marine organisms near the intake structure. The most significant impacts can be broadly categorized as impingement and entrainment (I&E). Each represents an interaction between the organisms in the source water body and the desalination feedwater system and each is dependent on the size of the organism and the screen mesh of the intake screening technology. Impingement refers to the pinning of larger organisms (typically juvenile and adult stages) against the screen mesh by the flow of the withdrawn water while entrainment refers to the passage of smaller organisms (typically early life stages—eggs and larvae) through the screen mesh (Fig. 4.1). Another term, entrapment, refers to organisms that have entered a component of the intake system. These organisms have not yet been impinged on or entrained through the final downstream screening structure, but have no means of escape from the intake water system.

Commonly accepted definitions of entrainable and impingeable organisms, as they are used in the U.S., are given as:

> *Impingeable organism*—organism large enough to be retained by a mesh with a maximum opening of 14.2 mm—includes 9.5-mm mesh and 6.35 by 12.7 mm mesh (EPA 2014). This group includes larger, actively moving juvenile and adult organisms.
> *Entrainable organism*—organism small enough to pass through a mesh with a maximum opening of 14.2 mm—includes 9.5-mm mesh and 6.35 by 12.7 mm mesh (EPA 2014). This group includes small organisms with limited to no

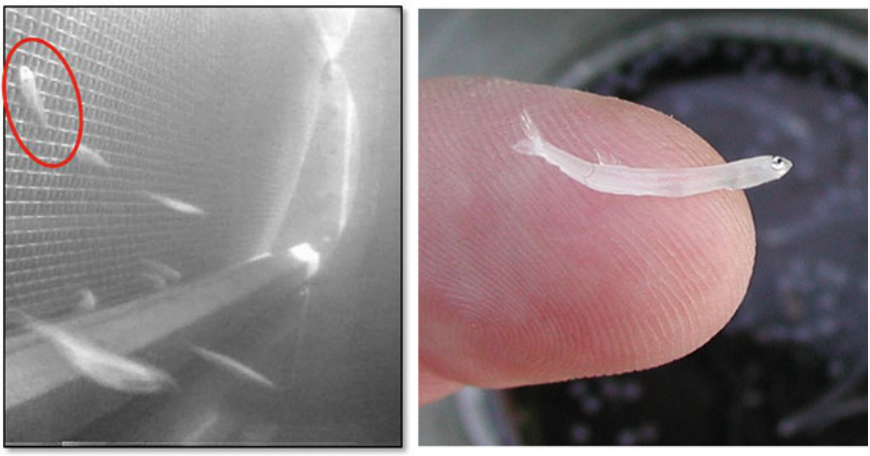

Fig. 4.1 Impingement of juvenile striped bass on a traveling water screen (*left*) and a larval fish representing a size that is potentially at risk of entrainment (*right*)

swimming ability. Some of these organisms (e.g., fish eggs) may be completely passive, lacking the ability to avoid the intake flow regardless of velocity.

The magnitude of impingement losses for any species from intake operation is a function of the organism's risk of exposure to the intake screen (number or proportion impinged and entrained) and the subsequent mortality of those organisms that were exposed (referred to as impingement or entrainment mortality). Impingement survival is very species-specific, with species that are considered "hardy" (e.g., species with heavy skeletal structure, thick scales, protective slimes) typically experiencing higher survival and those considered "fragile" (e.g., species with lighter skeletal structures, thinner scales, a tendency to lose scales readily when handled) (EPRI 2003a). In the desalination process, entrainment mortality is assumed to be 100 % (Foster et al. 2013; Pankratz 2004) except in cases where a portion of the withdrawn flow is diverted away from the treatment systems for brine dilution.

There are a number of factors that can directly or indirectly affect the probability and magnitude of I&E at seawater desalination intakes, most of which are interrelated. These include:

- *Intake location*—An intake in a more biologically productive area poses a greater risk of exposing marine life to I&E than one located outside of a biologically-productive area.
- *Ambient hydraulics*—An intake in an area with low ambient currents (e.g., tidal or ocean currents) poses a greater risk of I&E than one located in an area with relatively strong ambient currents that can sweep non-motile organisms away.
- *Water quality*—Extremes of temperature and low dissolved oxygen can negatively impact marine organism health, in turn compromising their ability to avoid exposure to the intake.
- *Species-specific morphology and physiology*—Physical attributes of the marine organisms can affect both their ability to avoid impingement and entrainment and to survive impingement.
- *Intake system design and operation*—An active intake screening system that collects and returns impinged organisms poses a greater risk of impinging organism than a passive intake screening system operating at a low velocity, which nearly eliminates the risk of impingement.

Minimizing environmental impacts to marine resources is often a regulatory concern, particularly in the U.S., but can also be driven by other mechanisms such as corporate environmental policy or project financing requirements (e.g., the Equator Principles). Given the high priority placed on preserving marine resources by many countries, it is important to have both accurate measurements of I&E impacts as well as effective mitigation approaches. Consideration of these impacts during pre-design phases for new SWRO facilities is also critical because the potential for I&E can be minimized through the careful selection of an intake location and intake screening technology. The location, screening technology, and intake design are also important

from an economic perspective, as each can significantly impact capital and operational expenditures. For example, an intake constructed in a poorly selected location may result in greater than expected impingement. Such a scenario may require the facility operator to make either a physical or operational modification, typically at a high cost, to the intake to reduce impingement.

4.2 Environmental Regulation in the U.S

The U.S. is often considered to be one of the most environmentally-conservative countries and impingement and entrainment have received intense scrutiny, particularly at thermal electric power plants, since the 1970s. Although not explicitly covered by the same federal regulations developed for the thermal power industry, desalination facilities are commonly held to the same environmental performance standards; therefore, the following review of the principal federal regulation governing I&E in the thermal power industry is warranted.

Cooling water intake structures (CWIS) at thermal power plants fall under the federal Clean Water Act (CWA) which is administered by the U.S. Environmental Protection Agency (EPA). Section 316(b) of the CWA requires "*that the location, design, construction, and capacity of cooling water intake structures reflect the best technology available for minimizing adverse environmental impacts*" (EPA 2011). In 2004, rulemaking by the EPA established new guidelines for the implementation of Sect. 316(b) (the Rule), which required all CWIS to meet national performance standards relative to impingement mortality and, in some cases, entrainment. The rulemaking was parsed into several phases: Phase I covered new power plants, Phase II covered existing power plants, and Phase III covered new offshore oil and gas extraction facilities that withdraw 7575 m^3/d or more and use at least 25 % of the water exclusively for cooling. The Rule laid out benchmark performance standards for the reduction of impingement mortality (IM) and entrainment.

The Rule for existing thermal power plants was recently rewritten and a final 316(b) Rule was released in May of 2014 (EPA 2014). This final Rule supersedes the Phase II and Phase III rules and covers all facilities withdrawing at least 7575 m^3/d of cooling water from waters of the U.S. of which 25 % is used exclusively for cooling. All facilities falling under the final Rule have to address IM. The EPA has provided seven pathways for IM compliance; they include:

- Operate a closed-cycle recirculating system.
- Operate at a design through-screen velocity less than or equal to 0.15 m/s.
- Operate at an actual through-screen velocity less than or equal to 0.15 m/s.
- Operate an existing offshore velocity cap (i.e., those installed before October 14, 2014 and has to be 244 m offshore to qualify)
- Operate modified traveling water screens (requires a 2-year optimization study to ensure screens are working as best they can to minimize IM of non-fragile species)

- Operate a combination of technologies, management practices, and operational measures that meets the standards set forth in the following compliance alternative (also requires a 2-year optimization study as compliance alternative 5).
- Achieve a specific IM performance standard of no more than 24 % mortality of all non-fragile species for 12 months. The EPA stated that they do not expect many facilities to choose this compliance option; rather, this is a compliance path that can be used for innovative technologies developed in the future.

Due to site-specificity, the EPA has not issued a national entrainment performance standard. Instead, the EPA has left the determination for what constitutes best technology available (BTA) for entrainment to the permit writers. CWIS permitting in the U.S. is generally decentralized with most states having been delegated the authority to issue permits under the Clean Water Act. While all facilities are subject to a BTA determination relative to entrainment, only those facilities withdrawing greater than 473,176 m^3/d are required to submit additional studies that include evaluation of entrainment reducing technologies. These studies must evaluate closed-cycle cooling, the use of recycled water (to reduce intake flow and associated entrainment), and the technical feasibility of fine-mesh/narrow slot (2-mm) screens.

The biggest factor affecting whether an intake will be held to an entrainment performance standard is the location of the intake. Given that desalination facility intakes, by design, withdraw seawater, they are located in coastal marine and estuarine areas. Since coastal and estuarine areas are widely recognized as highly biologically productive (Agardy and Alder 2005) and are used for spawning and rearing of early life stages of marine organisms, protection against entrainment of early life stages is likely to be required.

The details of the final Rule and the approaches utilized by power generators to comply with the regulations are important to the desalination industry in the U.S. In nearly every case in the U.S., state regulators with jurisdiction over the desalination industry draw from the federal 316(b) Rule. Since the regulation of desalination impacts is handled at the state level in the U.S., there is potential for the regulations to vary among states.

4.3 Typical Intake Studies Required

A suite of biological studies are typically required by permitting authorities to support the assessment of potential intake-related I&E impacts as well as to determine the effectiveness of the intake screening system for minimizing these impacts. The studies can be broadly grouped into two categories: studies that provide data on the populations of organisms occurring near the intake that may be at risk of I&E (i.e., baseline characterization) and studies that provide data on the organisms that actually impinge on or entrain through the intake screening system (i.e., I&E characterization). Each study type is described briefly here, though greater detail on standard I&E studies is provided in Sect. 4.4.

4.3.1 Baseline Characterization Study

A baseline characterization study is designed to yield data on the species and life stages occurring in the source water body and which may be at risk of I&E. Baseline data are critical for setting the benchmark against which I&E impacts can be measured. Typical baseline characterization studies include the following components (EPA 2012):

- A review of existing pertinent data that would aid in identifying the species and life stages present;
- Identification of the species and life stages in the area and their relative abundance near the proposed intake location;
- Identification of the species and life stages most susceptible to impingement and entrainment (I&E);
- Identification of the primary periods of reproduction, larval recruitment, and peak abundances;
- Identification of the temporal (daily, seasonal) variations in abundance; and
- Supplemental field studies conducted to collect data that were not available must document the study methods, statistical power, QA/QC process, and data analysis approach.

4.3.2 Impingement and Entrainment Characterization Studies

Impingement and entrainment studies are designed to quantify the magnitude of I&E of organisms at an intake screening system. In the case of impingement, many studies are also designed to estimate the survival of organisms after impingement. Typical I&E studies include the following general components (EPRI 2004b):

- Review and summary of any historical I&E data that are available for the site under consideration;
- Identification of the species and life stages in the area that may be susceptible to I&E;
- Quantification of the current impingement and entrainment levels at the intake in question; and
- Characterization of the spatial and temporal variation (e.g., annual, seasonal, diel) in abundance.

Of impingement and entrainment, entrainment has been receiving greater scrutiny in the U.S. desalination industry. Since many entrainable-sized organisms are passive, planktonic particles, lacking the capacity to swim away from the hydraulic zone of influence of an intake, there is often a greater focus on designing intake systems with screening mesh/slot sizes sufficient to physically exclude these early

life stages. Subsequently, much effort is expended addressing entrainment concerns in the U.S. In general, other countries put less of an emphasis on intake-related impacts as a whole, instead focusing on the potential impacts of concentrate discharge.

4.4 Measuring I&E

Direct measurements of I&E can be made through the collection of impingement and entrainment samples at a facility's seawater intake. Typically, impingement sampling studies are conducted over a sufficient time period (minimum of 12 months) to account for natural variations in abundance associated with seasons, time of day, tidal stage, etc. However, collecting two years of data can account for interannual variability in natural populations. Sampling frequency and magnitude will vary based on the study-specific objectives.

4.4.1 Impingement Sampling

Impingement sampling provides the opportunity to quantify the number of organisms impinged at a seawater intake. The difficulty in collecting impingement samples varies among screening technologies. For example, collecting impingement samples from a traditional traveling water screen which actively collects impinged organisms is much less difficult than trying to quantify impingement on cylindrical wedgewire screens that are designed to passively prevent impingement.

Collecting impingement samples from a traveling water screen is relatively straightforward. Debris and fish that impinge on and are subsequently rinsed from the screen are diverted into a sample collection system. Typically, the collection system is a mesh basket or net placed in the return sluiceway (Fig. 4.2), but can be more elaborate if it is not feasible to install impingement sampling equipment in the screen house (Fig. 4.3). Impinged organisms and debris are collected, sorted, and counted. The impingement rate can then be calculated based on the numbers of impinged organisms collected and the duration of sampling. It is also wise to collect water quality and environmental data as environmental conditions can impact impingement rates (EPRI 2004b).

In cases where the traveling water screens being sampled have been modified to include fish-friendly features, there is often interest in assessing impingement survival. Impingement survival requires that, after collection, the impinged organisms are held over a sufficient time period (e.g., 48 h) to determine any latent mortality attributable to the impingement and collection process.

Fig. 4.2 Impingement sampling equipment used inside a screen house (*left*)—traveling water screen housing is at left with fish return trough exiting through the side; collection basket is suspended in discharge of return trough. Post-collection latent impingement mortality holding system (*right*)

Fig. 4.3 Impingement survival sampling study. Impinged organisms are diverted from the screen's fish return trough (*left*) to a collection net (*middle*). Collected organisms are transferred to a holding facility (*right*) where they are held in flow-through tanks to assess latent impingement mortality. (Images courtesy Alabama Power Company)

4.4.2 Entrainment Sampling

As with impingement sampling, entrainment sampling provides the opportunity to quantify the number of smaller organisms that are entrained through the intake screening technology. Entrainment data are used to estimate the total annual impact of entrainment on the local populations of marine organisms.

In desalination plants, entrainment samples must be collected from locations upstream of the pumps. There are two upstream locations from which desalination facility entrainment samples can be collected: (1) with plankton nets from an area directly upstream of the intake screens (Figs. 4.4 and 4.5) or (2) with pumps from

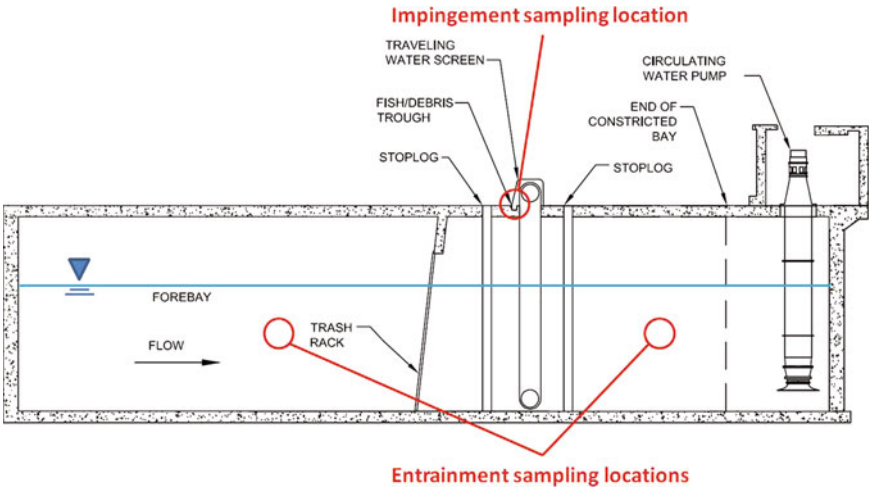

Fig. 4.4 Generalized entrainment sampling locations (impingement sampling location given for reference) within a typical seawater intake structure equipped with a trash rack and traveling water screens

an accessible area within the intake structure downstream of the screens, but still upstream of the pumps (Figs. 4.4 and 4.5). In cases where a portion of the withdrawn flow may be used for brine dilution and entrainment survival may be greater than zero, entrainment samples may be collected from a location downstream of the circulating water pump. Regardless of the sampling location, sampled water is typically filtered through a collection device with sufficiently small mesh (typically 335-μm mesh plankton nets) based on the size of the target organisms. An in-line flow meter is used to record the volume of water sampled. Entrained organisms are rinsed from the collection device, concentrated, and preserved. Samples are then transported to an ichthyoplankton processing laboratory where they are sorted, identified to the lowest taxonomic level practicable, and enumerated. Entrainment densities are then calculated based on organism abundance and sample volume (e.g., number of organisms per cubic meter).

Ideally, entrainment sampling is conducted over multiple years in order to account for inter-annual variability in organism abundance. Typically, samples are collected once per week or once every two weeks over a 12-month period in order to capture any seasonal variations in organism abundance. Sampling may be less frequent during time periods when ichthyoplankton are not present or only occur in very low abundances (e.g., winter months in temperate climates) (EPRI 2005). Daytime and nighttime sampling is also conducted to capture diel variations in organism abundance. Diel sampling also provides data on variations in organism abundance related to tidal cycle. Samples can also be composites comprised of multiple depths or discrete-depth samples which can aid in determining whether there is any vertical stratification of the entrained organisms. It may also be

Fig. 4.5 Entrainment sampling equipment. Bongo plankton nets for collecting ichthyoplankton samples upstream of the intake structure (*top left*); barrel sampler with integral plankton net for collecting pumped samples from within intake structure (*bottom left*; image courtesy ASA Analysis and Communication, Inc.); and fish eggs and larvae collected during entrainment sampling studies

desirable to monitor ambient current velocities near the intake so that any relationships between organism abundance and ambient hydraulic conditions can be determined.

In addition to sampling from the intake system, ambient biological samples should also be collected in the source water body near the intake location. These ambient samples serve to establish a concurrent baseline to which densities of entrained organisms can be compared and can serve as the basis for assessing the impacts of entrainment on local populations of organisms (see Sect. 4.6 for more on estimating impacts).

4.5 Predicting I&E

Predicting the potential biological effectiveness of an intake technology is important to facility operators, particularly given the high cost of modifying an intake after construction to provide greater protection to marine organisms. Using existing data, it is possible to estimate the potential biological efficacy of various intake screening alternatives.

The methods used to estimate an intake technology biological efficacy depends upon its mode of action (e.g., exclusion [passive mode] versus collection [active mode]). In addition, the site-specific intake design and operating characteristics, and the morphological, physiological, and behavioral characteristics of the organisms involved at the intake will impact the efficacy of a screening technology. Determining the potential efficacy of various intake screening technologies takes into account two principal components for which empirical data are often available: (1) physical exclusion and (2) impingement survival. The following sections describe these components in greater detail.

4.5.1 Physical Exclusion

For passive screening systems [e.g., cylindrical wedgewire screens (see Chap. 5)], physical exclusion is the principal factor to consider when estimating biological efficacy. It is commonly accepted that impingement on passive screens, which utilize low through-slot velocities, is virtually eliminated (Gulvas and Zeitoun 1979; Zeitoun et al. 1981), obviating the need to determine the potential for impingement survival.

The key factor in determining physical exclusion is organism size in relation to the screen mesh size or slot width. Several methods have been used to estimate physical exclusion by screens (e.g., Schneeberger and Jude 1981; Turnpenny 1981; PSEG 2004). All of these methods rely upon the sizes of organisms exposed to the intake and the underlying assumption that organisms with body depths greater than opening size of the screening mesh will not fit through the mesh. Often the larval head capsule depth (HCD) is used as the limiting dimension, because it is the widest non-compressible portion of the larval body (Fig. 4.6); (EPRI 2014).

Exclusion is a species-specific measure, as there is substantial variation in the morphometric characteristics among species. With larvae, the orientation of the organism at the time of contact with the screen will also influence its likelihood of being entrained. In addition, the ratio of ambient velocity to through-mesh velocity and the swimming ability of the larvae can impact the probability of entrainment

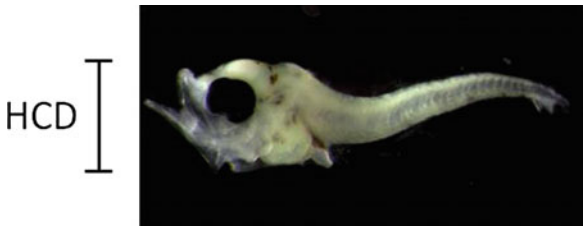

Fig. 4.6 Head capsule depth (HCD) of a larval fish

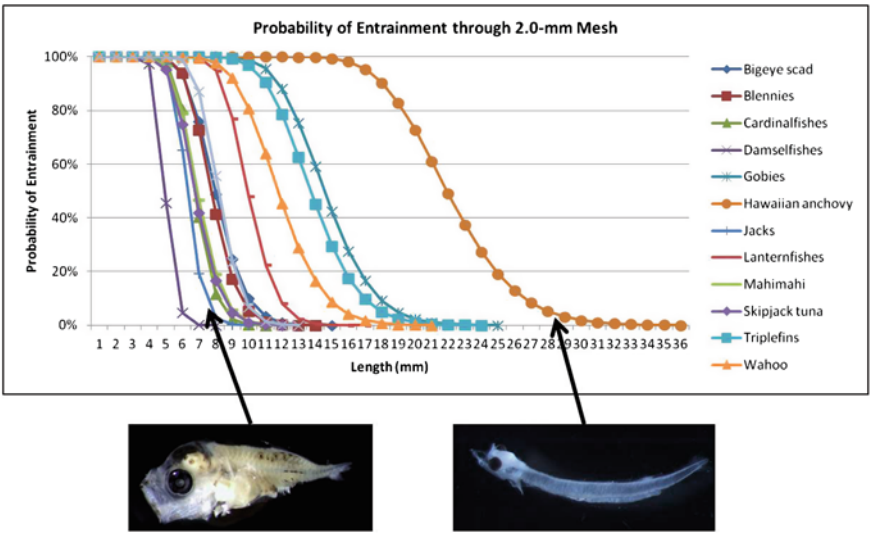

Fig. 4.7 Probability of fish entrainment through 2.0-mm mesh screening. Larvae with larger HCDs relative to body length (e.g., jacks, *bottom left*) are excluded at smaller lengths than larvae with smaller HCDs relative to body length (e.g., anchovies, *bottom right*). (Modified from Oney et al. 2013)

with wedgewire screens. In the case of juvenile and adult fish, exclusion can be estimated using the limiting body depth of the organisms (not always the HCD).

As fish length (or egg diameter) increases, the probability of entrainment decreases (Fig. 4.7). As shown in Fig. 4.7, species-specific differences in morphology factor heavily into determining the probability of entrainment. Fish with large HCDs are excluded at a shorter total body length than fish with small HCDs. It is important to note that other factors have been shown to increase exclusion (e.g., organism behavior, orientation of organisms, ambient hydraulics (EPRI 2003b; Heuer and Tomljanovich 1978; NAI 2011a, b; Weisberg et al. 1987); therefore, the physical exclusion component should be considered a conservative estimate.

4.5.2 Impingement Survival

Collection technologies, such as modified traveling water screens, handle the organisms during the collection and transfer process back to the source water body. This handling may impart additional stress, injuries, scale loss, or mortality to the organisms. Therefore, the second component of evaluating the effectiveness of a collection technology, is determining how well organisms survive the impingement, collection, and return process. The survival of these impinged organisms is

dependent upon their biology (e.g., life stage, relative hardiness) and the screen operating characteristics (e.g., rotation speed, spraywash pressure) (WRRF 2014).

Impingement survival data are readily available for many species that are typically of concern at conventional thermal power plants in the U.S. (EPRI 2003a); however, other sites may have substantially fewer or no data on species that are targeted for protection near their intakes. The presence of existing data is also a function of the regulatory requirements for industrial water intake permits; parts of the world that have stringent regulatory requirements (e.g., the U.S.) are likely to have more historical impingement survival data than countries that are not required to monitor for intake-related impacts.

Ideally, impingement survival data is available for the intake technology under consideration and for each of the species and life stages of concern. However, this is seldom the case. More often, data are available for some species and lacking for others. In cases where impingement survival data are lacking for a particular species or life stage, surrogate data can be used provided the surrogate organism shares similarities with the species of concern.

4.6 I&E Impact Assessment

I&E monitoring studies collect raw data on the numbers or weight of organisms impinged or entrained. These raw numbers are converted to densities based on the sample volumes and can then be used to estimate total annual impacts. Total annual losses can be calculated for a full-scale intake under actual or maximum design withdrawal by multiplying the densities by the total volume of water withdrawn. Thus, three components are included in determining the impact of I&E; they are: (1) an estimate of the number of organisms impinged or entrained, (2) an estimate of survival after impingement or entrainment (assumed to be zero in the desalination process), and (3) an estimate of the population in the source water body (Cannon and Lauer 1976).

With total I&E losses calculated for a given intake, the next step is to convert those numbers to a value. Total annual losses are used to assess the impacts of I&E on local populations through a number of well-established impact assessment models. The resulting impact assessments can then be put in the context of their effect on local populations. EPRI (2002) categorizes, in increasing level of analysis complexity, the various levels of prospective (predictive) assessments as those that define I&E losses in terms of numbers of individuals or biomass lost ("individual loss"), in terms of the fractional loss in annual production from a population ("fractional loss"), or in terms of population-level changes resulting from long-term exposure to I&E loss. Of these three approaches, the most frequently used impact assessment models in the U.S. have been those that define impacts as individuals lost (demographic approach) or as a fractional loss to populations (proportional mortality approach). Table 4.1 provides a summary of the commonly-used demographic and proportional mortality approaches to assessing I&E impacts.

4.6.1 Demographic Approach

Demographic models convert lost organisms to equivalent numbers of adults. Demographic approaches are germane to assessing entrainment impacts. Projecting a certain number of adults that equate to a certain number of eggs or larvae requires the use of detailed life history data such as natural mortality rates for each life stage, fecundity, age-at-maturity, and life span (EPRI 2004a). The principal demographic approaches include those that equate the numbers of eggs and larvae lost to entrainment to an equivalent number of adults (adult equivalent loss), equivalent biomass lost (biomass foregone), or to the number of mature females that would be required to compensate for the loss (fecundity hindcast).

Demographic approaches are relatively simple provided there are sufficient life history data available for the species of concern (Table 4.1). Converting losses of early life stages of organisms makes estimating the value of the loss easier since adult organisms are more easily understood in fisheries management terms and typically have a true market value (i.e., commercial and recreational).

4.6.2 Conditional Mortality Approach

The conditional mortality approach, also known as the empirical transport model (ETM) was originally proposed in the 1980s to estimate losses from power plant cooling water intakes (Boreman et al. 1978). The ETM compares the number of organisms entrained to the total number at risk of entrainment in the source water body and results in an estimate of the proportional mortality caused by entrainment (Steinbeck et al. 2007).

The ETM approach has a distinct advantage in that it does not require the detailed life history data of demographic approaches (Table 4.1). However, upfront data collection may be more intensive since sampling must also be conducted in the source water body to: (1) characterize the abundance and composition of source water larval populations and (2) characterize the hydrodynamic/oceanographic conditions that could impact a larva's risk of being exposed to entrainment.

Once I&E impacts have been defined, a determination will be rendered on whether the magnitude of the impacts warrants mitigation. The outputs from impact assessments provide the basis for conducting a cost-benefit analysis to determine whether changes to the intake are justified. For impacts that cannot be addressed with intake modifications, compensatory mitigation is typically used. Such mitigation of I&E impacts is typically achieved through restoration of spawning or nursery habitat for the affected organisms. The size of habitat is designed to offset for the numbers of organisms lost due to the operation of the intake.

Table 4.1 Description of the common I&E impact assessment approaches, their data requirements, and their advantages and disadvantages

	Demographic approach		Conditional mortality approach
	AEL	FH	Empirical transport model
Description of model	Uses larval losses (entrained organisms) to estimate the equivalent number of adult fishes that would have been lost to the population	Uses larval losses (entrained organisms) to estimate the number of sexually-mature adult females whose reproductive output has been lost	Estimates the proportion of organisms in the source water body population that will be lost to entrainment, while accounting for spatial and temporal variability in distribution and vulnerability of each life stage to water withdrawals
Requires biological sampling of entrained organisms?	Yes		Yes
Requires biological sampling of organisms in source waterbody?	No		Yes
Requires oceanographic data on currents near intake?	No		Yes
Requires life history data?	Yes		Limited
Advantages	Adult fish are easily understood in fisheries management context		Model output lends itself well to calculating mitigation in terms of area of production foregone (APF)
	Does not require biological sampling of organisms in source water body		Requires only limited life history information, specifically, an estimate of the duration over which an organism is vulnerable to entrainment
Disadvantages	Requires detailed life history data that are sometimes unavailable, incomplete, or uncertain		Requires collection of oceanographic data (currents) as model input (if not otherwise available)
	Accurate data on the status of the adult population are required to assess the impact of lost adults		Requires biological sampling of source water body in addition to intake sampling

4.7 Minimizing I&E

I&E impacts resulting from the operation of seawater intakes cannot be eliminated; however, they can be minimized through the proper location, design, and selection of the best performing intake screening technology. In the recently released final 316(b) Rule, EPA (2014) describes four approaches for reducing I&E at existing power generating facilities: (1) reduce flow, (2) install technologies or operational procedures to gently exclude organisms or collect and return them to the source water body without harm, (3) locate the intake to a less biologically rich area (i.e., greater distance offshore or greater depth), or (4) reduce intake velocity.

4.7.1 Flow Reduction

Reducing flow is a viable means for reducing entrainment impacts since entrainment is proportional to flow when considering passive life stages of organisms with no swimming ability. Whether reducing flow has a similar benefit for reducing IM remains to be conclusively demonstrated. Nieder (2010) concluded that, in general, volumetric flow rate is not a strong predictor of adverse environmental impacts. In particular he states "*there is little direct, proportional relationship between impingement and cooling water capacity use*". Rather, impingement has been shown to be more episodic and more closely related to other environmental variables such as temperature (EPRI 2003c).

Reducing flow at a seawater desalination facility may not be a viable option as reduced inflow will result in reduced production of potable water. However, the following approaches could be considered to reduce seawater needs at desalination facilities:

- Increase recovery rates such that less feedwater is required
- Reduce ancillary water demands (e.g., additional flow withdrawn for concentrate dilution)
- Consider other feedwater sources that have no real potential for I&E impacts (e.g., subsurface intakes)

4.7.2 Exclusion and Collection Technologies

Intake technologies designed to reduce I&E can generally be categorized into four groups based on their mode of action (WRRF 2014). These categories include: behavioral systems, which take advantage of natural behavior patterns to attract or repel fish; exclusion systems, which physically block fish from passage; collection systems, which actively collect fish and return them to a safe release location; and diversion systems, which divert fish to a bypass for return to a safe release location.

Exclusion and collection technologies have received the greatest focus for their application in reducing I&E at seawater intakes. These two categories of intake technologies are discussed below in greater detail.

4.7.2.1 Exclusion Technologies

Exclusion technologies include systems that passively prevent the passage of organisms based on their size. Their potential effectiveness can be determined based on the size distribution of the organisms that may come in contact with it, i.e., exclusion technologies function on the premise that a screen will physically exclude organisms equal to or greater than its mesh size. Exclusion systems are also typically designed with low intake velocities to minimize the risk of impingement.

Cylindrical wedgewire screens are one of the most popular exclusion technologies for reducing I&E impacts at large seawater intakes (Fig. 4.8). Cylindrical wedgewire screens are typically designed with a small slot size (≤3 mm) and a low through-slot velocity (e.g., 0.15 m/s) to reduce entrainment impacts (see Chap. 5 for more on passive screens). By nature of the low through-slot velocity and small hydraulic zone of influence, these screens have also been shown to essentially eliminate impingement (Gulvas and Zeitoun 1979; Zeitoun et al. 1981; Tenera 2010). The biological and engineering performance of cylindrical wedgewire screens is optimized when there is sufficient ambient velocity to carry organisms and debris away from the screen face (EPRI 2006).

A number of pilot-scale studies have been conducted to determine the potential for cylindrical wedgewire screens to minimize I&E at seawater desalination facilities on the California coast. Tenera (2007) completed a pilot-scale biological evaluation of a 2.4-mm cylindrical wedgewire screen (0.09 m/s through-screen velocity) for the Marin Municipal Water District proposed desalination facility in northern California. Results from the pilot-scale testing indicated that the risk posed by entrainment resulting from a full-scale desalination facility (30 MGD) would be low to ambient populations of fish (0.02–0.06 % entrainment-related mortality). Tenera (2010)

Fig. 4.8 Cylindrical wedgewire screen designs. Bilfinger Water Technologies screen with Hydroburst backwash cleaning system (*left*) and Intake Screens, Inc. screen with rotating, brush-cleaned screen drums (0.5-mm slot width) (*right*)

completed a similar pilot-scale evaluation of a 2.0-mm cylindrical wedgewire screen (0.10 m/s through-screen velocity) in Santa Cruz, California. While the results indicate that the screens were very effective at reducing the potential for impingement, the magnitude of entrainment reduction was limited to approximately 20 % compared to an open intake. The authors concluded that the abundance of very small larvae (with HCDs less than the 2-mm slot size) may have affected the results.

4.7.2.2 Collection Technologies

Collection technologies are designed to either actively or passively collect organisms or direct them to a bypass. Their potential effectiveness can be determined in much the same way as discussed above for exclusion systems; however, since the organisms are being actively collected, it is necessary to know how well they survive the collection and return process. Therefore, while the potential efficacy of exclusion systems can be determined based on the size of the organisms in relation to the size of the mesh, the potential efficacy of collection systems also has to take into account injury and mortality that may be imparted by the collection and return process.

Modified traveling water screens (TWS) are one of the most commonly used collection technologies for reducing I&E impacts at large seawater intakes. Modified TWS represent an improvement over conventional TWS in that they include various fish-friendly components including fish lifting buckets at the bottom of each screen basket, low-pressure spray wash systems, and fish return systems (Fig. 4.9). In addition, such screens are designed to rotate continuously to reduce impingement duration and improve survival. The survival of organisms through a collection system is species- and life stage-specific, but in many cases can be high (EPRI 2003a). Modified TWS utilizing smaller mesh sizes may reduce entrainment of early life stages, though survival of impinged early life stages is generally poor (EPRI 2010).

Modified TWS are used extensively throughout the U.S. to reduce impingement mortality and entrainment (IM&E). The mesh size selected will determine the size of the organisms that will be retained (i.e., impinged). Recent moves towards the use of finer-mesh modified TWS means that the numbers of impinged organisms increases. For example, organisms that would entrain through a coarse-mesh (e.g., 9.5-mm) screen would impinge on a mesh of 3 mm. In the case of seawater desalination facilities where entrainment mortality is assumed to be 100 %, using smaller mesh to impinge smaller organisms could constitute an overall improvement in biological performance provided IM is less than 100 %.

4.7.3 Location

The location of the withdrawal point can confer an environmental benefit to marine organisms. Offshore withdrawal points have been shown to reduce I&E impacts simply by moving the intake to a place where there are fewer organisms (EPA 2014).

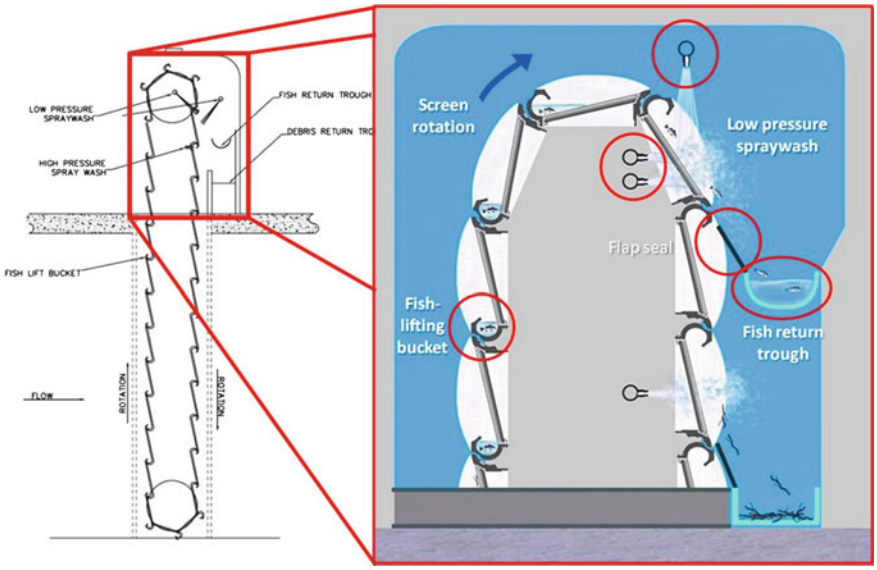

Fig. 4.9 Modified traveling water screen (through-flow design) with fish-friendly features indicated in the exploded view. (Image Courtesy Evoqua Water Technologies)

It is commonly accepted that the nearshore and estuarine zones where many large industrial water intakes are located are more biologically productive and are likely to have higher densities of organisms that could become impinged or entrained in the intake flow (EPA 2014). Moving an onshore withdrawal point offshore can have a beneficial biological effect provided the offshore location is in an area of low fish density (i.e., not a valuable spawning or nursery area). The offshore location has potential to reduce entrainment due to its location in less productive water.

Relative to impingement, nearly all offshore intakes include a velocity cap of some sort. A velocity cap is a behavioral deterrent technology that changes what would otherwise be vertical flow vectors at an uncapped offshore intake riser to horizontal flow vectors. A velocity cap is an effective means for reducing IM because it has been shown that horizontal flow vectors are more easily sensed and avoided by fishes (Beck et al. 2007; Lifton and Storr 1978; Weight 1958). A velocity cap, however, does not reduce entrainment of free-floating eggs and larvae, which are unable to distinguish the hydraulic cues or do not sufficient swimming ability to avoid them.

4.7.4 Intake Velocity

Reducing intake velocity can reduce IM. A through-screen velocity of 0.15 m/s has been determined to be protective of impingeable sized fishes (EPA 2014; EPRI 2000).

Practically speaking, for the same flow rate, reducing the intake velocity means that the open screening area must be increased. Screening area can be increased either through use of larger mesh or more screens.

4.8 Discussion and Conclusions

Impingement and entrainment have received intense focus in the thermal power generating industry in the U.S. and have become an increasing concern at other industrial water intakes, including at SWRO desalination facilities. As was presented in this chapter, the majority of the information available on the topic of I&E has been obtained by power generators, typically in response to permit requirements. Nonetheless, SWRO desalination facilities are likely to be held to similar environmental performance standards and in some cases will have to comply with standards that could be more restrictive. This scenario is currently playing out in California and New York, as some SWRO desalination plant developers face I&E-related state regulations that are more stringent than the federal-level 316(b) ones. Beyond the U.S., the topic of impacts associated with the operation of large SWRO desalination intakes has also been receiving greater attention of late, particularly in countries that rely heavily on seawater desalination, such as the Kingdom of Saudi Arabia and Australia (Chaps. 2 and 3).

The withdrawal of seawater has impacts that cannot be eliminated; however, they can be minimized. The presence and magnitude of I&E at a given site need to be documented with biological sampling. Biological sampling at the intake and in the source water body provides the basis upon which the magnitude of the I&E can be determined. In the absence of site-specific empirical data, it is also possible to estimate the biological performance of various intake technologies by considering existing data. Ultimately, though, the magnitude I&E must be defined to be able to determine what it means on a population-scale for the species being affected.

The body of knowledge surrounding I&E and the means to minimizing its impacts on natural populations of marine organisms is extensive. Various technological and operational methods have undergone comprehensive laboratory and field evaluations to refine their biological efficacy.

References

Agardy, T. & Alder, J. (2005). Coastal systems. Chapter 19, In R. Hassan & R. Scholes, N. Ash (Eds.), *Ecosystems and human well-being: Current state and trends* (Vol. 1).

Beck, S., E., Miller, D., Bailey, D. & Steinbeck, J. (2007). Quantification of effectiveness of velocity caps. Presented at: American Fisheries Society's 137th Annual Meeting, San Francisco, CA. September 2–6, 2007.

Boreman, J., Goodyear, C. P. & Christensen, S. W. (1978). An empirical transport model for evaluating entrainment of aquatic organism by power plants. U.S. Fish and Wildlife Service FWS/OBS-78/90, Ann Arbor, MI.

Cannon, T. C. & Lauer, G. (1976). Conceptual approaches for the evaluation of biologic Impact from entrainment and impingement at power-generating stations. In L. D. Jensen (Eds.). *Proceedings of the Third National Workshop on Entrainment and Impingement: Section 316(b)—Research and Compliance*. EA Communications, Melville, New York.

EPA (United States Environmental Protection Agency) (2011). National pollutant discharge elimination system—Cooling water intake structures at existing facilities and phase I facilities. Federal Register 76(76), April 20, 2011.

EPA (United States Environmental Protection Agency) (2012). General permit for discharges from the offshore subcategory of the oil and gas extraction point source category to the territorial seas off Texas. Permit No. TXG260000.

EPA (United States Environmental Protection Agency) (2014). National pollutant discharge elimination system—Final regulations to establish requirements for cooling water intake structures at existing facilities and amend requirements at phase I facilities; Final Rule. Federal Register 79(158), Aug. 15, 2014.

EPRI (Electric Power Research Institute) (2000). *Technical evaluation of the utility of intake approach velocity as an indicator of potential adverse environmental impact under clean Water Act Section* 316(*b*). Palo Alto, CA: EPRI 1000731.

EPRI (Electric Power Research Institute) (2002). *Evaluating the Effects of Power Plant on aquatic communities: Guidelines for selection of assessment methods.* Palo Alto, CA: EPRI 1005176.

EPRI (Electric Power Research Institute) (2003a). *Evaluating the effects of power plant operations on aquatic communities: Summary of impingement survival studies*. Palo Alto, CA: EPRI 1007821.

EPRI (Electric Power Research Institute) (2003b). *Laboratory evaluation of wedgewire screens for protecting early life stages of fish at cooling water intakes.* Palo Alto, CA: EPRI 1005339.

EPRI (Electric Power Research Institute) (2003c). *Impacts of volumetric flow rate of water intakes on fish populations and communities.* Palo Alto, CA: EPRI 1005178.

EPRI (Electric Power Research Institute) (2004a). *Extrapolating impingement and entrainment losses to equivalent adults and production foregone.* Palo Alto, CA: EPRI 1008471.

EPRI (Electric Power Research Institute) (2004b). *Impingement abundance monitoring technical support document*. Palo Alto, CA: EPRI 1008470.

EPRI (Electric Power Research Institute) (2005). *Entrainment abundance monitoring technical support document*. Palo Alto, CA: EPRI 1011280.

EPRI (Electric Power Research Institute) (2006). *Field evaluation of wedgewire screens for protecting early life stages of fish at cooling water intake structures: Chesapeake Bay studies*. Palo Alto, CA: EPRI 1012542.

EPRI (Electric Power Research Institute) (2010). *Laboratory evaluation of fine-mesh traveling water screens*. Palo Alto, CA: EPRI 1019027.

EPRI (Electric Power Research Institute) (2014). *Fish protection technical brief: Estimating physical retention on traveling water screens*. Palo Alto, CA: EPRI 3002002526.

Foster, M. S., Cailliet, G. M., Callaway, J., Vetter, K. M., Raimondi, P. & Roberts, P. J. W. (2013). Desalination plant entrainment impacts and mitigation. Report to the State Water Resources Control Board.

Gulvas, J. A. & Zeitoun, I. H. (1979). Cylindrical wedge-wire screen investigations in offshore Lake Michigan for the J.H. Campbell Plant, 1979. In Passive intake screen workshop, Chicago, IL., December 4–5, 1979. Prepared by Consumers Power Company, Jackson, Michigan.

Heuer, J. H. & Tomljanovich, D. A. (1978). A study on the protection of fish larvae at water intakes using wedge-wire screening. TVA technical note B26.

Lifton, W. S. & Storr, J. F. (1978). The effect of environmental variables on fish impingement. In L. D. Jensen (Ed.), *Proceedings of the Fourth National Workshop on Entrainment and Impingement*. EA Communications. ISBN: 0-931842-01-8.

NAI (Normandeau Associates, Inc.) (2011a). *2010 IPEC Wedgewire screen laboratory study*. Buchanan, NY: Prepared for the Indian Point Energy Center.

NAI (Normandeau Associates, Inc.) (2011b). *2011 IPEC Wedgewire screen laboratory study*. Buchanan, NY: Prepared for the Indian Point Energy Center.

Nieder, W. C. (2010). The relationship between cooling water capacity utilization, electric generating capacity utilization, and impingement and entrainment at New York State steam electric generating facilities. New York State Department of Environmental Conservation Technical Document. Albany, NY. July 2010.

Oney, S. K., Hogan, T., & Steinbeck, J. (2013). *The potential impacts of OTEC intakes on aquatic organisms at an OTEC site under development on Kauai*. HI: Prepared for the U.S. Department of Energy. doi:10.2172/1092416.

Pankratz, T. (2004). An overview of seawater intake facilities for seawater desalination. *The future of desalination in Texas*, Vol. 2.

PSEG (Public Service Enterprise Group). (2004). Salem generating station NJPDES permit no. NJ0005622—Custom Requirement G.9.b.ii—Entrainment Exclusion Studies Task #1, Morphometric Analysis.

Schneeberger, P. J., & Jude, D. J. (1981). Use of fish larva morphometry to predict exclusion capabilities of small-mesh screens at cooling-water intakes. *Transactions of the American Fisheries Society, 110*, 246–252.

Steinbeck, J.S., Hedgepeth, J., Raimondi, P., Cailliet, G. & Mayer, D. (2007). Assessing power plant cooling water intake system impacts. Prepared for the California Energy Commission. CEC-700–2007-010.

Tenera (Tenera Environmental) (2007). Marin Municipal Water District desalination facility intake effects. Appendix C of Final Environmental Impact Report (EIR), Marin County, California.

Tenera (Tenera Environmental) (2010). City of Santa Cruz Water Department and Soquel Creek Water District SCWD2 desalination program. Open ocean intake study effects. ESLO2010–017.1.

Turnpenny, A. W. H. (1981). An analysis of mesh sizes required for screening fishes at water intakes. *Estuaries, 4*(4), 363–368.

Weight, R. H. (1958). Ocean cooling water system for 800 MW power station. *Journal of the Power Division of the American Society of Civil Engineers*. Paper 1888.

Weisburg, S. B., Burton, W. H., Jacobs, F., & Ross, E. A. (1987). Reductions in ichthyoplankton entrainment with fine-mesh, wedge wire screens. *North American Journal of Fisheries Management, 7*, 386–393.

WRRF (WateReuse Research Foundation) (2014). Impingement mortality and entrainment (IM&E) reduction guidance document for existing seawater intakes. 10–04-1. Prepared by T. Hogan, C. Fay, D. S. Beck, S. Lattemann and T. Pankratz.

Zeitoun, I. H., Gulvas, J. A., & Roarabaugh, D. B. (1981). Effectiveness of fine-mesh cylindrical wedge-wire screens in reducing entrainment of Lake Michigan ichthyoplankton. *Canadian Journal of Aquatic Sciences, 38*, 120–125.

Chapter 5
Passive Screen Intakes: Design, Construction, Operation, and Environmental Impacts

Thomas M. Missimer, Timothy W. Hogan and Thomas Pankratz

Abstract Passive screen intake systems provide a higher degree of reduction in impingement and entrainment compared to open-ocean intake structures, such as channel and velocity cap intake systems. The system consists of a wedgewire screen structure with a conveyance pipeline to the plant facility and a pumping station. Commonly, the screen structure contains a semi-automated cleaning system that uses bursts of compressed air. Passive screen intake systems exclude a large part of the marine biota by using a relatively small screen aperture and a low inflow velocity. Screen slot aperture is commonly less than 3 mm and depends on environmental regulations pertaining to the specific site location. The range in design intake velocities through the screen ranges from 10 to 15 cm/s, again depending on local regulations. The current motion across the screen structure also sweeps small organisms off the screen and helps exclude them from entrainment into the inflowing water. The degree of environmental impact on entrainment of ichthyoplankton is greatly dependent on the design of the passive intake system and the current velocity. Some environmental impacts occur when constructing the connecting pipeline across or beneath the seabed and surface zone of the shoreline. Passive screen intake systems can provide a high-capacity SWRO plant with the required feed water. However, when the passive screens are located offshore, there is some complexity in the maintenance of the screens that can limit use of the technology.

T.M. Missimer (✉)
U.A. Whitaker College of Engineering, Florida Gulf Coast University, 10501 FGCU Boulevard South, Fort Myers, FL 33965-6565, USA
e-mail: tmissimer@fgcu.edu

T.W. Hogan
Alden Research Laboratory, Holden, Massachusetts
e-mail: thogan@aldenlab.com

T. Pankratz
Water Desalination Report, 75064 Houston, Texas, USA
e-mail: pankratztm@gmail.com

T.M. Missimer et al. (eds.), *Intakes and Outfalls for Seawater Reverse-Osmosis Desalination Facilities*, Environmental Science and Engineering,
DOI 10.1007/978-3-319-13203-7_5

5.1 Introduction

Most large-capacity seawater reverse osmosis (SWRO) desalination facilities use conventional surface-water intake systems, such as a velocity cap attached to a large diameter pipeline which conveys raw seawater to an onshore screenhouse and a series of other pretreatment processes (Gille 2003; Missimer 2009; Chap. 1). Finer screening of debris and marine life at the intake in such systems can present hydraulic (e.g., head loss) and environmental (e.g., impingement) difficulties as the design intake velocities can be high. A passive screen intake system offers an alternative approach that minimizes hydraulic and environmental challenges through an innovative system design. This intake system has a series of primary components, including the screen, commonly an automated screen cleaning system, the pipeline connecting the screen to the shoreline (in offshore applications), and a pump with controls.

Conventional screening at large seawater intakes typically includes active collection of impinged debris and marine life. Depending on the design of the active screening system, the collected debris and marine life is either disposed of or rinsed into a collection system that returns it to the source water body. Passive screening, however, is a fundamentally different approach, relying on a combination of small screen slot size and low through-slot velocity to passively exclude debris and marine life from the intake flow. Indeed, passive screens are so-named because they have no moving parts. There are several names applied to passive screens, which are barrel screens, cylindrical wedgewire screens, "Tee" screens, and perhaps others, but in this chapter we use the term passive screens throughout the text to avoid confusion.

Passive screens have been used for cooling water intake structures (CWIS) in the power industry for decades (Cooke 1978; Gulvas and Zeitoum 1979; Hanson 1979; Otto et al. 1981; Zeitoun et al. 1981; Weisberg et al. 1983, 1984a, b; Stefan et al. 1986; Weisberg et al. 1987; Erhler and Raifsnider 1999; EPRI 1999, 2003, 2005). There is considerable experience in the design and operation of this intake technology in freshwater and some estuarine CWIS. There is, however, far less experience in passive screen intake system design and operation in the marine environment (Bechtel Power Corporation 2012), especially for use as SWRO intake systems (Pankratz 2008). A list of SWRO facilities that use passive screen intakes is given in Table 5.1.

Table 5.1 SWRO facilities using passive screen intake systems

Facility name	Location	Plant capacity (m^3/d)	Intake capacity (m^3/d)	Type of system	Distance offshore (m)
Test bed	Busan, South Korea	45,460	108,000	Offshore	300
Beckton	London, England	150,000	350,000	Platform	0
Chennai	India	100,000	265,000	Offshore	600

Unfortunately, many passive screen intake systems are located in dead-end canal channels attached to seawalls bordering tidal water with only a few offshore installations. Locating a passive screen system in a dead end canal is generally a poor practice as there is no exposure to ambient cross-currents that minimize debris accumulation and marine life interaction. Furthermore, when backwashed, without ambient cross-currents, debris will simply re-impinge on the screen face or accumulate as sediment on the bottom, requiring periodic removal. The results of previous studies that have evaluated multiple ambient and through-screen velocities indicate passive screens should be protective of most species and life stages when ambient velocities are equal to or greater than through-slot velocities (Cooke 1978; Hanson et al. 1978; Heuer and Tomljanovich 1978; Lifton 1979; EPRI 2003). Under these hydraulic conditions, passive screen intakes should also be optimized to shed debris efficiently. The Water Research Foundation (2011) suggested that passive screen intakes are most effectively used when the current velocity passing adjacent to the screen is >30 cm/s which allows debris in the water column to pass by the screen without impinging upon it, but this report does not document where this velocity has been used in a design and does not report any data on the effectiveness of the criterion.

Passive screen intakes can serve large capacity SWRO facilities, such as the Beckton SWRO facility in London, England which has a total raw water intake capacity of 150,000 m^3/day. This site does have tidal currents which do allow some sweeping of debris away for the intake screens.

Some of the most important issues in the design of passive screen intake systems include: (1) overall system capacity, (2) distance between the shoreline and intake screen, (3) tidal and ocean bottom current strength, (4) water depth at the site, (5) the strength of storm wave orbital motion on the marine bottom, (6) screen composition for corrosion prevention, (7) screen material for anti-fouling prevention, (8) ease and frequency of screen cleaning based on water depth, biological productivity of the area around the intake, and distance offshore, (9) conveyance pipeline design from the facility to the offshore intake including materials and provisions for cleaning, and (10) pumping system design. The design, construction, maintenance, and environmental impacts of passive screen intakes for SWRO facilities are covered in this chapter with some suggested innovations in design of offshore systems.

5.2 Design and Construction

5.2.1 Passive Screen Intake System Location

Passive intake screens are feasible for both onshore and offshore applications and can also be used at new and existing intake structures (i.e., as a retrofit). The design of each passive screen intake generally depends on the design intake flow rate, the

expected biofouling and debris loading conditions at the intake location, the ambient hydraulic conditions (e.g., ocean and tidal currents), and the extent to which marine life must be protected against impingement and entrainment. Care must be taken in the consideration of the field conditions where a passive intake system is to be installed. Water flow past the screens is a key factor controlling the effectiveness of the system to remove debris and living organic matter, and to allow effective cleaning.

5.2.1.1 Onshore/Bulkhead, Channels, Docks, or Proximal Restricted Waters

There are many SWRO facilities that share a common intake structure with power plants. Typically, power plant intakes connected to tidal water are used to convey water through the condenser system for cooling purposes. There is a water conveyance structure abstracting flow from the sea, passing it through the power plant condenser, and discharging the warmed water through a separate outfall structure located outside the hydraulic influence of the intake (to prevent recirculation). The water conveyance structure may be a channel, a tunnel, or a large-diameter pipeline depending on the design and capacity of the facility. Passive screen intakes may be mounted on a seawall adjacent to the outflow discharge structure where some of the natural debris in the seawater may have been screened out in the power plant facility, the water temperature is warm (treatment process enhancement), and where sufficient current velocity is maintained to allow the passive screen intake to function normally.

In these co-located channel intake systems and other stand-along SWRO plants with shoreline or channel intakes, an array of passive screens is mounted directly on the seawall or mounted directly above the channel bottom with the conveyance pipe located beneath the screen with a concrete pad to provide a stable structure (Fig. 5.1). This arrangement is rather simple and the design of the intake pipeline, cleaning system, and pumps is straight forward with all of the components located in close proximity.

A key design issue is to place the screens at locations where there is a continuous water current passing across them. Placement of a passive screen array at a dead-end canal is not usually a viable design solution, because a greater percentage of debris occurring within the water column will become impinged on the screen (no shear-force of the current to keep in clean). Also, the cleaning of the screen would not be effective because the debris would remain in the water column for an extended time before settling to the bottom. The debris would accumulate on the bottom and would require periodic physical removal to prevent cycling into the intake screens. In systems where the water in the intake channel is quite clear and free of debris, passive screens could be used in dead-end channels to reduce fish entrainment.

Fig. 5.1 Passive screen intake along a seawall or channel edge (Courtesy of Gap Technology Limited)

5.2.1.2 Offshore Locations

Nearshore seawater quality can be quite poor in many areas, especially near urban areas, estuaries, coastal wetlands, or stream discharge points (e.g., wadi discharge locations in the Middle East). Poor quality is defined as water with relatively high concentrations of organic compounds and suspended sediments. Algae, bacteria, dissolved organic compounds and organic polymers along with clay-sized suspended sediments will pass through the passive screen system into the pretreatment process, where they will have to be removed. Therefore, intake locations should be given careful consideration in regards to the quality of feedwater available; the intake should be located in an area yielding the best possible raw water quality. To that end, many intakes are designed to draw feedwater from an offshore location where water clarity is better and it is a greater distance from the source of sediment.

Most offshore intakes are located in water depths ranging between 5 and 15 m depending on the offshore bottom slope (Missimer 2009). Deeper intakes can be designed and constructed, but the issues involving maintenance must be carefully considered. If manual maintenance will be required, then depths suited for scuba diving should be considered or perhaps the maximum depth that does not require decompression for an extended work effort. For example, if the intake is located at a depth of about 10 m, then a diver can work on the intake for about 160 min using normal compressed air before decompression is required on ascent (U. S. Navy Dive Tables, Table 5.2). Manual screen cleaning becomes more complex at greater depths and typically is considered to be a design limit based on cost and safety risk

Table 5.2 U. S. navy dive tables for decompression

Depth feet / metres		Doppler No-Decompression Limits (minutes)	No-Decompression Limits and Repetitive Group Designation Table For No-Decompression Air Dives										
10	3.0		60	120	210	300							
15	4.5		35	70	110	160	225	350					
20	6.0		25	50	75	100	135	180	240	325			
25	7.5	245	20	35	55	75	100	125	160	195	245		
30	9.0	205	15	30	45	60	75	95	120	145	170	205	
35	10.5	160	5	15	25	40	50	60	80	100	120	140	160
40	12.0	130	5	15	25	30	40	50	70	80	100	110	130
50	15.0	70		10	15	25	30	40	50	60	70		
60	18.0	50		10	15	20	25	30	40	50			
70	21.0	40		5	10	15	20	30	35	40			
80	24.0	30		5	10	15	20	25	30				
90	27.0	25		5	10	12	15	20	25				
100	30.0	20		5	7	10	15	20					
110	33.0	15			5	10	13	15					
120	36.0	10			5	10							
130	39.0	5			5								

issues. Very deep intakes, as being touted by the Megaton research initiative in Japan, could require the operation of a submersible vehicle to allow cleaning.

The distance from the shoreline to the passive screen intake is another important design consideration. It affects the type of pump that can be used, the horsepower of the pump, and the ability to use automated air-bust cleaning of the screens. In an analysis of passive screen use for a SWRO facility at Candelaria, Chile, it was found that at 200 m offshore, a single pipe airburst cleaning system using a normal compressor (8.5 m^3/min) and conveyance pipe (100 cm in diameter) would be inadequate to clean both sides of a passive screen using a "t" air cleaning configuration. At this distance, a design solution was to place two air conveyance pipes inside the intake pipe and clean the barrel screens one-half at a time. Distances beyond 600 m offshore and 10 m of water depth were found to be quite problematical. Such distances would require radical resign change in the compressor capacity, storage tank (higher pressure and capacity), and the strength and diameter of the airline to use the air burst technology. The Test Bed SWRO plant located in Gijang-gun, South Korea uses a passive screen intake that is located 300 m offshore, but still uses an air-burst cleaning system (Woo et al. 2013).

Another potential design solution to this problem would be to redesign the passive screen configuration to have the airline "t" at the opposite side of the barrel screen from the offshore conveyance pipe (Fig. 5.2). This airline would contain a nipple with a quick-connect fitting. The compressed air source would be a compressor/air tank assembly located on a boat or barge that would be sent offshore to the intake site. A diver would convey the airline from the boat to the screen quick connect fitting, hook it up, and allow the air burst operation to occur. The maintenance barge and airline system could be used at any location. Mooring rings could be installed in the seabed to allow the boat or barge to remain on-station during the cleaning operation.

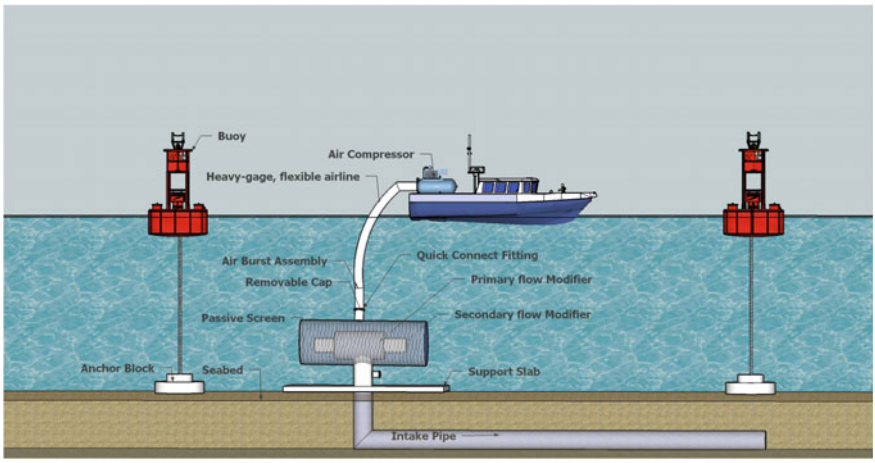

Fig. 5.2 Airburst system modified for boat-based maintenance of an offshore passive screen intake system

An elevated offshore platform could be constructed to house the compressor, air tank, and an electric generator as used at the Beckton site. This type of tower could serve multiple purposes, such an a navigation marker, air bust cleaning system housing, and perhaps to stabilize the passive screen intake underwater by using the tower pilings as attachment points for a rigid structure that holds the screen assembly (Fig. 5.3). This would prevent the settling of the structure into the marine bottom during intense storms.

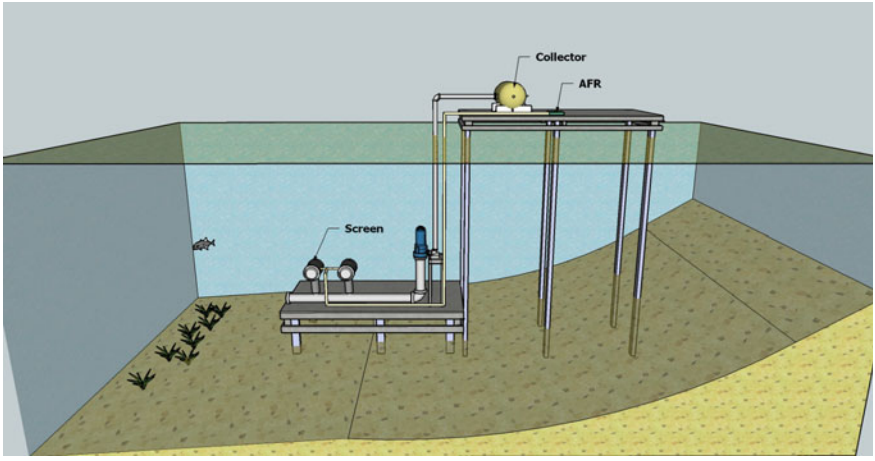

Fig. 5.3 Tower structure for location of a navigation station, housing of the air bust cleaning system and compressor, and to stabilize the passive screen intake structure underwater (Beckton SWRO plant example)

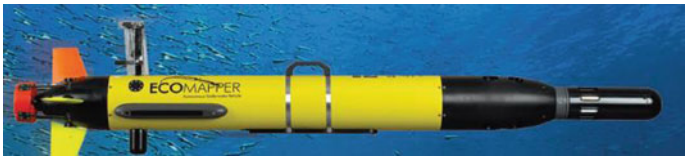

Fig. 5.4 Untethered submersible data collection device for collection of bathymetric and water quality data (Courtesy of YSI)

The bottom slope and roughness is another design consideration when deciding where to locate barrel screens in offshore areas. Obviously, the location of a steep or unstable bottom slope would cause risk for failure of the system. A pre-design side-scan sonar survey of the offshore bottom should be conducted before a location decision is made. This survey should be run coincident with environmental surveys that are needed to assess potential environmental impacts which could include some type of pilot testing to assess impingement and entrainment of marine organisms. Other issues, such as navigation and associated water depth, must be considered to avoid ship damage to the intake structure either by collision or prop turbulence. Today, there are automated devices that can be used to collect detailed bathymetry, water physical properties, water chemistry, dissolved oxygen, turbidity, and certain organic parameters, such as chlorophyll A (Fig. 5.4). A flat spot could be located to place the barrel screen intake assembly. Test borings offshore will likely to be required to assess bottom stability at the screen site as well as the conveyance pipeline.

Strong tidal or offshore ocean currents and storm wave orbital motion can also provide a design challenge for passive screen intakes. Uneven current motion or undulatory motion (wave orbital induced) could produce torque on a typical "t" screen and eventually cause some structural damage to base of the mount assembly. A passive screen intake that has a more rounded geometry (one-half screen, rounded and standing upright) could be used. There are several other potential design solutions. One is to brace the "t" design with welded struts between a basal plate and the terminations of the screen assembly (Fig. 5.5). In an extreme case, the passive screen and offshore infrastructure could be constructed onshore on a pre-fabricated concrete pad and sent offshore on a barge. The assembly could be lowered onto the seabed and anchored. This would provide a very high degree of strength and stability. This however assumes that there is an adequate seabed substrate to do so. A pilot scale passive screen study for South Padre Island in Texas used a similar approach with a screen mounted to a pre-fab concrete gravity base. After a few months, wave action sunk the assembly into the sand and the screen became completely occluded. Therefore, the slab may have to be anchored to driven or drilled cement pilings. The design also must be coordinated with the pipeline design and construction methodology.

The passive screen design at the Beckton facility located at London, England uses a rather interesting design for installation of the passive screen intake. The screens are mounted on the river bottom adjacent to a platform which is used for the

Fig. 5.5 Passive screen with steel frame to stabilize it and prevent torque damage (Courtesy of Screen Services)

collection pump and cleaning system (Fig. 5.3). Platform use could be a design solution for cleaning and pumping at locations where the water offshore is very shallow, causing the distance from the shore to be large to achieve better raw water quality.

5.2.2 Passive Screen Design

5.2.2.1 Introduction

The screen design must be carefully considered to maximize water inflow while minimizing the risk of both impingement and entrainment of biological organisms and debris blockages. Also, the screen material is a critical design choice because of corrosion issues and the potential for sessile organism attachment and growth on the screen and support structure.

The passive screen is constructed using the wedgewire screen configuration that has a classic "v" configuration with the aperture increasing in the inward direction (Fig. 5.6). Most passive screens have a "t"-shaped geometry with screened sections located on either side of a central intake to maximize flow capacity (Fig. 5.7). Johnson Screens has developed a flow stabilizing system that creates a uniform head loss across the slots, thereby producing a relatively uniform flow pattern (Figs. 5.8 and 5.9). Currently, there are a number of manufacturers that make barrel screens globally, including Johnson Screens, Hendrick Screen Company, Intake Screens Inc., Delta Screens, Ovivo, StaticOrb, and several others (Pankratz 2005). In recent years, some additional configurations for passive intake systems have been developed by Taprogge (Tapis-Taprogge Air Powered Intake System) and others.

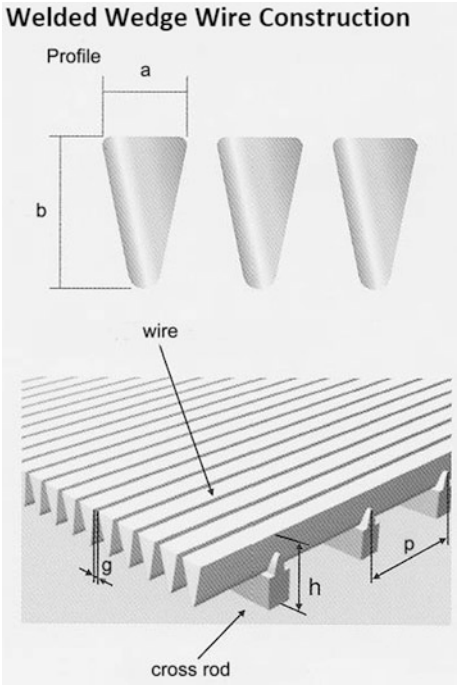

Fig. 5.6 Close-up of the wedgewire screen geometry. The width of the wire is *a* and the thickness is *b*. The aperture width is *g*. The total thickness of the screen plus the cross rod is *h*. (Courtesy of Johnson Screens)

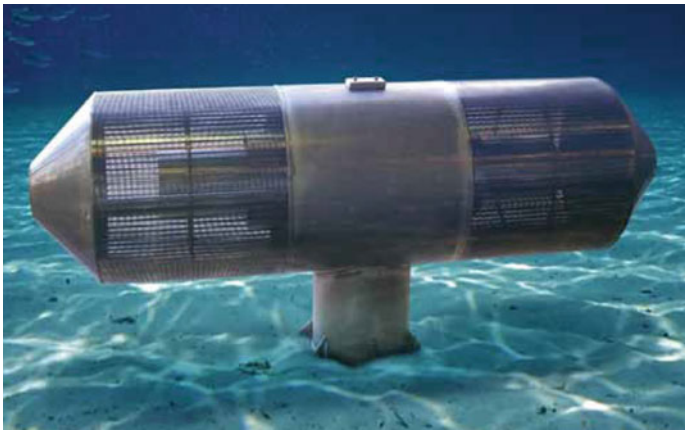

Fig. 5.7 Classical "T"-shaped barrel screen at an the offshore showing the components (Courtesy of Johnson Screens)

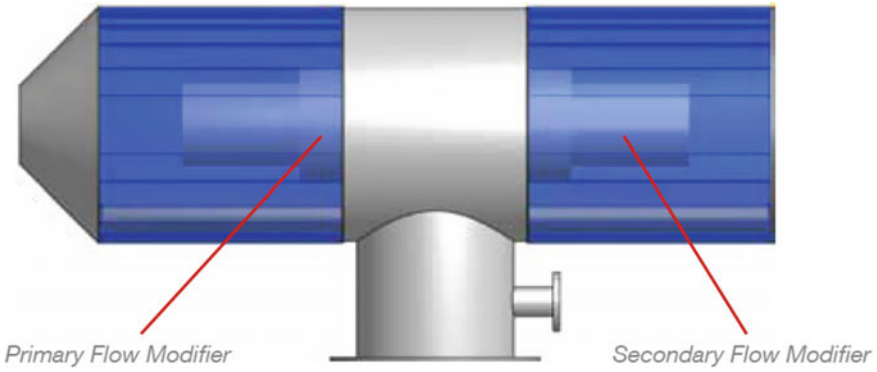

Fig. 5.8 Patented johnson screens flow stabilizer in a barrel screen (Courtesy of Johnson Screens)

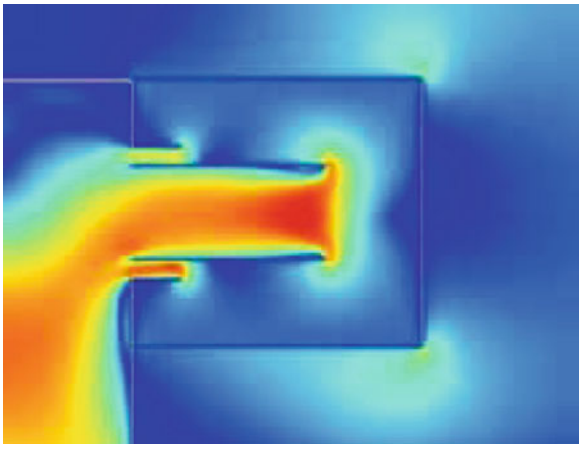

Fig. 5.9 Hydrodynamic model of the flow uniformity through the barrel screen intake using the flow stabilizer (Courtesy of Johnson Screens)

5.2.2.2 Hydraulic Design and Operation

A design balance must be achieved to meet the water flow rate requirement of the facility, while minimizing the potential for fouling of the screen slots with living or dead organic material and meeting environmental regulations to minimize impingement and entrainment. A rather conservative set of passive screen criteria has been suggested by the Northwest Region of the National Marine Fisheries Service in the United States (NMFS 1996, 2008a, b). It is important to note that these criteria were originally developed to address concerns over Pacific salmon species at the migration barrier, rather than guidelines for all species potentially interacting with each type of industrial water user (e.g., hydroelectric, steam electric, irrigation, desalination). The criteria are given in Table 5.3. In this case, the suggested maximum approach velocity for passive screens is 6.1 cm/s.

Table 5.3 Pump intake screen intake design criteria recommended by the National Marine Fisheries Service (NMFS 1996, 2008a, b)

Screen approach velocity (**How to calculate**): The approach velocity must not exceed 12.2 cm/s (0.40 ft./s) for *active screens*, or 6.1 cm/s (0.20 ft./s) for *passive screens*. Using this approach, velocities would minimize screen contact and/or impingement of juvenile fish. For pump intake screen designs for water drafting, *approach velocity* is calculated by dividing the maximum screened inflow (cm^3/s) by the entire *effective screen area*. *Approach velocity* should be measured as close as physically possible to the boundary layer turbulence generated by the screen face
Effective screen area: The minimum *effective screen area* must be calculated by dividing the maximum screened flow by the allowable *approach velocity* (12.2 cm/s for *active screens*, or 6.1 cm/s for *passive screens*)
Specific criteria and guidelines for pump intake screen mesh material
Circular screens: Circular screen face openings must not exceed 2.46 mm (3/32 in) in diameter. Perforated plate must be smooth to the touch with opening punched through in the direction of approaching flow
Slotted screens: Slotted screen face openings must not exceed 1.75 mm (3/32 in) in the narrow direction
Square screens: Square screen face openings must not exceed 2.46 mm (3/32 in) on a diagonal
Material: The screen material must be corrosion resistant and sufficiently durable to maintain a smooth uniform surface with long term use
Other components: Other components of the screen facility (such as seals) must not include gaps greater than the maximum screen opening defined above
Open area: The percent open area for any screen material must be at least 27 %

The approach velocity is calculated by dividing the screen inflow by the effective screen area. Using this design criterion, flow balance through the screen slots is very important so that the flow is uniformly below the maximum approach velocity. NMFS also suggests that the maximum slot aperture should be 1.75 mm in the narrowest section of the wedgewire "v" screen. There are several other criteria listed with regard to a different screen types (e.g., square slots) and the need to construct the screens with corrosion resistant material.

The State of California has some regulations under development regarding the use of passive screen intakes for SWRO applications. Guidelines provided by the California Department of Fish and Game suggest the maximum approach velocity measured perpendicular to the screens shall not exceed 10 cm/s and the screen slot size shall not exceed 2.38 mm. This is not as stringent as the NMFS guidelines. The maximum through-screen velocity considered protective by the U. S. Environmental Protection Agency is 15 cm/s (USEPA 2011).

Most international SWRO facilities using passive intakes use a moderately conservative approach to the inflow design criteria. For example, the Test Bed Gijang-Gun SWRO plant, located at Busan, South Korea (45,460 m^3/d), uses a passive offshore intake that has a design capacity of 4,500 m^3/h with a screen length of 5,540 mm, a screen diameter of 1,675 mm, a screen slot aperture of 3 mm, and a through-slot intake of 0.13 m/s or 13 cm/s (Woo et al. 2013). This facility has an

approach velocity of nearly two times the NMFS recommended standard, but is reasonably close to the California guideline.

Some of the velocity regulatory terms can be somewhat confusing and are not always consistently defined. There is some back and forth between the use of "approach velocity" and "through-screen velocity". NMFS describes the approach velocity as that measured within 7.6 cm of the screen face. Through-screen velocity is the velocity of the water as it passes between the structural components of the screen (slot apertures) and by definition will always be greater than approach velocity measured in front of the screen.

5.2.2.3 Screen and Exposed Fittings Materials

Seawater is exceptionally corrosive having high dissolved chloride and oxygen concentrations. Also, seawater moving through the screen slots tends to promote the rapid growth of sessile organisms, such as mollusks, tunicates, corals, calcareous red or green algae, and others. Therefore, these issues must be taken into consideration in the barrel screen design.

To minimize corrosion, some high grade of stainless steel must be used. Some barrel screens have been installed using 316L stainless steel, but some corrosion was experienced or in other seawater applications of this grade of stainless steel (Malik and Al-Fozan 1994). A duplex or super-duplex stainless steel type is preferred over lower grades, but this material is quite expensive. The design challenge is to strike a balance between a resistant grade of stainless steel and the useful life expectancy of the screen. All of the higher grade standard stainless steels, excluding 304 and 316, do resist marine corrosion, but have no significant impact on retarding marine organism growth within the screen. Stainless steel alloys containing molylibdinum (Mo), such as 904L at 4.5 % Mo and 254 SMo and 4565S which have 6 % Mo, have resistance to marine corrosion. Detailed assessments of metals that can be successfully used in the marine environment are contained in Tuthill (1988) and Malik et al. (1991, 1995, 2001). A recently constructed SWRP plant at Chennai, India used superstainless steel alloy 2507 for the passive screens (http://www.johnsonscreens.com/contetn/johnson-screens-supplies-c…). Materials research on passive screen conducted at West Basin Water District in California showed good results using 1910 duplex stainless steel. However, there was rapid growth of mussels on the screen face and within the lighted inflow pipe when chlorine was not used.

Retardation of marine sessile organism growth can be achieved by using special stainless steel alloys that contain copper. Johnson Screens uses such an alloy, referred to as a "Z-Alloy". There are a number of similar or equivalent types of materials on the market. There may be a trade off by using these alloys with greater resistance to marine organism growth, but less resistance to marine corrosion. Careful research and a life-cycle cost analysis should be performed when developing the design criteria for the screen material.

5.2.2.4 Design Approach to Cleaning

The air burst cleaning system (*Hydroburst*™) was developed by the Johnson Screens, currently owned by Bilfinger Water Technologies. This system consists of an air compressor attached to a conveyance pipe which connects to a "t" within the barrel screen assembly (Fig. 5.10). The system delivers a high volume surge of compressed air to the inside of the screen assembly and is quite effective at removing most of the debris that has become lodged on the screen face. For example, the pressure in the tank at the Test Bed SWRO facility (South Korea) is 8 bars which is sufficient to allow cleaning of the screen located 300 m offshore at a depth of 10 m.

Air burst cleaning systems are particularly effective and easy to design for installations located at the shoreline, such as those attached to a seawall bordering a channel that has adequate water flow velocity (see Sect. 5.2.1.1). The key design complication is the distance between the air compressor and the barrel screen. The issue is the diameter and strength of the air transmission line and the capacity of the compressor. Long transmission distances between the compressor and barrel screens may compromise the effectiveness of the system if an insufficient volume of air is released during a cleaning event. This requires a detailed analysis of the air compression loss along a horizontal pipe which can be calculated using a form of

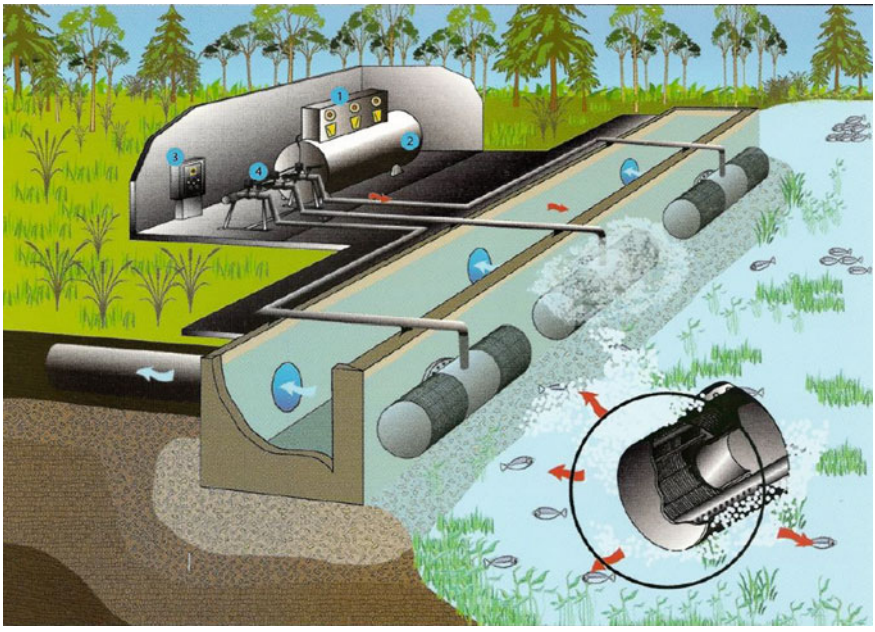

Fig. 5.10 Diagram showing the components of the Johnson air burst cleaning system (Courtesy of Gap Technology)

Boyles Law adapted for calculation of pressure loss with transmission (Sahu 1998; Nayyar 2000).

As previously presented (Sect. 5.2.2.2), another design solution to use air burst technology to clean barrel screens involves use of a boat or barge-mounted compressor and air tank. This would allow the passive screens to be located at any distance offshore, but there still is some reasonable economic depth limitation. A diver would have to attach the airline to the nipple at the front of the barrel screen or the airline could be suspended and attached to a floating buoy, so that the boat could hook up the airline to the compressor without a diver. The airline has to be purged of water before it will function properly or a ball valve could be used to keep water out.

5.2.3 *Design Criteria for Offshore to Onshore Transmission Pipe*

There are a number of important issues that must be addressed during the design of the pipeline(s) that connects the intake screen(s) with the shore treatment facility. These issues are: (1) pipe capacity and diameter, (2) pipe strength and material, (3) pipeline construction methodology, (4) coordination with the pump design, (5) possible pipeline redundancy that would allow maintenance to clean internal biofouling, (6) possible pigging infrastructure, and (7) real and perceived environmental impacts.

There are four different strategies that can be used for design and construction of the pipeline, all of which affect the final design. The pipeline can be installed in an open trench and buried, in an open trench onshore and laid on the bottom offshore (exposed on the seabed), can be placed inside of a pre-constructed tunnel (Baudish et al. 2011), or can be installed using micro-tunneling technology.

The most common material currently being using for SWRO facility intake pipes is high-density polyethylene (HDEP). This material is non-metallic, flexible to a degree, somewhat buoyant, strong, and can be welded effectively from shorter segments. However, intense wave activity can cause it to be damaged, so it must be anchored to the seabed and must be buried beneath the littoral zone, especially in high energy coastlines where breaking waves during storms could damage or destroy the pipe. Sometimes HDEP pipe is placed into a caisson in the high-energy area of construction or inside of a tunnel to the location of the passive wave inlet (see Chaps. 2 and 3).

An emergent HDEP pipeline can be easily installed by welding the segments at the shoreline, plugging the ends and then using a boat to float the pipe seaward to the connection location with the passive screen with subsequent sinking of the pipe (Fig. 5.11). The final connections to the screen assembly at the distal end and the connector pipe beneath the surf zone are accomplished using divers. Concrete anchors are installed on the pipeline either before towing and sinking or afterward

Fig. 5.11 Installation of conveyance pipeline for an intake system using the float, transport and sink method at Abutaraba, Libya

when the pipe sets upon the bottom. Emergent HDEP pipelines must have a rather uniform bottom slope with no rocky ledges that could cause the pipe to shear or tear during installation or storm events. Therefore, some preparation of the bottom may be required (e.g., dredge and filling) to properly "bed" the pipe.

5.2.4 Pump Design and Configuration

There are two general design approaches that can be used to install the conveyance pumps. A deep vertical caisson can be constructed near the SWRO facility that is at a depth greater than that of the installed screen. In this case, the pumps could be placed beneath land surface, so that the pumping head would be minimal. Centrifugal pumps could be used in this type of design. Another method is to design and construct a vertical pool that is sufficiently deep to allow vertical-life turbine pumps to create sufficient head loss at the proximal end of the pipeline to overcome gravity head losses and friction head losses for the pipeline and screens. Care must be taken to allow sufficient design flexibility to overcome head losses in the screens between cleaning times when some buildup of impinged material and attached sessile organisms partially block the screen slots.

Seawater corrosion potential necessitates the use of some duplex stainless steel alloy for the pump materials. Therefore, the most efficient pump type and materials must be carefully coordinated with the design of the inlet for the pumping station to assure that pump replacement time is maximized and that the electric operational cost is minimized.

Where a pigging system is required to control biofouling of the transmission pipe interior, the pumping station design will be required to include a pig catching assembly. This will complicate the overall system design.

5.3 Operation and Cleaning

5.3.1 Screen Clogging and Cleaning Methods

There are a number of potential mechanisms that can cause screen clogging, including straining of organic material onto the screen face, growth of marine sessile organisms on the screen face or within the interior of the screen near the connection to the conveyance pipe. The strategy concerning management of the cleaning or fouling suppression process depends on the local marine conditions (local biological assemblage), the inflow velocity through the screens, the screen material, and the water depth and location at which the passive intake is installed. Local conditions control the frequency of cleaning and the most economic methods to be employed. Soft, impinged material can be removed by air burst or by physical bushing. Hard growth of calcareous organisms will require mechanical cleaning when they reach a certain size, so this type of growth needs to be controlled early before it becomes a chronic problem.

Passive screen intakes located at a dead-end canal or along a seawall that has a very low current velocity can create some special problems. Air burst cleaning (Sect. 5.3.2) alone will not likely solve the normal maintenance condition, because the material removed will tend to remain in the water column for some period of time after being cleared from the screen surface and the cleared debris will accumulate on the bottom adjacent to the screen. These sites will likely require the physical removal of the cleared debris from the water column which can be accomplished by using a vacuum pumping system with onsite filtration and recycling of the seawater back into the water body. The filtrate collected would require disposal as solid waste. The vacuuming process would also prevent the accumulation of debris on the floor of the canal. Where there is a minor current, the timing between cleaning and return to normal operation would have to be extended to allow the debris in the water column to settle. In this case, there would likely need to be periodic dredging and removal of the organic sediment that accumulates on the bottom. Where numerous screens are located side-by-side, the cleaning process may require plant shut-down during a cleaning cycle to prevent recycling of debris into the adjacent intake. Therefore, the spacing between the screens is a design issue in which maintenance must be considered.

Passive screen cleaning offshore can require some special equipment and scheduling can be rather complex. Where the passive screen system is located offshore and the distance is not too great from the shore-mounted compressor and air tank, the air burst system can be effectively used to clean impinged debris and some sessile attached organisms. A key issue is the timing between cleanings. If the water is relatively clean and the growth rate of sessile organisms is slow, then cleaning may be required every several weeks. It is important, however, to physically inspect the screen(s) often to be sure that hard growth is not occurring. Where hard growth on the screen occurs, air burst cleaning should be scheduled frequently to disrupt the attaching organisms before they become well-established and cover a

large area of the screen. If attachment has occurred, then a diver should physically clean the screen to remove the juvenile organisms.

During air burst cleaning, the pump should be shut off to avoid impinging the removed debris and to lessen the probability of entraining the finer debris through the screens. The cleaning cycle time requirement, therefore, controls the need for redundancy of screen capacity and the actual timing of the maintenance activity. Air burst cleaning could be performed during daily low-flow periods during nighttime hours. Physical cleaning requiring divers to perform the work must be conducted during daylight hours. Since the velocities through the screens are quite low, this activity could be conducted while during pumping. There would be some fine debris entrained during cleaning.

One key fouling issue that must be considered is marine growth at a location that cannot be accessed for cleaning and removal. This may occur inside of the screens, inside of the screen structure, or within the photic zone of the conveyance pipe. Such growth occurred at the West Basin test passive screen site in California. Rapid growth of sessile organisms may occur in these locations and could require another approach to keeping them clean or the entire screen assembly would have to be periodically lifted off of the pipe inlet for manual cleaning.

5.3.2 Continuous or Episodic Chlorine Feed

One option to keep the interior screen and pipeline head clear of sessile organism growth is to install a chlorine feed line within the conveyance pipe. Chlorine delivery could be continuous or periodic depending on the growth rate of marine organisms inside of the screen the head of the pipeline, and perhaps within the pipe interior. In a system with a relatively high organic load, the chlorine would be consumed fully via oxidation of the organics before reaching the end of the conveyance pipe and would be create a problem at the treatment facility.

5.3.3 Pipeline Cleaning: Pigging or Manual

The highest potential for the requirement to manually clean the pipeline is at the distal end in the photic zone where sessile marine organisms, such as mollusks, corals, or tunicates, will tend to attach to the pipe and grow. This could be prevented by the use of a chlorine feed, but this is expensive and not environmentally friendly. Another possible is the use of a coating, such a copper based marine paint that would prevent attachment of the organisms. Unfortunately, coatings have a limited useful life and would have to be re-applied in a wet condition which presents a challenge concerning the availability of a product that could be applied under such conditions. Periodic manual cleaning of the pipeline head by a diver

may be required. This would be a time-consuming process and would require the pumping system to be inactivated during the cleaning procedure.

It is likely that a biofilm will develop on the walls of the pipeline downstream from the photic zone to the pumping station. In most cases, the biofilm will not affect the operation of the treatment process or the pipeline conveyance. The friction head loss in HDPE pipe may increase to a minor degree. In an extreme case where there is a high influx of organic carbons and/or storm activity sufficiently intense to cause sediment to enter the pipeline, periodic pigging of the pipeline may be necessary to remove debris and to strip off most of the biofilm layer. This would be a complex process and would require that special permanent or temporary structures would need to be installed to allow launching and catching of the pig without damaging the pump. The operation of the passive intake would have to be shut down during this process. This issue again affects the design of the intake system and the need for redundancy of inflow capacity, especially went onsite or distribution system product water storage is insufficient.

5.3.4 Pump Cleaning and Maintenance

All pumps used in the marine environment require regular maintenance because of the extremely corrosive nature of seawater. As a primary part of the intake system, an estimate must be made on the timing of the required maintenance and the duration of the activity. This issue may necessitate some redundancy in the installed number of pumps, pipelines, and passive screens used in a system. In no case should a single intake pump and passive screen be used for a SWRO system unless a spare pump and fittings are maintained on site in the event of a failure. Onsite storage of treated water is another factor to be considered within the overall intake system design with maintenance considerations.

5.4 Environmental Impacts

As with any intake structure, the construction and operation of a passive screen array can create a number of potential environmental impacts. The impacts are related to the construction activity, the physical presence of the intake system, and the operation of the intake system. Construction impacts are those associated with the temporary disturbance or permanent destruction of benthic habitat. The magnitude of these impacts depends wholly on whether the screens are installed onshore or offshore. The physical presence of the intake structure also has potential to create negative environmental impacts. The magnitude of operational impacts (I&E) depends, in part, on the location of the screening array and the characteristics of the marine organisms in the area.

5.4.1 Impacts During Construction and Related to Physical Presence of Infrastructure

Some impacts to the marine environment will occur during construction of passive screen intake systems. The intensity of impacts depends on the location of passive screen intake system (coastal or offshore), the capacity of the intake, the number of screens and pipelines required, and the design of the conveyance pipe (e.g., emergent on bottom, buried in a trench, within a tunnel constructed below the bottom).

In general, construction impacts will be less severe for onshore passive screen systems because without the need for an offshore water conveyance or a large submerged support structure, there is comparatively little disturbance or destruction of the benthic substrate. In-shore impacts are not likely to be significant. If the passive screen is to be constructed at an existing system, the conveyance canal or waterway is already in existence and will not cause dredging and potential turbidity and bottom impacts. Installation can usually be accomplished from the shore, precluding the need for extensive in-water construction equipment; however, some dewatering may be required to install the passive screens in a dry condition. This would require turbidity control and the need to use temporary sheet piling or a coffer dam. Turbidity screens and monitoring can be used to minimize impacts. The composite construction of a new canal system with a passive screen intake would have potential impacts to benthic marine organisms and possible turbidity impacts to the full water column. The dredging and filling would require an extensive number of environmental permits in the United States and the European Union, mostly for the canal construction and little for the passive screen construction.

Construction impacts for an offshore passive screen array, however, will create greater potential impacts associated with the physical disturbance of the sea floor. An offshore intake location would require an offshore support structure for the screening array as well as a water conveyance structure to deliver water to the SWRO facility onshore. The order from highest to lowest of potential impacts associated with construction of the conveyance pipeline are: (1) burial of a pipeline below the seabed, (2) an emergent pipeline on the seabed, and (3) placement of the pipeline in a tunnel beneath the seabed. In most cases, the construction of a trench in the seabed with subsequent burial of the pipeline (aka “trench and fill”) is not technically feasible and the environmental consequences would be significant in terms of disruption of the marine benthic community by excavation or dredging and burial with excess sediment produced, and impacts on the marine environment as a whole caused by uncontrolled turbidity. The least expensive conveyance with the least risk of environmental impact is the emergent pipeline lying on the seabed. It can be easily installed by towing the floating pipeline from land to the sea and sinking it into place. Stabilizer or ballast weights can be attached before it is towed or after it is sunk to the seabed. The concrete collars are necessary to keep the pipeline from moving during storms. The principal impact is on the benthic marine community lying directly below the pipeline. This system can be used in many

locations, but could be problematic in areas where frequent or very intense storms cause disruption of the marine bottom to significant water depths. In very shallow water and through the intertidal (surf) zone the pipeline must be buried to depth below the reach of storm (excavation up to 2 m in some areas). Placement of the conveyance pipeline inside of a tunnel is a very expensive option, but has a very low environmental impact. Also, several pipes could be placed in the tunnel for connection to a corresponding series of passive screen intakes. Tunnels are used for the large Australian SWRO facilities for connection to velocity cap systems containing coarse bar screening (see Chaps. 2 and 3).

Construction of the passive screen structure typically creates less environmental impact than the construction of the water conveyance system. The supporting vertical riser pipe may have a maximum diameter of about 1.5 m. If the assembly is mounted on a prefabricated concrete slab, the slab dimensions should be no greater than 10 m by 10 m in an extreme case. The only impacts would be to the marine benthic community located directly below the slab.

In many areas, marine growth will occur on the pipeline anchors in a very short time period and may occur on the HDPE pipe over an extended period. Coral reef growth will help stabilize and hide the pipe. A system designed in Thailand used concrete pipe instead of HDPE pipeline to cross a coral reef complex. The reason was to encourage regrowth of corals on the pipeline to make it become part of the reef, to hide it, to mitigate reef impacts, and to stabilize the pipeline and protect it from storms. Concrete constitutes a hard ground composition that encourages coral polyp attachment and growth. It is important to also note that in some cases components of the passive screening system (e.g., screens, pipeline, pipeline armoring) can act as aggregating devices for structure-oriented marine species. If these structures become spawning habitat, the offspring could be at risk of entrainment.

5.4.2 Impingement and Entrainment Impacts

Impingement and entrainment impacts of passive screen intakes systems are generally lower than other common intake screen systems when designed properly. The potential for impingement and entrainment is dependent on the screen slot aperture, flow velocity, and the current passing by the screen. Each factor affects the rates of impingement and entrainment which need to be discussed separately.

Approach and through-screen velocities are designed and regulated to minimize (and in many cases eliminate) impingement. However, there is potential for some impingement of young fish larvae with limited swimming capabilities; though this impact must be considered to be minimal.

The impact of entrainment is of greater concern compared to impingement. Weisberg et al. (1987) suggest that wedgewire screens exhibit two different

mechanisms for reduction of entrainment which are physical exclusion based on the screen aperture and hydrodynamic exclusion which is the result of rapid diffusion of the flow field immediately surrounding the screen. An additional exclusion mechanism is produced by the transverse velocity of ocean currents across the screen face. The current produces a deflection of the flow field and possible turbulence at the screen slot depending upon the intensity of the current.

The marine organisms at greatest risk of entrainment in intake flows are the early life stages of fishes (i.e., eggs and larvae), also referred to as ichthyoplankton due to their small size and limited swimming capabilities. There are other marine organisms occurring in the same general size range at specific locations, such as coral polyps, during certain seasons in tropical regions. The potential for entrainment of fish larvae depends on the life stage of the organism, morphology, overall size, and swimming ability (EPRI 2005). Older fish larvae are generally physically excluded based on size, but can also avoid the hydraulic zone of influence of the intake as a result of greater swimming ability (EPRI 2003).

Field data collected at freshwater and estuarine sites suggest that there is a significant reduction in the concentration of larvae with sizes greater than the slot aperture width (exclusion width) when comparing ambient versus through-screen densities (Zeitoun et al., 1981; Weisberg et al. 1987; EPRI 2005). It should be noted that caution should be used in evaluating these results based on some differences in plankton collection techniques (EPRI 2005). Laboratory and field studies suggest that the predominant factor controlling the percentage of fish larvae and eggs excluded from entrainment is the slot width with the smaller excluding the largest percentage. However, the hydrodynamic exclusion of individuals smaller than the slot aperture was significant. More recent laboratory evaluations confirmed that hydrodynamic bypass and active avoidance are also important factors in the overall efficacy of passive cylindrical screens and that larval length is an important determinant of avoidance capability (NAI 2011a, b).

Slot velocity has a significant impact in reducing entrainment of selected species of fish larvae (EPRI 2003). The entrainment rates generally increase with an increase in slot velocity. However, the impacts of slot velocity are smaller than that of the screen slot width. EPRI (2005) found that slot velocity, tested in the range from 0.15 to 0.30 m/s, did not significantly affect the entrainment rates. In subsequent field evaluations at different sites with different species, however, EPRI (2006) found that entrainment of eggs and larvae were significantly reduced at the lower slot velocity.

Ambient velocity of current across the screen face has a significant impact on reducing impingement and the rate of entrainment (Hanson et al. 1978; Heuer and Tomljanovich 1978; EPRI 2003). There is a conflict in results concerning the effect of ambient velocity on the density of entrained organisms. Sometimes at higher velocities, the recorded density of entrained organisms is higher in the samples collected after passage through the screen compared to the average ambient condition. It is believed that the issue is related to the greater volume of water coming in contact with the screen and consequently, the greater number of organisms exposed to the screen face. Therefore, a real comparison would be to assess the total

volume of seawater passing by the screen with a known concentration of organisms and compare it to the volume of water passing through the screen with the concentration of organisms, and then normalize the density versus volume. Laboratory testing suggests that under lower velocities, swimming larvae will orient themselves to avoid entrainment and at higher velocities, they become passive particles and will pass through the screen. Eggs are always passive particles (EPRI 2003).

Most of the past impingement and entrainment investigations to assess impacts on ichthyoplankton were conducted on freshwater or estuarine species. However, with increasing interest in SWRO in California, a number of pilot-scale studies have been recently conducted to evaluate the biological performance of cylindrical wedgewire screens in a fully marine environment. Based on biological sampling conducted with a 2.4 mm slot width, pilot-scale cylindrical wedgewire screen at the Marin Municipal Water District pilot desalination plant in San Francisco Bay, CA, Tenera (2007) concluded that the risks posed by entrainment resulting from a full-scale desalination facility (30 MGD) would be low (probability of entrainment-related mortality ranging between 0.02 and 0.06 %). The City of Santa Cruz Water Department and Soquel Creek Water District ($SCWD^2$) have also been jointly studying the feasibility of an SWRO facility in Santa Cruz, CA. In 2009–2010, they conducted a pilot-scale study of the biological performance of a cylindrical wedgewire screen in the Pacific Ocean near Santa Cruz, CA. Tenera (2010) concluded that the 2.0 mm slot width screen operating at a maximum of 10 cm/s effectively eliminated impingement of larger organisms and reduced entrainment by almost 20 %. The reduction in entrainment, however, was not significantly different from samples collected through an unscreened intake port.

The general principles involved in estimating the biological performance can be applied from site to site; however, various site-specific characteristics can affect performance. Attention should be paid to such site-specific biological details such as species composition, morphologies and life stages, and swimming capabilities. Site-specific hydrodynamic characteristics such as wave, ocean, and tidal currents, shipping traffic, and storm exposure must be considered carefully during the design process to ensure optimal biological performance. Overall, research has indicated that a passive screen intake will produce a significant reduction in impingement and entrainment impacts compared to many classes of open-ocean intakes.

5.4.3 Impact on Treatment Cost and Energy Consumption

Removal of organic material before the pretreatment system does have a positive impact on the operational cost of SWRO treatment. Infrastructure design and construction to exclude fish and other marine organisms and to recycle them back into the marine environment is a significant capital and operating cost. The operation of traveling screens with collection of marine debris also creates a solid waste

disposal cost and at some large SWRO facilities that are plagued by season seaweed or jellyfish infestations, the disposal cost for processing and disposal of the waste can be quite high. Therefore, the use of passive screen intakes which reduce some aspects of pretreatment, have some positive impact on reduction of treatment intensity and energy consumption. The magnitude of actual cost savings is quite site-specific.

5.5 Discussion and Conclusions

Passive screen systems are a design option lying between conventional open-ocean intake systems (e.g., velocity caps) and a subsurface intake system. They do reduce the potential impingement and entrainment of large fish and reduce the impact to some degree of larvae and eggs. Even fish larvae and eggs may be excluded to a degree based on the natural current velocity in the vicinity of the screens and the design of the passive screen system, including the slot aperture, the approach and slot-entry velocities, and hydrodynamic exclusion. The environmental impact of passive screen intakes must be considered to be lower than open-ocean intakes, but higher than subsurface intakes.

Advantages of using passive screen intakes include the ability to develop large capacity systems using multiple screen assemblies, the ability to remotely clean the screen face using compressed air systems, and the generally lower environmental impacts. These systems have the potential to lessen the in-plant pretreatment system by precluding the requirement to use bar and traveling screen systems to remove large-scale debris and living organisms. This also lowers the need for disposal of large volumes of marine debris which commonly occurs during seasonal jellyfish infestations and other events that periodically plague some SWRO facilities.

Disadvantages of passive screen intake systems include some limitation on operational capacity, maintenance issues including the potential need to feed chlorine into the system at the screen to inhibit sessile marine group within the interior of screen the photic part of the pipeline, requirement to use expensive duplex stainless steel or an anti-fouling duplex stainless steel alloy as screen material, possible requirement to pig the intake pipelines to control biofilm development on the pipeline interior, periodic replacement of the screens based on operational life-expectancy due to marine corrosion, and variable head loss in the system based on the screen fouling rate. Within the context of the regulatory environment, passive screen intakes may be used when there is a strict preclusion of using open-ocean intake systems because of perceived impingement and entrainment impacts. While these impacts may be significant or not, they still may be irrelevant because the cost and time for completion of extensive marine environmental impact assessments may cause passive screen intake systems to be a viable alternative system (Figs. 5.9 and 5.10).

References

Baudish, P., Lavery, N., Burch, R., Pain, D., Franklin, D., & Banks, P. (2011). Design considerations and interactions for tunneled seawater intake and outfall systems. In *Proceeding, International Desalination Association World Congress on Desalination and Water Reuse*, Perth, Australia.

Bechtel Power Corporation. (2012). Offshore modular wedge wire screens for San Onofre Nuclear Generating Station. Consultant's report prepared Southern California Edison and the Stae Water Resources Control Board, Nuclear Review Committee.

Cooke, L. E. (1978). The Johnson screen for cooling water intakes. In R. K. Sharma & J. B. Palmer (Eds.), Larvel exclusion systems for power plant cooling water intakes, Argonne National Laboratory Report ANL/ES-66.

Electric Power Research Institute (EPRI). (1999). *Fish protection at cooling water intakes*. EPRI Report No. TR-114013 (Prepared by Alden Research Laboratory, Inc.).

Electric Power Research Institute (EPRI). (2003). *Laboratory evaluation of wedgewire screens for protecting early life stages of fish at cooling water intakes*. EPRI Report No. 1005339, Palo Alto, CA (Prepared by Alden Research Laboratory, Inc.).

Electric Power Research Institute (EPRI). (2005). *Field evaluation of wedgewire screens for protecting early life stages of fish at cooling water intakes*. EPRI Report No. 1010112, Palo Alto, CA.

Electric Power Research Institute (EPRI). (2006). *Field evaluation of wedgewire screens for protecting early life stages of fish at cooling water intakes*: *Chesapeake Bay studies*. EPRI Report No. 1012542, Palo Alto, CA.

Erhler, C., & Raifsnider. (1999). Evaluation of the effectiveness of intake wedge wire screens. In *Proceedings of the Power Impacts on Aquatic Resources Conference*, Atlanta, GA, 12–15 April 1999 (sponsored by the Electric Power Research Institute (EPRI).

Gille, D. (2003). Seawater intakes for desalination plants. *Desalination, 156*, 249–256.

Gulvas, J. A., & Zeitoun, I. H. (1979). Cylindrical wadge-wire screen investigations in offshore Lake Michigan for the J. H. Campbell Plant. In *Proceedings of the Passive Intake Screen Systems Workshop*, Chicago, Illinois, December, 1979.

Hanson, B. N. (1979). Studies of three cylindrical profile-wire screens mounted parallel to flow direction. *Proceedings of the Passive Intake Screen Systems Workshop*, Chicago, Illinois.

Hanson, B. N., Bason, W. H., Beitz, B. E., & Charles, K. E. (1978). A practical intake screen which substantially reduces the entrainment and impingement of early life stages of fish. In: L. D. Johnson, (Ed.), *Proceedings of the Fourth National Workshop on Entrainment and Impingement*, Chicago, Illinois, 5 Dec 1977.

Heuer, J. H., & Tomljanovich, D. A. (1978). A study on the protection of fish larvae at water intakes using wedge-wire screening. Tennessee Valley Authority (TVA) Technical Note B26.

Lifton, W. (1979). Biological aspects of screen testing on the St. Johns River, Palatka, Florida. In *Proceedings of the Passive Intake Screen Systems Workshop*, Chicago, Illinois, December, 1979.

Malik, A. U., Ahmad, S., Andijani, I. N., & Al-Fozan, S. (1991). Corrosion behavior of steels in Gulf seawater environment. *Desalination, 123*, 205–213.

Malik, A. U., & Al-Fozan, S. (1994). Localized corrosion of AISI 316L SS in Arabian Gulf seawater. *Desalination, 97*, 199–221.

Malik, A. U., Prakash, T. L., Ahmad, S., Andijani, I. N., Al-Musaili, F., & Jamaluddin, A. T. M. (2001). Crevice corrosion of high alloy stainless steels in SWRO plant. Saline Water Conversion Corporation (SWCC), Technical Report TR 3804/APP 93003, Saudi Arabia. www.swcc.gov.sa/Files%Cassets%5CTTechnical%20Papers. Accessed 3 Mar 2014.

Malik, A. U., Siddiqui, N. A., Ahmad, S., & Andijani, I. N. (1995). The effect of dominant alloy additions on the corrosion behavior of some conventional and high alloy stainless steels in seawater. *Corrosion Science, 37*, 1521–1535.

Missimer, T. M. (2009). *Water supply development, aquifer storage, and concentrate disposal for membrane water treatment facilities*. Sugar Land, Texas: Sugar Land, Texas, Schlumberger Water Services.

National Marine Fisheries Service (NMFS). (1996). *NMFS juvenile fish screen criteria for pump intakes addendum*. Portland: Oregon, NMFS Environmental and Technical Services Division.

National Marine Fisheries Service (NMFS). (2008a). *Anadromous salmonoid passage facility design*. NMFS Northwest Division.

National Marine Fisheries Service (NMFS). (2008b). *National Marine Fisheries Service (NMFS) pump intake screen criteria for water drafting*. www.fs.usda.gov/Internat/FS-DOCUMENTS/stelprdb5366394.pdf. Assessed 26 Feb 2014).

Nayyar, M. L. (2000). *Piping handbook* (7th ed.). New York: McGraw-Hill.

Normandeau Associates, Inc. (NAI). (2011a). *2010 IPEC wedgewire screen laboratory study*. Buchanan, NY: Prepared for the Indian Point Energy Center.

Normandeau Associates, Inc. (NAI). (2011b). 2011 IPEC Wedgewire Screen Laboratory Study.

Otto, R. G., Hiebert, T. I., & Kranz, V. R. (1981). The effectiveness of s remote profile-wire screen intake module in reducing the entrainment of fish eggs and larve. In P. J. Dorn & J. T. Larson (Eds.), *Proceedings of the on Workshop Advanced Intake Technology*, San Diego, CA, April, 1981.

Pankratz, T. (2005). *Screening equipment handbook for industrial and municipal water and wastewater treatment* (2nd ed.). Boca Raton, Florida: CRC Press.

Pankratz, T. (2008). Global verview of seawater desalination intake issues. In *Alden Desalination Intake Solutions Workshop*, Holden, Massachusetts.

Sahu, G. K. (1998). *Handbook of pipe design*. New Delhi, India: New Age International Limited.

Stefan, H., Dahlin, W., Winterstein, T., & Fournier, P. (1986). Passive screen intake design studies. *Journal of Energy Engineering, 112*(2), 115–126.

Tenera Environmental (Tenera). (2007). *Marin municipal water district desalination facility intake effects*. Prepared by Tenera. Appendix C of Final Environmental Impact Rerport (EIR) Marin.

Tenera Environmental (Tenera). (2010). City of Santa Cruz Water Department & Soquel Creek Water District SCWD2 Desalination Program: Open Ocean Intake Study Effects. ESLO2010-017.1.

Tuthill, A. H. (1988). Usage and performance of Nickel-concerning stainless steels in both saline and natural waters and brines. *Materials Performance, 27*, 49–50.

United States Environmental Protection Agency (USEPA). (2011). National pollutant discharge elimination system—cooling water intake structures at existing facilities and phase I facilities. *Federal Register 76*(76), 20 April 2011.

Water Research Foundation (2011) *Assessing seawater intake systems for desalination plants*, Water Research Foundation, Denver

Weisberg, S. B., Burton, W. B., & Ross, E. A. (1984a). *The effects of biofouling on the exclusion efficiency of 2-mm wedge-wire screens*. Report CP-84-2, prepared for the Maryland Department of Natural Resources. Annapolis, MD.

Weisberg, S. B., Burton, W. H., Ross, E. A., & Jacobs, F. (1984b). *The effects of screen slot size, screen diameter, and through-slot velocity on entrainment of estuarine ichthyoplankton through wedge-wire screens*. Report CP-84-1 prepared for the Maryland Department of Natural Resources, Annapolis, MD.

Weisberg, S.B., Jacobs, F., Burton, W. H., & Ross, R. (1983). *Report on preliminary studies using the wedge-wire screen model intake facility*. Report PPSP-CP-83-1, prepared for the Maryland Department of Natural Resources, Annapolis, MD.

Weisberg, S. B., Burton, W. H., Jacobs, F., & Jacobs, F. (1987).*Reductions in ichthyoplankton entrainment with fine mesh, wedgewire screens*. North American Journal of Fisheries Management, *7*, 386–393.

Woo, S. W., Park, B. S., Lee, W. N., Park, Y. H., Min, J. H., Park, S. W., et al. (2013). Seawater intake system in Test Bed seawater reverse osmosis (SWRO) project. *Desalination and Water Treatment, 51*(31–33), 6238–6247.

Zeitoun, I. H., Gulvas, J. A., & Rorabaugh, D. B. (1981). Effectiveness of fine mesh cylindrical wedge-wire screens in reducing entrainment of Lake Michigan ichthyoplankton. *Canadian Journal of Fisheries and Aquatic Science, 38*, 120–125.

Chapter 6
Effects of Intake Depth on Raw Seawater Quality in the Red Sea

Abdullah H.A. Dehwah, Sheng Li, Samir Al-Mashharawi, Francis L. Mallon, Zenon Batang and Thomas M. Missimer

Abstract It has been suggested that using a deep open-ocean intake would improve feed water quality and would reduce the cost of SWRO water treatment by lessening membrane biofouling potential. The feasibility of developing deep intake systems for large-capacity SWRO plants located on the Red Sea was assessed. A bathymetric survey showed that the continental shelf along the Red Sea nearshore has a nearly vertical drop into deep water beginning at depths between 20 and 40 m. The vertical nature of the bathymetric profile and the issue of active seismicity make the development of a SWRO intake at a depth of greater than 100 m below surface a very risky venture along the Red Sea coast of Saudi Arabia. Detailed assessment of temperature and salinity with depth show a decrease of 5 °C and an increase of 1100 mg/L respectively over 90 m. Concentrations of algae, bacteria, total organic carbon, particulate and colloidal TEP, and the biopolymer fraction of natural organic carbon all showed declines in concentration. However, the general water quality improvements in reduced concentrations of organic matter were insufficient to reduce the intensity of pretreatment for an SWRO system. Overall,

A.H.A. Dehwah · S. Li · S. Al-Mashharawi
Water Desalination and Reuse Center, King Abdullah University of Science and Technology, Thuwal, Saudi Arabia
e-mail: abdullah.dehweh@kaust.edu.sa

S. Li
e-mail: sheng.li@kaust.edu.sa

S. Al-Mashharawi
e-mail: samir.almashharawi@kaust.edu.sa

F.L. Mallon · Z. Batang
Coastal and Marine Resources Core Lab, King Abdullah University of Science and Technology, Thuwal, Saudi Arabia
e-mail: francis.mallon@kaust.edu.sa

Z. Batang
e-mail: zenon.batang@kaust.edu.sa

T.M. Missimer (✉)
U.A. Whitaker College of Engineering, Florida Gulf Coast University, FL, USA
e-mail: tmissimer@fgcu.edu

T.M. Missimer et al. (eds.), *Intakes and Outfalls for Seawater Reverse-Osmosis Desalination Facilities*, Environmental Science and Engineering,
DOI 10.1007/978-3-319-13203-7_6

the Red Sea does not appear to be a good location for the use of deep SWRO intakes because of the structural risk of installing and maintaining an intake at near or below 100 m of water depth.

6.1 Introduction

It has been suggested that seawater to be used as feed water for seawater reverse osmosis (SWRO) facilities improves with depth because of lower primary productivity caused by light absorbance and a lower concentration of suspended sediment in the water column (Gille 2003; Cartier and Corsin 2007). Therefore, some have concluded that "deep water" intakes can produce a higher quality feed water that has potential to reduce the pretreatment requirements and to lower the cost of SWRO desalination.

It is important to first define the difference between "deep water" and "shallow water" intakes. Cartier and Corsin (2007) suggest that shallow water intakes range between depths of 0–15 m while deep intakes range from 20 to 35 m. They further suggest that the feasibility of deep water intakes is limited to geographic locations where deep water is found adjacent to the physical SWRO plant location and that there is no limit to the intake depth caused by water temperature. Cooler feed water can cause a significant increase in SWRO treatment cost (Goosen et al. 2002; Wilf 2007). The Japanese government funded Megaton project research suggests that deep water intakes can be feasible to depths >100 m (Ito et al. 2013). Both of these investigations assume that seawater quality actually improves with depth; the intake design will be secure and not subject to failure during normal operation; and routine maintenance can be performed on an intake structure, regardless of depth.

Biofouling of SWRO membranes has been linked to the concentration of transparent exopolymer particles (TEP) and other sticky polysaccharides in raw seawater (Berman and Passow 2007; Bar-Zeev et al. 2009; Berman 2010; Berman et al. 2011). TEP tends to coat or condition SWRO membranes and promote the formation of a biofilm by creating a sticky substrate that encourages attachment of bacterial cells and also provides a food source. Therefore, if a deep water intake truly provides a better feed water quality, then the concentrations of TEP, mono- and polysaccharides, biopolymers, and other organic substances should be lower to lessen the potential for membrane biofouling.

TEP is formed predominantly by the self-assembly of precursor substances, such as dissolved acidic polysaccharides, that are produced by algae and bacteria (Passow and Alldredge 1994; Passow 2000; Passow et al. 2001; Passow et al. 2002b). TEP acts as part of the sedimentary flux that produces flocs and marine "snow" which move downward in the marine water column (Alldredge et al. 1993; Passow et al. 2001; Passow 2002a), but also can migrate upward by buoyancy to the sea surface (Azetsu-Scott and Passow 2004; Mari 2008). The primary source of TEP and

precursors has been considered to be phytoplankton with some bacterial production (Passow and Alldredge 1994; Passow 2002a). Abiotic polymerization of dissolved precursor compounds along with sedimentation remove TEP from the euphotic zone (Engle 2004). Bacteria play an important role in the release, creation, or coagulation of TEP at depth in the sea (Van Loosdrecht et al. 1989; Johnson and Kepkay 1992; Stoderegger and Hernl 1998, 1999; Radic et al. 2006; Sugimoto et al. 2007). Therefore, the concentration of TEP and other organic substances that contribute to membrane biofouling does not strictly decrease with water depth and has an irregular occurrence profile as found in the Southern Ocean (Ortega-Retuerta et al. 2009), Hudson Bay (Michel et al. 2006), northeast Atlantic Ocean (Engle 2004) and at other locations (Wurl et al. 2001).

It has been suggested that deep ocean intakes will produce a higher quality feedwater based on some oceanographic investigations at various locations (Hayashi et al. 2003; Takahashi and Ikeya 2003; Takahashi and Yamashita 2005; Takasashi and Huang 2012). The purpose of this research is assess the use of potential deep water SWRO intakes along the Red Sea coast of Saudi Arabia by providing data on the bathymetry from the shoreline to deep water (>100 m), and the concentrations of algae and bacteria, TEP, and other organic fractions of natural organic matter (NOM) from a series of profiles collected offshore to 90 m below sea level or greater, and to assess an operating SWRO facility that extracts feed water from a depth of 9 m with a comparison to the surface seawater at the same site (Fig. 6.1). These data will provide some insight into algae, bacteria, TEP and organic carbon dynamics in the Red Sea and the feasibility of using deep water intakes.

6.2 Methods

6.2.1 Measurement of Red Sea Depth Profiles

A detailed bathymetric survey of a section of the Red Sea near Thuwal, Saudi Arabia was conducted. A three-dimensional depth projection from the beach to water depths greater than 100 m was developed using data collected from a programmed marine data collection device. Three bathymetric profiles were constructed to show the width of the inner reef low slope area, depth changes seaward of the coral reef, and the bottom slopes.

The bathymetric survey data were collected using a EK60 3 KHz scientific echo sounder manufactured by Simrad-Kongsberg Maritime Subsea. Surveys were conducted during the period of April to May, 2014. Compilation of the data and graphics preparation was accomplished using the Fledermaus and ArcGis 10 computer programs.

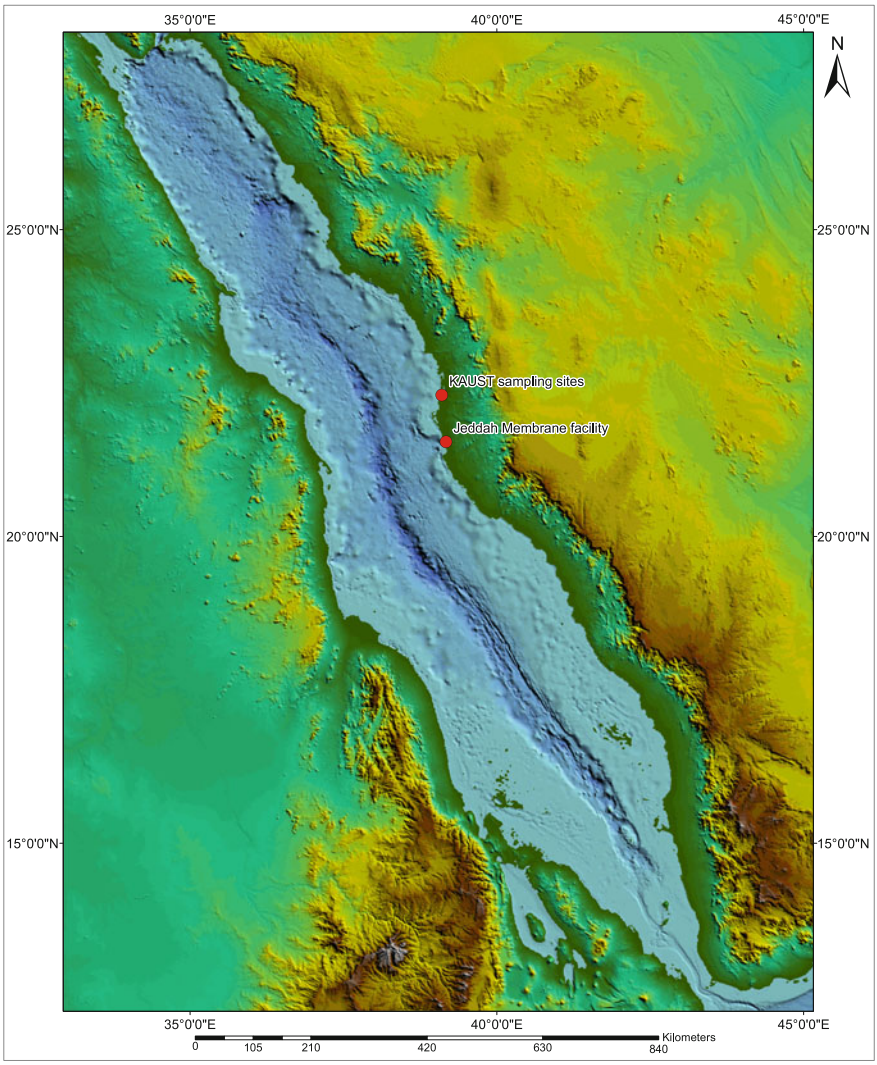

Fig. 6.1 Map showing the location in the Red Sea of the bathymetric profiles and profile sampling sites, and the membrane treatment facility where sampling was conducted

6.2.2 Water Sampling Methods

Water samples from the Red Sea were collected at 10 m depth increments from the sea surface to 90 m at three different sites in the vicinity of the King Abdullah University of Science and Technology which is located about 85 km north of Jeddah. Approximate 3 L of water was collected at each depth increment using a Seabird Carousel collection system. Physical parameters, including temperature,

conductivity, TDS, turbidity, and pH, were measured on the water samples. The water samples were immediately chilled to 4 °C to preserve the organic compounds and to lessen the potential for biological activity that could adversely affect measurement of the organic components.

Water samples collected for the purpose of TEP analysis were fixed using a 0.02 % (w/v) solution of sodium azide. For samples collected for algae and bacterial quantification, glutaraldehyde was added for preservation. Care was taken to carefully label and store all samples in opaque containers. The samples were quickly transported to the laboratory where the analyses were performed.

6.2.3 TEP Measurement

Analysis of TEP was performed using the Alcian Blue staining techniques developed by Passow and Alldredge (1995). Two types of TEP exist in the marine environment; particulate TEP with a size >0.4 μm and colloidal TEP with a size range from 0.05 to 0.4 μm (Villacorte et al. 2009).

A staining solution was prepared using a 0.06 % (m/v) Alcian Blue 8GX (Standard Fluka) solution that contains an acetate buffer (pH = 4) and the solution was pre-filtered through a 0.2 μm polycarbonate filter prior to staining. About 500 mL of seawater from each sample was filtered through a polycarbonate membrane with a pore size of 0.4 μm using an adjustable vacuum pump at a low constant vacuum. The membrane was then rinsed with 10 mL of Milli-Q water to avoid the coagulation of Alcian Blue once it comes in contact with the seawater during the staining process. Subsequently, the retained TEP on the membrane surface was stained with the Alcian Blue dye for 10 s. After staining, the membrane was flushed with 10 mL of Milli-Q water to remove the excess dye. The prepared membrane was then transferred into a small beaker, where it was soaked in 80 % sulfuric acid for 6 h to extract the Alcian Blue dye that is bound to the TEP. Finally, the absorbance of the resultant solution was measured using a UV spectrometer at 752 nm wavelength to measure the TEP concentration. For determination of the colloidal TEP concentration, the same general procedure was used, but 250 mL of the permeate water from filtering the seawater through the 0.4 μm polycarbonate filter was passed through a 0.1 μm polycarbonate membrane. Extraction of the colloidal TEP followed the same procedure as that for the particulate TEP.

To relate the UV absorbance values to TEP concentrations, a calibration curve was established. Xanthan gum solutions with different volumes, such as 0, 0.5, 1, 2, and 3 mL, were used to obtain a calibration curve. The total organic carbon (TOC) concentrations of xanthan gum before and after 0.4 μm filtration were analyzed (or 0.1 μm filtration for the colloidal TEP), and the TOC concentration difference was used to calculate the gum mass on each filter. The TEP mass was calculated based on the calibration curve as shown in Fig. 6.2. Note that curves for both particulate

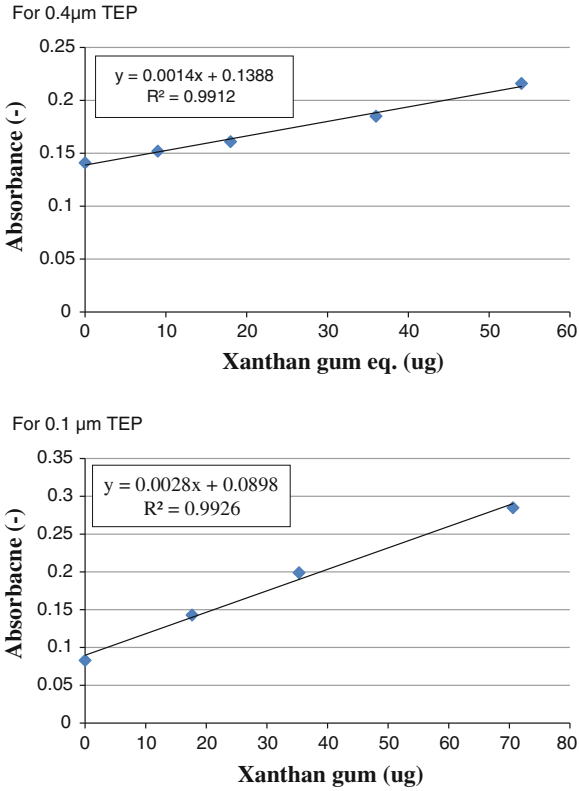

Fig. 6.2 Xanthan gum standard calibration curves for particulate and colloidal TEP

TEP and colloidal TEP are shown in the figure. Because of the methodology including the use of xanthum gum as a proxy, the estimated concentration of TEP is considered to be semi-quantitative.

6.2.4 Algae and Bacteria Quantification

Counts of the number of algae in the water samples were determined using a flow cytometer manufactured by BD Bioscience FACSVerse and bacteria concentrations were measured using a device manufactured by BD Accuri (C6). Algal cell counting was performed by combining 500 μL of each sample with a 1 μL standard containing 1 μm beads into a standard 10 mL tube. The tube was then vortexed and measured using a medium flow with a 200 μL injection volume. The counting procedure was repeated three times to assess the precision of the measurements.

For bacterial counts, a comparative staining protocol using SYBR® Green was used. A volume of 500 μL from each sample was transferred to a standard 10 mL tube, incubated in a 35 °C water bath for 10 min stained with the SYBR® Green dye

(5 µL into 500 µL aliquot), vortexed, and incubated for another 10 min. After that, 200 µL of the incubated sample was transferred into the measurement plate. The prepared samples were then analyzed in a medium flow setting with a 50 µL injection volume. Triplet measurements were made on each sample to assess precision.

6.2.5 Organics Analyses: Total and Fractions

A Shimadzu TOC-VCSH instrument was used into determine the bulk organics concentration (TOC) in the samples. In order to determine the detailed fractions of organic carbon, a Liquid Chromatography Organic Carbon Detector (LCOCD) from DOC-Labor was used. The method developed by Huber et al. (2011) was used to measure the various fractions of the NOM.

The samples for the LC-OCD were pre-filtered using a 0.45 µm syringe filter to exclude the non-dissolved organics. Before analyzing the samples, a system cleaning was performed by injection of 4000 µL of 0.1 mol/L NaOH through the column for 260 min. Following the cleaning step, 2000 µL samples were injected for analysis with 180 min of retention time. The analysis result is a chromatogram showing a plot of signal response of different organic fractions to retention time. Manual integration of the data was then performed to determine the concentration of the organic fractions including biopolymers, humic substances, building blocks, low molecular weight acids and low molecular weight neutrals.

6.3 Results

6.3.1 Depth Profiles from the Beach to Offshore Deep Water Along the Red Sea Coastline

The bathymetric survey data are shown in Fig. 6.3. Figure 6.3a shows the location of the survey and the three depth profiles. Figure 6.3b shows a three-dimensional aerial view of the bathymetric data. Extreme variations in relief occur with water depths of 1–3 m occurring in the nearshore area with a low slope moving seaward from the shoreline and then a very steep slope (virtually vertical) occurs from 10 to 12 m to a depth of 400–500 m within an inner trough. A peninsular shallow area occurs from the shoreline to the south-southwest into deep water. This flat-topped feature contains some mud banks, seagrass flats, and reef corals, particularly along the seaward margin. The depth profiles illustrate the extreme slopes from shallow to deep water and some addition bottom features (Fig. 6.3c). The center profile shows a step within the depth profile from very shallow water flat-inner reef area with

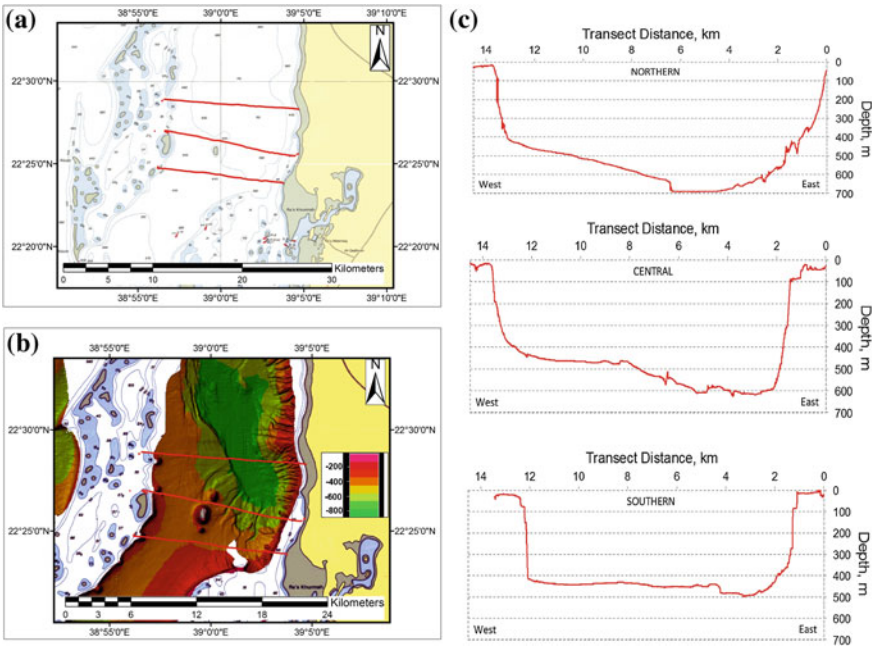

Fig. 6.3 Three-dimensional bathymetric projection of the bathymetry in the Red Sea near Thuwal, Saudi Arabia. **a** Map showing the location of the bathymetric survey and selected profiles. **b** Three-dimensional expression of the bottom bathymetry. **c** Selected profiles of the bottom topography from the shoreline to an offshore shelf area

depths range from 1 to 12 m to a depth of about 85 m, and then a near vertical cliff to a depth of almost 600 m. The 100 m depth at all locations occurs on a very steep slope or a vertical cliff.

6.3.2 Changes in Temperature, Salinity, Turbidity, Dissolved Oxygen, and PH with Depth in the Red Sea

Water temperature and salinity were continuously measured from sea surface to a depth of 90 m at three locations offshore from KAUST (Figs. 6.4). Temperature decreases in a regular manner about 5 °C with the lowest temperature being 24.3 °C at 90 m (Fig. 6.5). Salinity rises slightly with depth from about 38.9 ppt at surface to 40.0 ppt at the bottom (Fig. 6.6). Turbidity decreases very slightly by 0.02–0.05 NTU which is nearly insignificant. Differing trends of dissolved oxygen (DO) occur between sites. DO decreases at site A from 3.45 at surface to 2.25 ppm at 90 m, but at site B there is an increase from 2.20 to 4.20 ppm and at site C DO concentration increases from 2.10 to 4.07 ppm at 90 m (Fig. 6.7). Variation in pH is quite minimal at all sites with a very minor increase with depth.

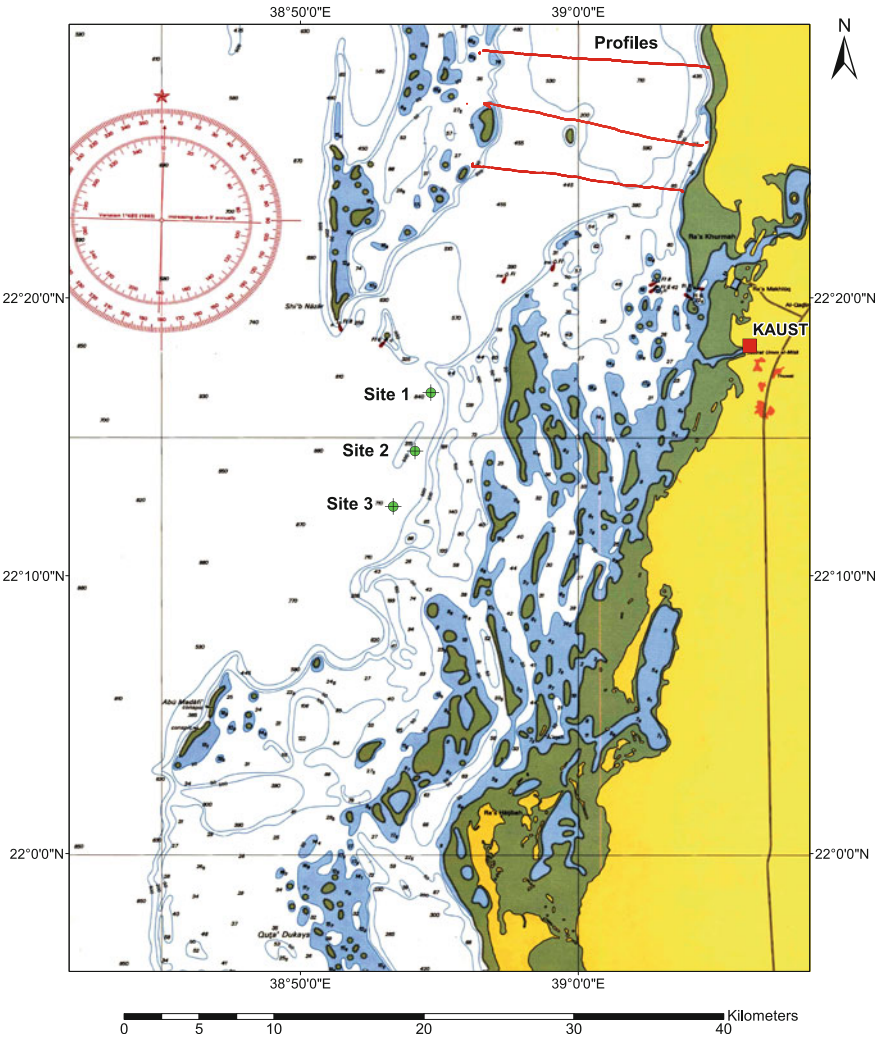

Fig. 6.4 Locations of depth profiles in Fig. 6.3 and sampling site locations A, B, and C

6.3.3 Distribution of Algae, Bacteria, TEP and the Biopolymer Fraction of NOM with Depth in the Red Sea

The concentration of total algae varied considerably with depth. The highest concentrations occurred at 50 m below surface instead of near surface (Fig. 6.8). The lowest algae concentrations were measured at the 90 m depth, which were about 2000 cells/mL. The surface algae concentrations ranged from about 30,000–60,000 cells/mL.

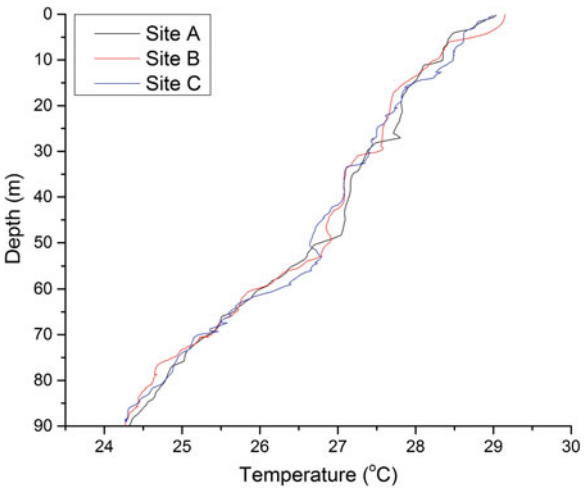

Fig. 6.5 Profiles of the Red Sea water column showing variation in water temperature with depth

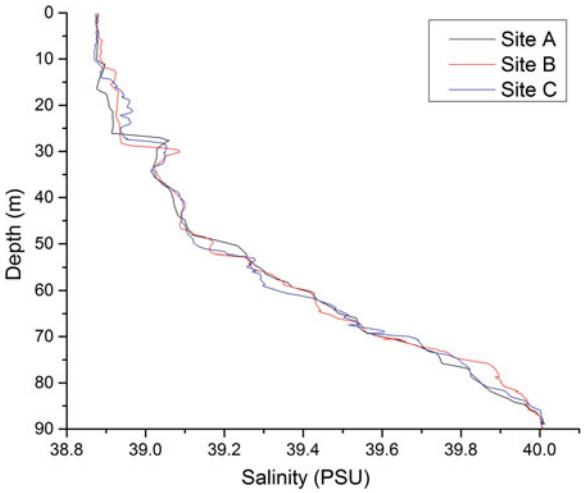

Fig. 6.6 Profiles of the Red Sea water column showing variation in salinity (conductivity) with depth

Total bacteria concentration trended downward from the sea surface to 90 m (Fig. 6.9). The data show an irregular decline in concentration with a decrease of about 79 %. The full range in concentrations for the three sites was found to be about 95,000–450,000 cells/mL.

Measured TOC profiles show a quite irregular variation with depth, but the trend is downward as would be expected. A spike in TOC occurs between 30 and 50 m below surface, but it is lower than surface except at site B where the surface concentration is quite low. The average of the three profiles is roughly 1.2 mg/L at surface and decreases to 0.95 at 90 m below surface (Fig. 6.10).

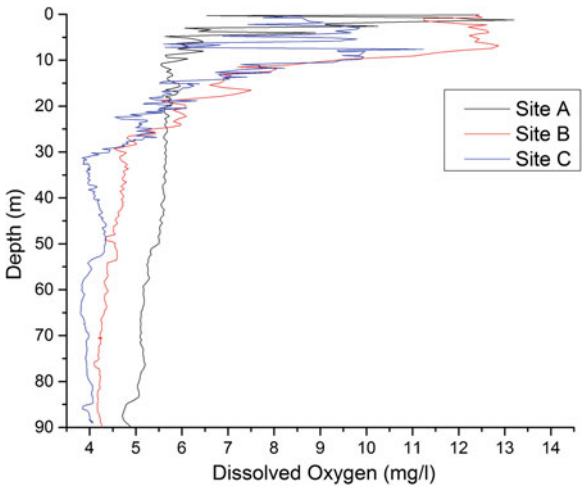

Fig. 6.7 Profiles of the Red Sea water column showing variation in dissolved oxygen with depth

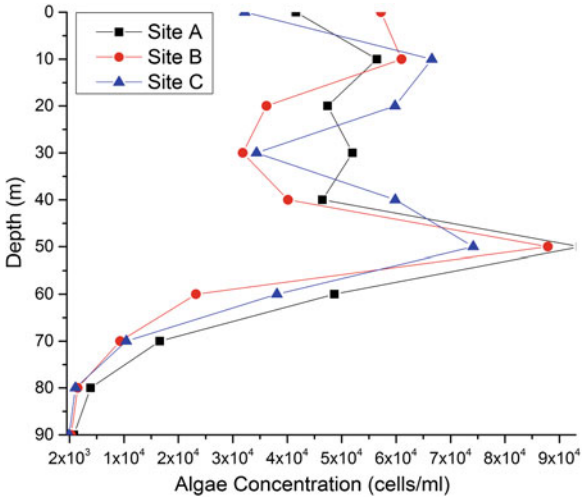

Fig. 6.8 Profile of the Red Sea water column showing total algal concentration with depth

Concentration of particulate and colloidal TEP are quite variable between the different sites with the highest concentrations occurring at surface, and generally decreasing with depth with the exception of colloidal TEP (Figs. 6.11 and 6.12). There is an upward spike in the concentration of both particulate and colloidal TEP at 40 m in all profiles except at site B.

The biopolymer fraction of NOM showed a steady decline from the sea surface to a depth of 90 m (Fig. 6.13). The highest concentrations were found at the B and C sites at a depth of 10 m below surface. Overall, the average concentration at surface was about 170 ppb and declined to about 100 ppb at 90 m below surface for an average decline of about 41 %.

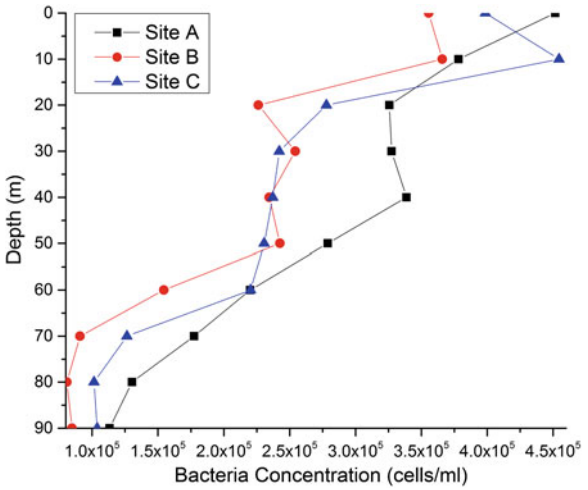

Fig. 6.9 Profile of the Red Sea water column showing total bacteria concentration with depth

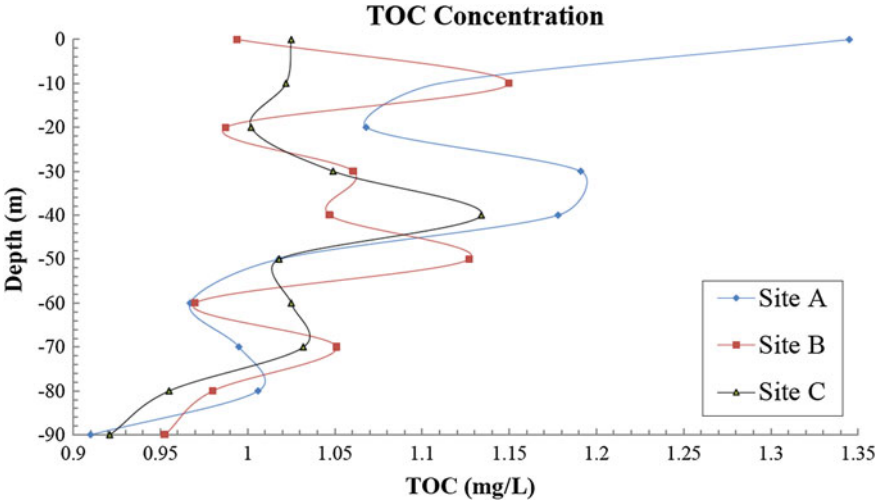

Fig. 6.10 Profiles of the Red Sea water column showing variation in concentration of TOC with depth

6.3.4 Comparison of Algae, Bacteria, Organic Carbon Fractions, and TEP at a 9 m Intake Depth with the Surface Seawater

A SWRO facility located near Jeddah uses an open-ocean intake that is located 9 m below the sea surface. While the depth of this intake is not really an example of a

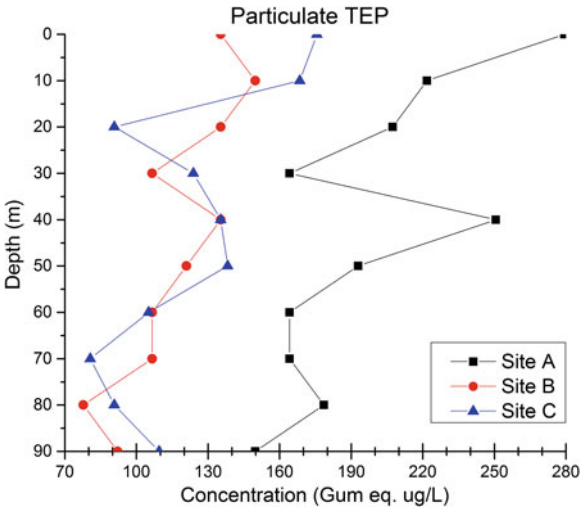

Fig. 6.11 Profiles of the Red Sea water column showing variation in concentration of particulate TEP with depth

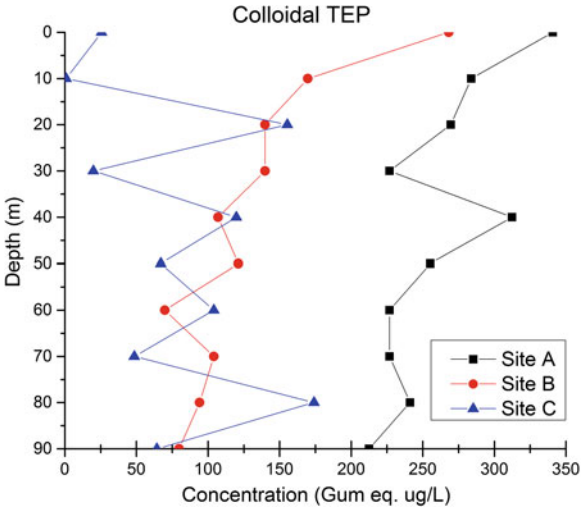

Fig. 6.12 Profiles of the Red Sea water column showing variation in concentration of colloidal TEP with depth

true "deep ocean" intake, it does allow some contrasts to be made on water quality changes with depth in the Red Sea. There are some interesting differences between the seawater at surface and at the 9 m depth. These data were extracted in part from Dehwah et al. (2014).

The flow cytometer analysis of the size and number of the algae shows that the overall concentration is rather low at 23,773 cells/mL at surface and 10,801 cell/mL at 9 m or a 55 % lower count with depth (Table 6.1). The dominant algae type is *Synechococcus*, which constitutes more than half of the population. The difference between concentration at the surface and the 9 m depth shows that all three algae

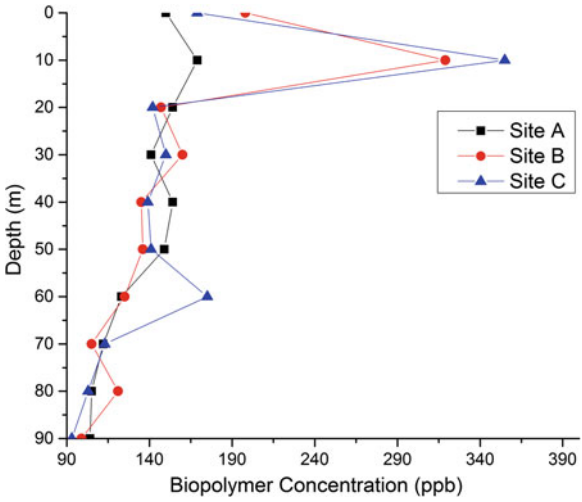

Fig. 6.13 Profiles of the Red Sea water column showing variation in concentration of the biopolymer fraction of total NOM with depth

Table 6.1 Measured algae concentrations at the sea surface and at a depth of 9 m (cells/mL)

Sampling Site	Synechococcus	Proclorococcus	Pico/nanoplankto	Total
Surface	14,488	8,590	695	23,773
9 m	6,823	3.735	243	10,801
Difference (5 less)	63	57	65	55

Table 6.2 Particulate, colloidal, and total TEP at surface and at a 9 m depth (μg/L of xanthan gum)

Sample location	Particulate TEP	Colloidal TEP	Total TEP
Surface	52.96	56.27	109.23
9 m	15.00	73.60	88.60
Percentage difference from surface	−72 %	+23 %	−19 %

types have a lower concentration with depth at this site which is located very close to the shoreline.

Concentrations of bacteria also show the same general pattern as the algae with surface seawater having a substantially higher concentration than seawater at the 9 m water depth (Fig. 6.13). Bacterial counts were relatively low at 317,174 and 210,761 cells/mL at the surface and bottom 9 m depth respectively, compared to concentrations that are commonly near 1 million cells/mL in seawater at other locations. The deeper water has a 34 % lower bacteria concentration.

A comparison of the particulate, colloidal, and total TEP shows that the variation with depth in the relatively shallow nearshore water is irregular (Table 6.2). Particulate TEP is substantially higher (72 %) in surface seawater than at 9 m, but the colloidal TEP is 23 % higher at 9 m compared to the surface. There is a 19 % difference between total TEP between the surface (higher) and the 9 m depth (Fig. 6.14).

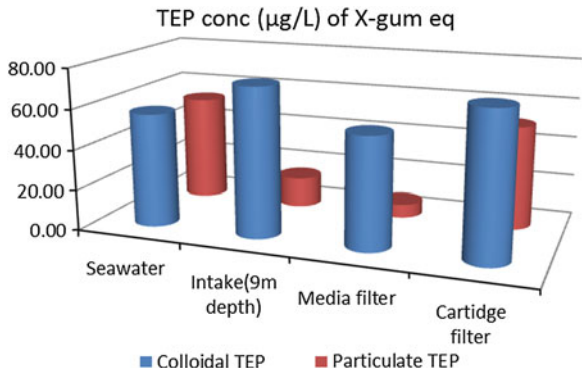

Fig. 6.14 Comparison of bacteria concentration between the surface and a 9 m depth (from Dehwah et al. 2014)

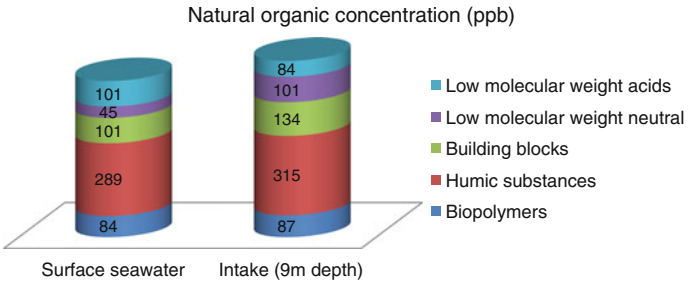

Fig. 6.15 Comparison of NOM fraction concentrations between the surface and 9 m (from Dehwah et al. 2014)

The concentration of TOC was nearly equal at the surface compared to the 9 m depth with the values of 0.88 and 0.83 mg/L respectively. Total NOM shows very little variation in composition between the surface and a depth of 9 m (Fig. 6.15). Each of the organic carbon fractions also shows a very similar concentration pattern with depth. Particularly noteworthy is that the biopolymer fraction, which contains the higher molecular weight polysaccharides and other organics that promote membrane biofouling, have nearly equal concentrations.

6.4 Discussion

6.4.1 Physical Bottom Bathymetry and the Feasibility of Using Deep-Ocean Intakes

The nearshore margin of the Red Sea along a section of the Saudi Arabia coastline has rather extreme relief with a narrow low-slope continental shelf. From the

shoreline water depth reaches a depth of 2 m between 150 and 250 m offshore. The bottom slope increases slightly to a depth of up to 12 m which occurs between 300 m and 2 km offshore. At this depth there is a steep drop to a narrow, flat shelf at about 85 m or a very steep slope (nearly vertical) to depths ranging between 420 and 600 m (middle transect in Fig. 6.3). The width of the continental slope is very narrow, perhaps 100 m to 2 km. The other transects show a nearly vertical wall occurring on the seaward margin of the reef tract with water depths reaching 500–600 m.

Based on the extremity of the nearshore topography, development of a deep ocean intake at a depth of about 100 m or a greater depth is not possible in this area of the Red Sea. The narrow step at a depth of 85 m at one location could be sufficiently wide and stable to support some type of bottom intake structure, but the connecting pipeline would have to be constructed with some very high strength material that is resistant to damage caused by downslope sediment transport during off-shelf transport events. This region is also subject to earthquakes which would cause sediment turbidity slides and would create shear forces on the pipeline (El-Isa and Shanti 1989).

The extreme steepness of the transition from shallow water to deep water along the coastline of the Red Sea of Saudi Arabia is common. Therefore, successful development of a deep water intake at a water depth greater than perhaps 20 m along the Saudi Arabia coastline is unlikely with the exception of perhaps a few limited areas. Construction and maintenance of a deep intake would be problematical based on the observed conditions.

6.4.2 Changes in Temperature, Salinity, and Turbidity with Depth and Effects on the SWRO Treatment Process

The general decrease in water temperature with depth in the Red Sea of <5 °C near the shoreline will not likely change the efficiency of the SWRO process. However, the observed increase of overall salinity of between 1100 and 1600 mg/L will have a slight impact on conversion efficiency because of a slight increase in the pressure required for the process. While there is a very minor decline in the turbidity, it appears to be insignificant in affecting the SWRO treatment process. Dissolved oxygen concentration shows an irregular change with depth. In two of the three profiles, the concentration decreases with depth by 50–70 % to an average of about 4.5 ppm at 90 m. These concentrations will not likely have a significant impact on SWRO treatment.

6.4.3 Potential Impacts of Organic Compounds in the Deep Sea Versus Shallow Water on Membrane Biofouling

The algae concentration generally declined with depth, but the highest values were found at a depth of 50 m below surface. Bacteria concentration declined relatively uniformly with depth and did not show any increase at 50 m.

The variation in TOC is between about 1.2 mg/L at surface and 1.0 at 90 m. There is generally a significant decrease in the concentration of both particulate and colloidal TEP with depth, but the trend is very irregular and profile B shows an increasing trend in colloidal TEP concentration. The biopolymer fraction of NOM shows a steady decline in concentration with depth. The spike in TOC and TEP concentrations at 40 m could be related to a high marine productivity zone.

It is interesting to note that there is some correlation of increased TOC concentration with the increase in algae concentration at between 40 and 50 m below surface. Particulate TEP seems to correlate to a degree with the spike in algae concentration between 40 and 50 m below surface. It appears that the particulate TEP may be moving upward in the water column. A spike in colloidal TEP occurs at 40 m below surface at 2 of the 3 sites tested.

Based on the data collected, the potential for SWRO membrane biofouling using the deeper water at 90 m would be somewhat decreased compared to the surface, but would still require the same general pretreatment train design compared to the surface seawater. Perhaps there would be less potential for membrane biofouling, but it is not possible to ascertain what impact it would have on the overall operation of a SWRO plant because the pretreatment processes would not be varied based on the data collected to date. This analysis of the organic compounds was conducted only to 90 m and seawater at greater depths may have a different trend. It is clear, however, that depth could be a significant issue in intake design, especially if the raw water was extracted from a high productivity zone, similar to that found between 40 and 50 m below surface.

6.5 Conclusions

Based on the observed bathymetric conditions, earthquake hazard, and the measured concentrations of bacteria, organic carbon, and TEP, it is concluded that design and construction of a deep water intake at over 90 m is not feasible in the segment of the Red Sea investigated. Furthermore, the very steep wall occurring seaward of fringing reef is a common feature along large segments of the Red Sea in coastal Saudi Arabia. This would make the construction of a deep intake very difficult and operational maintenance nearly impossible without using some type of submersible vehicle (below divers' depth range).

The water quality variation in temperature, salinity, turbidity, and dissolved oxygen between surface and a depth of 90 m in the Red Sea would not have a

significant impact on a SWRO plant operation. There is an overall decrease in algae, bacteria, TOC, TEP, and biopolymer concentration with depth, which could reduce the potential for membrane biofouling, but not to a large degree. A high productivity zone occurs between 40 and 50 m below surface, which would make this depth interval a poor option for locating a SWRO intake system.

Although a deep intake option may be a viable option at other locations, based on the data collected from the Red Sea, there is no clear advantage for using a deep sea intake system in the Red Sea. Also, there would be considerable construction and operational risk based on the extreme depth profile from the marine shelf to the deep water of the basin.

Acknowledgments Funding for this research was provided by the Water Desalination and Water Reuse and the Red Sea Centers at King Abdullah University of Science and Technology. The authors thank the ownership and staff at the Moya Bushnak Company for access to the SWRO facility with the deep intake and engineer Mohamed Arfin for allowing facility access and giving water sampling assistance. The authors thank the Center for Marine Operations and Research (CMOR) led by Dr. Abdulaziz Mohammed Al-Suwailem and the Red Sea Center for providing equipment of bathymetric surveying and the vessel and assistance in collection of offshore water quality data and samples.

References

Alldredge, A. L., Passow, U., & Logan, B. E. (1993). The adundance and significance of a class of large, transparent organic particules in the ocean. *Deep Sea Research, Part 1, 40*(6), 1131–1140.

Azetsu-Scott, K., & Passow, U. (2004). Ascending marine particles: significance of transparent exopolymer particles (TEP) in the upper ocean. *Limnology and Oceanography, 49*(3), 741–748.

Bar-Zeev, E., Berman-Frank, I., Liberman, B., Rahav, E., Passow, U., & Berman, T. (2009). Transparent exopolymer particles: Potential agents for organic fouling and biofilm formation in desalination and water treatment plants. *Desalination and Water Treatment, 3*, 136–142.

Berman, T. (2010). Biofouling: TEP-a major challenge for water separation. *Filtration and Separation, 47*(2), 20–22.

Berman, T., Mizrahi, R., & Dosoretz, C. G. (2011). Transparent exopolymer particles (TEP): A critical factor in aquatic biofilm initiation and fouling on filtration membranes. *Desalination, 276*, 184–190.

Berman, T., & Passow, U. (2007). Transparent exopolymer particles (TEP): An overlooked factor in the process of biofilm formation in aquatic environments. *Nature Precedings*. doi:10.1038/npre.2007.1182.1.

Cartier, G, & Corsin, P. (2007). Description of different water intakes for SWRO plants. In *Proceedings of the International Desalination Association World Congress on Desalination and Water Reuse*, Gran Canaria, Spain, October 21–26, 2007, Paper IDAWC/MP07-185.

Dehwah, A. H. A., Li, S., Al-Mashharawi, S., Rachman, R. M., Winters, H., & Missimer, T. M. (2014). The influence of beach well and deep ocean intakes on TEP reduction in SWRO desalination systems, Jeddah, Saudi Arabia. *AWWA/AMTA Membrane Technology Conference Proceedings*, Las Vegas, Nevada, March 10–13, 2013, 18 pp.

El-Isa, Z. H., & Shanti, A. (1989). Seismicity and tectonics of the Red Sea and western Arabia. *Geophysical Journal, 97*, 449–457.

Engle, A. (2004). Distribution of transparent exopolymer particles (TEP) in the northwest Atlantic Ocean and their significance for aggregation processes. *Deep Ocean Research Part 1, 51*(1), 83–92.

Gille, D. (2003). Seawater intakes for desalination plants. *Desalination, 156*(1–3), 249–256.
Goosen, M. F. A., Sablani, S. S., Al-Maskari, S. S., Al-Belushi, R. H., & Wilf, M. (2002). Effect of feed temperature on permeate flux and mass transfer coefficient in spiral-wound reverse osmosis systems. *Desalination, 144*, 367–372.
Hayashi, M., Ikeda, T., Otsuka, K., & Takahashi, M. M. (2003). Assessment on environmental effects of deep ocean water discharged into coastal sea. In: Saxena, N. (ed.) *Marine Science and Technology, PACON International*, 535–546.
Huber, S. A., Balz, A., Abert, M., & Pronk, W. (2011). Characterisation of aquatic humic and non-humic matter with size-exclusion chromatography—organic carbona detection—organic nitrogen detection (LC-OCD-OND). *Water Research, 45*(2), 879–885.
Ito, Y., Hanada, S., Kitade, T., Tanaka, Y., & Kurihara, M. (2013). Clarification of impact of biofouling triggered by chemical addition for designing of Mega-Ton SWRO plant. In *Proceedings of the International Desalination Association World Congress 0n Desalination and Water Reuse*, Tianjin, China. Paper IDAWC/TIAN13-062.
Johnson, B. D., & Kepkay, P. E. (1992). Colloid transport and bacterial utilization of oceanic DOC. *Deep-Sea Research, Part A, 39*(5A), 855–869.
Mari, X. (2008). Does ocean acidification induce upward flux of marine aggregates? *Biogeosciences, 5*(4), 1023–1031.
Michel, C., Lapoussiere, A., LeBlanc, B., & Starr, M. (2006). Transparent exopolymeric substances (TEP) in Hudson Bay during fall. Significance and potential roles. *Reunion Scientifique Annuelle d'Arcticnet*, Victoria, Colombrie-Britanique (one sheet).
Passow, U. (2000). Formation of transparent exopolymer particles, TEP, from dissolved precursor material. *Marine Ecology Progress Series, 192*, 1–11.
Passow, U. (2002a). Production of transparent exopolymer particles (TEP) by phyto- and bacterioplankton. *Marine Ecology Progress Series, 236*, 1–12.
Passow, U. (2002b). Transparent exopolymer particles (TEP) in aquatic environments. *Progress in Oceanography, 55*(3–4), 287–333.
Passow, U., & Alldredge, A. L. (1994). Distribution, size and bacterial-colonization of transparent exopolymer particles (TEP) in the ocean. *Marine Ecology Progress Series, 113*(1–2), 185–198.
Passow, U., & Alldredge, A. L. (1995). A dye-binding assay for the spectrophotometric measurement of transparent exopolymer particules (TEP). *Limnology and Oceanography, 40*, 1326–1335.
Passow, U., Shipe, R. E., Murray, A., Pak, D. K., Brzezinski, M. A., & Alldredge, A. L. (2001). The origin of transparent exopolymer particles (TEP) and their role in the sedimentation of particulate matter. *Continental Shelf Research, 21*(4), 327–346.
Ortega-Retuerta, E., Reche, I., Pulido-Villena, E., Agusti, S., & Duarte, C. M. (2009). *Marine Chemistry, 115*, 59–65.
Radic, T., Ivancic, I., Kuks, D., & Radic, J. (2006). Marine bacterioplankton production of polysaccharidic and proteinaceous particles under different nutrient regimes. *FEMS Mircobiology Ecology, 58*(3), 333–342.
Stodergger, K., & Herndl, G. J. (1998). Production and release of bacterialcapsular material and its subsequent utilization by marine bacterioplankton. *Limnology and Oceanography, 43*(5), 877–884.
Stodergger, K., & Herndl, G. J. (1999). Production of exopolymer particles by marine bacterioplankton under contrasting turbulence conditions. *Marine Ecology Progress Series, 189*, 9–16.
Sugimoto, K., Fukuda, H., Baki, M. A., & Koike, I. (2007). Bacterial contributions to formation of transparent exopolymer particles (TEP) and seasonal trends in coastal waters of Sagami Bay. *Japan. Aquatic Microbial Ecology, 46*(1), 31–41.
Takahashi, M., & Ikeya, T. (2003). Ocean fertilization using deep ocean water (DOW). *Deep Ocean Water Research, 4*, 73–87.
Takahashi, M., & Huang, P.-Y. (2012). Novel renewable natural resource of deep ocean water (DOW) and their current and future practical applications. *Kuroshio Science, 6*, 101–113.

Takahashi, M., & Yamashita, K. (2005). Clean and safe supply of fish and shellfish to clear the HACCP regulation by use of clean and cold water in Rausu, Hokkaido, Japan. *Japan Journal of Oceanography, 4*, 219–223.

Van Loosdrecht, M. C. M., Lyklema, J., Norde, W., & Zehnder, A. J. B. (1989). Bacterial adhesion-a physicochemical approach. *Microbial Ecology, 17*(1), 1–15.

Villacorte, L. O., Kennedy, M. D., Amy, G. L., & Schippers, J. C. (2009). Measuring transparent exopolymer particles (TEP) as indicator of the biofouling potential of RO feed water. *Desalination & Water Treatment, 5*, 207–212.

Wilf, M. (2007). *The guidebook to membrane desalination technology*. Balaban Desalination Publications, L'Aquila, Italy.

Wurl, O., Miller, L., & Vagle, S. (2001). Production and fate of transparent exopolymer particles (TEP) in the ocean. *Journal of Geophysical Research Oceans* 116(1) C00H13, doi:10.1029/2011JC0077342.

Chapter 7
Coastal Evaluation and Planning for Development of Subsurface Intake Systems

Abdullah H.A. Dehwah, Samir Al-Mashharawi and Thomas M. Missimer

Abstract The feasibility of using a subsurface intake system for a seawater reverse osmosis (SWRO) water treatment plant is based on the site-specific hydrogeologic conditions which control the type of intake design that can be used and the capacity of the intake. Planning for future development of subsurface intake systems requires a careful analysis of the shoreline and shallow offshore area. Example regions, the Red Sea coast of Saudi Arabia and the shoreline of Florida (USA), were investigated to develop general feasibility criteria for possible development of SWRO intake systems. Within the Red Sea, it was found that various well intake systems could be feasible for low-capacity SWRO facilities and high capacity intake systems would be limited to seabed gallery intakes. Coastal Florida had more subsurface intake options available, including wells, beach galleries, and seabed galleries which could be used based on the required capacity and the specific site conditions. The presence of high transmissivity carbonate aquifers containing seawater in Florida would allow medium capacity SWRO systems to use conventional vertical wells. High capacity systems could be developed using beach gallery systems in many locations. The methods developed for shoreline and nearshore evaluation contained herein could be applied to any coastal region of the world for subsurface intake evaluation.

A.H.A. Dehwah · S. Al-Mashharawi
Water Desalination and Reuse Center, King Abdullah University of Science and Technology, Thuwal, Saudi Arabia
e-mail: abdullah.dehweh@kaust.edu.sa

S. Al-Mashharawi
e-mail: samir.almashharawi@kaust.edu.sa

T.M. Missimer (✉)
U.A. Whitaker College of Engineering, Florida Gulf Coast University, Fort Myers, FL, USA
e-mail: tmissimer@fgcu.edu

T.M. Missimer et al. (eds.), *Intakes and Outfalls for Seawater Reverse-Osmosis Desalination Facilities*, Environmental Science and Engineering,
DOI 10.1007/978-3-319-13203-7_7

7.1 Introduction

The intake system for a seawater reverse osmosis (SWRO) desalination facility is a critical part of the overall system design in that a specific volume of seawater must be delivered to the plant. Feed water flow to the plant must be reliable and have the best possible quality at all times of operation. Variation in water quality caused by extreme natural events, such as harmful algal blooms (HABs), or anthropogenic events, such as an oil spill, can lead to plant shutdowns or damage to the treatment process. SWRO facilities using surface or open-ocean intakes (Chap. 1) are subject to temporary shutdown during these events. An HAB occurred in the Arabian Sea and Arabian Gulf in 2009 and shut down many large SWRO plants by overwhelming the pretreatment processes (Berktay 2011).

Natural seawater contains a wide range of constituents. Variable concentrations of algae, bacteria, and organic compounds occur in seawater, which tend to cause operating difficulties in SWRO plants, in particular biofouling. Feed water quality ranges from quite high with a minimal concentration of organic material to greatly impaired with high turbidity and concentrations of bacteria and biopolymers. Variations in organic compound concentrations are very common on a season or even daily basis. Therefore, feed water obtained via open-ocean intakes requires extensive pretreatment before it can be transmitted into the primary membrane process, otherwise the facility will suffer difficulties with membrane fouling, either physical or biofouling (Flemming 1997; Flemming et al. 1997). The intensity of pretreatment is a major cost factor in the operation of SWRO facilities, and despite extensive pretreatment, many SWRO plants still have problems with membrane biofouling (Matin et al. 2011).

Subsurface intake systems used for SWRO facilities have been proven to provide significant feed water quality improvement and reduced pretreatment requirements resulting in operational and economic benefits (Missimer 2009; Missimer et al. 2013; Rachman et al. 2014). However, use of subsurface intake systems is highly dependent on the geology and hydrogeology of the coastal area including the beach and nearshore belt paralleling the shoreline. Use of subsurface intake systems for SWRO feed water development should be considered in all facilities regardless of capacity, because of reduced cost of treatment, reduced environmental impacts, and lower chemical usage (Missimer et al. 2013).

The shoreline and nearshore environments are perhaps the most dynamic areas on Earth. Therefore, the location and construction of any intake system in this area (even open-ocean intakes) requires careful analysis and planning with particular attention given to the changes that can be anticipated during the operational life-expectancy of a SWRO facility which is a planning horizon normally ranging from 20 to 30 years. It is the purpose of this chapter to develop an approach for coastal mapping and system development planning to assess the general feasibility of using various types of subsurface intake systems, including vertical wells, angle wells, horizontal wells (or collectors), Ranney wells (or collector wells), water tunnels

with laterals, beach galleries, and seabed galleries. This technical approach must be considered as screening and once a general intake location is determined, a site-specific investigation would be required.

7.2 Methods

Coastal mapping for an initial assessment of the feasibility of specific types of subsurface intakes requires detailed analysis of the coastal geomorphology and the development of a coastal classification scheme relating specific environments to the use of various intake types. Coastal geomorphology reference texts provide classifications of coasts based on shoreline geology, offshore conditions, bottom profiles, intensity of normal wave activity, frequency and intensity of potential storm impacts and other factors (Sunamura 1992; Davis and Fitzgerald 2003; Davidson 2010). Classification schemes have been developed from the geology and process assessments at a number of global locations, such as coastal California and Florida (Inman and Nordstrom 1971; Tanner 1960). Each coastline contains a unique set of environments that characterize it and no single classification can be uniformly applied to all global shoreline systems. A second aspect is to superimpose and assess the desired intake system within a framework of engineering design within the coastal zone. This requires consultation with a standard coastal engineering reference (e.g., Sorensen 2005; Kamphuis 2010).

As an example, a combination of methods was used by Dehwah et al. (2014) to characterize the geomorphology of the Red Sea coastline of Saudi Arabia. The Red Sea contains a large number of seawater desalination facilities ranging in capacity from 5,000 to 200,000 m^3/day and numerous additional facilities are being planned and constructed (Hoepner and Lattemann 2002). Therefore, this is an important region for study of subsurface intake system feasibility.

The scope of the research included a literature search, field visits to 105 sites (Fig. 7.1), collection and analysis of 485 sediment samples, use of archived satellite images to classify various segments of the coast with groundtruthing provided by field site visits, photographs of the shoreline and nearshore bottom, and data georeferencing. Aerial mapping was used to compile and classify the coastline. Field inspection, review of geologic maps, and analysis of satellite photographs were collectively used to define the large-scale features of the coastline, such as the occurrence of rocky headlands associated with active tectonism, marine carbonate terraces (limestone) with a cliffed geometry, presence or absence of fringing coral reefs, occurrence of ephemeral stream intersections with the coast, the occurrence of beachrock, the occurrence of marine hardgrounds in the shallow subtidal areas, and any evidence of erosion or accretion of the beach. Sensitive environmental features were mapped, such as the distribution and density of corals and seagrasses. Finer details were also assessed on a limited scale, such as the thickness and composition of unlithified sediment at various locations. Sediment samples were collected at representative sites for laboratory analysis of grain size distribution, hydraulic

Fig. 7.1 Map showing the Red Sea coast of Saudi Arabia with the sites visited and sampled (from Dehwah et al. 2014)

conductivity, and porosity. Overall, the Red Sea coastline of Saudi Arabia is very complex, containing a large number of geomorphological environments.

The characteristic geomorphological environments of the coastal area were assessed with respect to each type of subsurface intake system that could be potentially designed and constructed to provide feed water to a SWRO facility. A qualitative, planning-level assessment was also made concerning the possible range of systems capacities that may be feasible. Site-specific, detailed feasibility assessments were conducted at five locations and were used to test the planning-level assessments (Sesler and Missimer 2012; Dehwah and Missimer 2013; Lujan and Missimer 2014; Mantilla and Missimer 2014; Al-Mashharawi et al. 2014). Progressively, the information base on this coastal area was improved to allow a general classification scheme to be developed with a relatively high degree of accuracy for initial feasibility screening.

A second classification scheme was developed for a much less complex shoreline, the full coastline of Florida. This is another region that has very large population growth in the coastal zone with limited future development of freshwater resources caused by saltwater intrusion and potential wetlands impacts. Evaluations were based on the past work of Tanner (1960) linked with various subsurface intake types.

7.3 Coastal Mapping and Subsurface Intake Evaluation of the Red Sea Coast of Saudi Arabia

7.3.1 Geologic and Geomorphological Setting

The Red Sea is a restricted-circulation water body that is characterized by low tidal fluctuation ranges, minimal wave activity at the shoreline, and a low frequency of comparatively low-intensity storms (Morcos 1970; Pedgley 1974; Sofianos et al. 2002; Sofianos and Johns 2003). Therefore, it is considered to be a low-energy system in terms of wave transport of sediment in the coastal zone. However, the Red Sea coastal area of the Saudi Arabia has a large number of geomorphological environments, because it is an area of active tectonism associated with the Red Sea spreading center (Bosworth et al. 2005). The tectonism is responsible for the occurrence of grabens and horst features in the offshore areas (Chap. 6, Fig. 6.3) and the occurrence of steep rocky headlands and uplifted marine terraces at the shoreline (Figs. 7.2 and 7.3). Steep-gradient and low-gradient ephemeral streams drain the Precambrian craton into the nearshore and deep water of the Red Sea (Chap. 6, Fig. 6.3).

The tropical nature of the Red Sea stimulates fringing coral reef growth along nearly the full-length of the coastline (Bemert and Ormond 1981; Colontani and Taviani 1982; Head 1987; DeVantier and Pilcher 2000). Active carbonate sediment production, transport, and marine lithification occur within and landward of the reef system and in some cases to the shoreline. The beach is commonly covered with beachrock and the nearshore area from the beach seaward to the inner margin of the reef tract is commonly a marine hardground.

7.3.2 Coastal Geomorphological Classification System

The coastal environments of the Red Sea were grouped into 17 different classifications based on the topography at the shoreline, the type of sediment (rock, sand, mud), the vegetation type at the shoreline, the general composition of sediment (or rock) in the nearshore, and the presence or absence of coral reefs. If was necessary to group a number of similar sub-environments into a single category, because of their similarities and the objectives of the research.

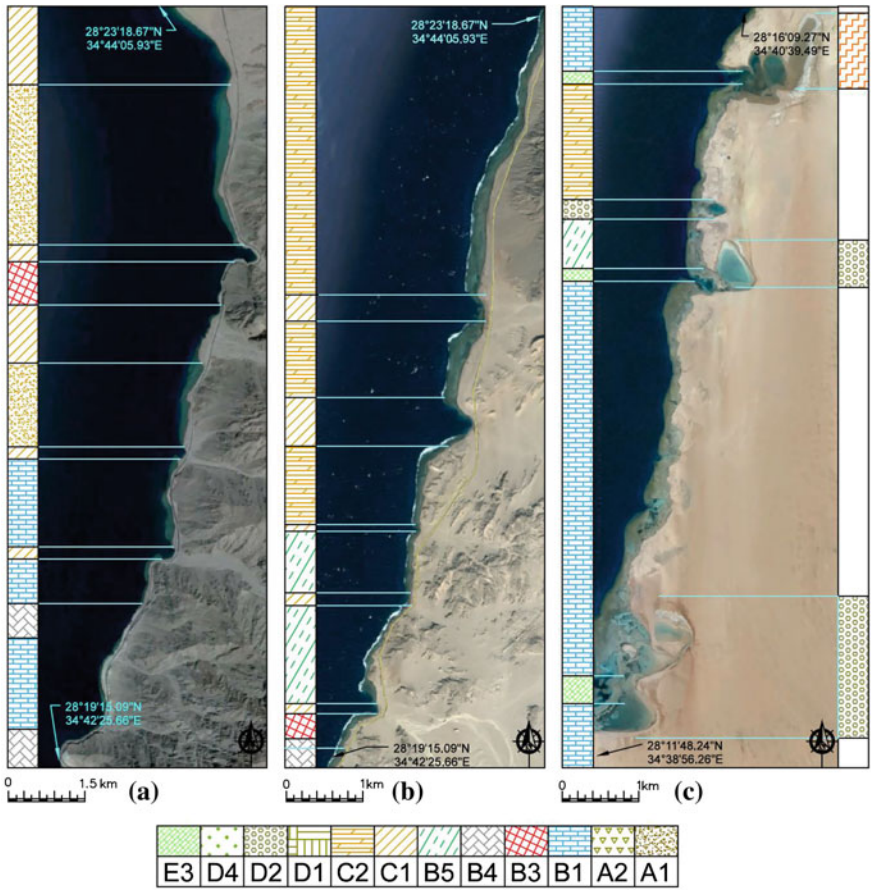

Fig. 7.2 Examples of the coastal mapping and resulting classifications along the Red Sea coastline of Saudi Arabia (from Dehwah et al. 2014)

The five general classifications include sandy beaches, rocky shorelines, wadi intersections, muddy shoreline (sabkhas, lagoons, and mangroves), and others. Each major classification is subdivided into two to five subcategories based on other criteria. A summary of the classifications is presented in Table 7.1 and a detailed description of each environment is contained in Dehwah et al. (2014). An example showing part of the Red Sea coastline of Saudi Arabia with the associated classification is given in Fig. 7.2. Note that the letter and number in the figure correspond to the key in Table 7.1.

7.3.3 Linkage Between Subsurface Intake Type and the Geomorphological Coastal Classification

The geomorphological classifications and assessments of the various subsurface intake types are given in Table 7.2. The data in the table has been modified to a degree from that originally presented by Dehwah et al. (2014). New data have been obtained at some sites and some re-evaluation was done. Also, the water tunnel subsurface intake type was omitted from the evaluation, because the equipment to construct this type of intake structure is not readily available in this region and this type of system is not appropriate for the general geology.

There are obvious and tenuous linkages between the coastal geomorphological environments and the development of subsurface intakes. For example, all of the environments within general classifications D and E in Table 7.1 contain muddy, low permeability sediments and some contain sources of hypersaline water, such as sabkhas (Gavish 1980; El Abd and Awad 1991; Missimer et al. 2014b). These

Table 7.1 Geomorphological classifications of the Red Sea coastline of Saudi Arabia (from Dehwah et al. (2014))

A. Sandy beaches
A1. Sandy beach with corresponding nearshore sand or slightly muddy sand, coral reef complex offshore
A2. Sandy beaches, restricted, with no reef
A3. Offshore island with nearshore sandy sediments and reef
B. Rocky shorelines
B1. Limestone rocky shoreline with corresponding nearshore sand, and offshore coral reef complex
B2. Limestone rocky shoreline with nearshore muddy sediments
B3. Limestone rocky shoreline, nearshore deep water, no reef
B4. Rocky headland with offshore rocky bottom, no reef
B5. Rocky shoreline, wadi sediments nearshore, offshore reef
C. Wadi intersections
C1. Wadi sediments (boulders, pebble, and gravel)at shoreline, variable sand, gravel and mud offshore with no reef
C2. Wadi shoreline sediments, nearshore marine hard ground, minor nearshore sand, coral reef offshore
D. Sabkha, lagoons, and mangrove
D1. Coastal sabkha shoreline and nearshore muddy sediments
D2. Muddy shoreline with lagoonal muddy sediments, nearshore sand and offshore reef complex
D3. Muddy shoreline /lagoon/supratidal sabkha with no reef complex
D4. Mangrove shoreline with nearshore muddy sediments
E. Others
E1. Shoreline reef complex dropping to deep water in the nearshore off-reef area
E2. Artifical channels or urban shoreline with artificially filled nearshore dropping to deep water nearshore
E3. Natural channel

Table 7.2 Correlation between coastal environment and feasibility of using various subsurface intakes along the Red Sea coastline of Saudi Arabia (modified from Dehwah et al. 2013)

Intake type	Subsurface intake system					
Well/gallery	Well system				Gallery system	
Environments	Vertical	Horizontal	Radial (collector)	Angle	Beach gallery	Seabed gallery
A. Sandy beaches						
A1	1(b)	2	2(b)	2(b)	1(d)	1(d)
A2	1(a)	3	2(b)	2(a)	4	1(c)
A3	1(a)	2	2(b)	2(b)	1(d)	1(d)
B. Rocky shorelines						
B1	1(b)	2	1(b)	1(c)	1 (c)	1(d)
B2	4	4	4	4	4	2(c)
B3	4	4	4	3	4	4
B4	4	4	4	4	4	4
B5	1(a)	3	2(b)	2(a)	2(c)	2(c)
C. Wadi intersections						
C1	4	4	4	4	4	4
C2	1(b)	3	2(c)	2(b)	2(c)	2(c)
D. Sabkha, lagoons, and mangrove						
D1	4	4	4	4	4	4
D2	4	4	4	4	4	4
D3	4	4	4	4	4	4
D4	4	4	4	4	4	4
E. Others						
E1	4	4	4	4	4	4
E2	4	4	4	4	4	4
E3	4	4	4	4	4	4

Feasibility factor: *1* Excellent, *2* Possible, *3* Questionable, *4* Not feasible
Estimated Capacity (m^3/day): (a) Capacity <20,000, (b) 20,000–50,000, (c) 50,000–100,000, (d) Unlimited

coastal environments are not conducive to the development of a subsurface intake system. Only an offshore, open-ocean intake could potentially be developed where these environments dominant the coastline. However, in some locations there are islands located offshore from lagoonal or sabkha environments. These islands, such as Um Al Misk Island, may contain very good sites for one or more subsurface intake types (Sesler and Missimer 2012).

To understand the limitations of some of the well intakes, it is necessary to provide additional information on the nature of some of the sandy beach and rocky shoreline environments. For example, the beachrock and marine terrace limestones located along the coast are limited in thickness within a range of 5 to 60 m in general. Therefore, vertical wells will tend to have limited yields based on aquifer thickness and likely transmissivity. At wadi intersections with the coast, the sediment consists

of particle sizes ranging from boulders to mud. Vertical and horizontal wells can be constructed using normal drilling methods through this material. However, the construction of horizontal wells through material containing boulders up to 25 cm in diameter creates potential deviation issues during drilling and potential for breakage of equipment and the primary screen. Even where the coastal aquifer contains limestone or a combination of limestone and unlithified carbonate sand, the feasible use of horizontal drilled wells is open to question because there are breaches through the limestone in the offshore area, which could cause short-circuiting of water into the wells, thereby providing no significant treatment. The breakthrough of algae into the horizontal intake system at Alicante, Spain is likely caused by vertical conduits into the limestone aquifer (Rachman et al. 2014).

Rocky headlands, classified as sub-environments B4 and B5, are outcrops of Precambrian shield rocks. This material has a very low hydraulic conductivity and the development of any type of subsurface intake in these environments is not feasible.

Another issue that affects well construction along the Red Sea coast is the occurrence of hydersaline water in the coastal plain near the shoreline and, in some cases, under the beach (Missimer et al. 2014a). The origin of this high salinity water is the common occurrence of the sabkha environment which is a supratidal system in which spring high tide water is trapped landward of a shallow berm. The water does not completely circulate back to the sea and intense evaporation takes place, causing the development of hypersalinity and precipitation of salt and gypsum. Some of this hypersaline water tends to flow in the subsurface toward the sea and beneath the beach area. Use of conventional vertical wells can pull this water into the wells, rendering it unusable as feed water to a SWRO system. Perhaps a solution to this issue would be the use of an angle well if the aquifer is sufficiently thick to produce enough distance from the beach to create primarily vertical recharge to the well through the seabed with little or no capture of water from the landward direction. Dehwah et al. (2014) and Al-Mashharawi et al. (2014) describe a hybrid well intake system constructed upon an artificial fill area jutting seawater onto the reef tract with subsequent construction of vertical wells on the fill. The production wells are actually located offshore and away from the source of hypersalinity (Fig. 7.3). Such a solution would not be viability in many parts of the world due to environmental permitting restrictions that prohibit filling of marine bottomlands, especially on a reef tract.

The coastal classification scheme developed for the Red Sea shoreline of Saudi Arabia provides general guidance to the location of subsurface intakes. However, it does not fully define any capacity limitations that may occur at a specific site. To supplement the database on subsurface intake feasibility, a series of field and laboratory investigations were conducted at 5 locations within the beach and nearshore areas (to water depths of 2 m) (Sesler and Missimer 2012; Dehwah and Missimer 2013; Lujan and Missimer 2014; Mantilla and Missimer 2014; Al-Mashharawi et al. 2014). These investigations were conducted near sites containing large-capacity SWRO facilities and were used to assess the feasibility of primarily seabed galleries. The strategy of mapping and limited-scope site-specific field investigations could be used to improve the database of any coastline that has potential use for SWRO intake development.

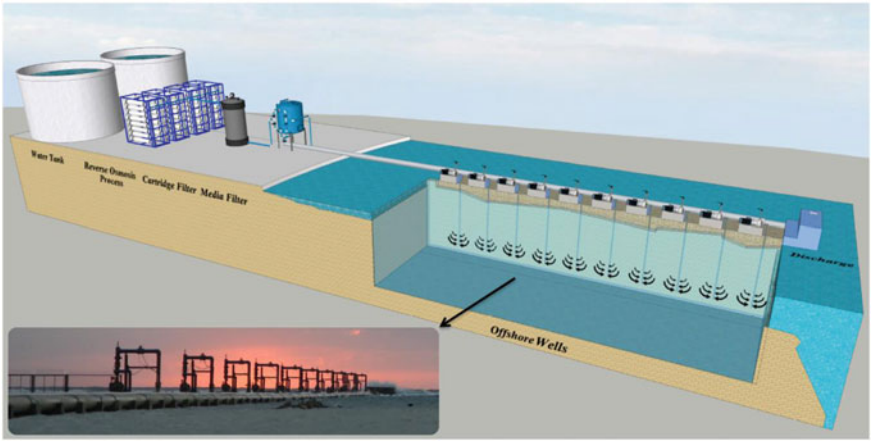

Fig. 7.3 Offshore wellfield intake (SAWACO facility) located south of Jeddah along the Red Sea coast of Saudi Arabia (from Al-Mashharawi et al. 2014)

7.4 Coastal Mapping and Subsurface Intake Evaluation of Coastal Florida, USA

7.4.1 Introduction

Florida lies within a subtropical area that receives an average annual rainfall of about 1,500 mm/year. Compared to the average rainfall of the Red Sea coastline at less than 60 mm/year, one could question why the State of Florida would require seawater desalination to meet water supply requirements. Currently, Florida faces water management challenges associated with rapid urban growth in its coastal zone, saline-water intrusion into coastal freshwater aquifers, and a rather sensitive internal environment with issues related to wetland impacts (Florida Council of 100, 2003). Florida is one of the leading regions globally in the use of brackish groundwater desalination and has one large capacity SWRO facility. The Tampa Bay Water facility is the only desalination system that uses a surface intake system in Florida and the plant has been plagued with membrane fouling problems.

It is anticipated that Florida will develop a number of SWRO systems in the future to diversify water supplies. Therefore, it is important to make a preliminary assessment of the coastlines to ascertain the potential development of subsurface intakes for SWRO facilities. Also, HAB's are common along the shoreline of the Gulf of Mexico and a subsurface intake system is a good method to avoid system shutdowns.

7.4.2 Coastal Geology and Geomorphological Classification Based on Energy and Depositional Environment

A summary of major and minor geomorphological classifications for the coastline of Florida is presented in Table 7.3. There are five major classifications and 1–3 subcatagories under each major one. The classification system is primarily based on geomorphology and shallow geology. However, the underlying deep geology also must be considered when assessing potential subsurface intakes in Florida.

The vast majority of the shorelines of Florida are sandy beaches along the eastern coast facing the Atlantic Ocean and the western coast bounding the Gulf of Mexico. These beaches can be classified based on energy (A1 − A3) using the average wave heights and associated induced littoral processes. Tanner (1960) developed a useful coastal classification and demonstrated that most coastal areas contain sandy beaches with variable rates of sediment transport, but a low energy shoreline lies along the Gulf of Mexico shoreline north of Tampa within an area known as the "Big Bend" (Fig. 7.4). This area contains muddy sediments along the shoreline and contains the delta of the Suwannee River which along contributes some fine-grained sediment to the coast during floods. This area also contains some coastal marshes. An expansion of the Tanner (1960) classification system is given in Table 7.3.

A small segment of the Florida East Coast in Martin and Palm Beach counties contains a cliffed shoreline. The Anastasia Formation outcrops along the beach in some areas and the associated beach profile shows a beach sloping to a 1–2 m wave-cut bench and a rapid decline into deep water from the bench to the offshore area (Fig. 7.5). This is only a minor area within the entire coastline.

Table 7.3 Coastal classifications of Florida

A. Sandy beaches
A1. High energy beaches (Atlantic) A2. Moderate energy beaches (Gulf of Mexico) A3. Low Energy beaches (Gulf of Mexico and islands in Florida Bay and Ten Thousand Islands)
B. Rocky shorelines
B1. Limestone cliffed
C. Shallow shelf with fringing reef
C1. Restricted low energy beach C2. Restricted muddy lagoon and mangrove swamps
D. Muddy or mixed mud and sand
D1. Lagoonal/deltaic shorelines D2. Mangrove shorelines D3. Coastal marshes
E. River or channel intersections
E1. River intersections E2. Natural inlet intersections E3. Man-made channel intersections

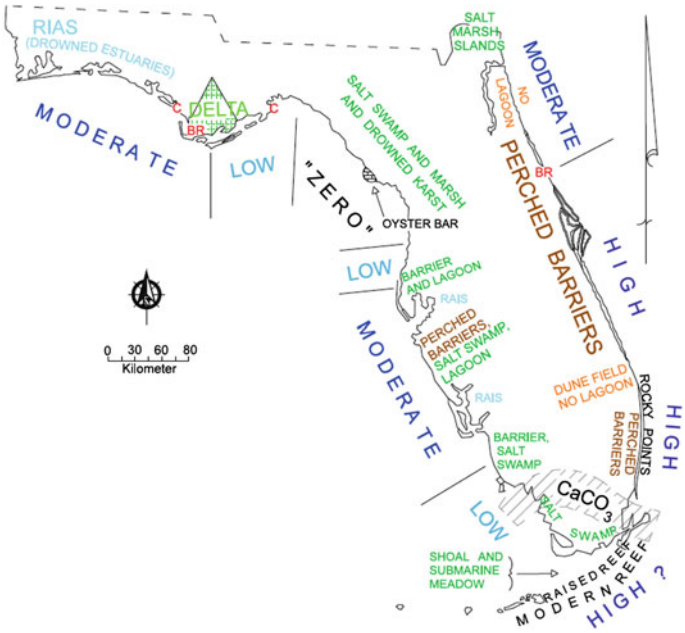

Fig. 7.4 Coastal classification of Florida based on wave energy (modified from Tanner 1960)

Fig. 7.5 Photograph of the outcrop of the Anastasia Formation in Martin County, Florida

The Atlantic margin of the Florida Keys contains some restricted-circulation low energy beaches with an offshore fringing reef. The shorelines along the land mass of the island chain has some sandy beaches and the offshore contains carbonate sands. However, some of the areas between islands and the shorelines of some islands contain mangroves and some muddy sediment. The western margin of the Florida Keys borders Florida Bay which contains predominantly muddy sediments.

There are a large number of lagoons and mangrove forests lying along the coastal areas of Florida. Most of these areas are bounded on the seaward margin by barrier islands that contain high to moderate energy beaches. However, along the southwest coast of Florida south of Marco Island to Florida Bay, the coastal lagoons and mangrove forest environments lie directly along the coast and contain a considerable amount of muddy sediment. Within the Big Bend area north of Tampa, some segments of the coast contain saltwater marshes (*Spartina*) north of the growth range for mangroves. This area also contains muddy sediments.

There are a number of channel or stream intersections with the shoreline along the Florida coast. These intersections with the coast are commonly unstable in terms of beach sediment movement, particularly in high energy areas (e.g., Florida East Coast). Some of the river intersections like the Suwannee and Caloosahatchee rivers contain mud deposition at their mouths. Overall the areas immediately near the associated high-energy unstable shoreline or within mud deposition areas are not viability for subsurface intake development.

A unique feature of the Florida peninsula is that many coastal areas are underlain either at shallow or deep depths by high permeability carbonate aquifers. Therefore, when assessing the viability of subsurface intakes, these aquifers, which commonly contain seawater, are highly productive in terms of yield and can support the use of a well intake system regardless of the nature of the surficial sediments. However, while conventional shallow, vertical "beach" wells can be used in places like the Florida Keys, deep vertical or angle wells might be used to develop feed water in areas like the "Big Bend" where the shallow sediments are muddy.

7.4.3 Linkage Between Coastal Classifications and Subsurface Intake Feasibility

A preliminary assessment of feasibility for development of subsurface intakes for SWRO facilities in Florida is given in Table 7.4. There are three key criteria that are considered within the assessment given; the intake type must produce the desired quantity of water reliably over the life-cycle of the facilities, the water quality must be stable and must show improved quality in comparison to surface seawater, and it must not impact coastal freshwater resources (particularly groundwater).

Development of SWRO intakes in the high to moderate energy shorelines of Florida has a high degree of feasibility over a wide range of capacities. Shallow wells could be used in certain areas where the underlying aquifer contains seawater and

Table 7.4 Correlation between coastal environment and feasibility of using various subsurface intakes along the coastline of Florida

Intake type	Subsurface intake system						
Well/gallery	Well systems					Gallery systems	
Environments	Vertical (deep)	Vertical (shallow)	Radial collector	Horizontal	Angle	Beach	Seabed
A. Sandy beaches							
A1. High energy	1(a–c)	1(a, b)	1(b, c)	2	1(b, c)	1(d)	1(b–d), 3
A2. Moderate energy	1(a, b)	1(a, b)	1(a–c)	1(a–c)	1(a, b)	1(a–c)	1(a–d)
A3. Low energy	1(a, b)	3	3	4	1(b, c)	1(b–d)	1(b–d)
B. Rocky shorelines							
B1. Limestone cliffed	1(b–d)	1(a, b)	1(b–d)	4	3	4	3
C. Shallow shelf with fringing reef							
C1. Restricted low energy beach	1(a)	1(a, b)	1(c)	2	3	4	1(a–c)
C2. Restricted lagoon and mangrove swamp	4	4	4	4	4	4	4
D. Muddy/mixed							
D1. Lagoonal/ deltaic	4	4	4	4	4	4	4
D2. Mangrove	4	4	4	4	4	4	4
D3. Coastal marshes	1(a, b)[a]	4	4	4	1(a, b)[a]	4	4
E. Channel intersections							
E1. River	4	4	4	4	4	4	4
E2. Natural inlet	4	4	4	4	4	4	4
E3. Man-made channel	4	4	4	4	4	4	4

Feasibility factor: *1* Excellent, *2* Possible, *3* Questionable, *4* Not feasible
Estimated Capacity (m^3/day): (a) Capacity <20,000, (b) 20,000–50,000, (c) 50,000–100,000, (d) Unlimited
[a]In locations where the underlying Floridan Aquifer Systems contain high permeability and seawater

has adequate hydraulic conductivity. Large capacity wells could be developed along the southeast Florida coast and areas further to the north. Care would have to be taken not to impact the freshwater resources. High-capacity seawater wells could be used in conjunction with saline-water intrusion control in some areas (Fig. 7.6).

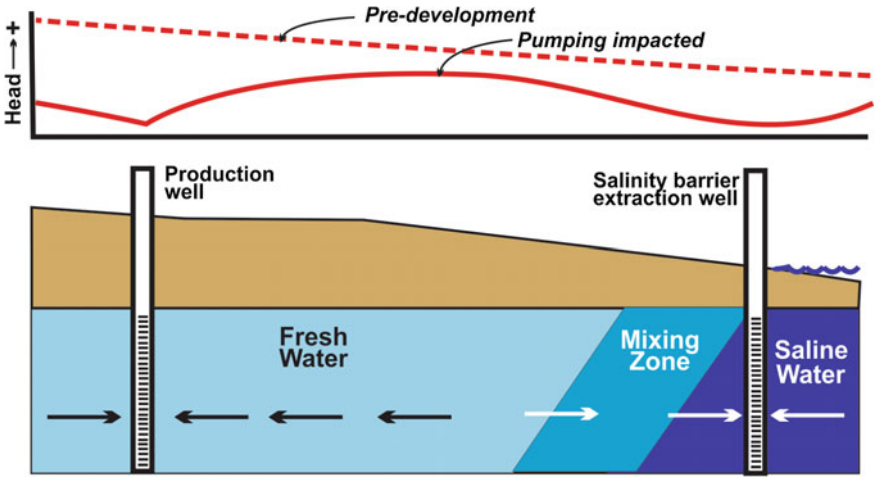

Fig. 7.6 Diagram showing the use of seawater extraction in the coastal zone to inhibit saltwater intrusion into shallow aquifers

Shallow well development would be more limited along the western Florida coastline and would tend to be feasible for only low capacity systems because of potentially low aquifer yields. The use of deep aquifer seawater wells would be feasibility along a large part of the Florida coastline, but the depths may have a wide range from perhaps 350 to 1,000 m. Also, the well capacities would vary greatly depending upon which aquifer with the Floridan Aquifer System that could be used. For example, the Boulder Zone in southern Florida could yield very large quantities of raw water, sufficient to supply SWRO plants with capacities over 100,000 m^3/day. High yield aquifers from Tampa northward along the west coast could also produce very high capacities. The key issue is to carefully develop the Floridan Aquifer System without interfering with freshwater resources lying further inland. For example, the Tampa Bay SWRO facility uses a surface intake system, but a deep Floridan Aquifer System series of seawater wells could have been installed to meet the required capacity and would not have interfered with management of the freshwater resource. Angle wells could have been used to keep the intake of the wells further seaward from the freshwater/seawater interface if necessary.

Radial collector wells are another potential intake solution along a large part of the Florida coastline. Placement of the caisson at depths ranging from 20 to 60 m below surface could allow laterals to be extended into shallow, high-productivity aquifers, such as the Biscayne Aquifer, to create very large yield wells (e.g., 25,000–80,000 m^3/day).

Galley intake systems could be very productive, especially beach galleries located along reasonably stable parts of the shoreline (see Chap. 10) (Missimer et al. 2014b). The use of offshore seabed galleries, which can be developed to meet virtually any capacity system, is perhaps most suited for moderate energy shorelines where there is no significant quantity of mud deposition. The location of seabed

galleries is limited in areas that have a steep offshore profile because of construction limitations based on economics. Some areas of the rocky shoreline along the Florida East Coast contain some steep offshore profiles that would not be conductive to seabed gallery development.

The only segment of the coastline containing a fringing reef system is located in the Florida Keys. Along the eastern margin of the islands that constitute the Florida Keys, there are a series of low energy sandy beaches and a low gradient seaward sloping, sandy bottom. The offshore area could be used to develop seabed gallery intakes where these is no significant occurrences of coral or seagrass. A seabed gallery intake could serve virtually any capacity SWRO plant if located in this area.

Development of subsurface intakes in areas that contain muddy sediments is unlikely with a few exceptions. The coastal marsh sediments located in the "Big Bend" area with a low energy shoreline are underlain by high permeability carbonate rocks occurring with the Floridan Aquifer System. Within upland environments, deep wells could be drilled into the aquifer system where it contains seawater. These wells would likely contain very high capacities that could support a wide range in SWRO plant capacities.

Development of large-scale SWRO facilities along the northeast Florida coastal area has been under consideration for many years. Because of the issue of impingement and entrainment and the overall cost of SWRO, these plans have been delayed. Since the cost of treatment would be lowered if a subsurface intake system would be used, it is timely to ascertain what types of intakes could be developed. In this area, deep angle wells tapping seawater in the upper Florida aquifer would be an option as well as high capacity beach galleries (Maliva and Missimer 2010). Seabed galleries may also be considered if the offshore bottom slope is sufficiency low to allow economic construction.

7.5 Discussion

7.5.1 Geological Control of Coastal Aquifer Yields and Potential Use of Well Intakes

Classification of coastal environments is a useful exercise to allow preliminary screening of the overall feasibility and potential viability of various types of subsurface intake systems. The occurrence and potential yield characteristics of coastal aquifers can be used to assess feasibility of conventional vertical wells, which are commonly termed "beach wells". The study areas chosen for analysis, the Red Sea coast of Saudi Arabia and the Florida coastlines, have mixed results in terms of potential use of shallow well systems. Along the Red Sea coast of Saudi Arabia, well intake systems with low yields may be developed if the local aquifer does not contain hypersaline water. In Florida, high capacity wells could be locally used for feed water supply, if they have no impact on interior parts of the aquifer system that

contain fresh water. Both angle wells and radial collector wells have high potential in Florida for development of SWRO intakes. However, these subsurface intake types do not appear to be useful for development of high capacity systems along the Red Sea coastline of Saudi Arabia. The issues that primarily control the use of shallow wells for SWRO intake use are the potential well yields, aquifer water quality (e.g., presence of hypersaline water), and impacts to inland fresh water and wetlands.

Use of deep wells completed in parts of the Floridan Aquifer System that contain seawater has a high potential for use as a feed water source. However, these saline zones are also used for concentrate disposal using injection wells, so the systems would have to be located and designed to avoid recycling of the concentrate into the feed water. Along coastlines that do not contain high permeability carbonate aquifer systems (e.g., Red Sea), use of deep wells is not feasible, except for very low capacity systems. Other areas of the Middle East-North Africa MENA arid region, such as the Levant coast, contain carbonate aquifer systems that may be suitable for beach well development. Again, the role of local geological conditions is paramount in assessing the viability of any subsurface intake option using wells.

Horizontal well intakes have a great appeal based on the ability to use a single site to drill a "fan" of wells under the seabed. Both the Red Sea and parts of the Florida shoreline contain areas that have a reasonable potential for successful development of horizontal well intakes with high capacity. In Saudi Arabia, the nearshore, thin (< 20 m) carbonate system is the environment with the greatest potential and in Florida, the areas containing a sandy offshore bottom with a low slope have some potential for horizontal well implementation. The use of this technology is still open to question based on lack of operating experience at high capacities, the issue of oxidation/reduction reactions in the seawater as it passes from oxic to anoxic conditions in the aquifer, and the issue of long-term maintenance of the well screens. Therefore, it is considered to be a possible intake system option, but requires considerable further investigation.

7.5.2 Geologic and Process Controls on Siting and Operation of High Capacity Gallery Intakes

Beach and seabed gallery intake systems generally have the greatest potential to meet the feed water requirements for a wide range of SWRO plants capacities. A great advantage of these types of systems is that they use an engineered sand filter and thus have greater flexibility to be successfully implemented in settings where local geological conditions are less than ideal. Therefore, several chapters of this book are dedicated to describing the latest research in siting and designing gallery intake systems. While the fundamental design concept for these galleries is similar, the intensity of the process controls on sedimentation is different. In both cases, serious technical assessment is required to understand the shoreline and nearshore processes that control stability.

Beach galleries are constructed within the littoral zone of the beach, which is the most dynamic part of the shoreline. Sediment movement along the shoreline is controlled by the incident angle of the wave as it breaks across the shoreline and the energy is released based on wave height (Inman and Bagnold 1963; Komar and Inman 1970; Longuet-Higgins 1970; Inman and Dolan 1989). Even stable beaches undergo seasonal changes in profile, due changes in the direction and intensity of wave energy released at the shoreline (Inman 1953). These changes can completely rearrange the nearshore bottom bathymetry with temporary erosion of the beachface and storage of sand in offshore bars. The seasonal climate changes affecting beach sedimentation may occur both near the site and at great distance in the bounding sea, because waves can travel thousands of kilometers after being generated.

Siting of gallery intakes is the key to success for long-term operation. For beach galleries, the shoreline can be either stable or can be undergoing some minor degree of erosion (see Chap. 10). Therefore, the dynamics of the ocean offshore and along the beach must be clearly understood. Jenkins and Wasyl (2005) constructed a model that can be used to predict shoreline changes, which need to be understood before siting and design of either gallery type. Directed wave energy at the shoreline is derived from the behavior of approaching waves as they are refracted and redirected across the bottom and are affected by natural offshore obstructions and the bottom bathymetry (Jenkins and Wasyl 2005). An illustration showing the movement of waves approaching and impinging on the beach is shown in Fig. 7.7. It can be clearly observed that parts of the beach with focused erosion could be problematical for location of a beach gallery intake. Changing beach and nearshore

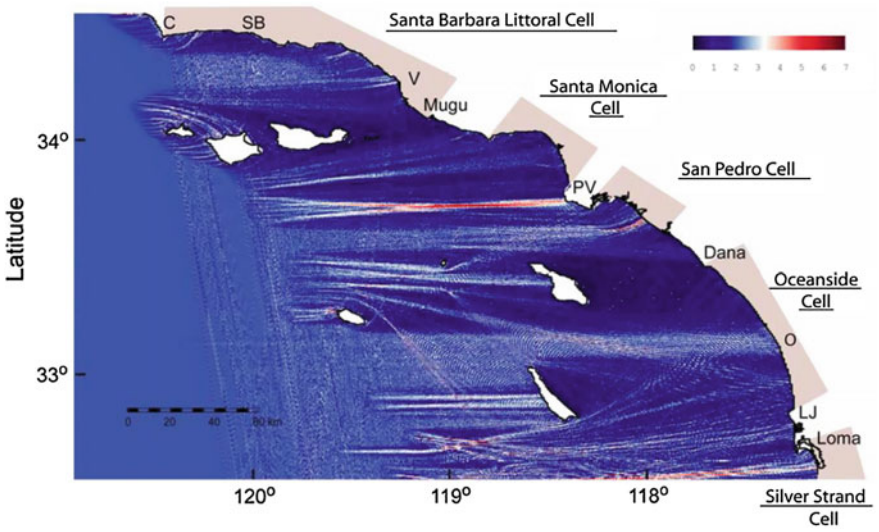

Fig. 7.7 Refraction/diffraction analysis for erosion hot-spot analysis on the 5 largest storms to strike Southern California in the El Nino winter of 1998 (from Jenkins and Wasyl 2005)

profiles can also affect the performance of seabed filters depending upon the distance a seabed gallery is constructed from the shore. A more detailed analysis of the methodology used in siting of gallery intakes is included in Chap. 12.

7.6 Conclusions

Coastal mapping of geomorphic and geological environments and relating them to the feasibility of developing various types of subsurface intakes is an important planning mechanism for the siting and development of SWRO systems. Since the feed water quality variation affects virtually all of the downstream process design and operation, an important design aspect is to deliver the highest and most consistent quality feed water possible to a SWRO plant, which can be accomplished by using subsurface intake systems.

A coastal mapping methodology was applied to two global regions with quite different geologic settings; the Red Sea coastline of Saudi Arabia and the coastline of the state of Florida, USA. It was concluded that the use of well intakes along the Red Sea coastline is limited to small to medium capacity SWRO systems. Further, the presence of sabkha features (coastal evaporation basins) causes the common occurrence of hypersaline groundwater along the beach, which does not allow use of shallow wells in some areas, despite favorable aquifer hydraulic properties. Seabed galleries are the intake system design most favorable for the Red Sea coast area.

The coastline of Florida contains primarily high to moderate energy sandy beaches, some limited coastal segments of rocky limestone out crops, restricted water with fringing coral reefs, and muddy environments associated with mangrove and coastal marshes. A large portion of the coastal part of the Florida peninsula is underlain by high permeability aquifers, some of which contain seawater. Therefore, Florida has a greater number of feasible subsurface intake options compared to Saudi Arabia. Many options are available to meet the demands for low to moderate capacity facilities. Subsurface intake options for large capacity facilities include high-capacity radial collector wells in some areas, high-capacity deep wells in southern Florida (boulder zone), high-capacity deep wells in areas such as the Big Bend, beach galleries in stable shorelines, and seabed galleries where the offshore bottom contain the appropriate characteristics.

Coastal mapping is useful in providing planning level assessments for feasibility determination of using various subsurface intake systems for SWRO facilities. However, detailed site-specific investigations are required for all final designs with the detail of the investigation necessary being related to the proposed system capacity. High-capacity SWRO facilities will require a greater scope of investigation to assure that the subsurface system of choice will meet the primary feasibility criteria consisting of the need to meet the required capacity and water quality requirements of the treatment facility under all conditions with no significant environmental impacts.

References

Al-Mashharawi, S., Dehwah, A. H. A., Bandar, K. B., & Missimer, T. M. (2014) Feasibility of using a subsurface intake for SWRO facility south of Jeddah, Saudi Arabia. *Desalination and Water Treatment*. doi:10.1080/19443994.2014.939870

Bemert, G., & Ormond, R. (1981). *Red Sea coral reefs*. London: Kegan Paul International.

Berktay, A. (2011). Environmental approach and influence of red tide to desalination process in the Middle East region. *International Journal of Chemical and Environmental Engineering, 2* (3), 183–188.

Bosworth, W., Huchon, P., & McClay, K. (2005). The Red Sea and Gulf of Aden basins. *African Journal of Sciences, 43*, 334–378.

Colontani, P., & Taviani, M. (1982). Morphological and ecological observations in the Sharn Obhor area and nearby coral reefs (Saudi Arabia, Red Sea). In *6th International Science Symposium Underwater Fed Troc Heriot-Watt* (pp. 183–192).

Davidson, R. (2010). *Introduction to coastal processes and geomorphology*. Cambridge: Cambridge University Press.

Davis, R. A, Jr, & Fitzgerald, D. M. (2003). *Beaches and coasts*. New York: Wiley-Blackwell.

Dehwah, A. H. E., & Missimer, T. M. (2013). Technical feasibility of using gallery intakes for seawater RO facilities, northern Red Sea coast of Saudi Arabia: The king Abdullah Economic City site. *Desalination and Water Treatment, 51*(34–36), 6472–6481. doi:10.1080/19443994.2013.770949.

Dehwah, A. H. A., Al-Mashhawari, S., & Missimer, T. M. (2014). Mapping to assess feasibility of using subsurface intakes for SWRO, Red Sea coast of Saudi Arabia. *Desalination and Water Treatment, 52*, 2351–2361. doi:10.1080/19443994.2013.862035.

DeVantier, L., & Pilcher, N. (2000). The status of coral reefs in Saudi Arabia. Global Coral Reef Monitoring Network (GCRMN).

El Abd, Y. I., & Awad, M. B. (1991). Evaporitic sediment distributions in Al-Kharrar sabkha, west Red Sea coast of Saudi Arabia, as revealed from electrical soundings. *Marine Geology, 97*, 137–143.

Flemming, H.-C. (1997). Reverse osmosis membrane fouling. *Experimental Thermal and Fluid Science, 14*, 382–391.

Flemming, H.-C., Schaule, G., Griebe, T., Schmitt, J., & Tamachkiarowa, A. (1997). Biofouling—the Achilles heel of membrane processes. *Desalination, 113*, 215–225.

Florida Council of 100 (2003). *Improving Florida's water supply management*. Tallahassee, FL: Florida Council of 100, September 2003.

Gavish, E. (1980). Recent sabkhas marginal to the southern coasts of Sinai, Red Sea. In A. Nissenbaum (Ed.), *Hypersaline brines and evaporative environments* (pp. 23–51). Amsterdam: Elsevier.

Head, S. M. (1987). Coral and coral reefs of the Red Sea. In A. J. Edwards & S. M. Head (Eds.), *Red Sea* (pp. 128–151). Oxford: Pergamon Press.

Hoepner, T., & Lattemann, S. (2002). Chemical impacts from seawater desalination plants—a case study of the northern Red Sea. *Desalination, 152*, 133–140.

Inman, D. L. (1953) *Areal and seasonal variations in beach and nearshore sediments at LaJolla, California*. Beach Erosion Control Board Technical Memorandum 39, (134 p). Washington, DC: Army Corps of Engineers.

Inman, D. L., & Bagnold, R. A. (1963). Littoral processes. In M. N. Hill (Ed.), *The sea, v. 3, The Earth beneath the sea*. New York: Wiley.

Inman, D. L., & Nordstrom, C. E. (1971). On the tectonic and morphologic classification of coasts. *Journal of Geology, 79*(1), 1–21.

Inman, D. L., & Dolan, R. (1989). The outer banks of North Carolina: Sediment budget and inlet dynamics along a migrating barrier island system. *Journal of Coastal Research, 5*(2), 193–237.

Jenkins, S. A., & Wasyl, J. (2005) *Coastal evolution model*. Scripps Institution of Oceanography Technical Report 58. La Jolla: Scripps Institution of Oceanography.

Kamphuis, J. W. (2010). *Introduction to coastal engineering and management*. London: World Scientific Publishing and Imperial College.

Komar, P. D., & Inman, D. L. (1970). Longshore sand transport on beaches. *Journal of Geophysical Research, 75*(30), 5914–5927.

Longuet-Higgins, M. S. (1970). Longshore currents generated by obliquely incident waves. *Journal of Geophysical Research, 75*(33), 6778–6789.

Lujan, L. R., & Missimer, T. M. (2014). Technical feasibility of a seabed gallery system for SWRO facilities at Shoaiba, Saudi Arabia and regions with similar geology. *Desalination and Water Treatment*. doi:10.1080/19443994.2014.909630.

Maliva, R. G., & Missimer, T. M. (2010). Self-cleaning beach gallery design for seawater desalination plants. *Desalination and Water Treatment, 13*(1–3), 88–95.

Mantilla, D., & Missimer, T. M. (2014) Seabed gallery intake technical feasibility for SWRO facilities at Shuqaiq, Saudi Arabia and other global locations with similar coastal characteristics. *Journal of Applied Water Engineering and Research*. doi:10.1080/2349676.2014.895686.

Matin, A., Khan, Z., Zaidi, S. M. J., & Boyce, M. C. (2011). Biofouling in reverse osmosis membranes for seawater desalination: Phenomena and prevention. *Desalination, 281*, 1–16.

Missimer, T. M. (2009). *Water supply development, aquifer storage, and concentrate disposal for membrane water treatment facilities* (2nd ed.). Sugarland, TX: Schlumberger Water Services.

Missimer, T. M., Ghaffour, N., Dehwah, A. H. A., Rachman, R., Maliva, R. G., & Amy, G. (2013). Subsurface intakes for seawater reverse osmosis facilities: Capacity limitation, water quality improvement, and economics. *Desalination, 322*, 37–51. doi:10.1016/j.desal.2013.04.021.

Missimer, T. M., Jadoon, K. Z., Li, D., Hoppe-Jones, C., & Al-Mashharawi, S. (2014a) Hydrogeology and water quality of a coastal alluvial aquifer and its potential use as an intake system for a seawater reverse osmosis water treatment system, Thuwal, Saudi Arabia. *Hydrogeology Journal*. doi:10.1007/s10040-014-1168-3.

Missimer, T. M., Maliva, R. G., Dehwah, A. H. A., & Phelps, D. (2014b) Use of beach galleries as an intake for future seawater desalination facilities in Florida and globally similar areas. *Desalination and Water Treatment*, *52*(1–3), 1–8. doi:10.1080/19443994.2013.808406.

Morcos, S. A. (1970). Physical and chemical oceanography of the Red Sea. *Journal of Oceanography and Marina Biology, 8*, 73–202.

Pedgley, D. E. (1974). An outline of the weather and climate of the Red Sea. In: *L'oceanography physique de las Mer Rouge* (pp. 9–27). Paris: CNEXO.

Rachman, R. M., Li, S., & Missimer, T. M. (2014). SWRO feed water quality improvement using subsurface intakes in Oman, Spain, Turks and Caicos Islands, and Saudi Arabia. *Desalination*. doi:10.1016/j.desal.2014.07.032.

Sesler, K., & Missimer, T. M. (2012). Technical feasibility of using seabed galleries for seawater RO intakes and pretreatment: Om Al Misk Island, Red Sea, Saudi Arabia. *IDA Journal: Desalination and Water Reuse, 4*(4), 42–48.

Sofianos, S. S., Johns, W. E., & Murray, S. P. (2002). Heat and freshwater budgets in the Red Sea from direct observations at Bab el Mandeb. *Deep Sea Research Part III, 49*, 1323–1340.

Sofianos, S. S., & Johns, W. E. (2003). An oceanic general circulation model (OGCM) investigation of the Red Sea circulation, three-dimensional circulation in the Red Sea. *Journal of Geophysical Research: Oceans, 107*(C11), 17-1–17-11.

Sorensen, R. M. (2005). *Basic coastal engineering* (3rd ed.). New York: Springer.

Sunamura, T. (1992). *Geomorphology of rocky coasts*. New York: Wiley.

Tanner, W. F. (1960). Florida coastal classification. *Gulf Coast Association of Geological Societies Transactions, 10*, 259–266.

Chapter 8
Well Intake Systems for SWRO Systems: Design and Limitations

Robert G. Maliva and Thomas M. Missimer

Abstract Well intake systems are used globally for intakes to hundreds of medium to low capacity seawater reverse osmosis (SWRO) systems. Conventional vertical wells are the most commonly used type. Other types of well intake systems include slant wells, horizontal wells, and radial collector wells (Ranney wells). Selection of the well design type that best meets the feed water capacity requirement at a given site is based on the local hydrogeology, shoreline conditions, potential interference with other water users, and the capacity of the SWRO treatment plant. Selection of any type of well system or other subsurface intake requires that the operational risk for future performance must be carefully evaluated. Conventional vertical wells have exhibited long-term successful operation and therefore, have a low risk profile. Radial collector wells have been successfully operating for decades at locations where the hydrogeologic conditions are suitable for their use. Slant and horizontal wells are relatively new innovations as applied to use for SWRO intakes and few large-scale facilities are operating. These well types have a higher risk in terms of long term operation.

8.1 Introduction

The two main types of subsurface intakes are wells, and galleries and trenches. A well is defined by the U.S. Environmental Protection Agency as a bored, drilled, or driven shaft, or a dug hole, whose depth is greater than its largest surface dimension. Galleries or trenches, on the contrary, have shallow depths relative to their

R.G. Maliva (✉)
Schlumberger Water Services, 1567 Hayley Lane, Suite 202, Fort Myers, FL 33907, USA
e-mail: rmaliva@slb.com

T.M. Missimer
U.A. Whitaker College of Engineering, 10501 FGCU Boulevard South, Fort Myers FL 33965-6565, USA
e-mail: tmissimer@fgcu.edu

T.M. Missimer et al. (eds.), *Intakes and Outfalls for Seawater Reverse-Osmosis Desalination Facilities*, Environmental Science and Engineering,
DOI 10.1007/978-3-319-13203-7_8

largest surface dimension. Trenches are long narrow excavations, whereas galleries are wider features. Wells currently are by the far the most common type of subsurface intake in use for seawater water reverse osmosis (SWRO) desalination systems. Well intake systems can be divided into three main types; vertical wells, directionally drilled wells, and radial collector (Ranney) collector well systems. Directionally drilled wells include slant or angle wells and horizontal directionally drilled (HDD) wells. Vertical well and radial collector well seawater intake systems are essentially an application of long-used water well drilling techniques to produce seawater instead of freshwater. Slant and HDD well intake systems largely utilize (in some cases with modifications) existing drilling technologies developed for the oil and gas, utility (pipe installation), and water well and geotechnical industries.

The advantages of subsurface intakes for SWRO facilities in terms of reducing environment impacts (e.g., impingement and entrainment of marine organisms) and pretreatment costs are now widely recognized. Surface and subsurface intakes, including well systems, were reviewed by Missimer (1994, 2009), Voutchkov (2005), National Research Council (2008), Bartak et al. (2012), Mackey et al. (2011), WateReuse Association (2011) and Missimer et al. (2013). The above references include data presented herein on the locations and capacities of existing well and other intake system types. The fundamental challenge for the implementation of well intakes, and subsurface intakes in general, lies in selecting, designing, and constructing the intake types that can properly function based on given site physical, environmental, and hydrogeological constraints. These systems must cost-effectively provide the required feed water flow while also meeting feed water quality requirements.

8.2 Water Quality

Seawater produced from vertical wells tends to lower suspended solids concentrations, algae, bacteria, and organic compound fractions due to relatively long flow paths (and thus filtration potentials) and hydraulic retention (i.e., travel) times, provided that there is not significant bypass flow (Rachman et al. 2014; Chap. 9). Reported silt density indices from operational beach wells systems are on the order of 0.3–1 (Barak et al. 2012).

8.2.1 Oxygen-Reduction Issues in Wells

The quality of produced water can be impacted by the mixing of chemically dissimilar waters in production well fields. Redox (oxidation–reduction) reactions due to the mixing of chemically reducing and oxidizing waters can be particularly

problematic. Groundwater that is chemically reducing (i.e., has negligible dissolved oxygen) may have elevated concentrations of dissolved iron, which is in the soluble reduced ferrous (Fe^{2+}) state. Oxic groundwater, on the contrary, normally has very low dissolved iron concentrations, as iron in oxidizing environments tend to occur in the relatively insoluble ferric (Fe^{+3}) state. The mixing of anoxic and oxic waters can result in the precipitation of ferrous iron out of solution as iron oxyhydroxides, which can clog the well, piping, and the cartridge filters. The mixing of waters with different redox states can also result in the precipitation of other metals (e.g., manganese) and elemental sulfur. Iron precipitate has been reported as a problem in two of the SWRO facilities operating in Malta.

There are a number of different scenarios that could result in the mixing of waters with different redox states. Infiltrated seawater and landward derived waters could, for example, have different redox states. Aquifers may also be stratified with respect to dissolved oxygen concentration, with the shallowest groundwater (closed to the water table) having relatively high dissolved oxygen concentrations, whereas water produced towards the bottom of a well may be chemically reducing. Where more oxic groundwater enters a well from above, a solution to reduce the potential for adverse redox reactions is to case wells deeper to isolate the shallower oxic groundwater. Oxygen may also enter the feed water stream from the piping system not being air tight (Fig. 8.1).

Fig. 8.1 Elemental sulfur coating the cartridge filters at a SWRO plant in the Bahamas. An air leak in the centrifugal pump caused mixing of the raw water containing hydrogen sulfide with air, causing the precipitation of elemental sulfur that caused shutdown of the plant

8.2.2 Occurrence of Hypersaline Water in Some Coastal Aquifers

Coastal aquifers in arid regions may locally contain hypersaline water, which could be drawn into well intake systems (Missimer et al. 2014). It is therefore, important, to obtain information on the three-dimensional distribution of salinity in the vicinity of project sites. It is also important to determine if there are any known or potential areas of groundwater contamination that could impact a SWRO system (e.g., petroleum product spills) in the project site vicinity, which might be drawn into production wells. If hypersaline or contaminated groundwater is present, then an intake type would have to be selected and designed (e.g., beach or seabed gallery) that produces water essentially only from downward seawater infiltration.

8.2.3 Reduction in Organic Substances Achieved in Well Intake Systems

Recent research has demonstrated that well intakes tend to produce seawater having much lower concentrations of algae, bacteria, and organic compounds compared to surface seawater (Rachman et al. 2014; Dehwah et al. 2014; Chap. 9). Since bacteria and organic compounds in high concentrations in the feed water tend to cause membrane biofouling, it is very important to remove them before they enter the primary membrane process. Recent investigations have shown that using well intake systems that do not have breakthrough of unfiltered seawater can produce feed water with no detectable algae, a 95 % plus lower bacterial concentration, and substantial reductions in total organic carbon, transparent exopolymer carbon (TEP), and the biopolymer fraction of natural organic matter (Rachman et al. 2014; Dehwah et al. 2014).

8.3 Vertical Wells

Vertical wells constructed near the shoreline, commonly referred to as beach wells, are the least complex surface intake design. The wells are completed with an open hole or screen in a transmissive interval (production zone) that is hydraulically connected to the adjoining sea (Fig. 8.2). The pumping of the well draws in water radially from all directions within the production zone (including the landward direction), and vertically from above and below. However, where the production zone is hydraulically well connected to the sea, most of the water will be produced by induced infiltration (recharge) from the sea. If the connection to the sea is moderate or poor (e.g., semiconfining strata are present above the production zone), then the produced water could include a large fraction of landward derived fresh or

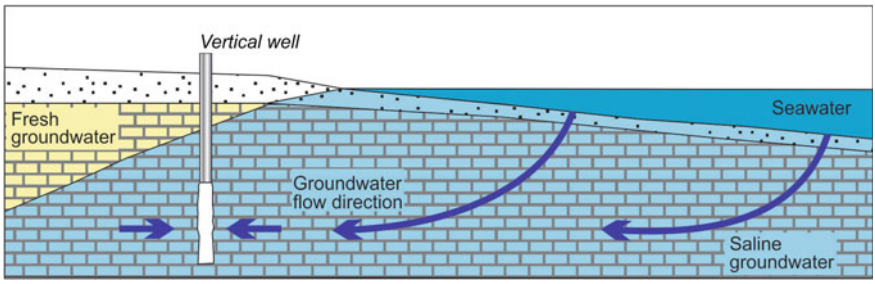

Fig. 8.2 Vertical well conceptual diagram

brackish groundwater. The production of water from landward aquifers could cause local environmental impacts (e.g., dehydration of wetlands) and contribute towards aquifer overdraft. The mixing of waters from different sources could result in adverse geochemical reactions (Sect. 8.2.3).

Vertical wells have the advantages of a minimal surface footprint, little or no environmental impact during construction and operation, low cost, and the availability of well drillers in most areas with the equipment and experience to construct the wells. Another important advantage of vertical wells is that they inherently have a modular design. Additional feed water capacity can be obtained by the installation of additional wells. Vertical wells also have the great advantage that their feasibility and performance at a given site can usually be evaluated by the installation of one or several relatively inexpensive test wells. The basic limitation of vertical wells is that their capacity is largely controlled by local hydrogeology, particularly aquifer transmissivity. An economically unviable large number of wells and shore frontage may be required to obtain the required feed water supply for large capacity SWRO systems or for SWRO systems constructed in areas where the local aquifers are poorly transmissive and individual well yields are low. Therefore, vertical wells are usually only considered as intakes for small to medium capacity SWRO facilities.

8.3.1 Implementation of Vertical Wells for SWRO Water Supply

Vertical wells are by far the most common type of subsurface intake currently in operation for SWRO systems. The finished water capacity of some of the larger systems is provided in Table 8.1. The vertical well feed-water capacity is typically twice or more (with back-up wells) of the finished water capacity. The largest operational system constructed to date is the 80,200 m^3/d capacity SWRO facility located in Sur, Oman (David et al. 2009). There are numerous small capacity systems constructed in coastal areas where the feed water supply is obtained from one or two shallow wells.

Table 8.1 Large SWRO plants that use vertical wells for feed water supply

Facility	Permeate capacity (m^3/d)
Sur, Oman	80,200
Pemroke Plant, Malta	54,000
Bay of Palma, Mallorca, Spain	42,000
Blue Hills, Nassau, Bahamas	45,000
W.E.B. Aruba (Phase I and II)	32,000
Gap Lapsi, Malta	24,000
Cirkewwa, Malta	18,600

A common denominator of the large vertical well intake systems listed in Table 9.1 is that they are all constructed in areas in which the shallow geology consists predominantly of carbonate (limestone) strata. Groundwater flow in carbonate aquifers is dominated by secondary (karstic) porosity, which may result in high transmissivities and thus high well yields. Vertical wells completed in karstic limestones often have yields of 3,800 m^3/d per well or greater. The largest system using vertical wells completed in siliciclastic strata is located near Jeddah, Saudi Arabia, with a permeate capacity of 10,000 m^3/d, which is supplied by 10 wells.

8.3.2 Vertical Well Construction

The drilling and construction of vertical intake wells for SWRO facilities is essentially the same as that for freshwater production wells. Water well construction and testing procedures have been reviewed by Driscoll (1986), Roscoe Moss Company (1990), Misstear et al. (2006) and Sterrett (2007). Missimer (2009) provided a detailed analysis of well construction design and construction for SWRO application. As is the case for freshwater production wells, vertical intake wells should be constructed to maximize well efficiency. Saltwater is corrosive and, therefore, SWRO intake wells should be constructed with corrosion resistant materials. Inasmuch, as subsurface intakes wells are normally shallow, polyvinyl chloride (PVC) or fiberglass casings are suitable and recommended. Well screens, if needed, should also be constructed of non-metallic materials or corrosion resistant steel alloys (e.g., Duplex 2205 stainless steel or another super duplex stainless steel alloy).

Bentonite-based drilling muds can result in the direct fouling of membranes by passing through the cartridge filter (fine clay size) or through the formation of colloidal silica. Bentonite-based drilling muds should, therefore, be avoided for the completion interval of wells to be used for a SWRO intake. However, bentonite-based drilling muds may be safely used for drilling of boreholes for cemented casing strings. Reverse-air rotary, dual-rotary (dual-tube), and combination air rotary and percussion hammer methods are preferred for drilling boreholes in the production zone. The mud-rotary methods could also be used with biodegradable

drilling fluids. However, organic drilling fluids, if not completely removed, could result in biological clogging of wells or problems with bacterial clearance for certification by local health agencies.

Where vertical intakes wells are installed in lithified strata, such as carbonate rock, the preferred construction method is to set a casing at the top of the production zone and then complete the well using an open hole drilling method that utilizes only water or air as a drilling fluid. For wells with a screened completion, a dual-tube drilling method is attractive in that the outer casing supports the borehole during screen and filter pack installation and well grouting, as opposed to using drilling mud to stabilize the borehole.

8.4 Directionally Drilled Wells

Directionally drilled wells that have been or potentially may be used for well intakes for SWRO facilities include:

- Slant or angle wells
- Horizontal directionally drilled wells with dual pits or surface access points (utility-type directional drilling)
- Horizontal directionally drilled wells with a single surface access point (oilfield-type directional drilling.

The advantages of directionally drilled wells include:

- Greater exposure of the borehole (screen) to the production formation, which allows for greater well yields
- Drilling pad and wellhead can be offset from the shore (beach) and thus be positioned in a safer and less visually obtrusive location
- Multiple wells can originate (fan out) from a single surface location, which reduces surface disturbance, reduces land requirements, and reduces costs
- Well screen or liner can be positioned offshore to reduce the production of landwards derived water, and associated geochemical incompatibility challenges.

The principal disadvantages of directionally drilled wells are that they are more complex to construct, and thus much more expensive than vertical wells. A potential cost saving lies in that a horizontal well may have the yield of multiple vertical wells. A basic challenge in directional drilling is that boreholes are prone to collapse under gravity and difficulties occur in emplacing gravel and sand packs and to achieve proper development. The availability of local drillers with the appropriate equipment and expertise and experience may also be a constraint in some locations.

8.4.1 Slant Wells

Slant or angle wells, as the names implies, are straight wells that are drilled at an angle (Fig. 8.3). Slant well technology including the results of a test well program at Dana Point, California, was reviewed by Williams (2008, 2009) and Chap. 13 of this volume. Use of slant wells for feed water supply for SWRO plants is a new application of existing technologies. Indeed, angled wells have a long history in the oil and gas industry, including as a disreputable means of tapping oil reserves on neighboring properties (early days). As discussed by Williams (2008, 2009), the preferred means for installing slant wells, especially in unconsolidated strata, is use of the dual-rotary method, in which the outer casing supports the borehole while the screen and filter pack is installed. "Barber" dual-rotary drilling rigs (developed by in 1979 by Barber Industries, now Foremost Industries) have slant well capabilities suitable for seawater intakes and are fairly widely available (Herrick 1994; Henahan 1999; Foremost Industries 2003).

To the author's knowledge, slant wells are currently not in operation at any SWRO plant globally, but they are under consideration for several desalination projects in California where environmental concerns are a major constraint on desalination projects.

8.4.2 Utility-Type HDD Wells

HDD has been used in the utility industry since the 1970s for long subsurface crossings of underground pipes, conduits, and cables. Boreholes are drilled at a shallow angle from an entry (launch) point to a distant exit point. The drilling process typically involves three steps (Fig. 8.4). A small diameter pilot hole is drilled from the entry to exit point. The pilot hole is next reamed to achieve the target borehole diameter. Finally, the pipe, conduit or cable, is installed by pulling from the exit point to the entrance point. Shallow horizontal wells can be constructed using this method by installing a screen in the borehole. Neodren® drain

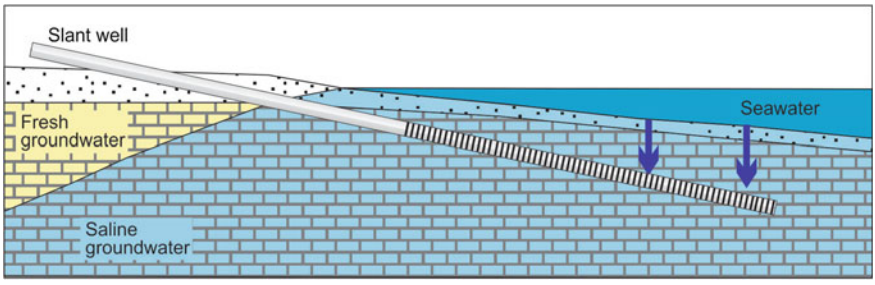

Fig. 8.3 Slant well conceptual diagram

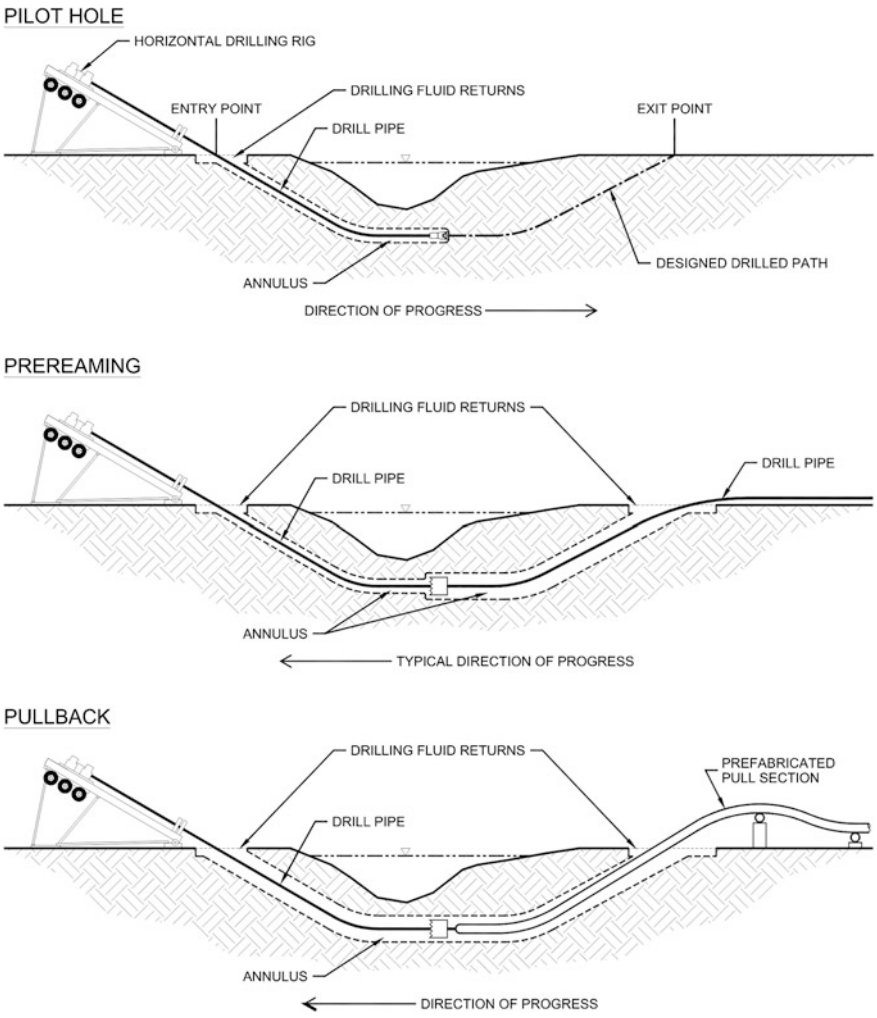

Fig. 8.4 Utility-type HDD well construction sequence *Source* U.S. Fish and Wildlife Service

technology is essentially a modification of the utility-type horizontal direction drilling in which a porous and permeable pipe filter is installed at a shallow depth (typically ≈ 4–7 m) below the seabed (Peters et al. 2007; Peters and Pintó 2010). The produced water reportedly requires pretreatment by ultrafiltration, minimizing the need for chemical use. The exit point is located subsea, which requires the use of boats and divers to construct the system. The distal end of the annulus between the pipe and borehole is sealed with cement.

Noedren® wells can be installed in a radial fan pattern from a single drilling pad and pump station site, which minimizes the surface footprint of the systems.

The largest SWRO facility currently using Neodren drain technology is the San Pedro del Pinatar Phase I system in Alicante, Spain, which has a permeate capacity of 65,000 m^3/d. The feed water system for the plant was provided by 20 drains, which is equal to a design average feed water production rate of 6,500 m^3/d per drain. Published data are not available on the long-term performance of Neodren drain systems. Half or more of the feed water for the San Pedro del Pinatar Phase I system is now provided by a water tunnel system. Recent research at the site on water quality has found that the Neodren system is not operating well compared to the vertical wells and water tunnel located on the site (Rachman et al. 2014).

Key feasibility and design issues are that a transmissive formation must be present at shallow depths below the seabed. The intervening strata between the seabed and production zone must have a sufficiently high hydraulic conductivity to allow for an adequate filtration rate while also provide sufficient filtration for removal of suspended sediments, algae, bacteria, and some organic compounds.

8.4.3 Oilfield-Type HDD Wells

Horizontal direction drilling has revolutionized the oil and gas industry, but has much less application to date for water supply projects. An oilfield-type HDD well would be drilled in a similar manner as the pilot hole for a utility-type well, but without the emergence from the aquifer (Fig. 8.4). After completion of the borehole drilling, the drill string would be removed and the casing and string installed. Depending on the turn radius of the drilling equipment and desired depth of the horizontal segment, the well may be started either as a vertical or slant well. Oilfield-type HDD wells would work best in lithified strata in which borehole integrity can be more readily maintained (less risk of collapse), such as in lithified aquifers. An important technical challenge would be developing the well to remove all introduced drilling fluids.

8.5 Radial Collector Wells

Radial collector wells, which are often referred to as horizontal collector wells and "Ranney®" wells, after their inventor Leo Ranney, have been used to produce freshwater in riverbank filtration systems since the 1930s. Radial collector well intake systems are in essence a variation of riverbank filtration in which saline water, rather than freshwater, is produced. The characteristic features of a radial collector well is a large-diameter reinforced concrete caisson (shaft) through which radially-oriented, screened laterals are installed (Fig. 8.5). The laterals are constructed in relatively high-transmissivity strata in order to maximum yields. For riverbank filtration systems, laterals are commonly installed in gravel intervals. The great advantage of radial collector wells is that a single well can produce the same

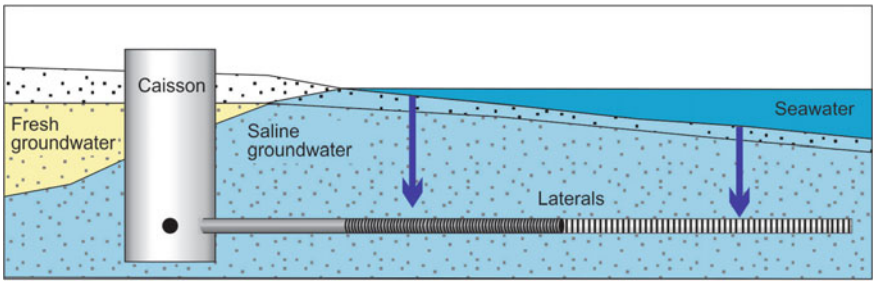

Fig. 8.5 Radial collector well conceptual diagram

volume of water as several vertical wells with a smaller footprint. Radial collector wells are a well-proven technology with hundreds of wells globally installed and there is ample operational data on their ability to removed suspended particles, including pathogenic microorganisms.

Radial collector wells are used to a much more limited extent as a subsurface intake for SWRO systems. A design modification is that laterals may be installed only in the seawards direction, so as to minimize production of landward-derived water. The largest radial collector system for an operating SWRO facility is the Pemex Salina Cruz refinery plant, which has three 15,000 m^3/d collector wells and a permeate capacity of 15,000 m^3/d. A planned seawater radial collector system for backup cooling water supply for a nuclear power plant expansion in Miami-Dade County, Florida, will consist of four wells each with a design capacity of 163,600 m^3/d. Hence, where local hydrogeological conditions are favorable, radial collector wells are capable of meeting the feed water demands for very large SWRO facilities.

The location of a radial collector well on the beach is a significant issue. There is a construction limit on the length of the radials that can be installed for a given caisson diameter. One contractor will not bid on any design that contains a radial length greater than about 60 m. This would require the well to be located very close to the intertidal zone of the beach, making it subject to storm damage and erosion, separation from the shore by beach progradation, and may appear as a visual nuisance. If the well were to be constructed further away from the sea, the water yielded to it would be a combination of seawater and landward derived freshwater or brackish water. This could cause landward aquifer impacts or problem with mixing water qualities within the well (geochemical reactions).

Another issue in the use of a high capacity radial collector well is in maintaining it during operation. Maintenance would likely require shutdown of the well and therefore, would cause the necessity to construct at least one standby well to allow continuous operation of the SWRO facility. The construction of a backup system would greatly raise the system cost.

8.6 Selection of Well Intake Types

The optimal well intake design option for a given site will depend upon a variety of site hydrogeological, and logistical factors, which ties into economic considerations. The optimal intake system for a given site is that which reliably provides, at the lowest cost, the required volume of feed water at the target quality, while meeting all site environmental and logistical constraints. Intake system costs are highly site-specific and no meaningful generalizations can be made. A vertical well is the least expensive intake element to construct, but a HDD or radial collector well may provide as much water as several vertical wells. There is no generic conversion factor between the different well types.

A key issue in the selection of intake type is performance risk, which is essentially the degree of uncertainty over whether or not the intake will meet performance criteria over the operational life of the facility. Performance risk includes the probability that a system can be constructed with its target water capacity and water quality requirement, and the likelihood that the system can be cost-effectively maintained over its operational life. Risk can be reduced through the collection of additional data, particularly through pilot testing. Performance risk thus ties into investigation costs, which is the investment required to determine whether or not an intake system type is feasible at a site and to obtain data needed for system design. Vertical wells have a relatively low performance risk, because their performance can be readily and economically evaluated through a test well program. Vertical wells, in general, are also a very well-established technology and the various methods to construct and maintain them are understood.

Slant, HDD, and radial collector wells have a greater performance risk, because of the much greater costs to test these systems, which may preclude adequate pilot testing. For example, pilot testing of a radial collector well requires a very large financial commitment to install a caisson and one or more laterals. In the absence of long-term operational data, the long-term reliability of slant and HDD wells is also open to question. Rehabilitation of these wells would be expected to be far more complex and expensive than that of vertical wells. Some question arises whether effective maintenance can be performed on non-vertical wells surrounded with an artificial filter pack, because of gravity fall of the gravel during standard compressed air or water jet cleaning.

Non-vertical (slant, HDD, and radial collector) wells have their greatest value at sites where shoreline access (e.g., beach frontage) is limited, which may preclude the use of numerous vertical wells. A series of slant or HDD wells constructed from single pad or a radial collector well may have a much smaller footprint than a series of vertical wells.

Water quality is an additional consideration in the selection and design of well intake systems. The objective of subsea intakes is to produce seawater derived from the local infiltration of seawater through the seabed. The mixing of infiltrated seawater with landward derived fresh and brackish water could result in adverse fluid-rock interactions. Slant, HDD, and radial collector well systems completed

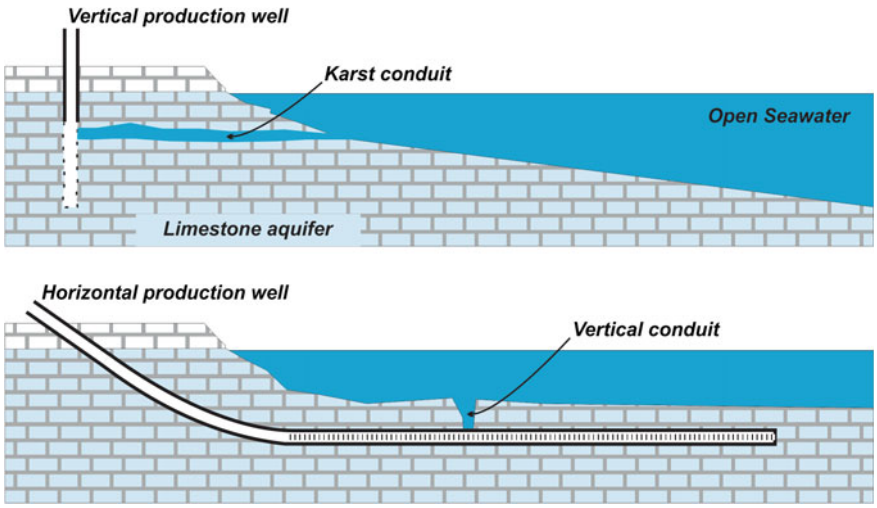

Fig. 8.6 Bypass flow may occur due to horizontal (*top*) or vertical (*bottom*) conduits

subsea may be geochemically more stable as they would tend to induce vertical (downward) flow of infiltrated seawater, provided that the subsea completion zone is hydraulically well connected to the seabed. If intervening confining or semi-confining strata are present, then vertical flow would be reduced and more land-ward-derived water produced. Also, in semi-confined aquifers located beneath the sea, the water may have adverse redox conditions that can produce high concentrations of dissolved iron or manganese (experienced at a California test site) and/or contain brackish-water with a changing water quality in time.

The hydraulic connection between the production zone and the seafloor should not be so good that filtration is bypassed. Bypass flow is a possibility in karstic limestone aquifers, where conduits might directly connect vertical wells with the sea, and thus, avoiding the filtration provided by seabed sediments and aquifer rock (Fig. 8.6). The potential for bypass flow may be reduced by setting vertical well casings at a greater depth than any near-shore subsea outcrop of the production zone. The same issue can cause bypassing of flow in horizontal wells where vertical karst conduits are present in carbonate aquifer systems.

8.7 Investigation of Well Intake Options

Investigation of well intake options starts with an aquifer characterization, which can be divided into desktop and field testing phases (Chap. 7). The desktop phase involves review of available existing information on the hydrogeology of the project site vicinity, which may include technical reports prepared by governmental agencies, consultants, and academic researchers, unpublished reports (e.g., geotechnical

studies), governmental databases, historical aerial photographs and bathymetric maps. Usually well data along the coast is limited, because there is little interest in the parts of the aquifers that contain seawater. However, useful data on the hydrogeology of coastal aquifers may be available from more inland areas where the aquifers contain freshwater. A site visit is also recommended to evaluate logistical issues (e.g., availability of potential well sites) and to obtain information about local geology (e.g., from examination of nearby outcrops). The main objective of the desktop investigation is to obtain an initial estimate of potential well yields and water quality. Bathymetric information is important for evaluating the outcrop depths of potential production zones and thus, travel distances offshore.

The scope of field investigations is project specific and quite variable. Typically, the first element is the drilling of test wells to obtain information on site-specific geology. Single-well pumping tests are usually performed to obtain initial information on potential well yields and aquifer hydraulic properties. The test well program is often followed by the installation of a large diameter vertical test production well and perhaps some additional monitor wells. An aquifer performance (pumping) test is then performed to obtain more accurate data on aquifer hydraulic parameters and water quality. Silt density index (SDI) should be measured during the test to determine an estimate of the filtration capacity of the system. The produced water during the test should also be sampled and analyzed for the SW RO design parameters and organic constituents to determine the biofouling potential. For an HDD well system, subsea test borings will be required to obtain information on aquifer properties along potential well tracks.

The preliminary design phase of well intake projects should involve groundwater modeling, which is used to evaluate various design options. Density-dependent solute-transport modeling should be the performed if the aquifer locally contains water of varying salinity. Variables to be evaluated by modeling are potential wellfield configurations (number of wells, well separation and locations), drawdowns (which would affect pumping rates and pump depths), and the source of produced waters (e.g., induced seawater infiltration versus flow from landwards direction).

8.8 Conclusions

Well intake systems, which include vertical, directionally drilled (slant and HDD), and radial collector (Ranney) wells, are the preferred option for subsurface intakes for SWRO systems where a coastal aquifer is present that has a high enough transmissivity to allow for economic well yields (i.e., an unreasonably large number of wells is not required to obtain the required feed water volume).

Vertical wells are generally the preferred option where they have sufficient yields, because of their low performance risk. The vertical well intake option can be readily pilot tested and the wells can be constructed and maintained using standard methods. However, an unfeasibly large number of vertical wells may be required for large-capacity SWRO systems.

Slant, HDD, and radial collector wells have the advantages of larger capacities and thus, smaller footprints, which may be a key issue for sites in which shoreline access is limited. Determination of the optimal intake system type and design for a given site requires a detailed aquifer characterization including groundwater modeling, and economic analysis. Water chemistry stability (i.e., absence of adverse fluid-mixing and fluid-rock interactions) is also a consideration, and the extent to which this is an issue is highly site-specific.

References

Bartak, R., Grischek, T., Ghodeif, K., & Ray, C. (2012). Beach sand filtration as pre-treatment for RO desalination. *International Journal of Water Sciences, 1*(2), 1–10.

David, B., Pinot, J., & Morillon, M. (2009). Beach wells for large-scale reverse osmosis plant: The Sur case study. Proceedings of the International Desalination Association World Congress on Desalination and Water Reuse. Dubai, UAE, DB09-16, 10 pp.

Dehwah, A. H., Al-Mashharawi, S., Kammourie, N., & Missimer, T. M. (2014). Impact of well intake systems on bacterial, algae, and organic carbon reduction in SWRO desalination systems, SAWACO, Jeddah, Saudi Arabia. Desalination and Water Treatment, (ahead-of-print), 1-7 pp.

Driscoll, F. G. (1986). *Groundwater and wells* (2nd edn.). St. Paul, Minnesota: Johnson Filtration Systems, 1089 pp.

Industries, Foremost. (2003). *Benefits of dual rotary drilling in unstable overburden formations*. Calgary, Canada: Foremost Industries. 19 p.

Herrick, D. (1994). Dual-rotary drilling—is it for you. *Water Well Journal*, *48*, 50–54.

Henahan, M. (1999) Dual rotary drilling in unconsolidated overburden. *Water Well Journal*, *53*, 66–68.

Mackey, E. D., Pozos, N., James, W., Seacord, T., Hunt, H., & Mayer, D. L. (2011). *Assessing seawater intake systems for desalination plants*. Denver, CO: Water Research Foundation. 172 p.

Missimer, T. M. (1994). *Water supply development for membrane water treatment facilities*. Boca Raton, Florida: Lewis Publishers. 253 p.

Missimer, T. M. (2009). *Water supply development, aquifer storage, and concentrate disposal for membrane water treatment facilities* (2nd ed.). Methods in Water Resources Evaluation Series No. 1 Houston, Texas, Schlumberger Water Services, Sugar Land, Texas.

Missimer, T. M., Ghaffour, N., Dehwah, H. A., Rachman, R., Maliva, R. G., & Amy, G. (2013). Subsurface intakes for seawater reverse osmosis facilities: Capacity limitation, water quality improvement, and economics. *Desalination, 322*, 37–51.

Missimer, T. M., Jadoon, K. Z., Li, D., Hoppe-Jones, C., & Al-Mashharawi, S. (2014). Hydrogeology and water quality of a coastal alluvial aquifer and its potential use as an intake system for a seawater reverse osmosis water treatment system, Thuwal, Saudi Arabia. *Hydrogeology Journal*, Doi: 10.1007/s10040-014-1168-3.

Misstear, B., Banks, D., & Clark, L. (2006). *Water wells and boreholes*. Chichester, England: Wiley. 498 p.

National Research Council. (2008). *Desalination—A National Perspective*. Washington, D. C.: National Academies Press. 298 p.

Peters, T., Pintó, D., & Pintó, E. (2007). Improved seawater intake and pre-treatment system based on Neodren technology. *Desalination, 201*(1–3), 134–140.

Peters, T., & Pintó, D. (2010). Seawater intake and partial pre-treatment with Neodren—results from investigation and long-term operation. *Desalination and Water Treatment, 24*(1–3), 117–122.

Rachman, R. M., Li, S., & Missimer, T. M. (2014). SWRO feed water quality improvement using subsurface intakes in Oman, Spain, Turks and Caicos Islands, and Saudi Arabia. *Desalination 351*, 88–100. Doi: 10.1016/j.desal.2014.07.032.

Roscoe Moss Company. (1990). *Handbook of ground water development*. New York: Wiley. 493 pp.

Sterrett, R. J. (2007). *Groundwater and wells* (3rd ed.). St. Paul, Minnesota: Johnson Screens, 812 pp.

Voutchkov, N. (2005). SWRO desalination: On the beach—seawater intakes. *Filtration and Separation, 10*, 24–27.

WateReuse Association. (2011). Overview of desalination plant intake alternatives. White Paper, June 2011, WateReuse Association, Alexandria, VA, 19 p.

Williams, D. E. (2008). *Research and development for horizontal/angle well technology*. Desalination and Water Purification Research and Development Program Report No. 151, U.S. Department of the Interior Bureau of Reclamation, Denver CO, 62 p.

Williams, D.E. (2009). *Results of drilling, construction, development, and testing of Dana Point ocean desalination project test slant well*. Research and Development for Horizontal/Angle Well Technology, Desalination and Water Purification Research and Development Program Report No. 152, U.S. Department of the Interior Bureau of Reclamation, Denver CO, 62 p.

Chapter 9
Effects of Well Intake Systems on Removal of Algae, Bacteria, and Natural Organic Matter

Rinaldi Rachman, Abdullah H.A. Dehwah, Sheng Li, Harvey Winters, Samir Al-Mashharawi and Thomas M. Missimer

Abstract Analyses of the changes in concentration of algae, bacteria, transparent exopolymer particles (TEP), and the fractions of natural organic matter (NOM) impacts between surface seawater and the discharges of well intake systems were evaluated at seven different seawater reverse osmosis water (SWRO) treatment plants. In nearly all cases, travel of the raw seawater through the seabed into the aquifer and into the wells removed all of the algae. Bacteria removal was up to 98.5 %, but varied greatly between sites and in different wells at each site. The TEP concentration was significantly lowered compared to the natural seawater. The biopolymer fraction of NOM was significantly lowered at all sites, but the lighter fractions of the NOM were removed at lower percentages. The removal percentage of NOM fractions appears to be based on molecular weight (and size) with the lighter weight fractions removed at lower percentages. A key factor controlling the removal of organic material appears to by the hydraulic retention time which is controlled by the length of the flowpath and the type of aquifer porosity. Specific

R. Rachman · A.H.A. Dehwah · S. Li · S. Al-Mashharawi
Water Desalination and Reuse Center, King Abdullah University of Science and Technology, Thuwal, Saudi Arabia
e-mail: rinaldi.rachman@kaust.edu.sa

A.H.A. Dehwah
e-mail: abdullah.dehweh@kaust.edu.sa

S. Li
e-mail: sheng.li@kaust.edu.sa

S. Al-Mashharawi
e-mail: samir.mashharawi@kaust.edu.sa

H. Winters
Fairleigh Dickinson University, Teaneck, USA
e-mail: harvey@fdu.edu

T.M. Missimer (✉)
U.A. Whitaker College of Engineering, Florida Gulf Coast University, Fort Myers, FL, USA
e-mail: tmissimer@fgcu.edu

T.M. Missimer et al. (eds.), *Intakes and Outfalls for Seawater Reverse-Osmosis Desalination Facilities*, Environmental Science and Engineering,
DOI 10.1007/978-3-319-13203-7_9

site geology does not seem to be a significant factor. Vertical well systems showed greater organic materials removal compared to horizontal and tunnel intake systems. Again, this appears to be related to the length of the flowpath and the hydraulic retention time. The horizontal well system at Alicante, Spain showed poor removal of organic matter and breakthrough of algae occurred in the system.

9.1 Introduction

The marine environment is biologically active and productive, containing a variety of living organisms and natural organic compounds. Seawater reverse osmosis (SWRO) water treatment systems extract raw feed water from the sea, in most cases via open-ocean intakes that provide no real degree of pretreatment. Organic matter in seawater has a significant effect on the operation of seawater reverse osmosis membranes with the common result being biofouling (Flemming 1997; Flemming et al. 1997). There are relationships between concentration of organic matter in the feed water entering a SWRO facility, the type of pretreatment, the biological activity within the pretreatment and process trains, and the rate of membrane biofouling (Dehwah et al. 2014b).

In recent years, research on biofouling has focused on membrane conditioning and subsequent attachment of bacteria to the deposited substrate, leading to biofilm creation. The role of sticky polysaccharides and biopolymers on membrane conditioning as the precursors for membrane biofouling has been explored and many scientists conclude that transparent exopolymer particles (TEP) may be a key substance that has the most impact (Berman and Passow 2007; Bar-Zeev et al. 2009; Berman 2010; Berman et al. 2011). TEP is produced by algae and bacteria as an extracellular excretion of a "soup" of organic compounds which undergo self-assembly with the water column (Passow and Alldredge 1994; Passow 2000). Once TEP attaches to the membrane surface, it facilitates the attachment of bacteria which also use it as a food source (Villacorte et al. 2009b). An important issue is to remove as much of the dissolved natural organic material, TEP, and bacteria as possible in the pretreatment process to lessen the rate of biofouling.

Pretreatment in SWRO facilities can be quite intense (Kumar et al. 2006; Vedavyasan 2007). It commonly involves numerous processes ranging from conventional screening and mixed media filtration to use of conditioning filters followed by membrane filtration. Another strategy is to use a prefiltering stage followed by dissolved air flotation coupled with the use of a coagulant, such as ferric chloride, followed by additional filtering. The intensity of the pretreatment process train and cost of operation associated with it is based on the overall concentration of the organic matter in the feed water (Ghaffour et al. 2013). Therefore, any improvements that can be made to the quality of the feed water will lessen the complexity of the pretreatment process and reduce cost. Despite the use of quite extensive pretreatment processes, many SWRO facilities still suffer a high rate of biofouling with the necessity for frequent membrane cleaning.

Use of subsurface intake systems is known to improve the quality of feed water and lessen the environmental impacts in SWRO systems (Missimer 2009; Missimer et al. 2013; Table 9.1). The most common type of subsurface intake system uses various types of wells (Chap. 8). Pumping of wells located near the shoreline forces water in the sea to pass vertically through the seabed into the underlying aquifer, and then through the aquifer horizontally into the well (Fig. 9.1). The passage

Table 9.1 Comparison between bacteria, algae, organic carbon compound concentrations in natural seawater verses well intakes from select sites (modified from Missimer et al. 2013)

Location	Parameter	Seawater	Well 1	Well 2	Well 3	Well 4
Dahab, Egypt (Hassan et al. 1997)	DOC (mg/L)	1.6	1.2	2.3	0.6	0.8
	UV-254 (m^{-1})	1.4	0.8	0.9	0.8	0.6
Fuerteventura Island, Spain (Teuler et al. 1999)	TOC (mg/l)	0.5	0.7			
	UV-254 (m^{-1})	0.36	0.55			
	Phytoplancton, cell/L	57,720	0			
Al-Birk, Saudi Arabia (Jamaluddin et al. 2007)	Dissolved protein (mg/L	2.73 ± 0.78	0.75 ± 0.08	ND	ND	
	Dissolved carbohydrates (mg/L)	1.57 ± 0.23	0.52 ± 0.15	0.77 ± 0.10	0.50 ± 0.14	
SWCC Al-Jubail Test Site (Hassen et al. 1997)	TOC (mg/L)	2	1.2–2			
	Bacteria (CFU/mL), 0, 24, and 72 h	1.8×10^3	1.3×10^3			
		1.1×10^5	3.3×10^5			
		5.6×10^4	4.0×10^6			
Daheb beach well system, Egypt (Bartak et al. 2012)	DOC (mg/L)	1.6	1.2	2.3	0.6	0.8
	UV-254 (m^{-1})	1.4	0.8	0.9	0.8	0.6
Mediterranean location-Spring (Choules et al. 2007)	Total Picophyto-plankton (cells/mL)	1.6×10^3	1.3×10^2			
	Synechococcus (cells/mL)	1.3×10^3	1.0×10^2			
	Picoeukaryote (cells/mL)	1.1×10^3	1.9×10^1			
	Nanoeukarote (cells/mL)	1.2×10^2	1.7×10^0			
Site 1 (LaParc et al. 2007)	TOC (mg/L)	1.2	0.9			
	Polysaccharides (mg/L)	0.12	0.01			
	Humic substances + building blocks (mg/L)	0.5	0.4			
	Low-molar mass acids and neutrals (mg/L)	0.25	0.16			
	Low molar mass compounds (mg/L)	0.33	0.29			
Site 2 (LaParc et al. 2007)	TOC (mg/L)	0.9	0.6			
	Polysaccharides (mg/L)	0.4	ND			
	Humic substances + building blocks (mg/L)	0.26	0.16			
	Low-molar mass acids and neutrals (mg/L)	0.22	0.13			
	Low molar mass compounds (mg/L)	0.38	0.3			

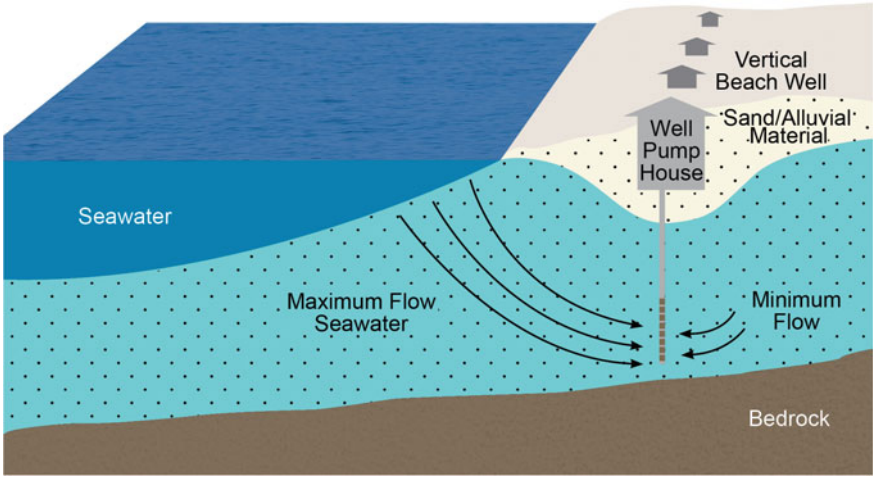

Fig. 9.1 Schematic diagram showing induced aquifer flow from the sea to a well (from Missimer et al. 2013)

through the aquifer system causes changes to occur in the feed water by removal of various substances, normally improving water quality by removal of particulates and some dissolved organic compounds (Missimer and Winters 2000, 2003; Schwartz 2003; Choules et al. 2007; Laparc et al. 2007; Missimer 2009; Missimer et al. 2013). Recently collected data show that well systems can be very effective in the removal of algae, bacteria, and natural organic matter (NOM), including TEP (Dehwah et al. 2014a, b, c; Rachman et al. 2014). It is the purpose of this chapter to summarize the most recent data on the effectiveness of well intake systems in the removal of algae, bacteria, TOC, NOM fractions, and TEP from the raw water.

9.2 Methods

9.2.1 Sampling Sites and Methods

Detailed research on organic substances removal by well intakes systems is reported for 9 systems located in Saudi Arabia (4), Spain (3), Turks and Caicos Islands (1), and Oman (1) (Dehwah et al. 2014a, b; Rachman et al. 2014). Most of these well intakes use conventional vertical wells with the exception of two sites in Spain which have a horizontal well system and a water tunnel containing radial collectors. The wells in Spain, the Turks and Caicos Islands, Oman and one system in Saudi Arabia are constructed into carbonate rocks or sediments. The other wells in Saudi Arabia were constructed into siliciclastic sediments consisting of alluvial outwash sands and gravels.

Water samples were collected from different locations within or near the facilities including surface seawater, at the well discharge, at the aggregated intake pipeline (blend of all wells), at the media filter outlet, and at the cartridge filter outlet and placed into the appropriate types of bottles, and transported to the lab facilities the same day inside coolers containing ice. Data reported in this chapter include only those collected from the raw seawater, at the wellhead discharges, and the aggregated well intake pipe.

After water sampling, a 0.02 % (w/v) sodium azide solution was added to the TEP sample bottles for fixation and to limit the bioactivity. For samples collected for bacterial and algae quantification, glutaraldehyde was added for fixation immediately after sampling. All the samples were stored at 4 °C and analyzed within 7 days of sample collection. Proper sampling, quality control and assurance measures were used based on the type of analyses to be performed.

9.2.2 TEP Measurement

In this research two types of TEP were investigated, particulate and colloidal. Particulate TEP has a size >0.4 μm, while colloidal TEP ranges in size from 0.05 to 0.40 μm (Villacorte et al. 2009a). Particulate TEP is formed predominantly by the self-assembly of precursor substances, such as dissolved polysaccharides and biopolymers, that are produced by algae and bacteria (Passow and Alldredge 1994; Passow 2000, 2002).

Analysis of TEP was accomplished based on the method developed by Passow and Alldredge (1995). A staining solution was prepared from 0.06 % (m/v) Alcian Blue 8GX (Standard Fluka) in an acetate buffer solution (pH 4) and freshly prefiltered through a 0.2 μm polycarbonate filter before usage. Between 150 and 300 mL of seawater from each water sample was filtered through a 0.4 μm pore size polycarbonate membrane using an adjustable vacuum pump at low constant vacuum. After filtration, the membrane was rinsed with 10 mL of Milli-Q water to avoid the coagulation of Alcian blue once it came into contact with the seawater in the staining process. The retained TEP particles on the membrane surface were then stained with Alcian Blue dye for 20 s. After staining, the membrane was flushed with 10 mL of Milli-Q water to remove excess dye. The flushed membrane was then placed into a small beaker, where it was soaked in 80 % sulfuric acid for 6 h to extract the Alcian Blue dye that was bound to the TEP. Finally, the absorbance of the acid solution was measured using a UV spectrometer at a 752 nm wavelength to determine the TEP concentration. The same methodology was applied to determine the colloidal TEP. The only difference is that, water sample permeate from the 0.4 μm polycarbonate membrane was filtered through a 0.1 μm pore size membrane to allow deposition of the colloidal TEP on the membrane surface.

In order to relate the UV absorbance values to estimated TEP concentrations, a calibration curve was established. Xanthan gum solutions with different volumes (0, 0.5, 1, 2, 3 mL) were used to obtain a calibration curve (Fig. 9.2). The TOC

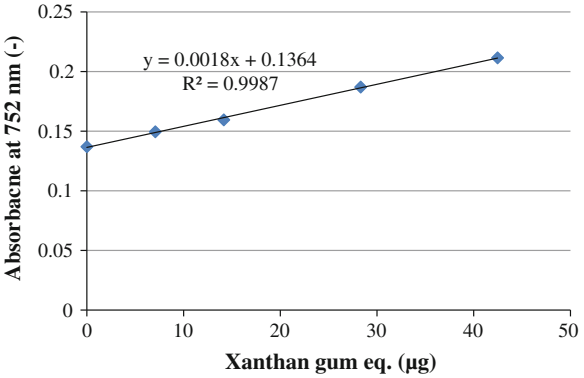

Fig. 9.2 Example of a xanthan gum calibration curve used to measure TEP concentration (from Dehwah et al. 2014c)

concentrations of xanthan gum before and after 0.4 µm filtration were analyzed, and the TOC concentration difference was used to calculate the gum mass on each filter. The TEP concentration then estimated using the calibration curve. The same procedures were used for the 0.1 µm membrane to establish the calibration curve for colloidal particles. Afterwards, the TEP concentration was expressed in terms of xanthan gum equivalent µg/L by dividing the TEP mass on the corresponding volume of TEP samples. Because particulate and colloidal TEP is measured indirectly, these values must be considered to be semi-quantitative.

9.2.3 Algae and Bacteria Quantification

Counts of the number of algae and bacteria in the water samples were determined using a flow cytometer manufactured by BD Bioscience FACSVerse. Algal cell counting was performed by combining 1 mL of each sample with a 2 µL volume of a standard containing 1 µm beads into a 10 mL tube. The tube was then vortexed and measured using high flow with a 200 µL injection volume. The counting procedure was repeated three times to assess the precision of the measurements.

For bacterial counts, a comparative protocol employing SYBR® Green stain was used. A volume of 1 mL from each sample was transferred to a 10 mL tube, incubated in a 35 °C water bath for 10 min and stained with the SYBR® Green dye (10 µL into 1 mL aliquot), vortexed, and incubated for another 10 min. The prepared samples were then analyzed in a low flow setting with a 9 µL injection volume. Triplet measurements were made on each sample to assess measurement precision.

9.2.4 Organics Analysis Using the LC-OCD Methodology

A Shimadzu TOC-VCSH instrument was used into determine the bulk organics concentration (TOC) in the samples. In order to determine the detailed fractions of

dissolved organic carbon, a Liquid Chromatography Organic Carbon Detector (LC-OCD) from DOC-Labor was used employing the method developed of Huber et al. (2011) to measure the various fractions of NOM.

The samples for the LC-OCD were pre-filtered using a 0.45 syringe filter to exclude the non-dissolved organics. Before analyzing the samples, a system cleaning was performed by injection of 2000 µL of 0.1 mol/L NaOH though the column for 260 min. Following the cleaning step, 2000 µL samples were injected for analysis with 130 min of retention time. The analysis result is a chromatogram showing a plot of signal response of different organic fractions to retention time. Manual integration of the data was then performed to determine the concentration of the organic fractions including biopolymers, humic substances, building blocks, low molecular weight acids and low molecular weight neutrals.

9.3 Geological Background and Description of SWRO Intake Well Sites

9.3.1 Sur, Oman

The SWRO plant located at Sur, Oman uses a series of 28 production wells to yield the required 160,000 m^3/day of feed water (Fig. 9.3; Table 9.2). This facility is currently the largest capacity SWRO facility using wells as an intake (David et al. 2009). The plant permeate capacity is 80,200 m^3/day.

A coastal carbonate aquifer system occurs along the segment of the Oman coast at Sur. The heterogeneous limestone aquifer occurs within early Tertiary age sediments (likely Eocene in age) lying within the Seeb Formation of the Hadhramaut Group and some sediments within the overlying Dhofar and Fars Group (Beavington-Penny et al. 2006; Fournier et al. 2006). The aquifer located along the coast is unconfined at surface and becomes semi-confined with depth. It is a dual- or tri-porosity aquifer that

Fig. 9.3 Location of SWRO plant and wells at Sur, Oman (modified from Rachman et al. 2014)

contains solution cavities, fractures, and some remaining intergranular porosity. Based on the geology of the aquifer, the flowpath from the sea is likely directed downward through the seabed and then follows either a tortuous path or more direct path following preferential flow conduits.

The wellfield generally parallels the coastline, but there are wells lying near the beach and others further inland with distances ranging from 30 to 250 m from the high tide line (Fig. 9.3). Depths of the wells range from 40 to 100 m below sea level and are completed with PVC screens. Each well is equipped with a submersible pump.

Water samples were collected from September 22–23, 2012 and March 19–20, 2013. The detailed analyses of algae, bacterial, TOC, organic carbon fractions and TEP are reported by Rachman et al. (2014). The site was chosen for analysis due to its high frequency of harmful algal blooms (HAB's).

9.3.2 Alicante, Spain

Wells systems are used to supply feedwater to two SWRO plants located at Alicante, Spain. The Alicante I and II facilities have permeate capacities of 50,000 and 65,000 m^3/day respectively. Three types of well intake systems are used to obtain feedwater, including conventional vertical wells, horizontal wells or drains, and a horizontal water tunnel containing lateral screens similar to those constructed on the horizontal plain in collector wells.

The conventional well system includes 30 individual production wells, each with a capacity of about 4,000 m^3/day that produce the 120,000 m^3/day required for Alicante I (Fig. 9.4). The combined yield of a horizontal well system and a water tunnel intake provide the feed water for Alicante II. The horizontal well system consists of 11 individual wells (differs between published papers and the numbers reported by the operators in the field) constructed using the Neodren configuration (Malfeito 2006; Farinas and Lopez 2007; Peters et al. 2007).

The vertical wells are constructed into Tertiary-age limestone (likely Miocene) containing some unlithified sediments (Gell et al. 1992). These wells are located between 60 and 110 m from the shoreline.

The horizontal drains or wells are constructed primarily into unlithified sediments that are carbonates with possibly some siliciclastic component (Gutierrez-Elorza et al. 2002). These wells may also penetrate soft limestone that occurs offshore. This carbonate unit does contain some solution cavities. The operators of the plant have suggested that the end of some horizontal wells may have been opened to the sea to allow greater capacity to occur. This has not been verified by observation. The horizontal wells are drilled at the ends of the water tunnel; three on the east side and 8 on the west side.

The water tunnel system is similar in concept to that developed by the City of Louisville in the United States as reported in Missimer (2009). It has a length of

Fig. 9.4 Location of SWRO plant and various well intake systems at Alicante, Spain (modified from Rachman et al. 2014)

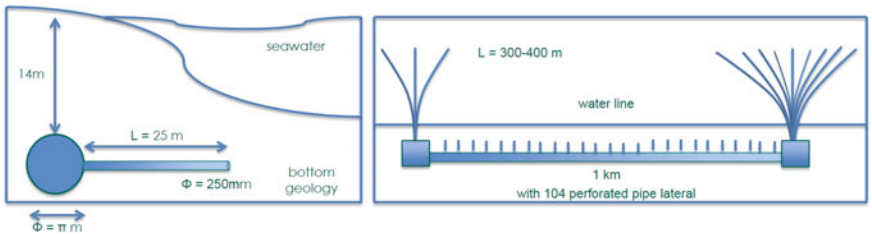

Fig. 9.5 Water tunnel intake system design at Alicante, Spain (from Rachman et al. 2014)

1 km and lies 14 m below the sea level. It is oriented parallel to the shoreline and has a diameter of 3.14 m (Fig. 9.5). Seawater enters the tunnel via 104 lateral wells drilled into the aquifer.

9.3.3 Turks & Caicos Water Company, Providenciales, Turks & Caicos Islands

The Turks & Caicos Water Company operates a SWRO facility that has a capacity of 10,000 m^3/day and uses conventional vertical wells that collectively produce about 24,000 m^3/day of feed water (Fig. 9.6). There are production wells that have maximum depths ranging between 30 and 50 m below surface. The wells contain PVC casings that are grouted between 15 and 20 m below surface. The wells are completed with open hole below the casing. The wells are located in the central part of the island, a distance of about 2000 m from the shoreline.

Little has been published concerning the subsurface geology of Providenciales. The surface geology was investigated by Kindler et al. (2008), and Wanless and Dravis (2008a, b, c). Based on a comparison to the geology of the Bahamas to the northwest beneath Andros Island, the age of the penetrated limestones is Pleistocene (McNeill et al. 2001). The aquifer is either semi-unconfined or semi-confined

Fig. 9.6 SWRO plant and wells at the Turks & Caicos Water Company, Provindenciales, Turks & Caicos Islands (modified from Rachman et al. 2014)

in nature based on the subsurface occurrence of low-permeability duricrusts. The production aquifer is karstic in nature, containing numerous large and small cavities and some preserved intergranular porosity.

9.3.4 Buhayrat City, Jeddah, Saudi Arabia

Four small to medium capacity SWRO facilities are being operated in the area within or near Jeddah, Saudi Arabia (Fig. 9.7). The Buhayrat city plant has a capacity of 6000 m^3/day and a feed water capacity of 12,400 m^3/day. Four production wells, located parallel to a tidal canal connected to the Red Sea, are used to produce the feed water. The wells are located between 70 and 80 m from the canal bank and have depths ranging from 30 to 40 m below surface and have a screened completion and three of the wellfields near Jeddah have a similar configuration, but with differing numbers of production wells (Fig. 9.8).

The shallow aquifer consists of siliciclastic sediments deposited as alluvial outwash. The aquifer is extremely heterogeneous with the aquifer containing sand and gravel with some large cobbles and a minor percentage of mud (silt and clay sized particles). Alluvial outwash aquifers in this region tend to have a high hydraulic conductivity and will effectively convey water from the canal into the wellbore (Missimer et al. 2012).

9.3.5 North Obhor, Jeddah, Saudi Arabia

The North Obhor SWRO facility has a permeate capacity of 13,350 m^3/day and the feed water capacity is about 33,375 m^3/day. The facility is using a well system that is constructed into a coral formation. A total of 13 vertical wells are used to supply the required capacity into the desalination facility. The wells range from 50 to 55 m in depth and are located 450 m from the seawater source. The wells were constructed in three different phases with the oldest being 13 years while the latest ones are 3 years old.

Fig. 9.7 Location of four SWRO plants that use vertical well intake systems in the Jeddah area, Saudi Arabia

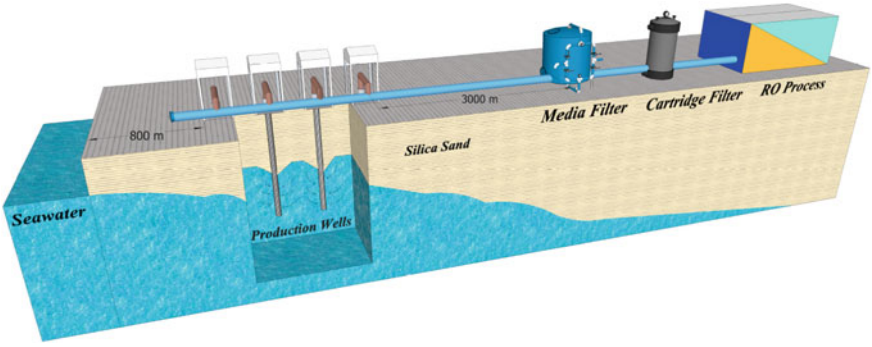

Fig. 9.8 Typical configuration of the SWRO facilities with well intake systems in the Jeddah area, Saudi Arabia

9.3.6 Corniche, Jeddah, Saudi Arabia

The SWRO plant located at the Corniche in Jeddah uses a series of 5 production wells to produce the required 11,250 m^3/day of feed water. This facility has a permeate capacity of 4,500 m^3/day. The vertical wells are constructed into siliciclastic sediments and the depth of these wells ranges from 46 to 50 m below sea level. These wells are located at a distance of 300 m away from the shoreline. The supplied water to this facility has a high iron concentration which causes a real problem for the pretreatment system. The cartridge filters used at this facility are replaced in a very short time due to an iron precipitation problem. The high iron concentration may be related to the water passage through the heterogeneous siliciclastic systems or some redox reaction.

9.3.7 South Jeddah Corniche, Jeddah, Saudi Arabia

The South Jeddah Corniche SWRO facility has a permeate capacity of 10,000 m^3/day and the feed water capacity is about 25,000 m^3/day. This facility utilizes a rather unique well intake system that consists of 10 production wells located on an artificial fill peninsula constructed into the Red Sea nearshore (Fig. 9.9).

During the initial construction of the plant, a series of wells were installed along the shoreline (beach wells), similar to many other low to medium capacity SWRO facilities in the region. After startup of the facility, it was discovered that the salinity of the feed water being produced from the wells was substantially greater that in the Red Sea. This is a rather common problem along the Red Sea coastline in areas where coastal sabkha environments are found. These environments contain trapped

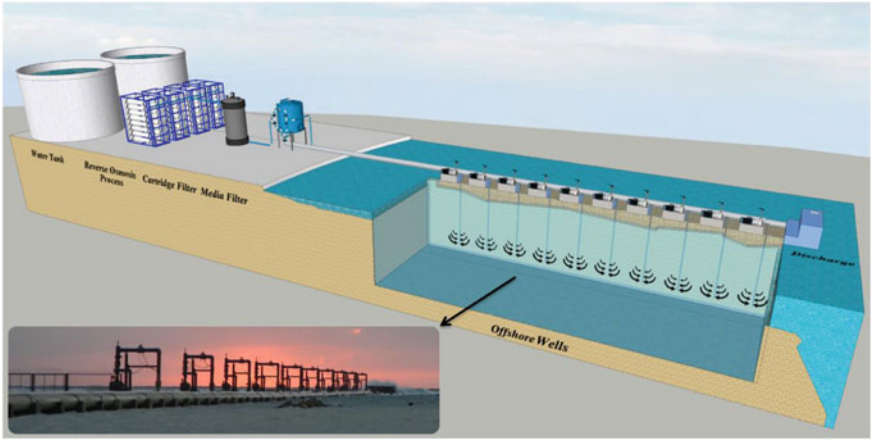

Fig. 9.9 Schematic diagram showing the offshore well system and SWRO plant constructed at South Jeddah, Saudi Arabia (from Al-Mashharawi et al. 2014)

seawater and are essentially evaporation basins that transmit hypersaline water toward the sea as density flows, thereby rendering the shoreline alluvial aquifer unusable for SWRO feed water development (Missimer et al. 2014). Therefore, an artificial peninsula was constructed from the beach seaward on the inner reef hardground. The wells are located 20 m apart and range from 40 to 50 m in depth. They have a screened completion. The aquifer beneath the Red Sea consists of interbedded limestone and carbonate sand.

9.4 Results

9.4.1 Introduction: Removal of Organic Particulates and Dissolved Compounds by Aquifer Transport to Wells

A relatively small quantity of data have been presented in the literature until recently on the effectiveness of aquifer removal of particulate and dissolved organic compounds within the marine environment. Most of the literature on aquifer treatment of organic compounds has occurred for freshwater systems associated with riverbank filtration and removal of organic compounds associated with aquifer treatment of domestic wastewater.

Missimer et al. (2013) summarized the historical data collected from SWRO well intake systems (Table 9.2). The early data suggest that significant reductions in

Table 9.2 Location and details of well intake systems investigated

System name	Location	Capacity (m^3/day)[a]	Well type	Aquifer type	No. wells
Sur	Oman	160,000	Shallow-beach	Carbonate	28
Alicante	Spain	130,000	Shallow-beach	Carbonate	30
Alicante[b]	Spain	130,000[b]	Tunnel with laterals	Carbonate	1
Alicante[b]	Spain	130,000[b]	Horizontal	Carbonate	11
Turk & Caicos I.	Providenciales	50,000	Shallow-inland	Carbonate	6
Buhayrat city, Jeddah	Saudi Arabia	12,500	Shallow-beach	Siliciclastic	4
North Obhor, Jeddah	Saudi Arabia	33,375	Shallow-beach	Siliciclastic	13
Corniche, Jeddah	Saudi Arabia	11,250	Shallow-beach	Siliciclastic	5
South Jeddah Corniche	Saudi Arabia	25,000	Shallow-offshore	Siliciclastic	10

[a]Capacity is defined as the capacity of the intake not the SWRO plant

[b]The required capacity for the combination of the horizontal wells and the tunnel is 130,000 m^3/day. Most of the time the tunnel is used and not the horizontal wells

organic compounds occurred, but these data were rather incomplete. The detailed analytical data included in this section were compiled from Dehwah et al. (2014a, b, c), Rachman et al. (2014a, b), and from unpublished data.

9.4.2 Algae and Bacteria Removal During Aquifer Transport

Data on algae within the surface seawater and in the discharge from wells was investigated at seven sites globally (Table 9.3). A large variation occurs in the natural concentrations of algae in seawater depending upon the climate, oceanic circulation, and nutrient balance of the site. The highest concentrations of algae in the investigated sites occurs al Sur, Oman, which shows a total algae concentration of nearly 200,000 cells/mL during one of the sampling periods. The lowest concentration occurred within the Red Sea at the South Corniche site with a total of 1,677 cells/mL.

Algae occurring in the water from the vertical intake wells sampled are labeled as numbers in Table 9.3. In all cases, the algae in the seawater were fully reformed during passage through the seabed and the aquifer feeding the wells. The detection limit varies based on overall algae concentration, but in all cases the measured concentration was less than the detection limit. The horizontal well intake at Alicante, Spain was the only subsurface intake system that showed any significant concentration of algae in the feed water. However, it was only 22.7 % of that in the surface seawater. The water tunnel intake system at the Alicante site was also 100 % effective in algae removal.

Bacteria occurrence within the marine environment varies greatly at the 7 sites sampled. The highest concentrations occur in the Arabian Sea at the Oman site at nearly a million cells/mL during the first sampling campaign and the lowest concentration was in the Red Sea near Jeddah at the North Obhor site at 112,790 cells/mL.

Vertical well intakes into coastal aquifers showed the highest percentage of bacteria removal in passage of seawater through the seabed and aquifer to the production wells (Table 9.4). The highest removal rates were found in the limestone aquifer system at Oman and the Turks & Caicos Islands site. The highest removal percentage achieved was 99.8 %. Within vertical well intakes at Alicante, Spain, removal percentages varied between 84.3 and 90 %. Vertical well intake systems in the Red Sea showed a reduced removal percentage with considerable variation between sites and within sites. In all cases, the reduction percentage was greater than 74.4 % and was as high as 96.5 %, The South Cornich Jeddah site, using the unique offshore well system, performed best.

Two different well intake systems at Alicante, Spain were also evaluated. The tunnel intake system produced a bacteria reduction of 69.9 %, close to the lowest reduction achieved using vertical wells within the 7 studied sites. The much-touted horizontal well or drain system produced only a 47.6 % reduction in bacteria

Table 9.3 Comparison of algae concentrations in surface seawater versus those in well intake discharges (values in cells/mL)

Samples	Prochlorococcus sp.	Synechococcus sp.	Cyanobacteria	Pico/Nanoplankton	Total algae
Sur, Oman					
SW	4,400	113,040	0	1,900	119,340
1	<100	<100	<100	<100	<100
2	<100	<100	<100	<100	<100
3	<100	<100	<100	<100	<100
4	<100	<100	<100	<100	<100
SW	2,810	194,310	0	435	197,555
1	<100	<100	<100	<100	<100
2	<100	<100	<100	<100	<100
3	<100	<100	<100	<100	<100
4	<100	<100	<100	<100	<100
Alicante, Spain					
SW	350	24,275	0	985	25,610
1	<100	<100	<100	<100	<100
2	<100	<100	<100	<100	<100
3	<100	<100	<100	<100	<100
4	<100	<100	<100	<100	<100
Hort.	135	5,460	0	225	5,820
Tunnel	<100	<100	<100	<100	<100
Turks & Caicos					
SW	770	37,225	0	250	38,245
1	<100	<100	<100	<100	<100
2	<100	<100	<100	<100	<100
3	<100	<100	<100	<100	<100
Buhayrat city					
SW	6,330	20,785	0	3,280	30,395
1	<100	<100	<100	<100	<100
2	<100	<100	<100	<100	<100
3	<100	<100	<100	<100	<100
4	<100	<100	<100	<100	<100
North Obhor					
SW	203	–	30,053	268	30,524
1	<50	–	<50	<50	<50
2	<50	–	<50	<50	<50
3	<50	–	<50	<50	<50
4	<50	–	<50	<50	<50
Corniche, Jeddah					
SW	243	0	3,300	60	3,603
1	<50	<50	<50	<50	<50
2	<50	<50	<50	<50	<50
3	<50	<50	<50	<50	<50

(continued)

Table 9.3 (continued)

Samples	Prochlorococcus sp.	Synechococcus sp.	Cyanobacteria	Pico/Nanoplankton	Total algae
South Jeddah Corniche					
SW	140	0	1,507	30	1,677
1	<5	<5	<5	<5	<5
2	<5	<5	<5	<5	<5
3	<5	<5	<5	<5	<5
4	<5	<5	<5	<5	<5

concentration. There is a question concerning this well system in terms of its possible opening to direct influx of seawater either at the well terminus (suggested by operators) or within a vertical solution cavity allowing direct enter of seawater without passage through the sediment.

9.4.3 TOC and DOC Removal During Aquifer Transport

There is a considerable difference in the concentration of TOC and DOC in the surface seawater at the 7 sampling locations (Fig. 9.4). TOC concentrations ranged from 0.88 to 1.677 mg/L with the highest concentration found at the Turks and Caicos Islands site and the lowest values occurring in the Red Sea sites (0.88–1.02 mg/L). Where DOC was measured, concentrations ranged between 0.890 and 0.997 mg/L.

TOC and DOC concentrations were reduced during aquifer transport in all wells sampled, but there were considerable variations in the percentage of removal (Table 9.5). The highest percentages of removal were achieved in the vertical wells at the Turks & Caicos Islands site with a reduction range of 76.9–82.8 % for TOC and 74.2–77.7 % for DOC. The lowest percentage of TOC concentration reduction occurred at the South Corniche Jeddah site (26.3–42.1 %). A very large difference between wells in terms of removal efficiency achieved occurred at the North Obhor site on the Red Sea (16.7–72.7 %). Seawater from the vertical wells at Alicante, Spain showed that reductions ranging between 53.0 and 60.2 % occurred for TOC and DOC. The water tunnel intake showed a reduction of only 23 % and the horizontal wells system only 6.5 %.

9.4.4 TEP Removal During Aquifer Transport

There are two types of TEP that occur in raw seawater; particulate and colloidal. The data from various sites show aquifer removal of particulate TEP during transport from the sea to the wells ranging from 36.9 to 92.1 %. Colloidal TEP

Table 9.4 Bacteria concentrations in surface seawater and the well intake discharges with the removal percentages achieved during transport

Site	Sample	Total bacteria concentration (cells/mg/L)	Percentage removal
Sur, Oman			
	SW	995,310	0
	1	3,270	99.7
	2	8,540	99.1
	3	13,630	98.6
	4	11,000	98.9
	SW	702,609	0
	1	5,109	99.3
	2	1,196	99.8
	3	3,043	99.6
	4	5,109	99.3
Alicante, Spain			
	SW	292,283	0
	1	29,348	90.0
	2	35,761	87.8
	3	45,870	84.3
	4	34,783	88.1
	Hor.	153,261	47.6
	Tunnel	89,891	69.2
Turks & Caicos			
	SW	698,152	0
	1	17,065	97.6
	2	20,978	97.0
	3	15,652	97.8
Buhayrat City			
	SW	320,870	0
	1	11,087	96.5
	2	10,978	96.6
	3	26,630	91.7
	4	13,804	95.7
North Obhor			
	SW	112,790	0
	1	10,054	91.1
	2	1,250	98.9
	3	8,370	92.6
	4	5,978	94.7

(continued)

Table 9.4 (continued)

Site	Sample	Total bacteria concentration (cells/mg/L)	Percentage removal
Corniche, Jeddah			
	SW	196,377	0
	1	30,652	84.4
	2	49,638	74.7
	3	38,804	80.2
South Corniche, Jeddah			
	SW	264,728	0
	1	9,185	96.5
	2	33,804	87.2
	3	12,283	95.4
	4	19,783	92.5

removal ranges from 40.5 to 78.5 % (Table 9.6). There is considerable variation in which form of TEP is removed at the greatest percentage with no consistent pattern. At Alicante, Spain, the average removal differences in the vertical wells between particulate and colloidal TEP is 68.15 to 51.45 % respectively. At the Corniche, Jeddah site the comparison is 60.1 to 55.1 % respectively. At the South Corniche, Jeddah site the removal percentage is nearly equal at 64.0 to 63.25 % respectively.

Aquifer removal during flow to vertical wells at the Turks & Caicos SWRO facility shows the highest removal of particulate TEP, averaging about 90 %. Removal of particulate TEP in water extracted from vertical wells at Sur, Oman and Alicante, Spain shows an average removal of 66.45 and 68.15 % respectively. Removal rates of particulate TEP using shallow wells along the Red Sea coast of Saudi Arabia show lower average rates ranging from 53.4 to 64 %. The South Corniche, Jeddah site has the average highest removal rate at 64 %. Also, there is considerable variation in the removal percentage between wells located on the same site. The worst performing intake system in terms of particulate TEP removal is the horizontal well system at Alicante, Spain.

9.4.5 NOM Fraction Removal During Aquifer Transport

Assessment of the aquifer removal of the NOM components including biopolymers, humic substances, building blocks, low molecular weight acids, and low molecular neutrals were determined for the seven sites. The general pattern of removal during aquifer transport from the sea to the wells was generally consistent (Table 9.7).

The highest removal rate of the NOM fractions occurred within the biopolymers. The range in average removal by site was 92.3 to 100 %. The highest removals occurred in the Alicante, Spain (vertical wells) and Turks & Caicos SWRO

Table 9.5 Organic carbon concentrations in surface seawater and from the well discharges with percentage of removal during transport

Samples	TOC (mg/L)	Percentage removal	DOC (mg/L)	Percentage removal
Sur, Oman				
SW	–	–	0.890	0
1	–	–	0.293	67.1
2	–	–	0.307	65.5
3	–	–	0.331	62.8
4	–	–	0.312	64.9
SW	1.053	0	0.957	0
1	0.266	74.4	0.210	78.1
2	0.478	54.61	0.442	52.8
3	0.533	49.38	0.481	49.7
4	0.514	51.19	0.425	55.6
Alicanti, Spain				
SW	1.12	0	0.856	0
1	0.568	49.3	0.396	53.7
2	0.560	50.0	0.392	54.2
3	0.602	46.3	0.402	53.0
4	0.567	49.4	0.374	56.3
Hor.	1.05	6.5	0.873	−2.0
Tunnel	0.714	23.0	0.548	36.0
Turks & Caicos				
SW	1.677	0	0.997	0
1	0.289	82.8	0.222	77.7
2	0.388	76.9	0.257	74.2
3	0.334	80.1	0.247	75.2
Buhayrat City				
SW	1.053	0	0.573	0
1	0.536	46.7	0.295	48.5
2	0.653	35.0	0.341	40.5
3	0.581	42.2	0.361	37.0
4	0.517	48.6	0.293	48.9
North Obhor				
SW	0.89	0	–	–
1	0.24	72.7	–	–
2	0.20	78	–	–
3	0.37	58.2	–	–
4	0.74	16.7	–	–

(continued)

Table 9.5 (continued)

Samples	TOC (mg/L)	Percentage removal	DOC (mg/L)	Percentage removal
Corniche, Jeddah				
SW	0.94	0	–	–
1	0.37	60.6	–	–
2	0.41	55.8	–	–
3	0.56	40.3	–	–
South Corniche, Jeddah				
SW	1.02	0	–	–
1	0.69	32.3	–	–
2	0.75	26.5	–	–
3	0.71	30.3	–	–
4	0.59	42.1	–	–

facilities with 100 % removal. Two sampling events at the Sur, Oman site produced about a 5 % difference in biopolymer removal, but the removal rate was still high. The average removals for all of the SWRO facilities located in the Jeddah, Saudi Arabia area showed high average rates of removal between 93.1 and 96.4 %. The horizontal well system at Alicante, Spain showed a reduction of 93 %, but the tunnel system produced only a 90.1 % removal.

Removal of humic substances was substantially lower compared to biopolymers. The range of sample group averages was 27.5 to 80.9 %. The highest removal occurred at Sur. Oman during the second sampling campaign. The first sampling at the site showed a much lower removal average of 58.4 %. Most of the sites showed removals between 43.9 and 45 % with the exception of the North Obhor site which averaged 70 %. The horizontal site system at Alicante, Spain was found to show a 24 % increase in humic substances compared to natural seawater and the tunnel intake system showed only a 24.3 % reduction in concentration.

The building blocks removal average percentage was lower at all sites compared to humic substances with the exception of the Turks & Caicos and Corniche, Jeddah sites. The range in average removal was 25.4 to 60.2 %. There was considerable variation within the groups of sampled wells at each site. Again, the horizontal well system at Alicante, Spain showed an increase in concentration of 11.8 %, similar to the increase found in the humic substances.

In most cases, the average removal percentages of the low molecular weight acids and neutrals were lower than the building blocks with the exception of the Turks & Caicos site (only acids), the Alicante site (vertical wells), and the Buhayrat site. The average removal percentage between the low molecular weight fractions varied with regard to which one was highest at a given site. The percentage of both low molecular weight fractions increased compared to the background seawater at the horizontal well site in Alicante.

Table 9.6 Particulate and colloidal TEP in surface seawater and from the well discharges with percentage of removal during transport

Samples	Particulate TEP (mg/L)	Percentage removal	Colloidal TEP (mg/L)	Percentage removal
Sur, Oman				
SW	0.036	–	–	–
1	0.007	80.4	–	–
2	0.008	77.4	–	–
3	0.011	70.2	–	–
4	0.015	58.9	–	–
SW	0.117	0	–	–
1	0.035	70.1	–	–
2	0.038	67.5	–	–
3	0.040	65.8	–	–
4	0.044	62.4	–	–
Alicante, Spain				
SW	0.521	–	0.171	0
1	0.147	71.8	0.080	53.2
2	0.156	70.1	0.090	47.4
3	0.177	66.0	0.074	56.7
4	0.184	64.7	0.088	48.5
Hor.	0.329	36.9	0.085	50.3
Tunnel	0.179	65.6	0.077	54.9
Turks & Caicos				
SW	0.642	–	–	–
1	0.051	92.1	–	–
2	0.066	89.7	–	–
3	0.053	91.7	–	–
Buhayrat City				
SW	0.058	–		
1	0.023	60.3		
2	0.038	34.5		
3	0.027	53.4		
4	0.020	65.5		
North Obhor				
SW	0.162	–	–	–
1	0.116	28.4	–	–
2	0.032	79.9	–	–
3	–	–	–	–
4	0.072	55.2	–	–

(continued)

Table 9.6 (continued)

Samples	Particulate TEP (mg/L)	Percentage removal	Colloidal TEP (mg/L)	Percentage removal
Corniche, Jeddah				
SW	0.121	–	0.073	
1	0.019	83.9	0.043	40.9
2	0.055	54.6	0.041	44.7
3	0.070	41.9	0.015	79.8
South Corniche, Jeddah				
SW	0.157	–	0.122	
1	0.038	75.7	0.071	42.2
2	0.069	56.1	0.032	73.8
3	0.057	63.8	0.026	78.5
4	0.062	60.4	0.051	58.5

9.5 Discussion

9.5.1 Processes Involved in Organic Removal Within Aquifer Systems

Removal of the particulates in the aquifer flowpath from the sea through the bottom and the connecting aquifer to the wells is likely caused by straining with some adsorption. The algae and bacteria loss is likely caused by straining, death and breakdown of the living organisms, and some adsorption, particularly onto subsurface biofilms within secondary porosity in the carbonate aquifers. Some of the bacteria may be removed by bacterial predation by groundwater species, but that is an unresolved issue.

Removal of TEP and the NOM fractions is likely a combination of physical, chemical, and biological processes. TEP and the biopolymer fraction of NOM contain large molecules, some of which are sticky polysaccharides that would tend to adsorb onto the aquifer matrix, particularly at the seawater/sediment interface. The largest molecules within the biopolymer fraction of NOM are also likely removed by straining and dispersion. Reduction in the overall TOC and the smaller NOM fractions is likely caused by chemical and bacterial activity with the aquifer. As the composition of the NOM becomes more refractory, the removal percentage of the NOM lessens. The NOM fractions data suggest that the large molecular weight fraction, biopolymers, have the highest removal with a reduction in removal percentage from the highest to lowest molecular weight.

It is likely that the uptake of organic matter within the aquifer system is somewhat dependent on operational time of the facility in that the bacterial activity in the aquifer will likely increase in time as more organic carbon flows through it.

Table 9.7 NOM fractions in surface seawater and from the well discharges with percentage of removal during transport

Samples	Biopolymers (ppb)	% removal	Humic substances (ppb)	% removal	Building blocks (ppb)	% removal	Low molecular Wt. acids (ppb)	% removal	Low molecular Wt. neutrals (ppb)	% removal
Sur, Oman										
SW	133		394		167		187		76	
1	8	93.98	74	81.22	38	77.25	68	63.64	22	71.05
2	13	90.23	180	54.31	85	49.10	120	35.83	44	42.11
3	11	91.73	215	45.43	97	41.92	110	41.18	48	36.84
4	9	93.23	186	52.79	88	47.31	96	48.66	46	39.47
SW	111		260		212.5		229		77.5	
1	1	99.25	85	78.43	80	52.10	95	49.20	32	57.89
2	8	93.98	41	89.59	59	64.67	150	19.79	49	35.53
3	0	100.00	91	76.90	77	53.89	125	33.16	38	50.00
4	2	98.50	84	78.68	83	50.30	117	37.43	26	65.79
Alicante, Spain										
SW	142		449		121		66		78	
1	0	100.00	238	46.99	70	42.15	41	37.88	47	39.74
2	0	100.00	243	45.88	70	42.15	33	50.00	46	41.03
3	0	100.00	259	42.32	72	40.50	29	56.06	42	46.15
4	0	100.00	247	44.99	59	51.24	26	60.61	42	46.15
Hor.	10	92.96	556	−23.83[a]	135	−11.57[a]	67	−1.52[a]	105	−34.62[a]
Tunnel	14	90.14	340	24.28	89	26.45	45	31.82	60	23.08

(continued)

Table 9.7 (continued)

Samples	Biopolymers (ppb)	% removal	Humic substances (ppb)	% removal	Building blocks (ppb)	% removal	Low molecular Wt. acids (ppb)	% removal	Low molecular Wt. neutrals (ppb)	% removal
Turks & Caicos										
SW	215		446		174		111		51	
1	0	100.00	142	68.16	52	70.11	3	97.30	25	50.98
2	0	100.00	163	63.45	60	65.52	4	96.40	30	41.18
3	0	100.00	158	64.57	58	66.67	3	97.30	28	45.10
Buhayrat City										
SW	47		343		82		16		85	
1	0	100.00	178	48.10	55	32.93	9	43.75	53	37.65
2	1	97.87	209	39.07	62	24.39	12	25.00	57	32.94
3	5	89.36	212	38.19	71	13.41	13	18.75	60	29.41
4	2	95.74	173	49.56	56	31.71	10	37.50	52	38.82
North Obhor										
SW	76		345		103		168		88	
1	2	97.4	110	68.1	55	46.6	103	38.7	52	40.9
2	2	97.4	89	74.2	33	68.0	107	36.3	41	53.4
3	4	94.7	145	58.0	53	48.5	105	37.5	71	19.3
4	3	96.1	70	79.7	23	77.7	120	28.6	44	50.0

(continued)

Table 9.7 (continued)

Samples	Biopolymers (ppb)	% removal	Humic substances (ppb)	% removal	Building blocks (ppb)	% removal	Low molecular Wt. acids (ppb)	% removal	Low molecular Wt. neutrals (ppb)	% removal
Corniche, Jeddah										
SW	90		360		91		192		94	
1	3	96.7	199	44.7	51	44.0	143	25.5	63	33.0
2	2	97.8	147	59.2	49	46.2	136	29.2	57	39.4
3	8	91.1	205	43.1	46	49.5	127	33.9	71	24.5
South Corniche, Jeddah										
SW	116		351		139		197		103	
1	7	94.0	247	29.6	99	28.8	146	25.9	84	18.4
2	6	94.8	282	19.7	114	18.0	158	19.8	87	15.5
3	3	97.4	244	30.5	120	13.7	191	3.0	117	−13.6
4	16	86.2	245	30.2	82	41.0	127	35.5	71	31.1

[a]Negative values of removal suggest that the measured concentration is higher than seawater at the site

Detailed sampling may indicate changes in aquifer assimilation based on seasonal changes in water temperature and dissolved oxygen concentrations in the aquifer. Further research would be required to assess this issue.

9.5.2 *Effects of FlowPath Length on Organic Substances Removal*

The length of the flowpath from the sea to the wells and the corresponding hydraulic retention time in the aquifer affects the removal percentage of bacteria and NOM. The longest flow pathway from the sea to the wells occurs at the Turks & Caicos SWRO facility. This site shows the highest percentage reduction in TOC, TEP, nearly all fractions of NOM, and the second highest reduction in bacteria. Wells at the Sur, Oman site contain a variation in flow pathway length and show a very high reduction in bacterial concentration, but a slightly lower TEP reduction. The depth of the screens at Alicante is deeper than most of the other sites investigated which increases the flowpath length and may be responsible for the relatively high removal percentage of bacteria, biopolymer fraction of NOM, and TEP.

The length of the flowpath of the sites sampled in the Jeddah area does not differ greatly, but there are observable differences in the removal percentages of organic matter between the sites. This may indicate difference in operational time or local changes in the biological activity within the aquifer.

The shortest flowpaths occur within the horizontal and tunnel intake systems at Alicante. Within the horizontal well system, breakthrough of algae is observed indicating a direct correction between the sea and the well system. These systems show the lowest percentages of bacteria removal. In addition, there is an increase in NOM within all fractions except the biopolymers.

9.5.3 *Effects of Aquifer Type and Matrix on Organic Substances Removal*

Three fundamental types of aquifers were investigated; carbonate systems with secondary porosity (Sur, Oman, Turks & Caicos, and North Obhor), combined lithified and unlithified carbonate (Alicante, Spain and South Corniche, Jeddah), and heterogeneous siliciclastic systems (Buhayrat City, Corniche, Jeddah). In general, there are no distinct differences in the removal of the organic matter between the different aquifer types. The highest bacteria removal percentages occur at the Turks & Caicos and Sur, Oman, but most of the other sites also exhibit high removal percentages. The carbonate aquifer types have a generally higher removal percentage for TEP compared to the siliciclastic aquifer sites. The results for removal of the NOM fractions are mixed and do not appear to be related to lithologic characteristics of the aquifer type.

9.5.4 Well Intake Design and Organic Substances Removal Efficiency

The design of the well system does have a significant impact on the removal of organic matter during the transport process. The sampling at Alicante, Spain allowed three types of well intake systems in close proximity to be evaluated; vertical wells, horizontal wells or collectors, and a water tunnel system with vertical collectors. Of the three intake types, the vertical wells significantly outperformed the other design types. Greater amounts of TOC, bacteria, TEP (with exception of the tunnel), and all NOM fractions were removed during transport from the sea to the wells. The horizontal well system performed quite poorly, showing a breakthrough of algae, less than 50 % removal of bacteria, only a 6.5 % removal of TOC, less than 40 % removal of TEP, and actual increases in most NOM fractions. The tunnel intake system produced significant removals of organic matter, but not as great as the vertical wells.

Based on the data collected and interviews with the operators, the horizontal wells system had operating problems and there may be some direct connection between the seawater and the installed wells at one or more locations. The transport distance of seawater to the horizontal well systems and the tunnel intake system were both much shorter compared to the transport distance from the sea to the vertical wells. The reduced distance and corresponding hydraulic retention time likely impact the removal percentage of the organic matter. The exact cause of the breakthrough of algae and poor performance of the horizontal well system is not known due to lack of detailed operational data.

9.6 Conclusions

Data collected from seven SWRO facilities in different geologic conditions and geographic locations clearly demonstrates that conventional vertical well intake systems provide a robust degree of pretreatment that significantly improves raw seawater quality. In all cases 100 % of the algae occurring in the raw seawater were removed and up to 99.8 % of the bacteria were removed during aquifer transport. Up to 92 % of the TEP was removed, but considerable variation occurred in TEP removal occurred between sites and internal within sites. Most of the biopolymer fraction of NOM was removed at all sites with reduction percentages ranging from 93.1 to 100 %. The removal of the NOM fractions appears related to molecular weight with the highest removal rates occurring in the biopolymer fraction and the lowest occurring in the low molecular weight acid and neutrals.

The combined removal of the bacteria, biopolymer fraction of NOM, and a significant amount of the TEP demonstrate that use of well intake systems tends to reduce the potential biofouling. The processes occurring within the aquifer during

transport produce both physical entrapment and biodegradation of the organic matter, similar to that occurring in a sophisticated engineered pretreatment systems.

Perhaps the key factor affecting the degree of treatment achieved within the groundwater system is the length of the flow pathway from the sea to the wells. The longer flowpath length generally increases the hydraulic retention time, allowing biological processes within the aquifer to achieve greater assimilation of organic compounds. In the case of similar flowpath lengths, the geological materials forming the aquifer framework do not appear to be a significant factor impacting organic matter removal.

Performance of vertical wells was found to be significantly greater compared to a horizontal well system at Alicante, Spain. An innovative water tunnel intake system at the same location achieved significant reductions in organic matter, but not as great as the horizontal wells. This lower reduction is likely caused by a shorter flowpath from the seabed to the tunnel.

References

Bartak, R., Grischek, T., Ghodeif, K., & Ray, C. (2012). Beach sand filtration as pre-treatment for RO desalination. *International Journal of Water Science, 1*(2), 1–10.

Bar-Zeev, E., Berman-Frank, I., Liberman, B., Rahav, E., Passow, U., & Berman, T. (2009). Transparent exopolymer particles: Potential agents for organic fouling and biofilm formation in desalination and water treatment plants. *Desalination and Water Treatment, 3*, 136–142.

Beavington-Penny, S. J., Wright, V. P., & Racey, A. (2006). The middle Eocene Seeb Formation of Oman: An investigation of acyclicity, stratigraphic completeness, and accumulation rates in shallow marine settings. *Journal of Sedimentary Research, 76*(10), 1137–1161.

Berman, T. (2010). Biofouling: TEP-a major challenge for water separation. *Filtration & Separation, 47*(2), 20–22.

Berman, T., Mizrahi, R., & Dosoretz, C. G. (2011). Transparent exopolymer particles (TEP): A critical factor in aquatic biofilm initiation and fouling on filtration membranes. *Desalination, 276*, 184–190.

Berman, T., & Passow, U. (2007). Transparent exopolymer particles (TEP): An overlooked factor in the process of biofilm formation in aquatic environments. *Nature Precedings*. doi:10.1038/npre.2007.1182.1.

Choules, P., Schotter, J.-C., Leparc, J., Gai, K., & Lafon, D. (2007) Operation experience from seawater reverse osmosis plants. In Proceedings, American Membrane Technology Conference and Exposition, Las Vegas, Nevada.

David, B., Pinot, J.-P., & Morrillon, M. (2009). Beach wells for large scale reverse osmosis plants: The Sur case study. In Proceedings of the International Desalination Association World Congress on Desalination and Water Reuse, Atlantis, The Palm, Dubai, UAE, November 7–12, 2009, Paper IDAW/DB09-106.

Dehwah, A. H. A., Al-Mashharawi, S., Kammourie, N., & Missimer, T. M. (2014a). Impact of well intake systems on bacterial, algae and organic carbon reduction in SWRO desalination systems, SAWAC), Jeddah, Saudi Arabia. *Desalination and Water Treatment*. doi:10.1080/19443994.2014.940639.

Dehwah, A. H. A., Al-Mashhawari, S., Missimer, T. M. (2014b). Impact of well intake systems on bacterial, algae, and organic carbon reduction in SWRO desalination systems, SAWACO, Jeddah, Saudi Arabia. In Proceedings, European Desalination Society Conference and

Exhibition, Desalination for the Environment: Clean Water and Energy, Grand Resort Hotel, Limassol, Cyprus, May 11–15, 2014.

Dehwah, A. H. E., Li, S., Al-Mashhawari, S., Rachman, R. M., Winters, H., & Missimer, T. M. (2014c). The influence of beach well and deep ocean intakes on TEP reduction in SWRO desalination systems, Jeddah, Saudi Arabia. In Proceedings, American Membrane Technology Association/American Water Works Association, 2014 Membrane Technology Conference & Exposition (18 p.), Las Vegas, Nevada.

Dravis, J. J., & Wanless, H. R. (2008a). Caicos platform models of Quaternary carbonate deposition controlled by stronger easterly Trade Winds—application to petroleum exploration. In W. Morgan & P. M. Harris (Eds.), *Developing models and analogs for isolated carbonate platform—Holocene and Pleistocene carbonates of Caicos Platform, British West Indies*. SEPM Core Workshop 22, Tulsa, OK, Society for Sedimentary Geology.

Dravis, J. J., & Wanless, H. R. (2008b). Pleistocene reefal and oolitic core sequences from West Caicos, Caicos Platform. In W. Morgan & P. M. Harris (Eds.), *Developing models and analogs for isolated carbonate platform—Holocene and Pleistocene carbonates of Caicos Platform, British West Indies* (pp. 171–177). SEPM Core Workshop 22, Tulsa, OK, Society for Sedimentary Geology.

Dravis, J. J., & Wanless, H. R. (2008c). Role of storms and prevailing energy in defining sediment body geometry, composition, and texture on Caicos Platform. In W. Morgan & P. M. Harris (Eds.), *Developing models and analogs for isolated carbonate platform—Holocene and Pleistocene carbonates of Caicos Platform, British West Indies* (pp. 13–20). SEPM Core Workshop 22, Tulsa, OK, Society for Sedimentary Geology.

Farinas, M., & Lopez, L. A. (2007). New and innovative sea water intake system for the desalination plant at San Pedro del Pintar. *Desalination, 203*, 199–217.

Flemming, H.-C. (1997). Reverse osmosis membrane fouling. *Experimental Thermal and Fluid Science, 14*, 382–391.

Flemming, H.-C., Schaule, G., Griebe, T., Schmitt, J., & Tamachkiarowa, A. (1997). Biofouling—the Achilles heel of membrane processes. *Desalination, 113*, 215–225.

Fournier, M., Lepvrier, C., Razin, P., & Jolivet, L. (2006). Late Cretaceous to Paleogene post-obduction extension and subsequent compression in the Oman Mountains. *GeoArabia, 11*, 17–40.

Geel, T., Roep, Th B, Kate, W., & Smit, J. (1992). Early-Middle Miocene stratigraphic turning points in the Alicante region (SE Spain): Reflections of western Mediterranean plat-tectonic reorganization. *Sedimentary Geology, 75*, 223–239.

Ghaffour, N., Missimer, T. M., & Amy, G. (2013). Technical review and evaluation of the economics of desalination: Current and future challenges for better supply sustainability. *Desalination, 309*, 197–207.

Gutierrez, M., Garcia-Ruiz, J. M., Javier Garcia, F., Goy, J. L., Gutierrez-Santolalla, F., Marti, C., et al. (2002). Quaternary, Chap. 14. In.: W. Gibbons & T. Moreno (Eds.). *Geology of Spain* (pp. 335–366). London: The Geological Society.

Hassan, A., Jamaluddin, A. T. M., Rpwaili, A., Abart, E., & Lovo, R. (1997). Investigating intake system effectiveness with emphasis on self-jetting well-point (SJWP) beachwell systems. In Proceedings of the 2nd Acquired Experience Symposium on Desalination plants O & M (p. 1350), Al-Jubail, Saudi Arabia, September 29–October 3, 1997.

Huber, S. A., Balz, A., Abert, M., Pronk, W. (2011). Characterisation of aquatic humic and non-humic matter with size-exclusion chromatography—organic carbon detection—organic nitrogen detection (LC-OCD-OND). *Water Research 45*(2), 879–885.

Jamaluddin, A. T. M., Hassan, A. M., Al-Reweli, A., & Saeed, M. O. (2007). Operation of Al-Birk plant intertucing beachwell intake system. In Proceedings of the International Desalination Associate World Congress on Desalination and Water Reuse, Singapore.

Kindler, P., Godefroid, F., & Samankassou, E. (2008). Pre-Holocene island geology of the Caicos and Mayaguana (Bahamas) Platforms: Similarities and differences. In W. Morgan & P. M. Harris (Eds.), *Developing models and analogs for isolated carbonate platform—*

Holocene and Pleistocene carbonates of Caicos Platform, British West Indies (pp. 211–213). SEPM Core Workshop 22, Tulsa, OK, Society for Sedimentary Geology.

Laparc, J., Schotter, J.-C., Rapenne, S., Croue, J. P., Lebaron, P., Lafon, D., et al. (2007). Use of advanced analytical tools for monitoring performance of seawater pretreatment processes. In Proceedings, International Desalination Association World Congress on Desalination and Water Reuse, Maspalomas, Gran Canaria, Spain, October 21–26, 2007, IDAWC/MP07-124.

Kumar, M., Adham, S. S., & Pearce, W. R. (2006). Investigation of seawater reverse osmosis fouling and its relationship to pretreatment type. *Environmental Science and Technology, 40*, 2037–2044.

Malfeito, J. J. (2006). San Pedro Del Pintar desalination plant: First year of operation with a horizontal drilled intake. In Proceedings of the International Desalination and Water Reuse International Forum and Exposition, Tianjin, China, September 6–8, 2006.

McNeill, D. F., Eberli, G. P., Lidz, B. H., Swart, P. K., & Kenter, J. A. M. (2001). Chronostratigraphy of a prograded carbonate platform margin: A record of dynamic slope sedimentation, western Great Bahama Bank. In R. N. Ginsburg (Ed.) *Subsurface geology of a prograding carbonate platform margin, Great Bahama Bank: Results of the Bahamas drilling project* (pp. 101–136). SEPM Special Publication No. 70, Tulsa, OK, Society for Sedimentary Geology.

Missimer, T. M. (2009) *Water supply development, aquifer storage, and concentrate disposal for membrane water treatment facilities* (2nd edn.). Sugarland, Texas: Schlumberger Water Services.

Missimer, T. M., Drewes, J., Amy, G., Maliva, R. G., & Keller, S. (2012). Restoration of wadi aquifers by artificial recharge with treated wastewater. *Ground Water, 50*(4), 514–527. doi:10.1111/j.1745-6584.2012.00941.x.

Missimer, T. M., Ghaffour, N., Dehwah, A. H. A., Rachman, R., Maliva, R. G., & Amy, G. (2013). Subsurface intakes for seawater reverse osmosis facilities: Capacity limitation, water quality improvement, and economics. *Desalination, 322*, 37–51. doi:10.1016/j.desal.2013.04.021.

Missimer, T. M., Jadoon, K. Z., Li, D., Hoppe-Jones, C., & Al-Mashharawi, S. (2014). Hydrogeology and water quality of a coastal alluvial aquifer and its potential use as an intake system for a seawater reverse osmosis water treatment system, Thuwal, Saudi Arabia. *Hydrogeology Journal* (in press).

Missimer, T. M., & Winters, H. (2000). Effects of well design and maintenance on biofouling at a seawater reverse osmosis plant, Grand Cayman Island, B.W.I. In Proceedings, American Desalting Association Meeting & Technical Program, Lake Tahoe, Nevada.

Missimer, T. M., & Winters, H. (2003). Reduction of biofouling at a seawater RO plant in the Cayman Islands. In Proceedings, International Desalination Association World Congress on Desalination and Water Reuse, BAH03-190.

Passow, U. (2000). Formation of transparent exopolymer particles, TEP, from dissolved precursor material. *Marine Ecology Progress Series, 192*, 1–11.

Passow, U (2002). Formation of transparent exopolmer particles (TEP) by phyto- and bacterioplankton. *Marine Ecology Progress Series*, *236*, 1–12.

Passow, U., & Alldredge, A. L. (1994). Distribution, size and bacterial-colonization of transparent exopolymer particles (TEP) in the ocean. *Marine Ecology Progress Series, 113*(1–2), 185–198.

Passow, U., & Alldredge, A. L. (1995). A dye-binding assay for the spectrophotometric measurement of transparent exopolymer particles (TEP). *Limnology and Oceanography, 40*, 1326–1335.

Peters, T., Pinto, D., & Pinto, E. (2007). Improved seawater intake and pre-treatment system based on Neodren technology. *Desalination, 203*, 134–140.

Rachman, R. M., Li, S., & Missimer, T. M. (2014a). SWRO feed water quality improvement using subsurface intakes in Oman, Spain, Turks and Caicos Islands, and Saudi Arabia. *Desalination, 351*, 88–100.

Rachman, R. M., Li, S., Al-Mashhawari, S., Dehwah, A. H. E., Winters, H., & Missimer, T. M. (2014b). Reduction in organic compound concentrations using well intakes for SWRO

facilities in the Caribbean and the Red Sea of Saudi Arabia. In Proceedings, American Membrane Technology Association/American Water Works Association, 2014 Membrane Technology Conference & Exposition (9 p.), Las Vegas, Nevada.

Schwartz, J. (2003). Beach well intakes improve feed-water quality. *Water & Wastewater International*, November.

Teuler, A., Glucina, K., & Laine, J. M. (1999). Assessment of UF pretreatment prior to RO membranes for seawater desalination. *Desalination, 125*, 89–96.

Vedavyasan, C. V. (2007). Pretreatment trends—an overview. *Desalination, 203*, 296–299.

Villacorte, L. O., Kennedy, M. D., Amy, G. L., & Schippers, J. C. (2009a). Measuring transparent exopolymer particles (TEP) as indicator of the (bio) fouling potential of RO feed water. *Desalination and Water Treatment, 5*, 207–212.

Villacorte, L. O., Kennedy, M. D., Amy, G. L., & Schippers, J. C. (2009b). Fate of transparent exopolymer particles (TEP) in integrated membrane systems: Removal through pre-treatment processes and deposition on reverse osmosis membranes. *Water Research, 43*, 5039–5052.

Chapter 10
Self-cleaning Beach Intake Galleries: Design and Global Applications

Robert G. Maliva and Thomas M. Missimer

Abstract Of the various subsurface intake systems available for use, gallery intake systems have the greatest potential to provide the feed water requirements of very large-capacity seawater reverse osmosis (SWRO) systems because of their scalability and flexibility as far as hydrogeological constraints. A beach gallery system is constructed beneath the intertidal zone of the beach where the wave action continuously cleans the face of the filter media. While it is designed similar to a slow sand filter, a clogging layer tends not to form at the sediment/water interface which allows it to be operated at a higher infiltration rate compared to a seabed gallery system. Design of a beach gallery system active layer (uppermost layer) must be compatible with the grain size characteristics of the beach into which it is constructed. It also must be constructed with sufficient thickness to avoid damage during storm events that produce large waves, which that can temporarily change the beach profile. The beach must be sufficiently stable so as not to have a prograding shoreline that could increase the distance from the gallery face to the sea which would decrease the rate of recharge and cause the intake to fail. This intake type is most suited for use on sandy beaches with moderate wave energy.

10.1 Introduction

It has become increasingly recognized that subsurface intakes for seawater desalination systems can provide significant cost savings, environmental benefits, and increased reliability compared to conventional open-ocean intakes (Missimer 2009).

R.G. Maliva (✉)
Schlumberger Water Services, Fort Myers, FL, USA
e-mail: rmaliva@slb.com

T.M. Missimer
U.A. Whitaker College of Engineering, Florida Gulf Coast University,
Fort Myers, FL, USA
e-mail: tmissimer@fgcu.edu

T.M. Missimer et al. (eds.), *Intakes and Outfalls for Seawater Reverse-Osmosis Desalination Facilities*, Environmental Science and Engineering,
DOI 10.1007/978-3-319-13203-7_10

Subsurface intakes serve both as a means to abstract seawater and to provide initial pretreatment primarily through filtration and, in some cases, also through sorption and biochemical processes (Missimer et al. 2013; Rachman et al. 2014). The primary advantage of subsurface seawater intakes is that they can reduce the capital and operational costs of pretreatment systems and, for some design options, avoid the costs associated with subsea construction. Subsurface intakes avoid the ecological impacts of open-ocean intakes, especially impingement and entrainment of marine life. Alternative intakes can provide improved reliability through a lesser vulnerability to contamination and by providing a time buffer between a contamination event and impacted water entering the desalination system.

A variety of design options are available for subsurface intakes including vertical (beach) wells, slant and horizontal wells, beach trenches and galleries, horizontal collector systems, and subsea galleries. An attractive aspect of subsurface intakes is that they are a modular design and thus readily expandable by, for example, installing additional wells or gallery cells. A disadvantage of the modular design is that there is low economy of scale compared to an open-ocean intake type.

Subsurface seawater intakes are proven technologies in that they are essentially a new application of the over 200 year-old riverbank filtration (RBF) technology. Over the past two decades there have been an increasing number of applications of subsurface intake systems to new operational desalination systems. The selection of the type of intake for a given desalination facility depends upon local hydrogeology, which influences system unit capacity (e.g., well capacity and water yield per square meter of gallery area) and the degree of filtration, and, in turn system costs and benefits. An additional consideration is the likely reliability of the intake system and operation and maintenance costs. The technical challenge for subsurface intakes lies not in the need to develop new technologies, but rather the optimization of the application of existing technologies. Given site-specific hydrogeological constraints and desalination plant raw water requirements, the challenge lies in developing a design that most cost-effectively and reliably provides the required volume and quality of water.

Beach galleries are, in essence, large slow-sand filters constructed along a beach, which take advantage of the natural filtration provided by the native beach sand and an engineered sand filter to provide high-quality water. While similar in design to slow sand filters, they differ in that slow sand filters operate by gravity feed, whereas beach galleries use a suction pump to produce the filtered water. This allows some flexibility in design. An advantage of beach galleries is that they are self-cleaning in the sense the action of waves and activities of burrowing and bottom-feeding organisms (i.e., bioturbation) prevent the build-up of a surficial clogging layer (Maliva and Missimer 2010). This self-cleaning process may make this intake type closer to a rapid sand filter, rather than a slow sand filter. Furthermore, beach and seabed galleries are often the only two subsurface intake types that can practically provide feed water for very large capacity seawater reverse osmosis (SWRO) facilities (Missimer et al. 2013; Dehwah et al. 2014a). This chapter explores the optimization of the design and operation of beach gallery intake systems.

10.2 Basic Beach Gallery Design

10.2.1 Introduction: Slow Sand Filtration

Beach galleries are essentially in situ slow-sand filters and have the same basic design principles. Slow filters normally operate at average rates of 1.2–4.8 m/d with higher rates (9.6 m/hr or greater) possible for high-quality (low suspended solids) water or during peak periods (Crittenden et al. 2005). The design of slow sand filters was addressed in detail by Huisman and Wood (1974), Crittenden et al. (2005), and Hendricks (1991, 2011). Slow sand filters contain two main elements, the sand filter and underlying underdrain, which includes the main and lateral screens and gravel support (Fig. 10.1).

The underdrain screen and gravel pack function to efficiently collect the seawater with a minimal loss of head. The gravel support does not serve a filtration purpose, but instead acts to support the screen and filter sand, and to efficiently transmit water to the screen. The gravel support should be coarse enough, and have a high enough hydraulic conductivity, so as to minimize head differences across the gallery. The objective is to have a near uniform infiltration rate through the overlying filter pack. The gravel pack normally extends below the screen to increase its transmissivity and to provide space for any fine-grain materials that settles or is drawn into the gravel to accumulate without covering the screen. The seabed filter differs from the slow sand filter in that it is pumped from the base, but it still shares similarity in that it cannot be back-flushed for cleaning. Pumping is necessary because natural tide changes cause the hydraulic head across the filter to vary in time, which requires the pump to adjust to maintain a constant pumping rate.

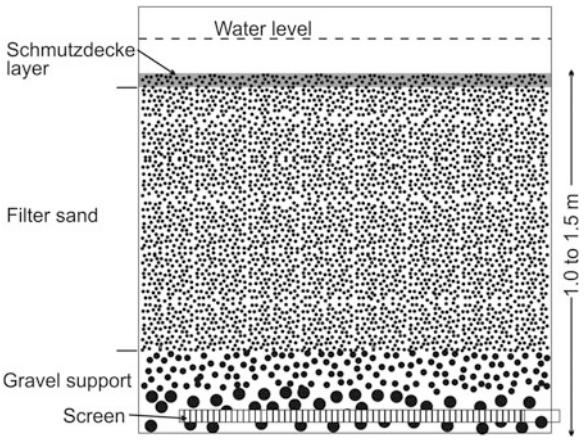

Fig. 10.1 Conceptual diagram of a slow sand filter

10.2.2 Design and Function of the Media and Hydraulic Retention Time

The filter sand needs to be fine enough to provide sufficient filtration of suspended materials of concern. Hendricks (1991, 2011) recommended that the d_{10} of the filter sand (sieve size that permits 10 % of the sand to pass through) be 0.2–0.3 mm with a corresponding uniformity coefficient (UC, d_{60}/d_{10}) between 1.5 and 2.0. Coarser sand may be used (0.3–0.4 mm) as long as the uniformity coefficient is less than 3. Crittenden et al. (2005) suggest that average grain size of the media can range from 0.3–0.45 mm and the bed depth is normally 0.9–1.5 m.

An important aspect of the slow sand filter design is the quality of the water to be treated and the hydraulic retention time of the water within the filter. There are limits on the turbidity of the raw water that can be effectively treated. Crittenden et al. (2005) suggest that the slow sand filtration process is effective for raw water with a turbidity range of 10–50 NTU. The hydraulic retention time of most slow sand filter systems ranges from 5 to 6 h. Hydraulic retention time from a set of slow sand filters with differing thicknesses and an assumed uniform hydraulic conductivity is given in Table 10.1. There is an offset between the lower hydraulic conductivity of the surficial layer and the increasing hydraulic conductivity with depth in the media. The key issues controlling the hydraulic retention time are the design infiltration rate and the bed thickness. Increased hydraulic retention time tends to increase the degree of water treatment.

In freshwater systems, a biologically active gelatinous mat, composed of deposited and synthesized material, forms at the top of the filter sand. This unit is called the schmutzdecke (German for 'dirty skin') layer. The schmutzdecke layer is an important part of the filtration process and is where much of the biological treatment occurs. Growth of the schmutzdecke layer increases hydraulic resistance across the slow sand filter and it must be periodically scrapped off in order to maintain acceptable filtration rates. To maintain the same degree of biological treatment, the scrapped filter must be given time to "ripen". This process can take between 12 h and several days in freshwater systems. Repeated cleanings by scrapping also reduces the thickness of the filter and changes the hydraulic retention

Table 10.1 Hydraulic retention time as a function of infiltration rate and bed thickness

Infiltration rate	Infiltration rate	Bed thickness	Hydraulic retention time
m/hr	m/d	m	hr
0.05	1.2	0.9	18
0.1	2.4	1.0	10
0.2	4.8	1.25	6.25
0.3	7.2	1.3	4.3
0.4	9.6	1.4	3.5
0.5	12.0	1.5	3.0

time. New sand can be added to the surface of the filter to replace the material removed. The typical run length before reconstruction of the full filter bed is 1–6 months. Because of the development of the schmutzdecke layer in freshwater systems, most of the water treatment occurs within the upper 10 cm of the filter, so the hydraulic retention time is not so important. This is not necessarily the case in in marine systems. Column experiments conducted using seawater from the Red Sea showed that a period of several months was required for the system to remove up to 50 % of the total organic carbon (TOC) entering the column (Dehwah et al. 2014b)

Design of the slow sand filter media requires that the grain size distribution of the created layers allow proper support without breakthrough of fine grains into the next lower layer. The gravel support consists of multiple layers with an upwardly decreasing grain size. The layers need to be design so that they are stable, minimizing settling of finer grained sand and gravel into underlying layers. Huisman and Wood (1974) proposed the following general rules for the design of the gravel support, which are still widely accepted:

1. d_{90}/d_{10} for a given layer ≤ 1.4
2. d_{10} lower layer/d_{10} upper layer ≤ 4
3. d_{10} top layers/d_{15} filter sand ≥ 4
4. d_{10} top layer/d_{85} filter sand ≤ 4
5. d_{10} bottom layers $\geq$ 2d (drain orifice or screen slot diameter)

Huisman and Wood (1974) noted that the requirement for a highly uniform sand ($d_{90}/d_{10} < 1.4$) may be too restrictive (i.e., expensive to meet) and that a ratio of 2 would be acceptable if the ratio of d_{10} values between layers is less than 3. The recommended minimum thickness of the gravel layers is three times the diameter of the largest grains or 5–7 mm for finer materials and 8–12 mm for coarse gravel (Huisman and Wood 1974). The use of fine sand in the top layer tends to provide a higher degree of removal of algae, bacteria, and viruses (Amy et al. 2006; Jenkins et al. 2011; Lujan and Missimer 2014). The upper sand layer, however, must be compatible with the natural beach sand or it would be rapidly scoured away. In some cases, a finer layer may have to be placed below the upper active layer with a downward coarsening below that level, or the uppermost layer must be significantly thickened, to increase hydraulic retention time.

Beach galleries have similar design as slow sand filters used for water treatment with the exception that they are topped with the natural beach sand, which may or may not be of an appropriate size for filtration purposes (Fig. 10.2). The sand filter needs to be designed to provide effective filtration of suspended solids and to meet water quality targets, such as maintenance of a silt density index of less than 3 and removal of all algae and most bacteria, and be stable. The suspended solids include silt and clay-sized siliciclastic sediment and organic matter, planktonic organisms, and any fine material within the surficial sand layer that may be mobilized. If the filter sand is too coarse, then filtration goals may not be achieved. If the sand is too fine grained, then it may provide excellent filtration, but too much flow resistance to provide adequate water production rates. The overall thickness of the filter should

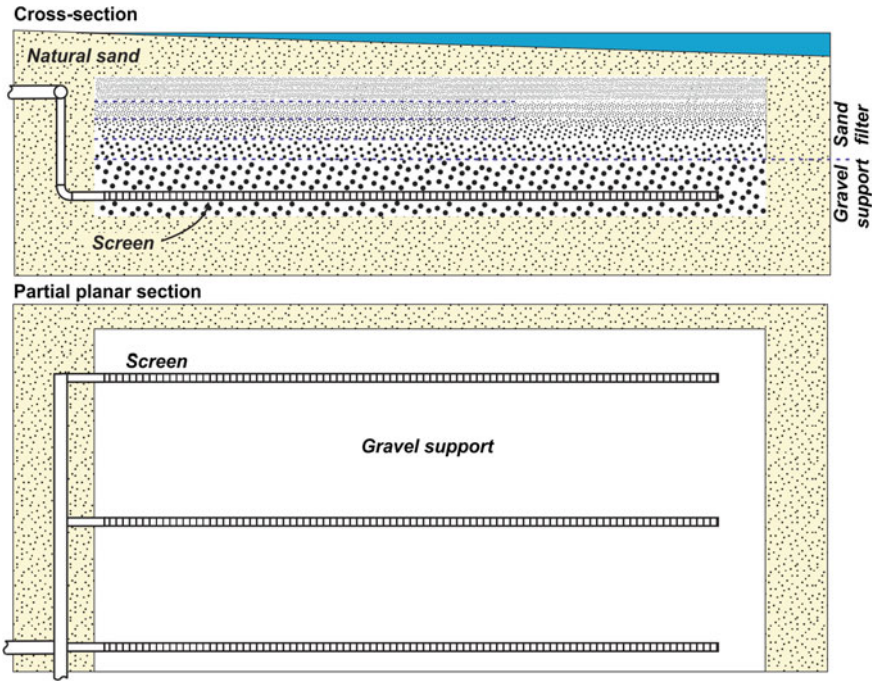

Fig. 10.2 Conceptual diagram of a beach gallery. Thickness of gravel support and sand filter is approximately 1.5–2 m

achieve a hydraulic retention time within the range of 6–8 h, which may require a greater thickness of constructed filter layers than the minimum thickness suggested Huisman and Wood (1974).

Proper design of a sand filter requires balancing filtration capability with system unit capacity, which is a function of the average vertical hydraulic conductivity of the filter. Thicker layers of finer-grained sediments improve filtration, but decrease the effective hydraulic conductivity, which requires the suction pumping to be increased to achieve the desired system capacity. The effective vertical hydraulic conductivity can also be reduced if there is mixing of sand between layers where the uppermost layer has a lower hydraulic conductivity compared to the next lower layer. This issue can necessitate a filter design using a thicker upper layer.

10.2.3 Use of Geotextile Fabrics in Design and Construction

Geotextile fabrics can be used to stabilize the walls of the gallery and minimize the mixing between layers, such as between the native beach sand and engineered filter sand and between the filter sand and underlying gravel pack. The pore size of the

geotextile fabrics should be selected to retain the finer grained sediments. The main potential drawback of the use of geotextile fabrics is that they can be preferential sites of biological growth and thus become clogging layers which would require periodic removal and reconstruction of the gallery cell. In general, the use of a geotextile fabric to line the sides of a gallery is recommended, particularly where there is high water production from lateral flow into the gallery. Internal use of a geotextile fabric is generally not recommended, because of the potential for clogging and associated impedance of vertical flow.

Commonly used geotextile fabrics are composed of polyester (PET), polypropylene (PP), polyethylene (PE) and polyamide or nylon (PA) and may have either a woven and nonwoven construction. Most common geotextile polymers are unaffected by microorganisms, bacteria, and fungi. Although bacteria and other organisms do not feed on geotextile polymers, they can destroy their function as a filter by growing on the surface of fabric, and/or blocking the pores (Kossendey et al. 1996; Cook 2003; Rollin 2004; Rowe 2005). Some nylon based geotextile fabrics have been damaged by consumption by marine isopods which was found during a beach erosion control experiment on Captiva Island, Florida. Burrowing macrofauna may also damage geotextile fabrics. Although both needle-punched nonwoven and woven geotextiles are used for filtering (e.g., in leachate collection systems); woven textiles appear to be a better choice for use in beach galleries because of a lower susceptibility to biological clogging. Needle-punched nonwoven geotextiles provide a particularly large surface area for biofilm development (Rowe 2005). Key variables in the selection of geotextiles for long term maintenance of permeability are maximizing the percent open area (POA) and apparent opening size (AOS). The AOS needs to be of an appropriate size to retain the adjoining sediment while maintaining the desired flow rate.

10.2.4 Design of the Underdrain or Collection System

A key design issue in any gallery cell is the maintenance of a uniform infiltration rate at the surface of the filter. Uneven infiltration can lead to areas of excessive infiltration that encourages clogging at the surface or below the depth of wave-agitation. Design of flow control in underdrain systems in marine galleries was addressed by Mantilla and Missimer (2014).

Design of the system requires that a uniform flow is maintained in the screen slots, which is related to keeping the suction heads in the collection system piping as constant as possible. Commonly, the applied suction head is highest in the proximal screens and lessens toward the distal boundaries of the piping. Head loss with the piping system is controlled to a degree by the pipe junction geometry and number of junctions. Careful design of the piping system to maintain an equal head loss requires some pipe modeling to balance the diameter of the collection pipes

with the intersection types and the screen locations. The density of screen slots and their apertures also play a role in achieving a proper balance (see Chap. 11).

10.2.5 Construction Materials: Sand, Gravel, and Pipes

The sand and gravel in the engineered filter should be well-rounded and not angular. It should be similar in density to the natural beach sand, so that it does not scour or leave an unnatural mound in the littoral zone. The upper layer that is in contact with the natural beach sediment is of primary concern. Therefore, gallery cells constructed within a predominantly quartz sand beaches should have an upper layer composed of quartz sand. Beaches can be composed of predominantly carbonate sands or a mix of carbonate and siliciclastic sands. The upper layer of the filter should be designed to generally match the composition with reasonable percentages based on the heterogeneity of beach sediment composition.

Seawater containing dissolved oxygen is extremely corrosive to any type of metallic material. Because beach galleries are always constructed with a bed thickness of less than 7 m, non-metallic materials, such as polyvinylchloride (PVC) and high density polyethylene (HDP) can be used for construction of underdrain screens and connecting pipes. These materials come in a variety of diameters and strengths that may be required based on field conditions.

10.2.6 Design of the Underdrain Screens

PVC screens used for underdrains should contain uniform-aperture, machined slots. Because of the coarse gravel in which the screens are placed, the slots do not necessarily have to be the wedgewire or "v" types used in the water well industry or used in passive screen intake systems (Chap. 6). There may be a limit to the diameter of PVC screens which can be used based on standard manufactured produce and compressive strength of the material. Machine slotted HDP can be used, but may be a special order material. The width of the screen slots must be less than the diameter of the smallest particular in the basal gravel unit because these screens cannot be easily "developed" to remove fine-grained material from the feeder pipes.

10.2.7 Design of High Capacity Beach Gallery Intakes

For medium to large-capacity systems (>1890 m^3/d), a modular design is preferred with each module or cell having an independent pumping system. A modular design can provide for redundant capacity, which allows for one cell to be taken off

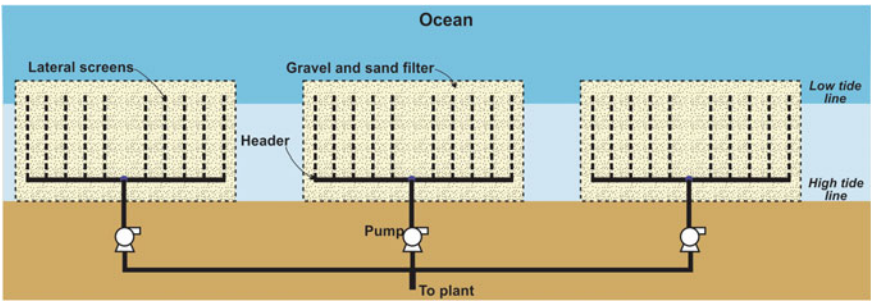

Fig. 10.3 Multiple cell beach gallery intake system configuration

line for maintenance activities without having to shut down the entire desalination system. The first cell should ideally be constructed and tested early in a project to obtain data on system capacity and water quality. Gallery cells could be pumped under suction using a variety of engineered pump scenarios. Each cell should be equipped with a dedicated pump to achieve high system reliability with redundant capacity. The configuration of the gallery cells should lie parallel to the beach and fully within intertidal and subtidal water to assure continuous vertical recharge (Fig. 10.3).

10.2.8 Alternative Beach Gallery Cell Design

An alternative to the standard design of beach gallery cells is the use of a modular plastic crate system instead of a gravel support. Modular crate systems, such as the polypropylene Flo-Tank® system developed by the Atlantis Corp, could be adopted for use in beach galleries (Fig. 10.4). The tanks are covered with a geotextile and then overlain with a sand filter consisting of engineered and/or natural beach sand. The advantages of this system include: the crates modules are light-weight, have a very large open area, and could be reused if the system requires maintenance.

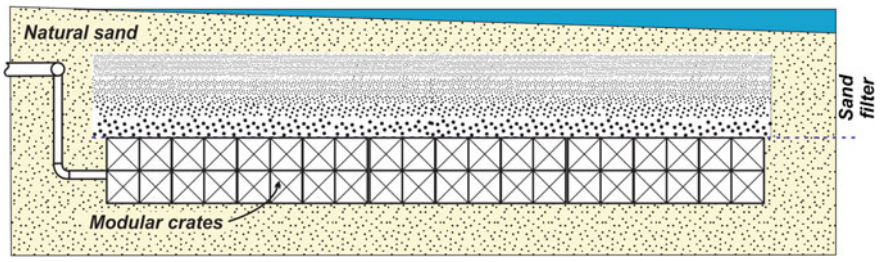

Fig. 10.4 Alternative beach gallery intake design using modular plastic crates

10.3 Optimization of Design

Variables that need to be incorporated into the beach gallery design include:

- area of each cell
- gallery media depth
- screen and gravel pack design (screen type, length, pattern, diameter, slot size and area, and gravel size)
- screen, collection pipe, and conveyance pipe dimensions and materials
- sand-and-gravel filter design (number, thickness, and grain size of layers)
- composition and shape of sand-and-gravel material
- geotextile fabric (whether or not to use and type)
- location of the gallery with respect to high and low tide lines

Additional design considerations include:

- source of water (flow paths)
- location of any sources of contamination or hypersaline water below the gallery
- constructability
- sedimentology of the project site (beach dynamics)
- ease of maintenance

The source of water refers to whether seawater is produced predominantly by vertical infiltration downward through the top of the gallery or if there is significant lateral flow from either the seaward or landward direction. In the former case, the gallery should be constructed either in the subtidal part of the beach (below the low tide line) or perhaps partly subtidal and partly in the lower part of the intertidal zone, so that it is submerged either all or most of the time. The key issue is that recharge to the gallery must be able to maintenance the required yield under all conditions, so that the gallery is never dewatered.

Occurrence of hypersaline water beneath the shoreline occurs in many parts of the Middle East and North Africa and in other areas, such as Australia and Cyprus. The source of the hypersalinity is commonly from sabhkas that are large supratidal flats that tend to trap seawater at spring high tides and become evaporation basins with a seaward trending density-driven flow. A beach gallery design from a medium capacity SWRO beach at Larnaca, Cyprus contained the gallery cells within concrete vaults to prevent any upward movement of high salinity water into the gallery structure (Missimer 2009).

Construction on a beach, in general, requires some knowledge of beach dynamics, such as whether the beach in retreating (being eroded) or prograding (growing seawards). Information about the history of a beach may be discerned from careful observations of current conditions and examination of a series of historical aerial photographs and maps. Some shorelines can be highly unstable. Figure 10.5 shows the location of the shoreline at Cape Hatteras, North Carolina (USA), which has migrated approximately one kilometer between 1860 and 1980 (Everts et al. 1983). The position of the shoreline can be determined relative to fixed

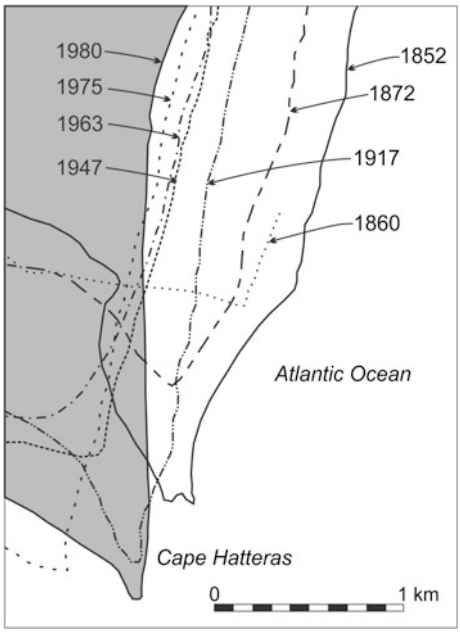

Fig. 10.5 Diagram showing changing position of mean high tide line at Cape Hatteras, North Carolina Island in 1980 is shaded gray (after Everts et al. 1983)

reference points. At Cape Hatteras, the shoreline adjacent to a lighthouse constructed in 1870 migrated 460 m inland. The lighthouse was moved inland in 1999 as the shoreline had retreated dangerously close to it.

It is important to appreciate that the erosion and growth of a beach may occur seasonally or during storm events, so conditions observed during a fair weather or single day visit may not be representative of what may happen in the future. In the case of a retreating beach, the concern is that erosion could expose and destroy the gallery. Progadation of a beach could strand the gallery future inland, causing the recharge flowpath to increase which, would decrease the yield of the gallery. Another issue is that seasonal beach profile changes occur on all beaches based on weather changes and these measured changes must be incorporated into the design of the gallery cells. In general, changes in the beach dynamics can be accommodated in the design of the gallery system. For example, if a beach is generally stable with the exception of potential severe storm impacts, the upper layer of the gallery could be increased in thickness to well below the maximum storm excavation depth. This would protect the gallery, but may increase the pumping head loss across the filter which would lead to some increase in operating cost. However, the thicker media would also lead to a higher degree of treatment of the inflowing water which may balance the overall cost.

Constructability is another important issue, particularly with respect to locally available resources and weather conditions. Public acceptance of some duration of beach closure may also be an issue. Locally available resources include both construction contractors and materials, such as properly graded sands. An important

cost issue is whether or not a gallery construction requires installation of temporary sheet piling or a coffer dam, which depends upon cohesiveness (stability) of the native sands, tidal range, and wave intensity. The preferred situation is where the excavation walls are stable and wave energy is minimal, which would allow for construction without sheet piling. Installation of the beach gallery could be performed using a backhoe and pumps to dewater the excavation during low tide periods. A sand barrier could be installed seawards of the excavation to allow for dewatering through the tidal cycle. Alternatively, temporary inflatable water barriers may be used. Construction scheduling is another important issue, because many beaches are intensively used for recreational activities. Because of the modular nature of a beach gallery design, construction can be staged to close only the segment of the beach where a single cell is being constructed. As each cell is finished, the construction site would be moved to the next location, thereby limiting the lateral extent of closure to the public.

Ability to maintain the intake is an often under-considered issue for all subsurface intake systems in general. Most wells require periodic maintenance. Similarly, various physical, chemical, and biological processes could impact the long-term performance of beach and subsea galleries. The selection of alternative intake options should consider the type, potential frequency, and costs of rehabilitation activities. For example, although horizontal wells can provide much greater flow rates than vertical wells, they may be much more difficult and expensive to maintain. In the case of beach galleries, clogging of screens, the gravel pack, and the sand-and-gravel filter may require re-excavation of the gallery. Subsurface intake systems should have robust designs that can accommodate some loss of performance over time and thus reduce the need for rehabilitation actions. The costs of rehabilitation activities should be considered in cost-benefit analyses. An example of a design to accommodate some degree of clogging is to use variable frequency drives (VFD's) on the production pumps to allow a constant flow rate during changes in head loss. Fluctuations in tides may requirement the use of VFD's anyway.

10.4 Design Process

Design of a beach gallery system requires the collection of detailed information on the hydraulic properties of shallow strata in and in the vicinity of the beach. The aquifer characterization program should be designed to obtain information of bulk aquifer properties and the degree and type of aquifer heterogeneity. The shallow aquifer testing program should include some or all of the following elements:

- test well installation and aquifer pumping tests
- slug testing
- grain-size analyses (in the geological profile and across the beach face)
- core collection and permeameter testing

Groundwater modeling is an indispensable tool for beach gallery design. A high-resolution model was developed using the MODFLOW (Harbaugh 2005) and MT3DMS (Zheng and Wang 1999) codes to simulate different beach gallery design options. A sub-meter grid size in the core area of the model allows for the incorporation of the individual layers of the sand-and-gravel filter (Fig. 10.6). The MT3DMS solute-transport code is used to trace the source of water that is produced from the gallery. By assigning the water above the gallery with a concentration of 100 and all other waters to a concentration of zero, the percentage of water that enters a gallery by downward flow can be calculated.

Simulations of an investigated gallery site consisting of fine-grained sand with a hydraulic conductivity of less than 1 m/d indicated that lateral flow into the gallery would be negligible. Nearly all of the water is produced by downward infiltration through the top of the gallery. The optimal design of the gallery would be to construct the system just below the low tide line where it could be continuously submerged. The depth of the standing seawater is not significant to the design of the filter media and system hydraulics (but affects the collection pump design). The modeling results also indicated that the depth of the gallery had a minimal effect on water production. The optimal design involves maximizing the surface area of the gallery to produce the desired capacity.

A key constraint of the design of galleries is the thickness of the upper native sand layer, where it has a low hydraulic conductivity. In layered systems, the effective vertical hydraulic conductivity of the sand-and-gravel filter depends upon the thickness and hydraulic conductivity of the least permeable layers, which in the modeled system was the native beach sand. Where the near-surface sediments have a moderate to high hydraulic conductivity, lateral flow may be important and a deeper trench may be a better design. The important issue is that a properly constructed groundwater model can be used to evaluate various design scenarios to

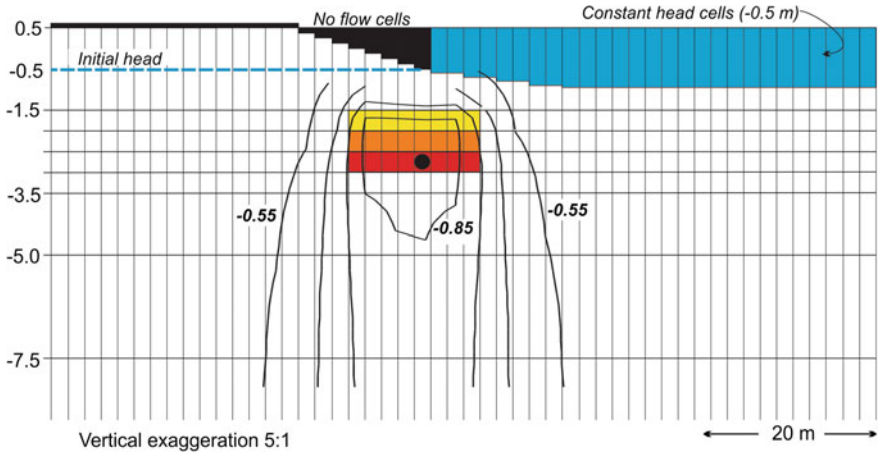

Fig. 10.6 Cross-section diagram of beach gallery showing modeled heads

understand the sensitivity of the system to different parameters and to determine the optimal design for a given site.

Once it is determined that a beach gallery is likely to be a technically feasible and economic option, then the next step in the design process is the construction and testing of a small-scale pilot system. The pilot system does not need to be very large (it could be as small as 10 m^2), but its design and location with respect to the beach should be a close as practical to that of a full-scale system. The objectives of the pilot testing program are to obtain proof of concept for the site and sufficient data to design a full-scale system. Pilot testing program data are normally used for calibration of the groundwater model for multiple cell systems. The sophistication of the test program needs to match the proposed capacity of the SWRO capacity desired with more data required for large capacity systems.

10.5 Potential Performance Issues

Beach galleries are based on the proven slow-sand filter technology, so there is a high probability that a properly constructed system will perform as expected. The filtration rate through slow-sand filters in freshwater systems declines over time due to the development of a biological clogging (schmutzedecke) layer. However, in the limited testing performed on seawater in the laboratory and at a pilot facility, no schmutzedecke layer formed at the filter surface (Desormeaux et al. 2009). However, regardless whether an upper biological layers forms or not, the self-cleaning nature of beach galleries (wave turbulence) would likely prevent the formation of a significant clogging layer. If a layer were to form, then it could be removed by raking or scraping the beach.

Beach galleries should ideally be constructed in locations where the beach is stable (i.e., neither significantly prograding or retreating) over the anticipated operational life of the gallery. If the position of the beach is unstable, then the gallery design needs to incorporate the likely range of shifts in the position of the beach with respect to the gallery. For example, if a beach is prograding, then the gallery design should incorporate future conditions in which the gallery is located further from the intertidal and subtidal zones. This may necessitate the construction seaward of the beach as a seabed gallery with transition to a beach gallery.

The integrity of the grain-size layering in the sand-and-gravel filter can be compromised by the activities of burrowing organisms, which are present in the intertidal and, to a greater degree, in subtidal zones. The mixing of sediments would tend to reduce their sorting and either increase or decrease their hydraulic conductivity (increase could be caused by burrow filling with coarse material), thereby changing the infiltration rate. In the beach environment, it is unlikely that significant quantities of fine-grained sediment would be incorporated into burrows. Filter-feeding infauna would tend to bind fine-grained sediments and organic residues into fecal pellets that would be hydraulically neutral (hard pellets). In warm tropical areas, the downward flow of seawater could result in calcium carbonate precipitation, which could

gradually clog the screen, gravel pack and sand-and-gravel filter. However, the rate of flow through the gallery is limited by the lower hydraulic conductivity sand at the top of the sand-and-gravel filter. Considerable clogging of the screen and gravel pack could occur without reducing system performance.

Beach galleries should have reliabilities comparable or favorable to that of other subsurface intake designs and conventional open-ocean intakes. It is recommended that all subsurface intakes have robust designs that can accommodate some loss of performance over time. The design should incorporate a substantial safety factor and reserve capacity to achieve a high system reliability factor. Gallery modules could be designed to operate at higher flow rates than the required rates. Another option is to plan on the installation of addition gallery modules, as needed to maintain the raw water supply. The overall system design would include plans for the location of the additional modules, including piping and instrumentation, especially if SWRO capacity expansion is being anticipated. The galleries should also be designed to facilitate future rehabilitation activities, if ever needed. For example, sheet piling might be left in place to facilitate the excavation and reconstruction of the galleries, if ever needed. This should occur only of the sheet piling will remain below the beach surface, because it could become a source of turbulence resulting in accelerated wave-induced erosion and disruption of the upper gallery layer.

10.6 Global Applications

Beach galleries are a potential feasible subsurface intake design anywhere in the world where there is a moderate to high-energy beach in which clean (clay-free) sands are deposited. Beach galleries have considerable design flexibility in that the engineered sand filter can compensate for sub-optimal sediment characteristics. This design option has a wide range of potential capacities and can accommodate very large systems depending on the available beach lateral area which may be a limiting factor. A key aspect of the design is that once constructed, the beach can be restored to essentially initial conditions with no significant visual impacts. Pumping stations and support infrastructure can be located off the beach.

A key issue is that a beach galley intake system must avoid the environmental issue of impingement and entrainment of marine organisms, which is a major political issue in the United States and the European Union. Also, similar to all subsurface intake systems, the beach gallery system would become part of the SWRO facility pretreatment process train and would reduce the need to use chemicals and the energy costs of the in-plant pretreatment systems used in open-ocean intake systems.

10.7 Discussion

10.7.1 Permitting and Public Involvement

In the United States and the European Union, there are rather stringent regulations that apply to constructed works along the shoreline and in the bottom of tidal water bodies. Construction of a beach galley system would require a variety of environmental permits to be obtained. Some of these permits may require the preparation of environmental impact assessments and all of them have access to public input and political approval. Therefore, many desalination facilities around the world are having difficulties in obtaining environmental permits for construction and operation of intake and outfall systems. Commonly, the objective of some stakeholders is to defeat the use of desalination in general, because they view it as an energy-intensive process and that expansion of the water supply may enable additional local population growth and development. This opposition is commonly focused on the axillary parts of the facilities that are most vulnerable to undefined impacts.

A key method of defusing public opposition is to clearly make the case of the reduced environmental impacts of using subsurface intakes and the long-term reduction in the cost of facility operation. A life-cycle cost analysis should be performed during the facility design to clearly assess a SWRO facility using an open-ocean intake with extensive pretreatment versus a beach gallery system with a much less intensive pretreatment system. Missimer et al. (2013) demonstrated that the amortized capital cost using a subsurface intake system, especially using periods from 15 to 30 years, will produce a lower cost of water treatment and a lower water cost to the consumer. Another key issue is that the lower use of chemicals during treatment (e.g., chlorine and ferric oxide) reduces impacts to the marine environment and the lower electric use in pretreatment reduces the carbon footprint of the facility.

Use of a beach gallery system must be presented to the public early in the design and permitting process to allow sufficient time to engage and educate the public. This should include the use of public involvement experts and the use of computer programs, such as STELLA, to allow interactive and informative presentations that may convince key societal groups to support the most environmentally sound intake type. The most common issues that tend to be raised include: (1) closed beach access during construction, (2) future impacts to intertidal infauna, (3) visual impacts to beach users, and (4) impingement of fish eggs. These issues can be reasonable addressed. Beach access limitation can be lessened by proper construction scheduling with phased construction, thereby closing only small parts of the beach. Certain beach infauna will be impacted during construction, but the filtration of organic material within the beach system will increase growth rates of many organisms, such as polycheates, and may improve the nearshore environment. Visual impacts should be minimal or non-existent because once the gallery cells are constructed there will show no surface expression. Pumping stations can be located

off the beach or be collocated with life-guard stations of changing facilities to hide them. The impingement issue is new and is addressed in the next section.

10.7.2 Environmental Issues

The newest criticism on subsurface intakes, gallery types in particular, is the inference that these systems cause impingement of fish eggs onto bottom sediments and "hide" the same impacts as open-ocean facilities. Fish eggs tend to be neutrally buoyant and are part of the ichthyoplankton within the marine water column. A key aspect of the maintenance of fish eggs within the water column is motion within the marine environment. The infiltration velocity in a beach gallery system is unlikely to be greater than 15 m/day. Therefore, the maximum inflow velocity into the sediments would be about 0.02 cm/s. To allow attachment of the eggs to the sediment in the beach intertidal zone, the wave breaking area, the water column would have to be essentially still with no wave orbital motion, no wave-generated turbulence, and no currents. The creation of a "still" condition in the intertidal zone of a beach may be limited to some types of very restricted water bodies that are likely to have a muddy shoreline, not geologically conducive to the development of a beach gallery intake system. Brownian motion may be sufficient to keep the fish eggs in motion without causing attachment, even in a relatively still environment.

10.7.3 Innovative Designs

Beach gallery systems are a relativity new design concept for seawater SWRO, introduced in a series of publications between 1991 and present (Missimer and Horvath 1991; Missimer 1994, 2009; Maliva and Missimer 2010). A few small SWRO systems currently use these systems, which are located at island facilities in the Caribbean. As more sophisticated and larger capacity designs are constructed and operated, design innovations will evolve that will produce some economies of scale and will involve innovative construction methods, not yet utilized. This will tend to reduce cost and will give SWRO facility owners and operators more confidence in the technology and design concept.

10.8 Conclusions

Beach galleries are a viable subsurface seawater intake design option that is particularly advantageous in locations with a small thickness of transmissive near surficial sediments, which precludes wells as a design option. The galleries can be constructed to be unobstrusive and thus not interfere will use of beach. The key

design and construction issues are obtaining a sand filter that provides sufficient yield (rate divided by gallery area) to economically meet plant raw water requirements while also meeting treatment requirements. The sand filter also needs to be stable in that infiltration rates do not decline over time. Although a beach gallery is self-cleaning, its performance may decline if it is buried by beach progradation (addition of sediment causing the length of the infiltration flow pathway to increase) or if vertical hydraulic conductivity is reduced due to sediment and filter material mixing by bioturbation (i.e., introduction of fine sediments into coarse sand layers) or subsurface clogging by biological growth and/or carbonate cement precipitation. If the vertical hydraulic conductivity is increased in burrows of marine infauna that are filled with coarse sediment, then the treatment function of the upper gallery layer would be reduced. Such issues can be adequately addressed in the system design to achieve the necessary modifications required for successful operation. The system design and cost-benefit analysis should also consider the potential requirement for system rehabilitation, which may require excavation and reconstruction of the galleries. However, the simple design and low material costs may make beach galleries an economically viable option even if major rehabilitation work is periodically required. A key issue is to make the beach gallery design robust to deal with a variety of natural system events and processes that could affect performance.

References

Amy, G., Carlson, K., Collins, M. R., Drewes, J., Gruenheid, M., & Jekel, M. (2006). Integrated comparison of biofiltration in engineered versus natural systems. In R. Gimbel, N. J. D. Graham, & M. R. Collins (Eds.), *Recent progress in slow sand filtration and alternative biofiltration processes* (pp. 3–11). London: IWA Publishing.

Cook, D. I. (2003). Geosynthetics. *Rapra Review Reports No. 58*, Shrewsbury: Rapra Technology Limited, 132 pp.

Crittenden, J. C., Trussell, R. R., Hand, D. W., Howe, K. J., & Tchobanoglous, G. (2005). *Water Treatment*: *Principles and Design* (2nd ed.). Hoboken: Wiley

Dehwah, A. H. A., Al-Mashhawari, S., & Missimer, T. M. (2014a). Mapping to assess feasibility of using subsurface intakes for SWRO, Red Sea coast of Saudi Arabia. *Desalination and Water Treatment, 52*, 2351–2361. doi:10.1080/19443994.2013.862035.

Dehwah, A. H. A., Li, S., & Missimer, T. M. (2014b). Effects of slow sand filtration of seawater in removal of algae, bacteria, organic carbons fractions, and TEP. *Water Research*.

Desormeaux, E. D., Meyerhofer, P. F., & Luckenbach, H. (2009). Results from nine investigations assessing Pacific Ocean seawater desalination in Santa Cruz, California. *Proceedings of the International Desalination Association World Congress on Desalination and Water Reuse, Atlantis, The Palm, Dubai, UAE*, November 7–12, 2009, Paper IDAW/DB09-291.

Everts, C. H., Battley, J. P., Jr., & Gibson, P. N. (1983). Shoreline movements. Report 1, Cape Henry Virginia to Cape Hatteras, North Carolina, 1849–1960. Technical Report CERC-83-1, Washington, D.C.: U.A. Army Corps of Engineers and National Oceanic and Atmospheric Administration, 111 pp.

Harbaugh, A. W. (2005). *MODFLOW-2005, the U.S. Geological Survey modular ground-water model–the Ground-Water Flow Process*. U.S. Geological Survey Techniques and Methods 6-A16.

Hendricks, D. W. (Ed.). (1991). *Manual of design for slow sand filtration*. Denver: AWWA Research Foundation and American Water Works Association.

Henricks, D. W. (2011). *Fundamentals of water treatment unit processes: Physical, chemical, and biological*. Boca Raton: CRC Press.

Huisman, L., & Wood, W. E. (1974). *Slow sand filtration*. Geneva: World Health Organization.

Jenkins, M. W., Tiwari, S. K., & Darby, J. (2011). Bacterial, viral and turbidity removal by intermittent slow sand filtration for household use in developing countries. *Water Research, 45* (18), 6227–6239.

Kosssendey, T. H., Gartung, E., & Schmidt, S. (1996). Microbiological influences on the long-term performance of geotextile filters. In *Proceedings Geofilters '96*, *Montreal*, pp. 115–124.

Lujan, L. R., & Missimer, T. M. (2014). Technical feasibility of a seabed gallery system for SWRO facilities at Shoaiba. Saudi Arabia, and regions with similar geology. Desalination and Water Treatment. doi:10.1080/19443994.2014.909630.

Maliva, R. G., & Missimer, T. M. (2010). Self-cleaning beach-gallery design for seawater desalination plants. *Desalination and Water Treatment, 13*, 88–95.

Mantilla, D., & Missimer, T. M. (2014). Seabed gallery intake technical feasibility for SWRO facilities at Shuqaiq, Saudi Arabia and other global locations with similar coastal characteristics. *Journal of Applied Water Engineering and Research*, *2*(1), 3–12.

Missimer, T. M. (1994). *Water supply development for membrane water treatment facilities*. Boca Raton: Lewis Publishers. 253 pp.

Missimer, T. M. (2009). *Water supply development, aquifer storage, and concentrate disposal for membrane water treatment facilities*. Houston, Texas, Schlumberger Water Services, Methods in Water Resources Evaluation Series No. 1, 390 pp.

Missimer, T. M., Ghaffour, N., Dehwah, A. H. A., Rachman, R., Maliva, R. G., & Amy, G. (2013). Subsurface intakes for seawater reverse osmosis facilities: Capacity limitation, water quality improvement, and economics. *Desalination, 322*, 37–51. doi:10.1016/j.desal.2013.04.021.

Missimer, T. M. & Horvath, L. E. (1991). Alternative designs to replace conventional surface-water intakes for membrane treatment facilities. *Technical proceedings of the International Desalination Association Conference on Desalination and Water Reuse*, Washington, D. C., pp. 131–140.

Rachman, R. M., Li, S., & Missimer, T. M. (2014). SWRO feed water quality improvement using subsurface intakes in Oman, Spain, Turks and Caicos Islands, and Saudi Arabia. *Desalination, 351*, 88–100.

Rollin, A. L. (2004). Long term performance of geotextiles. In *Proceedings 57th Canadian Geotechnical Conference, Quebec City, Quebec, Session 4D*, pp. 15–20.

Rowe, R. K. (2005). Long-term performance of contaminant barrier systems. *Géotechnique, 55*(9), 631–678.

Zheng, C., & Wang, P. P. (1999). *MT3DMS*: *A modular three-dimensional multi-species model for simulation of advection, dispersion and chemical reactions of contaminants in ground water systems: documentation and user's guide*. Vicksburg, Mississippi: U.S. Army Engineer Research and Development Center, report SERDP-99–1.

Chapter 11
Feasibility and Design of Seabed Gallery Intake Systems Along the Red Sea Coast of Saudi Arabia with Discussion of Design Criteria and Methods

Thomas M. Missimer, Abdullah H.A. Dehwah, Luis Lujan, David Mantilla and Samir Al-Mashharawi

Abstract Geological characteristics of the Red Sea coastline of Saudi Arabia were evaluated to assess the technical feasibility of designing and constructing seabed gallery intake systems to provide feed water for seawater reverse osmosis (SWRO) desalination plants. Five sites were investigated in detail at King Abdullah Economic City, Om Al Misk Island, Jeddah, Shoaiba, and Shuqaiq. It was found that a large part of the Red Sea nearshore area contains a low-sloping inner reef area from the beach seaward to the reef tract. Water depth ranges from 0 to 2 m in this shelf area and there is minimal coral growth and a small percentage of seagrass cover. There is a carbonate or siliciclastic sand cover over a moderately hard to soft limestone. It was found that seabed gallery systems could be designed and constructed at each of the sites investigated. The site-specific conditions varied which necessitated different designs of the filter with the upper, reactive layer varying with regard to the mean grain diameter of the media to match the site conditions and the layer thickness to provide adequate water treatment. Preliminary design infiltration rates varied between 5 and 10 m/d with hydraulic retention times ranging from 3.4

T.M. Missimer (✉)
U.A. Whitaker College of Engineering, Florida Gulf Coast University,
10501 FGCU Boulevard South, Fort Myers, FL 33965-6565, USA
e-mail: tmissimer@fgcu.edu

A.H.A. Dehwah · L. Lujan · D. Mantilla · S. Al-Mashharawi
Water Desalination and Reuse Center, King Abdullah University
of Science and Technology, Thuwal, Saudi Arabia
e-mail: abdullah.dehweh@kaust.edu.sa

L. Lujan
e-mail: luis.lujan@kaust.edu.sa

D. Mantilla
e-mail: david.mantilla@kaust.edu.sa

S. Al-Mashharawi
e-mail: samir.almashharawi@kaust.edu.sa

T.M. Missimer et al. (eds.), *Intakes and Outfalls for Seawater Reverse-Osmosis Desalination Facilities*, Environmental Science and Engineering,
DOI 10.1007/978-3-319-13203-7_11

to 7 h. Each gallery intake design was divided into a number of cells, each to be equipped with a pump to achieve overall high system reliability. The Saudi Arabia nearshore area of the Red Sea appears to be an ideal location for the development of seabed gallery intake systems based on the shallow water and relative ease of construction.

11.1 Introduction

The Red Sea coastline has a complex set of features that make the development of subsurface intake systems difficult in some areas (Dehwah et al. 2014). Of the many types of subsurface intake systems, the only design that can be used to supply large-capacity seawater reverse osmosis (SWRO) water treatment plants is the seabed gallery (Dehwah et al. 2014). Large-capacity SWRO plants are defined as those with a capacity >100,000 m^3/d.

Design of seabed gallery intakes has been documented beginning in the early 1980s, when a proto-type design was suggested in a draft tender for a SWRO plant on the coast of the Arabian Gulf (Missimer 2009). Preliminary design concepts for seabed filtration or a seabed galley intake system were published by Missimer and Horvath (1991), and Missimer (1994, 2009). After many years, the proposed use of seabed gallery intake systems has undergone renewed interest in Japan (Fukami 2002; Okamoto et al. 2005) and California (Wang et al. 2007, 2009; Allen et al. 2008). In 2005, the first large-scale seabed gallery intake system was installed at Fukuoka, Japan (Hamano et al. 2006; Pankratz 2006; Shimokawa 2012; Fig. 11.1). This facility has operated quite successfully for a period of nearly 8 years without the need to perform maintenance on the surface of the filter.

All subsurface intake systems tend to provide some degree of pretreatment of the feed water before it enters a SWRO plant. This concept is very important because the greatest challenge to operation of SWRO facilities is the control of membrane biofouling, which tends to reduce the life-expectancy of membranes, increase operational cost, cause the necessity to use large amounts of chemicals in the pretreatment process train (e.g., chlorine, ferric chloride, and others), increase the energy consumption of the facility by use of more energy expenditure in the pre-treatment process train, and increase labor cost due to the number of processes and some basic issues involving the handling and processing of marine waste, such as accumulated plant and animal matter entrained into the system.

Open-ocean intake systems also have the potential to create environmental impacts associated with the impingement and entrainment of living marine organisms in the facility (Missimer 2009; Chap. 4). The controversy and debate surrounding this issue necessitate the performance of long-term, very expensive environmental impact analyses on the marine environment in proximity to proposed intake systems. In Australia, large tunnels have been designed and constructed at

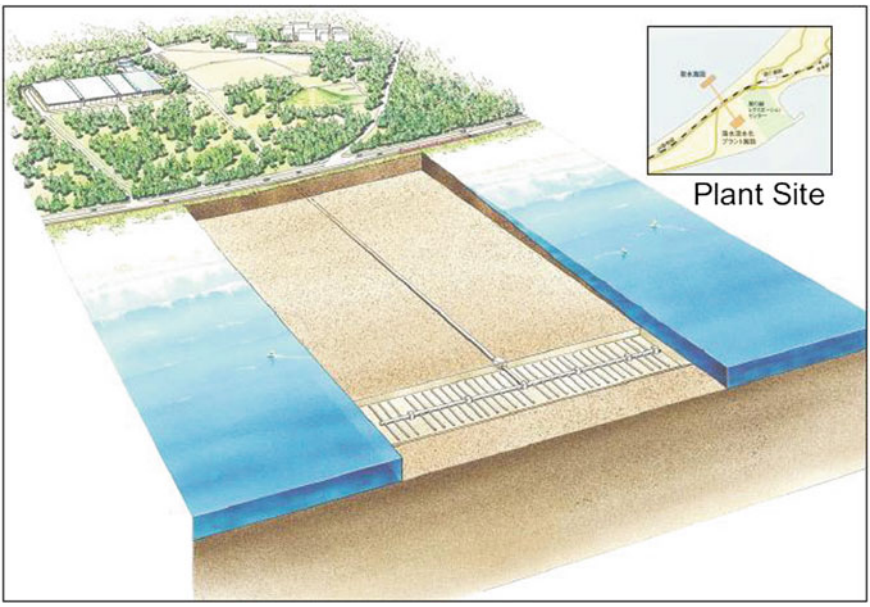

Fig. 11.1 Seabed gallery located at Fukouka, Japan with a capacity of 103,000 m^3/d

great cost to minimize the disruption of the marine bottom (Chaps. 2 and 3). In California, open-ocean intake systems have been nearly banned unless a subsurface intake system is deemed to not be technically feasible. Large-scale seabed gallery intake systems are being evaluated by the City of Long Beach (Wang et al. 2007, 2009) and by the California Coastal Commission at the City of Huntington Beach.

Despite great effort in design of pretreatment systems, biofouling is still a pervasive operational problem in many facilities. Recent research has suggested that the concentrations of algae, bacteria, total organic carbon (TOC), transparent exopolymer particles (TEP), and various fractions of natural organic matter (NOM) in the raw seawater are general indicators of biofouling potential. In particular, the occurrence of TEP and other biopolymers, which tend to coat and precondition the membrane surface, lead to the formation of biofilms on membrane surfaces (Berman 2010; Berman et al. 2011). TEP is formed by the self-assembly of precursor substances, such as dissolved acidic polysaccharides, that are produced by algae and bacteria (Passow and Alldredge 1994; Passow 2000). The engineered pretreatment process train is designed to remove as much of these organic substances as possible, but at great expense.

It is well known that subsurface intakes tend to improve the feedwater quality by removal of algae, bacteria, TOC, TEP, and various fractions of natural organic matter (NOM) with the highest molecular weight fraction being removed at the highest percentage (Missimer et al. 2013; Rachman et al. 2014). Most investigations on subsurface intake systems have focused on wells with little direct research

being conducted on gallery intake systems. Because there are inherent limitations on the capacity of all well intake systems, new research has been focused on gallery intakes because they have the potential to meet the intake requirements for virtually any SWRO treatment plant capacity.

While the basic concept of the seabed gallery is analogous to slow sand filtration, a technology used in the water industry for nearly two centuries, there are subtle, but significant differences in the design and operation of filters that treat seawater and are constructed within the marine environment. Slow sand filters operate by gravity feed, but seabed galleries operate by creating suction head loss across the filter media using a pumping system. Related aspects of design concepts for seabed filtration systems are presented herein, especially with regard to the design of the filter media and the balance of infiltration through the surface of the filter. General marine systems analysis is coupled with aspects of the function of benthic marine ecology as it affects the design and operation of seabed gallery intake systems.

This chapter provides a summary of the latest research on the feasibility assessment, design and construction of seabed gallery intake systems. The current greatest concentration of investigations being conducted on gallery intake systems is along the Red Sea coast of Saudi Arabia, because this region is projected to have the greatest increase in seawater desalination capacity over the next 20 years.

11.2 Methods

11.2.1 Site-Specific Investigations to Assess Technical Feasibility

In all natural system filtration methods, the site-specific geologic and hydrologic conditions dictate the feasibility of using a specific intake type. There are a number of issues that affect the feasibility of an intake design for any SWRO facility. To demonstrate feasibility an investigation needs to show that: (1) feed water flow will be provided under all operating conditions, (2) the intake system will operate under extreme natural system conditions, such as during harmful algal blooms (HAB's), (3) the intake will operate without causing significant environmental impacts or harm, (4) the intake can operate in coordination with the process design to minimize energy consumption, (5) the intake will minimize the use of chemicals in the pretreatment systems, (6) the intake will minimize interruption and/or maintenance caused by biofouling, (7) the intake will operate the entire system within a competitive economic mode, and (8) the intake design will convince the owners, operators, and financiers that the intake components meet an acceptable reliability standard.

A methodology for coastal classification and general screening for technical feasibility for all subsurface intake systems based on geologic and hydrologic conditions has been developed by Dehwah et al. (2014) (Chap. 7). Seabed gallery intakes, in general, have a larger range in site-specific conditions in which they can successfully operate. There are some fundamental feasibility issues that must be addressed when assessing any specific site. The gallery must be covered with water under all conditions so the filtration is constant. The selected marine bottom must not occur within an environmentally high-sensitivity zone, such as living coral reefs or heavy concentration of seagrass beds. The area of siting must have a limited rate of sediment deposition, especially with fine-grained muds, which could decrease the infiltration rate below operational minimums. The marine bottom at the selected site must not be subject to extreme excavation during storms. Construction of the seabed gallery must be feasible. A comprehensive checklist of factors that may need to be considered for assessment during the feasibility and design process is included in Table 11.1.

11.2.2 Literature Search and Site Inspection to Assess Tidal Range and Environmental Conditions

During the process of feasibility assessment and design for a seabed gallery intake system, a detailed literature search can be used to obtain general coastal characteristics and sometimes published coastal classifications are available (see Chap. 7). Perhaps the most useful tool today is Google Earth which allows reasonably recent, rectified satellite aerial photography to be viewed for almost any coastline of the world. This information can be used along with existing geologic and oceanographic studies to assess many of the issues raised in Table 11.1.

After the site screening process, it is necessary to conduct a physical inspection of the final sites being considered for a gallery intake. The site inspection should be conducted by a multi-disciplinary team, commonly consisting of an engineer (civil or with a coastal engineering specialty), a geologist, a marine biologist, and a land acquisition or access (easement) specialist. The specific composition of the inspection team will vary based on the capacity of the SWRO facility under consideration and the complexity of the coastline being evaluated. Where there are only a few sites under consideration, the team should begin the process of field data collection and possible bottom mapping to save field costs.

An example of a literature search containing relevant information for development of seabed gallery intake systems is contained in Dehwah et al. (2014). A series of marine biology, sediment, and geomorphology investigations were documented. These types of research are important to the siting and feasibility assessment for seabed gallery intake systems.

Table 11.1 Checklist of oceanographic, geologic, and geochemical investigations for evaluation of seabed gallery intake systems

Task	Information required
Oceanography/ marine biology	Assessment of wave energy, currents, and coastal dynamics
	Assessment of tide range
	Assessment of water quality changes (e.g., turbidity, algal blooms, nutrient concentrations)
	Assessment of water quality (biofouling compounds-TEP, TOC, NOM components)
	Assessment of historical storm impacts to marine bottom, including storm frequency
	Assessment of bottom stability
	Assessment of historical extreme events (tsunamis)
Geology/ hydrogeology	Assessment of sedimentation rate
	Characterization of surface sediment grain size distribution
	Assessment of shallow geology from the sea bottom to a depth of 6 m
	Assessment of climate change impacts (rising sea level)
Geochemical	Measurement of the inorganic chemistry of the seawater near the gallery (carbonate equilibria)
	Modeling of carbonate equilibria to assess potential for carbonate precipitation
Environmental/ biological	Assessment of benthic marine fauna (with impacts to filter operation)
	Assessment of impacts to marina flora and fauna during construction
	Assessments of impacts to endangered species
Permitting	Assessment of all potential government permits required (can they be issued?)
	Description of all environmental impact statement or assessments required
	Assessment of sediment disposal options during gallery construction
Constructability	Assessment of the possible construction methods and if it can be constructed
Economics	Assessment of capital cost of construction
	Assessment of operational costs based on life-cycle analysis

11.2.3 Sediment Investigations

There are several issues related to sedimentation rate and sediment grain size characterization that require assessment and analysis. The key issue is the long term viability of the surface and near-surface part of the gallery. Any sediment deposition that will potentially affect the hydraulic conductivity of the uppermost layer of the filter during future operation will require assessment. The excavation required for gallery construction must also be practically and economically possible at a feasible site. Therefore, the occurrence of a hard rock bottom or the occurrence of boulders would not be conductive for gallery development.

Deposition of fine-grained sediment is a major issue that affects site feasibility. If a site is subject to short-term mud deposition events, commonly associated with either storms or floods discharging sediment into the sea, then the site is unlikely to be useful for gallery development. Locations near perennial stream discharges to the sea, such as deltas, are large-scale mud depositional areas and should be screened out in the initial feasibility assessment stage. Some marine areas that are relatively remote from delta locations are also mud deposition areas caused by transport of fine sediments parallel to the coastline by ocean currents. Current maps and a remote inspection of the seafloor using side-scan sonar can reveal these "mud belt" areas.

The marine bottom should be relatively stable in terms of sediment deposition or erosion even if the bottom is predominately sandy. Seasonal changes in the bottom profile across a gallery site can be incorporated in a gallery design as long as the changes anticipated are not too extreme. For example, if the area is subject to slow erosion at a few centimeters per year, the upper gallery layer could be designed to have greater thickness. Seasonal oscillations in erosion and deposition can be expected in most areas and storm excavation with reestablishment of the original bottom profile is also common. Again, extreme change decreases the potential for a site to be feasible for gallery design and construction.

Since sandy sediment is expected to move across the seabed by current transport, oscillatory wave action, or storm wave drag on the bottom, it is important to understand and map the grain size characteristics of the surface sediments. This has two useful purposes; understanding of deposition patterns that may not be obvious from initial scans of the area and for design of the upper layer of the filter. The upper engineered filter layer should be compatible with the sediment grain size characteristics or the top of the gallery could be scoured or may stand high after extreme events. It is desirable to have the engineered filter blend in with the bottom sediments so that no bathymetric change on the bottom is produced across the filter during operation.

A relatively new consideration is the potential impact of sea level change related to global warming. Accelerated sea level rise should be considered within the gallery feasibility and design process. The typical life cycle maximum consideration for a SWRO plant is 30 years, so the sea level rise for this timeframe or up to 50 years may require analysis. Depending on which climate scenario is used, the expected sea level rise by the year 2100 will be somewhere between 0.4 and 1 m (IPCC 2013). This magnitude of increase will not likely change the sedimentation patterns along most coastlines within the offshore area. The gallery function will not be harmed based on increasing water depth, but could be harmed under shoaling depths in terms of storm excavation. Sea level change should be considered during system design to ensure that intakes are robust enough to accommodate variations in the rate of change. The pipeline connected an offshore seabed gallery could be at risk from sea level rise and should be designed to accommodate the projected range of change.

11.2.4 Red Sea Nearshore Sedimentology Investigation

The Red Sea shoreline has been studied in detail to assess the feasibility of developing seabed gallery intake systems (Fig. 11.2). A series of diverse sediment types occurs along the shoreline and nearshore areas of the Red Sea. Some pure carbonate sand environments occur where the fringing coral reefs are the predominant nearshore environment. Mixed carbonate and siliciclastic sediments occur adjacent to areas where wadi discharges have carried siliciclastic sediments into the nearshore marine environment and have mixed with the locally generated carbonate sediments. Pure siliciclastic sediments occur within channel discharge features located along the shoreline. Many of these features are a special type of alluvial fan (fan deltas) that intersects with the sea (Wescott and Etheridge 1980; Hayward 1985).

To establish a sedimentological assessment at site-specific locations, a linear section of the beach was selected. A sample grid was then established with the collection of samples beginning at the beach and moving seaward at horizontal

Fig. 11.2 Location of site-specific seabed gallery technical feasibility investigation along the Red Sea coats of Saudi Arabia

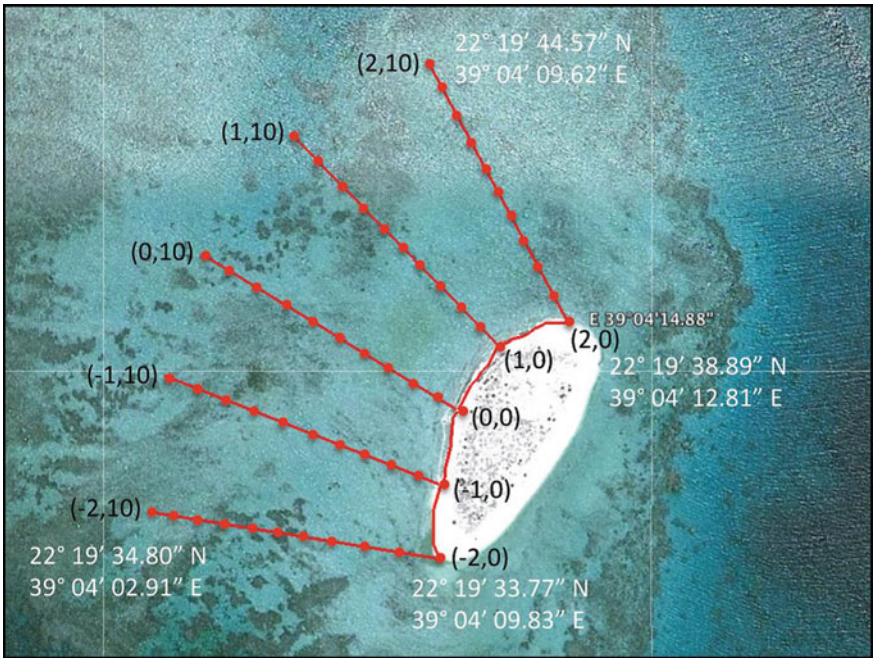

Fig. 11.3 Sediment sampling grids of the site-specific investigations along the Red Sea. Om Al Misk Island study (from Sesler and Missimer 2012)

increments of 10 or 20 m. Within the five sites investigated, between 50 and 91 sediment samples from the shoreline and offshore were collected along transects running perpendicular to the beach. The spacing between transects was based on the desired segment of the shoreline and nearshore area to be investigated (Fig. 11.3).

After collection, the sediment samples were carefully washed with fresh water in order to remove salts without removing any fine sediment. Washed samples were analyzed for hydraulic conductivity, porosity and grain size distribution using standard laboratory methods (ASTM 2006; Wenzel 1942; Tanner and Balsallie 1995).

11.2.5 Background Red Sea Water Quality

Data on background quality of the local seawater should be obtained regardless of the type of intake design is being considered. While a seabed gallery is perhaps a more forgiving intake design compared to a conventional open-ocean intake, it still can have operational difficulties related to seawater quality. The most significant issue is the average turbidity of the seawater over time and event-related turbidity, such as after storms. Also, the occurrence and impact of HAB's should be assessed. Therefore, some background turbidity measurements should be collected. However, the percentage of mud in the surface sediments is a good proxy for the potential impact of turbidity events or long-term turbidity impacts to the filter top.

The Red Sea has a restricted circulation, which results in seawater with a generally higher salinity than the global average of about 34,500 mg/L. It is necessary to assess the local seasonal variations in salinity and the nearshore circulation to be sure that the salinity does not vary outside of the acceptable range of SWRO treatment. Based on investigations conducted by Mantilla and Missimer (2014), Rachman et al. (2014), Dehwah et al. (2014), the common average salinity in the nearshore shallow water is 41,000 mg/L. Some offshore and deep water salinity data are presented in Chap. 6. Surface salinity offshore is about 38,000 mg/L and increases to about 40,000 mg/L at 90 m below surface.

At very shallow water sites along the shoreline, measurement of salinity during different seasons may be necessary to assure that periods of higher salinity do not occur. The evaporation loss rate along the nearshore area is up to 6.5 m/year (Lopez et al. 2014). In areas where very limited circulation occurs, the salinity may rise during the summer season, particularly when it is not windy. Fortunately, there is an onshore wind along the Red Sea shoreline during a large part of the year. This tends to cause nearshore mixing and limits short-term salinity increases.

11.3 Results of Investigations

11.3.1 Red Sea Water Quality and SWRO Treatment Facility Operating Difficulties

Operational difficulties have been reported from a number of SWRO facilities located along the Red Sea coastline. Membrane fouling has been a pervasive problem at the Shuqaiq facility as reported by operators. A number of smaller capacity SWRO plants in the Jeddah area have reported clogging of cartridge filters and some membrane biofouling. Facilities that use subsurface intake systems have had better operational experience compared to facilities using open-ocean intake systems (Dehwah et al. 2014; Rachman et al. 2014).

In order to assess the viability of seabed gallery intake systems along the nearshore region of the Red Sea, a detailed survey of the coastline was conducted and over a hundred sites were visited and sediment samples were collected. Based on the preliminary field data collected and proximity to various existing large-capacity SWRO plants, five site-specific investigations were conducted to perform detailed technical feasibility assessments targeted at seabed gallery intakes (Fig. 11.2).

11.3.2 Locations of Site-Specific Investigations

The five site-specific investigations were conducted at Om Al Misk Island (Sesler and Missimer 2012), King Abdullah Economic City (Dehwah and Missimer 2013), Shuqaiq (Mantilla and Missimer 2014), Shoaiba (Lujan and Missimer 2014) and

Table 11.2 Seabed gallery intake feasibility investigations along the Red Sea nearshore

Location	Design capacity (m^3/day)	Bottom type	Bottom sediment
King Abdullah Economic City	150,000	Hardground	Carbonate
Um Al Misk Island	105,000	Hardground	Carbonate
Shoaiba	375,000	Hardground	Carbonate
Shuqaiq	530,000	Sand	Siliciclastic
South Jeddah Corniche	60,000	Sand	Mixed siliciclastic and carbonate

near Jeddah (Al-Mashharawi et al. 2014). Each of these sites contains an existing SWRO plant that has a plan for expansion or has some type of operational difficulty (Table 11.2; Fig. 11.2).

11.3.3 General Offshore Bathymetry and Nearshore Bottom Conditions

Three of the five sites, Om Al-Misk Island, King Abdullah Economic City, and Shoaiba, contained a very low-gradient nearshore bottom profile from the beach seaward. The distance from the beach at mean low water to a depth of 1 m was roughly 100 m and to 2 m was an additional 100–150 m. The bottom was covered with a veneer of predominantly sandy carbonate sediments setting atop a soft to moderately hard marine hardground. The hardground can be classified as the inner reef and consists of modern marine cemented limestone. A fringing reef occurs seaward of the inner reef at a water depths ranging from 2 to 10 m. A very sharp increase in water depth occurs seaward of the reef. A vertical wall commonly drops into 450–600 m of water (see Chap. 6; Fig. 6.1). A generalized profile is shown in Fig. 11.4. A considerable percentage of the Red Sea beach and nearshore profile from Jeddah north to the Saudi Arabia-Jordan border shares a similar character.

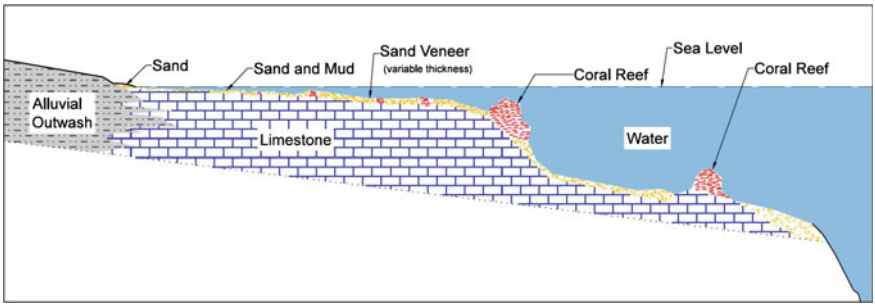

Fig. 11.4 Generalized bathymetric and geologic profile of the nearshore area of the Red Sea at Om Al Misk Island, King Abdullah Economic City, and Shoaiba

At two of the sites investigated, Shuqaiq and Jeddah, the nearshore bottom conditions and bathymetric profiles were different. These environments contained predominantly quartz sand with some skeletal carbonates. The profiles showed a rather abrupt change in water depth at about 1.2–2 m dropping to over 3 m. No hardground or inner reef environment exists across all or parts of these sites. Shuqaiq contained more seagrass compared to the other sites. These sites were located near intersections of wadi channels with the shoreline.

The inner reef in the sites investigated contained both non-sensitive and sensitive environments. The non-sensitive environments consist of barren sand or hard-ground bottoms with no significant coral or marine grass cover. There is a tendency for the bottom coral density to increase in water depths greater than 2 m, especially where the bottom is rocky. The density of seagrass is quite variable and occurs typically in patches where water circulation is enhanced (Fig. 11.5). Very large variations in the seagrass density occur within the inner reef area. Seagrass does not occur in bare hardground areas.

The sandy bottom contains a variety of infauna including mollusks, benthic foraminifera, some red and green (rare) algae, and polychaete worms. Sesler and Missimer (2012) reported that measured polychaete worm densities can be up to 2500 individuals/m^2. The high density of polychaetes occurs primarily where the bottom sediment is thickest and the water circulation is relatively good.

Areas with a low degree of environmental sensitivity were found at all five investigated sites that would allow the design and construction of a seabed gallery intake system without causing significant impacts. The sites contain shallow water with a relatively flat bottom. In all cases the season tide range was a maximum of

Fig. 11.5 Underwater photo of seagrass occurrence at the Shoaiba site

0.15–0.3 m. Therefore, the seabed gallery would be covered with seawater at all times of the year. Observed wave action, even during windy days, was rarely more than 0.5 m in height.

11.3.4 Sediment Properties at the Sites and Effects on Seabed Gallery Design

A large number of sediment samples were collected and analyzed from each site. The measured parameters included grain size distribution and mean grain diameter, porosity, mud percentage (sediment fraction with a grain size <0.0625 mm), and hydraulic conductivity. There was considerable variation in the mean grain diameter and mud percentage at each site. Examples of the spatial grain size distribution at two sites, one predominantly carbonate and the other siliciclastic, are shown in Fig. 11.6a, b. The sediment found is classified as medium to fine grained sand.

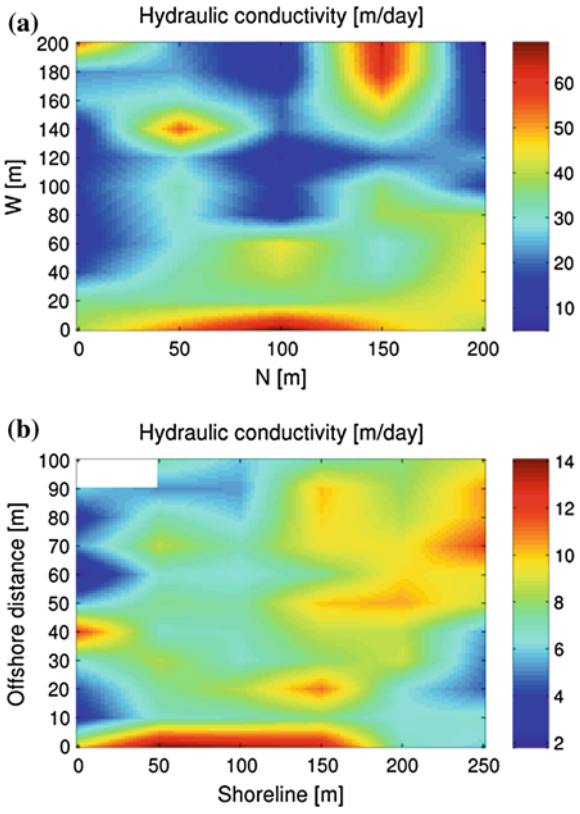

Fig. 11.6 Comparison of mean grain diameter at two of the sites investigated. **a** Om Al Misk Island (carbonate). **b** Jeddah site (siliciclastic)

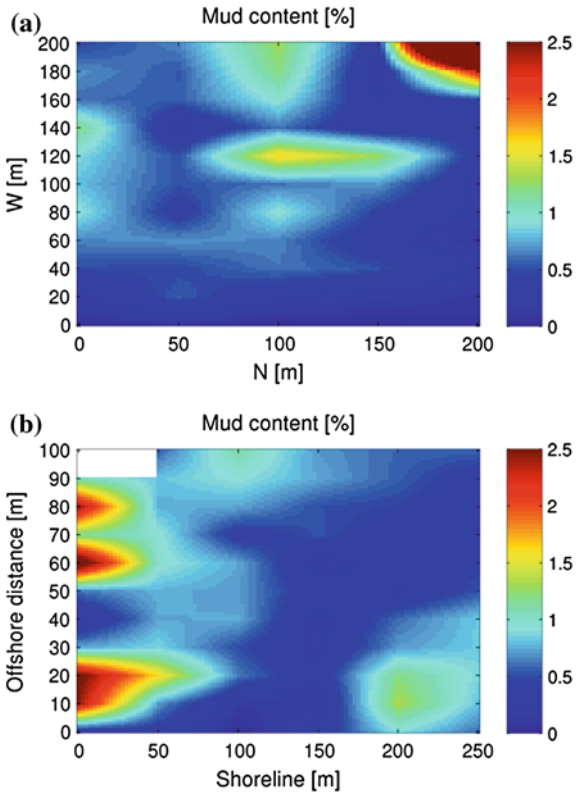

Fig. 11.7 Comparison of mud percentage at two of the sites investigated. **a** Om Al Misk Island (carbonate). **b** Jeddah site (siliciclastic)

Based on the predominantly sand-sized nature of the sediment, the percentage of mud was also mapped to locate any areas where fine-grained sediment is being deposited. The mud percentage at the Om Al Misk Island and Jeddah sites is shown in Fig. 11.7. In both cases, the percentage is relatively low, but there are a few areas where it is higher for some reason.

The sediment porosity was measured across the sites investigated. Generally, it ranged from 0.3 to 0.45 based on the laboratory methodology used. The porosity is related to the distribution of grain size found in the sediment. Commonly, fine-grained sediments have a higher porosity compared to sandy sediments, especially as packing density increases.

There are important relationships between all four sediment parameters measured. The spatial distribution of all four parameters are shown for a carbonate sand site (Om Al Misk Island) in Fig. 11.8 and a predominantly siliciclastic site (Jeddah) in Fig. 11.9. A distinct relationship between hydraulic conductivity and mud percentage is evident at both sites.

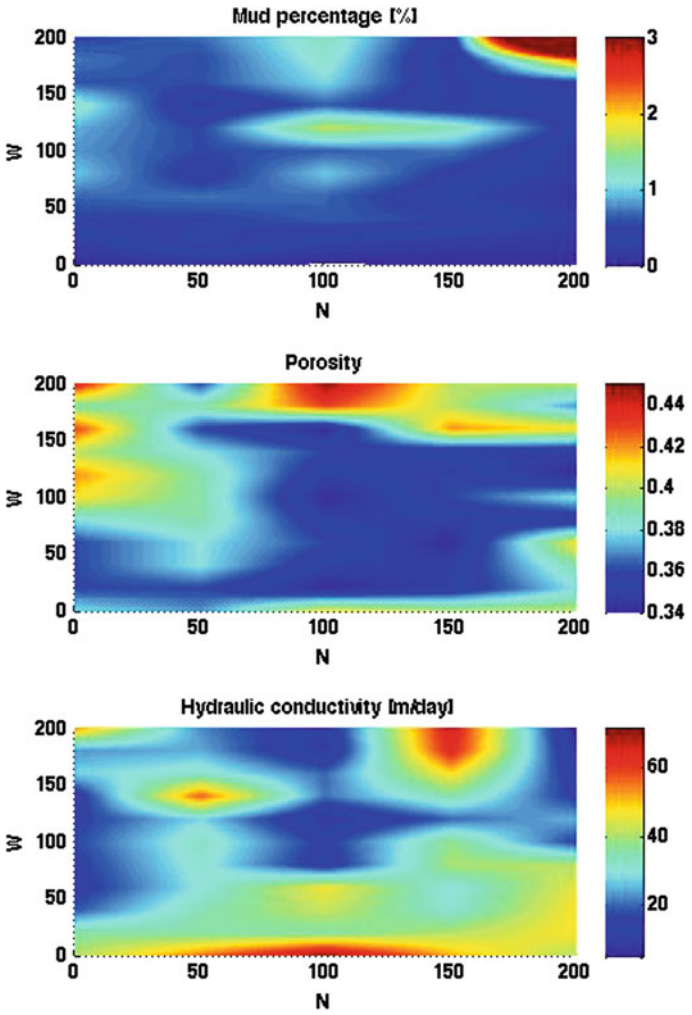

Fig. 11.8 Comparison of selected measured sediment parameters of a predominately carbonate sediment site at Om Al Misk Island (modified from Sesler and Missimer 2012)

11.4 Discussion

11.4.1 General Feasibility Criteria and Site Assessments Along the Red Sea Coast of Saudi Arabia

Based on the criteria listed in Table 11.1 and the findings of the five site-specific investigations conducted along the Red Sea coast of Saudi Arabia, the design and construction of seabed gallery intake systems was found to be technically feasible at each site. The geological conditions were demonstrated to be very good for gallery

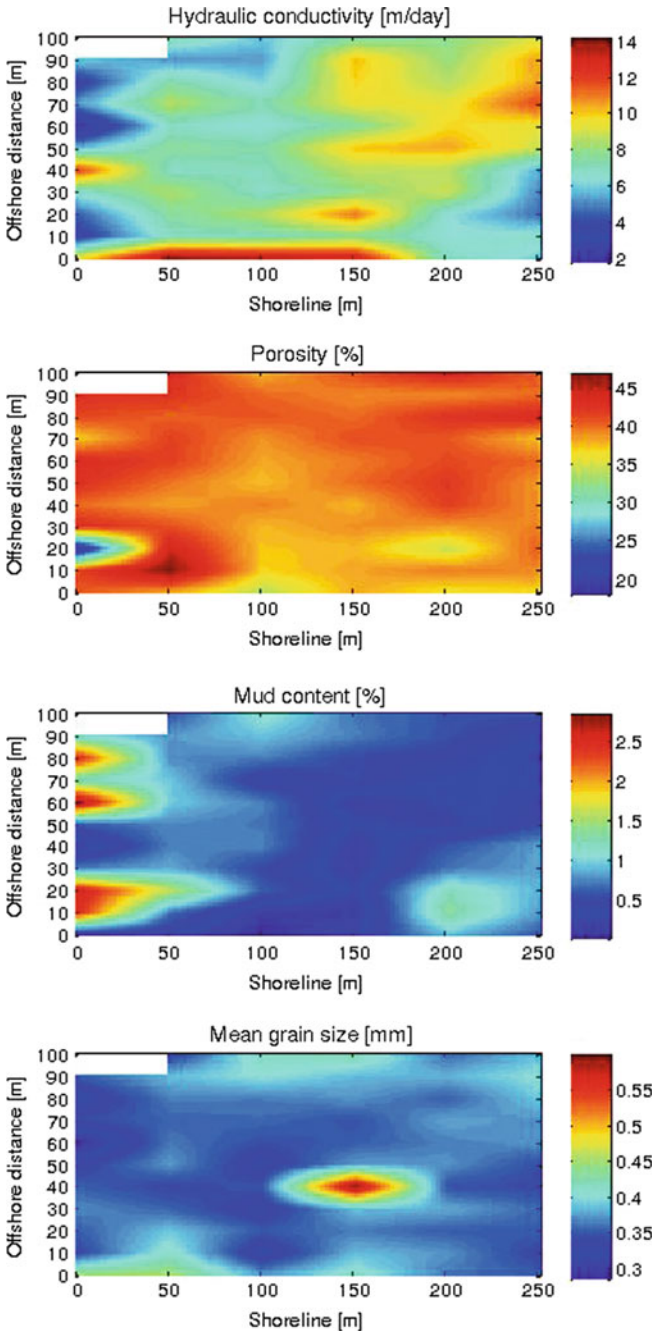

Fig. 11.9 Comparison of all four measured sediment parameters of a predominately siliciclastic sediment site at Jeddah (modified from Al-Mashharawi et al. 2014)

design at each site with the surface sediment consisting of medium to fine sand with a low mud percentage, which results in a moderate hydraulic conductivity. The unlithified sediment has properties that would not interfere with the operation of a gallery and the sedimentation rate is low. Minor areas of mud deposition were found, but the gallery cells could be constructed away from those areas.

The bottom contained a veneer of unlithified sand setting atop a carbonate marine hardground at three locations. This limestone could be easily excavated to create the depth required to construct gallery cells. In fact, the shallow water and stable bottom may allow construction without using sheet-piling. The water depth ranges from 1 to 1.5 m which would allow the placement of a temporary road seaward from the beach. This would facilitate construction and could be removed after completion. Water depth is sufficient to maintain submergence of the gallery cells under all tidal conditions.

The bottom sediment and water depth at the sites with occurrence of siliciclastic sands also showed technical feasibility for gallery construction. The sand generally contained a minimum percentage of mud, moderate hydraulic conductivity, and the water depth was sufficient in the nearshore area to maintain submergence of the filters. Construction would require sheet piling and dewatering at these sites, but temporary roads from the beach to the seaward maximum position of the gallery cells could be used to facilitate construction.

Based on data collected at the sites and nearby locations, water circulation appears to be sufficient to maintain the nearshore salinity of between 41,000 and 42,000 mg/L. Strong onshore winds causes mixing of the water to offset high evaporation rates, particularly during summer months. The calcium carbonate saturation will be high and careful monitoring of the uppermost gallery sand layer will have to be done to assess any potential lithification caused by marine cement formation.

The nearshore hardgrounds which form the inner reef contain very low density of corals from the beach to a water depth of about 2 m. The density of seagrass within the sites studied is minimal and higher density areas can be avoided by selective siting of gallery cells. Therefore, the construction of gallery cells would not have a high impact on the marine environment and after completion of the gallery cells, the productivity of the infauna may actually be improved based on the water movement through the sands of the filters (more food for the polychaetes).

11.4.2 Compatibility of the Gallery Type with the Coastal Geology and Sediment Deposition in Relationship to Siting

All of the sites assessed are compatible with the coastal geology and processes that affect the nearshore bottom. None of the sites investigated were located directly seaward of a wadi intersection where flash floods could discharge large quantities of sediment in a single event that could cover the gallery top. The sites are located in areas where longshore and nearshore transport of sediment would move over the

top of the gallery active layer. The continued survival of the offshore fringing reef and coral clusters in water depths of 1.5–2 m are indicators of the low sediment deposition rate.

11.4.3 Filter Media Design and Modification for the Site-Specific Condition

Seabed galleries are similar in design to slow sand filters that have been used in freshwater treatment since 1804 in Scotland and in 1829 at the Chelsea Waterworks Company in London (Huisman and Wood 1974; Christman 1998; Buchan 2003). The fundamental principle of the slow sand filter is to transmit water by gravity feed though a porous media to remove suspended solids, algae, and some bacteria by straining (and perhaps sedimentation), and small bacteria and some NOM via biological processes. A comparison between modern design of a slow sand filter versus a rapid sand filter is given in Table 11.3. Note that slow sand filtration only operates effectively with a range of natural turbidities ranging between 10 and 50 NTU within a freshwater environment. Note that no pretreatment of the water occurs within a slow sand filtration system and is required within rapid sand filtration. Operation of slow sand filtration for prolonged periods with influent turbidity above 50 NTU can cause breakthrough of poor quality water and/or system clogging.

An important aspect of the slow sand filter design is the quality of the water to be treated, and the hydraulic retention time of the water within the filter. There are limits on the turbidity of the raw water that can be effectively treated by slow sand filtration. Crittenden et al. (2005) suggest that the slow sand filtration process is effective for raw water with a turbidity range of 10–50 NTU. The hydraulic retention time of most slow sand filter systems ranges from 5 to 6 h. Hydraulic retention times for a slow sand filter with differing active layer thicknesses and an

Table 11.3 Design of slow sand filters (modified from Crittenden et al. 2005)

Process characteristic	Slow sand filtration	Rapid sand filtration
Filtration rate	1.2–4.8 (m/d)	120–360
Media diameter	0.3–0.45 (mm)	0.5–1.2
Bed thickness	0.9–1.5 (m)	0.6–1.8
Required head	0.9–1.5 (m)	1.8–3.0
Run length	1–6 months	1–4 days
Ripening period	Several days	15 min–2 h
Pretreatment	None required	Coagulation
Dominant filtration mechanism	Straining, biological activity	Depth filtration
Regeneration method	Scraping	Backwashing
Maximum raw water turbidity	10–50 NTU	Unlimited with pretreatment

assumed uniform hydraulic conductivity are given in Table 11.4. There is an offset between the lower hydraulic conductivity of the surficial active layer and the increasing hydraulic conductivity with depth in the media. The key issues controlling the hydraulic retention time are the design infiltration rate and the upper active bed thickness. The methodology for proper calculation of hydraulic retention time is discussed in Sect. 11.4.4. Increased hydraulic retention time tends to increase the degree of water treatment in that more NOM is removed.

In freshwater systems, a biologically active gelatinous mat, composed of deposited and synthesized material, forms at the top of the filter sand. This unit is called the schmutzdecke (German for 'dirty skin') layer. The schmutzdecke layer is an important part of the filtration process and is where much of the biological treatment occurs. Growth of the schmutzdecke layer increases hydraulic resistance across the slow sand filter and it must be periodically scrapped off in order to maintain acceptable filtration rates. To maintain the same degree of biological treatment, the scrapped filter must be given time to "ripen". This process can take between 12 h and several days in freshwater systems. Repeated cleanings by scrapping also reduces the thickness of the filter and changes the hydraulic retention time. New sand can be added to the surface of the filter to replace the material removed. A considerable amount of treatment occurs within this layer as water passes through it. Biological activity declined with depth within the filter. Huisman and Wood (1974) point out that in 1 m^3 of sand media, there is over 13,000 m^2 of surface area available for attachment of particulates and contaminants.

A recent discovery is that in seawater systems, a *schmutzdecke* layer does not form at the top of the filter and biological activity occurs throughout the active layer and perhaps into the lower support layers of the gallery filter (Abdullah Dehwah, personal communication, Water Desalination and Reuse Center, King Abdullah University of Science and Technology). Crittenden et al. (2005) suggest that the slow sand filter ripening period in freshwater systems requires a few days of operation, while column experiments conducted by Abdullah Dehwah at the King Abdullah University of Science and Technology determined that several months of ripening was required in seawater filtration before large quantities of the TOC were removed by biological activity. Therefore, there are some significant differences in the operation of slow sand filtration within difference salinity regimes.

The typical run length before reconstruction of the full filter bed is 1–6 months. Because of the development of the *schmutzdecke* layer in freshwater systems, most

Table 11.4 Hydraulic retention time as a function of infiltration rate and bed thickness

Infiltration rate (m/h)	Infiltration rate (m/d)	Bed thickness (m)	Hydraulic retention time (h)
0.05	1.2	0.9	18
0.1	2.4	1.0	10
0.2	4.8	1.25	6.25
0.3	7.2	1.3	4.3
0.4	9.6	1.4	3.5
0.5	12.0	1.5	3.0

of the water treatment occurs within the upper 10 cm of the filter, so the hydraulic retention time is not so important. The longer ripening period in seawater slow sand filtration suggests that increasing the hydraulic retention time may be useful in improving the pretreatment capabilities of the gallery.

The regeneration of a slow sand filter is by scraping of the uppermost layer to remove the *schmutzdecke*. Operational experience at the Fukuoka facility in Japan shows that no clogging of the filter has occurred during an 8 year run. Sesler and Missimer (2012) suggest that marine infauna that are sediment-deposit feeders may clean the upper part of the filter by the fixing of the organic carbon and fine-grain sediment as hard fecal pellets that act hydraulically similar to sand grains.

The filter media needs to be fine enough to provide sufficient filtration of suspended material of concern and NOM (Barrett et al. 1991). Hendricks (1991, 2011) recommended that the d_{10} of the filter sand (sieve size that permits 10 % of the sand to pass through) should be 0.2–0.3 mm with a corresponding uniformity coefficient (UC, d_{60}/d_{10}) between 1.5 and 2.0. Coarser sand may be used (0.3–0.4 mm) if the uniformity coefficient is less than 3. Crittenden et al. (2005) suggest that average grain size of the media can range from 0.3 to 0.45 mm and the bed depth is normally 0.9–1.5 m. Huisman and Wood (1974) point out that the bed thickness must also contain support media, graded sand and gravel layers, to facilitate the capture of the supernatant water at the base of the filter.

Design of the slow sand filter media requires that the grain size distribution of the created layers allow proper support without breakthrough of fine grains into the next lower layer. The gravel support consists of multiple layers with an upwardly decreasing grain size. The layers need to be designed so that they are stable, minimizing settling of finer grained sand and gravel into underlying layers. Huisman and Wood (1974) proposed the following general rules for the design of the gravel support, which are still widely accepted:

1. d_{90}/d_{10} for a given layer ≤ 1.4
2. d_{10} lower layer/d_{10} upper layer ≤ 4
3. d_{10} top layers/d_{15} filter sand ≥ 4
4. d_{10} top layer/d_{85} filter sand ≤ 4
5. d_{10} bottom layers $\geq 2d$ (drain orifice or screen slot diameter)

Huisman and Wood (1974) noted that the requirement for a highly uniform sand ($d_{90}/d_{10} < 1.4$) may be too restrictive (i.e., expensive to meet) and that a ratio of 2 would be acceptable if the ratio of d_{10} values between layers is less than 3. The recommended minimum thickness of the gravel layers is three times the diameter of the largest grains or 5–7 mm for finer materials and 8–12 mm for coarse gravel (Huisman and Wood 1974). The use of fine sand in the top layer tends to provide a higher degree of removal of algae, bacteria, and viruses (Amy et al. 2006; Jenkins et al. 2011; Lujan and Missimer 2014). The upper sand layer, however, must be compatible with the natural bottom sand or it would be rapidly scoured away. In some cases, a finer layer may have to be placed below the upper active layer with a downward coarsening below that level, or the uppermost layer must be significantly thickened, to increase hydraulic retention time.

Each of the preliminary gallery media designs developed for the five sites along the Red Sea contained differing layer thickness and sediment mean grain diameter based on the local conditions found at each site (Table 11.5). Four of the five sites used a five layer structure and the other used six layers. Three typical designs are shown in Fig. 11.10. A wide range of bed thicknesses were developed from 2.5 to 5 m. The active layer thickness in the designs ranged from 1.0 to 3.0 m. The design infiltration rates ranged from 5 to 10 m/d. The media mean grain diameter ranged from 0.1 to 0.45 mm based on the local site conditions.

These site assessments were completed as MS thesis projects at King Abdullah University of Science and Technology. The students developed preliminary designs based on the current knowledge of slow sand filtration processes in the marine environment at the time the research was completed. Therefore, the optimal design at each site would likely be different based on the current state of knowledge. However, the thick upper active layer, where most of the treatment occurs, and the graded sand and gravel support layer structure would be unchanged. The optimal infiltration rate for the Red Sea of Saudi Arabia, based on average turbidity measurements, would likely be between 7 and 8 m/d. The hydraulic retention time should likely be between 7 and 8 h to yield the optimal pretreatment result for the design infiltration rates.

Another design issue that requires careful attention is the need to maintain vertical flow within the seabed gallery and not to induce horizontal inflow from sediments outside of the constructed filter below the sea bottom. This horizontal flow could cause anoxic interstitial water to mix with oxygenated seawater within

Table 11.5 Preliminary designs of five seabed gallery intake system located along the Red Sea coastline of Saudi Arabia

Design parameters	Om Al Misk Island	King Abdullah Economic City	Shoaiba	Shuqaiq	Jeddah South
Media thickness (m)	4.25	4.50	3.00	5.00	2.50
Mean grain diameter, active layer (mm)	0.45	0.30	0.30 + 0.45	0.10	0.35
Active layer thickness (m)	2.00	1.25	1.75[a]	3.00	1.00
No. of layers	5	6	5	5	5
Infiltration rate (m/d)	8.0	5.0	7.0	10.0	7.0
Hydraulic retention time (h)	6.00	6.00	6.00	7.00	3.43[b]
Capacity (m^3/d)	105,000	150,000	375,000	530,000	60,000
Total surface area (m^2)	17,500	35,000	60,000	58,300	12,900
No. of cells, total	5	7	10	9	3
No. of cells, primary	4	6	9	8	2

[a]The calculated hydraulic retention time for Shoaiba would be for the first two layers based on the fine grain size of each

[b]An error was made in the calculation of hydraulic retention time at this site and would require a design modification

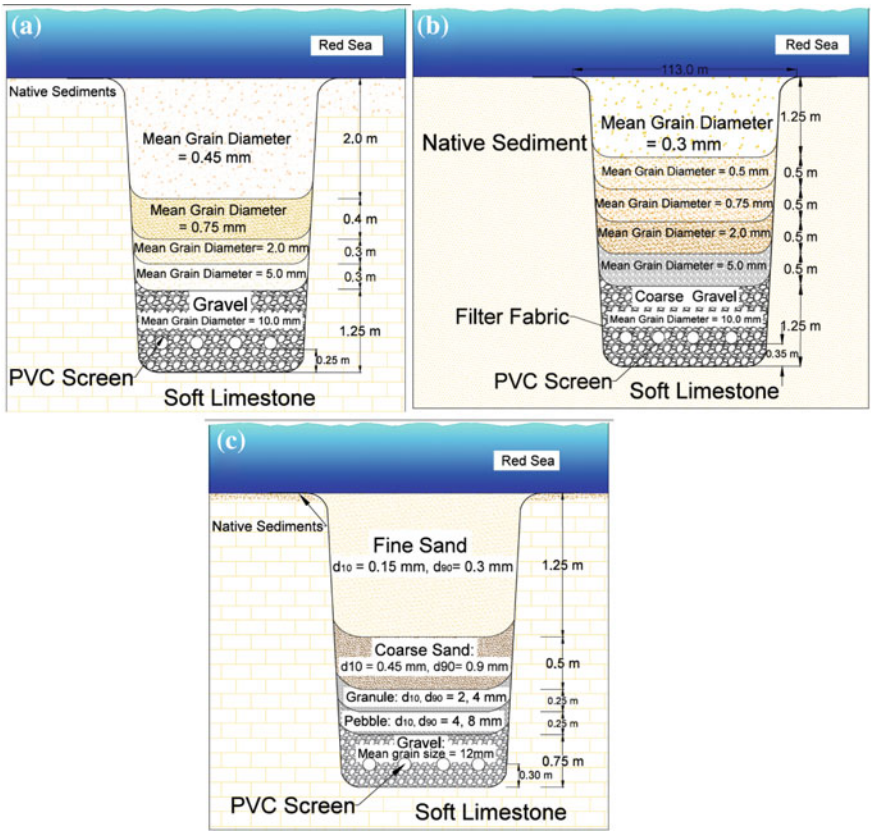

Fig. 11.10 Three preliminary seabed gallery filter designs from the Red Sea of Saudi Arabia. **a** On Al Misk Island. **b** King Abdullah Economic City. **c** Shoaiba (from Sesler and Missimer 2012; Dehwah and Missimer 2013; Lujan and Missimer 2014)

the filter and could lead to adverse chemical reactions that could impact the downstream membrane process. This issue can be avoided by using a geofabric liner at the bottom and edges of the gallery cells (Cook 2003; Rollin 2004). In extreme cases, the gallery cells could be pre-fabricated as cement vaults and placed on the seabed in excavated trenches or above the seabed, but below the wave orbital or current scouring depth.

11.4.4 Proper Calculation of the Hydraulic Retention Time for a Seabed Gallery Intake System

Hydraulic retention time in seabed filtration systems is important to maximize the removal of TEP and various fractions of NOM. As stated throughout this chapter, it is important to strike a balance between the infiltration rate and the degree of

pretreatment desired. Unfortunately, there is a discrepancy on the method of how to calculate the hydraulic retention time.

Within a slow sand filter, the gravel support layer lying beneath the primary media is quite thin and the simple estimate of the hydraulic retention time can be calculated by dividing the full bed thickness by the infiltration rate, so a slow sand filter with a bed thickness of 1.5 m and an infiltration rate of 4.8 m/d will have a hydraulic retention time of 0.3125 days or 7.5 h based on the mass balance of flow across the full thickness of the filter media. The head loss within a slow bed filter treating freshwater occurs mostly at the water-sediment interface where the *schmutzdecke* layer forms.

Seabed gallery designs tend to have greater thickness compared to conventional slow sand filters because they need to have a design robust enough to function under a wide variety of natural systems conditions, such as compatibility with the adjacent marine sediments that will move across the top of the gallery by various transport mechanisms, periodic excavation of the upper part of the filter media by storms, and bioturbation by burrowing and deposit feeding marine organisms. Therefore, the uppermost media layer will require a greater thickness compared to slow sand filters, may have a finer mean grain diameter, and will likely require a series of graded sand and gravel beds to allow a transition of grain size from the active upper layer through the lower collection layer to inhibit fine sediment infiltration.

Since the uppermost layer or layers of the seabed filter are the most active removal zone for all processes, including bacterial degradation of organic compounds, the best method to estimate hydraulic retention time is to use only the thickness of the active treatment layer(s) in the calculation. Therefore, a 2 m thick uppermost layer with an 8 m/d infiltration rate will yield an active zone hydraulic retention time of 6 h, even if the full filtration thickness is 4 m. The full thickness of the filter would yield a total hydraulic retention time greater that the active zone. The rate of volumetric flow through all layers will be the same (assuming no lateral flow) although average flow velocity may vary depending on effective porosity. To obtain an accurate estimate of the hydraulic retention time for the active layer, a Darcy flow model can be developed using all layers of the model design and could be coupled to the computer program used to estimate layer hydraulic conductivity and initial head loss through the filter.

11.4.5 Balance of the Surface Infiltration Rate with Proper Underdrain Design

Design of seabed gallery intake systems requires that the infiltration into the top of the filter media should be as uniform as possible. Since the head pressure loss within the basal collection layer induces the vertical flow of seawater, the pressure distribution with this layer must be carefully controlled. If the pressure is unevenly distributed, this will cause high, low, and perhaps no infiltration rates locally across the filter surface.

A critical part of the design is the configuration of the collection pipe, pipe intersections, the screen configuration, and the screen slot apertures. When a pipe is attached to a length of screen, the pressure head loss caused by pumping is transmitted from the pipe into some length of screen. Missimer (2009) showed that within a uniform screen cross-sectional diameter and uniform distribution of slots of the same aperture, the highest inflow will occur at the proximal end of the screen (Fig. 11.11). The friction head loss caused by flow of seawater across the rough screen and the inflow of water through the slots cause the available suction head to dissipate toward the distal end of the screen, thereby causing a very uneven inflow pattern and the probability that little or no inflow will occur at the distal end of the

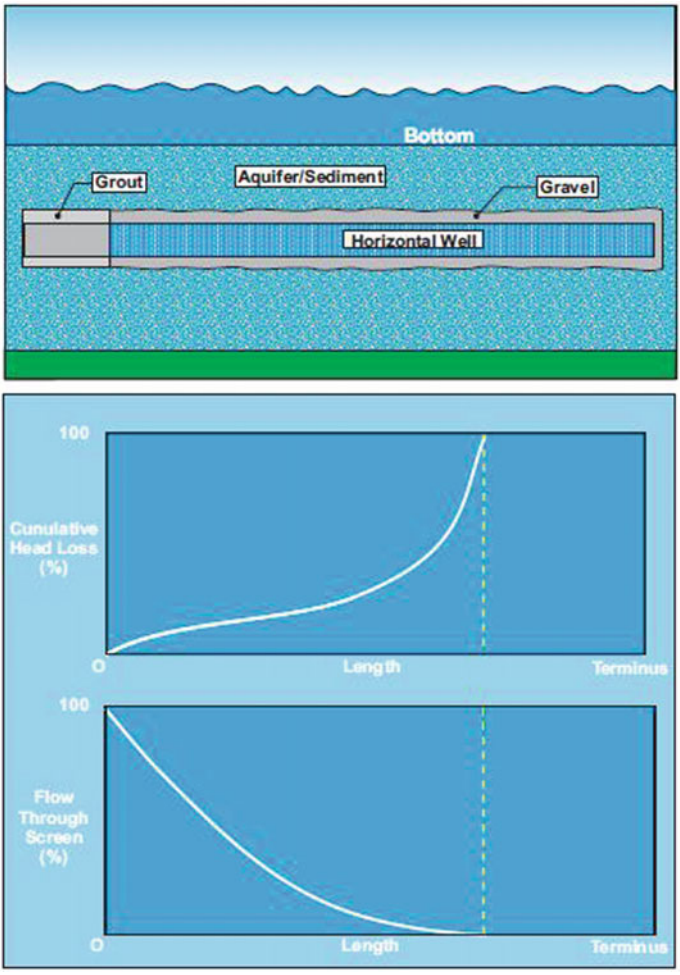

Fig. 11.11 Head loss and flow in a screen collector with a single proximal head loss (from Missimer 2009)

pipe. This problem becomes greater as the length of the screen is increased. Therefore, the screen length must be controlled so that flow stays relatively uniform.

Mantilla and Missimer (2014) found that the collection pipe diameter, configuration, and type of intersection also effects the internal head loss and the distribution of suction head that is transmitted to the screens. The collection pipe and screen system should be designed to minimize head losses. The piping system must be evaluated by dividing it into segments and evaluating each segment in terms of head loss, especially where there are transitions from laminar to turbulent flow (White 2011). The head losses within a given design can be evaluated using the Darcey-Weisbach equation for the pipeline and screen segments and the corrections developed by Hager (2010) for the intersections of pipes. A general approach to calculation of the friction head loss and the method to optimize the gallery design is contained in Mantilla and Missimer (2014).

Based on the research contained in Mantilla and Missimer (2014), it is clear that additional research is required in the development of a computer program to optimize the design of gallery cells for maintaining an equalized head within the collection layer. In the absence of this optimization program some basic principles should be applied in the design of the underdrain system which include: (1) the gravel within the collection layer should have a very high hydraulic conductively to effectively cause spreading of the pressure loss within layer away from the proximal pipe attachments to the screens, (2) the length of the screens from the header point to the distal end should be limited, (3) the area of slot within the screens could be expanded from the proximal to distal end of the screen to encourage uniform inflow of water, and (4) the slot aperture could be increased from the proximal to distal end of the screens to maintain uniform inflow.

Since there is only one large-scale seabed gallery intake system in operation today (Fukuoka, Japan), there is a small quantity of operational data available for evaluation of system hydraulic issues. Based on the research by Mantilla and Missimer (2014), it is clear that additional research is required to optimize the design of large seabed gallery intake systems in the future. Also, it can be concluded that using a single gallery cell with long headers and screen lengths is not a viable design in term of operational reliability. Breaking the system into multiple cells with individual pumps is more logical in terms of operational hydraulics and reliability.

11.4.6 Concept of Modular Gallery Cells, Coordination with SWRO Plant Design, and Reliability Design Issues

For many years, water treatment plant designers abided by a general rule that no part of the facility could cause a more than 10 % operational loss if a component failed. The issue of operational reliability of a SWRO plant must consider all of the internal facility components, but also must consider the intake. A seabed gallery can

be designed as a single feed water source to supply a pressurized header that conveys seawater to all of the high pressure pumps feeding the membrane trains. A single gallery with a very high capacity pump can be designed to meet the full feed water capacity requirement. This design type, however, is risky and does not meet an acceptable reliability standard.

The capacity required from any gallery intake system should be divided into a series of units in a modular configuration. A series of gallery "cells" should be designed and constructed to achieve reliable system hydraulics (see Sect. 11.4.5) and to subdivide the flow to improve operational reliability. An example of the gallery cell concept is shown for the Shuqaiq site developed in the site technical feasibility investigation (Fig. 11.12; Mantilla and Missimer 2014). A single cell would be equipped with a pump and could be used to feed a single corresponding

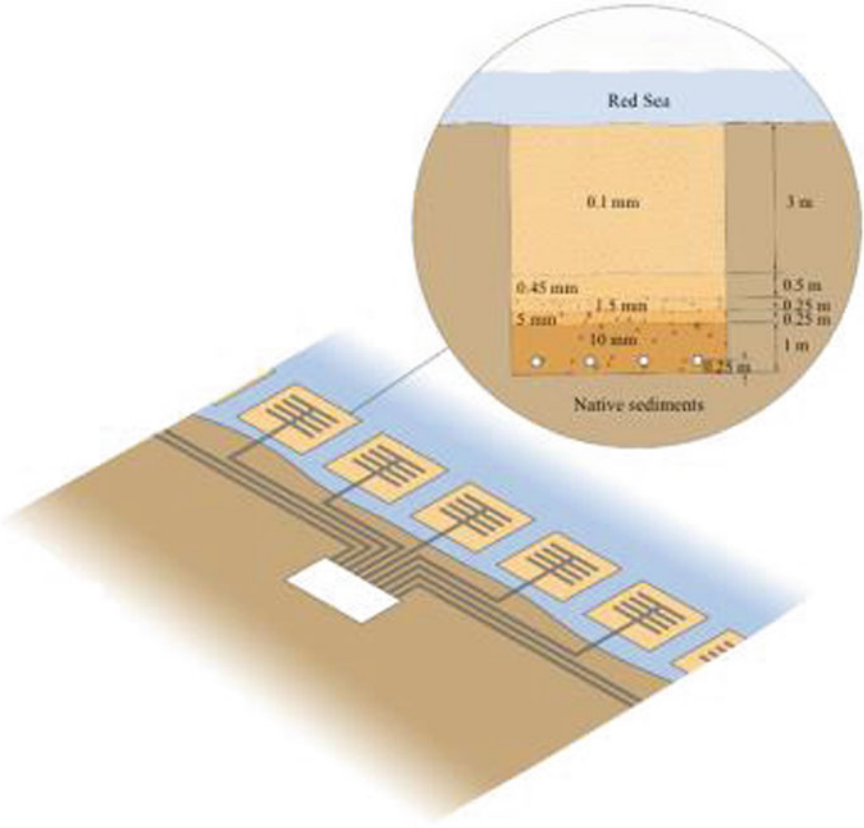

Fig. 11.12 Schematic diagram showing the design configuration of seabed gallery cells located along the coast of the Red Sea at Shuqaiq (from Mantilla and Missimer 2014). Each cell would be equipped with a single pump that would feed one SWRO train at this site

SWRO process train or perhaps two trains depending upon the plant capacity. The failure of a feed water pump or required maintenance of the gallery surface could be accommodated, especially if a standby gallery cell is constructed.

The number and configuration of gallery cells should be controlled by a combination of the site geological characteristics, environmental considerations, constructability or construction methods, and the SWRO plant design. Space limitations or the avoidance of high environmental impact areas could cause some significant separation distance between cells. Innovations in construction could also cause changes in the cell geometry and configuration. The correspondence between the number of cells and the SWRO plant design should consider the desired reliability factor.

11.4.7 Design Robustness to Overcome Possible Field Condition Changes

Seabed gallery intakes occur within the natural system are subject to the intense physical and biological processes of the nearshore marine environment. Depending upon the geographic location, a seabed gallery could be exposed to intense storm activity (hurricanes and typhoons), earthquakes, river or stream sediment discharges, harmful algal blooms, and man-induced contamination events. Each of these natural and anthropogenic factors should be considered in the design of the gallery intake system. The design needs to be robust enough to survive and remain operational during and after these events. Most of the possible impact events should have been considered during the technical feasibility and design phases of the project. However, not all factors can be considered, so the design should be robust enough to eliminate possible failures caused by unexpected events or such factors as sea level rise caused by global warming.

In regions where there are possible events that could cause temporary bottom excavation by storm activity, the upper active layer could be designed with a greater thickness to avoid damage to the graded filter. Some sediment deposition over the top of the intake may not cause a significant operational change unless the sediment is muddy or very thick. A slight increase in the upper bed thickness could cause a reduction in the head loss. Earthquake impacts, such as induced filter compaction, could also increase the head loss across the filter bed. A solution to this issue is to have the pump system designed to accommodate changes in the head loss by using a variable frequency drive (VFD) to maintain a constant flow rate. For extreme events, a small maintenance dredge may be required to clean a site while plant damage is being repaired. Many marine events would not only impact the intake, but would also impact the SWRO plant and support infrastructure. Therefore, the design considerations that affect the intake must be considered within the context of the entire SWRO facility.

11.4.8 Intake Pump Location, Design, and Operation

There are a variety of approaches to the design of a pumping system to withdraw seawater from an offshore gallery cell. The pump could be located close to the gallery near the shoreline and placed within a pump house or could be located at the SWRO plant site which could be some distance from the shoreline. A deep vault or sub-basement at the SWRO plant could be used to house the pumps and could also be used to produce the required suction head to maintain the inflow through the gallery cells. The key issue is to develop the least energy-intensive pump design that has high reliability.

11.4.9 Combining Rapid Infiltration with Membrane Filtration as a Complete Pretreatment System

Niizato et al. (2013) have recently suggested a hybrid pretreatment system consisting of a rapid seabed filter gallery system coupled with ultrafiltration and have termed the technology a high-speed seabed infiltration system (HiSIS). In a series of bench-scale column tests using a seawater feed, they tested infiltration rates ranging from 5 to 150 m/d. Some of their results are rather questionable in that the SDI reduction for a 5 m/d infiltration rate was only 5 % and increased to 22 % at 50 m/d and then declined to 12 % at 150 m/d. It is possible that some media compaction occurred due to the head loss experienced within the column. The experiment reductions in turbidity of the raw seawater ranged from 81 % at 5 m/d to 88 % at 50 m/d to 82 % at 150 m/d. A proxy for biofouling potential using ATP (Vesa et al. 2008) showed an average reduction at 5 m/d of 59 %, at 50 m/d of 79.4 %, and 70.6 % at 150 m/d. The head losses measured seemed to be rather low with all being less than 40 mm. However, only 200 m^3 of raw seawater was filtered during the experiments.

If larger-scale experiments are run at greater duration and produce similar results, the combined HiSIS system coupled with ultrafiltration could be a hybrid worth consideration. Pilot testing using the discharge from a HiSIS system should be conducted to ascertain if the system is truly producing a reduction in TEP concentration and the rate of membrane biofouling. Another question arises concerning its ability to operate during HAB's.

11.4.10 Constructability of Gallery Intake Systems Along the Red Sea Coast of Saudi Arabia

Comparative assessment of any subsurface intake versus a conventional open-ocean intake focuses on two primary issues; constructability and economics. Construction in the marine environment is generally complex and requires careful planning and

sometime innovative methods. Even offshore velocity-cap intake structures are not simple to construct and create challenges for placement of the connecting pipeline, particularly in locations where high-energy beaches must be crossed.

There are several different approaches that can be used to construct a seabed gallery intake system. Three different types are herein explored which include: (1) temporary road construction from the beach and excavation and installation of the gallery cells in wet conditions, (2) use of sheet piling and construction of the gallery cells in a dewatered condition, and (3) dredging of an offshore trench and placement of prefabricated cells into the trench with some emergence above the bottom.

Gallery construction along the Red Sea nearshore of Saudi Arabia is less complicated and costly compared to many other regions. Because the nearshore sites occur in very shallow water (1–1.5 m) and the bottom is relatively stable, consisting of soft limestone with a veneer of unlithified sediments, a temporary access road could be constructed to reduce construction difficulty. The option would exist as to whether to construct the gallery cells either in a dry mode or in the wet, if the soft rock is suitably stable to allow the excavated trenches to remain open during placement of the engineered filter material and collection system. Another configuration would be to use a concept similar to the South Jeddah Corniche wellfield intake system, which is constructed on a permanent offshore artificial fill area (Fig. 11.13).

Gallery cells constructed in deeper water would generally require the use of sheet piling to allow excavation and filter construction. This type of marine construction has been used for over a century in the construction of support structure

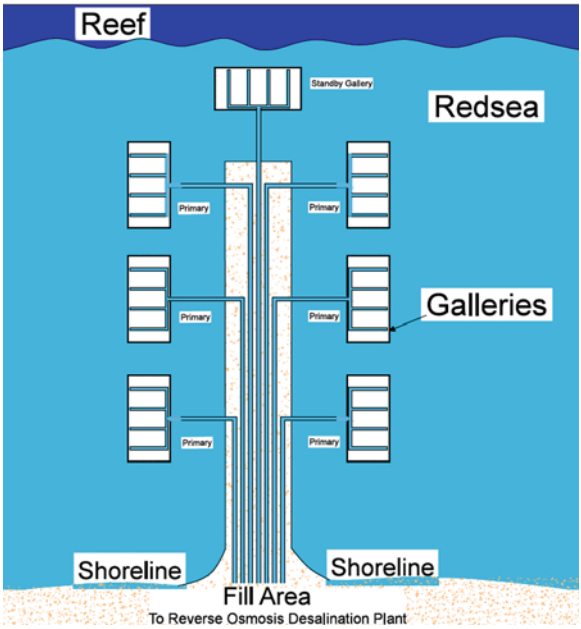

Fig. 11.13 Design concept for an offshore gallery system using an artificial fill peninsular for ease of construction and location of pipelines

Fig. 11.14 Construction of the City of Long Beach test seabed gallery cell using sheet piling and dewatering the excavation prior to filter emplacement

for large bridges across bay and shallow seas. An example is the City of Long Beach, California seabed gallery systems (Fig. 11.14). Perhaps an innovation would be to drive tong-and-groove concrete sheet piling with an upper fastener attachment that would extend from the concrete placed flush with the seabed to above the sea surface. This would allow dewatering during construction and would isolate the gallery walls from the subsea sediments.

Another approach would be to dredge a long linear area parallel to the shoreline with dimensions large enough to allow placement of a series of prefabricated

gallery cells constructed with pre-cast concrete (boxes without tops and holes from the collection pipe fittings). The dredging could be used to move some of the sediment to a stockpile location with some sediment stored near the site to be used to backfill the excavated gap between the hard galley cells and the far edges of the trench. The prefabricated cells could be lowered from a construction barge into the excavated trench with cranes. The prefabricated concrete walls of the gallery cells could be designed to be flush with the sea floor or could be elevated above the seafloor to some extent. The design would have to match the offshore energy condition and consider potential scouring of the filter face (top) or the sediment around the edges of the gallery structure.

As the use of seabed gallery intake structure becomes more common, construction innovation will occur to ease the process and to reduce cost. Each new large capacity system will allow design and construction improvements to be made that will affect the project capital cost.

11.4.11 Capacity Limitations and Economics

The issue of capacity limitation is raised commonly when considering a subsurface intake system to meet the feed water requirements of large-capacity SWRO facilities, defined as those with a permeate production of over 100,000 m^3/d. While all well intake types do have practical capacity limitations, gallery intakes can be effectively designed and constructed to meet very high capacities. The key issues in gallery capacity limitation involve constructability and economics, particularly the capital cost of seabed gallery construction.

Evaluation of construction cost should take into consideration the pre-treatment processes that occur with the gallery intake system versus the construction and operation of these processes at a SWRO water treatment facility. Therefore, a life-cycle cost analysis should consider the cost savings from the elimination of many or all of the pretreatment processes used to treat seawater coming from an open-ocean intake. Missimer et al. (2013) show a variety of pretreatment process trains for a SWRO facility and the goal process, which is the use of a subsurface intake system to treat the raw water for direct placement into the cartridge filters or use a fine mesh screen to eliminate the risk of particulates entering the cartridge filters or process train (Fig. 11.15).

A considerable volume of literature has documented the improvements in raw seawater quality that occur when using subsurface intake systems (Missimer and Winters 2003; Schwartz 2003; Bartak et al. 2012; Choules et al. 2007; Laparc et al. 2007; Missimer et al. 2013; Dehwah et al. 2014; Rachman et al. 2014). Therefore, many of the goals for reduction in the concentration of suspended solids, silt density index (SDI), algae, bacteria, NOM, and TEP are achieved by subsurface intake systems. The intensity of the in-plant pretreatment processes can be reduced with a consummate reduction in chemical usage, energy, and operational cost.

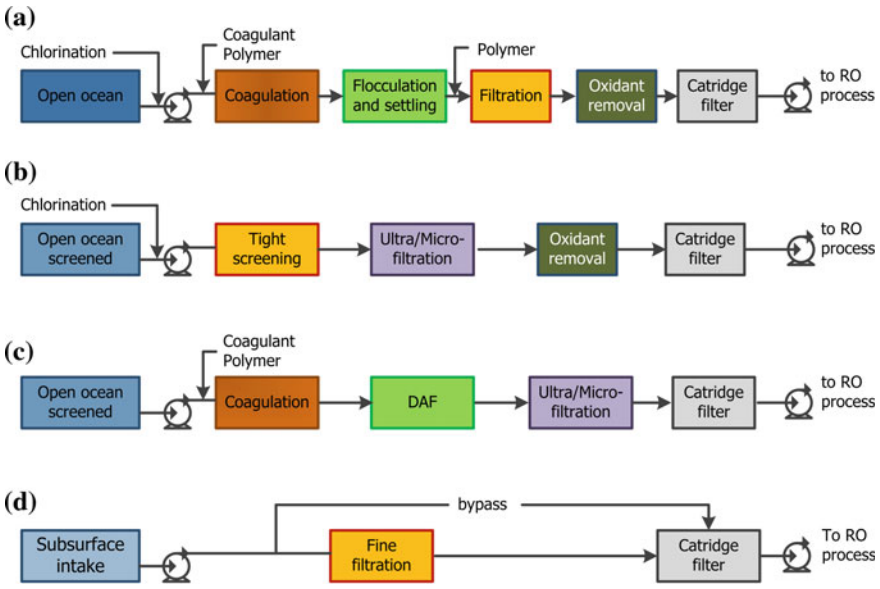

Fig. 11.15 Pretreatment complexity reduction using subsurface intake systems (modified from Missimer et al. 2013). **a** Conventional pretreatment. **b** Alternative pretreatment. **c** Alternative pretreatment. **d** Alternative intake

Within the life-cycle cost analysis, there will likely be a higher capital cost for constructing a seabed gallery intake system compared to any type of open-ocean intake system. However, the reduced operating cost over a 20 or 30 year operating period will make the seabed gallery system cost-effective depending on the percentage of operating cost saved by using this intake system. The reduced environment impacts associated with a reduction in impingement and entrainment of marine life also has an associated cost that should be factored into the life-cycle economic analysis. In conclusion, a life-cycle cost analysis should help justify the higher capital cost of the seabed gallery intake if there is real pretreatment cost savings included in the analysis.

11.5 Conclusions

Seabed gallery intake systems can be successfully designed and operated to meet the demands of virtually any capacity SWRO system. The feasibility of gallery development can be assessed at the screening level first and later at specific sites to assure that a gallery system can be successfully developed. A series of investigations of the Red Sea coastline and nearshore area were documented to illustrate the types of post-screening, site-specific feasibility investigations that should be

conducted and the parameters that need to be measured to assure feasibility. The Red Sea nearshore area contains a large number of feasible sites that could be used to design, construct, and operate seabed gallery intakes as evidenced by shallow water with a low offshore slope, moderate to low wave energy, low and predictable range in tidal fluctuations, generally sandy nature of the offshore bottom, ease of bottom excavation for gallery construction, lack of environmental sensitivity of the offshore marine environment, and constructability of gallery cells.

Considerable care must be used in the design of seabed galleries to assure operational reliability. The engineered filter media needs to be designed to assure that infiltration of finer sand from the upper to lower layers does not occur. While a geotextile fabric could be used to separate the active sandy upper layer from the underlying coarse gravel collection layer, this is not recommended because of concerns related to potential clogging caused by bacterial growth. The thickness of the uppermost, active filter layer must be considered to assure that the correct hydraulic retention time is achieved and that it is sufficiently thick to function after a storm excavation event and can withstand churning of the sediment caused by marine infauna, such as polychaete worms and burrowing shrimp.

Within the design of the gallery filter media, a balance must be achieved between the desired degree of treatment and the filter hydraulics. A range in active zone hydraulic retention time between 6 and 10 h is desirable. The hydraulic retention time can be estimated by dividing the active upper layer(s) by the infiltration rate. A hydraulic retention time in this range should allow the gallery intake to remove a large percentage of organic material and act as a part of the pretreatment system.

The hydraulic head loss based on the media hydraulic conductivity and design infiltration rate should be no greater than 1–1.5 m in most cases. The thickness of the upper active layer will generally range from 1 to 3 m depending of the site-specific conditions. The sediment grain size distribution in this layer must be compatible with the nature grain size distribution of the marine bottom in which it is placed (surface mobile sand).

Another key design aspect is the need to achieve as uniform as possible distribution of the infiltration rate across the surface of the gallery. The design of the underdrain system controls the head loss within the bottom layer that induces the vertical flow. The gravel in this lower collection layer must have a high hydraulic conductivity and the geometry of the collection header system and screens should be designed to keep the head loss with the system as uniform as possible. Extreme variation in the surface infiltration rate will cause the potential risk of clogging of the filter surface to increase, particularly in the surface areas overlying the proximal areas where the header attaches to the lateral screens.

The reliability of a seabed gallery system is a key design consideration. While the Fukuoka system uses a single gallery for its intake, it cannot be considered as the model design for reliability due to the potential failure of a single pipe or pump would curtail operation of the SWRO plant. Seabed gallery intakes should be designed using a series of “cells” which are independent galleries, each with a pump. The design of the SWRO plant should be coordinated with the gallery design so each train or set of trains receives feed water from a single gallery cell. At least

one standby or emergency cell should be constructed to improve reliability, especially if a pump failure were to occur. Also, additional capacity could be used to reduce the overall infiltration rate during extreme events, such as an HAB.

Seabed gallery intake systems will become an important class of SWRO intakes in the future. Design innovations will be required to reduce the construction costs and increase the reliability so that they are considered for use in the large-capacity SWRO systems of the future. As more research is completed on the degree of pretreatment achieved and operational experience is obtained, the risk factor perceived by project designers, operators, and owners will be reduced.

References

Allen, J. B., Tseng, T. J., Cheng, R. C., & Wattier, K. I. (2008). Pilot and demonstration-scale research evaluation of under-ocean floor seawater intake and discharge. *Proceedings of the American Water Works Association Water Quality Technology Conference*. Cincinnati, Ohio Nov 16–20, 2008.

Al-Mashharawi, S., Dehwah, A. H. A., Bandar, K. B., & Missimer, T. M. (2014). Feasibility of using a subsurface intake for SWRO facility south of Jeddah, Saudi Arabia. *Desalination and Water Treatment*. doi:10.1080/19443994.2014.939870.

American Society for Testing and Materials (ASTM). (2006). *Standard test method for permeability of granular soils*. Standard D2434-682006, ASTM, West Conshohocken, Pa.

Amy, G., Carlson, K., Collins, M. R., Drewes, J., Gruenheid, M., & Jekel, M. (2006). Integrated comparison of biofiltration in engineered versus natural systems. In R. Gimbel, N. J. D. Graham, & M. R. Collins (Eds.), *Recent progress in slow sand filtration and alternative biofiltration processes* (pp. 3–11). London: IWA Publishing.

Barrett, J. M., Bryck, J., Collins, M. R., Jamois, B. A., & Logsdon, G. S. (1991). *Manual of design for slow sand filtration*. Denver, Colorado: American Water Works Association Research Foundation and American Water Works Association.

Bartak, R., Grischek, T., Ghodeif, K., & Ray, C. (2012). Beach sand filtration as pre-treatment for RO desalination. *International Journal of Water Science, 1*(2), 1–10.

Berman, T. (2010). Biofouling: TEP-a major challenge for water separation. *Filtration and Separation, 47*(2), 20–22.

Berman, T., Mizrahi, R., & Dosoretz, C. G. (2011). Transparent exopolymer particles (TEP): A critical factor in aquatic biofilm initiation and fouling on filtration membranes. *Desalination, 276*, 184–190.

Buchan, J. (2003). *Crowed with genius: The Scottish enlightenment: Edininburgh's moment of the mind*. New York: Harper Collins.

Choules, P., Schotter, J.-C., Leparc, J., Gai, K., & Lafon, D. (2007). Operation experience from seawater reverse osmosis plants. *Proceedings, American Membrane Technology Conference and Exposition*. Las Vegas, Nevada.

Christman, K. (1998). The history of chlorine. *Waterworld, 14*(8), 66–67.

Cook, D.I. (2003). Geosynthetics. *Rapra Review Reports No. 58*, Rapra Technology Limited, Shrewsbury, 132 pp.

Crittenden, J. C., Trussell, R. R., Hand, D. W., Howe, K. J., & Tchobanoglous, G. (2005). *Water treatment: Principles and design*. Hoboken: Wiley.

Dehwah, A. H. A., Li, S., Al-Mashharawi, S., Rachman, R. M., Winters, H., & Missimer, T. M. (2014). The influence of beach well and deep ocean intakes on TEP reduction in SWRO desalination systems, Jeddah, Saudi Arabia. *AWWA/AMTA Membrane Technology Conference Proceedings*. Las Vegas, Nevada, March 10–13, 2013, 18 pp.

Dehwah, A. H. A., & Missimer, T. M. (2013). Technical feasibility of using gallery intakes for seawater RO facilities, northern Red Sea coast of Saudi Arabia: The king Abdullah Economic City site. *Desalination and Water Treatment, 51*(34–36), 6472–6481. doi:10.1080/19443994.2013.770949.

Fukami, H. (2002). Feature of the seawater infiltration water intake, and water quality variation at the time of pilot plant. *Journal of the Japan Society of Civil Engineers*, 75–76 (in Japanese).

Hager, W. H. (2010). *Wastewater hydraulics: theory and practice*. New York: Springer.

Hamano, T., Tsuge, H., & Goto, T. (2006). Innovations perform well in first year of operation. *Desalination and Water Treatment, 16*(1), 31–37.

Hayward, A. B. (1985). Coastal alluvial fans (fan deltas) of the Gulf of Aqaba (Gulf of Eilat), Red Sea. *Sedimentary Geology, 43*(1–4), 241–260.

Hendricks, D. W. (Ed.). (1991). *Manual of design for slow sand filtration* (p. 247). Denver: AWWA Research Foundation and American Water Works Association.

Henricks, D. W. (2011). *Fundamentals of water treatment unit processes: Physical, chemical, and biological* (p. 883). Boca Raton: CRC Press.

Huisman, L., & Wood, W. E. (1974). *Slow sand filtration* (p. 122). Geneva: World Health Organization.

Intergovernmental Panel on Climate Change (IPCC). (2013). Working Group I contribution to the IPCC Fifth Assessment Report (AR5), Climate change 2013: The physical science basis. Intergovernmental Panel on Climate Change. Geneva, Switzerland.

Jenkins, M. W., Tiwari, S. K., & Darby, J. (2011). Bacterial, viral and turbidity removal by intermittent slow sand filtration for households in developing countries: experimental investigation and modeling. *Water Research, 45*(18), 6227–6239.

Laparc, J., Schotter, J.-C., Rapenne, S., Croue, J. P., Lebaron, P., Lafon, D., et al. (2007). Use of advanced analytical tools for monitoring performance of seawater pretreatment processes. *Proceedings of the International Desalination Association World Congress on Desalination and Water Reuse*. Maspalomas, Gran Canaria, Spain, Oct 21–26, 2007, IDAWC/MP07-124.

Lopez, O., Stenchikov, G., & Missimer, T. M. (2014). Climate change water management using aquifer storage and recovery of stormwater: Environmental Research Letters 9, 075008, 8 p. doi:10.1088/1748-9326/9/7/075008.

Lujan, L. R., & Missimer, T. M. (2014). Technical feasibility of a seabed gallery system for SWRO facilities at Shoaiba, Saudi Arabia and regions with similar geology. *Desalination and Water Treatment*, doi:10.1080/19443994.2014.909630.

Mantilla, D., & Missimer, T. M. (2014). Seabed gallery intake technical feasibility for SWRO facilities at Shuqaiq, Saudi Arabia and other global locations with similar coastal characteristics. *Journal of Applied Water Engineering and Research*, http://dx.doi.org/10.1080/2349676.2014.895686.

Missimer, T. M. (1994). *Water supply development for membrane water treatment facilities* (1st ed.). Boca Raton, Florida: Lewis Publishers.

Missimer, T. M. (2009). *Water supply development, aquifer storage, and concentrate disposal for membrane water treatment facilities* (2nd ed.). Methods in Water Resources Evaluation Series No. 1. Schlumberger Water Services. Sugar Land, Texas.

Missimer, T. M., Ghaffour, N., Dehwah, A. H. A., Rachman, R., Maliva, R. G., & Amy, G. (2013). Subsurface intakes for seawater reverse osmosis facilities: Capacity limitation, water quality improvement, and economics. *Desalination, 322*, 37–51. doi:10.1016/j.desal.2013.04.021.

Missimer, T. M., & Horvath, L. E. (1991). Alternative designs to replace conventional water-water intakes for membrane treatment facilities. *Proceedings of the International Desalination Association World Congress on Desalination and Water Reuse*, pp. 131–140.

Missimer, T. M., & Winters, H. (2003). Reduction of biofouling at a seawater RO plant in the Cayman Islands. *Proceedings of the International Desalination Association World Congress on Desalination and Water Reuse*, Paper BAH03-190.

Niizato, H., Inui, M., Kira, N., Inoue, T., Oiwa, T., Cai, H., et al. (2013). Innovative SWRO desalination technology introducing high-speed seabed infiltration system (HiSIS).

Proceedings of the International Desalination Association World Congress on Desalination and Water Reuse. Tianjin, China, Paper IDAWC/TIAN13-033, Oct 20–25, 2013.

Okamoto, H., et al. (2005). Feature of the seawater infiltration water intake, and water quality variation at the time of test operation. *Journal of Japan Society of Civil Engineers,* 25–26 (in Japanese).

Pankratz, T. (2006). Seawater desalination technology overview. Presentation to the Georgia Joint Comprehensive Desalination Study Committee. St. Simons Island, Georgia, Aug 22–23, 2006.

Passow, U. (2000). Formation of transparent exopolymer particles, TEP, from dissolved precursor material. *Marine Ecology Progress Series, 192*, 1–11.

Passow, U., & Alldredge, A. L. (1994). Distribution, size and bacterial-colonization of transparent exopolymer particles (TEP) in the ocean. *Marine Ecology Progress Series, 113*(1–2), 185–198.

Rachman, R. M., Li, S., & Missimer, T. M. (2014). SWRO feed water quality improvement using subsurface intakes in Oman, Spain, Turks and Caicos Islands, and Saudi Arabia. *Desalination, 251*, 88–100.

Rollin, A. L. (2004). Long term performance of geotextiles. *Proceedings 57th Canadian Geotechnical Conference*. Quebec City, Quebec, Session 4D, pp. 15–20.

Schwartz, J. (2003). Beach well intakes improve feed-water quality. *Water & Wastewater International, 18*(8).

Sesler, K., & Missimer, T. M. (2012). Technical feasibility of using seabed galleries for seawater RO intakes and pretreatment: Om Al Misk Island, Red Sea, Saudi Arabia. *IDA Journal: Desalination and Water Reuse, 4*(4), 42–48.

Shimokawa, A. (2012). Fukuoka District desalination system with some unique methods. *Proceedings of the International Desalination Workshop on Intakes and Outfalls*. National Centre of Excellance in Desalination, Adelaide, Australia, May 16–17, 2012.

Tanner, W. F., & Balsillie, J. H. (1995). *Environmental clastic granulometry*. Tallahassee: Florida Geological Survey, Special Publication 40, 142 p.

Vesa, M. J., Ortiz, M., Sadhwani, J. J., Gonzalez, J. E., & Sanatana, F. J. (2008). Measurement of biofouling in seawater: Some practical tests. *Desalination, 220*, 326–334.

Wang, S., Allen, J., Tseng, T., Cheng, R., Carlson, D., & Henson, J. (2009). Design and performance update of LBWD's under ocean floor intake and discharge system. *Proceedings of the Alden Desalination Intake/Outfall Workshop*. Holden, Massachusetts, Oct 16, 2009.

Wang, S., Leung, E., Cheng, R., Tseng, T., Vuong, D., Carlson, D., et al. (2007). Under sea floor intake and discharge systems. *Proceedings of the Interbational Desalination Association World Congress on Desalination and Water Reuse*. Maspalomas, Gran Canaria, Spain, Paper IDAWC/MP07-104, Oct 21–26, 2007.

Wenzel, L. K. (1942). Methods for determining permeability of water-bearing materials with special reference to discharging-well methods. U.S. Geological Survey Water-Supply, Paper 887.

Wescott, W. A., & Ethridge, F. G. (1980). Fan-delta sedimentology and tectonic setting-Yallahs fan delta, southeast Jamaica. *Bulletin American Association of Petroleum Geologists, 64*, 374–399.

White, F. (2011). *Fluid mechanics*. New York: McGraw-Hill.

Chapter 12
Feasibility and Design of Seabed Gallery Intake Systems Along the Arabian Gulf Coast of Saudi Arabia with a Discussion on Gallery Intake Use for the Entire Arabian Gulf Region

Rinaldi Rachman and Thomas M. Missimer

Abstract The Arabian Gulf coast of Saudi Arabia contains a large number of existing desalination facilities of which many use the seawater reverse (SWRO) osmosis process. Many SWRO facilities have had historical operational problems with membrane biofouling. Subsurface intake system feasibility was assessed generally for the coastline of Saudi Arabia and a site-specific investigation was conducted at Ras Abu Ali Island. It was found that the common occurrence of sabkhas along the shoreline of Saudi Arabia causes the use of conventional vertical wells to be risky due to migration of hypersaline water into them. All well types do not appear to be feasible based on the shoreline and nearshore geological conditions. Beach galleries were assessed and are also subject to failure caused by migration of hypersaline water and possible burial by dune sands moving eastward from the desert into the Arabian Gulf. Seabed gallery intake systems were found to be the most technically feasible subsurface intake type which could provide high capacity SWRO facilities with feed water. However, the low slope from the beach seaward and the tide range necessitate that seabed galleries would have to be constructed over 500 m seaward of the beach. This distance would make the construction complex and would require future design and construction innovations. Perhaps the seabed gallery cells could be constructed adjacent to an artificial fill peninsula that would allow easier access and less expensive construction.

R. Rachman
Water Desalination and Reuse Center, King Abdullah University of Science and Technology, Thuwal, Saudi Arabia
e-mail: rinaldi.rachman@kaust.edu.sa

T.M. Missimer (✉)
U.A. Whitaker College of Engineering, Florida Gulf Coast University, 10501 FGCU Boulevard South, Fort Myers, FL 33965-6565, USA
e-mail: tmissimer@fgcu.edu

T.M. Missimer et al. (eds.), *Intakes and Outfalls for Seawater Reverse-Osmosis Desalination Facilities*, Environmental Science and Engineering,
DOI 10.1007/978-3-319-13203-7_12

12.1 Introduction

The Arabian Gulf contains the largest concentration of seawater desalination capacity in the world with a total installed capacity of 11 million m^3/d in 2008 (Lattamann and Hoepner 2008). Historically, thermal processes, in particular multi-stage flash (MSF) desalination, were the predominant methods used to desalt seawater. In recent years, seawater reverse osmosis (SWRO) has become an important component of desalination in the Arabian Gulf because of its lower energy usage and consummate lower cost (Ghaffour et al. 2013). Many MSF facilities are now being linked to SWRO plants in a hybrid configuration, because the high salinity of the Arabian Gulf water requires dilution if a single pass SWRO configuration is used (Awerbuch 2007). An MSF/SWRO blend produces an acceptable quality for potable use after post-treatment.

Operation of SWRO facilities using the Arabian Gulf for feed water has had a difficult history with all older facilities suffering from membrane biofouling to varying degrees (Hassan et al. 1989; Winters 1994, 1997; Winters and Isquith 1995; El Aleem et al. 1998). The very warm water temperature, limited circulation, and high degree of biological productivity collectively make the Arabian Gulf seawater difficult to treat; thereby, commonly resulting in membrane biofouling. Considerable research on pretreatment of Arabian Gulf seawater has been conducted to ascertain which methods provide the best results to control the rate of membrane biofouling (Winters and Isquith 1995; Matin et al. 2011; Nguyen et al. 2012). The open-ocean intake systems that are commonly used are also subject to fouling by marine growth at the intake and within the transmission pipeline. To control this growth, continuous chlorination has been used. Research on systems using continuous chlorination has shown that these systems have a greater rate of membrane biofouling (Applegate et al. 1989; Winters and Isquith 1995).

SWRO facilities in the Arabian Gulf almost exclusively use some type of surface-water intake system. Many of the hybrid plants use a common intake at the shoreline that is also used to supply cooling water to a co-located power plant and feed water for an MSF plant. Stand-alone SWRO facilities commonly use either a canal intake at the shoreline or a velocity-cap intake structure offshore. In all cases, the feed water is taken from the nearshore in relatively shallow water. The seabed slope is very low and it requires a pipeline of more than 10 km to get to deeper water of better quality. Harmful algal blooms are also a common occurrence in the Arabian Gulf and can cause temporary shut-down of SWRO facilities when they occur, such as the event that occurred in 2009 (Berktay 2011).

Another factor controlling membrane biofouling is the concentration of bacteria, natural organic matter (NOM), particularly the polysaccharides and transparent exopolymer particles (TEP). Biofouling of SWRO membranes has been linked to the concentration of TEP and other sticky polysaccharides in raw seawater (Berman and Passow 2007; Bar-Zeev et al. 2009; Berman 2010; Berman et al. 2011). TEP tends to coat or condition SWRO membranes and promote the formation of a biofilm by creating a sticky substrate that encourages attachment of bacterial cells

and by also providing a food source. It is a particularly significant issue in the Arabian Gulf.

Subsurface intake systems can provide a higher quality feed water by performing many of the pretreatment processes in the subsurface as water is forced through the seabed and travels in a coastal aquifer or artificial media to the pump intake (Missimer 2009; Missimer et al. 2013). Subsurface intake systems produce feed water with significantly lower concentrations of algae, bacteria, NOM, and TEP (Chap. 9). An investigation of the coastline of the Arabian Gulf of Saudi Arabia was conducted to assess the viability of using subsurface intake systems, either wells or galleries. A site-specific investigation was conducted to assess the technical feasibility of using a subsurface intake to supply a fish hatchery or a large SWRO facility.

12.2 Background on the Arabian Gulf

12.2.1 Geology of the Coast and Nearshore Zone of the Southern Margin of the Arabian Gulf

Because of the importance of the Arabian Gulf geology as a modern analog for ancient carbonate petroleum reservoirs, a considerable amount of data have been collected on the surficial carbonate and mixed carbonate and siliciclastic sediments. Purser (1973) provided a large number of technical papers that describe the shoreline geology and some of the nearshore bottom characteristics of the southern margin of the Gulf. Circulation and climate, including wind, temperature, and evaporation, play major roles in controlling sedimentation, diagenesis, and overall environmental conditions within the Arabian Gulf (Purser and Seibold 1973). The Arabian Gulf has a length of about 990 km, a maximum width of 370 km and an average depth of only 36 m (Kampf and Sadrinasab 2006). It is a very shallow water body with water over a depth of 70 m occurring only in a narrow zone through the Strait of Hormuz and running to the west off the coast of Iran and ending north of Qatar and many areas with a depth <20 m (Fig. 12.1). The surface area of the Arabian Gulf is about 239,000 km^2 (Emery 1956). It is generally classified as a semi-enclosed, marginal sea (Kamf and Sadrinasab 2006).

Overall, the Saudi Arabian coastline of the Arabian Gulf has not be studied in as much detail as coastal areas located further to the east, such as the Trucial Coast (United Arab Emirates). Emery (1956) produced a generalized map of the entire southern coast and nearshore of the Arabian Gulf. It shows areas of mud, sand, and rock along the Saudi Arabia shoreline and offshore. A later map shows the shoreline to be predominantly intertidal and supratidal flats with small bays containing muddy sediments and the shallow nearshore being covered with mixed carbonate and siliciclastic sands from an area parallel to the tip of Qatar and northward (Wagner and van der Togt 1973; Alsharhan and Kendall 2003). In the restricted water body between Saudi Arabia and Bahrain and southward into the area between Saudi Arabia and Qatar, the nearshore sediment types are more diversified and

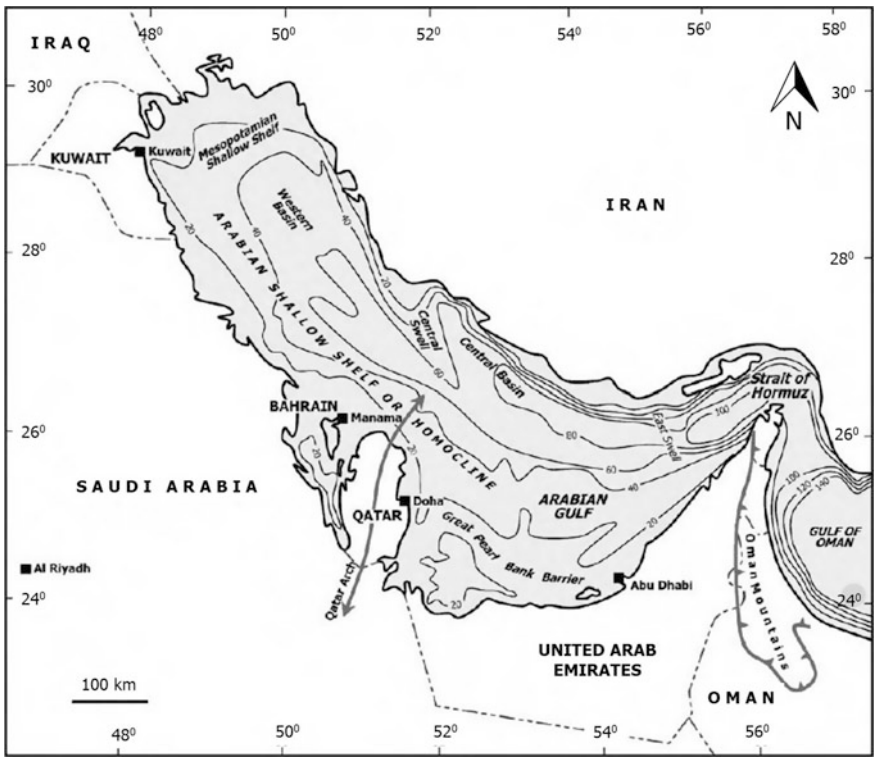

Fig. 12.1 General bathymetric map of the Arabian Gulf

muddier. Fryberger et al. (1983) describe the interplay at the shoreline of dune sand deposition, sabkha sediments, and offshore prograding mixed aeolian siliciclastic sand along the Saudi Arabia coast in the Dhahran area.

12.2.2 Circulation Within the Arabian Gulf and Impacts of Evaporation and the Freshwater Balance

Since the Arabian Gulf is a restricted water body, not open to typical oceanic circulation, it has some rather unique characteristics. Seawater travels from the Indian Ocean through the Arabian Sea Gulf and the Strait of Hormuz into the northern part of the Arabian Gulf off the coast of Iran (Kampf and Sadrinasab 2006; Fig. 12.1). The "fresher" seawater hugs the coast of Iran based on coriolis circulation. Since the Arabian Gulf has a very high evaporation loss rate and little freshwater enters it from ephemeral streams, much of the inflowing seawater evaporates and the more saline water leaves the Gulf as a density flow through the Strait of Hormuz (Swift and Bower 2003).

The nearshore area of Saudi Arabia has significant geographic and seasonal changes in salinity. The highest salinities found in the most restricted waters are over 46 ppt (Kampf and Sadrinasah 2006; Fig. 12.2). Yao (2008) found a similar pattern of the highest salinities in the western Gulf occurring in the winter months in a series of model simulations (Fig. 12.3). While the overall circulation patterns are greatly influenced by wind and salinity, the nearshore salinity pattern is influenced by the very high rates of

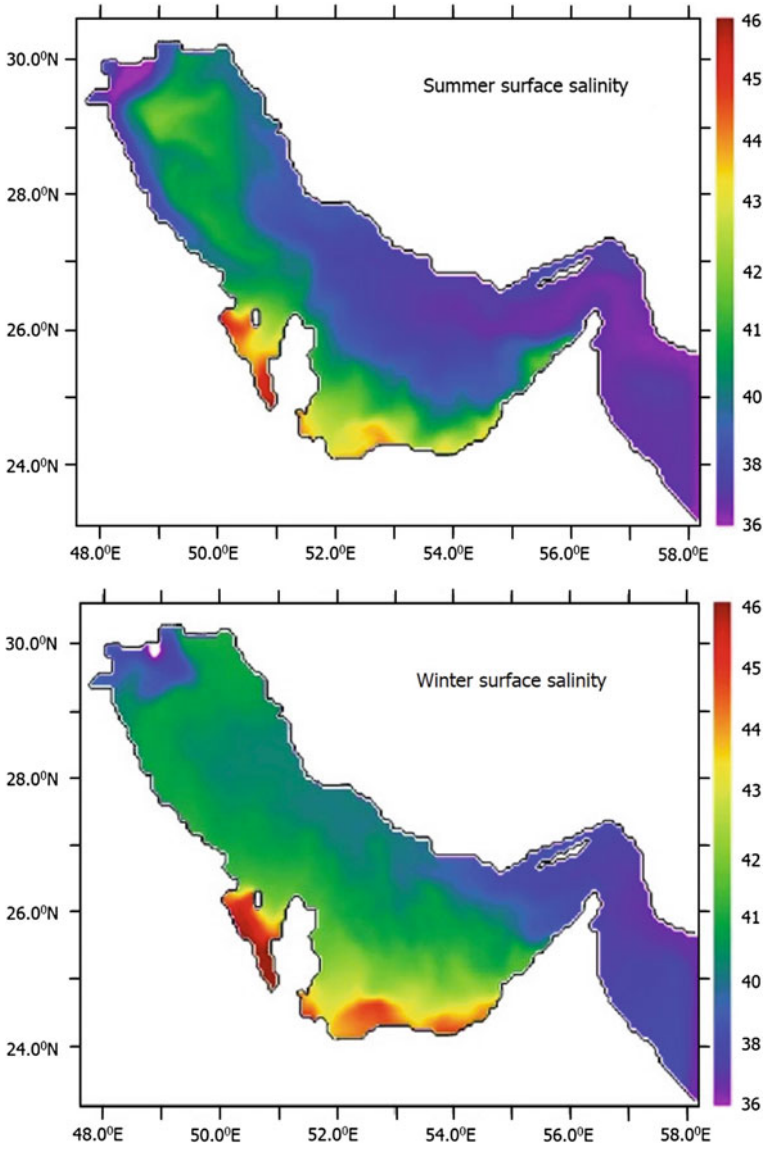

Fig. 12.2 Seasonal changes in distribution of salinity in the Arabian Gulf (Kampf and Sadrinasab 2006)

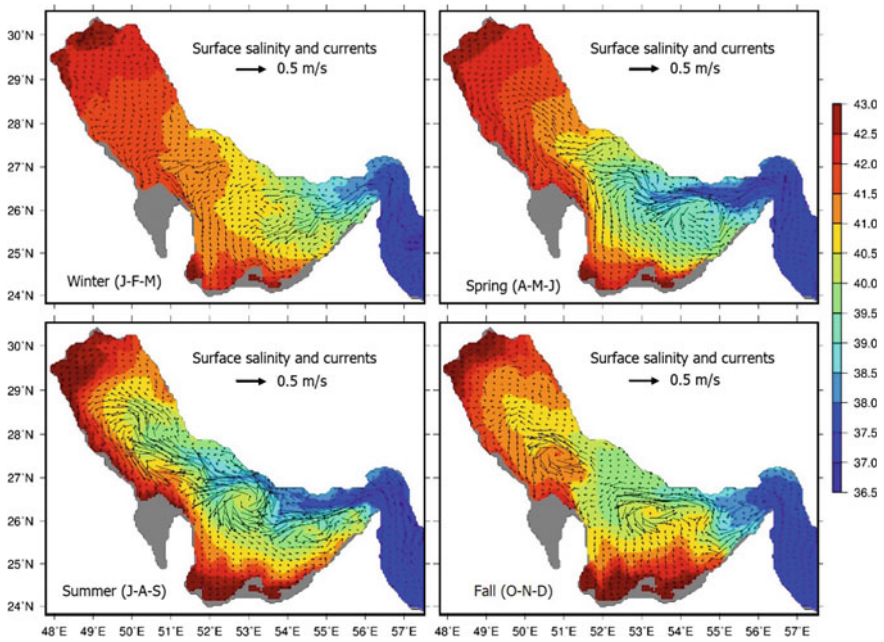

Fig. 12.3 Modelled salinity changes in the western Arabian Gulf showing the high nearshore salinities up to 46 ppt (from Yao 2008)

free-surface evaporation which can cause the formation of shallow water circulation cells. High evaporation rates can cause the formation of dense water flows along the bottom with seaward migration at calm periods or landward flows based on the predominant offshore wind direction during most of the year. The very high salinity and high saturation of calcium carbonate in the shallow seawater lead to the rapid marine cementation of bottom sediment with subsequent formation of extensive hardgrounds.

12.3 Methods

12.3.1 Literature Review on the Shallow Geology of the Shoreline and Nearshore Sediments of the Arabian Gulf with Emphasis on Factors that Affect Subsurface Intake Feasibility

A literature review was conducted on the surficial and shallow geology of the southern margin of the Arabian Gulf to assess shoreline and nearshore conditions. Particular emphasis was placed upon geological features that could potentially affect the development of a subsurface intake system that could be used to supply

feedwater for a SWRO facility. The key features for any coastal area were recently described by Dehwah et al. (2014). The type and mobility of the shoreline and nearshore sediments are very important as well as any coastal features that affect the quality of the groundwater near the beach and beneath the seabed (e.g., occurrence of sabkhas). The productivity in terms of coastal aquifer yield potential is another important issue. Also, oceanographic and climatic effects that may influence the quality of seawater in the nearshore also are of significance.

12.3.2 Investigation of a Specific Site Located at Ras Abu Ali Island, Saudi Arabia

A site-specific investigation was conducted by Rachman et al. (2014) at Ras Abu Ali Island, which is located north of Jubail between Ad-Dafi and Dawhats Al-Mussallamiyah, Eastern Province, Saudi Arabia (Fig. 12.4). The island has a

Fig. 12.4 Location of the site-specific field investigation at Ras Abu Ali Island, Saudi Arabia (from Rachman et al. 2014)

unique crescent shape with the outer section facing north where a proposed marine water intake system for a marine fish hatchery was proposed. The intake would have a required capacity of 6000 m^3/d and is being developed as part of a marine conservation program initiated by Saudi Aramco, the world's largest oil company.

Initially, a simple open-ocean pipeline or dredged open-channel intake was proposed for a fish hatchery water supply. During design, some problems were discovered for both intake types. Water temperature fluctuated between 35 °C during late summer and 15 °C during early spring, and red tides and oil spill contamination were identified as potential threats that could allow poor quality water to enter the sensitive seawater ponds. Marine biofouling control on inlet pipes, trash rack maintenance to remove marine debris, and extensive pretreatment to remove marine pathogens were also found to be necessary. A subsurface intake was then considered to resolve the issues related to impaired water quality. A 20 m deep monitoring well constructed on the beach revealed that the shallow groundwater, recharged by the sea, is hypersaline. The seaward-directed flow of brine from a sabkha causes the occurrence of hypersaline water that is inappropriate for fish larvae and hatchery conditions.

The offshore area near the hatchery and possible future SWRO plant facility was inspected to assess the bottom slope and condition (e.g., sediments, hardground, etc.). Also, the environmental sensitivity of the site was assessed by checking on the pattern of coral growth and occurrence of seagrass beds. The impact of tidal fluctuations on the site was also assessed (tidal range and exposed bottom at low tide).

Another subsurface intake option at the site is the use of a gallery-type intake which causes direct vertical flow of water from the sea through a media filter and does not allow horizontal water movement from the landward direction where the sabkha occurs. Therefore, a field investigation was performed to assess this possibility. The objectives of the investigation included the assessment of the shoreline and nearshore physical condition, including general characteristics of the marine bottom (sandy, muddy, rocky or combination), marine vegetation and coral distribution, wave action and tidal changes, and presence and thickness of unconsolidated sediment on the marine bottom. The latter evaluation is important because the upper layer of a gallery intake system would be affected by the native unlithified surface sediment as it moves across the gallery top. A preliminary engineering design of a system was made to assess the required surface area and for future cost estimates.

12.3.3 Field Sediment Collection and Laboratory Analyses

A predetermined sampling grid was established using an area with dimensions of 200 × 180 m for inspection and collection of sediment samples (Fig. 12.5). The sampling was organized within the grid system using a series of transects along which 35 samples were collected. At each point, unlithified surface sediment was collected and stored in a plastic container.

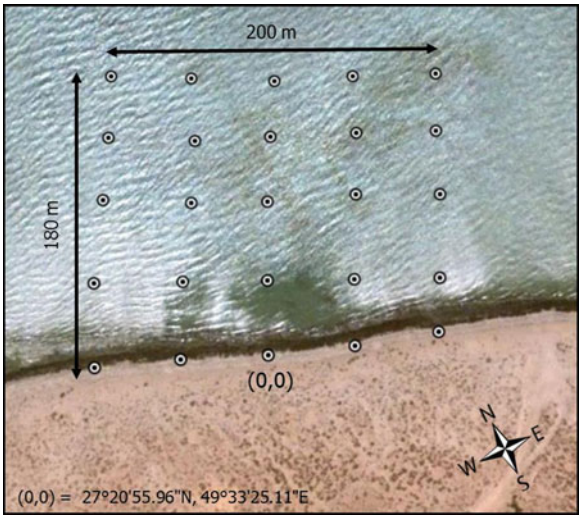

Fig. 12.5 Sampling grid used by Rachman et al. (2014) at Ras Abu Ali Island

Individual sediment samples were washed with fresh water having a neutral pH to remove the saline water and marine debris while conserving the mud content. After drying each sample, laboratory analyses of grain size distribution, sediment porosity, and hydraulic conductivity were made based on standard analytical methods as described in Tanner and Balsillie (1995), ASTM (2006), and Wenzel (1942).

12.4 Results of Initial Investigation

12.4.1 Site Description

The investigation conducted by Rachman et al. (2014) provided some very useful observations and results that have wide-spread use on ascertaining which subsurface intake types can be used along the coast and the nearshore of the Arabian Gulf. A preliminary field investigation revealed that the shoreline was covered with beachrock and an asphalt-like deposit (Fig. 12.6a). The beachrock was a tan color and was relatively hard. The black and gooey texture layer covered the beachrock and binded unlithified sediment in a layer 20–30 cm in thickness. The blacked area covered a belt within the intertidal zone about 10–20 m wide. It is believed that the oil spill during the Gulf War was the source of this material. Recent contracts have been awarded to remediate the beaches and intertidal area with removal of the oil contaminated sediments planned.

The nearshore marine bottom consists of predominantly a marine hardground with a veneer of unlithified muddy sand and carbonate sand (Fig. 12.6b). A subtidal (at high tide) marine-cemented limestone was observed all along the coast and seaward to the study area to water depths over 1 m. It extends at least 300–500 m

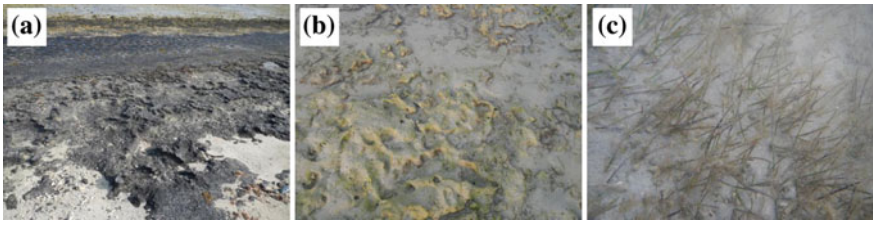

Fig. 12.6 Views of on-site conditions at Ras Abu Ali Island, Saudi Arabia. **a** Oil contamination deposited on the intertidal area of the beach. **b** Nearshore marine hardground with veneer of unlithified sediment. **c** Nearshore marine seagrass with generally sparse distribution (from Rachman et al. 2014)

from the shoreline (low tide point) seaward. Based on the field observations and literature review, the limestone is a marine-cemented, modern hardground. The thickness of the upper layer of limestone was observed to be about 30 cm in an excavation 1.5 m below the bottom at a location about 30 m seaward from the beach. The thickness of mixed carbonate and siliciclastic sand sediment lying atop the hardground was found to vary, but follows a trend of increasing from the shoreline vicinity (less than 50 cm) towards offshore (up to 100 cm). Parts of the hardground are devoid of sediment.

No living corals were observed on the hardground from the beach seaward to a distance of over 500 m. Seagrass occurs in low density in a belt from near the normal low tide position to a distance 100 m seaward (Fig. 12.6c).

12.4.2 Unconsolidated Bottom Surface Sediment Characteristics

Unlithified sediment tends to migrate across the top of the seabed and it can affect the operation of a seabed gallery. Detailed assessment of the size and hydraulic characteristics of the unlithified sediment is therefore important in the selection of a gallery site and in the design of the gallery media.

The variation in the mean grain size is shown in Fig. 12.7a. The mean grain diameter, which is the first statistical moment of the sediment, ranges from 0.24 to 1.72 mm with an average of 0.48 mm. The sediment is classified as medium-grained sand according to the Wentworth-Udden classification (Pettijohn et al. 1987). From the grain size distribution, the mud content of the samples was found to be relatively low at <0.5 % and generally low for all samples which is less than previously suggested compositions of the sediment (Fig. 12.7b; Wagner and van der Togt 1973).

Porosity was also measured on sediment samples and the results are shown in Fig. 12.7c. The values range from 0.29 to 0.41 with an average of 0.35.

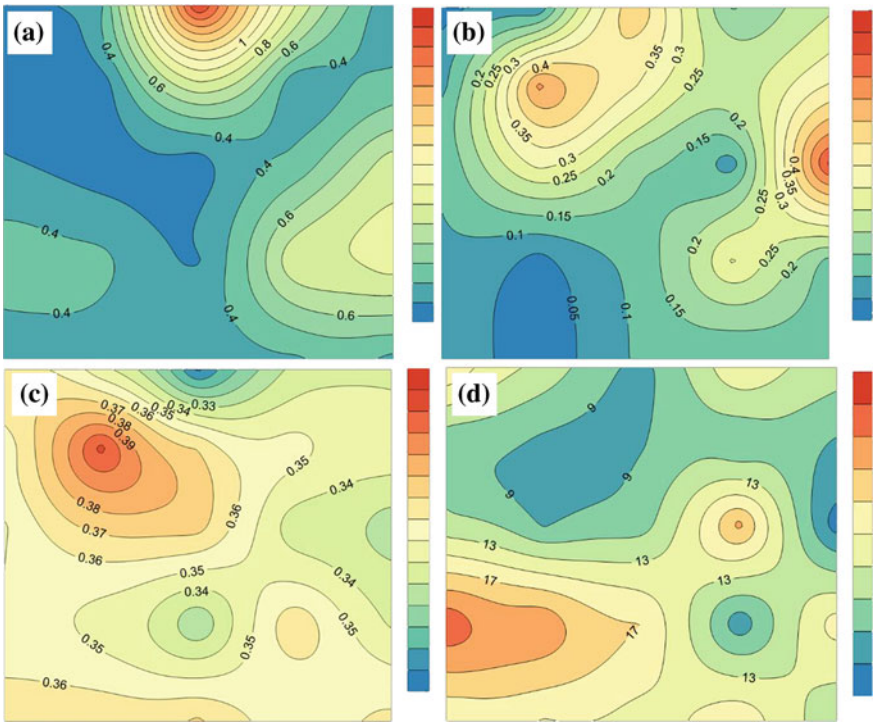

Fig. 12.7 Unconsolidated bottom surface sediment analyses results mapped in the study area **a** mean grain size, **b** mud percentage (decimal), **c** porosity (decimal), and **d** hydraulic conductivity (from Rachman et al. 2014)

The hydraulic conductivity measurements follow a similar pattern to the porosity values (Fig. 12.7d). Both properties are influenced by the percentage of mud in the samples. Hydraulic conductivity values range from 5.9 to 22.5 m/day and average 12.8 m/day.

12.5 Preliminary Seabed Gallery Design

12.5.1 General Site Feasibility for Seabed Gallery Intake Systems

Successful development of a seabed gallery intake system depends upon: (1) the type of the natural bottom sediments, (2) the sedimentation rate of fine sediments, (3) the tidal range (gallery must always be covered with water), (4) underlying site geology, (5) the impact on the marine ecosystem, and (6) stability of the nearshore marine bottom in terms of erosion and storm disturbance (Mantilla and Missimer 2014).

Table 12.1 Summary of study area characteristics in relation to key factors in development of gallery intake

Factors	Remarks
Natural bottom sediment	Medium-grained size sediment with relatively high hydraulic conductivity and low mud content
Tidal range	Low energy beach, wide intertidal zone, all-time covered water zone up to 500 m from low tide line
Sedimentation of fine sediment	Possibly high rate of hardground formation caused by rapid evapotranspiration
Marine ecosystem	Dead rocky coral (old) area with low density seagrass patches
Local groundwater system	Hypersaline groundwater found in the beach wells possibly caused by sabkha infiltrated water contamination

Groundwater quality issues can also have an impact on gallery design where hydersaline water can enter the gallery from the landward direction (Al-Mashharawi et al. 2014). Table 12.1 contains a summary of the site characteristics that are relevant to the design of a seabed gallery intake system at this location.

Two types of gallery intake systems are potentially feasible; beach and seabed (offshore) galleries. Beach galleries are constructed with the intertidal zone of a beach. The geology of the beach, in terms of the occurrence of certain sediments types, may not be significant because the gallery beds would have a fully engineered design developed to maximize efficient infiltration and treatment of seawater. However, rocky beaches or very high-energy beaches may not be appropriate locations for a beach gallery because the constructed filter bed could be eroded away. Also, some significant wave energy is required so that the mechanical energy of the breaking waves across the gallery surface causes cleaning of the gallery face. The risk of cementation calcium carbonate must be considered in areas where beachrock is actively forming.

The wide intertidal area and very low wave energy at the location investigated do not favor the construction of a beach gallery at this site. At low tide, the beach area would be located up to 500 m away from the gallery site, which would cause a short duration of the water covering the filter layer. This would give the facility a short daily duration of useful operation, would necessitate a greater gallery footprint to meet the required capacity, and may require onsite raw water storage. The absence of continuous flooding to promote continuous recharge of the gallery could promote preferential passage of hypersaline groundwater in the form of horizontal flow from the landward direction. Thus, the gallery option that is most suitable with the conditions in the study area is a seabed gallery intake type that maintains continuous flooding.

Despite the low slope of the nearshore, a seabed gallery system could be successfully constructed and operated at a location seaward of the low tide elevation. An essential factor for gallery operation is that the filter must be submerged in water at all times with a desired depth of at least 1 m to provide continuous recharge and to maintain an acceptable salinity. Based on the low offshore slope and the position

of the normal low tide line, the seabed gallery would have to be located >500 m from the shoreline to provide adequate water depth under all conditions. Since the sediment studies conducted in the field at this site did not survey the area seaward of 500 m, the natural bottom sediment characteristics seaward area must be extrapolated. Therefore, it is assumed that similar sediment characteristics favorable for the development of a seabed gallery system occur in the area of deeper water. Past geological investigations in this region support this assumption (Emery 1956; Wagner and van der Togt 1973).

Location of the seabed gallery system at a considerable distance from the shoreline does complicate the construction and can increase capital cost. However, the very shallow water depth may allow a temporary artificial fill area to be constructed from the beach to the seaward site of construction, thereby lessening construction cost compared to using barges, driving sheet piling and dredging in deeper water.

Maintenance of a slow sand filter is accomplished by manually by scrapping the filter top layer, which could also be accomplished in a seabed filter installed at a shallow water depth. Manual raking could be accomplished at low tide at this location. This effort becomes a challenging routine when the location is far offshore, especially if the water depth is great. In either case, special maintenance scheduling would have to be planned to allow safe access to the gallery (e.g., the low tide period providing that would provide temporary very shallow water between the filter location and the shoreline). Construction of a gallery intake at distance more than 500 m is technically feasible based on construction methodology, but may be very challenging based on capital cost.

12.5.2 Design of a Site-Specific Seabed Gallery Cell

A preliminary gallery design was proposed by Rachman et al. (2014) for Ras Abu Ali Island. The gallery filter system was designed similar to a slow sand filter, but with a thicker bed, greater hydraulic retention time and a generally more rapid infiltration rate. Typical slow sand filters operate at infiltration rates from 1.2 to 4.8 m/d and are constructed with media containing a mean grain diameter between 0.3 and 0.45 mm, and a head loss (gravitational) of 0.9–1.5 m (Huisman and Wood 1974). Slow sand filters in water treatment plants operate using gravity feed, but a seabed gallery filter is operated using pump suction. This allows more flexibility in terms of head loss and can allow greater variation in the design hydraulic retention time based on local water quality conditions.

Water treatment in a the gallery is determined to a large degree by the retention time inside the filter during which water undergoes physical and biological treatment by a series of processes, including size exclusion, adsorption, and bacterial breakdown (Huisman and Wood 1974; Ray et al. 2002; Missimer et al. 2013). The grain size and thickness of the uppermost layer and adequate retention time will collectively produce pretreatment. For example, the Fukuoka Desalination Plant

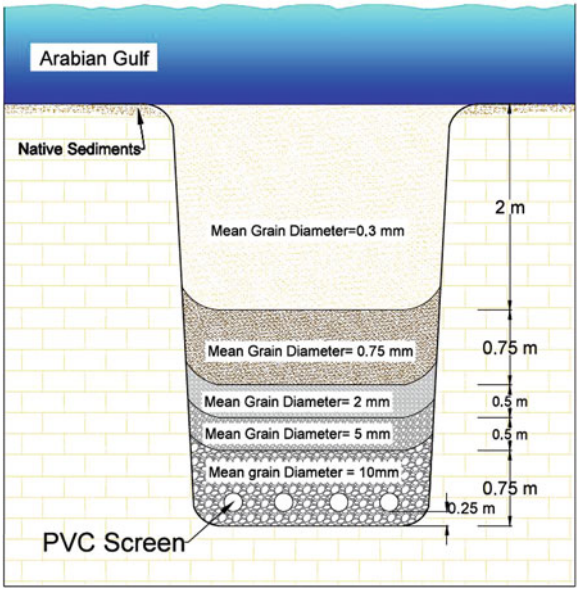

Fig. 12.8 Preliminary design of a seabed gallery for Ras Abu Ali Island, Arabian Gulf, Saudi Arabia (from Rachman et al. 2014)

utilizes seabed filtration with a 7 h retention duration, resulting in very high raw water quality with low silt density index, turbidity, and organic compound concentrations (Shimokawa 2012).

A preliminary design for the Ras Abu Ali Island seabed gallery system contains a 4.5 m gallery bed total thickness with the upper layer being 2 m thick (Fig. 12.8). The filter media design herein produces a retention time of 6 h, which was suggested by Rachman et al. (2014) because of the difficulty in treating Arabian Gulf seawater by SWRO. The retention time was estimated by considering the water passage through the upper 2 m active layer of the filter.

Design of the internal structure of the filter media was based on the average mean grain size of the natural bottom sediment. The composition of the unlithified sediment is a mix of skeletal carbonate sand and quartz sand with some coated grains. The mean grain diameter was about 0.3 mm, so the grain size of the media used for the top 2 m filter layer was also 0.3 mm to avoid any hydraulic intervention from clogging by smaller diameter grains. The lower layers of the filter are not very significant in treatment of the water, but have importance in supporting the filter and transitioning between the infiltration at the top and the extraction at the base. Design of the lower layers, including thickness and mean grain diameter, were based on the methodology described by Barrett et al. (1991). Care was taken to avoid top-down infiltration of finer sand into lower layers that would disturb uniform flow through the media (Barrett et al. 1991; Lujan and Missimer 2014). Therefore, the preliminary design contains 5 layers each with specific mean grain size and thickness. The head loss for passage of seawater through the media was estimated to be slightly less than 1 m based on the estimated hydraulic conductively of the layers and the design

infiltration rate. The hydraulic conductivity of the layers was estimated based on the proposed grain size distribution using the spreadsheet program developed by Rosas et al. (2014). A second program was developed to include the water density and the infiltration rate to further refine the head loss through the filter.

Another important design aspect is the lowermost layer of the filter where recovery of the filtered water is captured by an underdrain system. Detailed design issues involved in achieving flow balance at the infiltration interface as controlled by the design of the underdrain system is covered in Chap. 11. The base layer in this case contains large mean grain diameter gravel with a corresponding high hydraulic conductivity (up to 100 m/day). The gravel has a mean grain diameter of 10 mm media, which will allow constant intake pumping via the PVC screen underdrains. A design summary of the gallery cells is contained in Table 12.2.

Operation of a seabed gallery is assumed to be long with possible periodic scrapping of the upper sediment surface to maintain the hydraulic conductivity of the media to mitigate clogging or cementation with calcium carbonate in the Arabian Sea environment. However, the seabed filter in Fukuoka Japan has been operated for 8 years without the need for upper layer refreshing (Shimokawa 2012). The self-cleaning process is likely associated with the sediment stirring effect from the wave activity and ocean currents, and bioturbation caused by sediment-ingesting benthic organisms that degrade and bind fine particles and organics as fecal pellets. These hard pellets have no detrimental effect on the hydraulic conductivity of the sediments because they act hydraulically like sand grains (Sesler and Missimer 2012).

The most reliable design configuration for a large capacity seabed gallery is to divide the capacity into a series of gallery cells, each equipped with one pump. Such a design approach was chosen by Rachman et al. (2014) for the Ras Abu Ali Island site. The preliminary design contains a series of cells with design capacities that are coordinated with a SWRO facility design or to meet the need of the marine fish hatchery proposed. The cell capacities are designed based on the larger requirements of a SWRO plant. One or two cells could be used to meet the lower fish hatchery requirements. The overall SWRO facility design capacity

Table 12.2 Gallery cell specifications

Parameter	Specification
Filtration rate	8 m/day
Media diameter	0.3 mm
Bed depth	2 m upper layer, total bed 4.5 m
Run length	Unlimited
Pretreatment	None required
Dominant filtration mechanism	Straining, biological activity
Regeneration method	Mechanical scrapping of upper layer or none
Maximum water turbidity	None
Hydraulic retention time	6 h

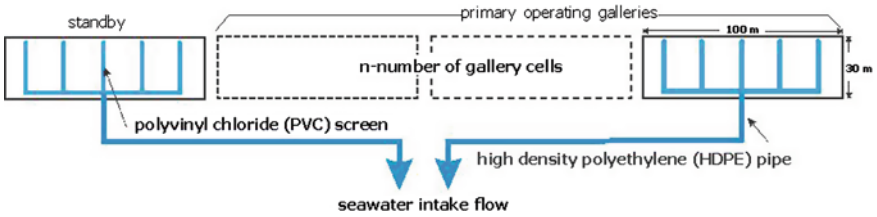

Fig. 12.9 Schematic showing a general configuration of multi-cell seabed gallery intake system (modified from Rachman et al. 2014)

considered is 54,000 m^3/day of permeate. At a 45 % recovery rate, this would require 120,000 m^3/day of raw seawater. Each cell was designed to provide 24,000 m^3/day of filtered seawater with conservative 8 m/day infiltration rate provided by pump suction. Consequently, the required surface area is 3000 m^2, which designed to form 100 m × 30 m rectangular cell areas with the 100 m axis running parallel to the shoreline, thereby minimizing construction distance from the low tidal point. There are a large number of possible cell configurations and the choice in a final design would be based on the most cost-effective solution (Fig. 12.9).

12.6 Discussion

12.6.1 Unique Features of the Arabian Gulf and Subsurface Intake Feasibility

The Arabian Gulf has some rather unique features that provide challenges for intake design and limitations on what types of subsurface gallery intake systems that can be used. Salinity of the seawater is affected by circulation on a large-scale basis, involving the entire Arabian Gulf, and on a smaller scale basis driven by high rates of evaporation from the very shallow nearshore water. The slope of the offshore bottom is quite low. Therefore, access to deep water of a higher quality is quite difficult because it is located many kilometers from the beach. Another significant issue is the common occurrence of coastal environments that contain hypersaline water. Sabhkas and other supratidal or intertidal bodies are shallow evaporation basins which cause high salinity water to migrate seaward or occur at a location at which any type of induced hydraulic gradient would move the hypersaline water toward the pumping center. The high evaporation rates and natural high salinities of the nearshore waters also create high alkalinity within the seawater that promotes marine cementation of unlithified bottom sediment and reduces the hydraulic conductivity of the uppermost layer (Shinn 1969).

These features preclude the use of any vertical well type along a large part of Arabian Gulf coast of Saudi Arabia. Well intakes require a constant recharge rate which is limited by the normal tide range and the seaward position of the seasonal low tide which can be over 500 m seaward from the shoreline. A second issue is the common occurrence of hypersaline water directly beneath the beach area, inland from the beach, and possibly seaward of the beach to an unknown distance. All vertical wells produce a cone of depression that induces radial flow which would cause the high salinity water to enter the well along with normal salinity seawater. Also, the seawater salinity near the beach will likely contain higher salinity than the offshore seawater due to the very high evaporation rate and lack of adequate circulation within the shallow water.

Use of horizontal well technology is also questionable based on the very long distance required to construct the wells. The well screens would likely have to begin at a distance of over 500 m from the beach to assure that the marine bottom is always covered with seawater to maintain continuous recharge. Therefore, the length of the required horizontal systems would be very difficult and expensive to meet the required feed water capacity for large SWRO facilities. Another issue that must be considered is the potential for calcium carbonate precipitation within the horizontal well system. In conventional shallow wells, it is relatively easy to clean the scale using an acid treatment. However, the cleaning of a horizontal well system would be quite difficult, especially at the distal end of a screen located more than 500 m from the wellhead. Also, the hardground layers have a moderate to low permeability and contain higher permeability unlithified sand between cemented layers. It would be difficult to design and construct a horizontal well system that can produce predominantly from a high permeability zone within the shallow sequence.

The only possible well solution would be to construct an artificial peninsula into the Arabian Gulf and drill a series of vertical production wells to obtain the necessary raw water supply. This would be a similar system to that located at the South Corniche site in Jeddah (see Chap. 10). This type of system could potentially yield between 10,000 and 100,000 m^3/d. The capacity would depend on a series of factors, including the seaward extent of the fill area, the number of wells constructed, and the yield of the individual wells. Additional capacity could be developed using a larger number of filled peninsulas.

A more flexible intake type for the conditions observed within the Arabian Gulf is some type of gallery intake system, either a beach or seabed design. Beach galleries would not likely be a widespread design solution because of limited area along the coast where suitable conditions are present based on normal design criteria as defined in Maliva and Missimer (2010). Some areas of the Arabian Gulf of Saudi Arabia do contain sandy beaches at which a beach gallery system could be feasible. Overall, the most likely subsurface intake system that is compatible with the geology of the Arabian Gulf is a seabed gallery system.

12.6.2 Compatibility of the Seabed Gallery with the Coastal Geology and Sediment Deposition in Relationship to Siting

It appears based on the geological literature that a significant part of the Arabian Gulf nearshore area of Saudi Arabia has high potential for development of seabed gallery intake systems. A large part of the area is covered by a marine hardground with a veneer of unlithified sediment lying on top of it. The seaward extent of the hardground has not been mapped, but at some sites the unlithified sediment component is more widespread and thicker. Production of carbonate sand offshore is not likely very fast, so there is a low potential for a seabed gallery to become buried with large quantities of carbonate sediment. Some areas of the coast do contain siliciclastic sand dunes that migrate to the shoreline and supply the offshore environment with sand due to the predominant offshore trending winds. Care would have to be taken in these dune areas to locate a seabed gallery a sufficient distance offshore to avoid being buried by aeolian sands.

Active areas of mud deposition occur within the restricted part of the Arabian Gulf located between Qatar and Saudi Arabia. Detailed oceanographic work in this area may be required before a seabed galley system could be deemed to be feasible. Significant sedimentation episodes allowing carbonate mud to accumulate on the bottom atop a gallery could rapidly clog the filter top. The deployment of offshore sediment collection pans and general sediment studies would needed in areas where the bottom contains muddy sediments.

12.6.3 Impacts of Marine Cementation on Gallery Placement and Design

Marine hardgrounds cover vast parts of the shallow nearshore of the Arabian Gulf (Shinn 1969). These areas are undergoing modern cementation with marine carbonate cements (aragonite and high-magnesium calcium carbonate). Some of the most active areas undergoing diagenesis are the beaches and intertidal zones where recent bottles and cans have been observed cemented into the limestone formed near the shoreline (Shinn 1969). A key design issue related to development of seabed gallery intake systems is to assess the position offshore where active cementation is either not occurring or is occurring at rates much lower than those in the intertidal areas. Typically, cementation occurs near the top of the sediment in offshore areas where active diagenesis is occurring with the most rapid rates occurring in the intertidal zones.

Since seabed gallery systems will move considerable volumes of seawater through the sediments, the calcium carbonate geochemistry of the water column

would need to be assessed at all times of the year. Slow cementation of the upper few centimeters of a gallery could be handled within the context of routine maintenance with the simple removal of the sediment or rock by mechanical or physical means. Robotic equipment has been designed to remove bottom hard precipitants from rapid infiltration ponds in the Orange County Replenishment District and such equipment could be used to control such a problem in the Arabian Gulf. The issue is the rate of rock formation, the degree to which formation lowers the vertical hydraulic conductivity (and thus infiltration rates) and the frequency of maintenance required.

12.6.4 Potential Salinity Issues in Design of Seabed Galleries

Very high evaporation rates in the shallow nearshore water of the Arabian Gulf could be a significant design factor in placement of a seabed gallery intake system. It is likely that a seabed gallery system would have to be sited at a location where some significant circulation of the water column occurs to disperse a higher salinity bottom layer. Along the southern shoreline of the Arabian Gulf, there is a seaward-directed density circulation with fresher seawater moving landward at the sea surface. Wind turbulence tends to mix the water as depth increases, so a balance must be achieved concerning the location of the gallery wherein "normal" seawater salinity occurs, which may be in the range of 38,000–45,000 mg/L. The area of the restricted circulation located between Qatar and the coastline of Saudi Arabia may tend to have high salinity compared to other areas of the Arabian Gulf and could affect the suitability for use as any intake for SWRO.

12.6.5 Capacity Limitations

A seabed gallery intake in the Arabian Gulf has no capacity limitation based on the existing geologic and water quality conditions. Using a modular design in coordination with the design of a SWRO facility, any number of cells could be developed to support a variety of intake capacities. Each cell could be equipped with a pump to give a system added operational reliability or more than one cell could be manifolded to one pump to reduce the number of pumps.

12.6.6 Pretreatment Economics

Successful operation of a seabed gallery intake in the Arabian Gulf will be based on the degree of organic matter removal and the savings in operating cost associated with the lesser degree of pretreatment required. Missimer et al. (2013) suggest that the complex pretreatment process train constitutes between 4 and 35 % of the

overall operating costs of a SWRO facility. The added capital cost associated with the design and construction of a seabed gallery system intake could be offset to a full degree if several pretreatment processes can be eliminated and the degree of membrane cleaning reduced. A thorough life-cycle analysis should be conducted to ascertain the overall cost reduction that would be experienced by using a seabed gallery intake. This would also assist in establishing the maximum capital cost that could be expended for the gallery intake versus a conventional open-ocean intake.

12.6.7 Research Needs for the Future

While considerable research has been conducted on the coastline of the Arabian Gulf in the United Arab Emirates, Qatar, Kuwait, and Bahrain, little research has been conducted on the Saudi Arabian coastline. Detailed mapping of the shoreline and nearshore areas needs to be conducted to ascertain the geological feasibility of using various subsurface intake systems. A recent investigation of the Red Sea coastline of Saudi Arabia has provided a planning level assessment of subsurface intake usage (Dehwah et al. 2014). This type of investigation along with some sediment data from the offshore environment would allow the use of subsurface intake options into new tender offers to construct and operate large SWRO facilities by reducing the tender risk.

Characterization of the organic chemistry of the Arabian Gulf needs to be accomplished to ascertain the not to optimum retention time for design of seabed gallery systems. This will require seasonal collection and analysis of water samples and analyses of algae, bacteria, TOC, NOM fractions, and TEP within the water column. Laboratory column experiments and local testing of one or more pilot systems should also be conducted to assess the effects of the media on rates of organic compound removal and degradation.

A life-cycle cost analysis should be conducted to provide guidance on the economic feasibility of seabed gallery intake systems for use in the Arabian Gulf. A series of scenarios could be developed to test the viability of replacing various pretreatment processes with consummate reduction in energy and chemical usage.

12.7 Conclusions

An analysis of the feasibility of using a subsurface intake system for SWRO facilities in the Arabian Gulf coastal region of Saudi Arabia shows that the most feasible method appears to be a seabed gallery system. Severe limitations occur, based on geologic and water quality conditions at the coastline, on use of all well intake systems. The only possible well intake type usable would be a multi-well system constructed on an artificial fill peninsula constructed into the sea. This design would also have some limitations.

The long-term difficulties in operating SWRO facilities using Arabian Gulf seawater suggests that using a type of subsurface intake system would provide a viable alternative to conventional open-ocean intake systems or a canal intake system. The reduction in algae, bacteria, TOC, NOM fraction, and TEP concentrations obtained using a gallery intake system suggest that such a system should be economically feasibility. An impediment to the implementation of seabed galleries is the limited documented operational history of such systems. Because of the very great costs of SWRO desalination of Arabian Gulf seawater, and operational advantages and cost savings of seabed galleries, a test system should be installed in the region as soon as practically possible. The system should be developed near one of the large capacity facilities with the intake water transported to a number of operating SWRO skids to conduct side-by-side testing.

References

Al-Mashharawi, S., Dehwah, A. H. A., Bandar, K. B., & Missimer, T. M. (2014). *Feasibility of using a subsurface intake for SWRO facility south of Jeddah*. Saudi Arabia: Desalination and Water Treatment. doi:10.1080/19443994.2014.939870.

Alsharhan, A. S., & Kendall, C. G. S. C. (2003). Holocene coastal carbonates and evaporites of the southern Arabian Gulf and their ancient analogues. *Earth-Science Reviews, 61*, 191–243.

American Society for Testing and Materials (ASTM). (2006). *Standard test method for permeability of granular soils, Standard D2434-682006* (p. 5). West Conshohocken, PA: ASTM.

Applegate, L. E., Erkenbrecher, C. W., & Winters, H. (1989). New chloramines process to control aftergrowth and biofouling in permasep B-10 RO surface seawater plants. *Desalination, 74*, 51–67.

Awerbuch, A. (2007). Hybrid systems and technology, Chapter 20. In M. Wilf (Ed.), *The guidebook to membrane desalination technology* (pp. 395–454). L'Aquila, Italy: Balaban Desalination Publications.

Barrett, J. M., Bryck, J., Collins, M. R., Janonis, B. A., Logsdon, G. S., et al. (1991). *Manual of design for slow sand filtration*. Denver, Colorado: AWWA Research Foundation, American Water Works Association.

Bar-Zeev, E., Berman-Frank, I., Liberman, B., Rahav, E., Passow, U., & Berman, T. (2009). Transparent exopolymer particles: Potential agents for organic fouling and biofilm formation in desalination and water treatment plants. *Desalination and Water Treatment, 3*, 136–142.

Berktay, A. (2011). Environmental approach and influence of red tide to desalination process in the Middle East region. *International Journal of Chemical Environmental Engineering, 2*(3), 183–188.

Berman, T. (2010). Biofouling: TEP-a major challenge for water separation. *Filtration and Separation, 47*(2), 20–22.

Berman, T., Mizrahi, R., & Dosoretz, C. G. (2011). Transparent exopolymer particles (TEP): A critical factor in aquatic biofilm initiation and fouling on filtration membranes. *Desalination, 276*, 184–190.

Berman, T., & Passow, U. (2007). Transparent exopolymer particles (TEP): An overlooked factor in the process of biofilm formation in aquatic environments. *Nature Precedings,*. doi:10.1038/npre.2007.1182.1.

Dehwah, A. H. A., Al-Mashhawari, S., & Missimer, T. M. (2014). Mapping to assess feasibility of using subsurface intakes for SWRO, Red Sea coast of Saudi Arabia. *Desalination and Water Treatment, 52*, 2351–2361. doi:10.1080/19443994.2013.862035.

El Aleem, A., Al-Sugair, K. A. A., & Alamand, M. I. (1998). Biofouling in membrane processes for water desalination and reuse in Saudi Arabia. *International Biodeterioration and Biodegradation, 41*, 19–31.

Emery, K. O. (1956). Sediment and water of the Persian Gulf. *American Association of Petroleum Geologists Bulletin, 40*, 2354–2383.

Fryberger, S. G., Al-Sari, A. M., & Clisham, T. J. (1983). Eolian dune, interdune, sand sheet, and siliciclastic sabkha sediments of an offshore prograding sand sea, Dhahran area, Saudi Arabia. *American Association of Petroleum Geologists Bulletin, 67*(2), 280–312.

Ghaffour, N., Missimer, T. M., & Amy, G. (2013). Technical review and evaluation of the economics of desalination: Current and future challenges for better supply sustainability. *Desalination, 309*, 197–207.

Hassan, A. M., Al-Jarrah, S., Al-Lohibi, T., Al-Mamdan, A., & Bakheet, L. M. (1989). Performance evaluation of SWCC SWRO plants. *Desalination, 74*, 37–50.

Huisman, L., & Wood, W. E. (1974). *Slow sand filtration*. Switzerland, Geneva: World Health Organization, Geneva.

Kampf, J., & Sadrinasab, M. (2006). The circulation of the Persian Gulf: A numerical study. *Ocean Science, 2*, 27–41.

Lattamann, S., & Hoepner, T. (2008). Environmental impact and impact assessment of seawater desalination. Desalination, *220*(1-3), 1–15.

Lujan, L. R., Missimer, T. M. (2014). Technical feasibility of a seabed gallery system for SWRO facilities at Shoaiba, Saudi Arabia and regions with similar geology. *Desalination and Water Treatment*. doi:10.1080/19443994.2014.909630.

Maliva, R. G., & Missimer, T. M. (2010). Self-cleaning beach gallery design for seawater desalination plants. *Desalination and Water Treatment, 13*(1–3), 88–95.

Mantilla, D., Missimer, T. M. (2014). Seabed gallery intake technical feasibility for SWRO facilities at Shuqaiq, Saudi Arabia and other global locations with similar coastal characteristics. *Journal of Applied Water Engineering and Research*. 10.1080/2349676.2014.895686.

Matin, A., Khan, Z., Zaidi, S. M. J., & Boyce, M. C. (2011). Biofouling in reverse osmosis membranes for seawater desalination: Phenomena and prevention. *Desalination, 281*, 1–16.

Missimer, T. M. (2009). *Water supply development, aquifer storage, and concentrate disposal for membrane water treatment facilities* (2nd ed.). Sugar Land, Texas: Schlumberger Water Services.

Missimer, T. M., Ghaffour, N., Dehwah, A. H. A., Rachman, R., Maliva, R. G., & Amy, G. (2013). Subsurface intakes for seawater reverse osmosis facilities: Capacity limitation, water quality improvement, and economics. *Desalination, 322*, 37–51. doi:10.1016/j.desal.2013.04.021.

Nguyen, T., Roddick, F. A., & Fan, L. (2012). Biofouling of water treatment membranes: A review of the underlying causes, monitoring techniques and control measures. *Membranes, 2*, 804–840.

Pettijohn, F. J., Potter, P. E., & Siever, R. (1987). *Sand and sandstone*. New York: Springer.

Purser, B. H. (Ed.). (1973). *The Persian Gulf: Holocene carbonate sedimentation and diagenesis in a shallow epicontinental sea*. New York: Springer.

Purser, B. H., & Seibold, E. (1973). The principal environmental factors influencing Holocene sedimentation and diagenesis in the Persian Gulf. In B. A. Purser (Ed.), *The Persian Gulf: Holocene carbonate sedimentation and diagenesis in a shallow epicontinental sea* (pp. 1–10). New York: Springer.

Rachman, R., Al-Mashharawi, S., & Missimer, T. M. (2014). Technical feasibility of a seabed gallery seawater intake at Ras Abu Ali Island, Arabian Gulf, Saudi Arabia. *Desalination and Water Treatment*. doi:10.1080/19443994.2014.940221.

Ray, C., Melin, G. R. B., & Linsky, R. B. (Eds.). (2002). *Riverbank filtration: Improving source water quality*. Dordrecht, Netherlands: Klumer Academic Publishers.

Rosas, J., Lopez, O., Missimer, T. M., Coulibaly, K., Dehwah, A. H. E., Sesler, K., et al. (2014). Determination of hydraulic conductivity from grain size distribution for different depositional environments. *Groundwater, 52*(3), 399–413.

Sesler, K., & Missimer, T. M. (2012). Technical feasibility of using seabed galleries for seawater RO intakes and pretreatment: Om Al Misk Island, Red Sea, Saudi Arabia. *IDA Journal: Desalination and Water Reuse, 4*(4), 42–48.

Shimokawa, A. (2012). Fukuoka District desalination system with some unique methods. In *International Desalination Intakes and Outfalls Workshop Proceedings*, *National Centre of Excellence in Desalination Adelaide, South Australia*, (May 16–17).

Shinn, E. A. (1969). Submarine lithification of Holocene carbonate sediments in the Persian Gulf. *Sedimentology, 12*, 109–144.

Swift, S. A., Bower, A. S. (2003). Formation and circulation of dense water in the Persian/Arabian Gulf. *Journal of Geophysical Research 108*(C1) 3005, 4–15.

Tanner, W. F., Balsillie, J. H. (1995). *Environmental clastic granulometry* (Vol. 40, 142 p). Tallahassee: Florida Geological Survey Special Publication.

Wagner, C. W., & van der Togt, C. (1973). Holocene sediment types and their distribution in the southern Arabian Gulf. In B. A. Purser (Ed.), *The Persian Gulf: Holocene carbonate sedimentation and diagenesis in a shallow epicontinental sea* (pp. 123–156). New York: Springer.

Wenzel, L. K. (1942). *Methods for determining permeability of water-bearing materials with special reference to discharging-well methods* (192 p). U. S. Geological Survey Water-Supply Paper 887.

Winters, H. (1994). Biofouling status of the Saline Water Conversion Corporation (SWCC) reverse osmosis (RO) plants in the Kingdom of Saudi Arabia, Unpublished consultant's report to SWCC, 23 pp.

Winters, H. (1997). Twenty years experience in seawater reverse osmosis and how chemicals in pretreatment affect fouling of membranes. *Desalination, 110*, 93–95.

Winters, H., & Isquith, L. (1995). A critical evaluation of pretreatment to control fouling in open seawater reverse osmosis—has it been a success? In *Proceedings of the International Desalination Association World Congress on Desalination and Water Reuse, Abu Dhabi, UAE* (Vol. 1, pp. 255–264), November 18–24, 1995.

Yao, F. (2008). *Water mass formation and circulation in the Persian Gulf and water exchange with the Indian Ocean*. Open-Access Dissertations Paper 183, Coral Gables, Florida, University of Miami (RSMAS).

Chapter 13
Slant Well Intake Systems: Design and Construction

Dennis E. Williams

Abstract In a recent amendment to the Water Quality Control Plan for Ocean Waters of California (Ocean Plan), the California State Water Resources Control Board staff recommended that subsurface intakes are the preferred technology for seawater intakes. A number of desalination projects in the planning and feasibility stage along the Coast of California are considering subsurface intakes for feed water supply. Some of these projects have product water requirements >190,000 m^3/day, with feed water requirements exceeding 380,000 m^3/day. Angled or slant wells, withdraw water from permeable deposits beneath the ocean floor and receive a high percentage of recharge from both vertical leakage (through the seabed) as well as horizontally in the subsea aquifers. Environmental advantages include no impacts to fish or marine life and minimal impacts to onshore water resources. Aquifers beneath the ocean also provide natural filtration from suspended organic matter and sediment, particularly during storm surges and heavy precipitation reducing or eliminating the need for pretreatment. Slant wells are drilled using the dual-rotary method of drilling in an angled cradle and have angles below horizontal typically ranging from a few degrees to a few tens of degrees. A telescoping design allows construction of angled wells up to 305 m completed with an artificial filter pack typically yielding 10,000–16,000 m^3/day. A slant well layout can be comprised of one well or a group of wells at a single wellhead location (i.e. pod). Multiple pods of slant well arrays are constructed until the cumulative total discharge rate meets the feed water supply demand. For slant wells, there is no theoretical limit on the maximum number of wells or the reliability of the source of supply (i.e. ocean). The only limitation is the permeability of the nearshore and offshore aquifers and areal and vertical extent of these deposits. Interference between wells and well pods governs the number and spacing of wells and geologic and coastline land

D.E. Williams (✉)
Geoscience Support Services, Inc., Claremont, CA, USA
e-mail: dwilliams@geoscience-water.com

T.M. Missimer et al. (eds.), *Intakes and Outfalls for Seawater Reverse-Osmosis Desalination Facilities*, Environmental Science and Engineering,
DOI 10.1007/978-3-319-13203-7_13

availability governs the limitation on spatial and vertical extent of the well fields. Limitations may also occur due to potential or unforeseen impacts to near shore and onshore habitat and water resources. Slant well angles can vary depending on site conditions to allow targeting specific aquifer thicknesses. Shallow angled slant wells also have higher discharge rates than vertical wells for the same formation loss drawdown and geohydrologic conditions. Water level distributions around a single or multiple pumping slant wells can be easily calculated from a discrete number of point sinks placed within the vertical projection of the well screen and utilizing the principle of superposition. Variable density groundwater flow and solute transport models calibrated to site specific historical water levels and geochemical data provide a reliable predictive tool for planning and operation of subsurface slant well feed water supplies.

13.1 Introduction

Water purveyors in coastal areas are more and more considering seawater desalination as a reliable source of water for municipal supply. This is accelerated by a lack of dependability on imported supplies and limited amounts of inland ground water or poor water quality. As such, seawater desalination is a workable alternative in many areas which has been made even more attractive through cost effective subsurface intake systems and water treatment technologies. Emerging technologies in feed water supply for SWRO include subsurface intakes as recently recognized in a draft amendment to the Water Quality Control Plan for Ocean Waters of California (SWRCB 2013). In that amendment, subsurface intakes were recommended as the preferred technology for seawater intakes. A number of desalination projects in the planning and feasibility stage along the coast of California are considering subsurface intakes for feed water supply. Some of these projects have product water requirements >190,000 m^3/day with feed water requirements exceeding 380,000 m^3/day.

A desalination intake using low angled wells (also called slant wells); produces groundwater from offshore aquifers located below the seabed and provides a number of important advantages over other subsurface and open-ocean intake systems (Fig. 13.1). These advantages include reduction or elimination of costly seawater reverse osmosis (SWRO) pretreatment processes and minimal environmental impacts. Drawing seawater from subsea and nearshore aquifers provides natural filtration from suspended organic matter and sediment particularly during storm surges and heavy precipitation. Field tests show the engineered artificial filter pack surrounding the screened portion of the intake wells results in low turbidity and silt density index (SDI) (Williams 2008, 2011, 2014).

A slant well SWRO feed water supply typically consists of shallow angled wells in a beach or near-coastal environment. The supply may consist of a single slant well, an array of wells or multiple arrays of wells extending beneath the ocean.

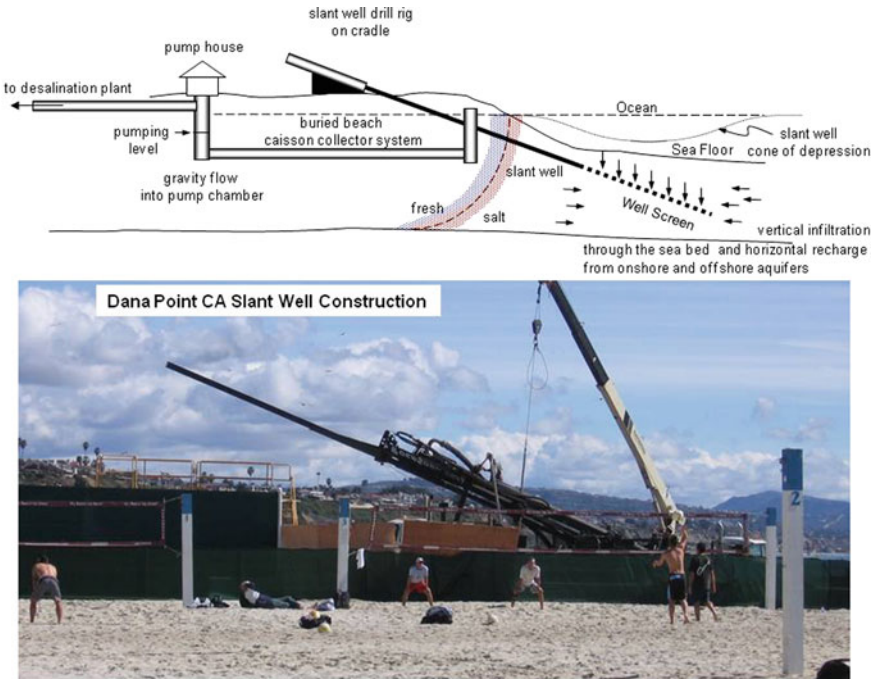

Fig. 13.1 Slant well feed water intake beneath the ocean floor—Dana Point California

Environmentally sensitive, slant well systems are buried systems completed below the land surface eliminating undesirable aesthetic impacts (i.e. no visual impacts on the surface). Tried and true well design and construction methods including an engineered artificial filter pack are employed in construction. Where offshore or near shore aquifer systems contain permeable alluvium, slant well intakes are viable alternatives to provide SWRO feed water supply. Slant wells are merely vertical wells drilled on an angle and produce water from subsea aquifers recharged from both horizontal and vertical flow (i.e. leakage through the sea floor). The same design criteria apply to slant wells and vertical wells alike (e.g. engineered filter packs and well casing and screen design). However, slant wells beneath the ocean pose more construction challenges than vertical wells due to borehole caving and shallow construction angles which reduces gravitational forces. Typically, slant wells are constructed at angles below horizontal ranging from a few degrees to a few tens of degrees. Drilling and completion challenges of shallow angled wells have been overcome using the dual-rotary method of construction which includes using temporary casing to maintain borehole integrity during well completion. A telescoping well design allows slant wells to extend to lineal lengths of 305 m or more into subsea aquifer systems and typically yielding 10,000–16,000 m^3/day. For slant wells, there is no theoretical limit on the maximum number of wells or the

reliability of the source of supply (i.e. ocean). The only limitation is the hydraulic conductivity of the nearshore and offshore aquifers, areal and vertical extent of these deposits, and siting, permitting and environmental factors.

13.2 Advantages of Using Slant Wells for Desalination Feed Water Supply

Slant well intakes have a number of advantages over other well intakes. Slant wells can be completed in relatively thin aquifers with potentially better production compared to some other types of wells. Ranney-type collector wells have lateral lengths typically limited to approximately 46 m or less. They also may draw a high percentage of recharge from inland supplies and require construction of a large diameter caisson which is visually offensive in a beach environment. Horizontal directional drilled wells (HDDW) could potentially be used for subsurface supply however; the main disadvantage is the inability to place an engineered artificial filter pack around the well screen which may result in clogging and limited well production in fine-grained alluvial formations. In addition to no impacts to ocean marine life, another important advantage of subsea slant wells is minimal impact to inland riparian habitat and inland water resources. Slant wells are completely buried, beneath the land and sea floor, receiving their recharge primarily through vertical leakage through the sea bed and horizontal recharge from offshore aquifers. Specifically, slant wells eliminate entrainment and impingement to marine life; can reduce or eliminate costly reverse osmosis pretreatment, do not have any ocean construction impacts, and do not have any permanent visual impacts.

13.3 Geohydrologic Conditions Favorable for Slant Wells

The purpose of a subsurface desalination feed water supply is to provide reliability as well as a supply which has a low fouling potential to SWRO treatment plants. Slant wells provide this when completed in subsea aquifers having high permeability, areal extent, and sufficient thickness and in hydraulic continuity with the ocean. Slant wells induce vertical recharge through the sea floor due to the hydraulic head difference between the slant well pumping level and the level of the ocean.

Good examples of permeable offshore aquifers can be seen in alluvial deposits which have resulted from aggradation or building up of the land surface or streambed through natural deposition of coarse-grained material (Fig. 13.2). The extent and thickness of these deposits vary widely and are a function of a number of geologic and hydrologic factors. Favorable subsurface aquifers may also consist of consolidated rocks (e.g. igneous, sedimentary or metamorphic) where these rocks contain sufficient secondary porosity features (joints and fissures) in hydraulic continuity with the ocean floor. However, production and filtration is generally not as efficient as alluvial systems.

Fig. 13.2 Offshore alluvial deposits

The quality and sustainability of a subsurface feed water supply is dependent upon:

- Hydraulic continuity with ocean sources—vertical leakage through the sea floor
- Horizontal recharge from offshore aquifers which are extensive or outcrop on the sea floor.
- Horizontal recharge from near shore aquifers
- Horizontal recharge from inland aquifers

Favorable conditions for permeable offshore deposits can be usually found near the mouths of rivers or streams. Coastal areas which have well developed alluvial plains or fans created by aggradation from nearby mountains generally extend beneath the ocean surface and offer good potential for subsurface intakes.

13.3.1 Unconsolidated Materials

The most favorable conditions for a subsurface feed water supply are those where permeable alluvial deposits extend offshore (typically near the mouths of streams and rivers-see (Figs. 13.2, 13.3 and 13.4). Where these deposits exist below the ocean floor and have sufficient thickness and permeability, reliable subsurface feed water supplies can be developed using slant wells. In addition, slant wells by virtue of their longer screened intervals, have higher well efficiencies and result in greater yields than vertical wells. With proper well design including engineered filter packs, fine-grained aquifers can be stabilized. Slant wells relying on a natural filter pack rarely

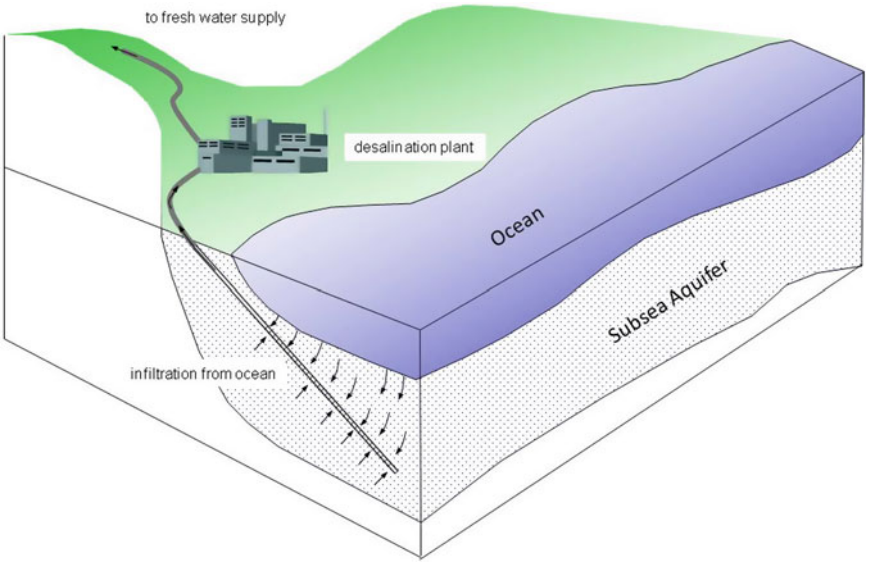

Fig. 13.3 Slant well completed in subsea alluvial aquifer

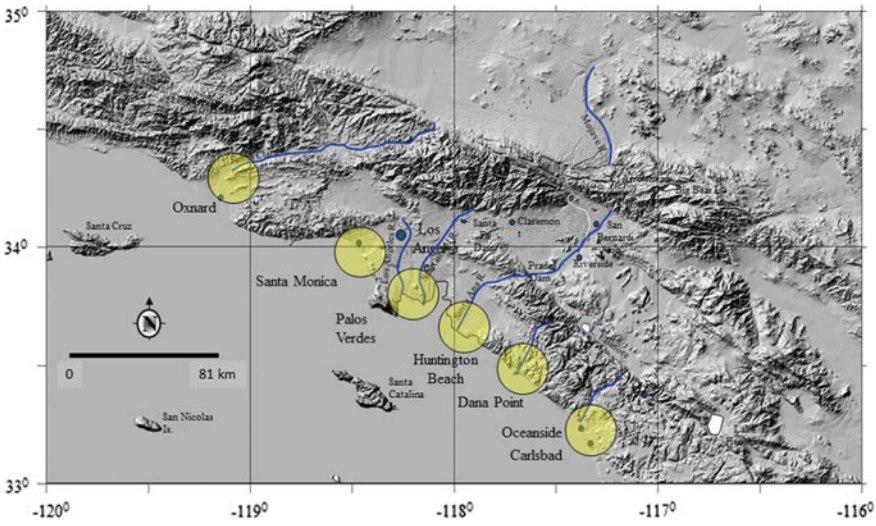

Fig. 13.4 Rivers discharging to the Pacific Ocean off the Coast of California are favorable geohydrologic conditions for slant well feed water supply wells

work in subsea strata due the inability to stabilize fine-grained sands and silts. Similarly, experience has shown that wells with a cemented type "pre-pack" screen design or a fixed filtering system (e.g. screens with very small slot openings), tend to clog due to the abundance of fine-grained particles and the inability to properly

develop (and redevelop) these types of wells. Slant wells tapping subsea alluvial aquifers can provide a high yielding and long-lasting sustainable water supply when designed, constructed and maintained properly. The unconsolidated nature of the subsea aquifer results in a natural filtration of the ocean water whether it is from vertical leakage through the sea floor (i.e. vertical leakage through the benthic zone), or from horizontal recharge from offshore aquifer systems.

13.3.2 Consolidated Materials

When nearshore or subsea materials consist primarily of consolidated rock (e.g. tightly bound geologic formations composed of sandstone, limestone, granite, or other rock), ocean water is supplied to wells through secondary porosity features (joints, fissures, faults etc.). If these secondary porosity features are interconnected and in hydraulic continuity with the ocean, there may be a possibility of a subsurface supply. However, in most nearshore and offshore deposits of consolidated or hard rock materials, with the exception of karstic limestones, the interconnectivity and more importantly the low transmissivity of the rock yields small quantities of water to wells. This is true for vertical wells and is the same for angled wells. The reason for this is the nature of the fracture or jointing system forming the secondary porosity, which is generally not interconnected with the ocean to the point where sufficient flow to wells can occur. For example, along the Central Coast of California, a 183 m horizontal well was constructed in consolidated rock under the ocean. The subsea materials consisted of a mélange (a body of rock characterized by lack of continuous bedding and the inclusion of fragments of rock of all sizes, contained in a fine-grained deformed matrix). The idea was to drill shallow enough to maintain hydraulic continuity between the fracture system of the rock and the ocean. Hydraulic fracturing (breaking or cracking the rock around the well screen area using high pressure), was also used to try and develop more secondary porosity. However, due to lack of an artificial filter pack, the well rapidly clogged with sand drastically reducing the discharge rate. Initially, 8176 m^3/day was obtained which quickly fell to zero as the fractures progressively clogged with fine-grain material.

Even if a supply can be developed, the nature of the consolidated or hard rock generally may not provide the necessary filtering necessary to reduce or eliminate pretreatment in shallow settings. However, Missimer et al. (2013) cites an example of a subsurface intake in Oman with a high degree of pretreatment for wells completed in limestone.

13.4 Siting Considerations

Slant well projects usually have high visibility with a good deal of public attention. As such, siting considerations need to consider a number of factors other than just feed water production and proximity to the desalination plant. For example, along

the coast of California these factors include the normal permitting land acquisition and access factors but are also dependent upon a number of environmental and operational factors, which if not complied with, could prohibit the project altogether. For example, many of these projects are tied to a maximum percentage of slant well recharge derived from inland water supplies, which if not met, may require expensive mitigation or provision of supplemental supplies, all of which add to the cost of supplied desalination product water.

13.4.1 Permitting Concerns

In some coastal areas, obtaining permits is the number one constraint in constructing a near shore or offshore subsurface feed water supply. In addition to the normal State and local well drilling permits, the following permits were required to construct the Doheny Ocean Desalination Project Test Slant Well located near Dana Point California:

California Environmental Quality Act (CEQA)
National Environmental Policy Act (NEPA)
California Coastal Commission Coastal Development Permit
California State Lands Commission Lease
California State Parks Right of Entry Permit
San Diego Regional Water Quality Control Board
NPDES Permit No. CAG919002
United States Army Corps of Engineers Nationwide Permit Number 7
San Diego Regional Water Quality Control Board Clean Water Act §401
Orange County Health Care Agency Well Construction Permit
California Department of Fish and Game Streambed Alteration Agreement

13.4.2 Wellhead Location

The location of the slant well wellhead may vary widely from site to site due to a number of permitting, site access, environmental and operational factors. In order to maximize recharge from ocean sources as well as minimize variations in salinity and impacts to inland resources, slant wells should be located as close to the ocean as possible. This results in both vertical leakage through the sea bed as well as horizontal recharge from offshore aquifers. Other factors affecting wellhead placement may include coastal erosion, 100-year flood event, sea level rise and proximity to sensitive habitat. The location should also consider well construction footprints and access to the well drilling site and equipment staging area.

13.4.3 Access and Maintenance

In addition to regular measurements within the well itself, all wells routinely need to be redeveloped and periodic access to the wellhead area is required. If the well is sited in an environmentally sensitive area, or areas where recreation exists (e.g. on a State Beach), provision must be made to minimize disturbance during routine measurements or during rehabilitation. If the construction footprint and access to a slant well is near or on a State Beach, then nearby parking lots or other areas could possibly be used for equipment storage and staging areas.

13.4.4 Wellhead Depth Below Land Surface

Typically slant well wellheads are buried 0.9–1.5 m below ground surface in order to minimize any nuisance and still allow access to the site (Fig. 13.5). The wellhead should be located in a stable area, and be sensitive to coastal erosion, flooding and sea level rise. The exact depth of burial is site specific and dependent upon both engineering wellhead completion features and the frequency of access needed.

Fig. 13.5 Wellhead burial 1.5 m below land surface

13.4.5 Environmental Concerns

In planning the location of the slant well intake, a number of environmental and operational factors need to be considered. Environmental factors during construction and operation are primarily concerned with adverse impacts to the natural environment (e.g. sensitive ecological or environmental areas inhabited by a particular species of animal, plant, or other type of organism). In areas of sensitive vegetation, fish habitat or other wildlife, well drawdowns (i.e. ground water level changes) from pumping may restrict placement or hinder construction and maintenance. Other environmental impacts may include visual impacts of facilities during construction or after completion such as unsightly facilities on the beach or in near shore areas where recreational or other high uses occur. Environmental impacts include:

- Impacts to fish and wildlife,
- Impacts to riparian vegetation,
- Impacts to onshore water supplies—percentage of inland recharge,
- Visual Impacts of facilities (permanent and during construction).

13.4.6 Operational Concerns-Potential Project Impacts

Siting slant well feed water supplies must be sensitive to near surface and subsurface water bodies. Impacts may occur from interference of the slant well cone of depression with onshore groundwater pumping levels which may cause static groundwater levels to lower inland well pumping rates. Also, if shallow aquifers are impacted, induced leakage from surface water bodies may result in loss of water from these water bodies with potential adverse impacts to sensitive habitat. Evaluation of project impacts to nearby water bodies and groundwater resources are most commonly predicted using a groundwater flow model calibrated to site-specific data. Impacts are monitored during feed water production through a comprehensive mitigation and monitoring plan.

13.4.7 Set-Backs Due to Coastal Erosion and 100-Year Flood Event

Other Important siting factors include coastal erosion (Hapke et al. 2006; Hapke and Reid 2006, 2007), the landward extent of a 100-year flood event and sea-level rise (Gill 2011; Flick et al. 2003). One or all of these factors must be considered in designing an adequate set-back distance from the ocean (Fig. 13.6). In California, the California Coastal Act (2003) requires that new development be sited in such a way that it will not be subject to erosion or stability hazard over the course of its design life (typically 30 years for SWRO facilities).

Furthermore, there is a finding that no seawall, revetment, jetty, groin, retaining wall, or other shoreline protective structure will be needed to shelter the development

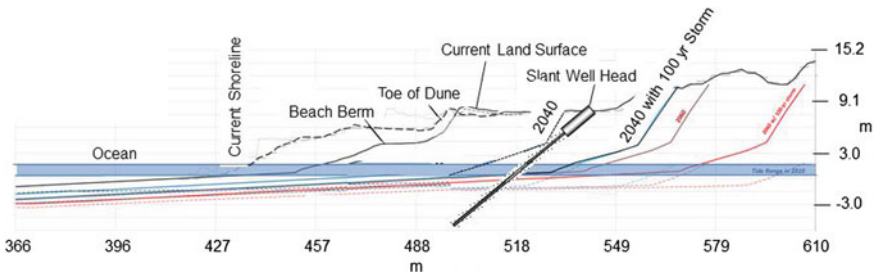

Fig. 13.6 Slant wellhead set back past 2040 coastal erosion prediction

over the course of its design. Bluff top and shoreline set-back requirements, based on coastal erosion rates, are used by Local Coastal Programs to help minimize coastal hazards. A 50-year economic lifetime set-back is required by the California Coastal Commission (2003) and is recommended by the Surfrider Foundation (2010). A coastal erosion study by the USGS and published in the Journal of Coastal Research (Hapke et al. 2009) calculated an average long-term shoreline erosion rate for the Monterey Bay area of California ranging approximately 0.6–1.8 m/year using Light Detection and Ranging (LIDAR) remotely sensed data.

13.4.8 Sea-Level Rise

Each slant well siting project should consider the risk of sea level changes to the project and environment during a 50-year life cycle (OPC 2011, 2013). Risks should include the likelihood of an impact and the consequences of that impact (NRC 2012). Climate change may result in increases in sea level as the result of global warming and associated extreme precipitation and storm events. Rising sea levels associated with global warming may contribute to an increase in the severity and duration of flooding and an acceleration of shoreline erosion. For example, in the Monterey area of California, the 30-year Monterey tide record shows a local sea level trend of approximately 12.7 cm per century (NOAA 2009). Also, the annual sea level rise between 2012 and 2073 is predicted to range from approximately 23–96.5 cm (NRC 2012). It is generally accepted that the uncertainty in these projections is large and the probability of a particular sea level rise occurring at a particular date is not known (USACE 2011).

13.4.9 Changes in Freshwater/Saltwater Interface

In accordance with the Ghyben-Herzberg principle (Todd 1980), the toe of the seawater intrusion front is stabilized under a 40:1 ratio (depth to fresh/salt interface below sea level: height of fresh water above sea level). In other words, the extent of

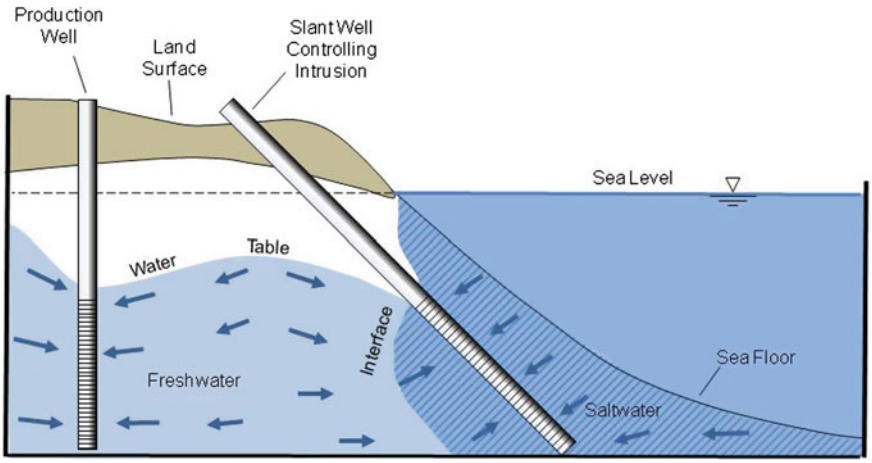

Fig. 13.7 Seawater intrusion control using slant wells

the seawater intrusion (i.e. toe of the sea water intrusion wedge) in an aquifer 61 m below sea level would be stabilized by fresh water heads 1.5 m above sea level. While the Ghyben-Herzberg relationship can be used to provide estimates, the interaction with the seaward directed flow rate alters the geometry of the interface to a significant degree. More precise solutions can be estimated based on flow interaction using methods developed by Cooper et al. (1964), Kemblowski (1987), and Todd and Mays (2005).

This relationship results in a freshwater/saltwater interface being highest at the coast and lowest inland. In reality, the interface is not a sharp line but a diffused zone where pure seawater is mixed with fresher inland waters and subject to tidal changes and onshore hydrologic cycles. Water pumped seaward of the interface is considered "new ocean water" and water pumped from the inland direction is considered to be "basin water". In reality, the water quality grades from pure sea water near the coast and offshore, to brackish water inland which eventually grades to inland ambient salinity. Where seawater intrusion exists (commonly measured by the landward extent of the 500 mg/L chloride front), slant well pumping from offshore aquifers can constitute a seawater intrusion control measure due to the interception of seawater and stabilization of the interface which otherwise would move inland causing or contributing to seawater intrusion (Fig. 13.7). However, some freshwater is also lost from the basin by using the wells to control saltwater intrusion.

13.4.10 Percentage of Ocean Water Recharge

The percentage of ocean water recharge to a slant well supply system can be calculated as the percentage of new ocean water pumped seaward of the fresh water/salt water interface. The location of the interface is found through depth specific

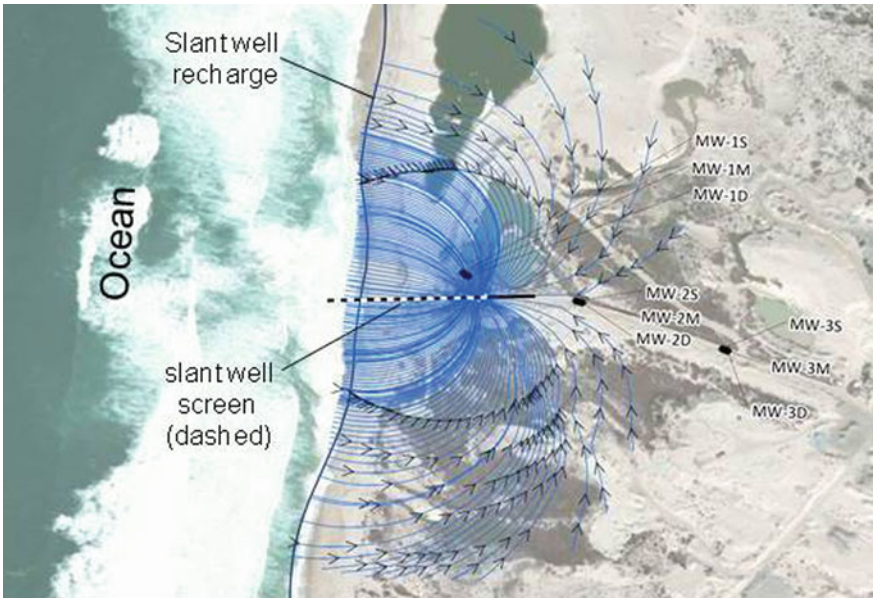

Fig. 13.8 Particle tracks to a slant well showing high percentage of recharge from ocean sources

sampling of well salinity or by measuring the extent of inland migration using the Ghyben-Herzberg principle using water level elevations and the depth to the base of the aquifer(s) in question.

Percentage of recharge from ocean sources (Charette 2012) is typically determined using a calibrated three-dimensional, solute transport groundwater model whereby model concentrations of the feed water supply are compared to ocean water concentrations. In addition, the model can calculate a water balance using a cell-by-cell budget in combination with particle tracking to determine percentage ocean water recharge (Fig. 13.8). Another key issue is the vertical leakage of the aquifer system in which the slant well lies. The leakance value or coefficient of leakage (Hantush 1964), between the shallow aquifer and the pumped zone plays an important role in determining the origin of the water, either infiltrated seawater or aquifer water moving in a horizontal direction.

13.5 Slant Well Design

Proper slant well design should maximize aquifer production, stabilize fine-grained materials and maintain as large a screen slot opening as possible (Fig. 13.9). This being said, the single most important design objective is prevention of fine-grained materials (sand and silt) from entering the well.

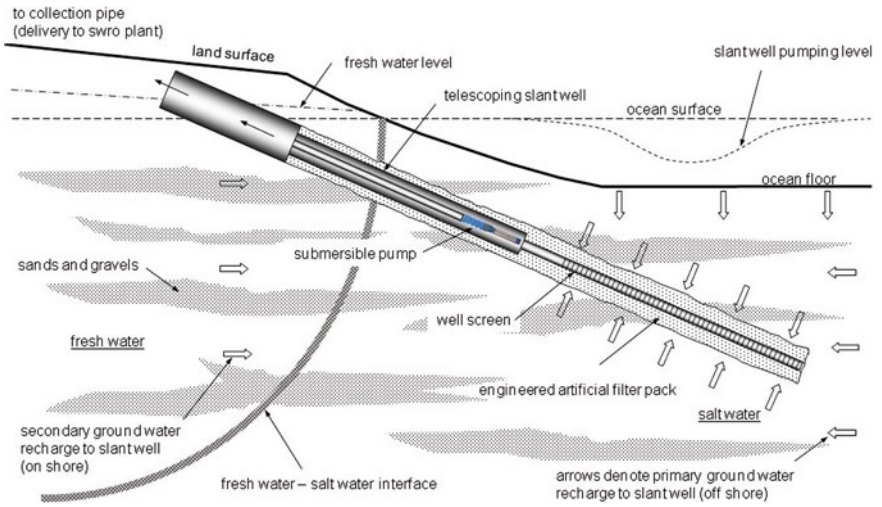

Fig. 13.9 Typical slant well design

Slant wells need to be:

- As simple as possible—but not too simple,
- Strong and long lasting,
- Provide a sustainable supply with a minimum of maintenance,
- Be completed in suitable aquifer types (i.e. productive with adequate thickness),
- Utilize proven artificial filter pack methodology,
- Incorporate proper well construction, completion, development and testing,
- Be composed of proper casing and screen materials for a sea-water environment.

13.5.1 Target Aquifers

Slant well drawdown is directly proportional to the discharge rate of the well as well as aquifer transmissivity which is the product of hydraulic conductivity and saturated aquifer thickness. Drawdown is also dependant on the vertical hydraulic conductivity and thickness of overlying sediments as this component of vertical leakage is a recharge source. Placement of well screen should maximize utilization of the aquifer transmissivity (e.g., maximize well screen placement into permeable sediments) in order to obtain the highest production possible from the subsea or nearshore aquifer system. Unless limited by environmental, operational or legal impacts, slant wells are designed to maximize overall production as well as have a high percentage of recharge from ocean water sources. As the geohydrology of the aquifer system at each location has site-specific conditions, slant well angles and lengths may vary within intake well fields.

13.5.2 Slant Well Angles and Lengths

The angle below horizontal and the length of the casing and screen are determined by the target aquifer(s), siting considerations, environmental constraints and potential operational impacts. All of these factors contribute to the geometry of the slant well. Specifically, the angle below horizontal and length of casing and screen must consider:

- Geometry of offshore (target) aquifers,
- Depth of top and bottom of producing zones,
- Productivity of producing zones,
- Wellhead siting constraints such as coastal erosion setbacks and sea level rise,
- Percentage of recharge from new ocean water sources.
- Environmental impacts during construction and operation

For example, consider the following scenario (Fig. 13.10). The base of the target aquifer lies at a depth of approximately 97.6 m below sea level. Due to siting constraints and coastal erosion setback requirements, the elevation of the slant wellhead is approximately 6.1 m above mean sea level. To transect the entire aquifer from the well head at +6.1 m to the base of the aquifer at −97.6 m and assuming a slant well length of 305 m, requires a slant well angle (α) of approximately 20° below horizontal [$\alpha = \mathrm{Sin}^{-1}$ (103.7/305)].

13.5.3 Casing and Screen Diameters

To maximize well yield, the minimum inside diameter of the well screen used for slant well completion should be at least 30.5 cm. This is based on allowing reasonable axial-flow head losses (3.5 m) for a discharge rate of 16,350 m^3/day with 305 m of well screen. As the slant wells are typically constructed using a telescoping design, a larger pump house casing is usually placed in the upper section of the well to accommodate as large a submersible pump as necessary (Fig. 13.11).

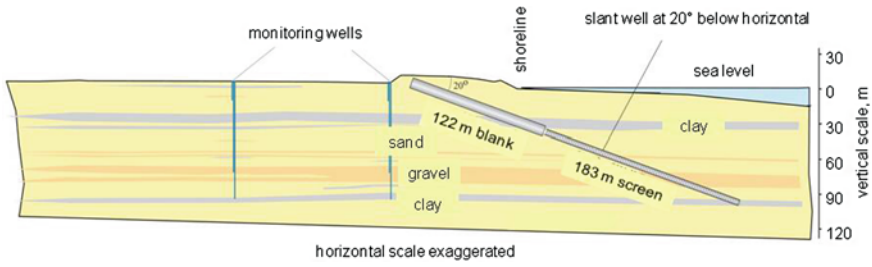

Fig. 13.10 Slant well design length and angle example

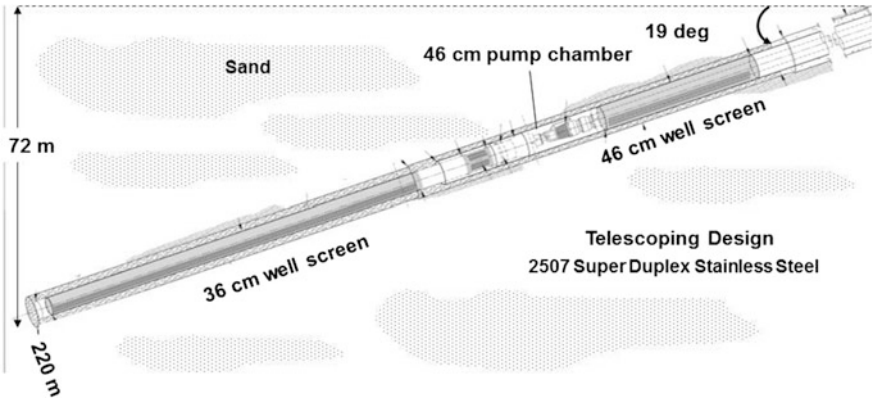

Fig. 13.11 Casing and screen diameters for a 220 m slant well equipped with a submersible pump

Calculations or model simulations should be made to determine the maximum probable pumping level under pumping conditions. For example, if the total feed water requirement is 113,600 m^3/day and each slant well is estimated to pump approximately 16,350 m^3/day, then seven slant wells will be required. In reality, more than the exact number of wells required is always constructed to allow for rotation of pumping and periodic rehabilitation of the well which should be routinely planned for every 3 to 5 years. Calculation of the combined interference from the wells needs to be made to determine the pumping levels in each of wells. Once this is made, the minimum diameter for the pump house chamber can be determined as well as the measured depth (i.e. length of casing). An example of water level interference around a three slant well pod is seen in the example shown in Fig. 13.12.

13.5.4 Well Screen Type

Proven well construction technology embraces the principle of "simple and strong". This principle is especially important in construction of subsea slant wells using the dual rotary drilling method. Of the available well screen types, a good choice for desalination slant well feed water supply is the pipe based horizontal louver shutter screen. Louvered screen consists of engineered slots punched into solid pipe forming small arches around the circumference of the screen. This type of well screen has good filter pack stabilizing qualities, sufficient open area, necessary yield and tensile strength, and is robust enough to withstand the normal abuse during construction and rehabilitation (Fig. 13.13). Although continuous wire-wrapped screens have a greater open area, field and laboratory tests have shown that above a

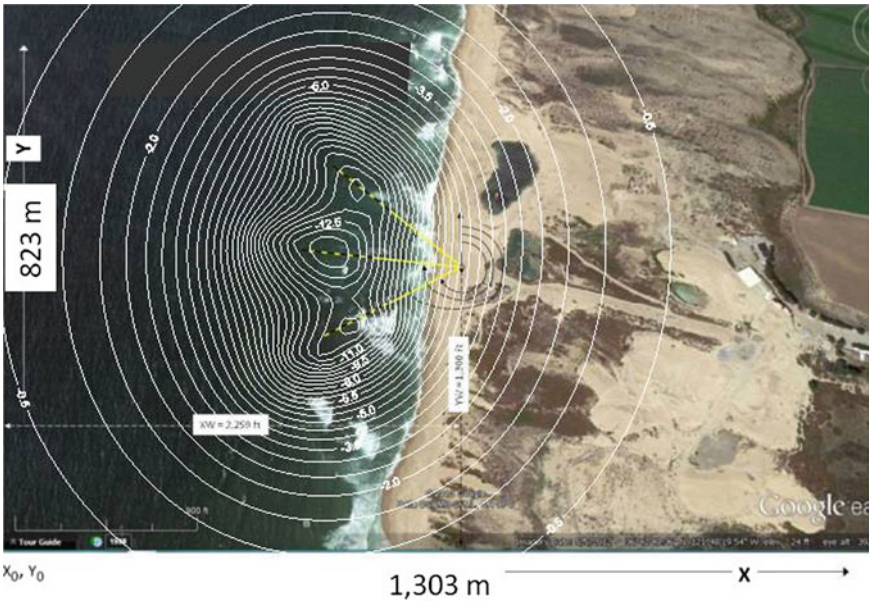

Fig. 13.12 Well field interference for a three slant well pod, drawdown in m

Fig. 13.13 Horizontal louver well screen

screen open area of 3–5 %, there is no significant increase in well efficiency (Williams 1985). In addition, wire wrapped screens are more susceptible to damage during installation and maintenance especially in a dual rotary drilling environment where rotational forces imparted to the filter pack and well screen during removal of the temporary casing may cause problems.

13.5.5 Silt Density Index—SWRO Membrane Fouling

Silt density index (SDI) (ASTM 2002), is one of the major design parameters in desalination feed water supply. SDI is a non-specific measure of the particulate and colloidal fouling potential of water and is the most widely used method for determining feed water quality for membrane desalting processes. As a general guideline, most membrane manufacturers recommend maintaining feed water SDI less than values of 3–5, depending on the membrane type and manufacturer. In natural water supplies, SDI values are controlled by the type and quantity of suspended sediments and colloidal particles, which are comprised of a wide range of constituents including clay, bacteria, algae, colloidal silica, transparent exopolymer particles, and other natural organic matter forms. Groundwater supplies high in dissolved iron and manganese result in formation of an iron and manganese hydroxide precipitate when water is exposed to oxygen or chlorine. When these precipitate, they may contribute to the colloid quantity and likely increase SDI levels. Feed water with SDI values consistently greater than 5 generally require pretreatment before entering the membrane desalting process. Typically, properly engineered artificial filter packed wells have SDI values between <1–3 (Table 13.1).

13.5.6 Casing and Screen Materials

For a long-lasting slant well intake system, the well and pump materials (casing, screen, centralizers, and tremie guides) should be manufactured using a high corrosion and pitting resistant steel suitable for the seawater environment such as super duplex stainless steel. For stainless steels to have a high pitting resistance, they should contain high chromium, molybdenum, and nitrogen content with sufficient nickel to maintain an austenitic structure (IMOA 2009). It is important that the material withstand both the corrosive environment of seawater (chloride and dissolved oxygen) and tensile and yield forces during well construction and maintenance.

Table 13.1 Well design parameters including SDI values for artificially filter packed wells

Location	Type of well	Total depth (ft bgs)	Screened interval (ft bgs)	Screen ID (in.)	Production (gpm)	Filter pack	Slot size (in.)	Terzaghi migration Factor	Terzaghi permeability Factor	Sorting factor	Turbidity (NTU)	SDI 15
Dana Point SL-1	Slant well	350	130–350	12	2100	4 × 16	0.094	3.2	3.6	0.5		0.1
City of Oceanside TW-1	Vertical well	180	70–130 140–170	6	31	6 × 20	0.050	3.6	6.1	0.4	0.4	0.5
Cab San Lucas Mexico PW-1	Vertical well	75	30–65	8.35	175	1/4 × 16	0.094	1.6	4.7	0.7	<1	
San Pasqual 4B	Vertical well	89	25–41 45–81	8.25	150	4 × 16	0.080	3.6	7.2	0.7	0.3	1.6
Hesperia RW-4	Vertical well	466	202–270 280–446	18	4041	1/4 × 16	0.094	0.3	1.9	0.4	0.4	0.9
Hesperia RW-5A	Vertical well	532	200–258 268–512	18	4052	1/4 × 16	0.094	1.4	6.0	0.5	0.1	0.4
Hesperia RW-3	Vertical well	548	200–254 264–528	18	4045	1/4 × 16	0.094	1.2	4.6	0.4	0.2	0.2
San Bernardino 9th Street South	Vertical well	1020	448–480 510–1000	20	3517	1/4 × 16	0.094	2.3	1.6	0.4	1.1	2.0
San Bernardino 9th Street North	Vertical well	1000	440–490 500–980	20	3445	4 × 14	0.070	3.1	3.4	0.4	0.5	0.9
Chino Desalter II-1	vertical well	410	155–288 308–390	16	2600	1/4 × 16	0.094	2.1	5.9	0.4	<0.20	0.0
Chino Desalter II-2	Vertical well	342	156–312	18	3000	1/4 × 16	0.094	2.8	11.8	0.3	<0.20	0.3
Chino Desalter II-3	Vertical well	355	160–325	16	3000	1/4 × 16	0.094	2.1	7.9	0.5	<0.20	0.0
Chino Desalter II-4	Vertical well	370	156–340	18	2000	1/4 × 16	0.094	2.5	12.8	0.6	<0.20	0.2

(continued)

Table 13.1 (continued)

Location	Type of well	Total depth (ft bgs)	Screened interval (ft bgs)	Screen ID (in.)	Production (gpm)	Filter pack	Slot size (in.)	Terzaghi migration Factor	Terzaghi permeability Factor	Sorting factor	Turbidity (NTU)	SDI 15
Chino Desalter II-6	Vertical well	315	150–295	16	2000	1/4 × 16	0.094	2.3	7.6	0.6	0.4	0.0
Chino Desalter II-7	vertical well	275	140–245	16	1500	1/4 × 16	0.094	2.9	8.8	0.5	0.3	0.0
Chino Desalter II-8	vertical well	260	130–230	16	1500	1/4 × 16	0.094	1.6	4.4	0.6	0.6	0.2
Chino Desalter II-9A	Vertical well	315	180–195 206–295	18	2000	1/4 × 16	0.094	0.6	2.9	0.3	<0.20	0.2
Chino Desalter I-16	Vertical well	170	100–140	18	252	1/4 × 16	0.094	1.1	5.3	0.6	1.1	1.8

13.5.7 Fundamental Principle of Well Design

The fundamental principle of well design is:

The purpose of the filter pack is to stabilize the aquifer.
The purpose of the well screen is to stabilize the filter pack

The single most important design parameter for desalination feed water supply for wells constructed in unconsolidated sediments is proper design and placement of an artificial filter pack between the well screen and borehole wall. "Tried and true" design criteria developed over seven decades and successfully demonstrated on vertical wells can be applied with equal success to slant wells.

13.5.8 Artificial Filter Pack Design

Artificial filter pack well technology has been perfected since the 1940s with excellent success leading to sand free water and high productivity (Williams 1985; Roscoe Moss 1990; Terzaghi and Peck 1948). Adapting this technology to slant well subsurface intake systems provides sand and silt free water with high productivity. Materials suitable for an artificial filter pack should be well-rounded rock composed primarily of silica with little silt, clay or organic matter. Calcareous gravels must be avoided or should not comprise more than 3–5 % of the total volume. The design of the pack must be compatible with the formation materials to be screened and the slot width of the screen which requires pre-design sampling and grain size analysis distribution to be made. Procedure for determining the optimal screen and artificial filter material are addressed in Roscoe Moss (1990) (Fig. 13.14). The annular space between the outside of the well screen and the borehole wall should be adequate for the filter pack to be installed without any "bridges" or voids and is typically 10–15 cm in thickness (Roscoe Moss 1990). Too large an annular filter will inhibit proper development (e.g. >20 cm) and too small a space may result in an inadequate or missing filter pack.

13.5.9 Well Screen Slot Opening and Entrance Velocity

The percentage of filter pack material passing the well screen slot opening should range from approximately 10 to 20 % Roscoe Moss (1990). The slot opening should be as wide as possible in order to allow the well to "breathe" while at the same time stabilizing fine-grained materials. Field and laboratory tests have shown that when percentage open area of the well screen is within 3–5 %, there is no significant loss in well efficiency (Fig. 13.15; Williams 1985). For properly designed and constructed wells, entrance velocity is not a primary design factor and turbulent flow losses (i.e. well losses) are not a significant drawdown component.

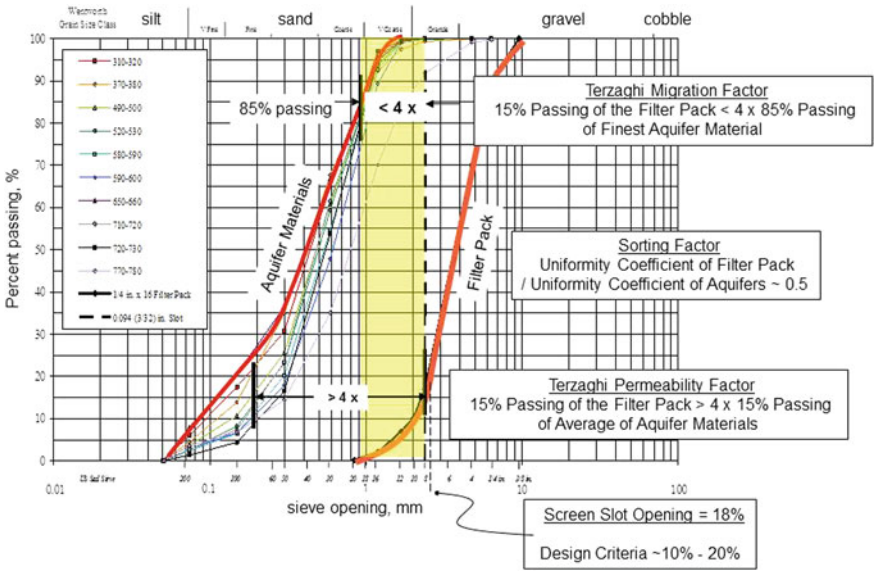

Fig. 13.14 Mechanical grading analysis showing filter pack and screen design parameters

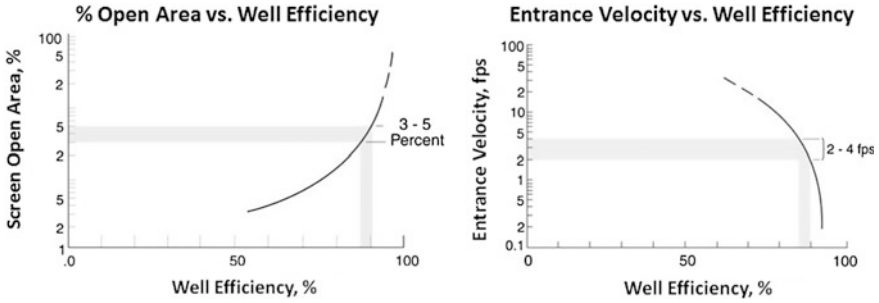

Fig. 13.15 Screen open area and entrance velocity versus well efficiency (Williams 1985)

13.6 Slant Well Construction and Testing

13.6.1 General

Construction of slant wells beneath the ocean creates special challenges in placing casings, screens and artificial filter packs. In vertical wells, borehole stability is maintained by pressure of the drilling fluid acting on the borehole sides. However, in a low angled well (slant well), the vertical depths are generally much less than in a vertical well and as such, borehole stability probably cannot be maintained with drilling fluid unless heavy mud additives are used. Addition of heavy mud additives

would compromise the ability to properly develop the well due to a heavy mud cake on the borehole walls. This impermeable mud cake is very difficult to remove and would most likely result in a sufficient loss in production. The dual-rotary method of construction solves this problem for subsea slant wells by placing a temporary solid casing extending to the total measured depth (i.e. lineal length) of the slant well casing and screen allowing completion of the well (casing, screen and filter pack) within the temporary casing.

13.6.2 Telescopic Construction

The dual-rotary method of construction involves construction of a temporary casing string to the total well completion depth. Once this depth is attained, the temporary casing is withdrawn exposing the artificial filter pack well to the subsea environment. In order to achieve the maximum slant well lengths ($\sim$305 m), the temporary casing needs to be installed in lengths which can be easily withdrawn and without the risk of getting stuck. Experience has shown that with conventional dual-rotary equipment, a 76.2 m section of casing can be withdrawn using the drill rig and anchor method. Thus, telescopic construction of slant wells involves advancing the borehole (using temporary casing) in progressive 76.2 m stages with each stage using a gradually smaller diameter telescoping downward (Fig. 13.16). As of this writing, a 220 m test slant well with a telescoping design is nearing completion in the Monterey area as part of the Monterey Peninsula Water Supply Project.

13.6.3 Anchor Installation and Site Set-up

To accommodate forces exerted during drilling (i.e., pushing down on the outer string of drill casing) and removal of the temporary casing (i.e., pulling back), a number of anchors are installed at both the front and the back of the drill skid (i.e., angled drill cradle). On a typical dual rotary (Foremost DR-24HD) drill rig, the top drive is capable of 38,102 kg of pullback and 11,748 kg of pull-down force, while the lower drive is capable of 53,070 kg of pullback and 19,051 kg of pull-down force. Typically, anchors consist of six or more 21.9 cm OD casings set in boreholes drilled to at least 6.1 m below ground surface. A typical installation includes two anchors installed at the back of the rig (i.e., adjacent to the well head entry point for use during drilling), and four anchors installed at the front of the rig for use during temporary casing removal.

To drill wells on an angle, an angled drilling platform (i.e., cradle) is fabricated to support the drilling rig mast at the desired angle below horizontal (Fig. 13.17). The angled drilling platform can be adjusted to any required drill angle from pure horizontal (0^o), to pure vertical (90^o).

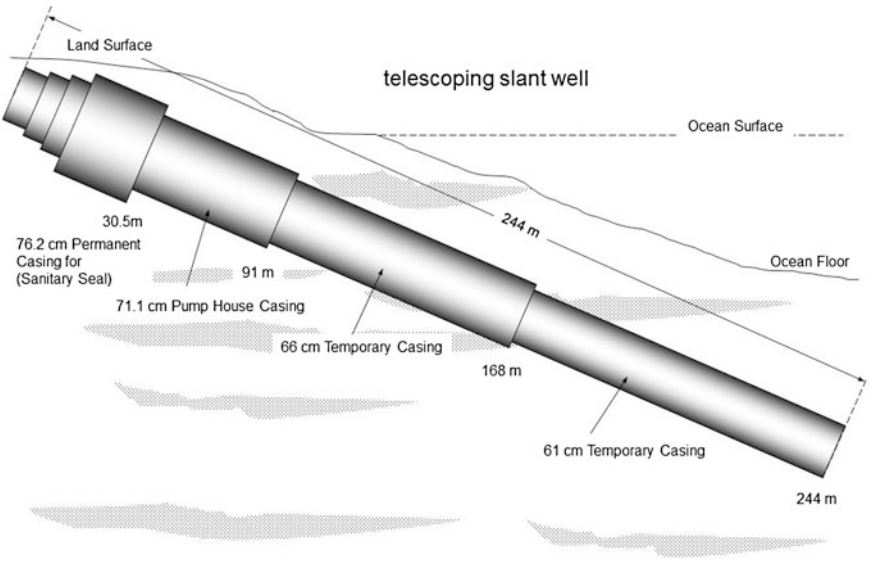

Fig. 13.16 Telescopic construction used in slant wells

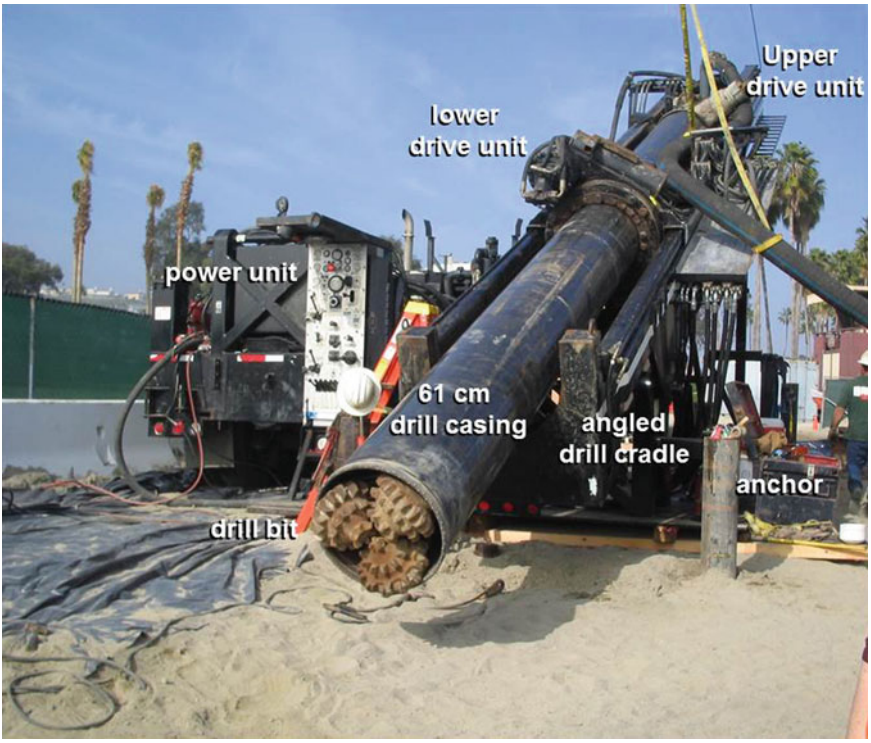

Fig. 13.17 Dual-rotary drilling cradle which can be adjusted for any slant well angle

Slant well construction typically requires a footprint of approximately 21 m × 43 m. However, this may also depend upon site characteristics and permitting. Some flexibility exists and final layout is based on a combination of factors determined to be feasible by the contractor. For example, in recreational areas near the beach, small footprints are required in order to minimize impacts to the beach-going public. A larger staging area (typically 30 m × 46 m) is located nearby. Trips to and from the staging area are kept to a minimum and work schedules adjusted so that essential equipment for the day's drilling activity is on-site at the start of the work day (Fig. 13.18).

13.6.4 Dual Rotary Drilling Method

The dual-rotary drilling method uses temporary casing that is rotated and advanced in combination with the inner drill string as formation materials are removed. Rather than the process resulting in an open borehole in which to construct the well as is done in other rotary drilling methods (e.g. reverse or direct mud rotary), the temporary casing holds loose formation material back as it is advanced. After reaching total depth, the well casing and screen is centered within the temporary casing. The artificial filter pack is then pumped under pressure into the annulus through multiple tremie pipes as the temporary casing is withdrawn.

The dual rotary method uses a lower rotational driving unit to advance temporary casing (up to 102 cm in diameter) through unconsolidated alluvial materials such as sand, gravel, and boulders. Dual rotary drilling units are very powerful, having very high pullback to weight ratios. The high pullback power is very useful when extracting the temporary drill casing from the borehole under difficult down-hole conditions. An upper (or top) rotary head is used to simultaneously drive a "dual-wall" drill string as the lower drive advances the temporary casing (Fig. 13.19). Two sizes of drill pipe, an inner string and an outer string are rotated and advanced simultaneously when drilling. A roller cone bit attached to the bottom of the dual wall drill string can break up large diameter formation materials while advancing the borehole. Compressed air is forced down the annulus between the outer and inner drill strings. Jets, or vents, placed within the inner drill string above the drill bit cause formation materials (drill cuttings) and water to be pushed to the surface through the interior of the inner drill string. The cuttings are then discharged at the surface through a flexible hose to a cyclone separator that is located over a roll-off box. Solid cuttings removed from the borehole remain in the roll-off box, while fluids are pumped to settling tanks for recirculation to the borehole during drilling.

The two driving units (upper and lower units) are able to work independently of one another in raising and lowering the temporary drill casing, as well as rotating the dual-wall drill string. Each drive may operate at a different rotational speed as down-hole conditions dictate. The lower drive can also rotate the casing in either direction because the temporary drill casing has welded rather than threaded connections. Pull down, pullback, clockwise and counter-clockwise rotational forces

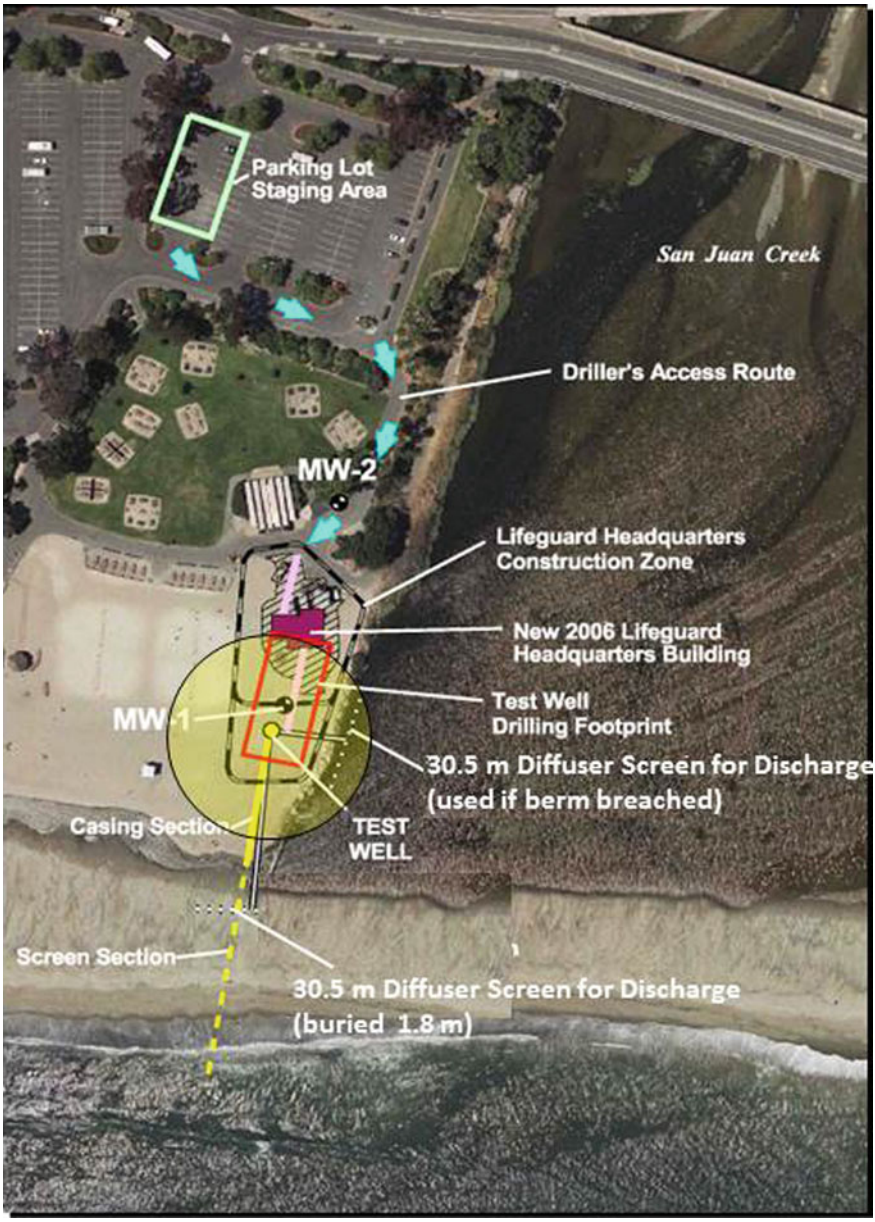

Fig. 13.18 Dual-rotary drill rig foot print and staging area for Dana Point test slant well

are effectively transmitted to the casing through hydraulically-operated jaws on the lower rotary unit. A carbide studded casing shoe is welded to the leading edge of each string of temporary drill casing, allowing the casing to be advanced through cobbles without being deformed (Fig. 13.17).

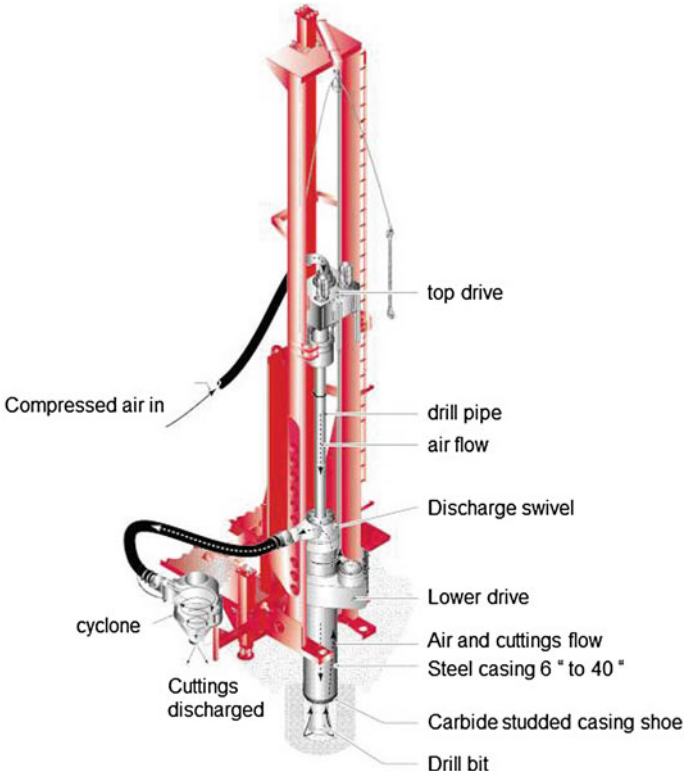

Fig. 13.19 Dual rotary drilling method (Foremost Industries, LP, 2003)

Each diameter of temporary drill casing may be advanced typically 76 m ahead of the preceding casing diameter. For example for a 305 m test slant well, four casing diameters are required, ranging from 76.2 to 61 cm in diameter. Once the total depth of the borehole has been reached, well screen and casing are installed and centralized within the temporary casing. Filter pack and seals are then placed around the well casing and screen as the temporary casing is gradually pulled up around the production casing, screen and filter pack.

13.6.5 Temporary Casing

Slant well drilling is accomplished by advancing temporary casing as the borehole is advanced. The temporary casing holds loose formation material back permitting advancement of the borehole. Temporary casing is limited to approximately 76 m lengths before telescoping to a smaller diameter. Once the targeted depth is reached, well casing and screen are installed within the temporary drill casing. The temporary outer casing is removed as the filter pack and seals are installed. During temporary

casing advancement, sections are attached onsite by welding. To avoid disruption, drill casing sections and other materials required for each day's work are generally transported from the staging area to the well site at the start of each day (Fig. 13.18).

13.6.6 Casing Collars and Centralizers

Installation of the louvered well screen and casing uses casing collars to provide extra strength and are manufactured from the same material as the casing and screen. Sight holes drilled at the midpoint of each collar and equally spaced around the circumference are used to maintain casing alignment. Collars are fabricated by slightly expanding a short section of casing so that it fits over the standard-sized casing. They are then welded to one end of the casing with the casing extending midway through the length of the collar. Centralizers are installed at selected increments to maintain the casing and screen in the middle of the temporary casing to allow uniform placement of the filter pack.

13.6.7 Logging Lithologic Samples

During the drilling process, lithologic samples are collected typically in 1.5 m intervals from the cyclone separator and placed in storage bags or containers. Samples are identified as to material type and potential as a productive aquifer by visually logging them in the field using the Unified Soil Classification System (USCS). Mechanical grading analyses are then performed on selected formation samples to obtain grain size distribution and to design the artificial filter pack and well screen aperture size.

13.6.8 Geophysical Borehole Logging

As the dual rotary construction method uses solid steel temporary casing, conventional geophysical logging methods are not possible. However, gamma ray logs may be successfully run in steel-cased boreholes to identify clay-bearing zones. Gamma ray logs are used to measure naturally occurring gamma radiation that is emitted from formation material surrounding the borehole, and are the result of the release of electromagnetic radiation from elements with unstable nuclei. The most common source of gamma radiation is potassium-40 (K40), uranium-238 (U238), uranium-235 (U235), and thorium-232 (Th232). Clay-bearing materials commonly emit relatively high gamma radiation due to weathering of potassium-bearing minerals such as potassium feldspar and other mica-bearing rocks. Placement of the gamma ray tool can be made on a cradle, trolley or other track mounted device to protect the tool.

13.6.9 Specific Coring and/or Water Quality Testing During Drilling

As the borehole for a slant well is advanced, core samples may be collected for the purpose of measuring hydraulic conductivity. Samples may be collected using a core barrel or other similar method however materials will most likely be disturbed and mechanical grading analyses should be used in conjunction to estimate hydraulic conductivity. As the temporary casing provides protection from borehole caving during advancement, water quality samples can be collected from inside the dual wall drill string.

13.6.10 Well Completion-Installing Casing, Screen and Filter Pack

Well casing and screen is installed and centralized within the temporary casing. An engineered artificial filter pack is then pumped under pressure into the annulus between the temporary casing and well screen through a number of gravel feed pipes (tremie pipes; Fig. 13.20). Placement of a temporary packer or bladder-type assembly within the bore of the well screen section helps facilitate placement of the artificial filter pack by forcing the water to stay in the annulus and not exit through the well screen. Water is pumped through the center of the well-screen packer assembly and exits the screen below the packer traveling out of the well screen and into and up the filter pack. This water injection through the well-screen packer assembly helps to settle the filter pack as well as ensure that the filter pack completely surrounds the well screen. As the filter pack is placed, the temporary casing is withdrawn by pulling and/or rocking and/or vibratory means. It is important to keep the level of filter pack approximately 1.5–3 m above the bottom of the temporary casing. This prevents "bridging" (i.e. entraining native material) or forming voids within the filter pack. If any cement grout seals are required, they are placed in a similar manner. As the filter pack and cement seals are being installed, the volume of material placed is checked against the calculated theoretical volume to ensure that voids have not formed, or bridging has not occurred within the annular space.

The key to proper placement of the filter pack around the well screen is pumping the filter pack under pressure with multiple tremie pipes, fluidizing the filter to settle and remove any voids, and carefully removing the temporary casing such that the filter pack stays in place (Fig. 13.21). Initial development consists of simultaneously airlifting and swabbing the screened interval to consolidate and clean the filter pack and near–well zone. To ensure maximum compaction of the filter pack within the annular space, a swabbing tool with packers is installed inside the well screen and mechanically swabbed and airlifted following placement of the filter pack (Fig. 13.22). A large quantity of water is added on a continual basis to the

Fig. 13.20 Installing the casing and screen

Fig. 13.21 Removal of Temporary Casing

Fig. 13.22 Air lift swab used for initial development

inside of the casing to assist in moving the filter pack downward, and to add hydrostatic pressure to the formation to prevent formation sand from disrupting the pack.

Having a sufficient filter pack thickness and properly placed and developed, minimizes the movement of coarse-grained materials away from the top of the well screen during development and redevelopment keeping the filter pack in place. This aspect of the slant well construction is the most challenging. Various combinations of gravel tremie placement, high pressure water injection, air lift pumping and a combination of all three may be necessary to properly place filter material and remove the temporary casing.

13.6.11 Initial Development—Airlifting and Swabbing

Well development removes results of drilling damage and fines in the near-well zone producing a smooth and progressively coarser gradation between the borehole-aquifer interface and the well screen. During the process of well development, compaction and settling of the filter pack occurs.

After drilling debris is removed from the well by airlifting with an open ended swab tool, swabbing and airlifting is performed using the swabbing tool in 3 m sections. Even though the target screen section is only 3 m, the swab is raised and lowered 12 m to generate sufficient force around the target screen section. Starting

at the top of the well screen, each 3 m section is repeatedly swabbed and stationary airlifted until sufficiently clean. This procedure is repeated from the top of the well screen to the bottom of the well screen and then repeated from bottom to top until the well is sufficiently developed (relatively clear water).

13.6.12 Final Development—Pumping and Surging

A submersible test pump is used for final well development. Development pumping should always start at the lowest rate and gradually increase. Pumping at a particular discharge rate should continue until the turbidity of the water has dropped to acceptable levels. The well pump is then typically surged (stopped and started) and the same discharge rate repeated until the water is clear. The number of surges required to produce low turbidity water at a specific discharge rate varies from site to site and well to well. Progressively increasing the development pumping in this fashion ensures proper development and stabilization of aquifer materials. This process is repeated until the development pumping is approximately 1.5 times the design pumping rate and the turbidity is acceptable. When the pump is stopped during surging, backwashing (i.e., adding water to the inside of the well bringing the level slightly above the static level) may be employed to help in the development process. An inflatable straddle packer assembly placed above and below the pump intake can also be used if required to focus development on particular screened intervals. For example, by inflating the lower packer and deflating the upper packer, the upper portion of the well screen will be isolated and developed separately from the lower screen thereby assuring a higher degree of development in this zone. The reversal is true to provide focused development of the lower zone.

13.6.13 Well and Aquifer Testing

Following completion of development pumping, step-drawdown and constant rate pumping tests are conducted. The purpose of pumping tests is to obtain information on well performance, efficiency and aquifer parameters. These data are used to determine the design discharge rate of the well and predict well and well field interference using analytical equations or ground water models. In addition to water level and discharge rate measurements, the sand content, silt density index, pH, conductivity, oxidation-reduction potential (ORP), temperature, dissolved oxygen and, turbidity are typically measured.

13.6.14 Step-Drawdown Test

The purpose of the step-drawdown test is to determine formation losses, well losses, and well efficiency. Time drawdown measurements are made to determine specific capacity and well efficiency relationships necessary to calculate the optimal discharge rate and pump design. Typically, three to four discharge rates are selected for step-drawdown testing, starting at the lowest rate, and progressing to the highest (Fig. 13.23). Pumping should continue at each rate for a sufficient length of time to show a predictable water level trend as determined by a semi-logarithmic plot of pumping level or drawdown versus time. Data from the step drawdown data are used to generate the following:

- Specific capacity diagram showing total well drawdown, formation loss, well loss and well efficiency for a range of discharge rates (Fig. 13.24),
- Recommended design discharge rate, total dynamic head and measured depth of pump setting (lineal length in slant wells).

13.6.15 Constant Rate Test and Pilot Testing

After recovery from the step drawdown test, and in order to predict long-term drawdown effects and feed water salinity, a constant rate pumping test is performed for a period typically ranging from one to a few days. Where there is a monitoring

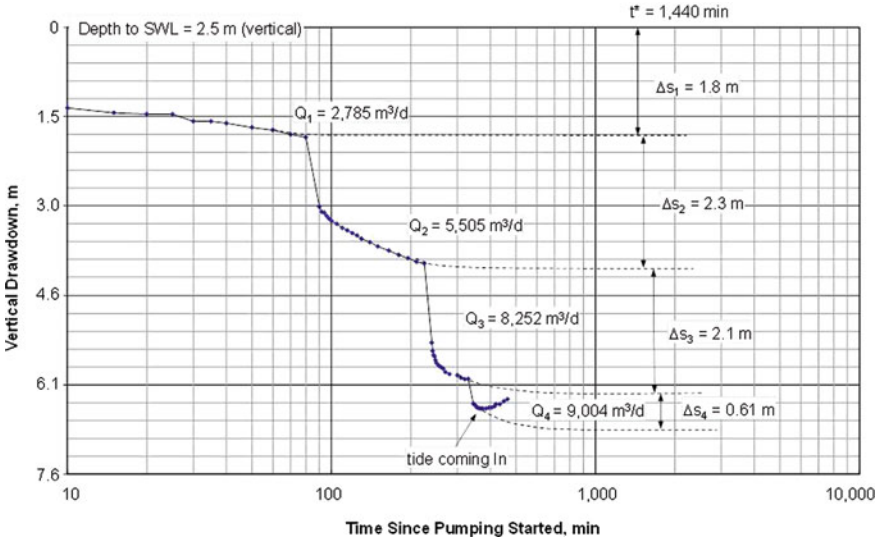

Fig. 13.23 Step-drawdown test

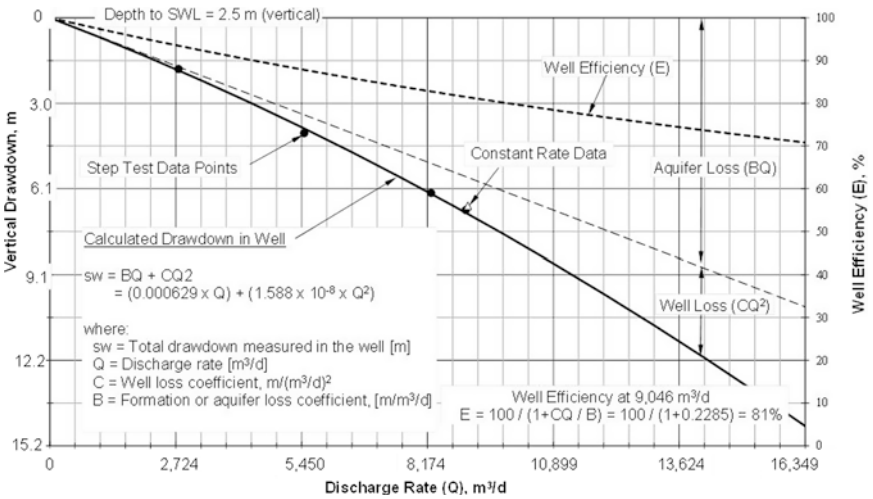

Fig. 13.24 Specific capacity diagram

well or wells available or a second production well which could be used for monitoring, the aquifer test should be conducted a sufficient length of time to obtain interference data from which formation parameters, transmissivity, storativity and leakance may be calculated. Depth to water during testing is typically measured using either wire-line sounders or more commonly, using continuous logging down-hole pressure transducers. In addition, other data logging devices may be used to continuously monitor key water quality parameters. During the constant rate tests, water quality samples are also periodically collected as necessary and tested for general mineral and physical properties and any other constituents as required (Fig. 13.25).

A long term pumping test may also be run for pilot testing the feed water supply parameters to develop long-term trends in salinity, overall water chemistry and water levels. These pilot tests may range from a few months to one or two years in order to obtain sufficient design information for the SWRO feed water supply. The duration of the testing depends on trends in well yield, salinity of produced water and other feed water quality factors that are site specific to each project.

13.6.16 Water Quality Sampling

Typical water quality measurements taken during pumping tests include:

- Analysis of feed water quality major inorganic chemical parameters along with TOC
- Analysis of dissolved trace metals
- Field measurements of water quality parameters (specific conductivity, salinity, TDS, oxidation reduction potential, dissolved oxygen, turbidity, temperature, and pH)

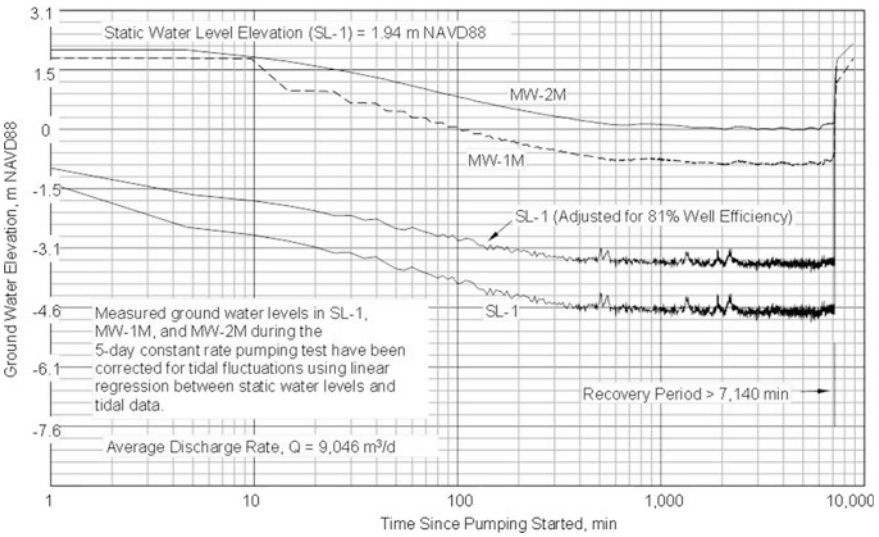

Fig. 13.25 Constant rate pumping test, Dana Point test slant well

- Field measurement of silt density index
- Analysis of parameters required by any discharge permit requirements for concentrate disposal

High iron and manganese concentrations may occur in subsea aquifers as "old marine water" in an anoxic state (depleted of dissolved oxygen) onshore or below the seabed offshore. Experience at the Dana Point project has shown that this water in the subsea alluvial fan off of Dana Point may be gradually removed and replaced with new ocean water during pumping of the full-scale subsea slant wells (113,600 m^3/day). In reality, the aquifer geometry, hydraulic properties and water chemistry will dictate the duration of time required to lower the concentration of iron and manganese at a site specific location. Great care must be taken to not allow dissolved oxygen to enter the system simultaneously with the anoxic water or damage could occur to the SWRO pretreatment and primary membrane system.

13.7 Well Field Design and Intake Salinity Management

13.7.1 Well Field Layouts

Once all necessary geohydrologic, geotechnical investigations and pumping tests are complete, well production can be adjusted using both areal layouts as well as slant well angles. Groundwater models calibrated to site specific data are typically used to accomplish this. Slant well layouts depend upon the quantity of supply and

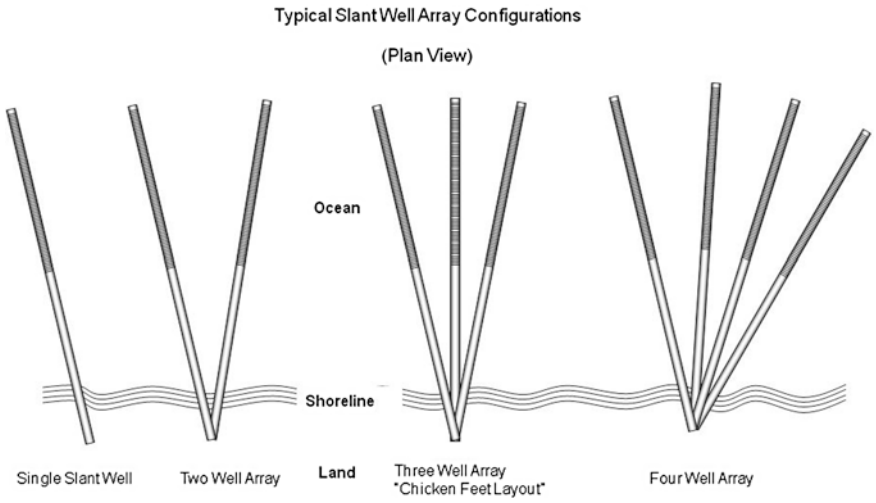

Fig. 13.26 Well field layouts

the variation in feed water salinity (total dissolved solids). Figure 13.26 shows typical slant well array configurations. Groundwater models are used to calculate interference between producing slant wells, the deepest pumping levels in each well, each well pod, and any impacts on inland water resources. Trial and error model runs are made to optimize the slant well layout and angles consistent with the feed water supply requirements.

13.7.2 Management of Intake Salinity

Nearshore aquifers are susceptible to tidal changes and changes in the fresh water/seawater interface as the result of onshore variations in groundwater levels from hydrologic changes. The productivity of the aquifers penetrated, the quality of the water, the sustainability of the supply are important factors in selection of a subsurface site. Subsurface feed water supply systems utilizing slant wells withdraw seawater or brackish water from offshore or nearshore materials below the land surface or seabed. In some cases, nearshore vertical wells producing brackish or seawater from aquifers close to the coast are subject to more tidal and onshore hydrologic variations than distant offshore subsea slant wells. Also, some desalination projects are sensitive to the percentage of inland groundwater recharge produced by the feed water supply wells.

When this condition occurs, the angle of the slant wells may be designed to enable pumping from higher or lower salinity zones which can theoretically minimize variation in feed water salinity (due to migration of the fresh-salt water interface (Fig. 13.27). Thus, shallow angle slant well arrays can produce water with

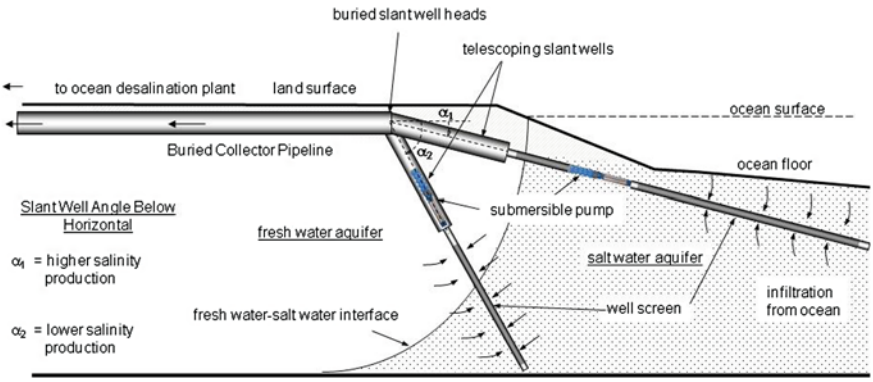

Fig. 13.27 Management of feed water salinity using variable angled slant wells

higher salinity to stabilize the feed water quality during wet hydrologic cycles (i.e. by mixing with the more saline portions of the subsurface aquifer). Steeper angled slant well arrays can produce water with lower salinity to stabilize the feed water quality during dry hydrologic cycles (i.e. by mixing with the less saline portions of the subsurface aquifer). Packers placed above and below pumps can also selectively pump higher or lower salinity concentrations in order to stabilize shifts in feed water salinity as required (Fig. 13.28).

13.8 Hydraulics of Slant Wells

The cone of depression in the vicinity of wells is a function of aquifer hydraulic properties, well field discharge rate, and time of pumping. In vertical wells the cone of depression is concentric (assuming homogeneity) with the highest drawdown in the vicinity of the well and declining outward. In angled wells, the cone of depression is ellipsoidal with the vertical projection of the drawdown distribution being oval-shaped. The major axis of the ellipse coincides with the alignment of the vertical projection of the slant well screen. The minor axis is perpendicular to the major axis and crosses at the center of the vertical projection of the well screen. Slant wells may produce more water than vertical wells in the same aquifer as the aquifer loss (i.e. formation loss component of the total drawdown), is "spread out" over the entire length of well screen and assumes a bowl shaped depression-like shape. Thus, higher discharge rates can be achieved with the same overall drawdown in the well (formation loss + well loss).

Mathematical support for this statement can be seen by comparing the non-steady state equation for a vertical well in a confined aquifer (using Jacob's approximation to the Theis equation) with the UDE for an angled well using Jacobs approximation (Eq. 6 Williams 2013 with ns = 4). When formation loss drawdowns are compared at the center of the vertical projection of the well screen, slant wells

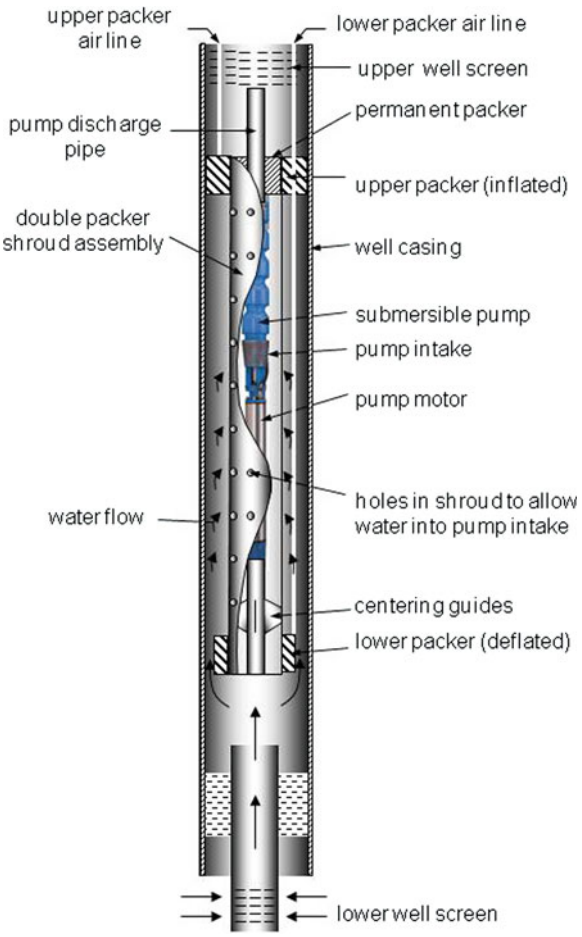

Fig. 13.28 Use of a dual-shroud packer assembly to selectively pump from upper or lower well screen sections

have discharge rates approximately 1.5–2 times greater than vertical wells (for the same drawdowns and for a typical range of aquifer parameters and slant well angles). Note that the following comparison is for the laminar flow loss component of the total drawdown (i.e. formation loss) at the effective well radius (Hantush 1964). Calculation of total drawdown in a pumping well requires determination of turbulent flow losses associated with the respective discharge values.

$$Q2/Q1 = \log(B)/\left[\log(B) - 0.5\log\left(XS^4/144\right)\right] \tag{13.1}$$

where

Q1 = vertical well discharge rate, m^3/day
Q2 = slant well discharge rate, m^3/day
B = (2.25 × T × t)/S, m^2

T = transmissivity, m^2/day
S = storativity
T = time, days
XS = vertical projection of slant well screen, LS × cos(α), m
α = slant well angle, degrees below horizontal

The drawdown distribution in the vicinity of an angled well is the algebraic sum of drawdowns for a finite number of point sinks distributed along the vertical projection of the well screen (Williams 2013). Each sink has a fractional discharge rate proportional to the total well discharge rate and number of sinks. A universal drawdown equation (UDE) for non-vertical wells (i.e. slant wells) developed by Williams (2013) enables a simple calculation of drawdown around slant wells or slant well fields.

13.8.1 Basic Notation and Coordinate System

A slant well typically consists of a blank casing section and a perforated section (well screen) within the production zone of the aquifer. Figure 13.29 shows a generalized cross section of a slant well along with the notation used to calculate slant well drawdowns. The angle below horizontal is denoted by (α). The total length of the slant well is (L) and the horizontal projection of the well screen is (XS). Figure 13.30 is a plan view of a slant well showing coordinate system notation. Coordinates for the wellhead (XW, YW) are shown relative to the origin of well field coordinates (X0, Y0). A number of point sinks are placed within the vertical projection of the well screen (XS) with the interval between the sinks denoted by (δ). The distances to each of the sinks from a desired drawdown point (X2, Y2) is also shown. The distances from each of the (i) sinks to the drawdown point in question is shown as RPi. Quadrant convention begins with quadrant I (0–90°) and successive quadrants increasing in a clockwise direction.

The number of sinks required for a smooth drawdown curve is primarily a function of the production well inclination angle, well screen length and radial distance from the well to the point where drawdown is calculated. For most problems of practical interest, a relatively few number of sinks (∼4) are required

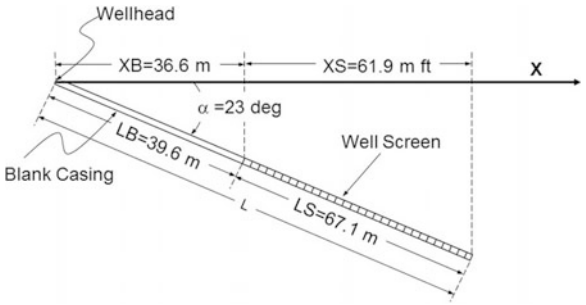

Fig. 13.29 Terminology for slant well hydraulics (*cross section view*)

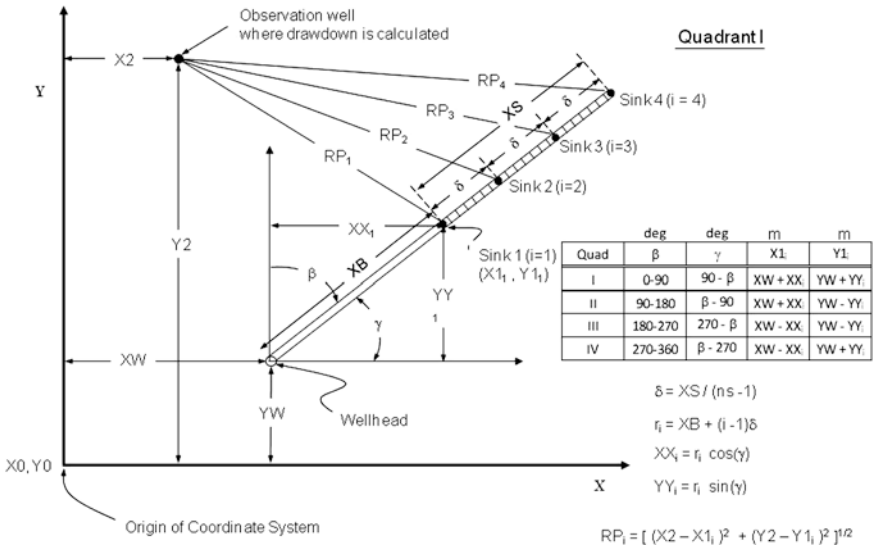

Fig. 13.30 Plan view of a slant well showing notation and coordinate system

for an adequate drawdown solution. A measure of the UDE accuracy is made using the discretization error (DE) relating the number of sinks and the radial distance to the point where drawdown is desired. For most cases, a low DE (<0.5) reflects a smooth drawdown profile.

$$\mathrm{DE} = [\mathrm{XS}/(\mathrm{ns} - 1)]/\mathrm{RPAve} \tag{13.2}$$

where

XS = horizontal projection of the well screen, m
RPAve = average distance from the point where drawdown is calculated and the point sinks, m
ns = number of point sinks

13.8.2 Drawdown Equations for Slant Wells

The following equation is the non-steady state universal drawdown equation (UDE) for slant wells completed in confined aquifers.

$$s = (0.1832Q/T)[\log(2.25Tt/S) - (2/ns)\log(RP_1 \times RP_2 \times RP_3 \times \ldots RP_{ns})] \tag{13.3}$$

where

s = drawdown, m
Q = well discharge rate, m^3/day
T = aquifer transmissivity, (K × b), m^2/day
S = aquifer storativity, (S_s × b), fraction
S_s = Specific storativity, m^{-1}
K = hydraulic conductivity, m/day
b = saturated aquifer thickness, m
t = time since pumping started, days
ns = number of sinks in the vertical projection of the well screen (integer)
RP_i = horizontal distance from point where drawdown is desired to the "ith" sink, m

Similarly, the drawdown calculation around a slant well in a leaky aquifer is:

$$s = [(0.0796Q)/(Tns)][W(u_1, r_1/B) + W(u_2, r_2/B) + W(u_3, r_3/B) + \ldots W(u_{ns}, r_{ns}/B)] \quad (13.4)$$

where:

$W(u_i, r_i/B)$ = Well function for leaky aquifers
r_i = radial distance to ith sink, m
B = leakage factor = sqrt [(Kb)/(K′/b′)], m
K′ = hydraulic conductivity of semi-pervious layer, m/day
b′ = thickness of semi-pervious layer, m
K′/b′ = leakance, day^{-1}
$u_i = r_i^2 S/4Tt$

Figure 13.31 shows the drawdown distribution around a slant well calculated using Eq. 13.3 for the parameters listed in the figure caption. To develop the drawdown distribution around a wellfield, individual slant well drawdowns can be calculated using either Eqs. 13.3 or 13.4 and algebraically added using the principle of superposition. Equation 13.4 was used to develop the drawdown distribution around the three well system shown in Fig. 13.12.

13.9 Sustainability of Supply

In order to maintain the feed water production, planned rehabilitation of the slant or vertical wells will be necessary. The frequency between rehabilitation episodes depends on both site-specific conditions and operational schedules. The same rehabilitation techniques from over 70 years of experience with maintaining sustainability in vertical water supply wells can be successfully applied to slant wells, including both mechanical and chemical rehabilitation. Based on the limited data

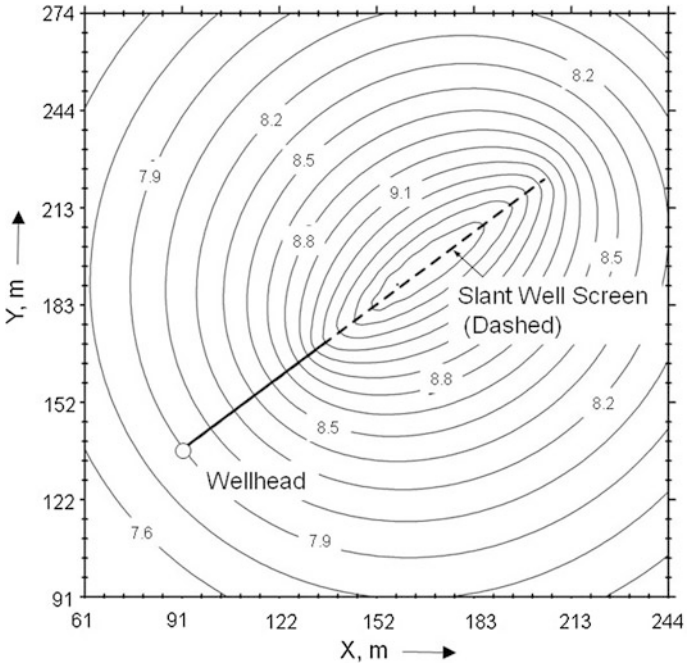

Fig. 13.31 Drawdown distribution, m in the vicinity of a pumping slant well after 1 year of pumping. $\alpha = 23°$, $\beta = 53°$, L = 152.4 m, LS = 91.4 m, ns = 4, K = 20.4 m/day, $S_s = 3.28 \times 10^{-6}$/m, b = 35.7 m, Q = 5,451 m^3/day

from the Dana Point Test Slant Well, it is expected that the frequency between well rehabilitation would be on the order of three to five years. However, depending on other constituents in the groundwater (e.g. iron and manganese), rehabilitation frequency may vary. Slant well rehabilitation utilizes essentially the same techniques and methods used in vertical wells. However, depending on the specific rehabilitation effort and global location, this equipment may not be available.

13.10 Summary and Conclusions

Proven design practices and procedures developed in the water well industry for the past seven decades, and routinely applied to high capacity municipal water supply wells, are equally applicable to desalination feed water supply wells. Nearshore and offshore permeable aquifer systems provide the sustainable supplies with low SDI values and can reduce or eliminate the need for pretreatment. Subsurface intake systems also eliminate impingement and entrainment issues and other environmental

impacts associated with conventional surface intake systems. SDI values are well below the RO design standard for wells which have used Terzaghi's migration and permeability formulas for design. The dual rotary method of drilling allows construction of artificially filter packed slant wells beneath the ocean floor to lengths of 305 m. Sustainability of feed water production can be accomplished using standard well rehabilitation methods such as air lift swabbing and pumping.

Limitation on the maximum number of wells or the reliability of supply (i.e. ocean) is dependent on the permeability of the near shore and offshore aquifers and areal and vertical extent of these deposits. Interference between wells and well pods governs the number and spacing of wells and geologic conditions and coastline land availability governs the limitation on spatial and vertical extent of the well fields. Limitations may also occur due to potential or unforeseen impacts to nearshore and onshore habitat, water resources and permitting issues.

Results from the successful completion and long-term testing of the Dana Point slant well (2010–2012) are being applied to design of subsurface intakes for other ocean desalination projects in California. In addition to the nine well 113,600 m^3/day slant well feed water supply designed for the Dana Point Project, a six slant well 83,000 m^3/day supply is planned for the Monterey Peninsula Water Supply Project and a 37,900–75800 m^3/day project is in the planning stage for the City of Oceanside California.

The main conclusions are:

- Slant wells eliminate entrainment and impingement to marine life; reduce or eliminate costly reverse osmosis pretreatment, do not have any ocean construction impacts, and do not have any permanent visual impacts.
- The most favorable conditions for a subsurface feed water supply using slant wells are where permeable alluvial deposits extend offshore (typically near the mouths of streams and rivers.
- Slant wells receive a high percentage of their recharge from ocean water sources including vertical leakage through the sea bed and horizontal recharge from offshore aquifers.
- For slant wells, there is no theoretical limit on the maximum number of wells or the reliability of the source of supply (i.e. ocean). The only limitation is on the permeability of the nearshore and offshore aquifers, areal and vertical extent of these deposits, and siting, permitting and environmental factors.
- In some coastal areas, obtaining permits is the number one constraint in constructing a slant well feed water supply.
- Environmental and operational factors need to be considered in planning slant well siting include: impacts to fish and wildlife, impacts to riparian vegetation, impacts to onshore water supplies, and percentage of recharge from ocean sources.
- Coastal erosion and sea level rise are also factors affecting the siting of slant well layouts.

- Percentage of recharge from inland and ocean water sources as well as potential aquifer and environmental (e.g., wetlands) impacts are typically determined using site specific calibrated groundwater models.
- Proven well design methods developed for vertical water supply wells may be applied to slant wells.
- Proven well construction technology embraces the principle of "simple and strong".
- Well casing and screens need to be strong and made of corrosion resistant materials capable of withstanding the initial construction as well as multiple rehabilitations in a sea-water environment.
- Slant wells constructed using the dual rotary method using temporary casing enables placement of artificial filter packs in subsea aquifers.
- Telescoping slant wells can extend to lineal lengths of 305 m with typical yields of 10,000–16,000 m^3/day.
- Use of pressure in the Installation of the artificial filter pack ensures proper filter pack placement and stabilization.
- Slant wells can be properly developed using conventional air lift swabbing and pumping techniques.
- The SWRO design SDI range of 3–5 is achievable using an artificial filter pack and the Terzaghi filter pack design principles.
- Slant well layouts can include multiple wells from one central wellhead area.
- Slant well angles and lengths can be varied as required for site specific aquifers.
- Slant well angles and lengths can be varied to minimize salinity variations.
- Slant wells can be pumped at high capacities using submersible pumps placed on an angle and centered within the pump house chamber.
- The cone of depression in the vicinity of slant wells is oval shaped with the highest drawdown occurring in the center of the vertical projection of the well screen.
- When formation loss drawdowns are compared at the center of the vertical projection of the well screen, slant wells have discharge rates approximately 1.5–2 times greater than vertical wells.
- Sustainability of a slant well supply includes periodic rehabilitation with an expected frequency ranging between three to five years depending on site conditions and operation.
- Use of slant well subsurface intakes is an emerging technology and as such, there are no wells in long-term operation and assessment of rehabilitation success is not yet known.
- An experienced "Team" is necessary for successful completion of a slant well project, including experts in ground water hydrology, well design, well construction, water quality, and project management.
- Consideration of SWRO feed water supplies using slant wells are in the planning and feasibility phases for a number of sites along the coast of California.

References

American Society for Testing and Materials (ASTM). (2002). *Standard test method for silt density index (SDI) of water* (pp. 4189–4195). American Society for Testing and Materials (ASTM) Standard D. West Conshohocken, PA: ASTM International. www.astm.org.

California Coastal Committee (CCC). (2003). *Establishing development setbacks from coastal bluffs*. Memorandum W11.5.

California Ocean Protection Council (OPC). (2011). *Resolution of the California Ocean Protection Council on sea-level rise*.

California Ocean Protection Council (OPC). (2013). *State of California sea-level rise guidance document*.

California State Water Resources Control Board. (2013). *Amendment to the water quality control plan for ocean waters of California*. Draft Staff Report.

Charette, M. A. (2012). *Natural isotope tracer study test slant well phase 3 extended pumping test South Orange Coastal Ocean Desalination Project*. Consultant's report prepared for the Municipal Water District of Orange County.

Cooper, H. H., Kohout, F. A., Henry, H. R., & Glover, R. E. (1964). *Sea water in coastal aquifers*. U.S. Geological Survey Water-Supply Paper 1613-C.

Flick, R. E., Murray, J. F., & Ewing, L. C. (2003). Trends in United States tidal datum statistics and tide range. *Journal of Waterway, Port, Coastal, and Ocean Engineering, 129*(4), 155–164.

Gill. (2011). *NOAA regional estimates—Estimating local vertical land motion from long-term tide gage records, version 2 draft*.

Hantush, M. S. (1964). Hydraulics of wells. In V. T. Chow (Ed.), *Advances in hydroscience* (pp. 281–432). New York: Academic Press.

Hapke, C. J., & Reid, D. (2006). *National assessment of shoreline change: A GIS compilation of vector shorelines and associated shoreline change data for the sandy shorelines of the California coast*. U.S. Geological Survey Open File Report 2006-1251.

Hapke, C. J., & Reid, D. (2007). *National assessment of shoreline change part 4: Historical cliff retreat along the California coast*. U.S. geological survey open file report 2007-1133.

Hapke, C. J., Reid, D., & Richmond, B. (2009). Rates and trends of coastal change in California and the regional behavior of the beach and cliff system. *Journal of Coastal Research, 25*(3), 603–615.

Hapke, C. J., Reid, D., Richmond, B. M., Ruggiero, P., & List, J. (2006). *National assessment of shoreline change part 3: Historical shoreline change and associated coastal land loss along sandy shorelines of the California coast*. U.S. Geological Survey Open File Report 2006-1219.

Kemblowski, M. (1987). The impact of the Dupuit-Forcheimer approximation on salt-water intrusion simulation. *Ground Water, 25*(3), 331–336.

Missimer, T. M., Ghaffour, N., Dehwah, A. H. A., Rachman, R., Maliva, R. G., & Amy, G. (2013). Subsurface intakes for seawater reverse osmosis facilities: Capacity limitation, water quality improvement, and economics. *Desalination, 322*, 37–51.

National Oceanic and Atmospheric Administration (NOAA) (2009). *Sea level variations of the United States 1854–2006*. Technical Report NOS CO-OPS 053, Silver Spring, Maryland.

National Research Council (NRC). (2012). *Sea-Level rise for the coasts of California, Oregon, and Washington: Past, present, and future.* Washington, D.C: National Academy Press (Prepublication).

Roscoe Moss, Co. (1990). *Handbook of ground water development* (2nd ed.). Hoboken, New Jersey: Wiley.

Stainless, T. M. R. (2009). *Practical guidelines for the fabrication of duplex stainless steel*. London, UK: International Molybdenum Association (IMOA).

Surfrider Foundation. (2010). *2010 Annual Report*.

Terzaghi, K., & Peck, R. B. (1948). *Soil mechanics in engineering practice*. Hoboken, New Jersey: Wiley.

Todd, D. K. (1980). *Ground water hydrology*. Hoboken, New Jersey: Wiley.
Todd, D. K., & Mays, L. M. (2005). *Ground water hydrology* (3rd ed.). Hoboken, New Jersey: Wiley.
United States Army Corps of Engineers (USACE). (2011). *Sea-level change considerations for civil works programs*. Circular EC 1165-2-212.
Williams, D. E. (1985). Modern techniques in well design. *Journal of the American Water Works Association, 77*(9), 68–74.
Williams, D. E. (2008). *Horizontal well technology application in alluvial marine aquifers for ocean feed water supply and pretreatment*. Prepared for State of California Department of Water Resources/Municipal Water District of Orange County.
Williams, D. E. (2011). Design and construction of slant and vertical wells for desalination intake. In *Proceeding, International Desalination Association World Congress on Desalination and Water Reuse, Perth, Australia*.
Williams, D. E. (2013). Drawdown distribution in the vicinity of nonvertical wells. *Ground Water, 51*(5), 745–751.
Williams, D. E. (2014). Subsurface intakes—Latest developments in slant well technology. *Proceedings of the AWWA/AMTA Membrane Technology Conference and Exposition, Las Vegas, Nevada*.

Chapter 14
Optimal Siting of Shallow Subsurface Intake Technologies

Scott A. Jenkins

Abstract Development of subsurface SWRO intake systems along the shoreline or in the nearshore environment requires careful evaluation before they can be successfully developed. These environments are zones of high energy and changes that impact the long-term viability of subsurface intake systems. A key aspect for evaluation is a detailed analysis of the sediment budget and transport system along the beach and nearshore environments. Erosion of the shoreline or rapid deposition could cause the failure of many subsurface intake systems, especially beach and offshore gallery intakes. Both the seasonal fluctuations in shoreline profiles and the long-term trends in sedimentation must be evaluated. Large capacity subsurface SWRO intake systems, such as that proposed at Huntington Beach, California, require an optimal siting and evaluation analysis to be conducted using modern modeling and analytical methods. A detailed summary of global littoral and nearshore processes as related to the design and construction of subsurface intake systems is presented with a detailed analysis showing how the natural system was evaluated to select a stable site for a seabed gallery (infiltration) system at Huntington Beach, California, which is a high energy shoreline that creates considerable challenges in siting and construction.

14.1 Introduction

In parts of the world where the political climate is hyper-sensitive to environmental concerns, (e.g., California), any subsurface intake that taps into deep coastal aquifers will probably have difficulty qualifying for environmental and development permits. This is due to water rights conflicts with existing groundwater programs and the potential for greenhouse gas emissions associated with extraction

S.A. Jenkins (✉)
Scripps Institution of Oceanography, University of California San Diego,
San Diego, CA, USA
e-mail: sjenkins@ucsd.edu

T.M. Missimer et al. (eds.), *Intakes and Outfalls for Seawater Reverse-Osmosis Desalination Facilities*, Environmental Science and Engineering,
DOI 10.1007/978-3-319-13203-7_14

from deep groundwater sources. Deep groundwater sources are cold and under high pressure and contain large quantities of dissolved CO_2 and methane (from the respiration of micro-organisms living in the aquifer sediments). These dissolved constituents subsequently out-gas from solution when the groundwater is recovered and exposed to the lower pressures and higher temperatures of surface conditions (Macpherson 2009; Kessler and Harvey 2001; Coudrain-Ribstein et al. 1998). Therefore we focus on shallow infiltration technologies that rely on minimal sediment cover (on the order of several meters) over the subsurface intake systems.

The characteristic of an optimal shallow subsurface intake site is one that is neither erosional nor depositional, and one that is within a feasible hydraulic pathway to the desalination facility. A feasible hydraulic pathway refers to one that is in reach of the desalination facility to accommodate hydraulic pressure losses with standard design practice, and one that can be built under the limitations of offshore construction methods. Finding such a site requires diagnosing the *sediment budget* of the *littoral cell* in which the desalination facility resides. A littoral cell is a coastal compartment that contains the complete cycle of sedimentation, including sources, transport paths, and sinks (Inman and Brush 1973). The cell boundaries delineate the geographical area within which the budget of sediment is balanced, thereby providing the framework for the quantitative analysis of coastal erosion and accretion. The sediment sources are commonly streams, sea cliff erosion, onshore migration of sand banks, beach disposal of dredge material (typically from harbor construction and maintenance dredging), and material of biological origin such as shells, coral fragments, and skeletons of small marine organisms. Typically, the infusion of new sediment from these sources is episodic and does not remain immobile, but migrates along the coast as *littoral drift*, and spreads out cross-shore throughout the shorezone of a littoral cell where the desalination facility is sited. The usual transport path is along the coast caused by waves and currents (longshore transport, longshore drift, or littoral drift). Cross-shore (on/offshore) paths may include windblown sand, over-wash, and offshore mining of beach nourishment material. The sediment sinks are usually offshore losses at submarine canyons and shoals or onshore dune migration, rollover, and deposition in bays, harbors and estuaries, (Fig. 14.1).

The boundaries between littoral cells are delineated by a distinct change in the longshore transport rate of sediment. For example, along mountainous coasts with submarine canyons, cell boundaries usually occur at rocky headlands that intercept transport paths (Fig. 14.1, upper panel). For these coasts, streams and cliff erosion are the sediment sources, the transport path is along the coast and driven by waves and currents, and the sediment sink is generally a submarine canyon adjacent to the rocky headland. In places, waves and currents change locally in response to complex shelf and nearshore bathymetry, giving rise to subcells within littoral cells. The longshore dimension of a littoral cell may range from one to hundreds of kilometers whereas the cross-shore dimensions are determined by the landward and seaward extent of the sediment sources and sinks.

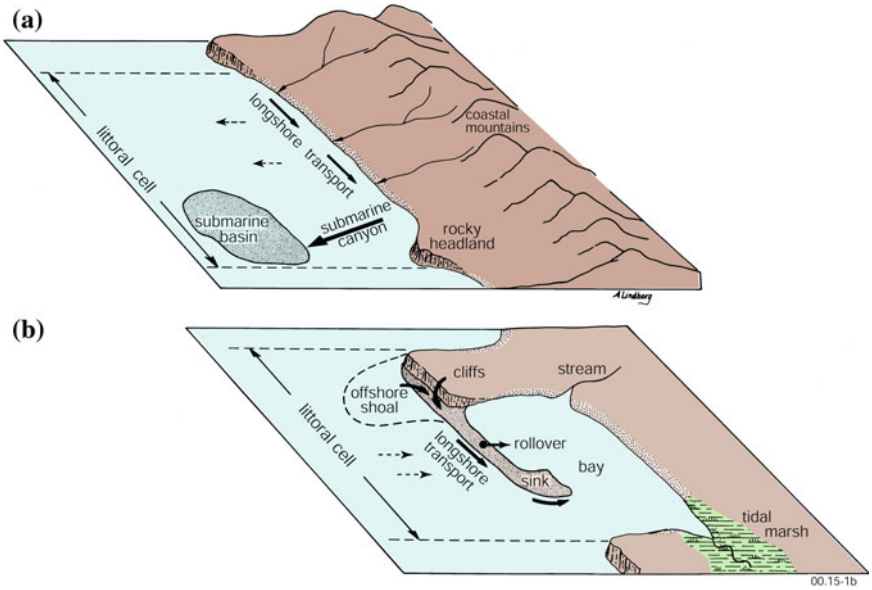

Fig. 14.1 Typical **a** collision and **b** trailing-edge coasts and their littoral cells. *Solid arrows* show sediment transport paths; *broken arrows* indicate occasional onshore and offshore transport modes (after Inman 1994)

14.2 Global Diversity of Littoral Cells

The configuration of littoral cells depends on the magnitude and spatial relations among the sediment sources, transport paths, and sinks. These in turn have been shown to vary systematically with coastal type. Because the large-scale features of a coast are associated with its position relative to the margins of the earth's moving plates, plate tectonics provides a convenient basis for the first-order classification of coasts (Inman and Nordstrom 1971; Davis 1996). This classification leads to the definition of three tectonic types of coast: (1) *collision coasts* that occur on the leading edge of active plate margins where two plates are in collision or impinging on each other, for example, the west coasts of the Americas; (2) *trailing-edge coasts* that occur on the passive margin of continents and move with the plate, for example, the east coasts of the Americas; and (3) *marginal sea coasts* that develop along the shores of seas enclosed by continents and island arcs, for example, coasts bordering the Mediterranean Sea, Red Sea and the South and East China Seas. It is apparent that the morphologic counterparts of collision, trailing-edge, and marginal sea coasts become, respectively, narrow-shelf mountainous coasts, wide-shelf plains coasts, and wide-shelf hilly coasts. However, some marginal sea coasts such as those bordering the Red Sea, Gulf of California, Sea of Japan and the Sea of Okhotsk are narrow-shelf, hilly, or mountainous coasts. A more complete coastal classification includes the latitudinal effects of climate and other coastal forming

processes such as reef-building organisms. The examples of the latter two coastal types described here are (4) coral reef form of *biogenic coasts*, and (5) arctic form of *cryogenic coasts.* Because sea ice is an easier alternative for source water than subsurface intakes, the cryogenic coasts will not be discussed further.

14.2.1 Collision Coasts

Collision coasts form at the active margins of the earth's moving plates and are represented by the mountainous west coasts of the Americas. These coasts are erosional and characterized by narrow shelves and beaches backed by wave-cut sea cliffs. Along these coasts with their precipitous shelves and submarine canyons, as in California, the principal sources of sediment for each littoral cell are the rivers that periodically supply large quantities of sandy material to the coast. The primary concern with a particular subsurface intake site on these types of coasts is the thickness of sediment cover, which is typically very thin (on the order of only several meters), other than in the neighborhood of a river mouth where paleo valleys have infilled with locally deep deposits of ancient fluvial sediments. The coarser sediments (primarily sand-size) are transported along the coast by waves and currents primarily within the surf zone like a *river of sand*, until intercepted by a submarine canyon. The canyon diverts and channels the flow of sand into the adjacent submarine basins and depressions (Fig. 14.1, upper panel). However, in southern California most coastal rivers have dams that trap and retain their sand supply. Studies show that in this area the yield of sediment from dredging projects, small streams and coastal bluff-lands has become a significant replacement for river sediment. Normal wave action contains sand against the coast and, when sediment sources are available, results in accretion of the shorezone. However, cluster storms associated with El Niño-Southern Oscillation events as occurred in 1982/83 produced beach erosion and broad-scale shorezone disequilibrium by downwelling currents that carried sand onto the shelf (Inman and Masters 1991). The downwelled sediment is lost from the shorezone when deposited on a steep shelf or it may be returned gradually from a more gently sloping shelf to the shorezone by wave action. The critical value of slope for onshore transport of sand by wave action varies with sand size, depth, and wave climate, but for depths of about 15–20 m it is approximately 1.5 % (1.0°).

14.2.2 Trailing-Edge Coasts

Trailing-edge coasts occur along the passive plate margins of continents and include the coasts of India and the east coasts of the Americas. The mid-Atlantic coast of the United States, with its wide shelf bordered by coastal plains, is a typical trailing-edge coast where the littoral cells begin at headlands or inlets and terminate at embayments and capes (Fig. 14.1, lower panel). This low-lying barrier island

coast has large estuaries occupying drowned river valleys. River sand is trapped in the estuaries and does not usually reach the open coast. For these coasts, the sediment source is from beach erosion and shelf sediments deposited at a lower stand of the sea, whereas the sinks are sand deposits that tend to close and fill estuaries and form shoals off headlands. The thickness of sediment cover is typically quite adequate for shallow subsurface intakes along these coasts; but can be quite variable relative to a given depth of system burial due to migrating large scale bedforms such as *sand waves*. Under the influence of a rise in relative sea level, the barriers are actively migrating landward by a rollover process in which the volume of beach face erosion is balanced by rates of overwash and fill from migrating inlets (e.g., Inman and Dolan 1989). For these coasts, the combination of longshore transport and rollover processes leads to a distinctively "braided" form for the *river of sand* that moves along the coast. The Outer Banks of North Carolina, made up of the Hatteras and Ocracoke Littoral Cells, extend for 320 km and are the largest barrier island chain in the world (Fig. 14.2). The Outer Banks are barrier islands separating Pamlico, Albemarle, and Currituck Sounds from the Atlantic Ocean. These barriers are transgressing landward with average rates of shoreline recession of 1.4 m/year between False Cape and Cape Hatteras. Oregon Inlet, the only opening in the nearly 200 km between Cape Henry and Cape Hatteras, is migrating south at an average rate of 23 m/year and landward at a rate of 5 m/year. The net southerly longshore transport of sand in the vicinity of Oregon Inlet is between one-half million and one million m^3/year. Averaged over the 160 km from False Cape to Cape Hatteras, sea level rise accounts for 21 % of the measured shoreline recession of 1.4 m/year. Analysis of the budget of sediment indicates that the remaining erosion of 1.1 m/year is apportioned among overwash processes (31 %), longshore transport out of the cell (17 %), windblown sand transport (14 %), inlet deposits (8 %), and removal by dredging at Oregon Inlet (9 %). This analysis indicates that the barrier system moves as a whole so that the sediment balance is relative to the moving shoreline. Application of a continuity model to the budget suggests that, in places such as the linear shoals off False Cape, the barrier system is supplied with sand from the shelf (Inman and Dolan 1989).

14.2.3 Marginal Sea Coasts

Marginal sea coasts front on smaller water bodies and are characterized by more limited fetch and reduced wave energy. Accordingly, river deltas are more prominent and are often important sources of sediment within the littoral cell. Elsewhere, barrier island rollover processes are similar to those for trailing edge coasts. Because of these types of depositional formations, thickness of sediment cover is not an issue for shallow subsurface intake technologies, although the grain size composition may be too fine to support high infiltration rates, and new deposition can easily defeat the higher infiltration rates of engineered fill over the subsurface intake systems.

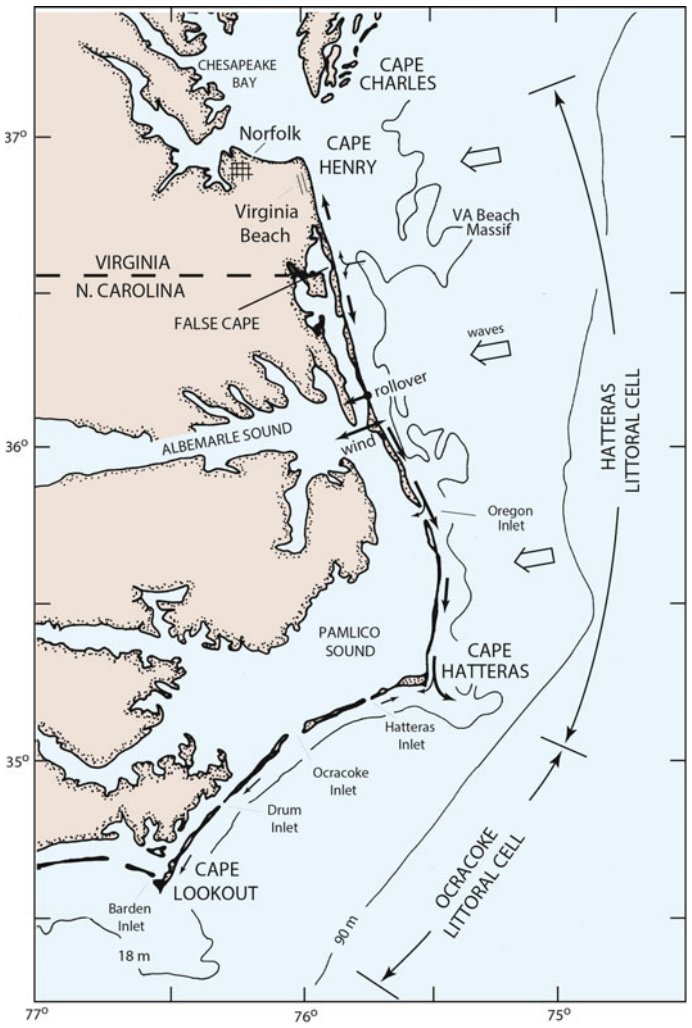

Fig. 14.2 Hatteras and Ocracoke littoral cells along the Outer Banks of North Carolina (after Inman and Dolan 1989)

Examples of marginal sea coasts include the shores of the Gulf of Mexico with the prominent Mississippi River delta, the seas bordering Southeast Asia and China with the Mekong, Huang (Yellow), and Luan river deltas, and the Mediterranean Sea coasts with the Ebro, Po, and Nile river deltas. Although the Mediterranean area is associated with plate collision, the sea is marginal with restricted wave fetch and prominent river deltas. The Nile littoral cell extends 700 km from Alexandria on the Nile Delta to Akziv Submarine Canyon near Akko, Israel, one of the world's longest littoral cells (Fig. 14.3). Before construction of the High Aswan Dam, the Nile Delta shoreline was in a fluctuating equilibrium between sediment supplied by

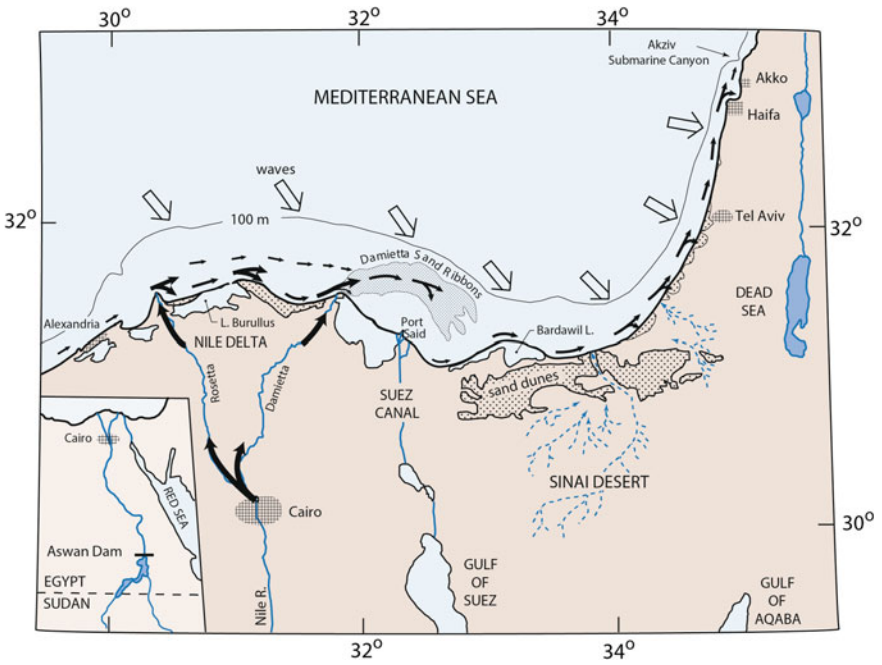

Fig. 14.3 The Nile littoral cell extends along the southeastern Mediterranean coast from Alexandria, Egypt to Akziv Submarine Canyon off Akko, Israel. Sediment transport paths shown by solid arrows (after Inman and Jenkins 1984)

the river and the transport along the coast. Now the sediment source is erosion from the delta, particularly the Rosetta promontory, in excess of 10 million m^3/year. The material is carried eastward in part by wave action but predominantly by currents of the east Mediterranean gyre that sweep across the shallow delta shelf with speeds up to 1 m/s. Divergence of the current down coast from Rosetta and Burullus promontories forms accretionary blankets of sand that episodically impinge on the shoreline. The sand blankets move progressively down coast at rates of 0.5–1 km/year in the form of accretion/erosion waves. Along the delta front, coastal currents augmented by waves transport over 10 million m^3/year, and the longshore sand transport by waves near the shore is about 1 million m^3/year (Inman and Jenkins 1984; Inman et al. 1992). The Damietta promontory causes the coastal current from the east Mediterranean gyre to separate from the coast and form a large stationary eddy that extends offshore of the promontory, locally interrupting the sediment transport path. The jet of separated flow drives a migrating field of sand ribbons northeasterly across the delta (Fig. 14.3). The ribbons arc easterly then southeasterly towards the coast between Port Said and Bardawil Lagoon (Murray et al. 1981). The Damietta sand ribbons form the eastern edge of a subcell within the Nile Littoral Cell. Off Bardawil Lagoon, the longshore sand transport is about 500,000 m^3/year and gradually decreases to the north with the northerly bend in

coastline. This divergence in the littoral drift of sand results in the buildup of extensive dune fields along the coasts of the delta, Sinai, and Israel. This sediment loss by wind- blown sand constitutes a major "dry" sink for sand in the Nile Littoral Cell.

14.2.4 Biogenic Coasts

Biogenic coasts are a subset of the broader category of *biogenous* coasts where the source of sediment and/or the sediment retaining mechanism is of biogenous origin as in coral reef, algal reef, oyster reef, and mangrove coasts. Coral reefs occur as fringing reefs, barrier reefs, and atolls and are common features in tropical waters of all oceans at latitudes within the 20 °C isotherm. Although the concept of the littoral cell applies to all types of biogenic coral reef coasts, the most characteristic are littoral cells along fringing reef coasts bordering high islands, where both terrigenous and biogenous processes become important. Reefs may be continuous along the coast or occur within embayments. In either case, the configuration of the fringing reef platforms themselves incorporates the nearshore circulation cell into a unique littoral cell (Fig. 14.4). The circulation of water and sediment is onshore over the reef and through the surge channels, along the beach toward the awas (return channels), and offshore out the awas. An awa is equivalent to a rip channel on the sandy beaches of other coasts (Inman et al. 1963). However, sediment cover is often very thin over underlying lithified reef structures, and in many places along

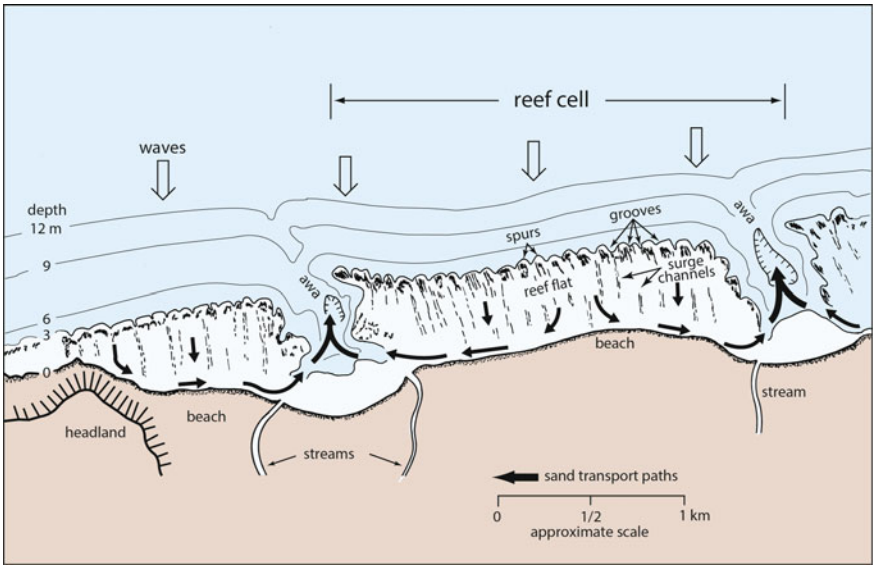

Fig. 14.4 Schematic diagram of littoral cells along a fringing reef coast (after Inman 1994)

the fringing reef systems may not be adequate to support shallow subsurface intakes, although the carbonate sediments are typically coarse and provide high infiltration rates for these kinds of buried systems.

Along biogenic coasts, the corals, foraminifera, and calcareous algae are the sources of carbonate sediment (as compared with quartz sediments more typical of collision, trailing edge coasts). The overall health of the reef community determines the supply of sedimentary material. Critical growth factors are light, ambient temperature, salinity, and nutrients. Turbidity and excessive nutrients are deleterious to the primary producers of carbonate sediments. On a healthy reef, grazing reef fishes bioerode the coral and calcareous algae and contribute sand to the transport pathway onto the beach. The beach behind the fringing reef acts as a capacitor, storing sediment transported onshore by the reef-moderated wave climate. It buffers the shoreline from storm waves and releases sediment to the awas. In turn, the awas direct runoff and turbidity away from the reef flats and out into deep water. Where the reef is damaged by excessive terrigenous runoff, waste disposal, or over-fishing, the continued local supply of carbonate sediments is imperiled.

14.3 Sediment Budget Boundary Value Problem

The sediment budget is a mass-balance boundary value problem in which the system boundaries are set by the littoral cell. The littoral cell is divided into a series of coupled computational cells referred to as *control cells*, (Fig. 14.5). Each control cell is a small coastal unit of uniform geometry where a balance is obtained between shoreline change and the inputs and outputs of mass and momentum. We sequentially integrate along-coast over these control cells in a down-drift direction so that the shoreline response of each cell is dependent on the exchanges of mass and momentum between cells, giving continuity of coastal form in the down-drift direction. Although the overall computational domain of the littoral cell remains constant throughout time, there is a different coastline position at each time step in sea level. The variation of the sediment cover with time is modeled by time-stepped solutions to the sediment continuity equation (otherwise known as the *sediment budget*) applied to the boundary conditions of the coupled control cell mesh diagramed schematically in Fig. 14.5. The sediment continuity equation is written (Jenkins et al. 2007):

$$\frac{\partial q}{\partial t} = \frac{\partial}{\partial y}\left(\varepsilon \frac{\partial q}{\partial y}\right) - V_l \frac{\partial q}{\partial y} + J(t) - R(t) \tag{14.1}$$

where q is the sediment volume per unit length of shoreline (m^3/m) and dq/dt is the sediment volume flux ($m^3/m/day$), ε is the mass diffusivity, V_l is the longshore current, $J(t)$, is the flux of new sediment into the littoral cell from watersheds or beach disposal of dredge material, and $R(t)$ is the flux of sediment lost to sinks. The first term in (14.1) is the surf diffusion term while the second is the advective term

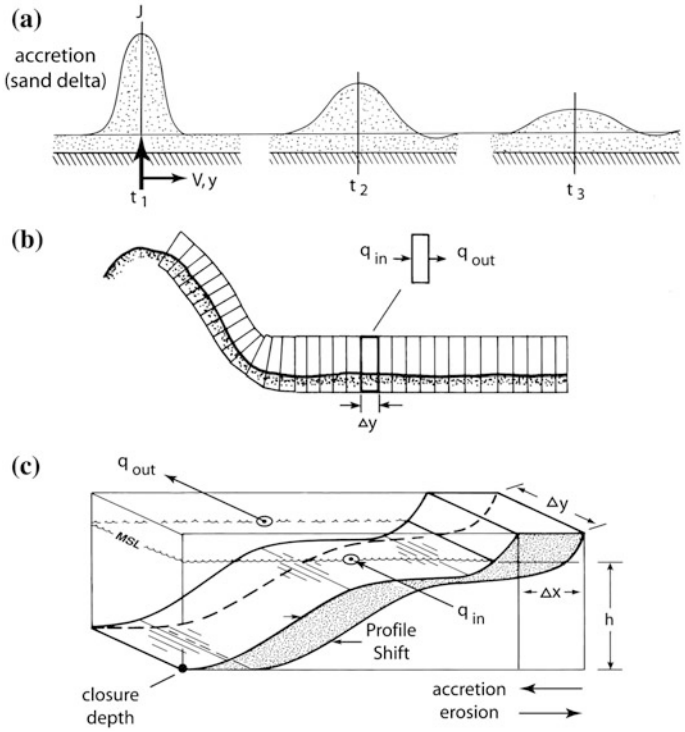

Fig. 14.5 Computational approach for modeling shoreline change (after Jenkins et al. 2007). **a** Accretion/Erosion wave. **b** Coupled control cells. **c** Profile changes

due to the longshore current. The net sediment volume flux out of or into a control cell (erosion or deposition, respectively) that results from the action of the advective term in Eq. (14.1) is related to the longshore transport rate Q_L by a functional known as the *divergence of drift*, $\nabla \cdot Q_L$, written as:

$$V_l \frac{dq}{dy} = \nabla \cdot Q_L \cong \int \frac{\partial Q_L}{\partial y} dy = KC_n \int \frac{\partial S_{yx}}{\partial y} dy \tag{14.2}$$

The formulation in Eq. (14.2) for the longshore transport rate of sediment, Q_L, due to the action of the longshore current, V_l, is taken from the work of Komar and Inman (1970) according to:

$$Q_L = K\left(C_n S_{yx}\right)_b \tag{14.3}$$

where C_n is the phase velocity of the waves; $S_{xy} = E \sin \alpha_b \cos \alpha_b$ is the along shore component of the onshore component of the radiation stress tensor; α_b is the breaker angle relative to the shoreline normal; $E = 1/8 \rho g H_b^2$ is the wave energy density;

ρ is the density of water; g is the acceleration of gravity; H_b is the breaking wave height; and, K is the transport efficiency equal to:

$$K = 2.2\sqrt{c_{rb}} \quad \text{with} \quad c_{rb} = \frac{2g\tan^2\beta_0}{H_b\sigma^2} \tag{14.4}$$

Here c_{rb} is the reflection coefficient which is calculated from the nearshore bottom slope, β_0 of the stationary bathymetry as determined from the break point coordinates and the position of the 0 MSL contour; and, σ is the radian frequency = 2π/T, where T is the wave period. The longshore transport velocity, $V_l = \overline{V_l(x)}$, is determined from the longshore current theories of Longuet-Higgins (1970), according to:

$$\bar{V}_l(x) = v_0\left(\frac{10x}{49X_b} - \frac{5}{7}\log\frac{x}{X_b}\right) \quad \text{if} \quad 0 \le x \le X_b \tag{14.5}$$

$$\bar{V}_l(x) = v_0\frac{10}{49}\left(\frac{x}{X_b}\right)^{5/2} \quad \text{if} \quad x > X_b \tag{14.6}$$

with:

$$v_0 = \frac{0.256\pi\beta}{C_D}\sqrt{gh_b}\sin\alpha_b \tag{14.7}$$

Here, X_b is the width of the surf zone derived from the coordinates of the break points (x_b, y_b) that are computed from numerical refraction/diffraction (REF/DIF) analysis. Highest rates of sediment flux are in the neighborhood of the break point, $(x = X_b)$, where the longshore currents approach a maximum value of $\bar{V}_l(x) = v_0$. These equations teach that the net erosion or deposition of sediment in a control cell due to advective transport by longshore currents (divergence of drift) is proportional to the along shore gradient of the radiation stress tensor component, $S_{xy} = E\sin\alpha_b\cos\alpha_b$, which is a quantity determined by directional wave climate and REF/DIF analysis. Positive values of radiation stress gradient indicate depositional tendencies, while negative values indicate erosion. Ideally, for a shallow subsurface intake site we seek sections of coast where the radiation stress gradient is small and trending to zero.

For any given control cell inside the littoral cell, Eq. (14.1) may be discretized in terms of the rate of change of cell sediment volume, Λ, in time increment Δt, given by:

$$\frac{d\Lambda}{dt} = \frac{q_{in} + q_{out}}{\Delta t} \tag{14.8}$$

Sediment is supplied to the control cell by the sediment influx from the up-drift control cell q_{in} while sediment is lost from the control cell due to the action of wave

erosion and expelled from the control cell by exiting littoral drift, q_{out}. Here fluxes into the control cell, $(q_{in}/\Delta t)$, are positive and fluxes out of the control cell, $(q_{out}/\Delta t)$, are negative.

The beach and nearshore sand volume change, dq/dt, is related to the change in shoreline position, dX/dt, according to:

$$\frac{dV}{dt} \cong \frac{d\Lambda}{dt} = \frac{dX}{dt} \cdot Z \cdot l \tag{14.9}$$

where: $Z = Z_1 + h_c$ and Z is the height of the shoreline flux surface equal to the sum of the closure depth below mean sea level, h_c, and the height of the berm crest, Z_1, above mean sea level; and l is the length of the shoreline flux surface (Fig. 14.5). Hence, beaches and the offshore bottom profile out to *closure depth* (the depth beyond which seabed profile change ceases) remain stable if a mass balance is maintained such that the terms on the right-hand side of Eq. (14.1) sum to zero; otherwise the shoreline will move during any time step increment as:

$$\Delta x(t) = \frac{1}{\Delta y(Z_1 + h_c)} \int \left(\frac{\partial}{\partial y} \left(\varepsilon \frac{\partial q}{\partial y} \right) - V \frac{\partial q}{\partial y} + J(t) \right) dt \tag{14.10}$$

where Δy is the alongshore length of the control cell, and Z_1 is the maximum run-up elevation from Hunt's Formula. River sediment yield, $J(t)$, is calculated from stream flow, Q_r, based on the power law formulation of that river's sediment rating curve after Inman and Jenkins (1999), or

$$J = \xi Q_r^{\omega} \tag{14.11}$$

Here, ξ, ω are empirically derived power law coefficients of the sediment rating curve from best fit (regression) analysis (Inman and Jenkins 1999). When river floods produce large episodic increases in $J(t)$, a river delta is initially formed. Over time the delta will widen and reduce in amplitude under the influence of surf diffusion and advect (move) down-coast with the longshore drift, forming an accretion erosion wave (Fig. 14.5, panel-a). The local sediment volume varies in response to the net change of the volume fluxes as this accretion erosion wave passes by as a consequence of divergence of drift, (see Fig. 14.5 panels-b and -c). The mass balance of the control cell responds to a non-zero divergence of drift with a compensating shift, Δx, in the position of the equilibrium profile (Jenkins and Inman 2006). This is equivalent to a net change in the beach entropy of the equilibrium state. The rate of change of volume flux through the control cell causes the equilibrium profile to shift in time according to Eq. (14.10). Therefore the time evolution of the equilibrium profiles between control cells becomes the controlling factor in the erosional or depositional states of the local shorezone.

14.4 Seasonal Equilibrium Bottom Profiles

It is well known that beach and nearshore bottom profiles change seasonally in response to seasonal wave climate variations as shown in Fig. 14.6, (Inman et al. 1993; Jenkins and Inman 2006); and that seasonal transitions between summer and winter equilibrium states cause seasonal changes in the mean shoreline, Eq. (14.10). Short period waves during summer cause the inner bar-berm section of the beach profile to build up and steepen; while long period storm swells during winter cause the bar-berm profile to flatten, and transfer beach sand to the outer shore-rise profile. These changes between summer and winter equilibrium states are predicted from long-term wave records applied to the well-tested elliptic cycloid solutions published in Jenkins and Inman (2006). The elliptic cycloid solutions were developed for beach profiles using equilibrium principles of thermodynamics applied to very simply representations of the nearshore fluid dynamics. Equilibrium beaches are posed as isothermal shorezone systems of constant volume that dissipate external work by incident waves into heat given up to the surroundings. By the maximum entropy production formulation of the *second law of thermodynamics* (the law of entropy increase), the shorezone system achieves equilibrium with profile shapes that maximize the rate of dissipative work performed by wave-induced shear stresses. Dissipative work is assigned to two different shear stress mechanisms prevailing in separate regions of the shorezone system, an outer solution referred to as the *shorerise* and a *bar-berm* inner solution. The equilibrium shorerise solution extends from closure depth (zero profile change) to the breakpoint, and maximizes dissipation due to the rate of working by bottom friction. In contrast, the equilibrium bar-berm solution between the breakpoint and the berm crest maximizes dissipation due to work by internal stresses of a turbulent surf zone. Both shorerise and bar-berm equilibria were found to have an exact general solution belonging to the class of elliptic cycloids.

To understand the formulation of the elliptic cycloid representation of the nearshore bottom profile and sensitivity to ocean conditions, we first review the nomenclature of the shorezone as shown schematically in Fig. 14.7a. The seaward boundary of the shorezone is a vertical plane at the critical closure depth $\hat{h}_c$

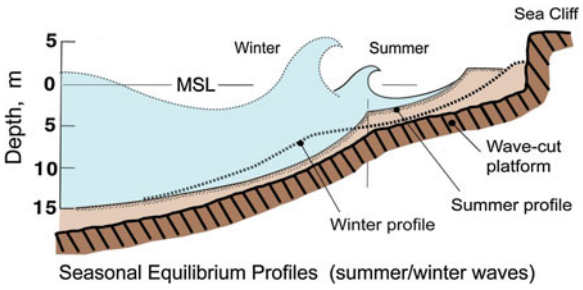

Fig. 14.6 Schematic of summer and winter equilibrium beach profiles (from Inman et al. 1993)

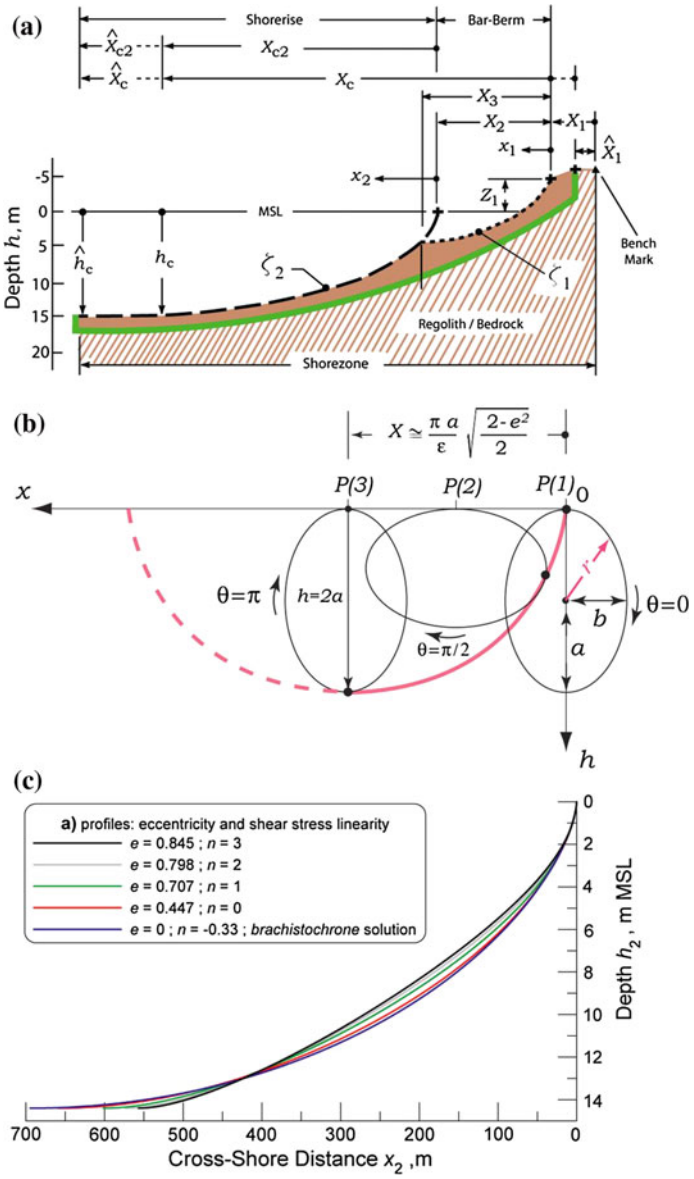

Fig. 14.7 Equilibrium bottom profile: **a** nomenclature, **b** elliptic cycloid, **c** type-a cycloid solution

(Fig. 14.7a,) corresponding to the maximum incident wave (e.g., Kraus and Harikai 1983). The landward boundary is a vertical plane at the berm crest (cross), a distance $\hat{X}_1$ from a bench mark. The cross-shore length of the system from the berm crest to closure depth is $\hat{X}_c$. The distance from the point of wave breaking to closure

depth is $\hat{X}_{c2}$ such that $\hat{X}_c = \hat{X}_{c2} + \hat{X}_2$, where $\hat{X}_2$ is the distance from the berm crest to the origin of the shorerise profile near the wave breakpoint. We consider equilibrium over time scales that are long compared with a tidal cycle and profiles that remain in the wave dominated regime where the relative tidal range (tidal range/H) <3 (Short 1999). Under these conditions, the curvilinear solution to the bottom profile which satisfies the maximum entropy production formulation of the *second law of thermodynamics* can be expressed in polar coordinates (r, θ) as:

$$x = x_2 = \frac{2rI_e^{(k_{1,2})}}{\pi\varepsilon}(\theta - \sin\theta) \tag{14.12}$$

where r is the radius vector measured from the center of an ellipse whose semi-major and semi-minor axes are a, b and $I_e^{(k)}$ is the elliptic integral of the first or second kind. This curve is what a point on the circumference of an ellipse would trace by rolling through some angle θ, (Fig. 14.7b); hence the name elliptic cycloid. The polar equivalent of the type-a cycloid shown in Fig. 14.7c has a radius vector whose magnitude is:

$$r = r_a = \left[\frac{a^2b^2}{a^2\sin^2\theta + b^2\cos^2\theta}\right]^{1/2} = \frac{a\sqrt{1-e^2}}{\sqrt{\sin^2\theta + (1-e^2)\cos^2\theta}} \tag{14.13}$$

where $a = h_c/2$; e is the eccentricity of the ellipse given by $e = \sqrt{1-(b^2/a^2)}$; and h_c is the closure depth (see next section). The eccentricity is proportional to the degree of non-linearity of the shear stress that is performing the dissipative work in the wave shoaling zone according to:

$$\begin{aligned} \tilde{\tau} &= \tau_0 \cos(\sigma t - kx + \varphi) \\ \tau_0 &= \rho c_f u_m^2 = \rho K_\tau u_m^n \end{aligned} \tag{14.14}$$

where τ_0 is the shear stress amplitude; φ is the phase angle between the bottom shear stress and the oscillatory potential flow velocity from Airy theory; c_f is the quadratic drag coefficient and n is the shear stress velocity exponent of the oscillatory velocity amplitude u_m. With this formulation for shear stress, the eccentricity becomes:

$$e = \left[1 - \frac{4}{(3n+5)}\right]^{1/2} \tag{14.15}$$

The polar form of the type-a cycloid in Fig. 14.7b, c is based on the elliptic integral of the second kind that has an analytic approximation, $I_e^{(2)} = (\pi/2)\sqrt{(2-e^2)/2}$, (see Hodgman 1947). The inverse of Eq. (14.15) for the

type-a elliptic cycloid gives the companion solution in terms of local water depth, h, as:

$$h = h_2 = \frac{\pi \varepsilon x_2}{2I_e^{(k_{1,2})}} \left(\frac{1 - \cos\theta}{\theta - \sin\theta} \right) = r(1 - \cos\theta) \tag{14.16}$$

The depth of water at the seaward end of the profile ($\theta = \pi$) is $h = 2a$ in the case of the type-a cycloid. The length of the profile X is equal to the semi-circumference of the ellipse,

$$X = \frac{2aI_e^{(2)}}{\varepsilon} \cong \frac{\pi a}{\varepsilon} \sqrt{\frac{2 - e^2}{2}} \quad \text{at} \quad \theta = \pi \quad \text{(type-a cycloid)} \tag{14.17}$$

The elliptic cycloids given by Eqs. (14.12)–(14.17) specify the bottom profile along the shore-normal boundary of each control cell, (cf., Fig. 14.5c).

14.5 Closure Depth

Closure depth is the most important parameter in the optimal siting of a shallow subsurface intake system. Closure depth represents the closest point to the shoreline where a stable seabed can be found, because it is the point beyond which all changes in the bottom profiles cease. It also represents the outer limit of the *critical mass*, the physical mass of sediment cover that can potentially be eroded or accreted over time. If a shallow infiltration gallery (SIG) were located inshore of closure depth, the engineered fill would suffer seasonal or episodic erosion, and subsequently be replaced by seasonal or episodic deposition of native sediments whose grain size may or may not be compatible with the original engineered fill material.

The closure depth relation is based on two premises: (1) closure depth is the seaward limit of non-zero net transport in the cross-shore direction; and, (2) closure depth is a vortex ripple regime in which no net granular exchange occurs from ripple to ripple. Inman (1957) gives observations of stationary vortex ripples in the field and Dingler and Inman (1976) establish a parametric relationship between dimensions of stationary vortex ripples and the Shield's parameter $\tilde{\Theta}$ in the range $3 < \tilde{\Theta} < 40$. Using the inverse of that parametric relation to solve for the depth gives (Jenkins and Inman 2006):

$$h_c = \frac{K_e H_\infty}{\sinh kh_c} \left(\frac{D_o}{D_2} \right)^{\psi} \tag{14.18}$$

where K_e and ψ are non-dimensional empirical parameters, D_2 is the shorerise median grain size; and D_o is a reference grain size. With $K_e \sim 2.0$, $\psi \sim 0.33$ and $D_o \sim 100\,\mu m$, the empirical closure depths reported in Inman et al. (1993) are

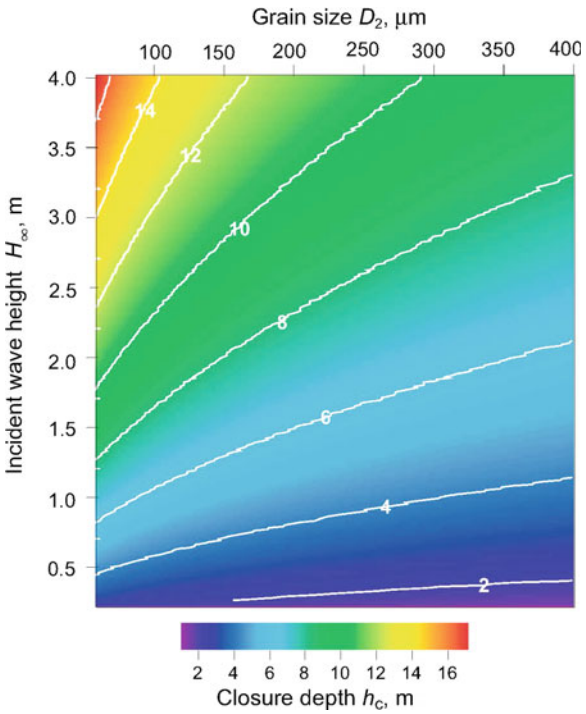

Fig. 14.8 Closure depth contoured versus incident wave height and sediment grain size for waves of 15 s period, with $K_e \sim 2.0$, $\psi \sim 0.33$ and $D_o \sim 100\,\mu m$. D_2 is the shorerise median grain size; and D_o is a reference grain size

reproduced by Eq. (14.18). From (14.18) we find closure depth increases with increasing wave height and decreasing grain size, as shown in Fig. 14.8. Because of the wave number dependence of (14.18), closure depth also increases with increasing wave period. Using Eq. 14.18, the distance to closure depth X_{c2} can be obtained from (Jenkins and Inman 2006),

$$X_{c2} = \frac{h_c I_e^{(2)}}{\varepsilon} \cong \frac{\pi h_c}{2\varepsilon}\sqrt{\frac{2-e^2}{2}} \tag{14.19}$$

where X_{c2} is measured from the origin of the shorerise located a distance X_2 from the berm and a distance $X_3 - X_2$ inside the breakpoint (Fig. 14.7a), $I_e^{(2)}$ is the elliptic integral of the second kind, and ε is a stretching factor proportional to the Airy wave mild slope factor N, and

$$\varepsilon = \frac{\sigma}{N}\left(\frac{H_b}{\gamma g}\right)^{1/2} \cong \frac{\sigma^{4/5}}{2^{1/5}N}\left(\frac{H_\infty}{g\gamma}\right)^{2/5} \tag{14.20}$$

14.6 Critical Mass of Sediment

When a long term collection of summer and winter equilibrium bottom profiles are superimposed for a broad range of wave heights, a well-defined envelope of variability, referred to as the *critical mass*, becomes apparent, as illustrated in Fig. 14.9. The critical mass represents the minimum volume of sediment cover required to maintain equilibrium bottom profiles and a stable seabed over the long-term, (where long-term is on the order of decades). The critical mass also determines the volume of engineered fill for a subsurface intake that can potentially be eroded and destroyed by the action of seasonal and episodic profile change or shoreline recession.

Generally, changes in profile shape between equilibrium states involve transitional shapes that are non-equilibrium in form. However, as a first order approximation, we assume the critical mass envelope consists of a set of incremented equilibrium profiles, (colored lines in Fig. 14.9) and the associated set of transitional profiles occurring between successive equilibrium states. Each profile in this set corresponds to a particular rms breaker height, H_b, that varies between some seasonal minimum H_{b0} and the critical maximum wave height $\hat{H}_b$, the highest wave condition for which the existing sand supply can accommodate equilibrium and transitional profile adjustments. The equilibrium profiles are incremented by infinitesimal changes in wave height, $H_{b0} \leq H_b + dH_b \leq \hat{H}_b$, giving a continuous envelope of beach profile change. The volume of this envelope can be calculated

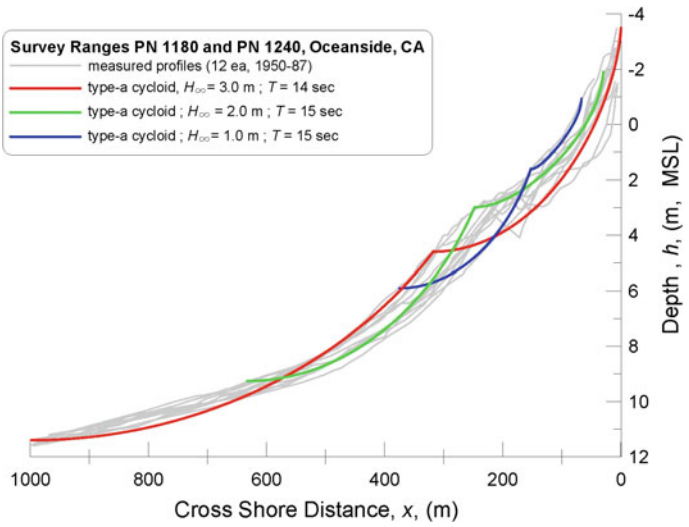

Fig. 14.9 Envelope of variability of measured beach profiles (1950–1987) at Oceanside CA (shown in *grey*), compared to an ensemble of elliptic cycloid solutions (*colored*) for selected wave heights and periods for average summer and winter wave climate (from Jenkins and Inman 2006)

from the elliptic cycloid solutions for the bar-berm profile and the shorerise profile to solve for the volume of critical mass, V_c, per meter of shoreline (m^3/m):

$$V_c = \int_{H_\infty}^{\hat{H}_b} \int_{X_1}^{X_3} \frac{\partial \zeta_1}{\partial H_b} dx dH_b + \int_{H_\infty}^{\hat{H}_b} \int_{X_3}^{X_c} \frac{\partial \zeta_2}{\partial H_b} dx dH_b \tag{14.21}$$

Analytic solutions to V_c are difficult because the thermodynamic solutions in curvilinear coordinates using elliptic cycloids are transcendental. Therefore solutions for the V_c envelope are obtained by numerical integration of (14.20) based on long term wave climate. Figure 14.10 gives the critical mass solution resulting from numerical integrations of (14.21). Because equilibrium and transitional profiles are grain size dependent through the closure depth condition, the volume of critical mass has a certain degree of sensitivity to grain size. Sensitivity analyses of (14.21) based on numerical integration show that finer grain sizes, particularly in the shorerise, tend to result in larger volumes of critical mass. However, the sensitivity of the volume of critical mass to grain size is second order relative to the dependence on wave height and period. A polynomial fit to the wave height dependence averaged over all grain sizes gives the following analytic approximation:

$$V_c \cong 500 H_b^{0.9} \tag{14.22}$$

where $\hat{H}_b$ is in meters, giving V_c in m^3 per meter of beach length.

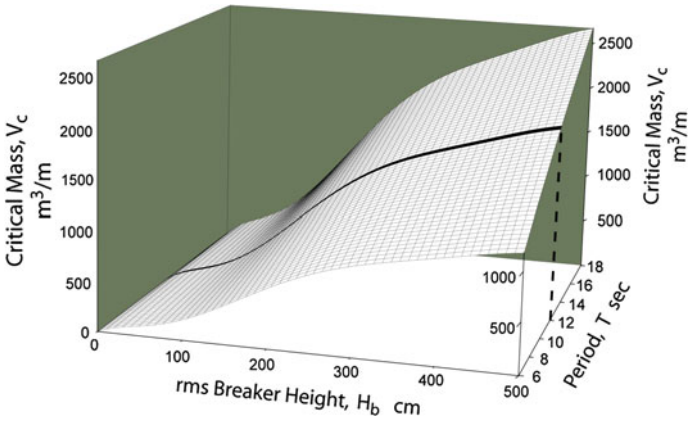

Fig. 14.10 Three-dimensional rendering of the total solution space of the critical mass. *Black line* corresponds to the solution in for D_1 = 225 microns and D_2 = 125 microns

14.7 Optimal Siting Example

This example seeks an optimal site for a seabed infiltration gallery (SIG) that can provide 480,000 m^3/d (127 million gallons) of feed water for the Huntington Beach Desalination Facility (HBDF), co-located with the AES Huntington Beach Generating Station (AES). Finding such a site in Huntington Beach is particularly challenging because it is located in the lower reach of the San Pedro Littoral Cell, between Anaheim Bay and the Santa Ana River (Fig. 14.11). The San Pedro Littoral cell resides on the collision coast of the Southern California Bight, and is not an ideal place to look for a SIG site because it is an intrinsically erosional section of coast, a characteristic aggravated by numerous flood works, coastal harbors and other hardened structures. For the last 50 years, the U.S. Army Corps of Engineers and the United States Congress has attempted to forestall this erosional trend with *San Gabriel River to Newport Bay Erosion Control Project*, which has placed 12.9 million m^3 (16.9 million cubic yards) of quasi beach-grade sediment at the northern end of this sub-cell at Surfside and Sunset beaches. This vast infusion of new sediment does not remain immobile, but migrates from north to south as *littoral drift*, and spreads out along the shorezone of Huntington Beach and the site of the HBDF. In addition, the HBDF is in close proximity to another major source of sediment, the Santa Ana River, (Fig. 14.12).

The advective (divergence of drift) term of Eqs. (14.1) and (14.2) is decisive to the SIG siting analysis because it is the mechanism that spreads out the large volumes of river deposition and beach-fill over many kilometers of coastline in southern portion of the San Pedro Littoral Cell between Anaheim Bay and the Santa Ana River. Divergence of drift and surf diffusion are wave driven, and their magnitudes and variations from place to place in the San Pedro Littoral Cell depend

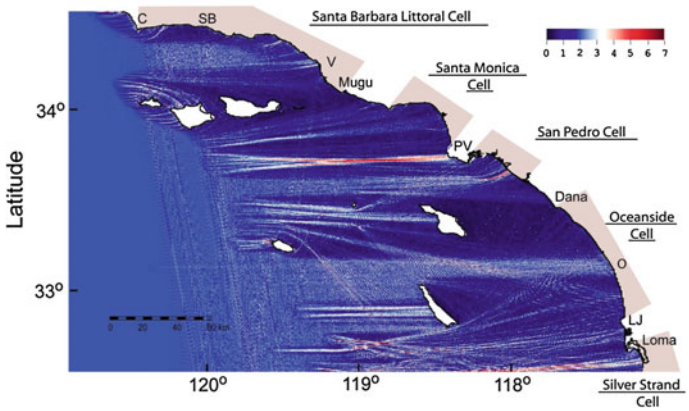

Fig. 14.11 Refraction/Diffraction pattern of the 5 largest storms to enter the Southern California Bight during the 1998 El Nino winter, showing the local intensification of wave energy (refraction bright-spot) in the southern portion of the San Pedro Littoral Cell

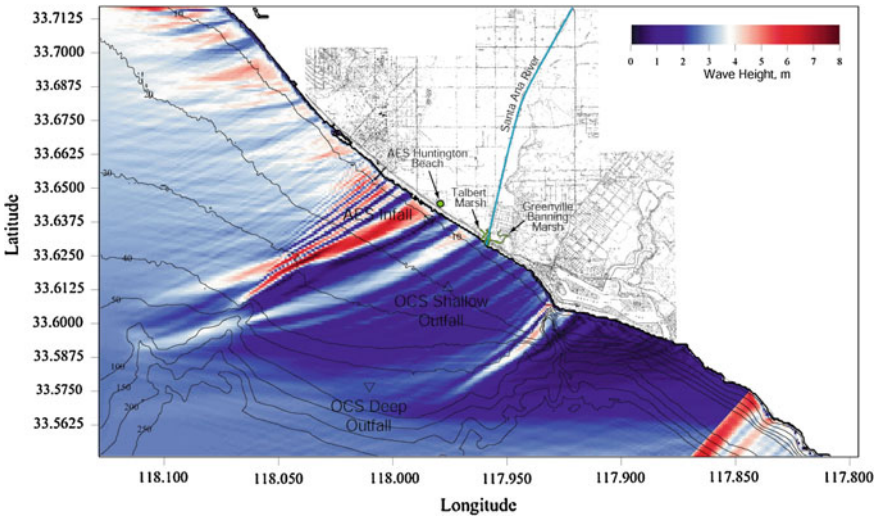

Fig. 14.12 Refraction/Diffraction pattern in over the San Pedro Littoral Cell due to the 5 largest storms during the 1998 El Nino winter, showing location of the Huntington Beach Desalination Facility (HBDF), co-located with the AES Huntington Beach Generating Station northwest of the Santa Ana River

on the wave refraction/diffraction pattern of the general region, beginning with the initial approach of waves into the Southern California Bight from distant storms. Figure 14.11 shows computations of the refraction/diffraction patterns of the 5 largest storms to enter the Southern California Bight during the 1998 El Nino winter. Many areas of the Bight are sheltered from these waves by the break-water effect of the offshore islands (referred to as *island sheltering*); but there is a significant gap between Catalina Island and the Channel Islands that leaves the southern portion of the San Pedro Littoral Cell open to waves from the west and north west, while waves approaching from southern hemisphere storms and Mexican hurricanes can freely travel inside of Catalina and San Clemente Islands to arrive at Huntington Beach. Of particular interest in Fig. 14.11 is the formation of a beam intensified of wave energy (refraction bright- spot, appearing as red), that begins at a twisted shoal in the outer continental margin and focuses wave energy on the southern portion of the San Pedro Littoral Cell. This bright spot is a one of several causal factors leading to the erosion problems experienced in the lower San Pedro Littoral Cell over the last 50 years, and is natural factor that has conspired with man's structural intervention in this region of the Bight that motivate Congress to authorize the on-going *San Gabriel River to Newport Bay Erosion Control Project*.

Zooming in on local wave shoaling tendencies in the lower San Pedro Littoral Cell, Fig. 14.12 shows the refraction/diffraction patterns of the same 5 largest storms during the 1998 El Nino winter that were mapped in Fig. 14.11 for the broad scale Bight. The refraction/diffraction pattern in Fig. 14.12 reveals that an abrupt

narrowing of the continental shelf seaward of the Huntington Beach Pier, (creating a large dog-leg in the −40 to −250 m depth contours), gives rise to an inner beam of intensified wave energy (red bright spot), that doubles shoaling wave heights between the Huntington Beach Pier and the AES Huntington Beach Generating Station. Immediately south of this bright spot, there is an area of greatly diminished wave energy (blue shadow zone) extending about a kilometer to the south of the AES property boundary. Additional bright spots in Fig. 14.12 are found at numerous places north of the Huntington Beach Pier up to Surfside Beach at Anaheim Bay. These bright spots at and to the north of the Huntington Beach Pier are consistent with its legacy reputation of Huntington Beach as *Surf City*, where numerous surfing championships have been held in the last 50 years.

Refraction/diffraction calculations were made over the January 1980–July 2000 period of record, from which the littoral drift parameters of longshore current, radiation stress, and radiation stress gradients were obtained for 167 coupled control cells along a 15 km reach of coast between the entrance to Anaheim Bay and the mouth of the Santa Ana River. Inputs for controlling variables in Eqs. (14.1)–(14.22) included CDIP monitored waves at Huntington Beach (CDIP 2001), grain size distributions (USACE 2001), Santa Ana River and San Gabriel River sediment flux from USGS (2001), and beach disposal of dredge material from the San Gabriel River to Newport Bay Erosion Control Project (USACE 1994; Shad and Ryan 1996; Weigel 2009; Gadd et al. 2006). These littoral drift parameters were averaged over the 20.6 year period of record and their variation along the coast is plotted in Fig. 14.13 in terms of distance from the Santa Ana River. Dashed red first-order trend lines are also overlaid on these plots. Several striking trends are revealed.

The variation of the longshore current is plotted in the upper panel of Fig. 14.13. The dashed trend line indicates the long-term average longshore current is on the order of 25–35 cm/s, and is directed toward the south everywhere from the receiver beaches at Sunset Beach down to the Santa Ana River. The longshore current will move (advect) sediment (primarily beach sands) by two transport mechanisms: suspended load transport where sand moves in suspension in the water column; and bedload transport where sand moves in traction along the seabed. Abrupt decelerations in the longshore current indicate locations of chronic rip currents, the best known of which is found immediately south of the Huntington Beach Pier, and is often exploited by surfers to access the breaker line-up. There is also another chronic rip current area in the neighborhood of the AES/HBDF where another noticeable deceleration in lonshore current speed is found. Longshore currents tend to be 10 cm/s stronger at the north end of this sub-cell, in the neighborhood of the Sunset and Surfside receiver beaches. This southerly persistence and the up-drift intensification indicates that, over time, the longshore current will induce potential transport of beach fill down-coast from Sunset and Surfside receiver beaches, dispersing it across other portions of shore zone to the south. This is confirmed by the long-term average of the radiation stress in the middle panel of Fig. 14.13. The radiation stress is proportional to the littoral drift, and its trend line is positive, indicating southward-directed transport everywhere between the receiver beaches to

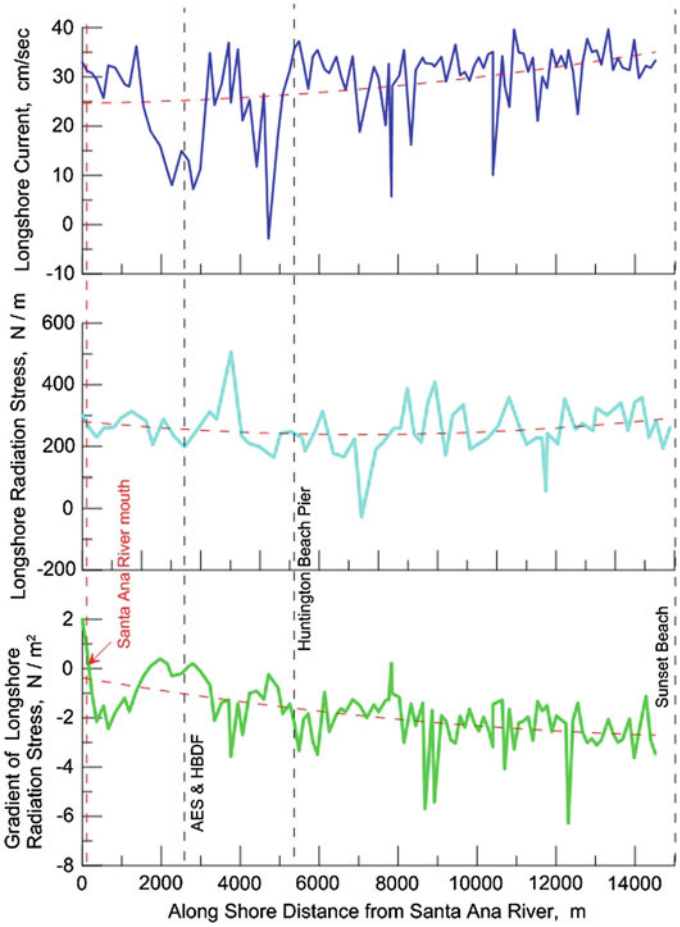

Fig. 14.13 Littoral drift parameters at 167 locations between the Santa Ana River and Sunset Beach, calculated over the 20.6-year period of record (1980–2000). *Upper panel*: longshore current (positive toward the south, negative toward the north). *Middle panel*: Radiation stress (positive toward the south, negative toward the north). *Lower panel*: gradient of longshore radiation stress (positive values are depositional and negative values are erosional)

the north, down-coast to the Santa Ana River to the south. This is a consequence of the beam of intensified wave energy that is formed in the refraction pattern beginning at the continental margin in the gap between Catalina Island and the Channel Islands (Fig. 14.11), and strikes the coast of the lower San Pedro Littoral Cell at a very oblique southward directed angle, thereby producing the significant southward directed (positive) component of the radiation stress throughout the region. The dashed trend line indicates the long-term average radiation stress on the order of 250–300 N/m. The alongshore continuity of the long-term average radiation stress indicates that the net littoral drift is a one-way, unidirectional transport

stream, a *river of sand* so to speak, flowing away from sediment sources of the receiver beaches at Surfside and Sunset, and flowing toward the Santa Ana River and the regional sediment sink a short distance beyond that is the Newport Submarine Canyon.

The gradient of the radiation stress in the lower panel of Fig. 14.13 adds another wrinkle to this transport mechanism. The radiation stress gradient is the dominant factor in determining the magnitude and sign of the divergence of drift. The trend line of the radiation stress gradient has a similar form as that for the longshore current, and is strongly negative in the northern end of the sub-cell indicating the receiver beaches near Anaheim Bay are erosional. This underscores the need for the continuance of the San Gabriel River to Newport Bay Erosion Control Project; because without the beach re-nourishment cycles under this program, the strong negative gradient of radiation stress in the neighborhood of Surfside and Sunset Beaches assures these beaches will be lost. The condition for *loss* of these beaches occurs after they erode to the point to where they no longer retain enough sediment to meet the required critical mass, whence they can no longer support a profile at equilibrium (Jenkins and Inman 2006). If that happens an *erosion wave* will develop and propagate southward, destabilizing other beaches of the Huntington Beach community (Inman and Jenkins 2004). This propagating erosion wave is supported by the fact that Fig. 14.13 shows the radiation stress gradient remains negative (erosional) long about 80 % of the coast south of Anaheim Bay and only begins to trend neutral to positive along the remaining reach of coast approaching the Santa Ana River.

Of particular interest to the problem at hand is the feature in the long-term gradient in radiation stress (Fig. 14.13) that trends weakly negative to neutral in the southern 20 % of the San Pedro Littoral Cell. It is here that the AES and HBDF facilities are located. In the lower panel of Fig. 14.13, the gradient in radiation stress approaches zero along a 1500 m section of coast near the AES/HBDF facility. This condition is referred to as *non-divergent littoral drift* and indicates a stable, steady-state condition that is neither erosional nor depositional, an optimal condition of a SIG site. To the south of this area, the gradient in radiation stress turns positive at the Santa Ana River indicating deposition; and to the north, the gradient in radiation stress is negative indicating erosional.

With this insight, we now turn to nested solutions to Eqs. (14.1)–(14.22) using a high-resolution inner grid with 180 coupled control cells along a 5.4 km reach of coast between Huntington Beach Pier and the mouth of the Santa Ana River. In this inner grid we perform the more complex calculations for sediment volume flux solutions to Eq. (14.1) for the complete sediment budget. Divergence of drift with its radiation stress gradient factor is only one of 4 terms contributing to sediment volume flux solution. Figure 14.14 gives the solution for the daily sediment volume flux between the Santa Ana River and the Huntington Beach Pier averaged over the 20.6-year period of record (1980–2000). Inspection of Fig. 14.14 reveals the sediment volume flux trends to zero over a 1300 m reach of coast in the neighborhood of the AES and HBDF facilities, indicating this section of coast is stable with minimal erosional or depositional tendencies. Among other lesser factors, this

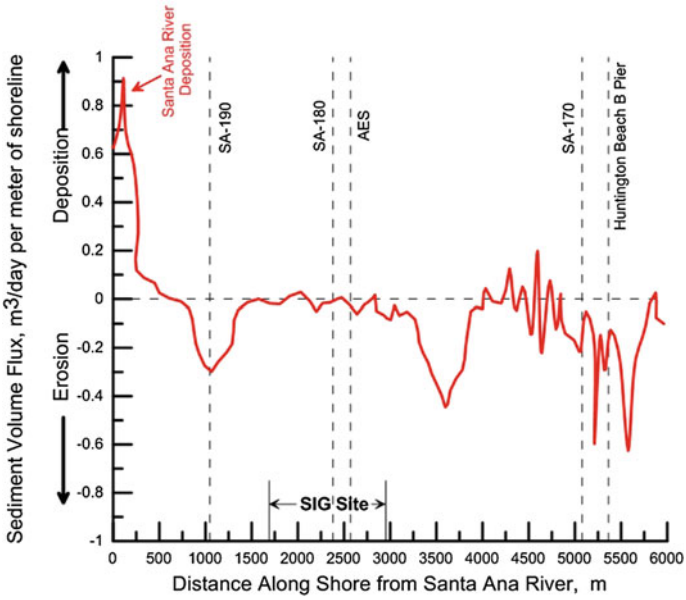

Fig. 14.14 Daily sediment volume flux, dq/dt, calculated by the calibrated from Eq. (14.1) and averaged over the 20.6-year period of record (1980–2000) for CDIP monitored waves at Huntington Beach (CDIP 2001), given grain size distributions after USACE 2001, Santa Ana and San Gabriel River sediment flux (USGS 2001), and beach disposal of dredge material from the San Gabriel River to Newport Bay Erosion Control Project, (USACE 1994; Shak and Ryan 1996; Weigel 2009)

condition arising at this particular location because the divergence of drift is almost nil, i.e., the same amount of littoral drift that arrives at the northern edge of this region also exits this region at the southern edge. Nowhere else is this stable condition found within 2.5 km to the north or to the south of the AES and HBDF facilities, (the practical maximum hydraulic path length of a gravity fed SIG). North or south of the potential SIG site identified in Fig. 14.14, there are erosional and depositional regions, interspersed at the cross-over points by very short segments of coastline with zero sediment volume flux. However, these cross-over coastal segments between depositional and erosional areas do not embrace sufficient coastline length for a usable SIG site. Also, the magnitudes of the non-zero sediment volume fluxes in these neighboring erosional or depositional areas are significant. When factored over 20 years, these non-zero sediment volume fluxes accumulate to 2000–4000 m^3 per meter of coast, on the order of all the total sediment volume in a critical mass envelope.

The results in Figs. 14.13 and 14.14 identify the location of a potential SIG site along the coastline, but do not provide guidance on how far offshore that site must be for a stable seabed. For that guidance we turn to the closure depth and critical mass solutions. Fortuitously, the potential SIG site is approximately bisected by one

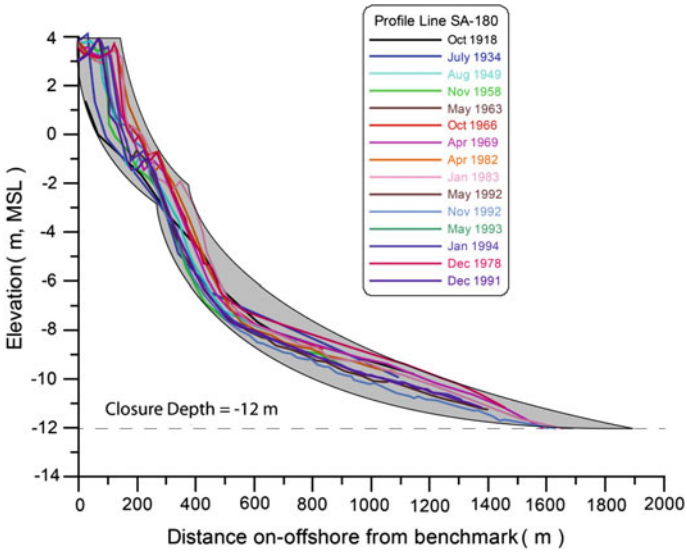

Fig. 14.15 Critical mass envelope at historic US Army Corps of Engineers survey range, SA-180, calculated by Eq. (14.14) for the 20.6-year period of record (1980–2000) for CDIP monitored waves at Huntington Beach, given grain size distributions after USACE (2001), Santa Ana and San Gabriel River sediment flux (USGS 2001), and beach disposal of dredge material from the San Gabriel River to Newport Bay Erosion Control Project, (USACE 1994; Shak and Ryan 1996; Weigel 2009). Measured beach profiles from USACE (1994). Closure depth = −12 m MSL calculated from Eq. (14.11). Critical mass volume = 2,845 m^3 per meter of shoreline calculated from Eq. (14.14)

of the historic US Army Corps of Engineers survey ranges, SA-180, that has been monitored between 1918 and 1994, with 7 profiles measured within the CEM 1980–2000 simulation period (Fig. 14.15). This overlap provides very high confidence to the solutions for closure depth and critical mass at the potential SIG site. Based on 7,523 solutions over the 1980–2000 simulation period, the Eq. (14.11) calculates in Fig. 14.15 that closure depth at SA-180 is at −12 m MSL, indicating that the SIG should be placed no closer to shore than the −12 m depth contour. The shoreward edge of its footprint should parallel the −12 m depth contour to avoid alongshore hydrostatic pressure gradients forming between the northern and southern ends of the infiltration gallery. Shoreward of the −12 m depth contour, Eq. (14.14) calculates that as much as 2,845 m^3 of sediment volume for every meter of shoreline (critical mass) may become unstable due to seasonal and episodic bottom profile changes, typically involving seasonal erosion in winter and deposition in summer. The maximum thickness of the critical mass envelope is 4.75 m in the surfzone, but most of this unstable layer of seabed is 1–2 m thick seaward of the surfzone (Fig. 14.15). Clearly, it would be unwise to site a SIG inshore of closure depth where seasonal profile change would destroy as much as 1/3–2/3's of the engineered fill placed outside the surfzone. However, Fig. 14.14 teaches that the net

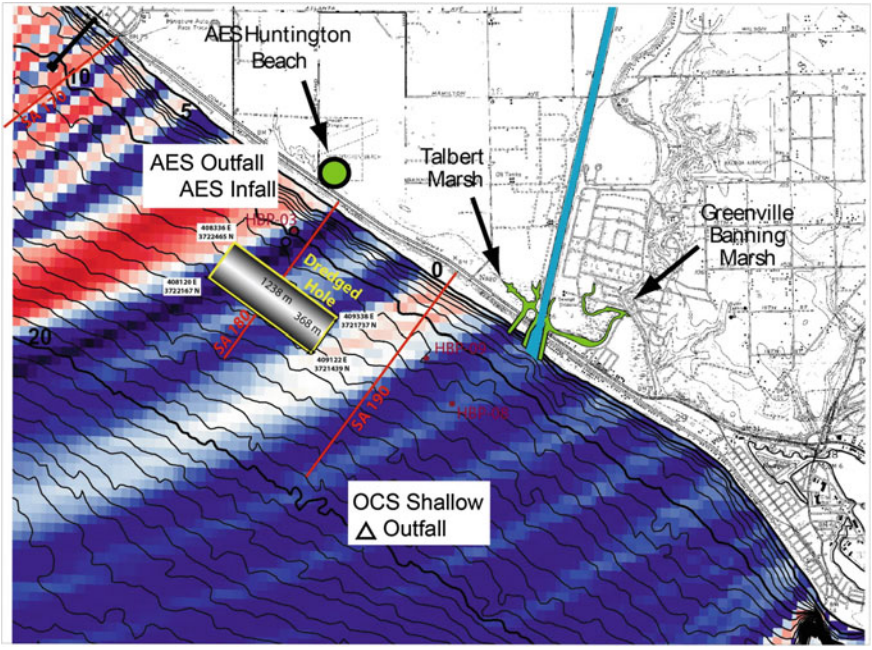

Fig. 14.16 Refraction/diffraction pattern of the 5 % highest waves for the period of record January 1980–July 2000. UTM coordinates shown for maximum SIG footprint at optima SIG site

long-term change in sediment volume at this location will be nil, thereby rendering it a favorable SIG site if one avoids the shorezone inside closure depth. Furthermore, the decelerations of the longshore current shown in the upper panel of Fig. 14.13 indicates that this potential SIG site is a chronic rip current area. This rip current activity will tend to prevent the fine-grained washload sediments discharged from Santa Ana River flood from dispersing inshore to closure depth, even though those sediments are too fine to settle and become immobile at this location.

We now seek to maximize the construction footprint at the optimal SIG site. The constraints on maximization are preservation of the largest continuous footprint of simple geometric proportions. Our analytic approach involves a refraction/diffraction analysis of the average of the highest 5 % waves for the period of record January 1980–July 2000, as shown in Fig. 14.16. We examine the shadow zone (area of diminished wave height delineated by blue and light blue) that cuts across the SA-180 range line, where sediment budget analysis has found a long-term null in sediment volume flux. We grow the boundaries of the potential SIG site in the along shore direction until meeting the adjacent bright spots in the refraction pattern (area of enhanced wave height delineated by white and red). This gives 1238 m of coastline available for a SIG site offshore of the −12 m closure depth. Maximization of the SIG footprint in the offshore direction is constrained by the bottom slope and the requirement to have a level bottom on the infiltration gallery so that on/offshore

hydrostatic pressure gradients do not occur between the onshore and offshore sides of the gallery. This requires dredging a deeper excavation for the infiltration gallery on the landward side of the SIG footprint than on the seaward side to compensate for the bottom slope. Since the SIG requires a 3 m thick layer of engineered fill over the infiltration gallery, it is sensible to not over-dredge the shoreward side of the footprint by more than that amount to compensate for bottom slope. Therefore the SIG footprint is grown offshore from closure depth to the −14 m depth contour. The resulting rectangular footprint for this maximized SIG at the optimal location is shown in Fig. 14.16 relative to the refraction/diffraction pattern of the 5 % highest waves for the period of record. The UTM coordinates for the SIG footprint are: (408336 E; 3722465 N), (409338 E; 3721737 N), (408120 E; 3722167 N), (409122 E; 3721439 N). The SIG site would have to be excavated 5 m below existing grade on its shoreward side, and 3 m below existing grade on its seaward ward side. The maximized SIG footprint could provide as much as 112.5 acres of construction of a SIG, but only 40 acres of seabed infiltration gallery are required to meet the 480,000 m^3/d (127 mgd) source water requirements of the HBDF.

Excavation of the SIG site represented in Fig. 14.16, and follow-on placement of the infiltration gallery hydraulics and engineered fill will be highly constrained by sea state conditions offshore of the HBDF. Altogether, a statistical sea state analysis for Huntington Beach indicates that average wave heights of between 0.9 and 1.2 m will prevail 87 % of the time during a typical year in an El Niño dominated climate period, occurring primarily during the spring, summer and fall seasonal periods. However, 13 % of the time during a typical El Niño year, average wave heights will increase to 2.4–2.7 m, with some waves reaching significant heights as large as 4–6 m (occurring primarily during winter months). These elevated sea states are sufficiently high and persistent as to present significant challenges to the excavation and placement of hydraulics and fill for a SIG at the optimal site off Huntington Beach identified in this study.

14.8 Discussion and Conclusions

The characteristics of an optimal shallow, subsurface intake site is one that is neither erosional nor depositional; and one that is within a feasible hydraulic pathway to the desalination facility and at water depths where offshore construction methods can be implemented in prevailing sea states. Finding such a site requires diagnosing the *sediment budget* of the *littoral cell* in which the desalination facility resides. The analysis should seek discovery of local nulls in the long-term divergence of drift. The kinds of data that are needed for this process-based approach are: (1) first and foremost, seismic reflection data to insure that there is adequate sediment cover over bedrock to maintain a permanently buried shallow infiltration system; (2) offshore bathymetry at a minimum of 3 arc-second resolution; (3) historic beach profile data; (4) vibracore data on sediment grain size to a minimum depth of 3.28 m (10 ft) below ambient seabed; (5) historic river flow rate data with

sediment rating curves, (6) historic dredging and beach disposal data, (7) historic wave height, period and direction data, (8) historic current data at closure depth, and (9) historic bluff retreat data. There should also be sufficient seismic data to identify aquatard formations to insure that the shallow infiltration systems will not tap into deeper aquifer formations.

References

CDIP. (2001). *Coastal data information program*. SIO Reference Series, 01–20 http://cdip.ucsd.edu.

Coudrain-Ribstein, A., Gouze, P., & de Marsily, G. (1998). Temperature-carbon dioxide partial pressure trends in confined aquifers. *Chemical Geology, 145*, 73–89.

Davis, R. A. Jr., (1996). *Coasts*. Upper Saddle River, NJ: Prentice Hall.

Dingler, J. R., & Inman, D. L. (1976). Wave-formed ripples in nearshore sands, In: *Proceedings 15th Coastal Engineering Conference*, ASCE (pp. 2109–2126) Honolulu, Hawaii.

Gadd, P. E., Leidersdorf, C. B., Hearon, G. E., Shak, A. T., & Ryan, J. (2006). Use of Statistical Depth of Closure to Resolve Historical Changes in Shoreline Position and Shorezone Volume in the Huntington Beach Littoral Cell, In: *Proc. 30th Coastal Engineering Conference*, San Diego (pp. 5302–5311), California, World Scientific, Singapore.

Hodgman, C. D. (1947). Standard Mathematical Tables, Cleveland (358 pp), Ohio: Chemical Rubber Publishing Co.

Inman, D. L. (1994). Types of coastal zones: Similarities and differences. In: *Environmental science in the coastal zone* (pp. 67–84). Ottawa: National Research Council.

Inman, D. L. (1957), Wave-generated ripples in nearshore sands, Technical Memorandum (Vol.100, 65 pp.) U. S. Army Corps of Engineers, Beach Erosion Board.

Inman, D. L., & Dolan, R. (1989). The Outer Banks of North Carolina: Budget of sediment and inlet dynamics along a migrating barrier system. *Journal of Coastal Research, 5*, 193–237.

Inman, D. L., & Jenkins, S. A. (1984). The Nile littoral cell and man's impact on the coastal zone of the southeastern Mediterranean. In: *Proceedings* 19th *Coastal Engineering Conference*. American Society of Civil Engineers, 2, 1600–1617.

Inman, D. L., & Nordstrom, C. E. (1971). On the tectonic and morphologic classification of coasts. *Journal of Geology, 79*, 1–21.

Inman, D. L., & Brush, B. M. (1973). The coastal challenge. *Science, 181*, 20–32.

Inman, D. L., & Masters, P. M. (1991). Budget of sediment and prediction of the future state of the coast. In State of the Coast Report, San Diego Region, Coast of California Storm and Tidal Waves Study. U. S. Army Corps of Engineers, *5*, 43.

Inman, D. L., Elwany, M. H. S., Khafagy, A. A., & Golik, A. (1992). Nile Delta profiles and migrating sand blankets. In: *Proceedings 23rd Coastal Engineering Conference*. American Society of Civil Engineers 3, pp. 3273–3284.

Inman, D. L., Elwany, M. H. S., & Jenkins, S. A., (1993). Shorerise and bar-berm profiles on ocean beaches. *Journal of Geophysical Research*, *98*(C10), 18, 181–199.

Inman, D. L. & S. A. Jenkins, (1999). Climate change and the episodicity of sediment flux of small California rivers. *Journal. of Geology*, *107*, 251–270.

Inman, D. L., Gayman, W. R., & Cox, D. C. (1963). Littoral sedimentary processes on Kauai, a subtropical high island. *Pacific Science, 17*, 106–130.

Inman, D. L. & Jenkins, S. A. (2004), Accretion and erosion waves on beaches (pp. 1–4), In M. Schwartz, (Eds.), Encyclopedia of Coastal Science, Kluwer Academic Publishers, Dordrecht, Netherlands.

Jenkins, S. A., & Inman, D. L. (2006). Thermodynamic solutions for equilibrium beach profiles. *Journal of Geophysical Research, 3*(C02003), 21. doi:10.1029/2005JC002899.

Jenkins, S. A., Inman, D. L., Richardson, M. D., Wever, T. F., & Wasyl, J. (2007). Scour and burial mechanics of objects in the nearshore. *IEEE Journal of Ocean Engineering, 32*(1), 78–90.

Kraus, N. C., & Harikai S. (1983). Numerical-model of the shoreline change at Oarai Beach. *Coastal Engineering 7*(1), 1–28.

Komar P. D. & Inman D. L. (1970). Longshore sand transport on beaches. *Journal of Geophyscial Research*,*75*(30), 5914–5927.

Kessler, T. J., & Harvey, C. F. (2001). The global flux of carbon dioxide into groundwater. *Geophysical Research Letters, 28*(2), 279–282.

Longuet-Higgins, M. S., (1970). Longshore currents generated by obliquely incident waves. *Journal of Geophyscial Research*,*75*(33), 6778–6789.

Murray, S., Coleman, J. M., Roberts, H. H., & Salama, M., (1981). Accelerated currents and sediment transport off the Damietta Nile promontory. Nature, *293*, 51–54.

Macpherson, G. L. (2009). CO_2 distribution in groundwater and the impact of groundwater extraction on the global C-cycle. *Chemical Geology, 264*, 328–336.

Shak, A. T., & Ryan, J. (1996). San Gabriel River to Newport Bay Erosion Control Project Orange County, California, 30 Years of periodic beach replenishment. In: *Proceedings of Coastal Eng*eering, Chapter 362, 4650–4664.

Short, A. D. (Ed.) (1999). Handbook of Beach and Shoreface Morphodynamics, (379 pp), Wiley, New York.

US Army Corps of Engineers (USACE). (1994). *Existing State of Orange County Coast* US. Army Corps of Engineers, Los Angeles District, Technical Report 93-1, 335pp.

US Army Corps of Engineers (USACE). (2001). Orange County Beach Erosion Control Project, San Gabriel River to Newport Bay, Orange County, California, Stage 11, Design Documentation Report. US Army Corps of Engineers, August 2001.

US Geological Survey (USGS). (2001). USGS Digital Data Series DDS-37 at INTERNET URL http://wwwrvares.er.usgs.gov/wgn96cd/wgn/wq/region18/hydrologicunitcode.

Wiegel, R. (2009). *History of the San Gabriel River to newport bay erosion control project*. Shore and Beach, American Shore and Beach Preservation Association, Awards Committee Presentation, August 13, 2009, 13 pp.

Chapter 15
Innovations in Design and Operation of SWRO Intake Systems

Thomas M. Missimer, Robert G. Maliva and Thomas Pankratz

Abstract Over the past several decades, many improvements have been made in the design and operation of seawater reverse osmosis desalination systems (SWRO), including the intakes that provide feed water. The invention of the velocity-cap offshore intake system reduced the entrainment of fish due to their sensing of horizontal flow versus vertical flow. Use of passive screen intakes further lessened the environmental impacts of open-ocean surface intake systems by near elimination of impingement and a reduction in entrainment caused by the low inflow velocity and the small slot size of the screens. Further reduction of environmental impacts of intake systems can be achieved by careful location of the intake systems (away from sensitive marine areas such as estuaries). Subsurface intake systems in the form of conventional vertical wells produced high-quality feed water for small and medium capacity SWRO plants. Well intake systems force seawater to infiltrate through the seabed into a porous aquifer. The transport of the raw seawater in the aquifer results in a significant reduction in the raw water organic matter content. Relatively new well types, such as slant wells, horizontal wells, and radial collectors, have been introduced to provide feed water for SWRO facilities. Some types performed better than others and experimentation is still ongoing. Gallery intake systems were developed for use in a wider range of required capacities from medium to large. A major seabed gallery intake system was constructed in Japan and has produced a very high-quality feed water and other similar systems are being planned for construction. The concept of the self-cleaning beach gallery intake was developed and has not yet been installed for use in a medium or

T.M. Missimer (✉)
U.A. Whitaker College of Engineering, Florida Gulf Coast University, 10501 FGCU Boulevard South, Fort Myers, FL 33965-6565, USA
e-mail: tmissimer@fgcu.edu

R.G. Maliva
Schlumberger Water Services, 1567 Hayley Lane, Suite 202, Fort Myers, FL 33907, USA
e-mail: rmaliva@slb.com

T. Pankratz
Water Desalination Report, PO Box 75064, Houston, TX 77234, USA
e-mail: pankratztm@gmail.com

T.M. Missimer et al. (eds.), *Intakes and Outfalls for Seawater Reverse-Osmosis Desalination Facilities*, Environmental Science and Engineering,
DOI 10.1007/978-3-319-13203-7_15

large capacity SWRO facility, but this intake design has high potential for success. Considerable additional research is merited on improving existing intake designs and creating new ones that can reduce SWRO operational costs by reducing the intensity of pretreatment.

15.1 Introduction

The quality of feed water entering a seawater reverse osmosis (SWRO) water treatment facility has significant impacts on facility operation, economics of treatment, and possibly also on environmental impacts. Many innovations have occurred over the past two decades that have improved feed water quality and have lessened environmental impacts in obtaining feed water from the sea. This remains a very important issue in the continuing quest to reduce the overall energy usage and cost of SWRO desalination.

Many SWRO plants use open-ocean intake systems either in channels at the shoreline, often collocated with power plants, or from offshore pipes. In these intake systems, marine life is carried into the plant and has to be removed by extensive pretreatment processes. Many of the early intake system designs had significant impacts caused by impingement and entrainment of marine organisms caught within the intake structure because the entrance velocities were generally high. The simple change to increased intake pipeline diameter to reduce the inflow velocity had a positive impact on reducing impingement and entrainment of marine organisms.

Over the years it has become apparent that the location of an intake has a significant effect on the environmental impacts, such as impingement and entrainment, and on the overall content of organic matter than enters a SWRO plant (Chap. 4). Placement of intakes within estuarine areas or other nearshore high marine productivity zones tends to increase impingement and entrainment, simply because of the higher density of marine organisms in these locations. Very high concentrations of total organic carbon (TOC) and natural organic matter (NOM) also occur in the estuarine areas. Placement of the intake in offshore areas that have sand bottoms with generally lower biological productivity tends to reduce impingement and entrainment and lessens real or perceived environmental impacts.

Use of subsurface intake systems was found to be quite effective in reducing environmental impacts and producing a higher quality feed water that requires less pretreatment. In the past, subsurface intake systems were considered only for small capacity (<10,000 m^3/d) systems, commonly located in carbonate aquifers in the Caribbean Islands. Application of subsurface intake systems to larger capacity SWRO systems is now occurring (Missimer et al. 2013).

15.2 Innovations in Open-Ocean Intake Systems

Improvement in the design and operation of open-ocean intake systems is on-going. Earlier innovations to reduce entrance velocity into SWRO facilities were to increase pipeline diameters and the invention of the velocity cap-type intake structure. A velocity cap is a behavioral deterrent technology that changes what would otherwise be vertical flow vectors at an uncapped offshore intake riser to horizontal flow vectors (see Chaps. 1 and 4). A velocity cap is an effective means for reducing impingement and entrainment because it has been shown that horizontal flow vectors are more easily sensed and avoided by fish (Beck et al. 2007; Lifton and Storr 1978; Weight 1958).

Various devices have also been installed within velocity cap intakes to "scare" the fish away. These devices include sound-emitting mechanisms and electrical currents. Few quantitative data are available on the effectiveness of these methods. Commonly, large fish will congregate within the upper layer of the intake below the cap and inside of the bar screen. The large fish can easy swim away from the low-velocity inflowing seawater. These large fish tend to scare away smaller fish that have limited ability to escape low-velocity inflows. The velocity cap intake design itself has been an environmental improvement in lowering entrainment of small fish.

Another innovation in reduction of environmental impacts is the use of conveyance tunnels from the SWRO plant site to the offshore intake. Offshore construction using trenching techniques to install the pipeline from the SWRO plant to the intake is a very disruptive process, which produces large volumes of suspended sediment and excess sediment excavated from the trench. Both can have impacts to the marine bottom ecology. In Australia, tunnels have been designed and constructed to convey the intake and outfall pipelines (Chaps. 2 and 3). These large-diameter tunnels are constructed using a tunneling machine and have no impact to the seabed. A vertical riser pipe is constructed from the seabed surface down to intersect with the tunnel and the velocity cap-type intake structure is attached. While the tunnel intake and outfall systems reduce environmental impacts, they adversely impact the project capital cost.

To exclude small fish and a significant part of the ictheoplankton, which includes larvae and eggs, the passive screen intake system, commonly used at power plant cooling water intakes, has been applied to SWRO intakes. This intake type is commonly used in surface water intake systems in freshwater rivers and streams. Passive screen intake technology has been extended to use for SWRO intakes in both onshore canal systems and offshore stand-alone systems. Passive screen systems can significantly reduce the impingement and entrainment of small fish and larvae by basic size exclusion and by shear forces caused by water currents passing over the screens (Chaps. 4 and 5). Impingement is virtually eliminated by use of passive screens intakes, but some entrainment of ictheoplankton will always remain.

A key issue in the use of passive screen intake systems, particular at significant distances offshore, is the ability to maintain the screens. New alloys have been

invented that are both corrosion resistant and anti-fouling in nature (copper-super duplex stainless steel alloys). Many of these intakes are located at a distance from the shore that makes air-burst cleaning using a shore-based compressor impractical. In Chap. 5, the use of an anchoring system to allow a boat-mounted cleaning system for air-burst cleaning of stand-alone passive screen intakes is suggested. This would facilitate cleaning and reduce the need for divers to perform the task.

Another issue that is being evaluated is the use of deep open-ocean intakes. It is generally recognized that oceanic biological productivity decreases with depth in the sea, but not regularly. If a reliable and structurally sound intake system could be designed and constructed to extract seawater from a depth >100 m, there is a reasonable possibility that the water would have generally lower concentrations of algae, bacteria, and other organic compounds that cause membrane biofouling. A study of deep intake system feasibility in the Red Sea indeed shows a significant decline in the concentrations of algae, bacteria, TOC, transparent exopolymer particles, and NOM between the sea surface and a depth of 90 m (Chap. 6). However, the bathymetry of the Red Sea (cliffed margins) would make the construction and maintenance of a deep intake system very risky and perhaps not feasible. Another key issue is the change of water temperature between the surface and the proposed depth of the deep intake. In the Red Sea, the decrease in temperature with depth is only about 5 °C, which is insignificant as far as its impacts on the SWRO treatment process. However, at other locations the decrease in temperature could materially increase the cost of SWRO treatment. Perhaps the most difficult element of deep intake development concerns how to maintain the intake below a depth to which normal scuba divers can safely work. Additional research on this issue will be required, probably in consultation with the offshore petroleum industry which uses deep submersible systems to maintain deep-water infrastructure. Cost would be a key feasibility issue.

15.3 Innovations in Well Intake Systems

Conventional vertical well intake systems have been used for decades to supply low capacity (<10,000 m^3/d) SWRO systems (Missimer 2009; Chap. 8). Vertical well intake systems have a demonstrated positive effect on feed water quality by resulting in significant reductions in algae, bacterial, transparent exopolymer particles (TEP), and fractions of NOM during transport of water from the sea into the wells (Chap. 9). While vertical well construction and maintenance is a mature technology, some innovations have occurred in materials that can be used for well casings and screen, as well as for the well pumps. Non-metallic fiberglass casing and screens can now be used in deep wells that previously required the use of more expensive stainless steel. New super duplex stainless steel alloys are now be used in well pumps. The corrosion resistance of duplex steel alloys increases the life-expectancy of the pumps, which was commonly 1–3 years in the past.

Slant and horizontal wells have the great advantage that multiple wells could be drilled from a single pad, which is an important consideration at the sites where shore access is limited. The use of slant wells and horizontal wells is relatively new for use as SWRO intakes. Slant well technology for SWRO intakes is being developed primarily in California (Chap. 13). Used in the proper type of hydrogeologic conditions, this emerging technology may have wide-spread application for medium capacity (10,000–50,000 m^3/d) SWRO facilities. As some new SWRO systems use this technology, data will become available concerning operational issues, such as the susceptibility of the wells to clogging, the ability to cost-effectively maintain (rehabilitate) the wells, and geochemical compatibility (redox reactions). Horizontal drilling technology has been a useful tool in the engineering world for over 50 years for the installation of pipelines, but it is new technology in applications for SWRO intake systems. The Neodren™ horizontal well technology has been used for medium-capacity intake systems in Spain, but the operational results are mixed at this time. Future refinement of drilling technologies may produce another useful intake type that may be applied under specific types of local geological conditions.

15.4 Innovations in Gallery Intake Systems

Gallery intake systems are another relatively new application for development of SWRO systems (Missimer et al. 2013). Seabed and beach gallery systems have the potential to provide feed water volumes to a larger range of SWRO plant capacities (Maliva and Missimer 2010; Chaps. 11 and 12). These intake types are based on the concept of slow sand filtration, which has been used in water treatment for nearly two centuries. Gallery intakes are engineered filters installed into the seabed or the active intertidal zone of the beach (surf zone). The concept of seabed galleries has been introduced over 25 years ago, but large-scale development of an SWRO intake in Fukuoka, Japan is a recent development (Shimokawa 2012).

Considerable effort has been conducted into the design and construction of seabed gallery intake systems with the Fukuoka, Japan system being the largest capacity system in operation to date. The City of Long Beach seabed gallery system was used for testing purposes, but is not in operation. Improved design of the seabed gallery intake systems is to divide the intake capacity into modules termed cells (Sesler and Missimer 2012; Dehwah and Missimer 2013; Lujan and Missimer 2014; Mantilla and Missimer 2014; Rachman et al. 2014; Al-Mashharawi et al. 2014; Chap. 12). The issue of proper filter design for these systems was discussed in Lujan and Missimer (2014) and the infiltration flow balance design problem was addressed in Mantilla and Missimer (2014). Key innovations for the future will be in developing better and more economic construction methods, such as the new concept of using an artificial fill peninsula in the Red Sea with bounding gallery cells (Fig. 11.13).

Beach gallery system intakes have been used in very small capacity SWRO systems in the Caribbean, but no other significant capacity systems have been developed elsewhere. The important innovation of this intake type is the self-cleaning nature of the face of the filter which is located in the surf zone. Wave turbulence tends to churn the sediments and particulate organic matter trapped in the sand and suspends it for transport longshore. Beach gallery intakes may be constructed in moderate energy, stable shorelines in regions requiring desalinated water.

Siting of gallery intakes must be based on sound science and knowledge of the processes acting on the shoreline and nearshore environments. A methodology is presented in Chap. 14 that illustrates the type of investigation that needs to be conducted when siting a high capacity gallery intake system. This is another technical innovation.

15.5 New SWRO Subsurface Intake Design Concepts

New innovations in SWRO intake systems design is occurring and will continue to grow. The tunnel intake system used in Alicante, Spain (Chap. 9) is a design modification based on the Louisville, Kentucky (USA) tunnel intake system described in Missimer (2009). Another design of this intake type has been proposed for use in southern California (RBF Consultants 2005; Fig. 15.1). Some basic design modifications will be required to improve the economics of construction of tunnel intakes and also, some innovations will be required in cleaning of the horizontal inflow "spines". Perhaps some type of tunnel isolation system could be used to take parts of it out of service during required maintenance.

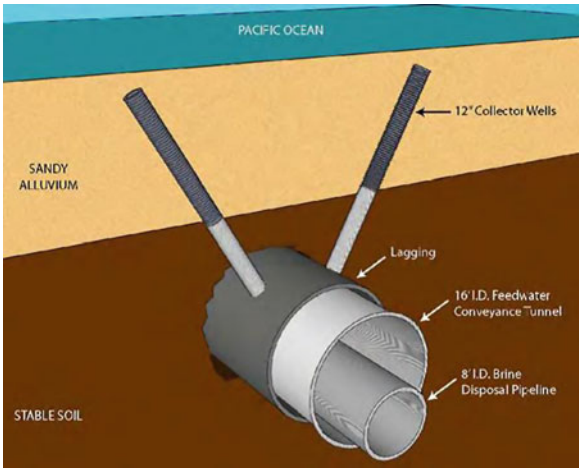

Fig. 15.1 Water tunnel intake system conceptual design (from RBF Consultants 2005)

Another type of subsurface/surface hybrid intake has been described by Pankratz (Chap. 1), which involves the excavation of the deep pit in limestone that is hydraulically connected to the sea. Seawater is extracted from the pit using high capacity pumps. The raw water is forced through the aquifer between the sea and the excavation, thereby receiving filtration and treatment. The excavation could be covered or not covered. Care would have to be taken to avoid the introduction of fish and other marine life into the excavation or there would be additional pre-treatment requirements.

15.6 Planning for Use of Subsurface SWRO Intake Systems

A major reason why subsurface intake systems have not been used to supply feed water to a larger number of medium to high capacity SWRO plants is the issue of contract and operational risk. Governmental bodies that manage design, construct, and operate a SWRO facility have the ability to evaluate all types of intakes in terms of environmental impacts and economics before a request for proposal for design is issued and construction bids are solicited. However, in most tenders for new SWRO facilities that involve coupled construction and long-term operation bids [build-own-operate (BOO) or build-own-operate-transfer (BOOT)], no information on local site subsurface conditions is provided in the bid package. Therefore, the bidder would have to accept the risk for using a subsurface intake system using few data, or absorb the cost of conducting the proper testing program before the bid is prepared which is commonly a short period of time. Often there is insufficient time for a program to pilot test alternative intake system design options.

Governments or regions that will require large-scale development of SWRO facilities have the ability to conduct coastal planning investigations that evaluate the use of subsurface intake. An example of a planning level investigation of subsurface intake use (or non-use where not feasible) is given in Chap. 7. The methods provided in this chapter, as well as in Dehwah et al. (2014), provide a method that can be applied to other coastal regions of the world. Maps could be produced that link specific locations along a shoreline or nearshore area with various feasible subsurface intake types. Also, the owner of the project could provide the bidders with sufficient site-specific data on which a bid could be developed that allows the bidder to develop innovations that could substantially reduce the cost of the water to the consumers.

15.7 Operational Innovations

One very important operational issue is the recognition that continuous chlorination of the intake water in an open-ocean intake facilitates biofouling of SWRO membranes (Winters 1994, 1997; Winters and Isquith 1995). The switch to episodic

chlorination of the intake pipeline from the intake to the plant for biofouling control has reduced the rate of biofouling at some SWRO plants. However, the total elimination of chlorination reduces the biofouling rate of the membranes even further. Subsurface intake systems require no chlorination to operate.

Various combinations of pretreatment systems with an intake could improve facilities operation in certain cases. For example, it has been proposed that using a rapid infiltration offshore gallery linked with a membrane filtration pretreatment process could improve the overall SWRO plant operational efficiency (Niizato et al. 2013; Chap. 11). The overall cost of this possible innovation has yet to be evaluated.

The concept of elimination of in-plant pretreatment processes when using a subsurface intake system must be considered to be an innovation. Well intakes have been used for decades to supply small capacity SWRO plants with the full elimination of any pretreatment, except for the cartridge filters positioned before the membrane trains. The seabed gallery operated at Fukuoka, Japan produces a very high quality feed water, which is the pretreated with a membrane filtration system before it enters the cartridge filters. Based on the quite low silt density index values coming from the feed water, it appears that the pretreatment process using membrane filtration could be bypassed without loss of plant efficiency. Continued research on the effectiveness of subsurface intake systems to actually provide pretreatment exterior to the SWRO plant needs to be conducted to ascertain the need for any in-plant pretreatment from the influent of the intake.

15.8 Discussion and Conclusions

The intake into a SWRO plant provides the feed water that controls the design and operation of many aspects of the plant, including the pretreatment process train and the desired flux through the SWRO membranes. Innovations in the development of intake systems that provide the highest possible feed water quality are key factors in reducing the environmental impacts, and cost of SWRO desalination.

In this section of the book, a number of innovations in intake design and operation of intake systems have been described including both open-ocean or surface intake systems and subsurface intake systems. The continued improvements and innovations that can be achieved in intake design and operation are in peril at this time. The danger of the “commodity engineering” approach to the design of SWRO plants is becoming an issue. As the SWRO industry becomes mature, and ‘standard’ SWRO designs are being used due to bidding schemes that are believed to lower costs, there is the danger of losing innovation which is the backbone of technological improvement and long-term energy and cost reduction in desalination.

References

Al-Mashharawi, S., Dehwah, A. H. A., Bandar, K. B., & Missimer, T. M. (2014). Feasibility of using a subsurface intake for SWRO facility south of Jeddah, Saudi Arabia. Desalination and Water Treatment, doi:10.1080/19443994.2014.939870

Beck, S. E., Miller, D., Bailey, D., Steinbeck, J. (2007). Quantification of effectiveness of velocity caps. In *Presented at American Fisheries Society 137th Annual Meeting*, *San Francisco*, *CA*. September 2–6, 2007.

Dehwah, A. H. E., & Missimer, T. M. (2013). Technical feasibility of using gallery intakes for seawater RO facilities, northern Red Sea coast of Saudi Arabia: The king Abdullah Economic City site. *Desalination and Water Treatment*, *51*(34−36), 6472–6481. doi:10.1080/19443994.2013.770949

Dehwah, A. H. A., Al-Mashhawari, S., & Missimer, T. M. (2014). Mapping to assess feasibility of using subsurface intakes for SWRO, Red Sea coast of Saudi Arabia. *Desalination and Water Treatment, 52*, 2351–2361. doi:10.1080/19443994.2013.862035.

Lifton, W. S., Storr, J. F. (1978). The effect of environmental variables on fish impingement. In: L. D. Jensen (Ed.), *Proceedings of the fourth national workshop on entrainment and impingement*. EA Communications. ISBN: 0-931842-01-8.

Lujan, L. R., & Missimer, T. M. (2014). Technical feasibility of a seabed gallery system for SWRO facilities at Shoaiba, Saudi Arabia and regions with similar geology. *Desalination and Water Treatment*, *52*(40–42), 7431–7442. doi:10.1080/19443994.2014.909630

Maliva, R. G., & Missimer, T. M. (2010). Self-cleaning beach-gallery design for seawater desalination plants. *Desalination and Water Treatment, 13*, 88–95.

Mantilla, D., & Missimer, T. M. (2014). Seabed gallery intake technical feasibility for SWRO facilities at Shuqaiq, Saudi Arabia and other global locations with similar coastal characteristics. *Journal of Applied Water Engineering and Research*, http://dx.doi.org/10.1080/2349676.2014.895686

Missimer, T. M. (2009). *Water supply development, aquifer storage, and concentrate disposal for membrane water treatment facilities*. Houston, Texas, Schlumberger Water Services, Methods in Water Resources Evaluation Series No. 1, 390 pp.

Missimer, T. M., Ghaffour, N., Dehwah, A. H. A., Rachman, R., Maliva, R. G., & Amy, G. (2013). Subsurface intakes for seawater reverse osmosis facilities: Capacity limitation, water quality improvement, and economics. *Desalination, 322*, 37–51. doi:10.1016/j.desal.2013.04.021.

Niizato, H., Inui, M., Kira, N., Inoue, T., Oiwa, T., Cai, H., Yanagimoto, Y., Nishimura, T. (2013). Innovative SWRO desalination technology introducing high-speed seabed infiltration system (HiSIS). In *Proceedings of the International Desalination Association World Congress on Desalination and Water Reuse*, October 20–25, Tianjin, China, Paper IDAWC/TIAN13-033.

Rachman, R., Al-Mashhawari, S., & Missimer, T. M. (2014). Technical feasibility for development of a seabed gallery intake for SWRO at Abu Ali, Arabian Gulf, Saudi Arabia. *Desalination and Water Treatment*, doi: 10.1080/19443994.2014.940221

RBF Consultants. (2005). *Camp Pendleton seawater desalination project feasibility study*. Consultant's report to the San Diego County Water Authority.

Sesler, K., & Missimer, T. M. (2012). Technical feasibility of using seabed galleries for seawater RO intakes and pretreatment: Om Al Misk Island, Red Sea, Saudi Arabia: IDA. *Journal: Desalination and Water Reuse*, *4*(4), 42–48.

Shimokawa, A. (2012). Fukuoka District desalination system with some unique methods. National Centre of Excellence in Desalination. In *International Desalination Intakes and Outfalls Workshop Proceedings, Adelaide, South Australia*, May 16–17, 2012.

Weight, R. H. (1958). Ocean cooling water system for 800 MW power station. *Journal of the Power Division of the American Society of Civil Engineers Paper, 1888*, 22.

Winters, H. (1994). Biofouling status of the Saline Water Conversion Corporation (SWCC) reverse osmosis (RO) plants in the Kingdom of Saudi Arabia, Unpublished consultant's report to SWCC, 23 pp.

Winters, H. (1997). Twenty years experience in seawater reverse osmosis and how chemicals in pretreatment affect fouling of membranes. *Desalination, 110*, 93–95.

Winters, H., & Isquith, L. (1995). A critical evaluation of pretreatment to control fouling in open seawater reverse osmosis—has it been a success? In *Proceedings of the International Desalination Association World Congress on Desalination and Water Reuse, Abu Dhabi, UAE* (Vol. 1, pp. 255–264), November 18–24, 1995.

Part II
Outfalls

Chapter 16
Overview of Coastal Discharges for Brine, Heat and Wastewater

Burton Jones

Abstract Environmental impacts of discharges into the marine environment have become a major issue in the United States and the European Union over the past decade. With the growing demand for freshwater, the capacity of seawater desalination systems using the reverse osmosis process is also rapidly growing. Therefore, the discharge of the concentrate (brine) from these facilities requires careful management to avoid the impacts of denser than seawater discharges that can adversely affect marine benthic communities. This section of the book covers new advances in the siting, design of discharge dispersion systems, evaluation of nearshore discharge systems locations, monitoring, and evaluation of environmental impacts of SWRO concentrate discharge systems.

16.1 Introduction

Discharges from coastal desalination facilities, power plants and municipal wastewater treatment plants are a major concern for a variety of environmental and public health related issues. Historically, wastewater and thermal discharges have been the major focus. Both are buoyant plumes, but the approach and management of these types of discharges have differed because of the different needs of exchanging heat and dispersing contaminated wastewater in ways that minimize both public and environmental health risks. Brine discharges from desalination facilities are considered less of an immediate public health risk, but are more likely to affect local water quality and environmental health, especially benthic and near-bottom marine communities (e.g., Lattemann and Amy 2013).

B. Jones (✉)
Red Sea Research Center, King Abdullah University of Science and Technology, Thuwal, Saudi Arabia
e-mail: burt.jones@kaust.edu.sa

T.M. Missimer et al. (eds.), *Intakes and Outfalls for Seawater Reverse-Osmosis Desalination Facilities*, Environmental Science and Engineering,
DOI 10.1007/978-3-319-13203-7_16

Regulations regarding seawater discharges are an important consideration in the design, implementation and monitoring of outfall discharges regardless of type of discharge. The requirements for thermal and wastewater discharges have been quite well worked out. Under the Clean Water Act of the United States, the National Pollutant Discharge Elimination System (NPDES) was established to regulate discharges into US coastal waters, lakes and rivers. The State of California enacted more stringent requirements for dischargers within the state under the California Ocean Plan (California Environmental Protection Agency (CEPA) 2012). Although the plan gives explicit guidelines for the regulation and monitoring of the discharge effects on the receiving environment, the only statement regarding concentrate (brine) discharges is that than that salinity should be monitored. Given the expected increase in demand for freshwater from desalination of seawater, California has been defining more specific guidelines for both intakes and discharges for desalination facilities (State Water Resources Control Board 2014).

While regulations continue to be developed and enacted, the processes for determining optimal designs, siting and monitoring for coastal desalination efforts need to be established. Much effort has already gone into the design and optimization of outfall characteristics. Siting of discharges for desalination, wastewater and thermal effluent continue to require optimization (e.g. Lattemann and Hopner 2008). This process includes the integration of policy requirements, modeling efforts that provide for optimal design and siting, and once constructed and operational, ongoing monitoring efforts that evaluate both short-term and long-term effects of the discharges.

16.2 Nearfield Considerations

The consideration of the nearfield dispersion of dense brine plumes is an extension of the preceding work on nearfield dispersion from buoyant wastewater and thermal plumes. The well known RSB model for wastewater effluent discharge was developed from a series of laboratory experiments that provided parameterization of key processes affecting the nearfield performance of buoyant plume discharges based on laboratory flume or tank models (Roberts et al. 1989a, b, c). Similar laboratory efforts were incorporated into the Cormix model developed by Jirka (e.g. Jirka and Harleman 1979; Donneker and Jirka 2001). More recent work on brine discharges has focused on the optimization of outfalls for discharge of dense brine effluents and attaining desired dilutions in the nearfield (e.g., Bleninger and Jirka 2008; Roberts et al. 1997). Comparison of field observations with the nearfield models has indicated that model performance is generally very good, and the scaling of the models from the small scale laboratory studies to the field scale of coastal discharges indicate that there may be discrepancies between in situ measurements of the effluent plumes and in situ plume measurements (e.g. Petrenko et al. 1998). But in general the nearfield models provide a reasonable prediction of the likely nearfield impacts.

A comprehensive overview of brine outfall configurations and their implications to the nearfield are presented in Chap. 17. Experimentation with various types of discharge ranging from single port to various configurations of multiport diffusers has provided a better understanding of how to design and implement dense water outfalls so that effective dilutions and zones of initial mixing can be achieved. Chap. 19 evaluates some basic configurations for brine water discharges that provide guidance in the design of these discharges. Numerical modeling of the complex flow associated with outfall diffuser jets remains to be a challenging effort. Therefore, laboratory modeling and dimensional analysis continue to be fundamental tools in evaluating the performance of marine outfalls.

16.3 Farfield Considerations

Farfield concerns have been much more difficult to assess, in part because they cannot be easily studied in laboratory and early coastal models were relatively coarse, and not necessarily verifiable. Connolly et al. (1999) published results from a coastal model that was locally driven to describe possible sources and pathways of transport of coliform bacteria onto Waikiki Beach in Honolulu, HI, USA. Simpler approaches for the same area used a progressive vector approach that assumes a uniform spatial distribution of the flow field relative to the measurement points (Roberts 2001). Significant improvements in computing resources and real-time and retrospective data assimilation of both atmospheric forcing and in situ observations have enabled sophisticated, highly resolved 3-dimensional computer models of the coastal environment. These models provide high spatial resolution and with realistic forcing and coupling to the regional and global ocean, more typical coastal dynamics. These models often rely on the nearfield models such as RSB (e.g. Roberts 1989a b, c; Roberts 1999; or Donneker and Jirka 2001) to provide the starting point of plume height, thickness and dilution. In shallow, well mixed coastal areas an integrated, two dimensional models may provide good evaluation of the farfield transport of the plume (see Chaps. 18 and 20). Various types of dynamic modeling are being used for coastal simulations where the models are incorporating the larger scale ocean circulation, regional and local wind fields, with various adaptations that provide advantages for particular questions. A recent paper by Uchiyama et al. (2014) uses the Regional Ocean Modeling System (ROMS) with a nested 75 m resolution model to examine the dispersion of effluent from two large southern California outfalls.

16.4 Monitoring and Environmental Assessment

Our ability to monitor and assess the impacts of coastal discharges has been rapidly evolving. The approach to monitoring and the likely impacts will differ based on whether the discharge becomes a buoyant, neutrally buoyant, or dense plume that

will collapse to near the seabed away from the discharge site (e.g., Bleninger and Morelissen, Chap. 18). Buoyant discharges, especially those from large wastewater treatment plants, will likely have two components that affect the approach to monitoring. Short-term, small-scale processes may affect the areas very close to the outfalls beyond the initial dilution field but before significant environmental dilution of the plume has occurred. Longer-term processes such as the mean circulation and integration of the discharge into the larger environmental area may make significant modifications to the area. A recent paper by Howard et al. (2014) outlines the contribution of major ocean wastewater outfalls to the regional nutrient budget for the Southern California. Surprisingly, the nutrient contribution from outfalls rivals the flux from coastal upwelling for regions within about 20–40 km from the mainland of the Southern California Bight. Despite years of sustained monitoring in the region, the scale and spatial extent of the effluent contribution to the regional nutrient budget has only become clear in recent efforts.

Lattemann and Amy (2013) lay out criteria and recommendations for establishing an adequate monitoring plan for brine discharges. Much of the suggested effort relates to long-term biological assessment of the discharges on the environment. However, assessment of the overall dispersion of these discharge plumes and their influence on the regional environment can only be achieved with long term sustained observations that are now feasible with the use of autonomous vehicles. Van der Merwe et al. (2014) described the used of short-term AUV deployments for evaluation of the dispersion of brined discharge plumes. Chap. 23 discusses longer term deployments to build a statistical resource that can be used for comparison with complex model statistics, evaluation of statistical impacts on the region, etc.

16.5 Conclusions

Despite many efforts, we are still in a stage of developing better resources for evaluation, design, implementation and monitoring of various types of discharges into the marine environment. Because of the complex coastal environment where there are multiple activities that include power plants, desalination facilities, and wastewater treatment plants, integrated planning, analysis and eventually monitoring should take into consideration the multiple uses of the coastal environment.

Both nearfield and farfield modeling provide valuable tools for planning the design of new facilities as well as evaluating the performance of existing facilities. Combining these with additional resources for site selection and integrated planning could provide the optimal strategies for efficiency, energy conservation, preservation of water quality and conservation of the invaluable natural coastal environments.

The tools for monitoring coastal environments are rapidly changing. We are now able to provide a view of the environment that was impossible ten years ago. How we use these observational tools and incorporate the results into future planning and management efforts is an ongoing process.

The chapters that follow provide some examples of the resources available for modeling, planning and monitoring of the coastal environment in the presence of various kinds of discharges.

References

Bleninger, T., & Jirka, G. H (2008). Modelling and environmentally sound management of brine discharges from desalination plants. *Desalination 221*(1–3), 585–597. doi:10.1016/J.Desal.2007.02.059.

California Environmental Protection Agency SWRCB. (2012). *Water quality control plan: Ocean waters of California*. CEPA State Water Resources Control Board, State of California, State Water Resources Control Board. 68 p.

Connolly, J. P., Blumberg, A. F., & Quadrini, J. D (1999). Modeling fate of pathogenic organisms in coastal waters of Oahu, Hawaii, *Journal of Environmental Engineering-Asce*, *125*(5), 398–406. doi: 10.1061/(Asce)0733-9372(1999)125:5(398)

Doneker, R. L., & Jirka, G. H (2001). CORMIX-GI systems for mixing zone analysis of brine wastewater disposal. *Desalination, 139*, 263–274.

Howard, M. D. A., Sutula, M., Caron D., Chao Y., Farrara J., Frenzel H., et al. (2014). Anthropogenic nutrient sources rival natural sources on small scales in the coastal waters of the Southern California Bight, Limnology and Oceanography, *59*(1), 285-297. doi:10.4319/lo.2014.59.1.0285

Jirka, G. H., & Harleman, D. R. F (1979). Stability and Mixing of a Vertical Plane Buoyant Jet in Confined Depth, *Journal of Fluid Mechanism*, *94*(02), 275–304. doi:10.1017/S0022112079001038

Lattemann, S., & Hopner, T (2008). Environmental impact and impact assessment of seawater desalination. *Desalination, 220*, 1–15.

Lattemann, S., & Amy, G (2013). Marine monitoring surveys for desalination plants—a critical review, Desalination and Water Treatment, *51*(1-3), 233-245. doi:10.1080/19443994.2012.694214

Petrenko, A. A., Jones, B. H., & Dickey, T. D. (1998). Shape and initial dilution of Sand Island, Hawaii sewage plume. *Journal of Hydraulic Engineering-Asce, 124*, 565–571.

Roberts, P. J. W., Ferrier, A., & Daviero, G (1997). Mixing in inclined dense jets, *Journal of Hydraulic Engineering*, *123*(8), 693-699. doi:10.1061/(Asce)0733-9429(1997)123:8(693)

Roberts, P. J. W. (1999). Modeling mamala bay outfall plumes. I: Near field. *Journal of Hydraulic Engineering-Asce, 125*, 564–573.

Roberts, P. J. W. (2001). Modeling mamala bay outfall plumes. II: Far field—Closure. *Journal of Hydraulic Engineering-Asce, 127*, 164–166.

Roberts, P. J. W., Snyder, W. H., & Baumgartner, D. J. (1989a). Ocean outfalls. 1. Submerged wastefield formation. *Journal of Hydraulic Engineering-Asce, 115*, 1–25.

Roberts, P. J. W., Snyder, W. H., & Baumgartner, D. J. (1989b). Ocean outfalls. 2. spatial evolution of submerged wastefield. *Journal of Hydraulic Engineering-Asce, 115*, 26–48.

Roberts, P. J. W., Snyder, W. H., & Baumgartner, D. J. (1989c). Ocean outfalls. 3. Effect of diffuser design on submerged wastefield. *Journal of Hydraulic Engineering-Asce, 115*, 49–70.

State Water Resources Control Board CEPA. (2014). *Draft staff report including the draft substitute environmental documentation: Amendment to the water quality control plan for ocean waters of California addressing desalinatin facility intakes, brine discharges, and the incorporation of other nonsubstantive changes*. Sacramento, California, USA.

Uchiyama, Y., Idica, E. Y., McWilliams, J. C., & Stolzenbach, K. D. (2014). Wastewater effluent dispersal in Southern California Bays. *Continental Shelf Research, 76*, 36–52.

van der Merwe, R., Bleninger, T., Acevedo-Feliz, D., Latteman, S., & Amy, G. (2014). In-situ monitoring and assessment of SWRO concentrate discharge. *Journal of Applied Water Engineering and Research,* in press.

Chapter 17
Near Field Flow Dynamics of Concentrate Discharges and Diffuser Design

Philip J.W. Roberts

Abstract The major physical aspects of near field mixing of dense jets resulting from diffuser discharges of concentrate are presented. It is proposed that any environmental impacts of such discharges will be local rather than regional, so initial mixing processes are an essential component of an effective disposal scheme. Typical international environmental criteria for concentrate are summarized; these can be readily met by well-designed diffusers. The major features of dense jets are presented, beginning with the simplest case of an inclined jet into deep stationary water, followed by the effects of shallow water. We then discuss merging jets from multiport and rosette diffusers and it is shown that their dynamic interaction can be critical and lead to significant changes in flow patterns and reduction in dilution. Design criteria are suggested to avoid impaired dilution. The effects of currents on single and multiport diffusers are then discussed. It is shown that small modifications in diffuser design can lead to significant changes in flow field and dilution. Some issues and difficulties with mathematical modeling of near field flows are discussed and how entrainment models may not adequately represent critical phenomena including dynamic jet and boundary interaction, re-entrainment, density current dynamics, and turbulence collapse. Finally, some open research issues are discussed.

17.1 Introduction

Concentrate resulting from seawater desalination can be safely discharged back to the ocean with minimal environmental impact if adequately diluted near to the source. This dilution can be accomplished by many means, of which a diffuser

P.J.W. Roberts (✉)
Georgia Institute of Tecnology, Atlanta, USA
e-mail: proberts@ce.gatech.edu

T.M. Missimer et al. (eds.), *Intakes and Outfalls for Seawater Reverse-Osmosis Desalination Facilities*, Environmental Science and Engineering,
DOI 10.1007/978-3-319-13203-7_17

is one. The objective of a diffuser is rapid dilution and mixing of the concentrate to reduce salinity to near background levels. The environmental impacts of well-designed operating diffusers have been studied in extensive field observations in Australia which show that any observable effects are confined to a small region, of order tens of meters from the diffuser (Roberts et al. 2010).

This might be expected when considering the primary processes involved in seawater desalination and their hydrometeorological fluxes. Desalination takes in seawater, concentrates it, and returns it to the ocean with no net addition of salt. There is some abstraction of freshwater, however, which could potentially lead to increases in background salinity.

These impacts will generally be very small and localized as can be illustrated by considering desalination effects on the Gulf of Arabia. The Gulf evaporates by about 1.5 m/year (Smith et al. 2007) (the Red Sea evaporates by about 2 m/year, Sofianos et al. 2002). The Gulf's surface area is about 250,000 km^2, therefore this evaporation corresponds to a freshwater abstraction of about 12,000 m^3/s. Total desalination production in the Gulf is currently of order 150 m^3/s (Lattemann and Höpner 2008). As this is very small (order 1 %) compared to evaporation, its effect would be swamped by natural variability and extremely difficult, if not impossible, to measure. Even anticipated future growth would not cause this effect to become significant. It is therefore clear that regional impacts should be minor. Similar conclusions would be expected for other coastal regions, where oceanographic fluxes far exceed those due to desalination plants.

Almost by definition then, any effects should be local, or near field, so providing rapid initial dilution should mitigate any environmental impacts of salinity. Of course, there are other potential effects such as from disposal of filter backwash or chemicals added during the desalination process as discussed by, for example, Lattemann and Höpner (2008). It has also been suggested that mortality of organisms due to turbulence and shear in the diffuser jets may also be a factor. We don't discuss these issues here as this chapter is concerned with the fluid mechanical aspects of near field mixing of typical brine diffusers and their design to meet environmental criteria.

Of course, there are other means of concentrate disposal, such as co-disposal with power plant cooling water whose volumes, particularly those associated with once-through cooling, are generally much greater than those due to desalination plants. Once-through cooling is being phased out in California, however, mainly because of its effect on entrained organisms and this may not be an option in the future.

The outline of this chapter is as follows. We first discuss typical regulatory criteria that apply to brine diffusers. We then review some general characteristics of discharges into stationary waters, first for single dense jets, then multiport diffusers with conventional designs and rosettes along with some guidelines for their design. Then some effects of flowing currents are discussed. We conclude with some discussion of mathematical modeling and some unresolved and future research issues.

17.2 Environmental Criteria

The potential environmental impacts of concentrate disposal have been discussed in many publications, such as Lattemann and Höpner (2008). They include concentrate and chemical discharges to the marine environment, air pollutants and energy usage. In this chapter, we are only concerned with the design of diffusers whose objective is rapid dilution and mixing. Criteria that have been adopted around the world for such discharges were recently reviewed for the proposed revision to the California Ocean Plan by Roberts et al. (2012) and are summarized in Table 17.1. They mostly involve limitations to salinity in the receiving water that are expressed as, for examples, an absolute level, an absolute increase over background of a few ppt, or an incremental increase of a few percent. These limits are to be met at the edge of a mixing zone, typically defined as extending a few tens or hundreds of meters from the source.

What are the implications of these regulations for diffuser design? The average salinity in the world's oceans is about 35 ppt, somewhat lower in areas of high freshwater input, and higher in areas of high evaporation and low precipitation such as the Gulf of Arabia. So an increment of 1 ppt over background would correspond to an increase of about 3 %. Typical recovery rates for reverse osmosis (RO) plants are of order 50 %, i.e. concentrate and potable water are produced in roughly equal quantities, so the salinity of the concentrate is doubled to about 70 ppt. For this case (50 % recovery, concentrate salinity twice the background level), the dilution required is directly related to the allowable percentage increase over background by:

Table 17.1 International brine discharge regulations (after Roberts et al. 2012)

Region/Authority	Salinity Limit	Compliance point (relative to discharge)
US EPA	Increment ≤ 4 ppt	–
Carlsbad, CA	Absolute ≤ 40 ppt	1,000 ft (304.8 m)
Huntington Beach, CA	Absolute ≤ 40 ppt salinity (expressed as discharge dilution ratio of 7.5:1)	1,000 ft (304.8 m)
Western Australia guidelines	Increment < 5 %	–
Oakajee Port, Western Australia	Increment ≤ 1 ppt	–
Perth, Australia/ Western Australia EPA	Increment ≤ 1.2 ppt at 50 m and ≤ 0.8 ppt at 1,000 m	50 m and 1,000 m
Sydney, Australia	Increment ≤ 1 ppt	50-75 m
Gold Coast, Australia	Increment ≤ 2 ppt	120 m
Okinawa, Japan	Increment ≤ 1 ppt	Mixing zone boundary
Abu Dhabi	Increment ≤ 5 %	Mixing zone boundary
Oman	Increment ≤ 2 ppt	300 m

$$S = \frac{100}{PC} = \frac{c_b}{c - c_b} \tag{17.1}$$

where S is the required dilution, PC the allowable percentage increase over background, c_b the ambient salinity and c the concentrate salinity. For example, an increment of 3 % requires a dilution of 33:1, an increment of 5 % a dilution of 20:1, etc. These dilutions can be readily achieved by a diffuser with high velocity jets, as discussed below.

17.3 Experimental Techniques

In the following sections we will rely heavily on laboratory experimental studies of dense jets in various flow situations. Such studies have formed the basis for much of our knowledge of the dynamics of dense jets and for diffuser design. They are also essential in validating and developing mathematical models of jet behavior. Visualization of flows can be as simple as adding dye to the discharges, or, more recently, by laser-induced fluorescence (LIF) dye techniques.

We will extensively use images obtained by LIF laboratory experiments to illustrate the mixing processes. In this technique, a fluorescent tracer dye is added to the flow and a laser causes the dye to fluoresce and emit light that is captured by a camera. By suitable calibration, quantitative tracer concentrations can be obtained from the images. It is beyond the scope of this chapter to describe this technique in detail, but descriptions are given in many publications, for example, Koochesfahani and Dimotakis (1985) and Crimaldi (2008).

In particular, we will show many three-dimensional LIF (3DLIF) images. In this technique a laser sheet is swept horizontally at high speed through the flow and sequential LIF images captured. The images are converted to tracer concentrations (and therefore dilution) and visualized to show three-dimensional distributions by computer graphics methods. The images can also be color-coded to show the concentration (and therefore dilution) distributions in the flows. For a discussion of the 3DLIF method used, see Tian and Roberts (2003).

17.4 Mixing of Single Dense Jets

17.4.1 Analysis

The main flow characteristics for a single dense jet in a stationary environment are shown in Fig. 17.1. The negative buoyancy of the jet causes it to reach a terminal rise height and then falls back to the lower boundary where it spreads as a density current. Vertical jets fall back onto themselves when discharged into a stationary

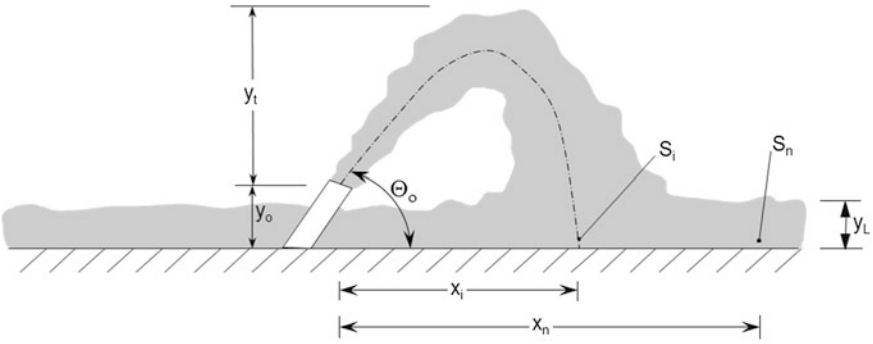

Fig. 17.1 Definition diagram for single dense jet

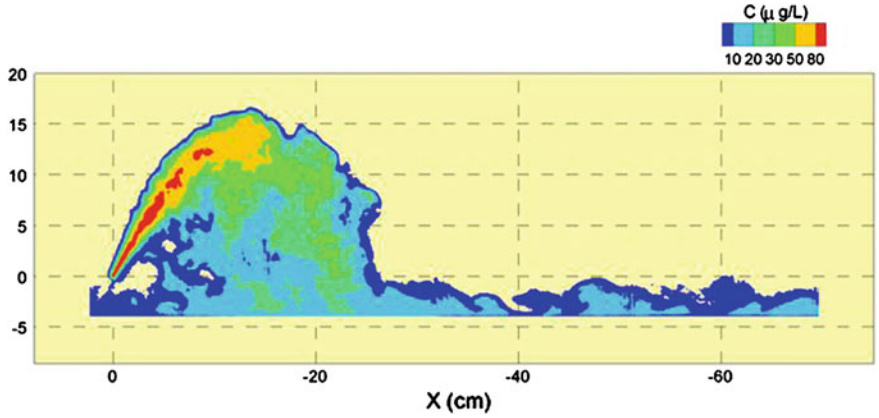

Fig. 17.2 Laser-induced fluorescence (LIF) image of a typical dense jet

environment, resulting in lowered dilutions, so inclined jets are more commonly used. A 60° nozzle inclination seems to have been adopted as the de facto standard for diffuser designs.

These essential flow processes are illustrated by the laser-induced fluorescence (LIF) image through the vertical central plane of a typical 60° dense jet shown in Fig. 17.2. The jet first ascends to a terminal rise height. As it rises, it entrains ambient water that mixes with and dilutes the discharges so that tracer concentrations (and therefore effluent salinity) decrease. It then begins to descend back to the floor, continuing to entrain and dilute as it falls. After impact it spreads horizontally as a density current which is still turbulent and thereby entrains more flow resulting in further dilution. This turbulence eventually collapses under the influence of its own density stratification, marking the end of the near field. The dilution at the end of the near field can be considerably higher than that at the initial jet impact point.

The analysis of this flow is well known, e.g. Roberts et al. (1997). The jet is primarily characterized by its kinematic fluxes of volume, Q, momentum, M, and buoyancy, B,

$$Q = \frac{\pi}{4} d^2 u; \quad M = uQ; \quad B = g_0' Q \tag{17.2}$$

where d is the port diameter, u the jet exit velocity, $g_0' = g(\rho_a - \rho_0)/\rho_0$, is the modified acceleration due to gravity, g the acceleration due to gravity, ρ_a the ambient density and ρ_0 the effluent density ($\rho_0 > \rho_a$).

As discussed in many publications, the most important length-scale of the flow is $l_m = M^{3/4}/B^{1/2}$ although this is essentially equal to and more commonly expressed as dF where F is the jet densimetric Froude number:

$$\mathrm{F} = \frac{u}{\sqrt{g_0' d}} \tag{17.3}$$

If the Froude number is greater than about 20, the volume flux Q is not dynamically significant (or, equivalently, the nozzle diameter is not an important length scale of the flow). For that case any dependent variable, such as the terminal rise height y_t, is a function of M and B only:

$$y_t = f(M, B) \tag{17.4}$$

which, following a dimensional analysis leads to:

$$\frac{y_t}{d\mathrm{F}} = \text{Constant} \tag{17.5}$$

Similar analyses lead to the following expressions for the other major jet geometric parameters:

$$\frac{y_t}{d\mathrm{F}} = 2.2; \quad \frac{x_i}{d\mathrm{F}} = 2.4; \quad \frac{x_n}{d\mathrm{F}} = 9.0; \quad \frac{y_L}{d\mathrm{F}} = 0.7 \tag{17.6}$$

and for dilution:

$$\frac{S_i}{\mathrm{F}} = 1.6; \quad \frac{S_n}{\mathrm{F}} = 2.6 \tag{17.7}$$

where the values of the constants are taken from Roberts et al. (1997). The variables in Eqs. 17.6 and 17.7 are defined in Fig. 17.1: y_t is the terminal rise height, x_i the location of the jet impact point (and location of the minimum dilution on the lower boundary), x_n the length of the near field, y_L the thickness of the spreading layer, S_i the dilution at the impact point, and S_n the near field dilution (termed the ultimate dilution in Roberts et al. 1997). Equations 17.6 and 17.7 apply when the jets are fully turbulent, i.e. the jet Reynolds number, Re = ud/ν where v is the kinematic

fluid viscosity is greater than about 2000, and the Froude number is greater than about 20, when the dynamical effect of the source volume flux becomes negligible. These conditions will be satisfied by the jets issuing from typical concentrate diffusers.

17.4.2 Effect of Water Depth

The results summarized above are applicable when the receiving water depth is much greater than the jet rise height so there is no interaction with the free surface. It is sometimes necessary to situate diffusers in shallow water, however, where the jets may interact with the water surface, modifying their flow dynamics and possibly reducing dilution.

This introduces another parameter: the water depth, H, and a dimensionless parameter, dF/H that determines its effect. If $dF/H \ll 1$ the flow is fully submerged and Eqs. 17.6 and 17.7 would be expected to apply. If $dF/H \gg 1$ the flow is strongly affected by the water surface.

Jiang et al. (2012) measured the minimum surface dilution for various water depths and delineated three flow regimes: deep water where the jet is unaffected by the water surface, surface contact where the top of the jet impacts the water surface, and shallow water where the jet centerline intersects the water surface. Jiang et al. (2014) extended this study by investigating flow trajectory, cross-sectional profiles, and surface and return point dilutions for 30° and 45° dense jets in limited depths.

Abessi and Roberts (2014c) report further 3DLIF experiments. The experiments were conducted with nozzles oriented at 30°, 45°, and 60°. Typical 3DLIF flow images of a 60° jet in shallow water are shown in Fig. 17.3. They reveal complex three-dimensional interactions with the free surface, especially for steep nozzle angles in the shallow water regime. Time-averaged concentration fields were extracted from the central planes and used to measure the major flow characteristics: Dilutions at the maximum rise height, bottom impact point, and near field, and their locations. Normalized expressions for each parameter were derived and plotted versus dF/H.

For the deep water condition, the results followed those previously reported for fully submerged jets. As the depth decreases the top of the jet begins to interact with the water surface. This occurs at $dF/H = 0.82$, 0.52, and 0.44 for nozzle angles of 30°, 45°, and 60°, respectively. As the depth decreases further dilution decreases and eventually the jet centerline intersects the water surface marking the transition to the shallow water regime. This occurs at $dF/H = 1.4$, 0.8, and 0.78 for nozzle angles of 30°, 45°, and 60°, respectively. Tracer concentration profiles in the surface contact region are truncated by the water surface and are unsymmetrical. In the shallow water regime they resemble half-Gaussian profiles similar to those of wall

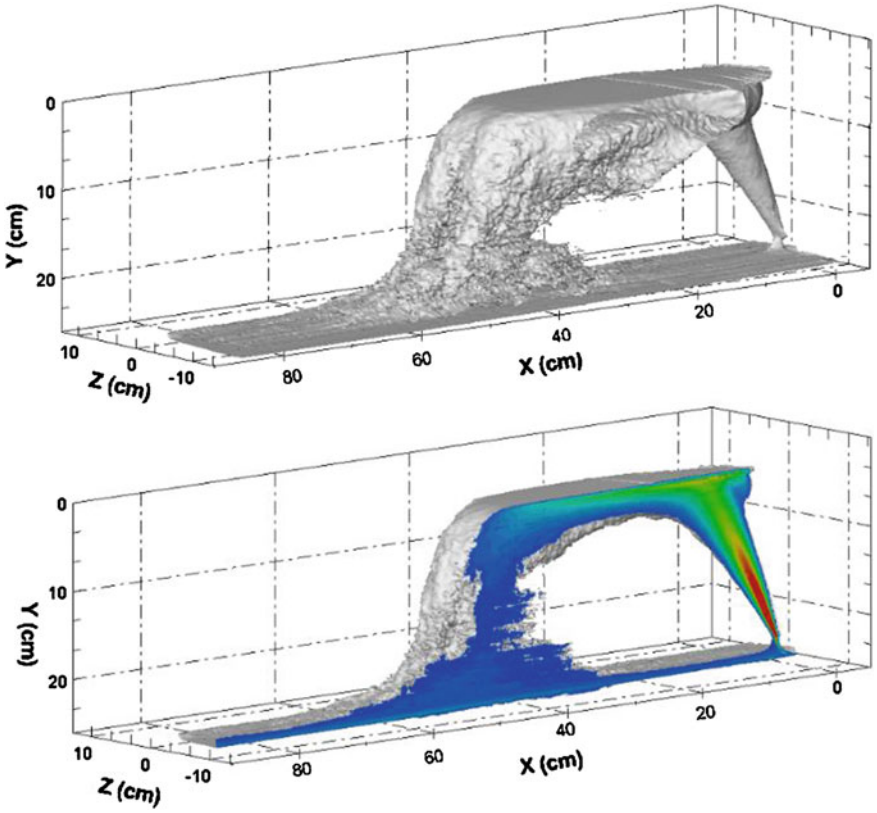

Fig. 17.3 3DLIF image of 60° dense jet in shallow water (from Roberts and Abessi 2014)

jets. The jets can cling to the water surface, although the locations of the bottom impact point and near field lengths are not significantly affected. The complex three-dimensional flows that can result with surface interactions may make them challenging to predict with mathematical models.

Of most importance for design are dilutions at the impact point and near field. In the deep water and surface contact regimes 60° nozzles gave the highest dilutions, as found in previous studies. As the depth decreases, however, the dilutions of the three nozzle angles become more similar, until for shallow water the 30° nozzle gives somewhat higher dilution. If it is necessary to situate a diffuser in shallow water, there may be advantages to the 30° nozzle because of its higher dilution and because there is less surface interaction and visual impact on the water surface.

17.5 Multiport Diffusers

17.5.1 Introduction

Most studies of the dynamics and mixing of inclined dense jets have been with single jets, but multiport diffusers have also been used and are becoming more common. Examples are Perth, Sydney, and Melbourne, Australia. Most designs have been based on formulae derived from experiments conducted with single jets. In a multiport diffuser the nozzles may discharge perpendicular to the diffuser axis and be uniformly distributed along either one or both sides of the diffuser. Or the nozzles may be clustered in rosettes each having multiple ports. The Perth diffuser has 40 ports distributed uniformly along one side of the diffuser at four meter intervals (Marti et al. 2011); the Sydney diffuser has two rosette risers spaced 25 m apart, each riser has four ports. Some hydraulic model tests of specific multiport diffusers have been made, for example Tarrade and Miller (2010).

Systematic studies of the effect of port spacing have been recently reported by Abessi and Roberts (2014a) to obtain guidelines to aid in the rational design of multiport diffusers. Their experiments were conducted on multiport diffusers that discharge from one or both sides and with rosette diffusers. The experiments were conducted with and without ambient currents and the various discharge parameters were systematically varied to cover a range expected for typical ocean outfall diffusers. Below we discuss some results of the studies on multiport diffusers with zero current. The experiments on multiport diffusers in flowing currents and on rosettes are discussed later.

17.5.2 Analysis

Consider the multiport diffuser shown in Fig. 17.4 (with discharge either from one or both sides) whose port spacing is s. For this case, the constants on the right hand sides of Eqs. 17.6 and 17.7 then become functions of $s/d\mathrm{F}$:

$$\frac{y_t}{d\mathrm{F}} = f\left(\frac{s}{d\mathrm{F}}\right); \quad \frac{x_i}{d\mathrm{F}} = f\left(\frac{s}{d\mathrm{F}}\right); \quad \frac{x_n}{d\mathrm{F}} = f\left(\frac{s}{d\mathrm{F}}\right); \quad \frac{S_i}{\mathrm{F}} = f\left(\frac{s}{d\mathrm{F}}\right); \quad \frac{S_n}{\mathrm{F}} = f\left(\frac{s}{d\mathrm{F}}\right) \tag{17.8}$$

The effect of the port spacing is therefore entirely encapsulated in the dimensionless parameter $s/d\mathrm{F}$.

Equation 17.8 has two asymptotic solutions. For $s/d\mathrm{F} \gg 1$ the ports are widely spaced and the jets do not interfere so the solutions should approach those for a single jet, Eqs. 17.6 and 17.7. For $s/d\mathrm{F} \ll 1$, the jets are close together and may behave as if emitted from a line, or slot, source. In that case, the relevant discharge parameters are not the individual jet momentum and buoyancy fluxes, but the volume, momentum, and buoyancy fluxes per unit diffuser length: q, m, and b:

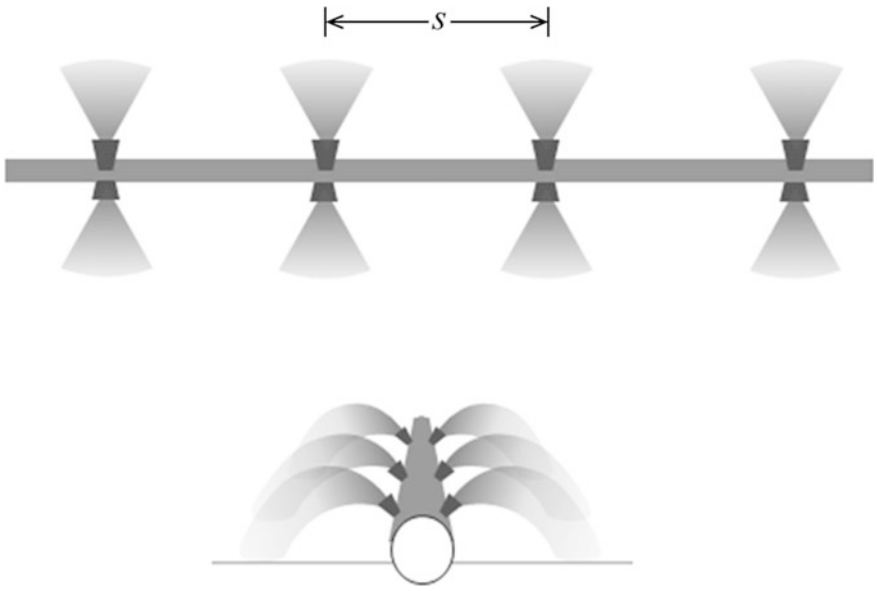

Fig. 17.4 Definition sketch for multiport dense effluent diffuser (from Roberts and Abessi 2014)

$$q = \frac{Q_T}{L}; \quad m = uq; \quad b = g_0' q \tag{17.9}$$

where Q_T is the total discharge from the diffuser and L the diffuser length. The analysis analogous to Eq. 17.4 for a line source is then:

$$y_t = f(m, b) \tag{17.10}$$

which, following a dimensional analysis becomes:

$$\frac{y_t b^{2/3}}{m} = \text{Constant} \tag{17.11}$$

For a long diffuser $b = B/s$ and $m = M/s$ and it can be shown that Eq. 17.11 becomes, after some manipulation, and using the definition of the Froude number, Eq. 17.3:

$$\frac{y_t}{d\text{F}} = C_1 \left(\frac{s}{d\text{F}}\right)^{-1/3} \tag{17.12}$$

Similar arguments apply to the other geometrical parameters, and for dilution:

$$\frac{S_n}{\mathrm{F}} = C_6\left(\frac{s}{d\mathrm{F}}\right)^{1/3} \tag{17.13}$$

where C_1 and C_6 are experimental constants. These equations should apply to diffusers with discharges from one or both sides, although the values of the constants may differ. As the jets are moved closer together, Eq. 17.12 implies that the rise height increases and Eq. 17.13 implies that the dilution decreases.

We would expect a transition between the single jet solutions ($s/d\mathrm{F} \gg 1$) and line jet solutions ($s/d\mathrm{F} \ll 1$) to occur at $s/d\mathrm{F} \sim \mathrm{O}(1)$. Systematic experiments were performed to test these hypotheses and to investigate the nature of these relationships.

The results for near field dilution are shown in Fig. 17.5; for other results see Abbessi and Roberts (2014a).

The results follow the expected point-source asymptotic solutions for $s/dF > \sim 2$ but for smaller spacings they do not follow the expected line source solutions. The rise height actually decreases as the spacing decreases rather than increases as predicted by Eq. 17.12. The impact and near field dilutions do decrease with spacing as expected, but much more rapidly than predicted by Eq. 17.13.

The following empirical equations were fitted to the results for $s/d\mathrm{F} < \sim 2$:

$$\frac{y_t}{d\mathrm{F}} = 1.9\left(\frac{s}{d\mathrm{F}}\right)^{1/2}; \quad \frac{x_i}{d\mathrm{F}} = 2.0\left(\frac{s}{d\mathrm{F}}\right)^{1/2}; \quad \frac{x_n}{d\mathrm{F}} = 6.0\left(\frac{s}{d\mathrm{F}}\right)^{1/2} \tag{17.14}$$

$$\frac{S_i}{\mathrm{F}} = 0.9\left(\frac{s}{d\mathrm{F}}\right); \quad \frac{S_n}{\mathrm{F}} = 1.1\left(\frac{s}{d\mathrm{F}}\right) \tag{17.15}$$

where the values of the constants are for diffusers discharging from one side.

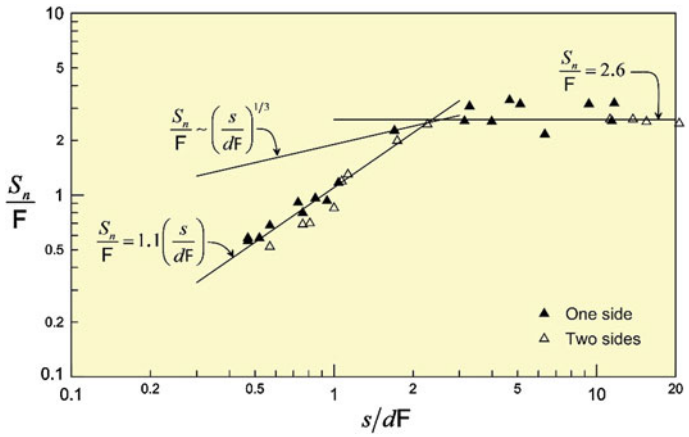

Fig. 17.5 Near field dilution of multiport dense effluent diffuser (from Roberts and Abessi 2014)

Even allowing for experimental scatter, Fig. 17.5 indicates that dilutions for diffusers with ports on both sides are systematically lower by about 20 % than for diffusers discharging to one side only (for otherwise similar values of F and s/dF). This reduction appears to be real despite the wide separation between the flows from each side (for example, Fig. 17.6). It is a secondary effect, probably mainly due to the slightly thicker bottom layer that forms with a discharge from both sides (which doubles the total discharge per unit diffuser length), thereby slightly increasing re-entrainment into the falling jet near the lower boundary. The corresponding constants for dilution for two-sided discharges would therefore be about 20 % lower than those given in Eq. 17.15.

Why the results did not follow those predicted for slot jets became evident from animations of the flows beginning at initiation of discharge. The jets at first rose much higher and then their rise height decreased to approach those shown in Fig. 17.6. The falling jets were re-entrained by the rising jets, filling the cavity between them and impeding their upward motion. The entrained flow could not penetrate through the jets to the interior, starving them and reducing dilution. This "sucking in" of the jets shortened the jet impact point distance and the length of the near field compared to similar single jets. This effect is also known as the Coanda effect. Clearly, the spacing must be large enough that entraining flow is freely available for the jets. According to Fig. 17.5 this occurs when $s/d\mathrm{F} > \sim 2$.

These results are generally consistent with the model studies that have been reported for multiport diffusers such as Miller et al. (2006). They are also consistent with the field observations for full flow of the Perth Stage 1 diffuser (discharge from

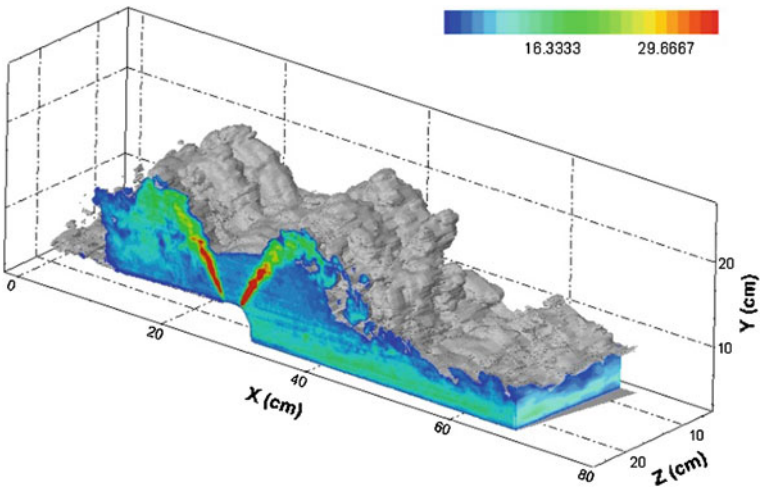

Fig. 17.6 3DLIF "instantaneous" image of flow from a multiport diffuser. F = 46, $s/(dF)$ = 0.6 (from Roberts and Abessi 2014)

one side) reported by Marti et al. (2011) correspond to $s/d\mathrm{F} \sim 1.3$, which is in the transition for port spacing effect.

Coanda dynamical interaction between buoyant jets from multiport diffusers can be important and has been noted in several contexts. It arises from the "Bernoulli" effect whereby proximity to a boundary or jet changes the entrained flow pattern resulting in a pressure force that deflects the jet towards it. If there is a boundary, such as the bed or water surface, the jet can cling to it; if there are adjacent jets, they entrain each other. An example for positively buoyant jets can be seen in Fig. 1a of Roberts et al. (1989). In the central region, the pressure force (or entrainment flow) is equally balanced on each side of the plumes and they rise vertically. The end plumes bend inwards, however, due to the unbalanced inward force acting on them.

Lai and Lee (2012) considered the dynamical interaction between multiple buoyant jets due to the induced pressure field. To predict the flow and pressure distribution they assume that the entrainment is due to distributed point sinks along the jet trajectory (the Distributed Entrainment Sink Approach, DESA, Choi and Lee 2007) and that the induced entrainment field is irrotational. The jet trajectories are then solved iteratively until a steady-state is achieved and the velocity and concentration fields are obtained by superposition. Although not specifically intended for dense jets with self-interaction between their rising and falling phases, this analysis may be applicable.

Similar dynamic interactions have also been noted for rosette diffusers with positively buoyant discharges. Roberts and Snyder (1993) found that increasing the number of ports per riser from 8 to 12 *decreased* dilution due to an inward bending of the plumes that resulted in merging and inhibited entrainment into the plumes' inner surfaces. Kwon and Seo (2005) also investigated rosette risers with four ports and reported inward bending due to "under pressure" in the flow core. These effects were further investigated in Tian and Roberts (2011) where rosette and "conventional" multiport diffusers were compared. Rosettes with eight ports resulted in inward bending of the plumes due to dynamic interaction, but did not significantly reduce dilution—provided the spacing is wide enough, which it is in the case of eight ports per riser but not twelve. It was also noted that the effect of dynamic interaction is more pronounced with zero currents and becomes less important in flowing currents.

This impaired dilution for merging dense jets is exacerbated by restricted entrainment at the diffuser ends. In the Abessi and Roberts' experiments, the channel walls are assumed to be planes of symmetry between ports, so the experiments represent the central section of a very long diffuser. For a diffuser of finite length, entrained flow can enter the inner core from its ends. For a single jet (or widely spaced jets) this issue does not arise as entrained flow is freely available, and any re-entrainment in the falling jet is already included in the dimensional analysis. The results of Fig. 17.4 are therefore probably conservative, and actual finite length diffusers should have higher dilutions.

These observations have significant implications for numerical modeling of multiport diffusers for dense jets. Integral entrainment models assume an unrestricted supply of entrainment water, neglect re-entrainment, and neglect dynamical

interaction (Coanda effect) between jets. All of these conditions are violated for the merged jets observed here and integral models may considerably overestimate dilutions. These deficiencies of entrainment models may be alleviated by including dynamic interaction such as by the DESA approach. CFD computations would also be very challenging as the entire flow field and restricted entrainment must be modeled. Physical modeling may be needed to predict these effects for complex diffuser geometries with multiple jets, for example, Miller and Tarrade (2010) and Tarrade and Miller (2010).

The increase in dilution from the impact point to the end of the near field is about 60 % for non-merged jets and 20 % for merged jets. For non-merged jets, that is similar to the observations on single dense jets in Roberts et al. (1997). No previous results have been reported for merged jets, but the increase in dilution from the impact point to the near field for positively buoyant fully merged (line plume) discharges was reported by Tian et al. (2004) to be also about 20 %. Point discharges show more increase because the bottom layer spreads in three dimensions approximately radially with ring-shaped entraining vortices whereas merged jets spread with entraining vortices that are more two dimensional.

In conclusion, for $s/d_F > \sim 2$ the jets do not merge and the geometrical and dilution results followed the expected asymptotic results for single jets. For $s/d_F < \sim 2$ the jets merged, but did not follow the expected line source solutions. The dilutions decreased as the spacing decreased, as expected, but much more rapidly than predicted. In order to prevent the reduction in dilution due to restricted entrainment, the jets must be sufficiently separated. To accomplish this it is recommended to maintain $s/d_F > \sim 2$.

17.6 Rosette Diffusers

Brine outfalls are frequently constructed as tunnels that discharge through risers. As risers and tunnels are expensive to construct, it is desirable to minimize the number of risers and the diffuser length by putting more ports on each riser and minimizing their spacing.

Rosette diffusers with dense discharges also show dynamic jet interactions. In stationary flows, Miller and Tarrade (2010) reported that risers with six ports had lower dilution than with four ports as the jets competed for clear water to entrain. With six risers the entrainment was primarily from above, and dilution was reduced if the tops of the jets were close to the water surface. Of course, there is a fundamental difference between rosettes with positively buoyant discharges compared to those with negatively buoyant discharges. Negatively buoyant flows allow entrainment from the top, as observed by Miller and Tarrade, whereas positively buoyant flows form a horizontal spreading layer that caps off the top. In that case the entraining flow can only come from gaps between the jets.

In a stationary environment, the dilution equation corresponding to Eq. 17.8 is:

$$\frac{S_n}{\mathrm{F}} = f\left(\frac{s_r}{d\mathrm{F}}\right) \tag{17.16}$$

where s_r is the riser spacing. Experiments to investigate the effect of s_r/dF were conducted by Roberts and Abessi (2014a) using single and multiple risers each containing four ports. Two different riser configurations were studied, as shown in Fig. 17.7. Each had four ports uniformly distributed around the perimeter (i.e. at 90° to each other in planform). The risers were rotated so that the ports were either perpendicular or parallel to the diffuser axis (Fig. 17.7a) or at 45° to the diffuser axis (Fig. 17.7b).

A typical 3DLIF image of a single rosette is shown in Fig. 17.8. Also shown is the concentration distribution along a central plane through two of the jets. The jets are similar to isolated ones although their dilution is somewhat reduced.

Results for near field dilution are shown in Fig. 17.9 along with results for an equivalent conventional diffuser that is assumed to have two ports per riser (in which case the equivalent port spacing is $s = s_r/2$). As for the multiport diffuser, the results become independent of riser spacing when $s_r/dF \gg 1$, in this case greater than about 2.5. The asymptotic value of dilution is less than that for a comparable conventional diffuser, however, because the jets interact even when the risers are widely separated (Fig. 17.8). Conversely, Fig. 17.9 shows that as the risers are moved closer together the dilution for a rosette is greater than that for equivalent two-port risers.

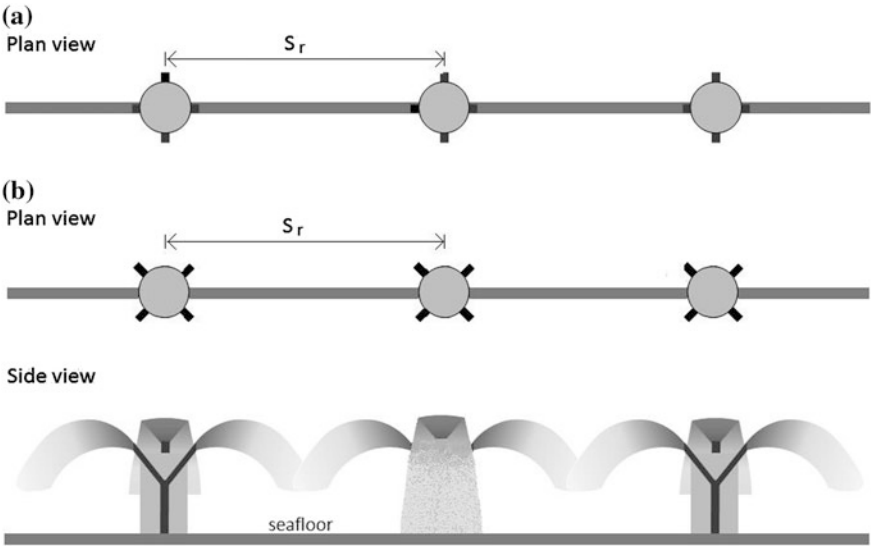

Fig. 17.7 Riser configurations tested (from Roberts and Abessi 2014)

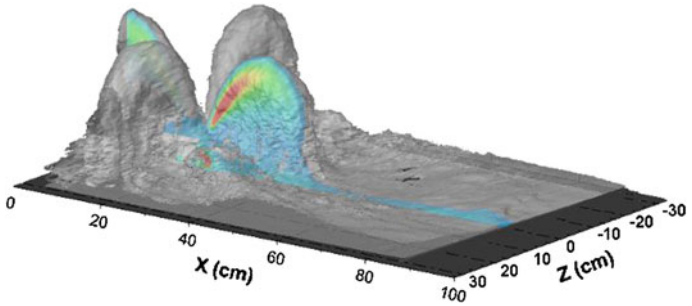

Fig. 17.8 3DLIF single rosette (from Roberts and Abessi 2014)

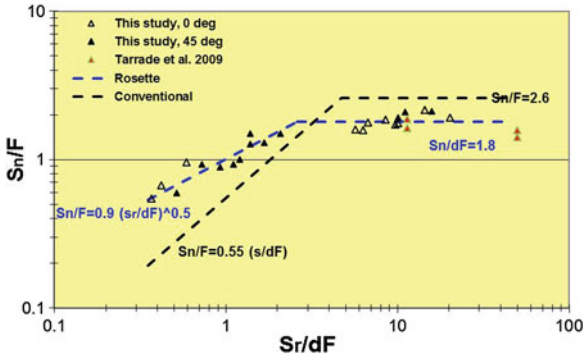

Fig. 17.9 Effect of riser spacing on near field dilution for 4-port rosettes (from Roberts and Abessi 2014)

The reason for this can be seen in Fig. 17.10 which compares images of a four-port riser and a two-port riser with approximately equal equivalent port spacings ($s_r/dF = 1.5$ for the four-port riser and $s/dF = 0.76$ for the two-port riser). As previously discussed, the two-port riser results in merging and restricted entrainment, significantly reducing dilution. The jets from the rosettes, however, remain distinct and able to entrain freely.

17.7 Effects of Flowing Currents

17.7.1 Introduction

The above discussions have been concerned with discharges into stationary environments. This is usually considered to be the worst case for dilution and is the usual basis for design. The ocean is rarely stationary, however, and, with a few notable exceptions, dilution generally increases with current speed. In this section we consider some aspects of the effects of flowing currents.

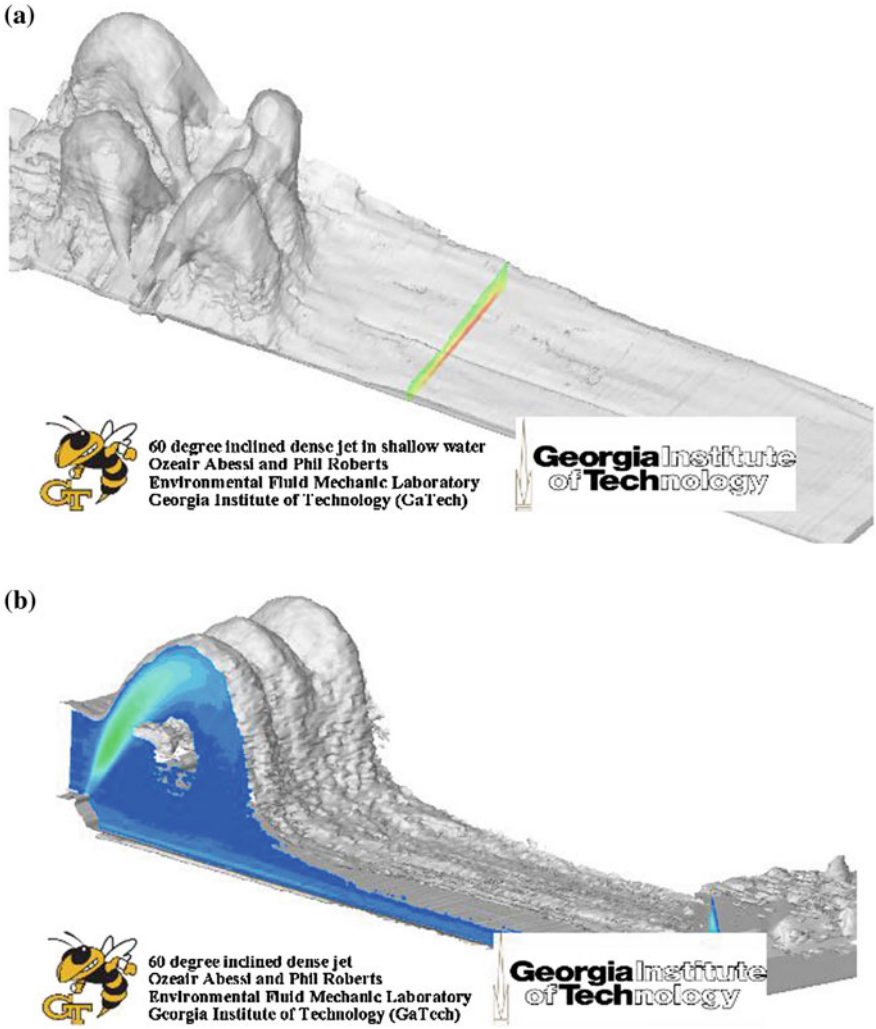

Fig. 17.10 Rosette and conventional diffusers with equivalent port spacings. **a** S_r/dF = 1.5 and **b** s/dF = 0.76 (from Roberts and Abessi 2014)

17.7.2 Single Vertical Jet

The simplest case, because it introduces only one new parameter, is the single vertical jet. The new parameter is the current speed, and because the jet is vertical its direction is immaterial.

The dynamical effect of the ambient current is mainly determined (Gungor and Roberts 2009) by the parameter u_rF where $u_r = u_a/u$ is the ratio of the current velocity u_a to the jet velocity u. Note that $u_r\mathrm{F} = u_a/\sqrt{g_0' d}$, which is itself a type of

Froude number based on the cross flow velocity, does not contain the jet velocity, u as a parameter. For $u_r\mathrm{F} \ll 1$, the current does not significantly affect the jet; the flow characteristics change as $u_r\mathrm{F}$ increases, however, as discussed below.

The terminal rise height y_t, the thickness of the bottom layer y_L, and the minimum dilutions at the impact point S_i, and at the terminal rise height S_t, can be written as:

$$\frac{y_t}{d\mathrm{F}}, \frac{y_L}{d\mathrm{F}}, \frac{S_i}{\mathrm{F}}, \frac{S_t}{\mathrm{F}} = f(u_r\mathrm{F}) \tag{17.17}$$

3DLIF Experiments on vertical dense jets to investigate the form of these equations are reported by Gungor and Roberts (2009).

Based on their studies, the following characteristics of a vertical dense jet in a cross flow emerge as sketched in Fig. 17.11. For zero current speed, the jet reaches a height $y_t \approx 2.2d\mathrm{F}$ and then falls back on itself, impairing dilution. This flow is sometimes called a fountain. The bottom layer flows radially in all directions as a density current and mixing continues in this layer beyond the impact point. With a current, the jet is bent downstream, and when $u_r\mathrm{F} \geq 0.2$ the ascending and descending parts of the flow separate. Because the ascending flow is now little influenced by the descending flow, the rise height increases and the dilution is higher than with no current. The bottom flow still intrudes as an upstream wedge against the current.

As the current speed increases further, the wedge becomes arrested and cannot propagate upstream. This occurs for a value of $u_r\mathrm{F}$ that lies somewhere between 0.24 and 0.37. The rise height is essentially constant over the range $0.2 < u_r\mathrm{F} < 0.8$. As $u_r\mathrm{F}$ is increased beyond 0.5, the rise height decreases slowly with increasing current speed, the jet is further bent over and impacts the lower boundary farther downstream. The trajectory of the ascending portion of the flow is generally quite steep, almost vertical, and the descending slope much more gradual. Further mixing still occurs in the bottom spreading layer, although it seems to be reduced compared to slower currents. For $u_r\mathrm{F}$ greater than about 1, the jet is significantly bent over and it becomes almost horizontal for $u_r\mathrm{F}$ greater than about 2. For this case, the jet will probably be dispersed by ambient turbulence in the receiving waters (Pincince and List 1973), i.e. it will go rapidly into the "far field," and/or be trapped by ambient density stratification. In either case, any impacts of the effluent on the seabed should

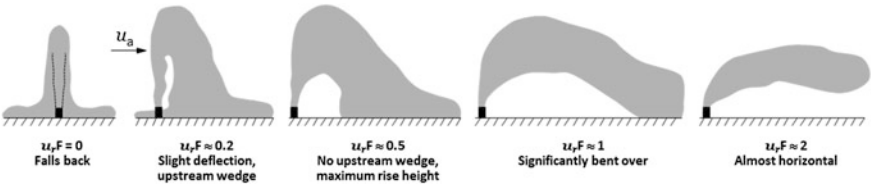

Fig. 17.11 Effect of currents on vertical dense jets (from Gungor and Roberts 2009)

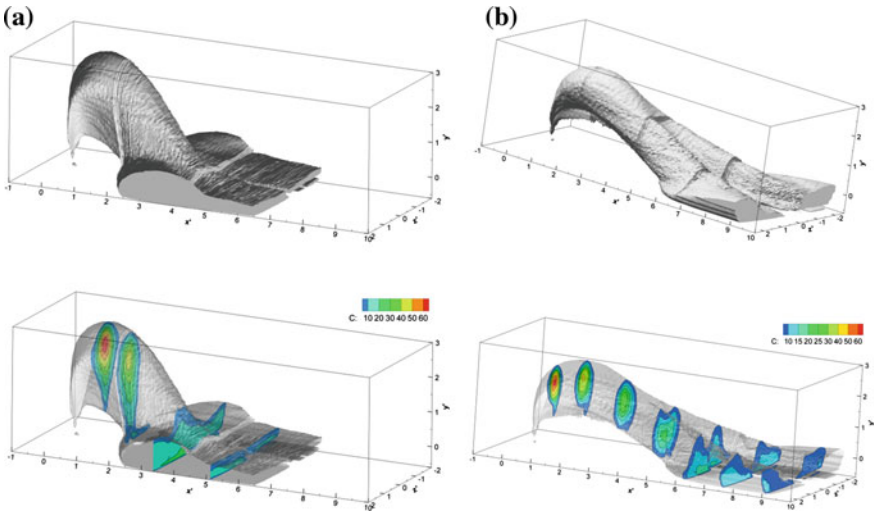

Fig. 17.12 3DLIF images of vertical jets in cross flows (from Gungor and Roberts 2009)

be minimal. The critical speeds of major interest are therefore u_rF < 1, which was the range investigated.

Some typical results for a moderate ($u_rF = 0.50$) and strong ($u_rF = 0.9$) currents are shown in Fig. 17.12.

For u_rF $\sim$ 0.5, the cross-sectional profiles of tracer concentration are neither axially symmetric nor self-similar. The jet is much taller than it is wide, and the peak concentration occurs much closer to the top. This results from a "gravitational instability" that causes fluid in the lower half of the jet to travel almost vertically and detrain from the jet. The detrained flow can be re-entrained back into the rising jet.

As the current speed increases to u_rF $\sim$ 0.9 this asymmetry decreases but other flow phenomena occur. The profiles in the rising portion are approximately radially symmetric but in the falling portion they develop a kidney shape due to formation of two counter-rotating vortices. These vortices cause the jet to almost completely bifurcate after impacting the bottom.

It was found that the rise height was essentially constant over the range of current speeds tested. The distance of the impact point and dilutions at the terminal rise height and impact point increased with current speed. The near field dilution is greater than the impact dilution due to additional mixing in the bottom layer.

The complexity of the flows and the different phenomena that dominate at different locations within the same jet and at different current speeds indicate that predicting these flows numerically will be quite challenging. Entrainment models are often used, but the experiments show flow features that violate some of their fundamental assumptions such as self and radial symmetry, and they also ignore mixing due to gravitational instability. Although entrainment models may predict trajectories reasonably well, their predictions of dilution should be viewed with caution.

17.7.3 Multiport Diffusers

Multiport diffusers in flowing currents involve more parameters than a single vertical jet. The discharge may be from one side of the diffuser only (e.g. Perth) in which case the current may be either co-flowing or counter-flowing relative to the jets, or it may discharge from both sides. Other variables are the port spacing and the angle of the current relative to the diffuser axis. Many experiments on various configurations of multiport diffusers are given in Roberts and Abessi (2014). Here we give just a few examples of the flows that may arise. The effects of port spacing and current are expressed by the dimensionless parameters u_rF and s/dF.

Co-flowing cases are illustrated in Fig. 17.13 which shows typical images for wide and narrow port spacings at various current speeds. The trajectories of a line source ($s/d\mathrm{F} \ll 1$) are different from a point source ($s/d\mathrm{F} \gg 1$); generally the trajectory is longer for point sources. The rise height decreases as $u_r\mathrm{F}$ increases with a break point near $s/d\mathrm{F} \approx 0.7$ for most $u_r\mathrm{F}$; beyond this point the maximum rise height does not change with $s/d\mathrm{F}$ and the flow behaves like a point source. The impact point moves farther downstream as $u_r\mathrm{F}$ increases.

Dilution at the maximum rise height and downstream both increase with $u_r\mathrm{F}$. For $s/d\mathrm{F} > \approx 0.7$ dilution does not change with $s/d\mathrm{F}$ and the flow approximates a point source. Impact point dilution increases with $u_r\mathrm{F}$ and also with $s/d\mathrm{F}$ which indicates that some merging occurs at some point downstream for smaller $s/d\mathrm{F}$.

Counter-flowing cases are illustrated in Fig. 17.14. Again the trajectories differ for line and point sources. The images also show an important phenomenon: at a particular current speed the jet can fall back directly on itself, which leads to reduced dilution. This occurs for $u_r\mathrm{F} \approx 0.67$. For higher current speeds, the maximum rise height decreases when $u_r\mathrm{F}$ increases.

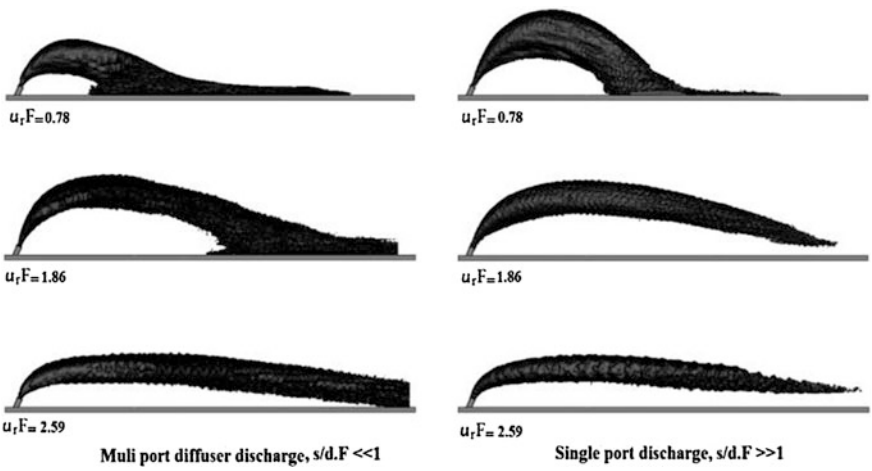

Fig. 17.13 Discharges in co-flowing currents for line sources ($s/d\mathrm{F} < 0.62$) and point sources ($s/d\mathrm{F} > 1.91$) (from Roberts and Abessi 2014)

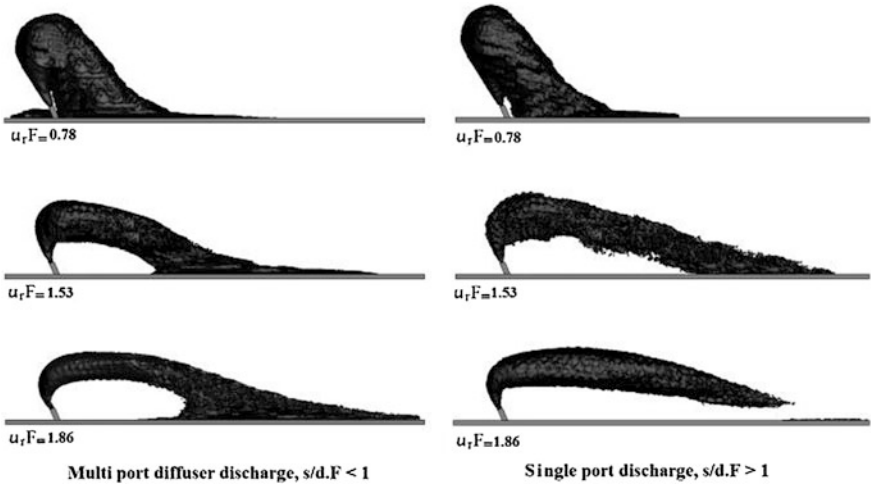

Fig. 17.14 Multiport and single port discharges in counter-flowing current (from Roberts and Abessi 2014)

The maximum rise height and dilution depend on port spacing (*s/d*F). They increase with *s/d*F up to *s/d*F ≈ 0.7 and then become independent of *s/d*F when the flows behave like point sources. The jet trajectories are influenced by merging; point source flows impinge the bed farther downstream than do line sources.

Finally, multiport diffusers with flows from both sides are illustrated in Fig. 17.15. Some experiments were conducted with a gap between the diffuser bottom and the channel bed to allow flow underneath the diffuser, and some with no gap. These two conditions are referred to as "blocked" and "unblocked."

The pattern of merging depends on the port spacing (*s/dF*) and the current speed (u_rF). For narrow spacing, the jets from both sides first merge with their neighbors and then with those from the opposite side of the diffuser. For wide spacing, the jets first merge with their corresponding jets from the opposite side, then with their neighbors. Figure 17.15 shows that the flow field can be significantly impacted by the presence or absence of the gap, which allows flow under the diffuser.

The wastefield geometric characteristics and dilution also depend on *s/dF* and u_rF. The rise height increases with *s/d*F in the range of 0.9–4.1, but differs for blocked and unblocked flows. The impact location for blocked and unblocked flows does not show any dependence on *s/d*F, although it is apparently shorter for the unblocked cases. The impact point dilution also increases with *s/d*F over the range of tested parameters and differs for blocked and unblocked cases. The flow trajectories show a significant influence of blocking; it increases the maximum rise height and decreases the impact point length. The blocked flow dilution at impact is less than when unblocked. These results show how a small gap beneath the diffuser and therefore relatively small changes in diffuser configuration can significantly impact the flow field in moving ambient waters.

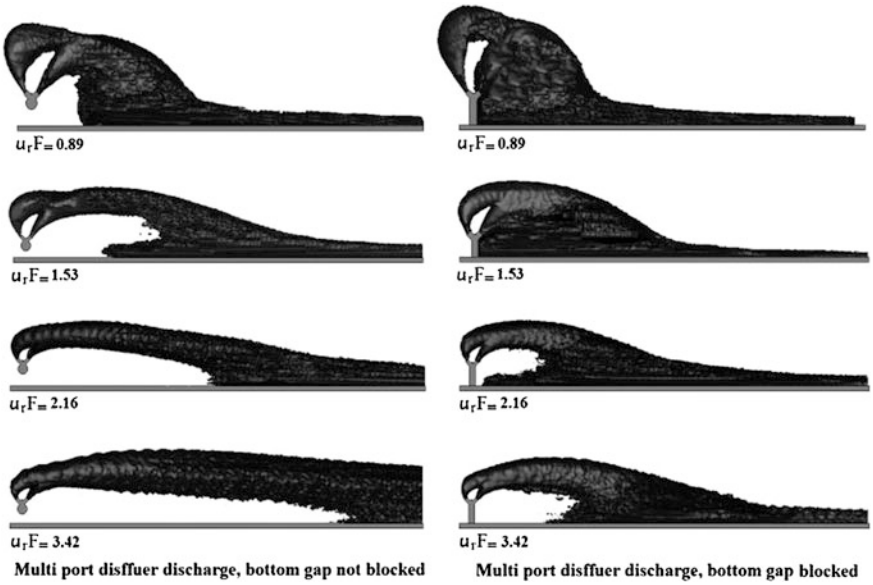

Fig. 17.15 Effect of flow blocking on discharges from multiport diffusers (from Roberts and Abessi 2014)

17.7.4 Rosette Diffusers

Experiments with single and multiple four-port rosettes in flowing currents are also reported in Roberts and Abessi. Again, multiple parameters are involved, including current speed, riser spacing, and rosette rotation (0° and 45°). Here we show just one example in Fig. 17.16. It is for a single riser with 0° rotation.

The four plumes merge downstream to a single one. For multiple risers, depending on the riser spacing, the jets may merge before interacting with those from a neighboring riser, or the jets issuing from adjacent risers may merge first. Examples are presented in Roberts and Abessi where results are given for dilutions and geometrical parameters for various flow conditions. Normalized trajectories for various u_rF show the importance of current on the flow behavior and how increases in ambient cross flow increase the distance of the impact point and dilution at this point. The influence of riser rotation is of secondary importance and can be ignored.

17.8 Mathematical Models

The above discussions have emphasized the physical aspects of near field mixing of dense jets. In many cases, satisfactory diffuser designs can be made by using the semi-empirical equations and "worst-case" conditions such as zero current speeds.

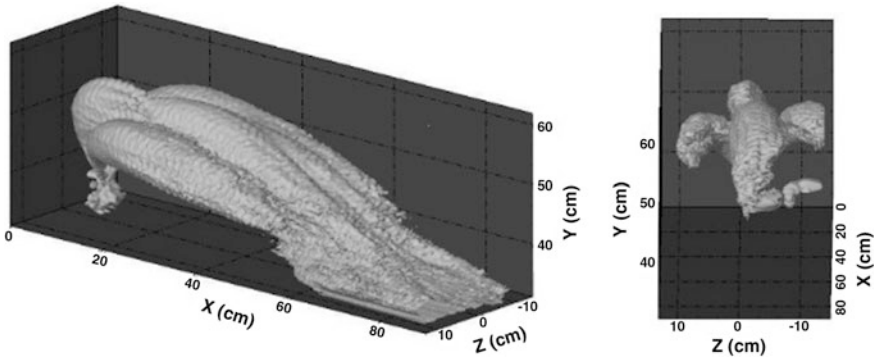

Fig. 17.16 Flow configuration for rosette diffusers in flowing water: 0° orientation (from Roberts and Abessi 2014)

Mathematical models are also essential of course, and means to couple the near field dynamics with far field hydrodynamic models to assess larger scale impacts are needed. Most near field models are of the entrainment, or integral, type or computational fluid dynamics (CFD).

Entrainment models are the most common ones used in engineering to predict near field dynamics of jets and plumes. Although they can be used for dense jets, their limitations should be kept in mind. They assume incorporation of external fluid into the jet by entrainment and the profiles of velocity and tracer concentration to be self-similar and axially symmetric. As shown here, however, dense jet flows often violate these assumptions, leading to unreliable predictions. For example, Pincince and List (1973) concluded that, although jet trajectories were reasonably predicted, dilutions were considerably underestimated. Anderson et al. (1973) concluded that the models can only predict trends, rather than exact dilutions and trajectories.

The vertical asymmetry in the tracer profiles, whereby the peak concentration is closer to the top (similar to Fig. 17.12a), has been observed in many previous studies of dense inclined jets in stationary environments and in cross flows. Lane-Serff et al. (1993) point out that the top half of the jet is gravitationally stable, with density decreasing upwards, but the bottom half is unstable, with heavier fluid above lighter fluid. This leads to the upper plume edge being sharp and well defined, but in the lower half fluid can detrain from the jet so the lower boundary is poorly defined. Lindberg (1994) also noted in his experiments with cross flows that low momentum fluid almost immediately descended after leaving the nozzle and this continued through the jet trajectory, and Kikkert et al. (2007) observed it in stationary inclined jets. This gravitational instability also leads to enhanced mixing within the jet and also between the jet and the environment.

Integral models do not usually include the additional mixing that occurs within the near field beyond jet impact. This can be substantial: for inclined jets in stationary environments, Roberts, et al. (1997) find the increase in dilution between the impact point and the end of the near field to be around 60 %.

Dynamical interaction of merging jets from multiport diffusers result in further complications. As discussed above, the jets entrain, or attract, each other, by the Coanda effect. If they are too close together (Fig. 17.6 for example), the supply of entraining water is restricted resulting in reduced dilution. In general, entrainment models do not predict the Coanda effect, which reduces jet rise height and dilution. For these cases, physical modeling may be more reliable.

Entrainment models may be Lagrangian, for example UM3 in the EPA model suite Visual Plumes, or VISJET, or Eulerian such as CORJET. For a recent extensive discussion and comparison of these models for simulating dense jets in stationary environments, see Palomar et al. (2012a, b). They found significant discrepancies between the models. Differences in dilution rate estimation were significant, motivating further review of the entrainment closure models and simplifying the assumptions made by integral models.

Computational fluid dynamics (CFD) models are now increasingly applied to a wide variety of turbulent flows in nature and engineering. There are several major CFD techniques; for a review, see Sotiropoulos (2005). One method is direct numerical simulation (DNS) where the unsteady, three-dimensional Navier-Stokes equations are solved over scales small enough to resolve the entire turbulence spectrum. The computational resources increase dramatically with Reynolds number, however, so DNS is not yet a practical modeling tool for simulating flows at engineering-relevant Reynolds numbers. Large Eddy Simulation (LES) solves the spatially filtered unsteady Navier-Stokes equations to resolve motions larger than the grid size, and models smaller-scale motions with a sub-grid model. For high Reynolds number flows of practical engineering interest very high grid resolutions and supercomputers are still required however. The most common CFD models are Reynolds-decomposition models. Flow quantities are decomposed into time-averaged and fluctuating values and the Navier-Stokes equations are then time averaged, producing what are known as the Reynolds-averaged Navier-Stokes (RANS) equations. Various adaptations of this model have been applied to many engineering flows.

There have been fewer applications of CFD to jet and plume-type flows. Hwang and Chiang (1995) and Hwang et al. (1995) simulated the initial mixing of a vertical buoyant jet in a density stratified cross flow. Blumberg et al. (1996) and Zhang and Adams (1999) used far-field CFD circulation models to calculate near field dilutions of wastewater outfalls. Law et al. (2002) used a revised buoyancy extended turbulence closure model to investigate the dilution of a merging wastewater plume from a submerged diffuser with 8-port rosette-shaped risers in an oblique current. Davis et al. (2004) used commercial codes to simulate several case studies of effluent discharges into flowing water, including a line diffuser, a deep ocean discharge, and a shallow river discharge. They concluded that CFD models are becoming a viable alternative for diffuser discharges with complex configurations.

The paucity of CFD applications to near field mixing is because of the challenges that they face. These arise from the geometrical complexity of realistic multiport diffusers, the large difference between port sizes and the other characteristic length scales, buoyancy effects, plume merging, flowing current effects, and

surface and bottom interactions. To overcome these difficulties, Tang et al. (2008) applied a three-dimensional RANS model using a domain decomposition method with embedded grids to model diffusers. CFD models of brine discharges have been reported by Muller et al. (2011), Oliver et al. (2008), and Seil and Zhang (2010). Although promising, the complexity of CFD models, the effort required to set them up and long run times suggests that entrainment and length-scale models will continue to be used for many years.

17.9 Concluding Remarks

In this chapter we have attempted to summarize and highlight some of the essential features of dense jets typical of those encountered in brine concentrate diffusers. It is possible to design a diffuser that will effect high initial dilution and safely dispose of concentrate with minimum environmental impacts. We have emphasized the physical aspects using laboratory experiments and visualizations to illustrate these processes. In many cases, the main features such as rise height, layer thickness, and dilution, can be estimated, and designs made, using the simple empirical formulae such as those presented here. More complex situations may require mathematical models. As pointed out, however, modeling is not simple. Entrainment models are frequently used, but they do not readily incorporate some flow features, in particular, lack of radial symmetry, changing flow characteristics along the jet trajectory, internal mixing due to gravitational instability, re-entrainment, dilution in the spreading layer, turbulence collapse and dynamical interaction between multiple jets. CFD models are being increasingly used in hydraulic engineering and their use will certainly increase in the future. They also face challenges, however, in simulating the features mentioned above and also their need to simulate the entire flow field, difficulty of grid and model setup, and long run times. Entrainment models will therefore probably be the mainstay of engineering calculations for some time with dynamical interactions possibly augmented by the DESA approach such as Choi and Lee (2007).

This dynamical interaction and Coanda effects should be acknowledged and incorporated into design, although they are difficult to predict mathematically. Experiments on multiport jets also show that small changes in diffuser design can result in significant changes in the flow field and therefore dilution. The difficulty of predicting these effects may indicate the need for physical models in complex situations.

Although the main features of dense jet dynamics are reasonably well understood, there remain many intriguing questions of a more fundamental research nature. For example, the dynamics of the bottom layer on sloping seabeds. This would probably increase dilution compared to the present results so the horizontal bed should be considered a “worst-case” for dilution. Bed forms could also have an impact.

Boundary interactions with the jet and its effect on dilution can also be important. Abessi and Roberts (2014b) report that as the descending jet approaches the lower boundary dilution tends to a constant value and then actually decreases in a thin boundary layer up to the wall. The presence of this thin layer may explain wide discrepancies in reported dilutions and may be environmentally important due to exposure of benthic organisms to high salinities. It does not persist far from the impact point, however, as it is swept up by the ring-like vortices that propagate radially from the impact point. The vortices entrain ambient fluid and increase dilution but they eventually collapse under their self-induced density stratification, marking the end of the near field. The dynamics of this collapse is not well understood.

Acknowledgments The author wishes to acknowledge and express his appreciation to Dr. Ozeair Abessi for his great expertise in tirelessly running many of the experiments discussed here and for many discussions on the mechanics of complex dense jet dynamics.

References

Abessi, O., & Roberts, P. J. W. (2014a). Multiport diffusers for dense discharges. *Journal of Hydraulic Engineering, 140*(8).

Abessi, O., & Roberts, P. J. W. (2014b). Effect of nozzle orientation on dense jets in stagnant environments. *Journal of Hydraulic Engineering* (Submitted).

Abessi, O., & Roberts, P. J. W. (2014c). Dense jet discharges in shallow water. *Journal of Hydraulic Engineering* (Submitted).

Blumberg, A. F., Ji, Z.-G., & Ziegler, C. K. (1996). Modeling outfall behavior using far field circulation model. *Journal of Hydraulic Engineering Division of the American Society of Civil Engineers, 122*(11), 610–616.

Choi, K. W., & Lee, J. H. W. (2007). Distributed entrainment sink approach for modeling mixing and transport in the intermediate field. *Journal of Hydraulic Engineering Division of the American Society of Civil Engineers, 133*(7), 804–815.

Crimaldi, J. P. (2008). Planar laser induced fluorescence in aqueous flows. *Experiments in Fluids, 44*(6), 851–863.

Davis, L., Davis, A., & Frick, W. (2004). Computational fluid dynamic application to diffuser mixing zone analysis—Case studies. In *3rd International Conference on Marine Wastewater Disposal MWWD 2004*, Catania, Italy, September 27–October 2, 2004.

Gungor, E., & Roberts, P. J. W. (2009). Experimental studies on vertical dense jets in a flowing current. *Journal of Hydraulic Engineering Division of the American Society of Civil Engineers, 135*(11), 935–948.

Hwang, R. R., & Chiang, T. P. (1995). Numerical simulation of vertical forced plume in a crossflow of stably stratified fluid. *Journal of Fluids Engineering, 117*, 696–705.

Jiang, B., Law, A. W.-K., & Lee, J. H.-W. (2012). Mixing of 45° inclined dense jets in shallow coastal waters: surface impact dilution. *Third International Symposium on Shallow Flows*, Iowa City, Iowa, USA.

Jiang, B., Law, A. W.-K., & Lee, J. H.-W. (2014). Mixing of 30° and 45° inclined dense jets in shallow coastal waters. *Journal of Hydraulic Engineering Division of the American Society of Civil Engineers, 140*(3), 241–253.

Kikkert, G. A., Davidson, M. J., & Nokes, R. I. (2007). Inclined negatively buoyant discharges. *Journal of Hydraulic Engineering Division of the American Society of Civil Engineers, 133*(5), 545–554.

Koochesfahani, M. M., & Dimotakis, P. E. (1985). Laser-induced fluorescence measurements of mixed fluid concentration in a liquid plane shear layer. *AIAA Journal, 23*(11), 1700–1707.

Kwon, S. J., & Seo, I. W. (2005). Experimental investigation of wastewater discharges from a Rosette-type diffuser using PIV. *KSCE Journal of Civil Engineering, 9*(5), 355–362.

Lai, A. C. H., & Lee, J. H. W. (2012). Dynamic interaction of multiple buoyant jets. *Journal of Fluid Mechanics, 708*, 539–575.

Lane-Serff, G. F., Linden, P., & Hillel, M. (1993). Forced, angled plumes. *J. Hazardous Materials, 33*(1), 75–99.

Lattemann, S., & Höpner, T. (2008). Environmental impact and impact assessment of seawater desalination. *Desalination, 220*(1–3), 1–15.

Law, A. W.-K., Lee, C. C., & Qi, Y. (2002). CFD modeling of a multi-port diffuser in an oblique current. In *MWWD2002,* Istanbul, Turkey, September 16–20, 2002.

Lindberg, W. R. (1994). Experiments on negatively buoyant jets, with and without cross-flow. In *NATO Advanced Research Workshop on "Recent Advances in Jets and Plumes" NATO ASI Series E* (Vol. 255, pp. 131–145). Viana do Castelo, Portugal: Kluwer Academic Publishers.

Marti, C. L., Antenucci, J. P., Luketina, D., Okely, P., & Imberger, J. (2011). Near-field dilution characteristics of a negatively buoyant hypersaline jet generated by a desalination plant. *Journal of Hydraulic Engineering Division of the American Society of Civil Engineers, 137*(1), 57–65.

Miller, B. M., Glamore, W. C., Timms, W. A., & Pells, S. E. (2006). *Physical modeling of desalination brine outlet, Perth (Stage 2).* The University of New South Wales, School of Civil and Environmental Engineering, Water Research Laboratory.

Miller, B., & Tarrade, L. (2010). Design considerations of outlet discharges for large seawater desalination projects in Australia. In *6th International Conference on Marine Wastewater Discharges, MWWD 2010,* Langkawi, Malaysia, October 25–29, 2010.

Muller, J., Seil, G., & Hubbert, G. (2011). Three modelling techniques used in Australia to model desalination plant brine dispersal in both the near-field and far-field. In *International Symposium on Marine Outfall Systems,* Mar del Plata, Argentina, May 15–19, 2011.

Oliver, C. J., Davidson, M. J., & Nokes, R. I. (2008). k-ε predictions of the initial mixing of desalination discharges. *Environmental Fluid Mechanics, 8*, 617–625.

Palomar, P., Lara, J. L., & Losada, I. J. (2012a). Near field brine discharge modeling part 2: Validation of commercial tools. *Desalination, 290*(0), 28–42.

Palomar, P., Lara, J. L., Losada, I. J., Rodrigo, M., & Alvárez, A. (2012b). Near field brine discharge modelling part 1: Analysis of commercial tools. *Desalination, 290*, 14–27.

Pincince, A. B., & List, E. J. (1973). Disposal of brine into an estuary. *Journal of WPCF, 45*(11), 2335–2344.

Roberts, P. J. W., Ferrier, A., & Daviero, G. J. (1997). Mixing in inclined dense jets. *Journal of Hydraulic Engineering Division of the American Society of Civil Engineers, 123*(8), 693–699.

Roberts, P. J. W., & Abessi, O. (2014). *Optimization of desalination diffusers using three-dimensional laser-induced fluorescence*. Final Report Prepared for United States Bureau of Reclamation. Georgia Tech, Atlanta, Georgia.

Roberts, D. A., Johnston, E. L., & Knott, N. A. (2010). Impacts of desalination plant discharges on the marine environment: A critical review of published studies. *Water Research, 44*(18), 5117–5128.

Roberts, P. J. W., & Snyder, W. H. (1993). Hydraulic model study for the Boston Outfall. II: Environmental performance. *Journal of Hydraulic Engineering Division of the American Society of Civil Engineers, 119*(9), 988–1002.

Roberts, P. J. W., Snyder, W. H., & Baumgartner, D. J. (1989). Ocean outfalls. I: Submerged wastefield formation. *Journal of Hydraulic Engineering Division of the American Society of Civil Engineers, 115*(1), 1–25.

Roberts, P., Jenkins, S., Paduan, J., Schlenk, D., & Weis, J. (2012). *Management of brine discharges to coastal waters: Recommendations of a science advisory panel.* Environmental Review Panel (ERP). Southern California Coastal Water Research Project (SCCWRP). Costa Mesa, CA. Technical Report 694. http://www.swrcb.ca.gov/water_issues/programs/ocean/desalination/docs/dpr.pdf.

Seil, G., & Zhang, Q. (2010). CFD modeling of desalination plant brine discharge systems. *Water*, September 2010. 79–83.

Smith, R., Purnama, A., & Al-Barwani, H. H. (2007). Sensitivity of hypersaline Arabian Gulf to seawater desalination plants. *Applied Mathematical Modelling, 31*(10), 2347–2354.

Sofianos, S., Johns, W. E., & Murray, S. (2002). Heat and freshwater budgets in the Red Sea from direct observations at Bab el Mandeb. *Deep Sea Research Part II: Topical Studies in Oceanography, 49*(7–8), 1323–1340.

Sotiropoulos, F. (2005). Introduction to statistical turbulence modeling for hydraulic engineering flows. In P. D. Bates, S. N. Lane, & R. I. Ferguson (Eds.), *Computational fluid dynamics*. New York: Wiley.

Tang, H. S., Paik, J., Sotiropoulos, F., & Khangaonkar, T. (2008). Three-dimensional numerical modeling of initial mixing of thermal discharges at real-life configurations. *Journal of Hydraulic Engineering Division of the American Society of Civil Engineers, 134*(9), 1210–1224.

Tarrade, L., & Miller, B. M. (2010). *Physical modeling of the victorian desalination plant outfall*. The University of New South Wales, School of Civil and Environmental Engineering, Water Research Laboratory.

Tian, X., & Roberts, P. J. W. (2003). A 3D LIF system for turbulent buoyant jet flows. *Experiments in Fluids, 35*, 636–647.

Tian, X., Roberts, P. J. W., & Daviero, G. J. (2004). Marine wastewater discharges from multiport diffusers I: Unstratified stationary water. *Journal of Hydraulic Engineering Division of the American Society of Civil Engineers, 130*(12), 1137–1146.

Tian, X., & Roberts, P. J. W. (2011). Experiments on marine wastewater diffusers with multiport Rosettes. *Journal of Hydraulic Engineering Division of the American Society of Civil Engineers, 137*(10), 1148–1159.

Zhang, X. Y., & Adams, E. E. (1999). Prediction of near field plume characteristics using a far field circulation model. *Journal of Hydraulic Engineering Division of the American Society of Civil Engineers, 125*(3), 233–241.

Chapter 18
Tiered Modeling Approach for Desalination Effluent Discharges

Tobias Bleninger and Robin Morelissen

Abstract The mixing behavior of desalination plant effluents in the receiving waters is significantly influenced by the effluent density, which is dominated by the varying effluent salinity and temperature. The dense RO (reverse osmosis) effluent flow has the tendency to fall as a negatively buoyant plume. The MSF (multi-stage-flash) effluent is distinguished by a neutral to positive buoyancy flux that causes the plume to rise. This chapter describes the principle steps to model effluent dispersion in the receiving environment and to improve discharge design and siting. The different modeling tools are described and applied for typical case studies. A modelling framework for the environmental-hydraulic design of the outfall system for desalination plants has been developed and combined with a tiered approach to facilitate discharge assessments. Furthermore, environmental regulations and opportunities for site-specific, ecologically relevant criteria are discussed. The tiers include initial screening methods, using rapid assessment tools to determine the significance of the discharge. Length-scale based flow classification, nomograms, and empirical dilution equations are applied for that. Subsequent application of mixing zone models improves the discharge design and allows for assessment of potential environmental impacts. The discharge siting is then improved by considering also water quality parameters using a combined modeling approach coupling a near-field model to a far-field model. The final tier presents a dynamically coupled modeling system, which is necessary for large discharge flows and complex environmental conditions, where a feedback mechanism is necessary to couple both models. Results indicate that the tiered approach applied to modeling methods is capable to assess potential impacts of desalination plant effluents on the receiving waters and to improve the discharge system.

T. Bleninger (✉)
Dpto. de Engenharia Ambiental (DEA), Universidade Federal do Paraná (UFPR), Curitiba, Brazil
e-mail: tobias.bleninger@gmail.com

R. Morelissen
Hydraulic Engineering, Deltares, Delft, The Netherlands
e-mail: Robin.Morelissen@deltares.nl

T.M. Missimer et al. (eds.), *Intakes and Outfalls for Seawater Reverse-Osmosis Desalination Facilities*, Environmental Science and Engineering,
DOI 10.1007/978-3-319-13203-7_18

Nomenclature

b	jet width (radial distance from centerline where 1/e of centerline quantity) (m)
C	substance concentration (mg/ℓ,kg/m^3)
D	internal pipe diameter (m)
F_o	initial (source) densimetric Froude number (–)
g	gravitational acceleration (m/s^2)
g'	reduced gravity, $g' = \Delta\rho/\rho g$ (m/s^2)
H	head above datum/water depth (m)
j_o	buoyancy flux per diffuser length, $j_o = g'q_o$ (m^3/s^2)
J_o	buoyancy flux (m^4/s^3)
h_o	height of discharge port (m)
ℓ	riser spacing (m)
L	length of the considered pipe section (m)
L_M	momentum length scale (m)
ℓ_M	slot jet/plume transition length scale $\ell_M = m_o/j_o^{2/3}$ (m)
ℓ_m	crossflow length scale $\ell_m = m_o/u_a^2$ (m)
ℓ_m'	stratification length scale $\ell_m' = m_o^{1/3}/\varepsilon^{1/3}$ (m)
ℓ_b'	stratification/plume length scale $\ell_b' = j_o^{1/3}/\varepsilon^{1/2}$ (m)
ℓ_a	stratification/crossflow length scale $\ell_a = u_a/\varepsilon^{1/2}$ (m)
m	momentum flux per diffuser length (m^3/s^2)
M	momentum flux (m^4/s^2)
Q	total flow through outfall system (m^3/s)
q	mass flux per diffuser length (m^2/s)
Re	Reynolds number $Re = VD/\nu$ (–)
S	dilution, $S = C_o/C$ (–)
t	time (s)
t_M	jet/plume time scale $t_M = m_a/j_o$ (s)
t_m	jet/crossflow time scale $t_m = m_a/u_a^3$ [s] (s)
T_{90}	the time taken for 90 % of the bacteria to die-off (h)
u, v, w	velocity (m/s)
U, V, W	mean velocity (m/s)
x, y, z	Cartesian coordinates (m)

Greek symbols

μ	dynamic viscosity (Ns/m^2)
ν	kinematic viscosity (m^2/s)
ε	stratification parameter, $\varepsilon = -(g/\rho_a)(d\rho_a/dz)$
θ	slope or discharge angle (°)
ρ	density (kg/m^3)

Indices

a	ambient
b	background
B	bottom/bed
c	centerline
e	effluent
ff	far-field
i	impingement point
min	minimal
max	maximum
nf	near-field
o	initial quantity
tot	total

18.1 Introduction

The impacts of a seawater desalination plant discharge on the marine environment depend on the physical and chemical properties of the desalination plant reject streams and the susceptibility of coastal ecosystems to these discharges depending on their hydrographical and biological features. Therefore, a good knowledge of both the effluent properties and the receiving environments is required in order to evaluate the potential impacts of desalination plants on the marine environment (Bleninger et al. 2009). This can be achieved by carrying out site- and project-specific EIA (environmental impact assessment) studies. This chapter provides required background information for the discharge related impact analysis using mathematical modeling systems. It supports the planning process by providing prediction tools to simulate and predict the distribution and fate of substances discharged from desalination plants.

The brine (or concentrate) is the waste stream produced by desalination plants and is usually discharged into the sea. The brine flow rates are large, generally up to 60 % (RO) and up to 90 % (MSF, including cooling water) of the intake flow rate, thus larger than the required drinking water flow rate considering the currently possible recovery rates of those technologies. The brine is characterized by its high concentration of substances taken out of marine waters (i.e. salt). Furthermore, and often more critical, the brine contains additives and corrosion products. Additives are chemicals used for biofouling control (e.g. chlorine), scale control (antiscalants), foam reduction, and corrosion inhibition that are added during the desalination process and discharged into the coastal waters as contaminants (Lattemann and Höpner 2003). In addition, next to the high salinity and contaminants, the brine

effluent might also show increased turbidity and temperature (the former mainly applies to RO, the latter mainly applies to MSF plants). Main problems arise due to the strongly limited mixing behavior in the receiving waters, which is significantly influenced by the effluent density, which is dominated by the varying effluent salinity and temperature (Fig. 18.1a, b). The dense RO (reverse osmosis) effluent flow has the tendency to fall as a negatively buoyant plume. The MSF (multi-stage-flash) effluent is distinguished by a neutral to positive buoyant flux causing the plume to rise. The impacts of these pollutants and brine characteristics on the marine environment can be diverse and must be mitigated by technical measures. *Discharge technologies* aim for enhanced effluent dispersion in the receiving environment and adequate discharge siting to avoid pollutant accumulation, to protect sensitive regions and to utilize natural purification processes. *Submerged, offshore, multiport diffuser outfalls* designed as efficient mixing devices installed at locations with high transport and purification capacities are capable to reduce environmental impacts significantly. However, modeling techniques are needed for the design and optimization of such installations.

The description and application of such tools is the overall objective of this chapter. A modeling framework for the environmental-hydraulic design of the outfall system for desalination plants has been developed and combined with a tiered approach.

18.2 Effluent Characteristics

The brine (or concentrate) is the waste stream produced by desalination plants. The brine is characterized by its high concentration of substances taken out of marine waters (i.e. salt). Furthermore, and often more critical, the brine contains additives and corrosion products (Bleninger et al. 2009). A sharp distinction in brine characteristics exists between the two major desalination processes. RO plants have a recovery rate from 20 to 50 %. In contrast, MSF plants have lower recovery rates (10–20 %) because of additionally having large cooling water demands (Goebel 2005). Thus, the effluent flow rate is 4–5 times higher for thermal desalination than for RO processes referring to the same amount of produced fresh water (Table 18.1). In the case of a MSF plant coupled with a power plant, the drinking water flow is only about 4 % of the total intake flow (Lattemann and Höpner 2003), which is illustrated generally in (Fig. 18.2). Those general flow distributions have to be considered in detail, when determining the final effluent characteristics. Simple mass balance calculations combined with a density calculator (e.g. Bleninger et al. 2010) would be sufficient for that purpose.

Salinity and temperature are essential properties that differ between the two processes. This causes differences in the effluent density since it varies with salinity and temperature—the higher the salinity, the higher the density; the higher the

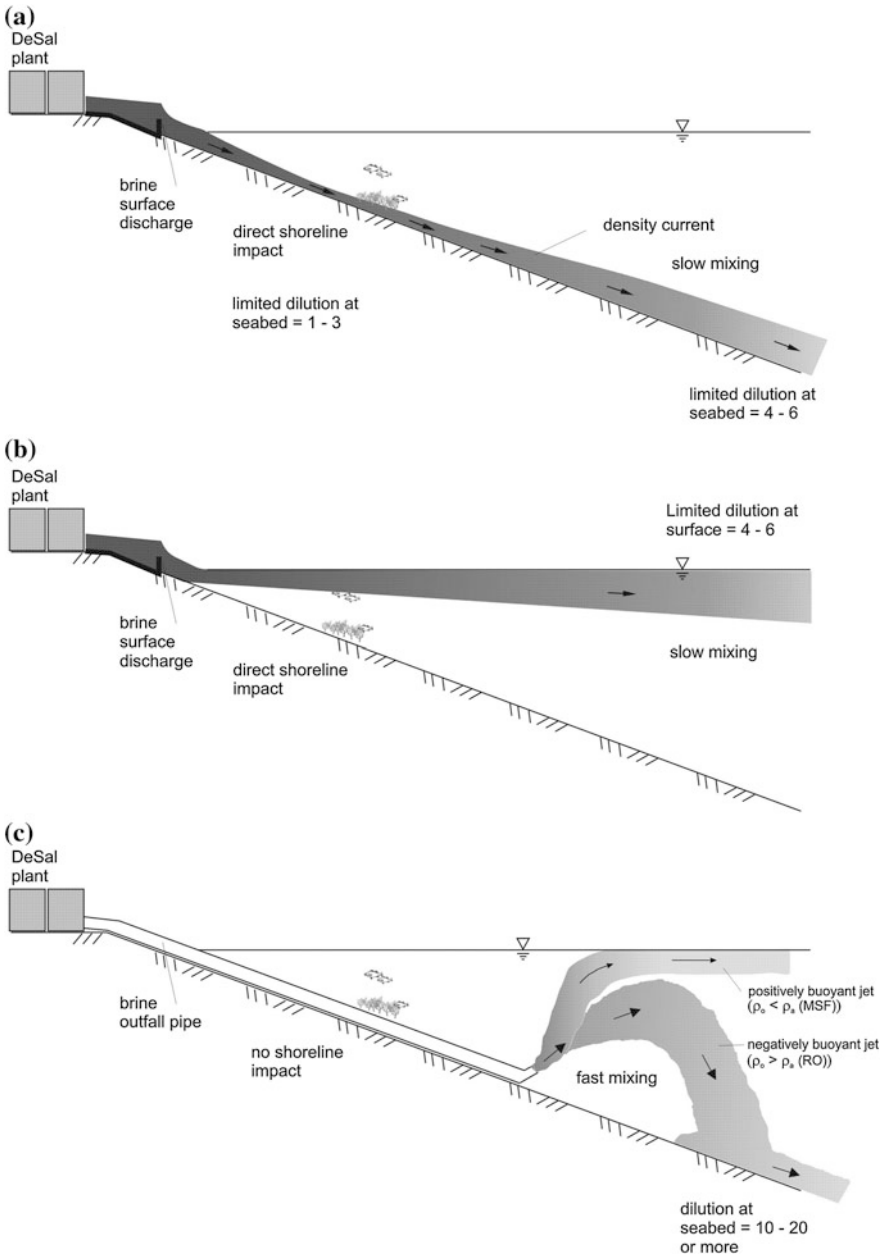

Fig. 18.1 Mixing characteristics and substance distributions for different brine discharge configurations and effluents (Bleninger and Jirka 2008). **a** RO plant (dense effluent) shoreline discharge via channel or weir, **b** thermal plant (dense effluent mixed with buoyant cooling water) shoreline discharge via channel or weir, **c** submerged discharge (dense effluent) via pipeline and nozzle or diffuser

Table 18.1 Comparison of properties of MSF and RO plants (following Goebel 2005)

	MSF	RO
Driving force	Increased temperature	Pressure
Energy demand	Thermal (95 %) ≡ 13–18 kWh_{el} plus thermal energy in the form of steam	Electrical 4–5 kWh_{el}
Recovery rate (Q_{fresh}:Q_{intake}) (%)	10–20	20–50
Cooling required	Yes	No
$\Delta T = T_o - T_a$ (°C)	5–15	ca. 0
Example study		
Q_{fresh} (m^3/s)	4	4
Q_{intake} (m^3/s)	39	12.5
Q_{cool} (m^3/s)	27	–
Q_{brine} (m^3/s)	8	8.5
$Q_o = Q_{brine} + Q_{cool}$ (m^3/s)	35	8.5
T_o (°C)	37.7	27.7
Sal_o	40.4	65.3
ρ_o (kg/m^3)	1022.9	1045.5

Discharge characteristics are assumed for a typical MSF plant (recovery: 10 %, $\Delta T = 10$ °C) and a RO plant (recovery: 32 %) with a fresh water production of $Q_{fresh} = 345$ Ml/d = 4 m^3/s according to Lattemann and Höpner (2003). "*o*" indicates the effluent characteristics. Ambient properties: $\rho = 1023.5$ kg/m^3; $Sal = 36.3$; $T = 27.7$ °C. Q = flow rate, T = temperature, Sal = salinity, ρ = density (Fig. 18.3)

temperature, the lower the density ($T > 4$ °C). In the case of RO, the salt concentration of brine can reach almost twice the concentration of seawater. No heating or phase change takes place in RO (Buros 2000). This results in a strongly increased effluent density. The brine of MSF plants is extremely hot ($T > 100$ °C) but is blended with cooling water from the MSF process, which reduces the overall effluent temperature to about 10 °C above the receiving water temperature. The increased effluent temperature minimizes the density difference arising from the elevated salt content (increased by 15 %). Usually coupled with power generation plants, the effluent produced by MSF is additionally mixed with cooling water from the power plant. As a result, the effluent is lighter than the receiving water (Lattemann and Höpner 2003). Summarized, this means that in contrast to a MSF plant, a RO plant rejects less water with a higher salinity and a higher density as illustrated in (Fig. 18.2).

According to the WHO guidance paper on desalination, more than 90 % of all large seawater desalination plants dispose of the concentrate into the ocean via an outfall system (WHO 2007), consequently being the option considered in the following sections. This applies particularly to seawater desalination plants with large discharge volumes (Mickley 2006).

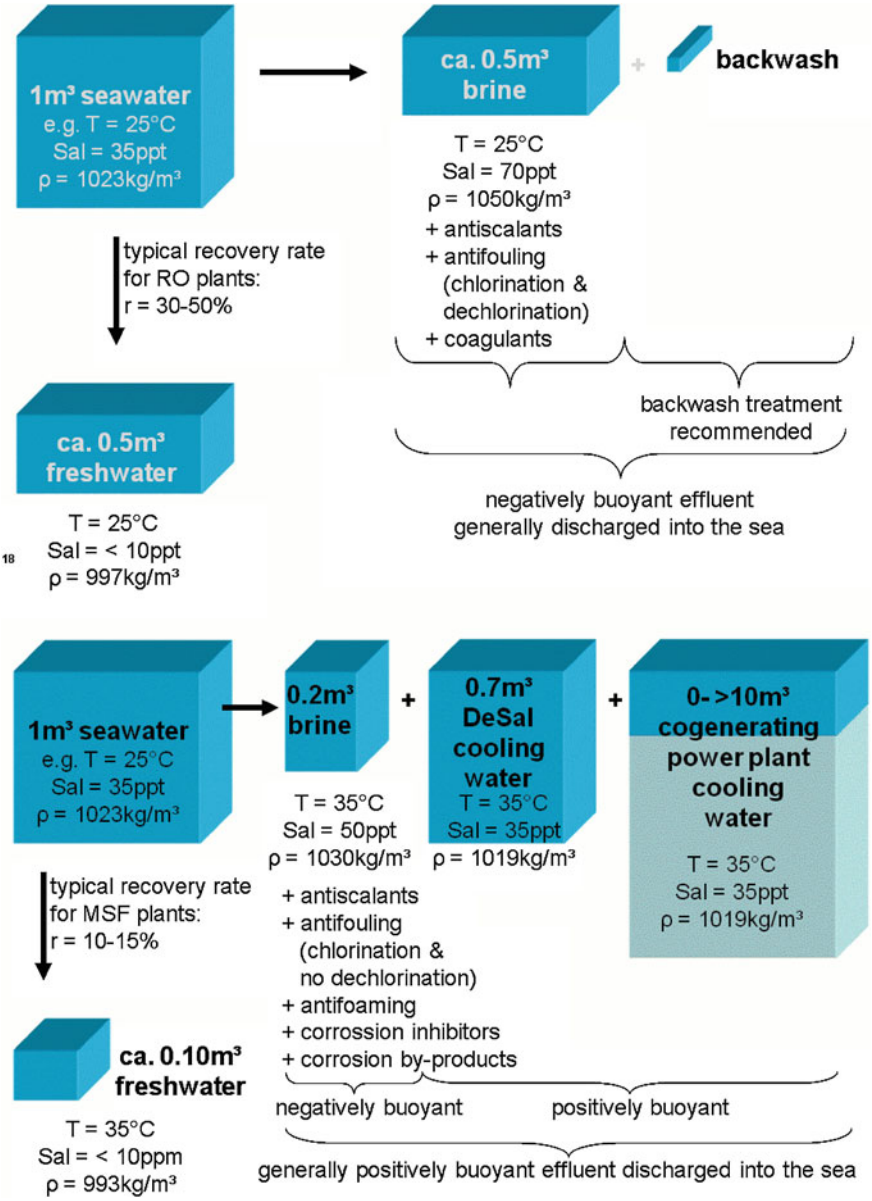

Fig. 18.2 Desalination effluent characteristics. *Top* RO-effluent, *down* MSF-effluent (Bleninger et al. 2009)

18.3 Discharge Systems

The various density differences between the brine and the receiving water represented by the buoyancy flux causes different flow characteristics of the discharge (Fig. 18.1). The dense RO effluent flow has the tendency to fall as a negatively buoyant plume. The MSF effluent is distinguished by a neutral to positive buoyant flux causing the plume to rise. Figure 18.3 illustrates the typical behavior of positively or negatively buoyant jet discharging into the receiving water through a submerged single port outfall.

Ocean outfalls are classified according to their location (onshore surface discharges/offshore submerged discharges), their mixing features (single port/multiport) and their effluent characteristics (positively buoyant, or negatively buoyant).

Onshore surface discharges have traditionally been installed due to their low costs. Examples are shown in Figs. 18.4, 18.5 and 18.6 summarized by Bleninger et al. (2009). However, such discharges should be analyzed carefully and generally be avoided due to their limited mixing characteristics, high visibility, their need for large scale coastal constructions, and thus generally larger impacts (Fig. 18.1).

Shoreline discharges may cause shoreline impacts by causing high concentrations accumulating in the near-shore region due to the limited mixing characteristics of these discharges. Further direct impacts are caused by the often-necessary large-scale discharge and protection structures (wave protection, stilling basins, etc.), and their effect on coastal currents and sediment transport characteristics.

Therefore, it is recommended to apply modern efficient mixing devices, which overcome the limitations of the traditional surface onshore discharges. Such single or multiport submerged diffuser systems are characterized by their flexible location and their high mixing rates (Fig. 18.7). These discharge technologies follow two main principles, aiming for *enhanced effluent dispersion* in the receiving environment and providing an *adequate discharge siting* to avoid pollutant accumulation, to protect sensitive regions and to utilize natural purification processes. Good examples for such mixing systems applied for large-scale desalination plants are illustrated in Figs. 18.8 and 18.9.

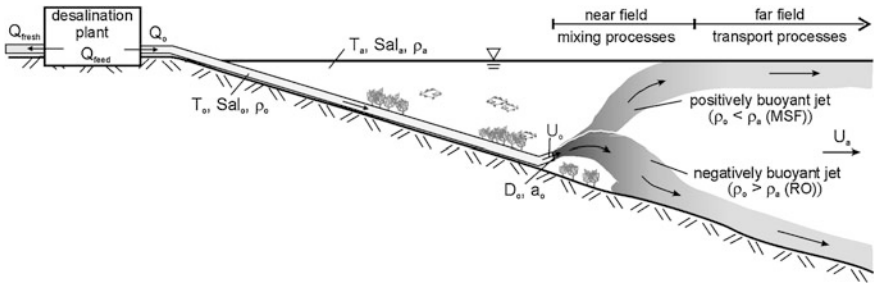

Fig. 18.3 Brine discharge characteristics of desalination plants

Fig. 18.4 Carlsbad RO plant, USA, positively/negatively buoyant discharge (*Source* Poseidon Resources)

18.4 Mixing Processes of Brine Discharges

When performing design work and predictive studies on effluent discharge problems, it is important to clearly distinguish between the physical aspects of hydrodynamic mixing processes that determine the fate and distribution of the effluent from the discharge location, and the administrative formulation of mixing zone regulations that intend to prevent any harmful impact of the effluent on the aquatic environment and associated uses.

Mixing processes are an interplay of ambient conditions and the outfall configuration. Different hydrodynamic processes drive and control the system. Most processes are running simultaneously, but with very clear dominance in different temporal and spatial regions, according to their predominant flow characteristics.

In the "*near-field*" (also called active dispersal region or initial mixing region), the initial jet characteristics of momentum flux, buoyancy flux, and outfall configuration (orientations and geometries) influence the effluent trajectory and degree of mixing. Source-induced turbulence entrains ambient fluid and dilutes the effluent. Though ambient characteristics affect the discharge once the effluent has left the diffuser openings, (in most cases) they are still only of minor importance until any bottom, surface or terminal layer interaction occurs. This characterizes the transition

Fig. 18.5 Ashkelon (Israel), RO plant with negatively buoyant brine discharge during backwash through an open channel at the coast into the Mediterranean (Courtesy of Rani Amir, Director of the Marine and Coastal Environment Division, Israel Ministry of the Environment) besides positively buoyant cooling water effluents

to the intermediate field. A general review of these processes has been given by Fischer et al. (1979), Wood et al. (1993), Roberts (1990, 1996) or Jirka and Lee (1994) and is covered in detail in Chap. 17.

The "*intermediate field*" (or zone of wastefield establishment (Ridge 2002)) is characterized by the impact of the turbulent plume with boundaries and the transition from the vertically rising (positively buoyant effluent) or falling (negatively buoyant effluent) plume characteristics to a horizontal motion generated by the gravitational collapse of the pollutant cloud. Source characteristics become less important. Generally, a pool of initially diluted effluent water is formed either at the

Fig. 18.6 Taweelah MSF plant, Arabian Gulf, 1.12 mio m^3/d, positively buoyant discharge (*Source* Google Earth)

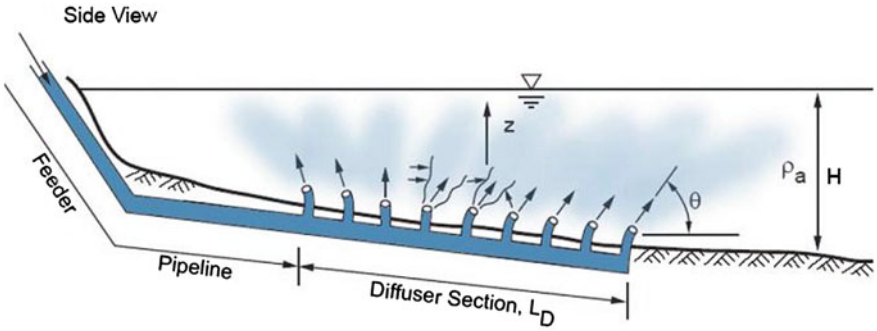

Fig. 18.7 Layout of an outfall pipeline with multiport diffuser (Bleninger and Jirka 2008)

surface (positively buoyant effluent) or at the bed (negatively buoyant effluent) or the level of submergence under stratification conditions, where the diluted plume reaches a level of equal density before reaching the surface, which also may occur with negatively buoyant effluents falling in stratified environments. Vertical and horizontal boundary conditions will control trajectory and dilution in the intermediate field through buoyant spreading motions and passive diffusion due to interfacial mixing. Such buoyant spreading motions are of specific interest for negatively buoyant effluents discharged on sloped sea-beds, where density currents

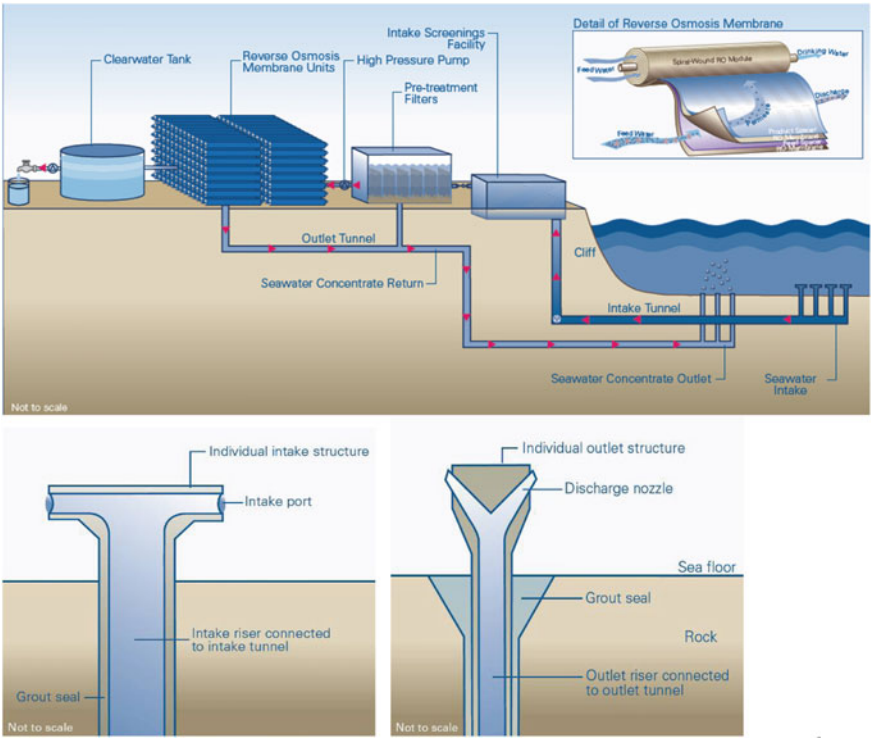

Fig. 18.8 Schematic designs for Sydney (Australia) RO plant, 125,000–500,000 m^3/d, similarly applied for Pearth RO plant, 140.000 m^3/d. Open intake towers located 200–300 m offshore in a depth of approximately 20–30 m. Outfall diffuser located 250–350 m offshore in a water depth of approximately 20–30 m. 20 risers spaced 25 m discharging through 2 ports with an angle of 60° to the horizontal (*Source* Sydney Water and Fichtner 2005)

of high velocities may develop. Intermediate field processes have often been neglected in practical applications (i.e. model formulations), because focus has been given to either the near-field or the far-field processes and not their combination. In addition, only a few laboratory and field studies have examined these processes in more detail (Jirka and Lee 1994; Akar and Jirka 1995). Although these works generally confirm negligible scales of intermediate field effects for discharges into reasonable strong turbulent current fields, they clearly show their importance in either stagnant or shallow waters, where large spreading processes or instabilities occur.

After the wastefield establishment, ambient conditions will control trajectory and dilution of the turbulent plume in the "*far-field*" (also called passive dispersal region), through passive diffusion due to ambient turbulence, and passive advection by the often time-varying, non-uniform, ambient velocity field. The flow is forced by tides and large-scale currents, wind stress at the surface, pressure gradients due

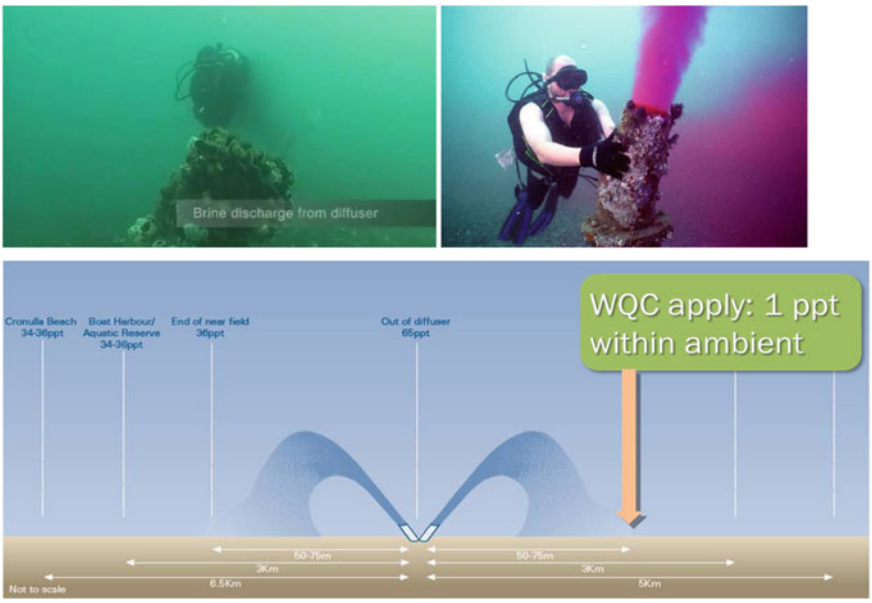

Fig. 18.9 Operating diffuser outfall port of Australian RO plants. *Left* Diver behind discharging outfall port (*Source* Alspach et al. 2009). *Right* Diver besides discharging diffuser port during tracer experiment to measure dilution characteristics (*Source* Christie and Bonnélye 2009). *Bottom* Results of model studies and measurements showing salinity concentrations in certain distances of discharge point, being in compliance with the water quality criteria (WQC) of 1ppt above ambient within 75 m distance from the discharge (*Source* Sydney Water and Fichtner 2005)

to free surface gradients (barotropic) or density gradients (baroclinic), and the effect of the Earth's rotation (Coriolis force). Dynamic discharge-related effects are unimportant in that region. Vertical mixing in stratified water bodies is dampened by buoyancy, so dilution is mainly due to horizontal mixing by turbulent eddies. Concentration reductions in the far-field are related to natural dispersion but also significantly to natural biological/chemical transformation processes. Far-field processes and their governing equations are presented in Chap. 22 (Zhan et al. 2014).

An overview of the physical processes is given in Fig. 18.10, including an example for their characteristic length and time scales for large discharges in the coastal environment. The combination of strong initial mixing induced by a multiport diffuser installation and adequate siting regarding high ambient mixing, transport and natural purification capacities reduces concentrations significantly. In total, the discharge plume and associated concentration distributions generated by a continuous efflux from a sea outfall can display considerable spatial detail and heterogeneities as well as strong temporal variability, especially in the far-field. This has great bearing on the application of any water quality control mechanisms.

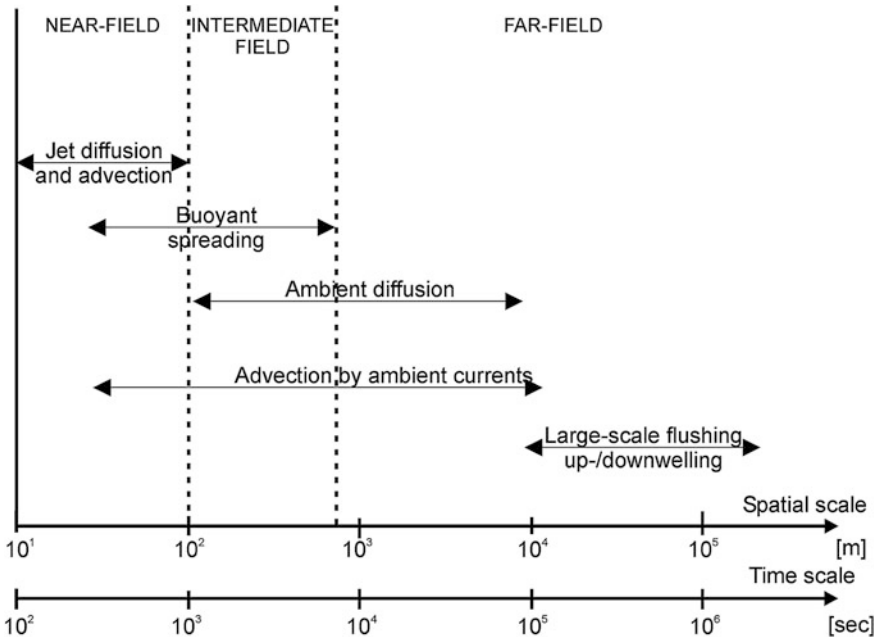

Fig. 18.10 Typical temporal and spatial scales for transport and mixing processes related to coastal wastewater discharges (Jirka et al. 1976; Fischer et al. 1979)

18.5 Environmental Regulations

An important way to control and restrict adverse environmental impacts of seawater desalination plants is to put up appropriate national laws or transnational agreements. These may regulate the brine discharge management, set up discharge limits or impose environmental standards and conditions mandatory for receiving operating permits. With respect to the worldwide desalination activities, the regulatory situation is very diverse and unclear. No common standards exist as each country has their own water regulations, which are more or less publicly accessible. Most regulations are abstract and do not apply specifically to desalination plants, but to industrial effluents in general. Furthermore, international standards such as World Bank Guidelines may be used as a reference. When national regulations differ from international guidelines, the World Bank recommends applying the more stringent regulations. The following gives an overview and comparison of regional and national regulations relevant for seawater desalination effluents in order to assess the level of regulatory protection of the marine environment.

Point-source discharges are usually controlled by setting environmental standards. Most common standards are effluent standards (ES), also called emission

limit values in European regulations, and ambient standards (AS), also called environmental quality standards in European regulations. There are existing different philosophies in applying either just one of these standards or combinations of them for pollution management, which is discussed as follows. ES encourage source control principles, such as effluent treatment and recycling technologies. AS require the consideration of the ambient response often associated with the concept of the "mixing zone", an allocated impact zone in which the numerical water quality standards can be exceeded (Jirka et al. 2004a, b). Ragas et al. (1997) have reviewed the advantages and disadvantages of different control mechanisms in the permitting processes of releases into surface water.

ES are preferred from an administrative perspective because they are easy to prescribe and to monitor (end-of-pipe sampling). From an ecological perspective, however, a quality control that is based on ES alone appears illogical and limited, since it does not consider directly the quality response of the water body itself and therefore does not hold the individual discharger responsible for the water body. To illustrate that point consider a large point source on a small water body or several sources that may all individually meet the ES but would accumulatively cause an excessive pollutant loading. ES are usually set as concentration values for pollutants or minimum required treatment levels.

AS, usually set as concentration values for pollutants or pollutant groups or set as maximum loads (e.g. TMDL = "total maximum daily load"—approach in the USA), may not be exceeded in the water body itself. They have the advantage that they consider directly the physical, chemical and biological response characteristics due to the discharge. They therefore put a direct responsibility on the discharger. But a water quality practice that would be based solely on AS could lead to a situation in which a discharger would fully utilize the assimilative capacity of the water body up to the concentration values or total loads provided by the AS. Furthermore, the water quality authorities would be faced with additional burdens because of more difficult monitoring—where in the water body and how often should be measured?—in the case of existing discharges or due to the increased need for a prediction modeling in case of new discharges.

Concentration or load limits for ES and AS can be found in state, national, and international legislations for different substances, effluents, and receiving water characteristics. Environmental standards for pollutants are generally determined from laboratory ecotoxicity tests conducted on a range of sensitive aquatic plant and animal species exposing the regionally occurring species to different pollutants and pollutant concentrations under regional climate and water body conditions and natural background concentrations. However, salinity and temperature are two stressors that are naturally very variable seasonally and among and within ecosystem types, and natural biological communities are adapted to the site-specific conditions. This suggests that trigger values for these three stressors may need to be based on site-specific biological effects data (ANZECC 2000).

18.5.1 Discharge and Site-Specific Environmental Criteria

It is noted that for many countries, environmental criteria (particularly AS, but also ES) are absent or inspired from another country or from worldwide criteria. As mentioned above, in particular for temperature and salinity increase due to the discharged effluent, such general criteria may not be effective for protecting the environment (i.e. ecology) at the project site. Since temperature and salinity levels can have complex effects on the ecology, criteria should be used that are relevant to the ecology found at the project site and for the natural conditions these species experience. For example, if at a project site the ecological variety and sensitivity is low, environmental criteria could be more flexible than at sites with sensitive species. If a project site contains predominantly benthic immobile species, criteria that apply to the bottom level are more relevant than criteria applied to the middle of the water column or water surface.

In general, it would be beneficial for the ecology at the project site if for each project site-specific, ecologically relevant criteria are derived as part of the project, to which the discharge is evaluated. The development of these site-specific criteria could contain the following steps:

1. Marine baseline survey to identify species at the project site and compose a habitat map.
2. Obtain from literature or experimental testing the response and tolerances of the identified species to the stressors (e.g. temperature and/or salinity levels), both chronic and peak stress levels.
3. Definition of site and species-specific criteria for the stressors in terms of both magnitude and duration, taking into account natural variations, seasonal dependencies (e.g. spawning seasons), etc. The regulatory mixing zone is defined on these criteria.
4. The mixing zone *extent* is subsequently computed e.g. on the basis of numerical modeling and using the regulatory mixing zone criteria/thresholds. This mixing zone extent is preferably computed in three dimensions to account for the vertical position of the species in the water column. Furthermore, the numerical modeling assessment should include all necessary scenarios to be representative for the conditions that could occur at the project site.
5. Subsequently, the computed mixing zone extent should be considered for acceptance by the regulatory body, e.g. by comparing this to a regulatory maximum extent of the mixing zone.

This mixing zone approach based on site-specific, ecologically relevant criteria ensures that ecology outside the mixing zone is not affected unacceptably by the discharge. The regulatory body typically decides on the maximum allowed extent of the mixing zone.

18.5.2 Discharge Permitting

A "combined approach" as for example described in the European Water Framework Directive, WFD (EC 2000), combines the advantages of both the ES and AS water quality control mechanisms while largely avoiding their disadvantages. Both criteria have to be met for a discharge permit.

Recently, a "Tiered Approach" has been developed to document the policy decision tree that may be adopted by EC Member States when setting Mixing Zones under Directive 2008/105/EC (EU 2008). At each tier the aim is to identify those discharges that do not give cause for concern, and also to highlight discharges that require action to reduce the size of the mixing zone.

The tiered approach may be summarised as follows (reproduced from EC Directive 2008/105/EC):

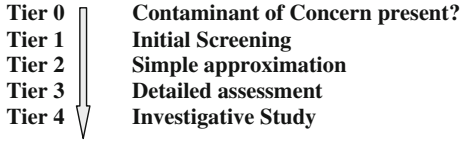

Tier 0—Contaminant of Concern present?
If the effluent does not contain substance concentrations above the required AS the discharge assessment does not need to consider mixing processes, and the environmental impact assessment can be based only on the discharge loads and assimilative capacities. Effluents with substance concentrations above the required threshold need to be analyzed in Tier 1.

Tier 1—Initial screening
Tier 1 is designed to define the significance of the discharge, using simple tests. Those tests are usually based on the flow and load information and simple dilution equations to exclude especially very small discharges into very large water bodies from unnecessary detailed mixing studies, thus avoiding an inappropriate burden for regulators and stakeholders.

Tier 2—Simple approximation
The purpose of Tier 2 is to eliminate those discharges that are clearly acceptable or clearly unacceptable. A number of suitable tools are available commercially for this. Acceptable discharges are usually small discharges into large and uniform water bodies. Unacceptable discharges are those that cannot reach even close to the required dilutions under normal conditions. All other discharges need to pass to Tier 3 for further analysis.

Tier 3—Detailed assessment
In complex cases, for example strongly varying or heterogeneous ambient conditions or multiple discharges, a more detailed assessment may be required. This usually involves unsteady and more dimensional models. Those are used to verify if

the dilution requirements can be achieved under most of the operational and ambient conditions.

Tier 4—Investigative Study
If Tier 3 cannot fully satisfy the required dilution criteria or requires even more detailed studies or measurements an investigative study and design optimization will be required to validate the final model result.

18.6 Tiered Brine Discharge Modeling

In order to demonstrate compliance within each tier for discharge permitting, it appears that both dischargers, as well as water authorities, must increase the application of quantitative predictions of substance distributions in water bodies (water quality parameters in general, mixing processes in particular). This holds for both existing discharges (diagnosis) as well as planned future discharges (prediction). There are several diagnostic and predictive methodologies for examining the mixing from point sources and showing compliance. Field or laboratory studies are hereby complemented by mathematical models.

Field measurements or tracer tests can be used for existing discharges in order to verify whether concentration values are indeed met. Field measurements are costly, often difficult to perform, and usually limited to certain discharge and ambient conditions. Frequently, they must be supported through mathematical model predictions: on one hand, to establish a clear linkage to the considered discharge (especially if more than one discharge exists); and on the other hand, to synthesize conditions allowing for variability in the hydrological or oceanographic conditions or in the effluent rates.

Hydraulic model studies replicate the mixing process at a small scale in the laboratory. They are supported by similarity laws and are quite reliable if certain conditions on minimum scales are met, as has been demonstrated in the past. But just like field tests, they are also costly to perform and inefficient for examining a range of possible ambient/discharge interaction conditions.

Regarding **mathematical models**, there is a huge number of different model types, ranging from simple analytical equations or nomograms to general flow, transport and water quality models. It is important to remember that mixing processes of brine discharges have widely varying length and time scales (Fig. 18.11). Since it is not possible to simulate them with one overall model, separate models are used in the near-field and far-field and then linked together. Existing “jet models” cover the near-field region, before boundary interactions take place. Regulatory mixing zones are usually larger than the jet regions, thus require further model applications. As shown later, the CORMIX model is the only modeling suite containing a jet model coupled to intermediate field models, being able to predict outfall performance under different limiting conditions. The far-field models instead are not necessarily required for showing compliance with outfall related mixing zones, but more for water body related general effects of the outfall on the coastal ecosystem.

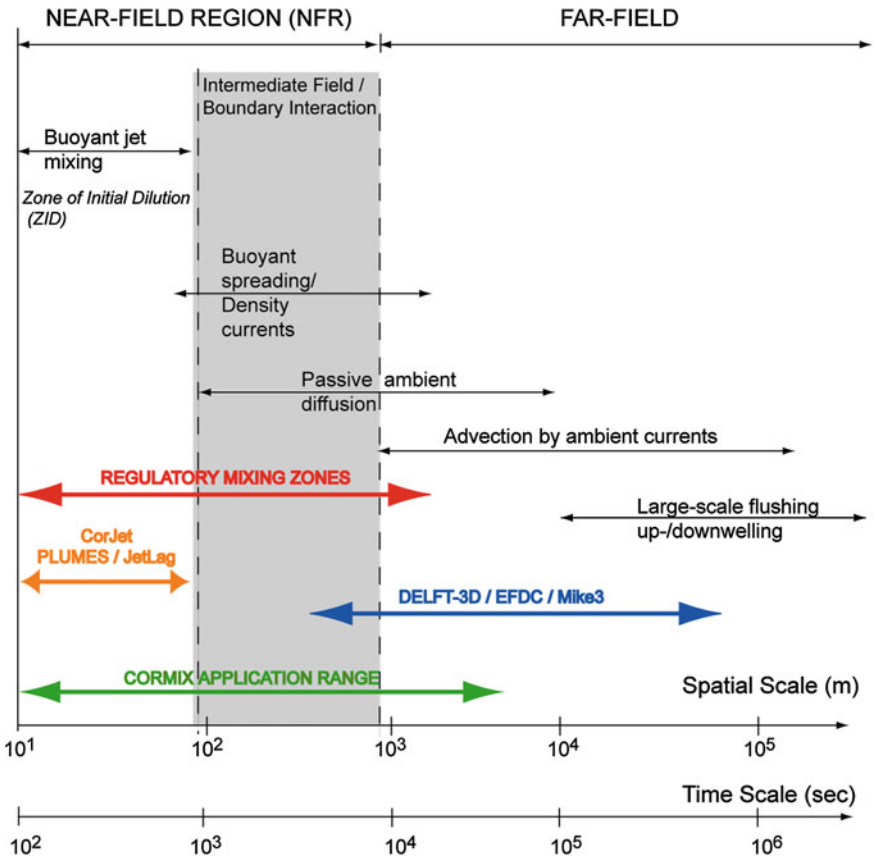

Fig. 18.11 Typical temporal and spatial scales for transport and mixing processes related to coastal wastewater discharges and model capabilities (Jirka et al. 1976; Fischer et al. 1979)

The tiered approach provides a good framework to include the different scales and levels of model complexity as follows in more detail in the subsequent sections.

Tier 0—Contaminant of concern present?
Simple spreadsheet models (e.g. Discharge Calculator as presented in Bleninger et al. 2010) are applicable for all type of discharges and ambient conditions to compute basic effluent characteristics to be compared to environmental standards.

Tier 1—Initial screening: rapid assessment tools, significance of discharge
Rapid Assessment Tools, including dilution equations, nomograms, screening equations included in simple modeling systems. Major limitations are usually associated to not considering any boundary interaction, unsteady motions, and assuming unlimited and quiescent ambient water. This screening allows defining the significance of a discharge situation.

Tier 2—Simple approximation: mixing zone modeling in the near-field
Using for example Mixing Zone Models, such as CORMIX, Plumes or VisJet. Major limitations are either missing boundary interactions and/or assumptions regarding steady and uniform ambient characteristics. This step allows to define concentration distributions under simplified conditions, thus to optimize the outfall design.

Tier 3—Detailed assessment: combined models for far-field and water quality
Using combined modeling approaches, usually linking a near-field information to a far-field model (e.g. a one-way coupling between CORMIX and Delft3D). Limitations are related to large discharges, where the discharge changes the ambient flow. This step allows to compute time-varying and spatially-varying concentration distributions and may include water quality analysis, such as transformation or decay processes on a larger scale. It is usually employed to determine the best siting of the discharge.

Tier 4—Investigative study: dynamically (two-way) coupled models for design optimization
Using combined and interacting modeling approaches, also (possibly) including extensive field studies and physical laboratory studies. Limitations are related to missing boundary condition information to run such complex modeling situations. This step allows study of complex details, such as the analysis of sensitive areas under extreme discharge and ambient conditions, and to optimize the discharge situation, such as design or operation.

18.6.1 Tier 0—Contaminant of Concern Present?

Simple spreadsheet models can be used (e.g. Discharge Calculator as presented in Bleninger et al. 2010). Those "calculators" are based on simple mass balance equations to compute basic effluent characteristics, such as effluent temperature, salinity, density and flow rate in addition to substance concentrations. The latter depend on the desalination processes applied, including pre- and post-treatment. Once the effluent concentrations are calculated, they can be compared with the existing ambient standards to check whether the discharge concentration is above or below it, as illustrated in the following equations:

Step 1: Compute effluent concentrations C_o of contaminants of concern, e.g. using spreadsheet programs based on mass balance (e.g. Bleninger et al. 2010).
Step 2: Check regulations for applicable standards (concentration limits Ca related to the contaminants of concern.
Step 3: Compare concentrations.
If $C_o < C_a$ for all substances → no further assessment necessary, eventually study discharged loads to check and avoid accumulation of substances.
If $C_o > C_a$ → tier 1

Interpretation and limitations: This tier does not consider any mixing processes, but serves as a pre-screening for the criticality of the discharged substance concentrations and allows to either "approve" the discharge upfront or to evaluate other desalination and pre- or post-treatment processes to reduce the most critical substance concentration before any mixing analysis in the following tier. This tier somehow represents former source-control approaches.

18.6.2 Tier 1—Initial Screening: Rapid Assessment Tools, Significance of Discharge

Rapid Assessment Tools, such as dilution equations, nomograms or screening equations are often available in simple modeling systems. Tier 1 is designed to define the significance of the discharge. Available modeling systems can be classified in (i) models computing mixing length scales via a flow classification or length scale analysis, and (ii) empirical dilution equations. The objectives of Tier 1 are to identify unproblematic discharges, for example very small discharges into very large water bodies. This, to avoid unnecessary detailed mixing studies, and thus inappropriate burden for regulators and stakeholders.

Interpretation and limitations: Typical simplifications can be summarized in the following assumptions:

- No consideration of source fluxes, the source is considered as passive. Most surface discharges have discharge velocities lower than 1 m/s, thus not considerably larger than ambient flows. Diffuser discharge velocities are much higher, thus cannot neglect those fluxes. As most brine discharges have considerable density differences, most times buoyancy fluxes cannot be neglected, thus further studies are required.
- single point discharges only (i.e. no diffusers)
- simplified ambient geometries (usually mean depth and unlimited ambient only)
- simplified ambient flow (uniform and steady flow)
- no consideration of substance decay or reactions
- discharge is always submerged

A first simple estimate to check significance under those conditions is the computation of the effective volume flux

$$V_{eff} = Q_o \frac{c_o}{c_a} \tag{18.1}$$

with Q_o being the discharge flow rate. Assuming coastal velocities being of the order of 0.1 m/s a maximum value for V_{eff} can be given by $V_{eff} < 5\ m^3/s$. Further approaches of that type can be found in the Technical Background Document on the Identification of Mixing Zones (CIS-WFD 2010) of the EC or in Bleninger and Jirka (2011) or Jirka et al. (2004).

The length scale approach and the empirical equations are summarized in the following sections.

18.6.2.1 Length Scale Analysis and Flow Classification

The computation of characteristic discharge parameters does not aim for computing dilutions or concentration profile distributions, but to distinguish between different flow regimes, namely a flow classification. The so-called length scale analysis allows distinguishing, for example, between dominating jet flow regions, thus classifying the flow itself and different flow regions, as illustrated in Fig. 18.12. Heretofore the initial source properties are used in a dimensional analysis to define characteristic length scales. The initial source fluxes have been mentioned earlier, but are repeated here for convenience:

- the initial volume flux $Q_o = U_o A_o$, for single port discharges, or $q_o = Q_o/L_D$ for multiport discharges with the initial discharge velocity U_o and the individual or total pipe discharge cross-section A_o and the diffuser length L_D
- the initial mass flux $Q_{co} = U_o C_o A_o$, or $q_{co} = Q_{co}/L_D$ with the initial concentration C_o
- the initial momentum flux $M_o = U_o^2 A_o$, or $m_o = M_o/L_D$
- and the initial buoyancy flux $J_o = U_o g_o' A_o$, or $j_o = J_o/L_D$ with the reduced gravity $g' = \Delta\rho/\rho g$ and $\Delta\rho = \rho_o - \rho_a$, with the initial effluent density ρ_o and the ambient density ρ_a.

General ambient characteristics further dictate the trajectory:

- the average ambient flow velocity u_a
- and the density stratification $d\rho/dz$

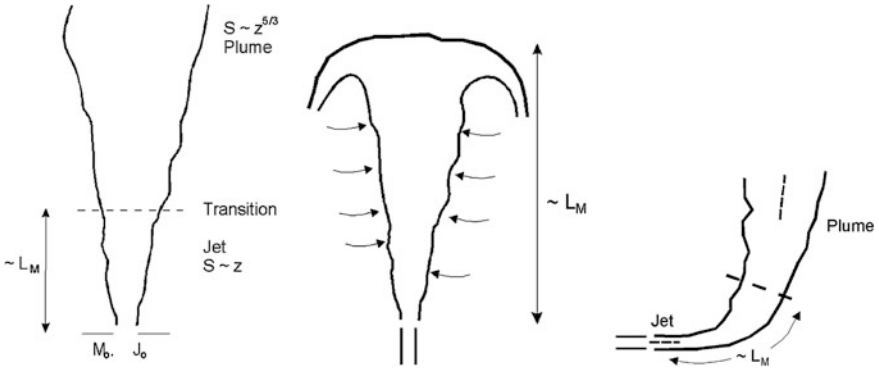

Fig. 18.12 Jet to plume transition length scale L_M for a single jet allows distinguishing between a jet like or plume like single jet behavior (reproduced from Jirka et al. 1996)

A consistent length scale based categorization of the different jet regimes in the presence of crossflow and/or stratification is summarized in Fischer et al. (1979) and modified for plane jets from multiport diffusers by Jirka and Akar (1991) resulting in the following length scales, which provide order of magnitude estimates of transitional locations.

Jet/plume transition length scale: the distance at which transition from jet to plume takes place (compare with Fig. 18.12)

$$L_M = \frac{M_0^{3/4}}{J_0^{1/2}} \quad \text{or} \quad l_M = \frac{m_0}{j_0^{2/3}} \text{ for multiport diffuser} \tag{18.2}$$

Jet-to-crossflow length scale: the distance beyond which the jet is strongly deflected by the crossflow

$$L_m = \frac{M_0^{1/2}}{u_a} \quad \text{or} \quad l_m = \frac{m_0}{u_a} \text{ for multiport diffuser} \tag{18.3}$$

Plume-to-crossflow length scale: the distance beyond which the plume is strongly deflected by the crossflow

$$L_b = \frac{J_0}{u_a^3} \tag{18.4}$$

Jet-to-stratification length scale: the distance beyond which the jet is strongly affected by the stratification

$$\begin{aligned} L'_m &= \frac{M_0^{1/4}}{\varepsilon^{1/2}} \quad \text{or} \\ \mathrm{l}'_m &= \frac{m_0^{1/3}}{\varepsilon^{1/3}} \text{ where } \varepsilon = -(\mathrm{g}/\rho\mathrm{a})(\mathrm{d}\rho\mathrm{a}/\mathrm{dz}) = \text{ambient buoyancy gradient.} \end{aligned} \tag{18.5}$$

Plume-to-stratification length scale: the distance beyond which the plume is strongly affected by the stratification

$$L'_b = \frac{J_0^{1/4}}{\varepsilon^{3/8}} \quad \text{or} \quad \mathrm{l}'_b = \frac{j_0^{1/3}}{\varepsilon^{1/2}} \tag{18.6}$$

Tidal currents are characterized by flows which reverse direction. During the reversal period, or the so-called slack tide, the ambient water may be momentarily stagnant. When the slack tide is approached, meaning $u_a = 0$, the steady state length scale L_m becomes unbounded and thus an unsatisfactory measure for the jet behavior (Nash 1995). A relationship between the ambient acceleration $|\mathrm{d}u_a/dt|$ and the discharge momentum flux M_o gives a measure for describing the unsteady trajectory leading to following scales:

Jet-to-unsteady crossflow length scale, a measure of the distance of the forward propagation into the ambient flow of a discharge during the reversal episode.

$$L_u = \left(\frac{M_0}{|du_a/dt|}\right)^{1/2} \quad \text{or} \quad \mathrm{l}_u = \left(\frac{m_0}{|du_a/dt|}\right)^{1/2} \tag{18.7}$$

Jet-to-unsteady crossflow time scale, a measure of the duration over which an effluent may be considered as discharging into stagnant water while the velocity field is reversing.

$$T_u = \left(\frac{M_0}{|du_a/dt|^{1/4}}\right)^{1/6} \quad \text{or} \quad \mathrm{t}_u = \left(\frac{m_0}{|du_a/dt|^3}\right)^{1/4} \tag{18.8}$$

Jirka et al. (1981) showed that buoyant jet deflection is primarily influenced by discharge momentum and not by buoyancy, thus scales for the interaction of the buoyancy flux J_o and $\mathrm{d}u_a/dt$ are not considered to be dominant.

Additional important numbers are the densimetric Froude Number

$$\mathrm{F_o} = \mathrm{U_o}/\sqrt{|\mathrm{g_o'}|\mathrm{D}} \tag{18.9}$$

and the Reynolds number

$$\mathrm{Re} = \frac{U_0 D}{\nu}, \tag{18.10}$$

to characterize the mixing characteristics of the discharging jet, where high Froude and Reynolds numbers indicate good turbulent mixing conditions.

A complete flow classification system based on the above length scale definitions have been established by Jirka and Akar (1991) and Jirka and Doneker (1991a, b), and briefly illustrated in Fig. 18.13 and Fig. 18.14. This classification system alone allows the definition of resulting flow classes without even starting a numerical computation. The near-field mixing model CORMIX (Doneker and Jirka 2007) is, in fact, a collection of several models for several sub-processes. These models are invoked through a length-scale based classification scheme that first predicts the discharge flow behavior (so-called flow classes) and then consecutively links (couples) the appropriate zone models (so-called modules) to provide near-field predictions. Also the near-field far-field coupling algorithm is initiated by a flow classification algorithm to provide appropriate coupling times and geometries.

The application of these classification schemes requires only very few and general input data related to the discharge and ambient characteristics. The simple quantitative comparison of the mixing length scales with the geometrical scales of the discharge and receiving waters is possible by following the guidance given in the classification trees, and the quantitative criteria. For example, sensitive

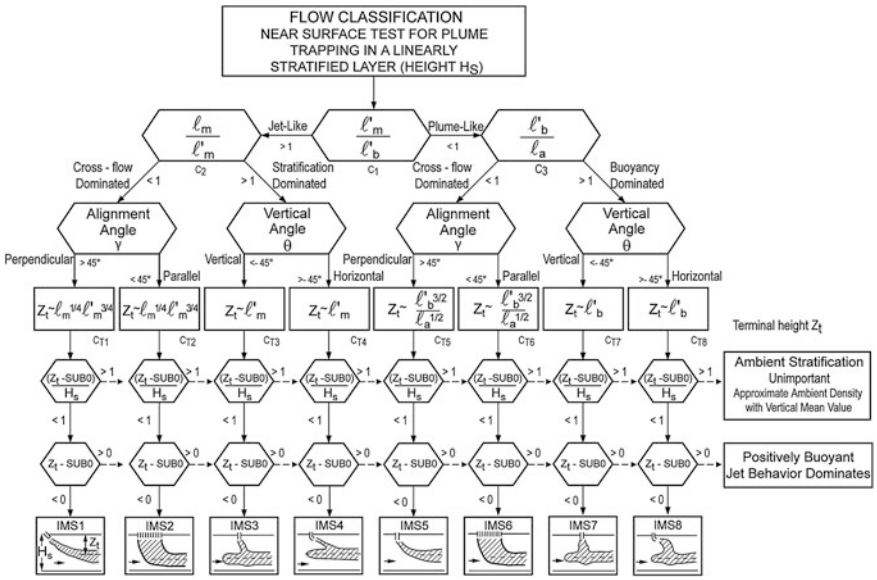

Fig. 18.13 CORMIX flow classification tree for a near-surface negatively buoyant multiport discharge into stratified ambient water (reproduced from Jirka et al. 1996)

coastlines or river banks may require that no plume contact with the bank occurs in the near-field, downstream vicinity. For a surface discharge with given buoyancy and momentum flux, only flow classes of type FJ (free jet, see Fig. 18.14) are in compliance with such a water quality protection criterion. The other flow classes will have downstream bank contact in the near-field region. Figure 18.14 shows that for the given example (grey shaded boxes) the discharge seems to be in compliance, predicting an FJ1 flow class. Furthermore it can be seen that buoyancy will keep the plume stratified in the surface layer (plan view in lowest shaded box), with no bed contact in the near-field region, in contrast to the situation in class FJ3 with bed contact.

The flow classification in addition can be used to decide whether conditions are met or special process considerations are needed within the application of more complex modeling systems. For example a large discharge into a small water body can create re-entrainment of discharged effluent and create so called near-field (Jirka 1982, 2006a, b). Large recirculation zones or vertically mixed currents that laterally entrain ambient water are typical examples for an unstable near-field. "Stable discharge" conditions, usually occurring for a combination of strong buoyancy, weak momentum, and deep water, are often referred to as "deep water" conditions. "Unstable discharge" conditions, on the other hand, may be considered synonymous with "shallow water" conditions, when a multiport diffuser represents a large source of momentum with a relatively weak buoyancy effect (i.e. for thermal

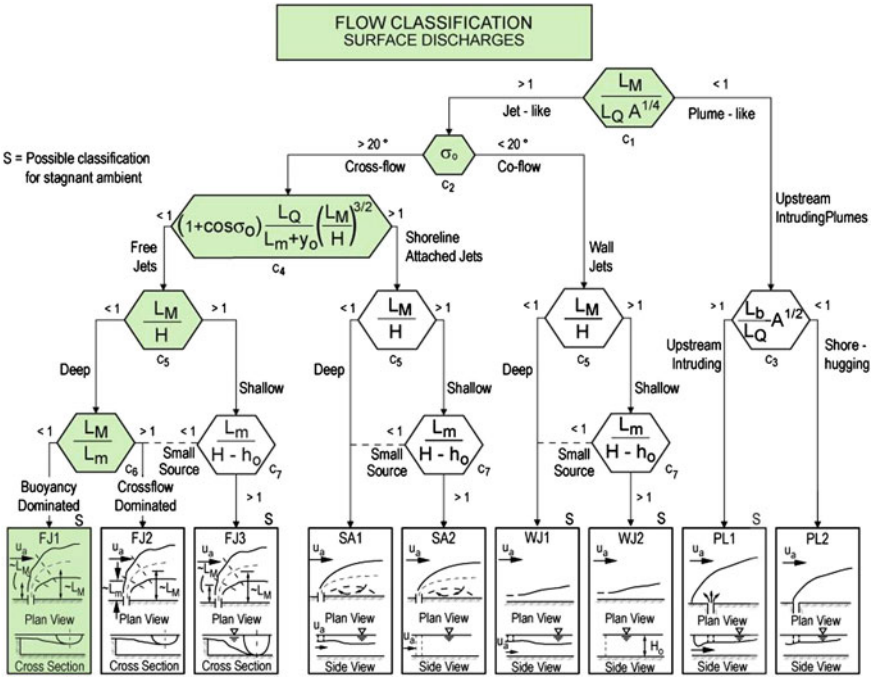

Fig. 18.14 Flow classification tree for positively buoyant surface discharge into uniform density layer (*Source* www.cormix.info)

plumes). Technical discussions on discharge stability are presented elsewhere (Jirka 1982; Holley and Jirka 1986), but fully based on length-scale approaches.

18.6.2.2 Nomograms and Screening Equations (RO)

Another advantage of characteristic length scale analysis is the normalization of different configurations and conditions, which is the base for nomograms. Whereas velocities and concentrations can successfully be normalized by their initial values, results for measured trajectories which are historically normalized by the individual jet diameter showed large scatter (Fig. 18.15, left for single buoyant jets). Numerous different solutions have hereby been obtained for different initial densimetric Froude numbers. The parameter combination based on the flux definitions instead resulted in the correct scaling (Fig. 18.15, right) using the momentum length scale $L_M = M_o^{3/4}/J_o^{1/2}$ (Jirka 2004). Such diagrams can be used to predict and estimate the trajectory location.

The geometric and mixing characteristics of the turbulent buoyant jet can be determined by two length scales, the discharge length scale L_Q and the momentum (jet/plume transition) length scale L_M. A related non-dimensional parameter is the

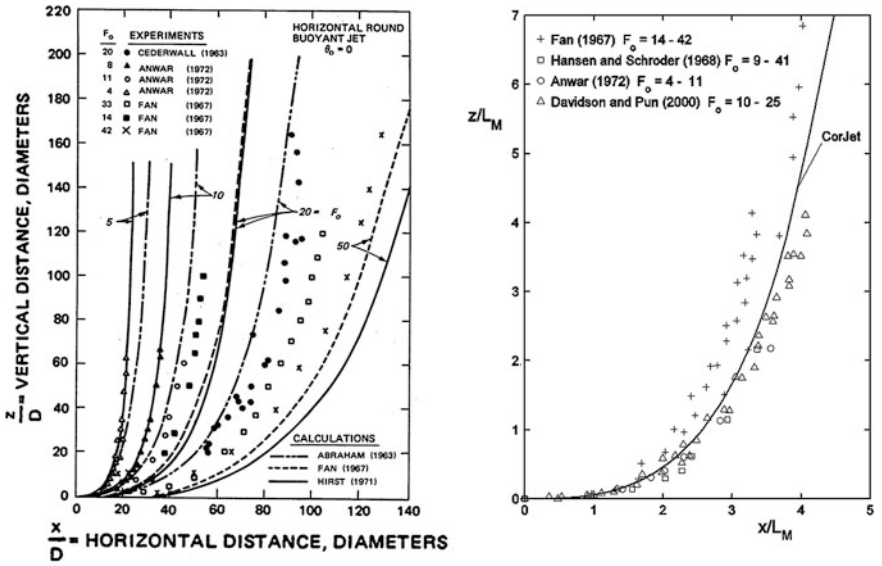

Fig. 18.15 3-dimensional horizontal buoyant jet trajectories for a single port discharge in stagnant ambient. Comparison between predictions and experimental data. *Left* normalized with port diameter. *Right* normalized with momentum length scale L_M (reproduced from Jirka 2006a, b)

jet densimetric Froude number F_o that is simply proportional to the length scale ratio, $L_M/L_Q = (\pi/4)^{-1/4} F_o$. Thus, for high Froude number discharges, $F_o \gg 1$, L_Q ceases to be a dynamically important parameter, as is well known for many other jet configurations (Jirka 2004). Detailed studies by Zhang and Baddour (1998) for a vertical negatively buoyant jet have shown that the dilution at the maximum level becomes independent of Froude number when $F_o \geq 10$. For smaller Froude numbers, the initial dilution becomes lower. A high Froude number discharge, $F_o > 10$, is assumed in the following so that L_M is the unique length scale for displaying jet properties.

Jirka (2008) applied the jet integral model CorJet in a preliminary parametric study of submerged negatively buoyant jets discharging over a flat or sloping bottom and covering the entire range of angles from 0° to 90° above the horizontal and compared the results with experimental data from literature. Resulting inconsistencies are generally larger among different experimental studies than the disagreement with the numerical model (Jirka 2008) because of deficiencies in the experimental set-up (e.g. flat bottom with possible recirculation effects after impingement; limited tank sizes) and in the measurement techniques (e.g. ambiguities in visual determinations; incomplete suction sampling in view of jet fluctuations). Considering other validation cases (trajectories and dilutions) for negatively buoyant jets with or without crossflow that have been reported in Jirka (2008), it is therefore concluded that CorJet can be used as a screening tool for

negatively buoyant jet discharge configurations covering a wider range of possible site conditions (Bleninger and Jirka 2008). However, CorJet, being a "jet model" is a strict near-field model and does not include any boundary interaction processes. Only more sophisticated mixing models like CORMIX, include the impingement dynamics and further intermediate field flows. The CorJet model has therefore been listed as screening tool in this chapter.

18.6.2.3 Empirical Dilution Equations (MSF)

Following considerations are based on positively buoyant discharge situations, as it is usually the case for thermal desalination discharges. Major contributions are from Brooks (1960, 1980, 1984, 1988) and Brooks and Koh (1965). Comprehensive reviews are given in Fischer et al. (1979), Wood et al. (1993) and Jirka and Lee (1994). Detailed discussions on buoyant jets were presented by Jirka (1979, 1994), Roberts (1980, 1986), Roberts et al. (1989a, b, c), Lee and Neville-Jones (1987). The resulting equations are all based on the near-field assumption and trying to calculate the minimum jet centerline dilution $S_c = c_o/c_c$ at the end of the near-field, i.e. after surface contact or at the terminal layer for trapped plumes. As stated previously, they do not consider the dynamics of boundary interactions or further intermediate field flows.

Larger flow rates usually require multiport diffuser installations. The individual jet discharges through each port of such a diffuser merge after a certain distance and create a 2D line plume, which further rises to the surface and then impinges with the surface and spreads horizontally. One of the key equations is the equation for a line plume in a stagnant unstratified ocean (Rouse et al. 1952):

$$S_c = 0.38 \frac{j_0^{1/3} H}{q_0} \tag{18.11}$$

For a given flow Q_o, the unit discharge q_o and unit buoyancy flux j are inversely proportional to the diffuser length L_D, and the above equation suggests that a higher dilution is obtained by increasing the length of the diffuser. For a line plume, the minimum dilution can be multiplied by a factor of $2^{1/2}$ to give the average dilution.

It has been demonstrated both theoretically and experimentally (Fischer et al. 1979) that maximum mixing can be achieved with closely spaced ports that allow some interference of adjacent jets. In relatively shallow coastal waters of typical depth 5–15 m, however, it is often the case that, given practical considerations (e.g. in order to maintain a minimum jet velocity and minimum diameter), multiport diffusers are designed to maximize interference of adjacent plumes. In such cases, the required spacing is about $H/3$.

In case of a linearly stratified ambient with a density gradient $d\rho_a/dz$ the maximum height of rise z_{max} to the terminal level and corresponding dilution S_c are given by

$$z_{max} = 2.84 j_0^{1/3} \left(-\frac{g d\rho_a}{\rho_a dz} \right)^{-1/2} = 2.84 l_b' \qquad S_c = 0.31 \frac{j_0^{1/3} z_{max}}{q_0} \tag{18.12}$$

In a linearly stratified ambient, the spreading layer is found to occupy about 40–50 % of the rise height. For computing bulk dilutions, one must allow for the thickness of the wastewater field. Simple models to account for blocking in the presence of an ambient current can be found in Fischer et al. (1979).

Roberts (1979, 1980) studied the mixing of a line source of buoyancy in an ambient current, and found that the shape of the flow field and the dilution are determined by the ambient Froude number $F_o = u_a^3/j_o$. F_o measures the ratio of the ambient current velocity to the buoyancy-induced velocity. For $F < 0.1$, the minimum surface dilution S_m is little affected by the current and is given by:

$$S_m = 0.27 \frac{j_0^{1/3} H}{q_0} \tag{18.13}$$

The smaller dilution coefficient reflects the effect of blocking of the surface layer. For higher crossflow, $F > 0.1$, however, the entrainment is dominated by the crossflow, and the alignment angle γ between the diffuser line and the current direction is important. Higher dilution results for a perpendicular alignment, $\gamma = 90°$, in which the maximum amount of flow is intercepted while the parallel alignment, $\gamma = 0°$, gives the lowest dilution. For $F \approx 100$, the perpendicular alignment results in a dilution

$$S_m = 0.6 \frac{u_a H}{q_0} \tag{18.14}$$

that is proportional to volumetric mixing between ambient (velocity u_a) and discharge flow, but with a reduced coefficient 0.6. For parallel alignment, the dilution is lower by a factor of about four. Experiments by Mendez-Diaz and Jirka (1996) have examined the different plume trajectories for various crossflow strengths.

The simple dilution equations given in the foregoing are useful for initial design screening of alternatives. They are limited to simplified ambient conditions. For final design evaluations and for more general and complex ambient oceanographic conditions, models like CORMIX that are more comprehensive must be employed.

18.6.3 Tier 2—Simple Approximation: Mixing Zone Modeling in the Near-Field

For a better knowledge of mixing characteristics and especially to obtain concentration distributions more comprehensive models as to those from Tier 1 are needed. Models, often called mixing zone models, such as CORMIX, Plumes or VisJet are representing the jet and plume characteristics of single port or multiport discharges. This step allows to define concentration distributions under simplified conditions, thus to optimize the outfall design and maximize dilution. In comparison to Tier 1, those models include the effects of momentum and buoyancy fluxes, as well as ambient stratification or ambient velocities.

Main computed characteristics are distances until contact with bed or surface or the coast, and related dilution values. Such information is useful to determine the areas affected by the discharge and related concentration values, under simplified conditions.

Interpretation and limitations: Models presented in the following may even be used beyond the near-field scales, if ambient conditions are rather uniform and steady or periodical (quasi-steady). Typical simplifications can be summarized in the following assumptions:

- pollutant built-up (returning plumes) not considered
- simplified ambient geometries (usually prismatic cross-section, which is working well in most cases, but is limited in different flow conditions, such as density currents on heterogeneous bed topography)
- simplified ambient flow (uniform and steady flow)
- no consideration of substance decay or reactions (still ok for near-field processes, because time-scales are shorter than substance transformation time-scales).
- single discharges only (no interaction of different discharges)

Mixing zone models are simple versions of more general water quality models. They describe with good resolution the details of physical mixing processes (mass advection and diffusion), but are limited to relatively simple pollutant kinetics by assuming either conservative substances or linear decay kinetics. This is acceptable for most applications, since residence times in the spatial limited mixing zones (see previously mentioned specifications) are typically short so that chemical or biological mass transformations are usually unimportant.

The screening equations of Tier 1 are useful for order of magnitude analysis, but are not applicable for the final design and analysis of discharge systems. Prediction models are needed, which include the effect of ambient currents, ambient density variations (i.e. stratified water bodies), and boundary interactions, as well as different discharge configurations, including multiport diffuser designs, and surface discharges.

Currently, there are only a few near-field models capable to model brine discharges, including dense discharges with negatively buoyant plumes. These are

CORMIX and VisJet and NR-Field (see Chap. 17). CORMIX in addition is capable to simulate boundary interactions. In summary, situations where VisJet and NR-Field can be applied would typically be deep ocean outfalls (e.g. sewage outfalls) and if only near-field mixing is of interest and there is no possibility of dynamic bottom attachments and surface interaction is unimportant. However, if discharge zone information after the near-field is desired, then the possibility of a density current in the far-field must be considered.

18.6.3.1 CORMIX System

The CORMIX system (Doneker and Jirka 1990; Jirka and Akar 1991; Jirka et al. 1996) addresses the full range of discharge geometries and ambient conditions, and predicts flow configurations ranging from internally trapped plumes, buoyant plumes in uniform density layers with or without shallow water instabilities, and sinking (negatively-buoyant) plumes. Boundary interaction, upstream intrusion, buoyant spreading, and passive diffusion in the far field are also considered. A flow classification system based on hydrodynamic criteria using length scale analysis and empirical knowledge from laboratory and field experiments provides a rigorous and robust expert knowledge base that distinguishes among the many hydrodynamic flow patterns that may occur. For every flow class, CORMIX assembles and executes a sequence of appropriate hydrodynamic simulation modules. The modules are based on buoyant jet similarity theory, buoyant jet integral models, ambient diffusion theory, stratified flow theory, and simple dimensional analysis. The basic tenet of the simulation methodology is to arrange a sequence of relatively simple simulation modules which, when executed together, predict the trajectory and dilution characteristics of a complex flow.

Additional features are contemporary 3D plume and diffuser visualizations, a comprehensive documentation and help system, GIS linkage, a benchmarking analysis and validation database, a far-field locator post-processor, sensitivity analysis, and a batch running mode and time-series, all fully linked within the expert-system interface. CORMIX results include design recommendations, flow class descriptions and reporting oriented on discharge zone analysis.

At the heart of CORMIX is the integral jet model CorJet developed by Jirka (2004, 2006). The model formulation includes the significant three-dimensional effects that arise from the complex geometric details that distinguish actual diffuser installations in the water environment. Local three-dimensional effects deal with the merging process to form the plane buoyant jet. A simple flux-preserving merging transition that considers geometric contact between adjacent individual jets is found to be sufficiently accurate for simple port arrangements with 2D plume like orientation. For complex port arrangements with opposing or rosette-like orientation, the highly complicated merging process is not considered in detail and a buoyancy flux-preserving equivalent slot jet assumption is made for the zone of flow establishment. A variable drag force formulation is introduced to provide an accurate representation of the merging and jet bending process under crossflow conditions.

Finally, proximity effects due to the presence of a horizontal bottom boundary near the level of the efflux are included in CorJet. These are related to a "leakage factor" that measures the combined effect of port height and spacing in allowing the ambient flow to pass through the diffuser line in order to provide sufficient entrainment flow for the mixing downstream from the diffuser. Multiport diffuser discharges with small leakage factors are thus predicted to have reduced plume rise trajectories in the crossflow. The model has been validated intensively and the range of applicability of the integral model has been carefully evaluated where a number of spatial limitations have been proposed beyond which the integral model necessarily becomes invalid. Whenever horizontal or lateral boundaries exist in the flow domain, e.g. the free surface or bottom of a water body, complex flow interactions may occur. Such resulting phenomena as jet impingement, attachment, internal hydraulic jumps, instabilities and recirculation are of course beyond the predictive powers of a simple integral model. In these instances, additional techniques for flow classification and prediction must be used, and are embedded in the CORMIX expert system structure.

18.6.4 Tier 3—Detailed Assessment: Combined Models for Far-Field and Water Quality

Tier 2 presented near-field mixing zone models, modeling the interaction of the discharge fluxes with the ambient flow conditions to obtain concentration distributions in region around the discharge. Discharge permits and outfall design studies are often assessing those relations. However, very often discharges either occur in sensitive or complex environments and information on the fate of the discharged substances beyond the near-field region are of interest. Furthermore, when the ambient conditions (such as bathymetry and flow conditions) cannot be schematised by simplified approximations to obtain reliable results for the discharge (as indicated in Tier 2), a combination of near field and far field models is typically necessary. This coupled modeling approach can compute the dispersion of the effluents more accurately in an irregular and dynamic environment. Furthermore, such modeling approach is very useful for recirculation assessments (i.e. to assess how much of the discharged effluent could reach the intakes for operational considerations), where the distance between outfall and intake is typically larger (and beyond the near field).

Near field models are most accurate in the initial mixing phase of the outfall plume (on spatial scales of metres) up to few hundreds of metres from the outfall. In this phase, turbulent mixing and non-hydrostatic effects play an important role on scales that can typically not be resolved by a (hydrostatic) far field model. Efficient near field models, such as CORMIX, are however typically limited in the complexity they can take into account regarding the ambient conditions around the outfall. The ambient geometry is strongly schematised, physical processes such as

temperature exchange with the atmosphere are simplified and these models typically provide steady-state solutions. These assumptions are very acceptable in the near and intermediate field region, close to the outfall, but become more limiting further away from the outfall.

At a larger distance from the outfall, larger scale dispersion processes become more dominant, such as those driven by ambient currents, wind effects, heat exchange with the atmosphere etc. These processes can be modeled accurately with a far field model such as Delft3D-FLOW (see Deltares 2013), EFDC or MIKE3. However, due to the typically used, feasible computational grid resolutions on the order of tens of metres around the outfall and the (commonly used) hydrostatic pressure assumptions, the smaller scale processes associated with the near field mixing of the outfall plume cannot be accurately included in a far field model.

Due to the large differences in scales and processes involved, when progressing from the near field, via the intermediate field to the far field, these different types of models are typically utilised for the simulation of near field and far field processes. Existing models that can theoretically cover this entire range of temporal and spatial scales in one integral computation (unsteady, baroclinic, non-hydrostatic models) are very computationally expensive and are not yet usable for most practical engineering applications.

However, by coupling the near field (e.g. CORMIX) and far field (e.g. Delft3D-FLOW) models at a location at which both models can compute and represent the plume accurately (i.e. a suitable coupling location), the full plume trajectory can be modeled in an adequate and physically accurate way.

18.6.4.1 Example of a Far Field Model—Delft3D

An example of a near field expert system, CORMIX, is presented above. An example of a far field model is the Delft3D modeling suite (in addition to other modeling systems, such as MIKE and EFDC).

Delft3D is the integrated flow and transport modeling system developed by Deltares for the aquatic environment. The flow module of this system, Delft3D-FLOW (Deltares 2013), provides the hydrodynamic basis for other modules such as water quality, ecology, waves and morphology.

The hydrodynamic module Delft3D-FLOW simulates two-dimensional (2D, depth-averaged) or three-dimensional (3D) unsteady flow and transport phenomena resulting from tidal and/or meteorological forcing, including the effect of density differences due to a non-uniform temperature and salinity distribution (density-driven flow). The flow model can be used to predict the flow in shallow seas, coastal areas, estuaries, lagoons, rivers and lakes. It aims to model flow phenomena of which the horizontal length and time scales are significantly larger than the vertical scales.

Three-dimensional modeling is of particular interest in transport problems where the horizontal flow field shows significant variation in the vertical direction. Wind forcing, bed stress, Coriolis force, bed topography or density differences may

generate this variation. Examples are dispersion of waste or cooling water in lakes and coastal areas, upwelling and downwelling of nutrients, salt intrusion in estuaries, fresh water river discharges in bays and thermal stratification in lakes and seas (see Lesser et al. 2004 and Deltares 2013).

Transport processes (i.e. for conservative substances) can be simulated either directly within the hydrodynamic module (Delft3D-Flow) or within the water quality module (Delft3D-WAQ), which allows including further transformation and decay processes of included substances. A simpler, but efficient type of transport model, namely a particle tracking model (Delft3D-Part) can be used to track substance distributions using the results from the hydrodynamic model, thus without a feedback between the transport and the hydrodynamic model. The latter is usually used for intermediate scale studies, thus outfall design and optimization, as large-scale analysis requires large computational efforts.

18.6.4.2 Coupling Near Field and Far Field Models

The aim of coupling near field and far field models is to allow for the modeling of the full plume trajectory, from the outfall to the sensitive receivers (e.g. ecological sensitive regions) up to kilometres away. For this, different model types (near field and far field) are used that are most appropriate and accurate for the different regions of the plume. These models are used in their applicable domains, where they are capable of describing the physical processes adequately. To obtain an accurate and efficient modeling assessment for the full plume trajectory, these models are coupled at a location where both types of models are able to compute the plume sufficiently accurately.

The criteria for a suitable coupling location between near field and far field plume models include both physical and numerical considerations.

Physical considerations include:

- The coupling location should be beyond the region where non-hydrostatic processes take place, since typically far field models are used with a hydrostatic pressure assumption.
- The coupling location should be beyond the region where initial turbulent mixing takes place based on physical processes that are not included in typical far field models.
- The coupling location should be beyond the region where small-scale processes take place that are smaller than the typical length-scales (and grid sizes) of the far field model.
- The coupling location should preferably be beyond the point of boundary interaction by the plume (in the intermediate zone), since these processes are typically not adequately represented by far field models. Typically selected coupling locations at the point of boundary interaction are less suitable (see Fig. 18.16).

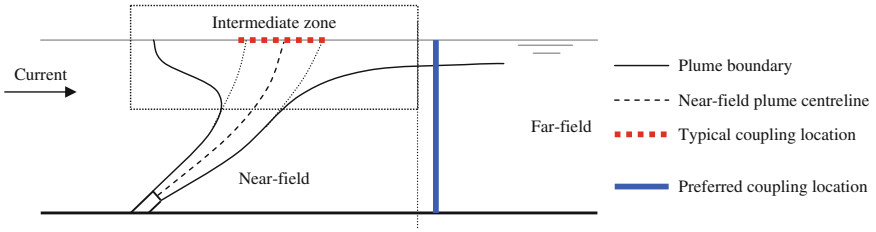

Fig. 18.16 Typical plume behaviour including boundary interaction and lateral spreading along the water surface. The typical and preferred locations for coupling the near and far field are indicated (Morelissen et al. 2013)

- The coupling locations, for example, can be estimated by the length-scale based flow classification scheme presented in Tier 1.

Numerical considerations include:

- The horizontal far field computational grid spacing should be able to describe the outfall plume properly at the coupling location (i.e. the plume should at least be resolved in the horizontal dimensions using several far field grid size at the coupling location)
- The far field vertical layer distribution should be able to describe the outfall plume's vertical dimensions at the coupling location by at least one or more layers

If the numerical criteria are not met, the plume will be subject to substantial numerical diffusion (i.e. it will mix directly over the volume of the far field grid cells) and will therefore change its physical (e.g. buoyancy) behavior.

For the translation of the near field plume to the far field model, an important consideration is on the (physical or model) parameters that should be translated from the near field plume assessment to the far field model. In this consideration, it is important to select the parameters necessary to describe the plume in the far field model adequately. On the other hand, to not overcomplicate the coupling, only parameters should be translated that can actually be resolved by the far field model grid size and implemented physical processes. Typically, for an outfall plume, the following parameters are translated:

- Plume trajectory (in X, Y and Z coordinates along the plume centre line)
- Dilution rate (in dilution factor S along the plume centre line)
- Plume dimensions at the coupling location (both width and height)

Concentrations of the effluent typically do not need to be translated, since these are the inverse of the dilution rate (for a conservative substance). As described below, the concentration is computed by the far field model based on the dilution information and initial outfall source. For fast decaying substances (even within the near field, i.e. within tens of metres and for travel times typically up to minutes), translating the concentrations could be considered.

Distributed Entrainment Sinks Approach (DESA)

To accurately schematise the outfall plume in the far field model, it is important to include the plume at the adequate coupling location as a diluted source. The dilution is computed by the near field model, based on the computed entrainment along the plume trajectory towards the coupling location. In particular for plumes with a different density (e.g. for heated effluent), the schematisation as a diluted source (as opposed to an undiluted source) is important to obtain a correct excess density at the coupling location and associated hydrodynamic (buoyancy) behavior. To include this dilution in the far field model in a mass-conserving way, the Distributed Entrainment Sinks Approach (DESA, see Choi and Lee (2007)) is implemented in the coupled modeling approach. This approach consists of defining entrainment sinks along the plume trajectory in the far field model grid where ambient water and substances are extracted according to the computed entrainment by the near field model for each plume section. The total amount of extracted (entrained) water is subsequently released together with the original outfall source at the coupling location, thereby obtaining a diluted source in the far field model. In Fig. 18.17 from Choi and Lee (2007) it is shown how the different entrainment sinks are defined along the plume trajectory.

The implementation of the DESA method in the coupling method also accounts for the possible re-entrainment of discharged effluent when the effluent is not effectively transported away from the outfall, which is typically not accounted for in steady state near field models. Since the DESA method in general improves the

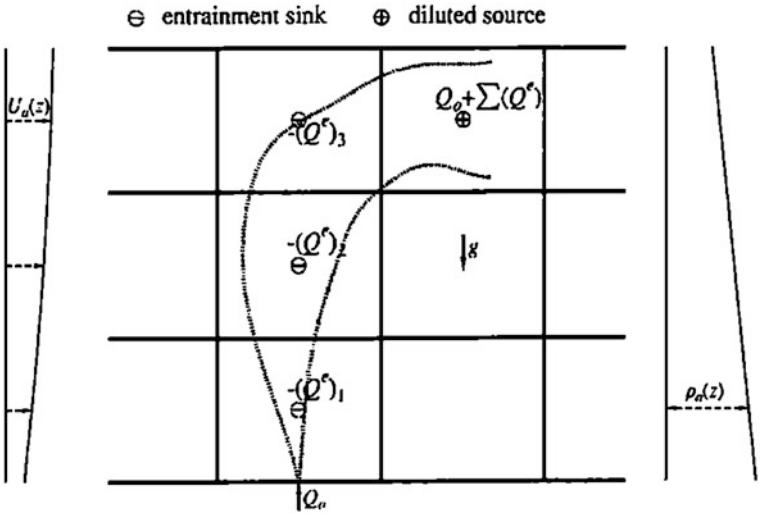

Fig. 18.17 Representation of diluted source flow and entrainment sinks along the jet trajectory (Choi and Lee 2007)

physical representation of the plume behavior in the far field model, the use of this method is recommended for any of coupling method.

Different Methods for Coupling Near Field Models to Far Field Models

The coupling between near field models and far field models can be done in different ways, with varying levels of comprehensiveness and include:

1. No coupling; undiluted, fixed source in the far field model
2. One-way coupling; fixed diluted source in far field model, based on near field modeling and possibly using the DESA
3. One-way coupling; time-varying diluted source in far field model, based on near field modeling for different ambient conditions (and possibly using the DESA)
4. Two-way, dynamic coupling; time-varying diluted source in far field model (and possibly using the DESA) and feedback to near field model, where the near field and far field models run in parallel.

Coupling method 1 (no coupling) is not recommended, particularly for submerged outfalls, due to the physical inaccuracy and large dependency on numerical aspects of the far field model but could be used as screening approach in Tier 1. Coupling method 2 (one-way coupling with fixed near field solution) should be used when the near field plume behavior (in terms of position of the coupling location, dilution and dimensions of the plume at the coupling location) remains fairly constant under the ambient conditions. Coupling method 3 (one-way coupling with time-varying near field solution) is most suitable for situations where the near field plume behavior varies over time under different ambient conditions (e.g. tidal flows or differences in summer and winter stratifications). Coupling method 4 is the most comprehensive method and is used in specific cases particularly when certain physical phenomena need to be reproduced and when the momentum of the outfall is generally larger than the ambient flow conditions (e.g. large outfalls in a low-current ambience, such as a lake). This latter method is described in Tier 4 and the other coupling methods are described in more detail below.

Coupling Method 1: No Coupling; Undiluted, Fixed Source in the Far Field Model

In this method, the outfall is included in the far field model directly, without any incorporation of near field processes. This means that the outfall source is included in the far field model as an undiluted source, in a selected model grid cell. Typically, single pipe or diffuser type outfalls have much smaller diameters than the far field model grid size. By including a smaller-scale outfall in a larger model grid cell, the effluent is immediately mixed over the grid cell volume, therefore changing the physical behavior of the effluent, such as buoyancy. The eventual behavior of the effluent therefore depends on the model grid cell size and not on actual mixing processes. Also including the outfall source not at the terminal vertical level

(e.g. inserting a buoyant plume source near the bottom), results in erroneous model behavior in a hydrostatic model and additional numerical diffusion.

Only for applications of open channel outfalls, where the outfall channel can be well represented by one or more far field model grid cells, this method could be used in certain conditions. It should however be carefully checked if the far field model is capable of representing the physical processes important for the modeled problem sufficiently well.

Advantages

- Simple approach, without need for a near field model
- Could be used under certain conditions for open channel outfalls

Disadvantages

- Does not include physical processes correctly
- Very sensitive to numerical diffusion and model (grid) assumptions
- Generally not recommended for use in outfall modeling

Coupling Method 2: One-Way Coupling; Fixed Diluted Source in Far Field Model

In this method, a near field assessment is carried out for typical ambient conditions at the outfall site. Based on this assessment, a typical near field behavior that is representative for most ambient conditions, is used as a constant source in the far field model. The schematisation of this source does however take into account the plume trajectory, dimension and dilution based on the near field assessment, preferably using the DESA method. This results in a diluted source, coupled at an adequate location to the far field model and with the correct dimensions. This approach takes into account certain important physical processes (e.g. with the DESA the entrainment processes and mass conservation) and is much less sensitive to numerical diffusion (if coupled at an adequate location).

This method consists roughly of the following steps:

1. Simulation of the ambient conditions with the far field model without the outfall
2. Definition of a representative selection of ambient conditions (i.e. climate), relevant to the near field behavior of the outfall plume
3. Near field assessment for the selected ambient conditions and discharge configuration
4. Definition of a representative near field source for inclusion in the far field model and a suitable coupling location
5. Inclusion of outfall source term with DESA in the far field model (i.e. defining a number of sinks along the plume trajectory that discharge at the coupling location together with the outfall source to obtain a correctly diluted source)
6. Simulation with the far field model with the diluted outfall source included

Advantages

- Inclusion of relevant physical processes in the far field model (e.g. diluted source, entrainment)
- Limited sensitivity for numerical diffusion (i.e. accounting for plume dimensions and adequate coupling location)
- Better representation of the plume behavior compared to Coupling method 1
- In general recommended to be the minimum level of coupling to use for outfall modeling

Disadvantages

- Fixed near field solution, so no variation of the plume behavior due to ambient dynamics included
- Expert judgement necessary for interpretation of near field assessment, selection of coupling location and adequate inclusion of plume sources (and sinks) in the far field model

Example case

In a case study carried out for a desalination brine discharge in Oman (Verbruggen et al. 2014), a near field assessment was conducted for the outfall diffuser. The ambient conditions at the project site and particularly near the bed, where the diffuser was located, were relatively mild in relation to the outfall dynamics. The near field assessment showed that for the different ambient conditions that occurred at the project site, the near field behavior (i.e. plume trajectory and dilution) did not vary substantially. In this case study, therefore a fixed near field solution could be used for the far field modeling. This consideration should be made in relation to the modeling objectives of the study (e.g. spatial scales under consideration and required comprehensiveness).

In the case study, a DESA implementation of the near field behavior was included in the far field that was a representative schematisation of the near field plume behavior. The case study has shown that by including the outfall source as a diluted source and by using the DESA method, certain (also less obvious) physical processes are included in the outfall modeling (see Verbruggen et al. 2014).

Coupling Method 3: One-Way Coupling; Time-Varying Diluted Source in Far Field Model

A further improvement to Coupling Method 2 is to use a time-varying outfall source in the far field model for the one-way coupling. In this method, the variation of the near field behavior in relation to the ambient conditions is taken into account adequately.

In this case, the far field model should first be run without the discharge (or with a simplified version of the discharge) to obtain time-varying ambient conditions at the discharge location. These ambient conditions are subsequently used to simulate these conditions with the near field model. Next, the far field model is run again

with the time-varying representation of the near field behavior as a diluted source. Depending on the type of near field model, this could be done as a time series of near field plume characteristics (Feitosa et al. 2013) or as a kind of look-up table with pre-computed plume characteristics, when a computationally intensive near field model is used, such as a CFD model (see also Botelho et al. 2013).

This method consists roughly of the following steps:

1. Simulation of the ambient conditions with the far field model without the outfall
2. Extract ambient condition time series at the outfall location (including water levels, three-dimensional currents and density profiles)
3. Near field modeling assessment to compute the outfall plume behavior for the discharge configuration, (a) for each time step in the ambient condition time series, use a detailed (CFD) near field model to model the outfall plume behavior for a climate of ambient conditions (based on the ambient condition time series) and store the results in a database. The near field results consist of the parameters to be translated to the far field model for the different ambient conditions.
4. Inclusion of the time-varying outfall source terms with DESA in the far field model (i.e. defining a number of sinks along the plume trajectory that discharge at the coupling location together with the outfall source to obtain a correctly diluted source). In the far field model, this means that the sinks and sources will vary over time, for each new near field solution. For example in Delft3D, this could be accomplished by defining each grid cell and layer that the plume trajectory reaches during the simulation as a potential source/sink. In the source/sink discharge time series input file, these potential sources have a zero discharge, unless it is part of the plume trajectory for a certain time step in which it obtains a positive (source at the coupling location) or negative (sink along the plume trajectory) value.

   It is important when discharging the extracted water from the entrainment sinks at the coupling location, to also extract/discharge the substances in the far field model to account for e.g. re-entrainment or adequate inclusion of ambient stratification in the plume dilution process. However, in these more complicated cases, a two-way coupling could be necessary to model these processes accurately (see Tier 4).
5. Simulation with the far field model with the time-varying, diluted outfall sources included

In some cases it could be appropriate to already include a simplified outfall source in Step 1 to account for some effects on ambient conditions by the outfall, if this is expected to be relevant (e.g. locally changed stratification due to the outfall). However, to adequately account for this type of more complex interactions, the two-way coupling method (Tier 4) would be more appropriate.

Advantages

- Inclusion of relevant physical processes in the far field model (e.g. diluted source, entrainment)
- Limited sensitivity for numerical diffusion (i.e. accounting for plume dimensions and adequate coupling location
- Good representation of the plume behavior, including varying plume behavior due to changing ambient conditions
- Recommended to use for outfall modeling in varying ambient conditions, where the ambient conditions result in differences in near field plume behavior

Disadvantages

- More complex method to use and possibly somewhat more time consuming

Example case

A comprehensive modeling study has been undertaken for the Olympic Dam discharge in Australia (Botelho et al. 2013 and BMT WBM (2013) reports for EIS). That study somehow reproduced the tiered approach for the different design steps. In a first step initial screening was done using simple dilution equations as shown in Tier 1 for still ambient conditions. That analysis allowed defining the number of required ports and the resulting diffuser length to obtain a minimal required dilution. A subsequent run of a near-field mixing zone model (CORMIX) for several different schematized ambient conditions (uniform and steady ambient velocity and density profiles, bathymetry) allowed pre-assessing the dilution values for different conditions and discharge characteristics.

Due to uncertainties in representing the near-field jet characteristics after impingement with the bed a complex computational fluid dynamics (CFD) simulation using Open-Foam has been undertaken. This showed a specific process not represented in the near-field models, a reentrainment within a 3–4 m stable salinity layer close to the bed, which have been observed in field monitoring studies too. Those comprehensive CFD studies are alternatives to conventional near-field models, once the discharge cannot be schematized as to the assumptions made in the near-field models. Examples for similar studies can be found in Law et al. (2002). However, limitations are: (i) long computation times (even using parallelized codes on multi-processors), (ii) stability issues and necessary validation, (iii) usually feasible only for steady conditions and small scales (near-field region only), (iv) simplifying the free surface as rigid lid, which is reasonable for dense discharges.

The far-field analysis for the Olympic Dam study were undertaken with the ELCOM model and using the CFD and CORMIX data as a near-field input using a one-way coupling Type 3 as described above, however, only translating pollutant mass fluxes as sources, as dynamic near-field parameters were small and not resolved in the far-field model.

18.6.5 Tier 4—Investigative Study: Dynamically (Two-Way) Coupled Models for Design Optimization

In Tier 4, investigative studies and design optimisation take place for specific cases that require a comprehensive (modeling) approach. Such cases are typically characterised by complex ambient conditions and near field—far field interactions that can influence the outfall plume behavior. The more simple modeling approaches do not satisfy the required accuracy for this type of outfalls. Those investigative studies are usually complemented with extensive field studies, and physical model studies.

Although coupling methods described in Tier 3 (especially Method 3) are already very comprehensive and accurate, especially when the DESA method is used, they do not fully account for feedback mechanisms of the far field outfall plume dispersion on the near field plume behavior. Particularly in areas with lower ambient dynamics (i.e. with a large outfall to ambient flow ratio) this is relevant. For example, a cooling water outfall in a lake could alter the (local) stratification, which in turn affects the near field plume behavior in terms of trajectory, dimensions and dilution. Coupling method 4, a two-way coupling, does account for this effect.

Similar to Tier 3, a far field model is used for the two-way coupling, which means that the modeling assessment requires more efforts than a simpler approach. In this section, a two-way coupling is illustrated between the CORMIX near field model and the Delft3D-FLOW far field model. In general, similar steps are taken as for the one-way coupling described in Tier 3, although many of these steps are included in the routines of the Delft3D-FLOW coupling interface. This makes this type of coupling more easy to use and less dependent on the choices made by the modeller.

Advantages

- Inclusion of relevant physical processes in the far field model (e.g. diluted source, entrainment)
- Limited sensitivity for numerical diffusion (i.e. accounting for plume dimensions and adequate coupling location
- Good representation of the plume behavior, including varying plume behavior due to changing ambient conditions
- Also includes feedback of far field changes by the plume on the near field computations (e.g. changed stratification by the outfall)
- Recommended to use for outfall modeling in varying ambient conditions, where the ambient conditions result in differences in near field plume behavior, but where also the near field can change the far field to an extent that the near field plume behavior is affected (i.e. large outfall compared to the ambient flow conditions).
- In general, this two-way coupled approach is appropriate for any type of (submerged) outfall, even though the particular requirements for such two-way

coupling are not present. Since the coupling steps are included in the software routines, this makes the coupling process more robust and easy to use for modellers.

Disadvantages

- Specific software necessary that includes the coupling routines (i.e. specific CORMIX and Delft3D-FLOW versions)
- Since the two-way coupling method is part of on-going research and development, additional developments could be necessary before application in certain outfall configurations.

18.6.5.1 The CORMIX—Delft3D-FLOW Two-Way Dynamic Coupling Algorithm

In Fig. 18.18, the general operation of the dynamically coupled CORMIX—Delft3D-FLOW modeling system is presented. Both models operate simultaneously and exchange information at set intervals. The Delft3D-FLOW computation

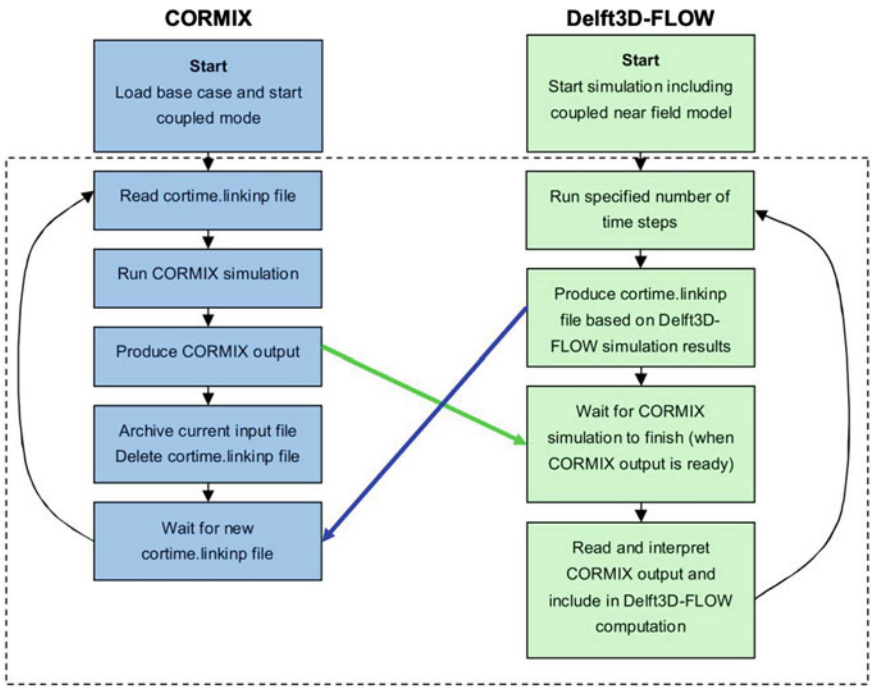

Fig. 18.18 The general operation of the dynamically coupled CORMIX—Delft3D-FLOW modelling system (Morelissen et al. 2014)

produces a CORMIX (CorTime 2008) input file with the ambient conditions near the outfall (at a so-called 'monitoring point'), after which a CORMIX computation is executed. CORMIX produces a prediction output file that is subsequently interpreted by Delft3D-FLOW and its results (in terms of plume trajectory, dimensions and dilutions) included in the far field model by means of the DESA method.

18.6.5.2 Example Case

The case study (in detail in Morelissen et al. 2014) consists of several large outfall situations in typically, relatively mild ambient conditions. Since these large discharges could (locally) alter the stratification of the water column and with that the initial plume behavior (e.g. effects on buoyancy), a dynamic two-way coupling of the near field and far field models is required.

The dynamically coupled modeling system was set up for the case study, including multiple, simultaneous coupled outfalls in the project area. The capabilities to model multiple outfalls, as well as the modeling of this type of diffuser outfalls (and coupling of the associated modules in CORMIX) were newly developed in this case study.

Due to the large momentum of the outfall ports (exit velocities of about 2.5 m/s at a port diameter of 2.5 m), the near field effects of initial momentum and buoyancy can cover a relatively large distance of hundreds of metres, depending on the ambient flow conditions. Furthermore, due to the relatively limited depth and large momentum, CORMIX predicted a temporarily mixing over almost the full water column at a certain distance from the diffuser before the plume re-stratifies towards the water surface, forming a plume of several metres thickness. The actual plume extent, dimensions and dilution depend substantially on the ambient flow conditions.

The dynamically coupled modeling system was used to assess various outfall configurations of different stages of development of the power plant extension. All these configurations were modeled for the four different seasons. The results were presented as the temperature increase at the intakes and as temperature increase footprints at surface (and several other vertical levels) for easy comparison with the criteria. Furthermore, impressions of the near field and far field results simultaneously were presented to indicate the interaction of the models.

The dynamical dependence of the models becomes apparent in Fig. 18.19 showing the outfall plumes during different stages of the tide in the coupled model simulation. It is hereby interesting to see that plume orientations not always necessarily follow the predominant velocity field, on one hand due to the far-field dynamics, on the second hand due to the near-field induced flow field. A comparison with field studies (Fig. 18.20), unfortunately during another period, thus not directly comparable, shows similar features occurring in reality.

Without a dynamic two-way coupling between the near field and far field model, those phenomena would not have been represented or underestimated. The fact that

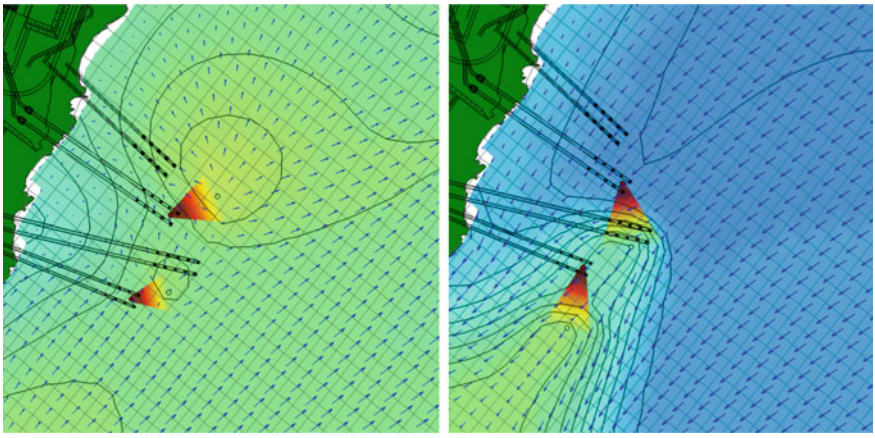

Fig. 18.19 Visualisation of the outfall plumes during different stages of the tide in the coupled model simulation; colours show temperature and vectors show currents (Morelissen et al. 2014)

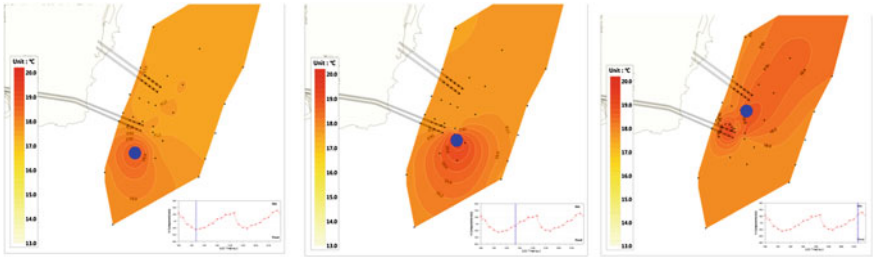

Fig. 18.20 Field measurements of the surface temperature showing different locations where the outfall plume surfaces (indicated by *blue dot*) during different stages of the tide (Morelissen et al. 2014)

the location with the highest temperature moves over different tidal stages has an influence on the shape of the thermal footprint that is relevant for permitting.

Since the dynamically coupled modeling system uses the near field modeling results (including dilution and plume dimensions) to define a source term in the far field model, the far field plume source term is a diluted source. In contrast to this approach, the traditional way of modeling is typically to include the heated cooling water effluent as an undiluted source in the far field model, e.g. at the top half of the water column. The latter method makes the initial effluent behavior in the model strongly dependent on the model grid resolution (numerical diffusion) and susceptible to processes that are not adequately included in a hydrostatic far field model. The modeling results for both methods also show different temperatures at the surface when thermal footprints are assessed. In Fig. 18.21, this difference between the coupled and traditional modeling methods is presented with regard to

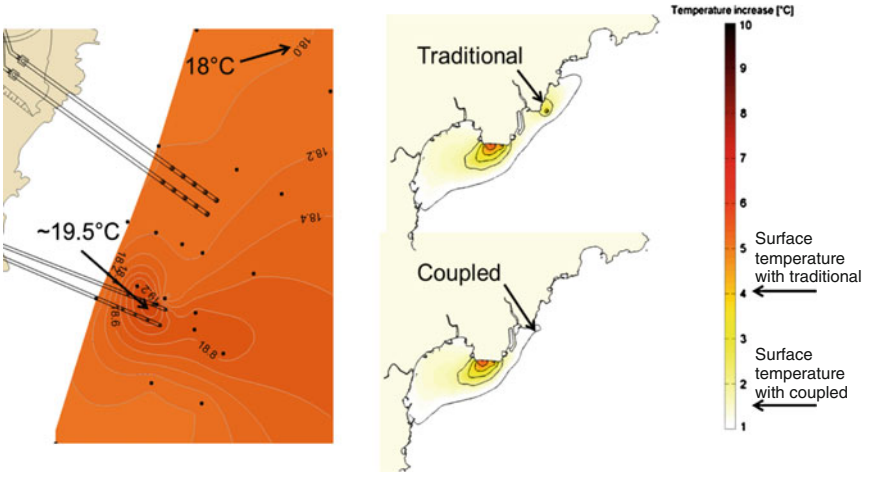

Fig. 18.21 Measured surface temperature (*left plot*) and different results for the coupled and traditional modelling methods in surface temperature increase and footprint size (*right plots*) for the submerged outfall indicated by the *black arrows* (Morelissen et al. 2014)

the (maximum) surface temperature increase and footprint size. This comparison shows that the coupled modeling system computes about 1–1.5 °C temperature increase at the surface (location of this plume indicated by the arrow) for this discharge of +9 °C at the sea bed. The traditional method, in which this discharge source is included in the far field model as an undiluted source divided over the top half of the water column (corresponding with the plume thickness at the coupling location for the coupled modeling approach), shows about 4 °C temperature increase at the surface and a larger thermal footprint. It is noted that the large temperature increase to the south is caused by open channel outfalls, which is modeled similarly in both approaches. When these different surface temperatures are compared to the field measurements (left plot in Fig. 18.21), it can be observed that the local temperature increase is about 1.5 °C, which corresponds well with the computed temperatures by the coupled modeling approach. The traditional approach with undiluted sources overestimates the surface temperature and footprint size substantially. It is noted that including initial dilution in the far field model source term will affect the surface temperature and footprint more strongly under stratified ambient conditions (see also the next section), but that not including dilution will generally lead to an overestimate of the (surface) temperatures.

The dynamically coupled modeling system uses the distributed entrainment sinks approach (DESA) to approximate the occurring near field entrainment effects in the far field model. This approach entrains the appropriate amount of ambient water to dilute the plume along the plume trajectory in the far field model. In this process, the entrainment also takes into account the actual temperature (and salinity, effluent concentrations etc., if applicable) of the entrained water, so that e.g. re-entrainment after a build-up of discharged effluent is accounted for, which is a

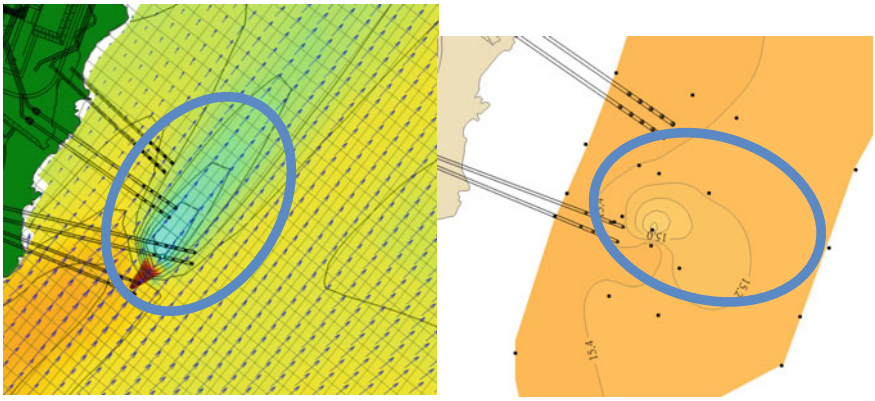

Fig. 18.22 Downstream 'wake' with lower temperatures at the surface during stratified conditions, *left plot* model results (colours and contours show temperature and vectors show currents), *right plot* field temperature measurements

unique feature of this coupled modeling approach. Also the possible stratification in background temperature (as is the case in the case study at times in spring and summer seasons) is accounted for this way.

In certain cases, the model results showed a temporary colder 'wake' at the surface downstream of the plume's surfacing location during stratified ambient conditions. Due to the large momentum of the outfall diffuser the outfall plume reaches the surface, regardless of the occurring background stratification. The CORMIX computations show that the plume becomes temporarily and locally mixed over a large part of the water column due to this large momentum, after which it re-stratifies. During the rising of the plume from the sea bed (where the outfall ports are located), the plume entrains colder water from the lower part of the water column during these stratified background conditions. The resulting temperature of the plume at the location of coupling is therefore at times colder than the ambient surface water temperature, which is shown Fig. 18.22 (left plot). This phenomenon could also be observed in the field measurements when stratified background conditions occurred, see Fig. 18.22, right plot. It is noted that the model showed this phenomenon more strongly than the field measurements, which could be explained by the fact that the model had a stronger background stratification (i.e. larger temperature difference over the water column) for the simulated period than in the period of the field measurements.

Although not presented here in detail, the field measurements of transects with vertical temperature and velocity profiles through the outfall plume confirmed the prediction by CORMIX that the plume mixes temporarily and locally over a large part of the water column before re-stratification, which is explained by the large outfall momentum.

The effects of plume recirculation with traditional (uncoupled) and dynamically coupled models is shown in Fig. 18.23, which shows a cross-section through the

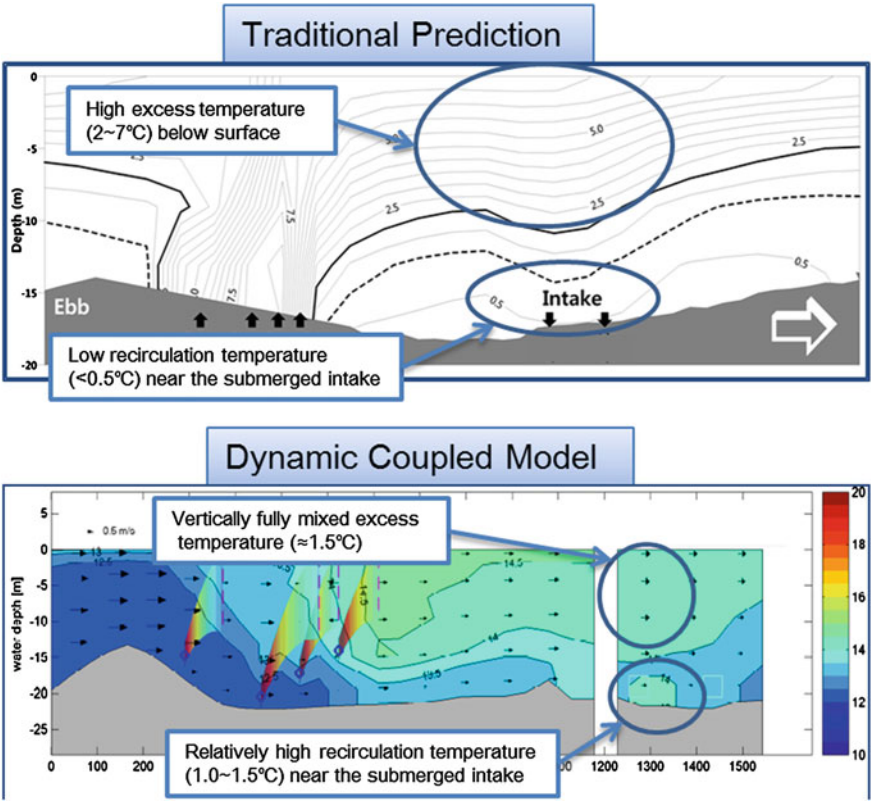

Fig. 18.23 Cross-section through the model from outfalls to intakes with the predicted temperatures in the traditional modelling approach (*upper plot*) and dynamically coupled approach (*lower plot*) (Morelissen et al. 2014)

model with the predicted temperatures in the traditional modeling approach (upper plot) and dynamically coupled approach (lower plot). The fact that the coupled model predicts a larger temperature increase at the intake is therefore more conservative (and realistic) and results in a safer design for the plant cooling water system.

Based on the case study, developments and validation of the dynamically coupled near field—far field modeling system, the following can be concluded:

- The two-way near field—far field coupling results in a good representation of physical processes associated with (large) outfalls.
- The validation against field data showed that accuracy has improved and that this improvement makes an important difference with design criteria of a (cooling water) outfall.
- The two-way coupled near field—far field modeling system is therefore an important technique in adequately modeling outfalls. For the case study, this improved modeling approach led to a more accurate and less conservative

prediction of the environmental impacts of the outfall and a more accurate and safer prediction of the design parameters of the intake and outfall configuration of these large-scale power plants.

18.7 Conclusions and Outlook

The tiered approach as proposed in recent water framework regulations has been applied to develop a tiered approach for brine discharge modeling. The presented steps showed that there are readily applicable tools and systems for all tiers available, and that complex multiple discharge situations of large volumes in shallow waters require a specific approach using a two-way coupled system.

It has to be noted however, that the required detail of necessary measurements (bathymetry, currents, tides, density profiles, etc.) increases considerably with every tier. The models however need that data, otherwise cannot be run satisfactorily. Considering the economic effects of a properly designed discharge system, and avoiding recirculation problems, definitely pay off those additional investments, and reduce risks.

Recent ongoing developments are promising in that regard, where most model systems are available as open-source and public domain, and still undergo considerable improvements, such as providing flexible mesh modeling, better access to environmental, publically available databases to obtain required boundary information, further developments on coupling different models for different scales and further validation of the different modeling techniques. This will result in an even more flexible, efficient and reliable set of modeling techniques and tools for the assessment of outfalls.

References

Akar, P. J., & Jirka, G. H. (1995). Buoyant spreading processes in pollutant transport and mixing. Part II: Upstream spreading in weak ambient current. *Journal of Hydraulic Research, 33*(1), 87–100.

Alspach, B., Burch, R., & Baudish, P. (2009). Seawater desalination in Australia: Water supply solutions without environmental cost. In *Proceedings of the IDA World Congress on Desalination and Water Reuse*—Atlantis. The Palm, Dubai, UAE, November 7–12, 2009.

ANZECC. (2000). *Australian and New Zealand Guidelines for Fresh and Marine Water Quality*.

Bleninger, T., & Jirka, G. H. (2008). Modelling and environmentally sound management of brine discharges from desalination plants. *Desalination, 221*(1–3), 585–597.

Bleninger, T., & Jirka, G. H. (2011). Mixing zone regulation for effluent discharges into EU waters. In *Proceedings of the ICE—Water Management 165*.

Bleninger, T., Jirka, G. H., Lattemann, S., Purnama, A., Al-Barwani, H.H., & Doneker, R.L. (2009). BrineDis: Environmental planning, prediction and management of brine discharges from desalination plants. Project Report, Middle East Desalination Research Center (MEDRC).

Bleninger, T., Niepelt, A., & Jirka, G. H. (2010). Desalination plant discharge calculator. *Desalination and Water Treatment, 13*, 156–173.

BMT WBM. (2013). Reports for EIS on Olympic Dam, Australia. Download from www.bmtwbm.com.au.

Botelho, D. A., Barry, M. E., Collecutt, G. C., Brook, J., & Wiltshire, D. (2013). Linking near- and far-field hydrodynamic models for simulation of desalination plant brine discharges. *Journal of Water Science and Technology* 67(6), 1194–207. doi:10.2166/wst.2013.673.

Brooks, N. H. (1960). Diffusion of sewage effluent in an ocean current. In *Proceedings of 1st International Conference on Waste Disposal in the Marine Environment*. University of California, Pergamon Press, New York.

Brooks, N. H. (1980). Synthesis of stratified flow phenomena for design of ocean outfalls. In *Proceedings of 2nd International Symposium on Stratified Flows* (pp. 809–831). Trondheim, Norway.

Brooks, N. H. (1984). Dispersal of wastewater in the ocean—a cascade of processes at increasing scales. In *Proceedings of Conference on Water for Resource Development*. Coeur d'Alene.

Brooks, N. H. (1988). Seawater intrusion and purging in tunneled outfall. *Schweizer Ingenieur und Architect, 106*(6), 156–160.

Brooks, N. H., & Koh, R. C. Y. (1965). Discharge of sewage effluent from a line source into a stratified ocean. *Proceedings of XI Congress IAHR, Leningrad*, Paper No. 2.19.

Buros, O. K. (2000). The ABCs of desalting. http://www.idadesal.org/pdf/ABCs1.pdf.

Choi, K. W., & Lee, H. W. (2007). Distributed entrainment sink approach for modelling mixing and transport in the intermediate field. *Journal of Hydraulic Engineering Division of the American Society of Civil Engineers, 133*(7), 804–815.

Christie, S., & Bonnélye, V. (2009). Perth, Australia: Two-year feed back on operation and environmental impact. *Proceedings of IDA World Congress on Desalination and Water Reuse —Atlantis*. The Palm, Dubai, UAE, November 7–12, 2009.

CIS-WFD. (2010). *Technical background document on identification of mixing zones*. Elektronisch verfügbar auf. https://circabc.europa.eu.

CorTime. (2008). *v2.0—user instructions*. September 29, 2008. MixZon Inc. (www.mixzon.com).

Deltares. (2013). *Simulation of multi-dimensional hydrodynamic flows and transport phenomena, including sediments*. User manual hydro-morphodynamics version 3.15.30059, September 6, 2013. Deltares, Delft.

Doneker, R. L., & Jirka, G. H. (1990). *CORMIX1: An expert systems for hydrodynamic mixing zone analysis of conventional and toxic submerged single port discharges.* Technical report. De Frees Hydraulic Laboratory, School of Civil and Environmental Engineering, Cornell University.

Doneker, R. L., & Jirka, G. H. (2007). *CORMIX user manual: A hydrodynamic mixing zone model and decision support system for pollutant discharges into surface waters*. Portland, OR: MixZon Inc.

European Union. (2008). Directive 2008/105/EC of the European Parliament on environmental quality standards in the field of water policy.

Feitosa, R. C., Rosman, P. C. C., Bleninger, T., & Wasserman, J. C. (2013). Coupling bacterial decay and hydrodynamic models for sewage outfall simulation. *Journal of Applied Water Engineering and Research, 1*, 137–147.

Fischer, H. B., List, E. J., Koh, R. C. Y., Imberger, J., & Brooks, N. H. (1979). *Mixing in Inland and coastal waters*. New York: Academic Press.

Goebel, O. (2005). Markets and desalination technologies in brief. DME seminar on the introduction to seawater desalination, Berlin.

Holley, E. R., & Jirka, G. H. (1986). *Mixing and solute transport in rivers*. Field Manual, U.S. Army Corps of Engineers, Waterways Experiment Station, Technical report E 86 11.

Jirka, G. H. (1979). Discussion of Roberts, P.J.W.: Line plume and ocean outfall dispersion. *Journal of the Hydraulics Division ASCE 102*(12), 1573–1575.

Jirka, G. H. (1982). Turbulent buoyant jets in shallow fluid layers. In W. Rodi (Ed.), *Turbulent jets and plumes*. New York: Pergamon Press.

Jirka, G. H. (1994). Shallow jets. In P. A. Davies & M. J. Valente (Eds.), *Recent advances in the fluid mechanics of turbulent jets and plumes*. Dordrecht: Kluwer Academics Publishers.

Jirka, G. H. (2004). Integral model for turbulent buoyant jets in unbounded stratified flows. Part 1: The single round jet. *Environmental Fluid Mechanics, 4*, 1–56.

Jirka, G. H. (2006a). Improved discharge configurations for brine effluents from desalination plants. *Journal of Hydraulic Engineering Division of the American Society of Civil Engineers* (submitted).

Jirka, G. H. (2006b). Integral model for turbulent buoyant jets in unbounded stratified flows. Part 2: Plane jet dynamics resulting from multiport diffuser jets. *Environmental Fluid Mechanics, 6*, 43–100.

Jirka, G. H. (2008). Improved discharge configurations for brine effluents from desalination plants. *Journal of Hydraulic Engineering Division of the American Society of Civil Engineers, 134*, 116–120.

Jirka, G. H., Abraham, G., & Harleman, D. R. F. (1976). An assessment of techniques for hydrothermal prediction. Department of Civil Engineering, MIT for US Nuclear Regulatory Commission, Cambridge.

Jirka, G. H., Adams, E., & Stolzenbach, K. (1981). Properties of surface buoyant jets. *Journal of the Hydraulics Division ASCE, 106*(11), 1467–1487.

Jirka, G. H., & Akar, P. J. (1991). Hydrodynamic classification of submerged single-port discharges. *Journal of Hydraulic Engineering Division of the American Society of Civil Engineers*, *117*, 1095–1111, HY9.

Jirka, G. H., Bleninger, T., Burrows, R., & Larsen, T. (2004a). *Environmental quality standards in the EC-water framework directive: Consequences for water pollution control for point sources.* European Water Management Online, European Water Association (EWA). www.ewaonline.de.

Jirka, G. H., Bleninger, T., Burrows, R., & Larsen, T. (2004b). Management of point source discharges into rivers. Where do environmental quality standards in the new EC-water framework directive apply? *Journal of River Basin Management*, *2*(3), 225−233.

Jirka, G. H., & Doneker, R. L. (1991a). Hydrodynamic classification of submerged multiport diffuser discharges. *Journal of Hydraulic Engineering Division of the American Society of Civil Engineers*, *117*, 1113–1128, HY9.

Jirka, G. H., & Doneker, R. L. (1991b). Hydrodynamic classification of submerged single port discharges. *Journal of Hydraulic Engineering Division of the American Society of Civil Engineers, 117*, 1095–1112.

Jirka, G. H., Doneker, R. L., & Hinton, S. W. (1996). User's manual for CORMIX: A hydrodynamic mixing zone model and decision support system for pollutant discharges into surface waters. US Environmental Protection Agency, Technical report, Environmental Research Lab, Athens, Georgia, USA.

Jirka, G. H., & Lee, J. H.-W. (1994). Waste disposal in the ocean. In M. Hino (Ed.), *Water quality and its control*. Rotterdam: Balkema.

Lattemann, S., & Höpner, T. (2003). *Seawater desalination: Impacts of brine and chemical discharge on the marine environment*. L'Aquila, Italy: Desalination Publications.

Law, A. W. K., Lee, C. C., & Qi, Y. (2002). CFD modeling of a multiport diffuser in an oblique current. *Proceedings of Marine Waste Water Discharges*. MWWD 2002, Istanbul, Turkey.

Lee, J. H. W., & Neville-Jones, P. (1987). Initial dilution of horizontal jet in crossflow. *Journal of Hydraulic Engineering Division of the American Society of Civil Engineers, 113*(5), 615–629.

Lesser, G. R., Roelvink, J. A., van Kester, J A Th M, & Stelling, G. S. (2004). Development and validation of a three-dimensional morphological model. *Journal of Coastal engineering, 51*, 883–915.

Mendez Diaz, M. M., & Jirka, G. H. (1996). Trajectory of multiport diffuser discharges in deep co-flow. *Journal of Hydraulic Engineering Division of the American Society of Civil Engineers, 122*(8), 428–435.

Mickley, M. (2006). Membrane concentrate disposal: Practices and regulation. Mickley and Associates, sponsored by the US Department of Interior, Bureau of Reclamation, Agreement No. 98-FC-0054.

Morelissen, R., van der Kaaij, T., & Bleninger, T. (2013). Dynamic coupling of near field and far field models for simulating effluent discharges. *Journal of Water Science and Technology* 67 (10), doi:10.2166/wst.2013.081.

Morelissen, R., Vlijm, R., Hwang, I., Doneker, R., & Ramachandran, A. S. (2014). Hydrodynamic modelling of large-scale cooling water outfalls with a dynamically coupled near field—far field modelling system. *Proceedings of the International Conference on Desalination, Environment and Marine Outfall Systems (ICDEMOS)*, Muscat, Oman.

Nash, J. D. (1995). Buoyant discharges into reversing ambient current. Masters thesis, DeFrees Hydraulics Laboratory, Cornell University, Ithaca, NY.

Ragas, A. M. J., Hams, J. L. M., & Leuven, R. S. E. W. (1997). Selecting water quality models for discharge permitting. *European Water Pollution Control, 7*(5), 59–67.

Ridge, M. M. (2002). Three-dimensional simulation of pollutant dispersion in coastal water. PhD thesis, Universitat Politecnica de Catalunya, Barcelona.

Roberts, P. J. W. (1979). Line plume and ocean outfall dispersion. *Journal of the Hydraulics Division ASCE, 105*(4), 313–331.

Roberts, P. J. W. (1980). Ocean outfall dilution: Effects of currents. *Journal of the Hydraulics Division ASCE, 106*(5), 310–313.

Roberts, P. J. W. (1986). Engineering of ocean outfalls. In G. Kullenberg (Ed.), *The role of oceans as a waste disposal option*. NATO ASI series C (Vol. 172, pp. 73–109).

Roberts, P. J. W. (1990). Outfall design considerations. In B. Le Mehaute & D. M. Hanes (Eds.), *The sea: Ocean engineering science*. New York: Wiley-Interscience.

Roberts, P. J. W. (1996). Sea outfalls. In V. P. Singh & W.H. Hager (Eds.), *Environmental hydraulics*. Dordrecht: Kluwer.

Roberts, P. J. W., Snyder, W. H., & Baumgartner, D. J. (1989a). Ocean outfalls. I. Submerged waste field formation. *Journal of Hydraulic Engineering Division of the American Society of Civil Engineers*, *115*(1), 1–25.

Roberts, P. J. W., Snyder, W. H., Baumgartner, D. J. (1989b). Ocean outfalls. II. Spatial evolution of submerged waste field. *Journal of Hydraulic Engineering Division of the American Society of Civil Engineers*, *115*(1), 26–48.

Roberts, P. J. W., Snyder, W. H., Baumgartner, D. J. (1989c). Ocean outfalls. III. Effect of diffuser design on submerged waste field. *Journal of Hydraulic Engineering Division of the American Society of Civil Engineers*, *115*(1), 49–70.

Rouse, H., Yih, C. S., Humphreys, H. W. (1952). Gravitational convection from a boundary source. *Tellus*, *4*, 201–210.

Sydney Water (2005). *Environmental assessment for Sydney's desalination project*. GHD, Fichtner (consultants report).

Verbruggen, W., Morelissen, R., & Freixa, C. M. (2014). Modelling of dense brine discharges in Oman: Recirculation and environmental aspects—a case study. *Proceedings of the International Conference on Desalination, Environment and Marine Outfall Systems (ICDEMOS)*, Muscat, Oman.

Water Framework Directive (WFD). (2000). Official publication of the European Community, L327, Brussels.

Wood, I. R., Bell, R. G., & Wilkinson, D. L. (1993). *Ocean disposal of wastewater*. Singapore: World Scientific.

World Health Organization (WHO). (2007). Desalination for safe water supply: Guidance for the health and environmental aspects applicable to desalination.

Zhan, P., Yao F., Kartadikaria A. R., Viswanadhapalli Y., Gopalakrishnan G., & Hoteit, I. (2014). Far-field ocean conditions and concentrate discharges modeling along the Saudi Coast of the Red Sea. In T. M. Missimer, B Jones & R. G. Maliva (this volume).

Zhang, H., & Baddour, R. E. (1998). Maximum penetration of vertical round dense jets at small and large Froude numbers. *Journal of Hydraulic Engineering Division of the American Society of Civil Engineers, 124*(5), 550–553.

Chapter 19
New Criteria for Brine Discharge Outfalls from Desalination Plants

Raed Bashitialshaaer, Kenneth M. Persson and Magnus Larson

Abstract An efficient method for increasing the dilution rate of brine water discharged into the sea is an inclined negatively buoyant jet from a single port or a multi-diffuser system. Such jets typically arise when brine is discharged from desalination plants. Two small-scale experimental studies were conducted to investigate the behaviour of a dense jet discharged into lighter ambient water. The first experiment concerned the importance of the initial angle of inclined dense jets, where the slope of the flow increased for the maximum levels as a function of this angle. An angle of 60° produced better results than 30° or 45°. An empirical predictive equation was developed based on five geometric quantities to be considered in the design of plants. The second experiment studied the near and intermediate fields of negatively buoyant jets. Dilution in the flow direction was increased by about 10 and 40 % with bottom slope, and bottom slope together with a 30° jet inclination, respectively. An over 16 % bottom slope experiment and more field work in the future are needed to compare with this result. It was found that an inclination of 30° with a 16 % bottom slope were optimal for the design of brine discharge outfall.

19.1 Introduction

In desalination, high-salinity brine is produced that needs to be discharged into a receiving water body with a minimum of environmental impact. Nowadays, brine discharge from desalination plants is the concern of all countries producing fresh water from desalination with different technologies.

R. Bashitialshaaer (✉) · K.M. Persson · M. Larson
Department of Water Resources Engineering, Lund University, Lund, Sweden
e-mail: ralshaaer@yahoo.com

K.M. Persson
e-mail: Kenneth_m.perrson@tvrl.lth.se

M. Larson
e-mail: Magnus.Larson@tvrl.lth.se

T.M. Missimer et al. (eds.), *Intakes and Outfalls for Seawater Reverse-Osmosis Desalination Facilities*, Environmental Science and Engineering,
DOI 10.1007/978-3-319-13203-7_19

The brine is typically discharged as a turbulent jet (Turner 1966) with an initial density that is significantly higher (salinity 4–5 %) than the density of the receiving water (ambient e.g. seawater). Thus, a rapid mixing of the discharged brine is desirable to ensure minimum impact, which requires detailed knowledge of the jet development. Since the density of the jet is greater than the density of the receiving water, the jet is negatively buoyant and it will impinge on the bottom some distance from the discharge point depending on the initial momentum, buoyancy, and angle of the discharge, as well as the bathymetric conditions. After the jet encounters the bottom it will spread out as a gravity current with a low mixing rate, making it important to achieve the largest possible dilution rate when the jet moves through the water column.

In an early study, Zeitoun et al. (1972) investigated an inclined jet discharge, focusing on an initial jet angle of 60° because of the relatively high dilution rates achieved for this angle. Roberts and Toms (1987) and Roberts et al. (1997) also focused on the 60° discharge configuration, where both the trajectory and dilution rate were measured. Cipollina et al. (2005) extended the work performed in previous studies on negatively buoyant jets discharged into calm ambient by investigating flows at different discharge angles, namely 30°, 45°, and 60°, and for three densities 1055, 1095 and 1179 kg/m^3. Kikkert et al. (2007) developed an analytical solution to predict the behavior of inclined negatively buoyant jets, and reasonable agreement was obtained with measurements for initial discharge angles ranging from 0° to 75° and initial densimetric Froude numbers from 14 to 99. Submerged negatively buoyant jets discharged over a flat or sloping bottom, covering the entire range of angles from 0° to 90°, were investigated by Jirka (2006) in order to improve design configurations for desalination brine discharges into coastal waters. Jet experiment measurement can be affected with possible related errors depending on the type and amount of dye, the illumination level, and the sensitivity of the recording method (Jirka 2008).

Christodoulou and Papakonstantis (2010) studied negatively buoyant jets with discharge angles between 30° and 85°. By fitting empirical equations to relevant experimental data they estimated that the trajectory of the upper boundary and the jet axis (centerline) could be approximated in non-dimensional form by a 2nd degree polynomial (parabola). Mixing and re-entrainment are both important in negatively buoyant jets. These phenomena have been experimentally studied and discussed by (Ferrari and Querzoli 2010). They found that re-entrainment tends to appear if the angle exceeds 75° with respect to the horizontal, and the onset occurs for lower angles as the Froude number increases. The re-entrainment makes the jet trajectory bend on itself, causing a reduction of both the maximum height and the distance to the location where entrainment of external fluid reaches the jet axis (Ferrari and Querzoli 2010). Papakonstantis et al. (2011) studied six different discharge angles for negatively buoyant jets from 45° to 90° to the horizontal. In their experiment they used a large-size tank and also measured the horizontal distance from the source to the upper (outer) jet boundary at the source elevation.

It was possible to investigate the effects of turbulent energy on the initial development and large scale instabilities of a round jet by placing grids at the

nozzle outlet to alter the jet initial conditions because the grids causes small scale injection of turbulent energy (Burattini et al. 2004). The jet lateral spreading and consequent dilution at the bottom is of considerable practical importance in assessing the environmental impact of the effluent on the receiving water at the discharge point (Christodoulou 1991). The behavior of a laterally confined 2-D density current has been considered in past but the numbers on a 3-D system are very limited (Ellison and Turner 1959; Benjamin 1968; Simpson 1987). Hauenstein and Dracos (1984) proposed an integral model based on similarity assumptions, which was supported by their laboratory experimental data of the radial spreading of a dense current inflow into a quiescent ambient.

Previous studies mainly focused on the separate analysis of near-field and intermediate-field properties of buoyant jets and plumes. Some hypotheses on how to connect the two different zones have also been proposed. Turner and Abraham were the first to analyze this kind of problem of a vertical negatively buoyant jet (Turner 1966; Abraham 1967). The dense layer spreads in all directions at a rate proportional to the entrainment coefficient (Alavian 1986). His result was obtained by flowing salt solution (4 g/l) on a sloping surface in a tank of freshwater and his experimental result was based on three different inflow buoyancy fluxes on three angles of incline of 5°, 10°, and 15° (Alavian 1986). Akiyama and Stefan (1984) developed an expression for the depth at the plunge point as a function of inflow internal Froude number, mixing rate, bed slope, and total bed friction. Christodoulou (1991) described theoretically the main factors affecting near-, intermediate-, and far-field properties, suggesting appropriate length scales for each zone. Suresh et al. (2008) investigated the lateral spreading of plane buoyant jets and how they

Table 19.1 Dispersion tanks with different sizes used in earlier experiments (excerpted from Bashitialshaaer and Persson 2012)

Previous study	Cross-section (m)	Depth (m)
Turner (1966)	0.45 × 0.45	1.40
Demetriou (1978)	1.20 × 1.20	1.55
Alavian (1986)	3.0 × 1.50	1.50
Lindberg (1994)	3.64 × 0.405	0.508
Roberts et al. (1997)	6.1 × 0.91	0.61
Zhang and Baddour (1998)	1.0 × 1.0	1.0
Pantzlaff and Lueptow (1999)	D = 0.295	0.89
Bloomfield and Kerr (2000)	0.40 × 0.40	0.70
Cipollina et al. (2005)	1.50 × 0.45	0.60
Jirka (1996, 2004, 2006)	CORMIX, CorJet	
Kikkert et al. (2007)	6.22 × 1.54	1.08
Papanicolaou and Kokkalis (2008)	0.80 × 0.80	0.94
Shao and Law (2010)	2.85 × 0.85	1.0
This study	1.50 × 0.60	0.60
	2.0 × 0.50	0.60

depend on the Reynolds number, suggesting and demonstrating that a reduction of the spreading occurs with an increase in the Reynolds number. Table 19.1 is the summary of different sizes that have been used for laboratory mixing tank dimensions (L × W × H) as found in literature.

19.2 Objectives and Procedures

The water intake to most of the world's desalination plants is located close to where the brine is discharged. Some chemicals and other parameters have to be considered as a function of the brine discharge from desalination plants to assist people from an environmental and economic perspective, e.g. fishing problems could increase in the future. More objectives were added to this study in order to find the relationships between an increase in desalination plant production and salinity increase in the recipient. Thus, the main objective of this study is to find out the most efficient way to reduce the impact of brine discharge from desalination plants by improving the mixing conditions in the discharged jet. Therefore, it was decided to perform small-scale laboratory experiments. Two sets of experiments were conducted for negatively buoyant jet, each with a total of 72 runs in order to:

- Understand jet behaviour when brine is discharged into a stagnant ambient and to find the maximum elevated level of the jet.
- Find the effect of the initial jet angle on the mixing between a denser fluid comprised of a sodium chloride solution and tap water.
- Evaluate the importance of bottom slope with and without inclination and the effect of lateral spreading and centreline concentration.
- Possibility to compare collected data with simulation results using hydraulic modelling software, e.g. CORMIX.

19.2.1 Laboratory Experiments

19.2.1.1 Experimental Setup

The experiments on inclined negatively buoyant jets were carried out in the laboratory of Water Resources Engineering at Lund University. The apparatus and major equipment used in the experiments included water tanks, a flow meter, a digital frequency recorder, a digital conductivity meter, pump to fill and empty the tanks, pipes, valves, nozzles and nozzle support, salt, and dye (Fig. 19.1). Several different tanks were used in the experiment: (1) a small tank to mix tap water with salt and a coloring dye for generating an easy to visualize negatively buoyant jet of saline water; (2) two elevated small tanks used to create the hydraulic head for generating the jet; and (3) a large tank made with glass walls filled with tap water

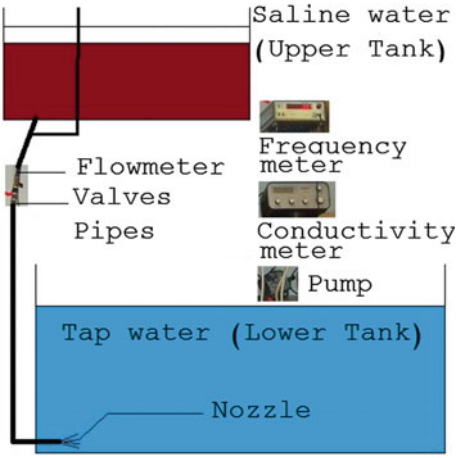

Fig. 19.1 Experimental setup and major components used (Bashitialshaaer et al. 2013)

(fresh water) where the jet was introduced through a nozzle. The small tanks were made of plastic and their volumes were 45, 70, and 90 L, whereas the maximum volume of the large tank was 540 L with bottom area dimensions of 150 cm × 60 cm and a height of 60 cm. Two of the smaller tanks were placed at a higher elevation compared to the large tank to create the necessary hydraulic head for driving the jet. These two tanks were connected by a pipe and together they had a sufficiently large capacity (i.e., surface area) to keep the water level approximately constant in the two tanks during the experiment to ensure a constant flow. The difference in elevation between the water levels of the upper tanks and the lower tank was about 100 cm. The colored saltwater from the upper tanks was discharged through a plastic, transparent pipe directly connected to the jet nozzle, which was fixed at the bottom of the large water tank. Between the elevated tanks and the nozzle there was a valve to control the flow to the nozzle. A flow meter was installed in the pipe between the valve and the outlet from the upper tanks in order to record the initial jet flow. This meter was connected to a digital frequency recorder, from which the readings were converted into flow rates based on a previously derived calibration relationship.

19.2.1.2 Experimental Procedure and Data Collected

Before starting an experimental case, it was crucial to empty the pipe leading from the upper tanks of air. This was done by attaching a special pipe to the flow meter and discharging tap water through this pipe, forcing out the air from the system. After each experimental case a submersible water pump was used to completely empty the large tank, so that each case started with water that was not contaminated by salt. With the capacity of the pump, it took about 12 min to empty the tank. Also,

the whole system was regularly washed to avoid accumulation of salt, which would disturb the experiment. Potassium permanganate ($KMnO_4$) was used to color the saline water and make the jet visible during the experiment. About 100 mg/L of dye gives the transparent water a distinct purple color. The use of a colored jet facilitated the observation of the jet trajectory and the mixing behavior in the larger water tank. The results of jar tests for different ($KMnO_4$) concentrations showed that at a concentration of 0.3 mg/L the water is still colored, whereas at a concentration of 0.2 mg/L no color was visible to the eye.

During a specific case, the jet was discharged for a sufficiently long time to allow steady-state conditions to develop, but short enough to avoid unwanted feedback from saline water accumulating in the tank (the duration of an experimental case was normally about 3–5 min). The jet trajectory and its geometric properties were determined by tracing the observed trajectory on the glass wall of the flume. The outer edges of the jet were traced and the center line was determined as the average between these two lines. In order to minimize the influence of the subjective element in tracing the jet, a number of different people were involved in this procedure to ensure that the results were consistent, in agreement, and reproducible. Also, the experimental cases were recorded with a video camera and subsequently viewed. Three cases did not produce satisfactory data due to malfunctioning, and here the results from 69 cases are reported.

19.2.1.3 Inclined Jet Experiment

Fine, pure sodium chloride was used with tap water to produce the saline water in the jet. The necessary water quantity was measured in a bucket and the mass of salt was measured using a balance to obtain the correct salt concentration. A conductivity meter was employed to measure the conductivity for the three different initial concentrations investigated. The density measurements for these concentrations yielded 1011, 1024 and 1035 kg/m^3 for 2, 4 and 6 %, (20, 40, and 60 g/L), respectively. The temperature of the tap water used in this experiment was in the range 20–22 °C for all cases, implying a density of about 995.7 kg/m^3. Each of the densities was the average of five different measurements based on the weight method. Differences in density were observed between the salt water used in this study and natural seawater. The chemical composition of seawater is different from the sodium chloride solutions used here, although the density varies only slightly in seawater compared to the pure sodium chloride solutions. The parameters of interest were:

- Diameter of nozzle, d_o (4.8; 3.3; 2.3, 1.5 mm)
- Initial jet angle, θ to the horizontal line (30°, 45°, 60°)
- Salinity of brine discharge S (2; 4; 6 %)

19.2.1.4 Near and Intermediate Zone Experiment

The apparatus and major materials used in the experiment in the laboratory were water tanks, flow-meter, digital frequency-meter, digital conductivity meter, pump, pipes, valves, nozzles and nozzle support, salt and dye (see Fig. 19.1). Preliminary measurements were conducted after calibrating the apparatus in order to obtain reference data and to check if our measurement tools (i.e. flow meter, conductivity meter) were reliable and coherent with literature data. These measurements included flows, water salinity, density, and conductivity, basic information about water density and conductivity variation as a function of salinity at a constant room temperature of 20 ± 1 °C. Each experimental run was characterized by a set of parameters, and the first step of each run was used to find the proper combination of parameter values. The parameters of interest were:

- Diameter of nozzle, d_o (4.8; 3.3; 2.3 mm)
- Initial jet angle, θ to the horizontal line (0; 30°)
- Bottom slope S_b (0; 16 %), the tank tilting
- Salinity of brine discharge S (4; 6; 8 %)

19.3 Theoretical Considerations

19.3.1 Inclined Negatively Buoyant Jets

An inclined negatively buoyant jet discharged upwards at an angle towards the horizontal (Fig. 19.2) represents the typical case of a brine jet discharged into receiving water. The jet describes a trajectory that reaches a maximum level, after which the jet changes its upward movement and plunges towards the bottom. Since the jet is negatively buoyant, the initial vertical momentum flux driving the flow upwards is continuously reduced by the buoyancy forces until this flux becomes zero at the maximum level and the jet turns downwards.

Knowledge of the shape of the jet trajectory is important in the design of brine discharge. Major variables that previously were employed to describe the jet trajectory (with respect to the location of the jet origin based on a *x*-*y* coordinate system) are: the maximum level of the jet centerline Y and its horizontal distance X_y, the maximum level of jet flow edge Y_m, and its horizontal distance X_{ym}, X_i is the jet centerline impact point distance and X_e the maximum horizontal distance to the jet flow edge point, where the jet returns to the discharge level (Fig. 19.2). In general, the location of the jet edge may be defined as the maximum jet height boundary at any particular location.

The jet is discharged at a flow rate Q_o through a round nozzle with a diameter d_o, yielding an initial velocity of u_o, and at an angle θ to the horizontal plane. The initial density of the jet is ρ_o and the density of the receiving water (ambient) ρ_a,

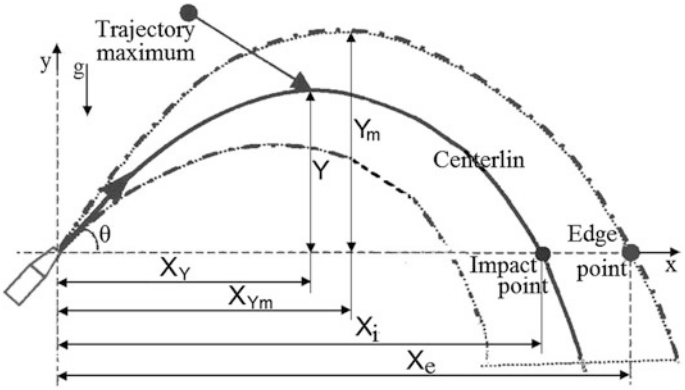

Fig. 19.2 Definition sketch for inclined jet parameters (after Cipollina et al. 2005)

where $(\rho_o > \rho_a)$, giving an initial excess density in the jet of $\Delta\rho = (\rho_o - \rho_a) \ll \rho_a$ (the Boussinesq approximation). Similar flow problems were previously analyzed through dimensional analysis (e.g., Turner 1966; Roberts and Toms 1987; Pincince and List 1973; Cipollina et al. 2005; Fischer et al. 1979). Most previous studies assumed that the Boussinesq approximation is valid and that the flow is fully turbulent. Thus, the initial jet properties can be characterized by the volume flux Q_o, the kinematic momentum flux M_o, and the buoyancy flux B_o, as defined by Fischer et al. (1979), together with the initial jet angle θ (the subscript o denotes conditions at the nozzle). The leading variables in the dimensional analysis may be written for a round jet with uniform velocity distribution at the exit:

$$Q_o = \frac{\pi d_o^2}{4} u_o, \quad M_o = \frac{\pi d_o^2}{4} u_0^2, \quad B_o = g \frac{\rho_o - \rho_a}{\rho_a} Q_o = g' Q_o \tag{19.1}$$

where g is acceleration due to gravity; and $g' = g(\rho_o - \rho_a)/\rho_a$ is the modified acceleration due to gravity. A dimensional analysis involving Q_o, M_o, and B_o yields two length scales that may be used to normalize the above-mentioned geometric quantities and to develop empirically based predictive relationships (Fischer et al. 1979):

$$l_M = \frac{M_o^{3/4}}{B_o^{1/2}} \quad \text{and} \quad l_Q = \frac{Q_o}{M_o^{1/2}} \tag{19.2}$$

By using the bulk quantities Q_o, M_o, and B_o, the nozzle shape and the initial velocity distribution is implicitly taken into account. For a uniform velocity distribution, $l_Q = \sqrt{A_o}$ and if the nozzle is circular $l_Q = d_0 \sqrt{\frac{\pi}{4}}$. In the two sets of experiments a densimetric Froude number F, is defined by $(u_0/\sqrt{g' d_0})$. More details and equations can be found in (Bashitialshaaer et al. 2012).

19.3.2 Near and Intermediate

Brine discharge from a desalination plant is an example of denser fluid discharge to a stagnant ambient from a single port or a multiport at angle θ, with bottom slope S_b. This flow may be conceptually divided into three connected regions, the near-field, the intermediate field and the far-field. The near-field is the initial flow or development region (named the potential core for a top-hat exit profile); it is usually found within ($0 \leq x/d_0 \leq 6$). The far-field is the fully-developed region where the thin shear layer approximations can be shown (with appropriate scaling); jet flows generally become self-similar beyond ($x/d_0 \geq 25$) (Christopher and Andrew 2007). The intermediate-field, or transition region, lies between the near- and far-fields of the jet. Method of understanding mixing in intermediate-field or transition was well defined qualitatively by flow visualization e.g. (Dimotakis 2000; Dimotakis et al. 1983). In the intermediate region of a round jet there was only Reynolds dependence of shear stress distributions as shown in (Matsuda and Sakakibara 2005). They used method of a stereo particle image velocity (PIV) system. The mean and fluctuating velocity curves were plotted for Re = 1500; 3000; 5000. The lateral spreading of the jet is shown in Fig. 19.3 in two dimensions x-axis and y-axis, in which b(x) was measured at three locations b_1, b_2 and b_3 at horizontal distances X_1, X_2 and X_3 for 20, 40 and 60 cm respectively (Bashitialshaaer and Persson 2012).

Considering a negatively buoyant jet, the dilution at the impact point S_d in the near-field from a single port into a stagnant ambient comes with some assumptions. For the jet to retain its identity, the discharge angle should not be too small to avoid attachment to the bottom or too large to avoid falling on itself (Christodoulou 1991). The terminal minimum dilution at the impact point can be written in terms of the main variables as:

$$S_d = f(Q_0, M_0, B_0, \vartheta) \tag{19.3}$$

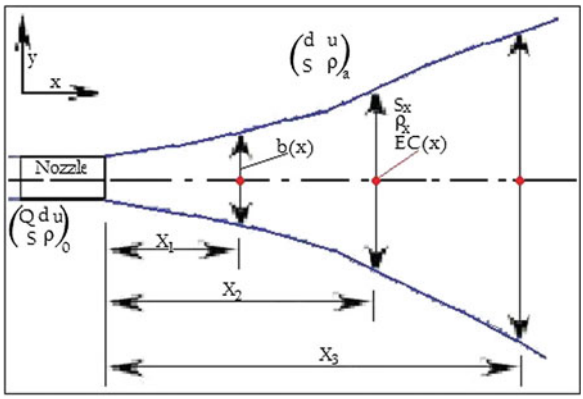

Fig. 19.3 Plan view of lateral jet spreading and the measurements locations (Bashitialshaaer and Persson 2012)

The effect of the initial discharge is normally small and negligible, after a simple dimensional analysis the initial dilution is given by $S_d = f_1\ (\theta, F)$, where F is a Froude densimetric number as defined before. A Froude number of 10 or larger simplifies the above equation to $(F/S_d) = c(\theta)$, where the constant c is a function of inclined angle θ. Previously this constant was determined experimentally by many people, e.g. (Roberts and Toms 1987) for a 60° inclined angle as a value of c = 1.03; for the same angle (Zeitoun et al. 1970) presented an earlier estimation for c of about 1.12. In the description of the intermediate field lateral spreading of the dense plume along a mildly sloping bottom, one should take into account that at small slopes, the entrainment is small and negligible (Ellison and Turner 1959; Alavian 1986; Britter and Linden 1980). Therefore, the width of the plume should depend mainly on the buoyancy flux, the bottom roughness (drag coefficient C_d) and the geometrical characteristics of the problem (Christodoulou 1991). Thus, the lateral spreading width b downstream a distance x can be written as:

$$b = f(x, b_0, B_0, S_b, C_d, g) \tag{19.4}$$

From dimensional analysis Eq. (19.4) can be written as:

$$\frac{b}{b_0} = f_1\left(\frac{x}{b_0}, \frac{B_0}{g^{3/2} b_0^{5/2}}, S_b, C_d\right) \tag{19.5}$$

Alavian (1986) suggested that the terminal to initial width ratio b_n/b_0 is essentially independent of the slope for $5° \le S_b \le 15°$, although the rate of approach to the normal state is faster for smaller slopes. From the above statement the determination of the terminal width b_n for relatively small slopes (less than about 15°), the explicit inclusion of S_b in, Eq. (19.5) can be omitted:

$$\frac{b_n}{b_0} \approx f_2\left(\frac{B_0}{g^{3/2} b_0^{5/2}},\ C_d\right) \tag{19.6}$$

A power law form for Eq. (19.6) yields:

$$\frac{b_n}{b_0} = K\left(\frac{B_0}{g^{3/2} b_0^{5/2}}\right)^a \tag{19.7}$$

where $K = k(C_d)$. Equation (19.7) has been tested against limited experimental data in (Alavian, 1986) and numerical results in Tsihrintzisand and Alavian (1986). They referred to a distance $x = 100b_0$, where the spreading width had not yet strictly reached a constant value, apparently due to the low drag coefficient employed. The value of the exponent was estimated in Christodoulou (1991), as a = 0.183, while k exhibits an increasing trend with decreasing C_d.

19.3.3 Model Assumptions

The modeling assumption of the jet and plume evolution was essentially divided into two sub-models, that is, the near field and the intermediate field. The near field is the proximity of the nozzle, where jet and plume development is driven by the initial conditions; i.e. the initial momentum flux, volume flux, and buoyancy flux, and there is no interaction with the bottom. In the intermediate field, the buoyant jet essentially becomes a plume (gravity current) and it is interacting with the bottom. The main forces to be considered are bottom drag force and bottom slope effects. The "intermediate field" begins when the buoyant jet reaches the bottom. To develop a simple model describing the situation in the proximity of the discharge nozzle, some assumptions were made (see Bashitialshaaer and Persson 2012).

19.4 Results and Discussion

19.4.1 General Development

A very strong correlation between Y_m and Y was found, lending some confidence to the accuracy of the measurements. The least-square fitted line through the origin yields a slope of about 1.25, implying that Y_m on average is about 25 % larger than Y. Similarly, between X_y and X_{ym}, a coefficient value of about 1.20 was obtained, which is somewhat lower than that in the relationship between Y and Y_m. Furthermore, the horizontal distance to the edge point of the jet (X_e) showed a rather good correlation with X_{ym} (or X_y), approximately 1.65. Thus, if the vertical and horizontal distance to the maximum centerline level (or, alternatively, the maximum jet edge level) can be predicted, other geometric quantities can be calculated from the following regression relationships:

$$\left.\begin{aligned} Y_m &= 1.25\,Y \\ X_{ym} &= 1.20\,X_y \\ X_e &= 1.65\,X_{ym} \end{aligned}\right\} \tag{19.8}$$

The relationship between the maximum levels and their horizontal distances displayed more scatter (Fig. 19.4) and included a dependence on the initial jet angle. However, a general equation of linear type could be fitted through the data points with reasonable accuracy ($Xy = k_\theta Y$), where k_0 is an empirical coefficient that takes on the value 2.3, 1.5, and 1.0 for the initial jet angle 30°, 45°, and 60°, respectively. If a simple ballistics model was employed to describe the jet trajectory (*i.e.*, constant g'), the ratio between X_y and Y would be given by $2/(\tan \vartheta)$, which yields the following slopes for the lines: 3.5, 2.0, and 1.2. A similar equation could be developed for X_{ym} and Y_m.

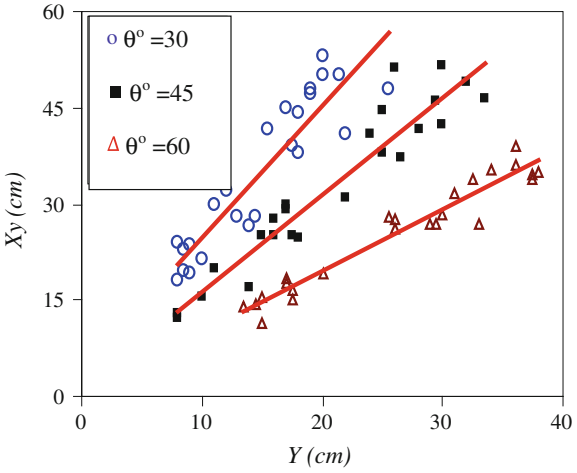

Fig. 19.4 Maximum jet centerline level versus its horizontal distance with respect to initial jet angle

19.4.2 Developing Relationships

Equation $(Y/l_M) = K$ indicates that there is a linear relationship between the normalized quantities that describe the jet trajectory and F. However, this is based on the assumption that $l_m \gg l_Q$, otherwise this equation $(Y/l_M) = f(l_m/l_Q)$ should be employed, developing this relationship by introducing the definition of the length scales yields:

$$\frac{Y}{d_0} = k * F * \Psi(F) \tag{19.9}$$

where Ψ = function and Y is used as an example of a geometric jet quantity. If F is small $\Psi(F) \rightarrow 1$, whereas for large F values $Y \rightarrow \infty$. The data indicates a relationship, where $Y/d_0 \propto F^n$, with $n < 1$. Based on the theoretical constraints and the empirical observations, the following equation was proposed to describe Y/d_o as a function of F over the entire range of experimental data:

$$\frac{Y}{d_0} = \frac{k * F}{(1 + \alpha F)^m} \tag{19.10}$$

where α and m are empirical coefficients obtained from fitting against data. Equation 19.10 can be approximated with a straight line in accordance with relation $(Y/d_0) = (k * F)$ for small values on α F. where $k = K(\pi/4)^{1/4}$. Similar equations may be developed for the other geometric jet quantities Y_m, X_y, X_{ym}, and X_e, but with different values of the coefficient k. Figure 19.5 shows an example of

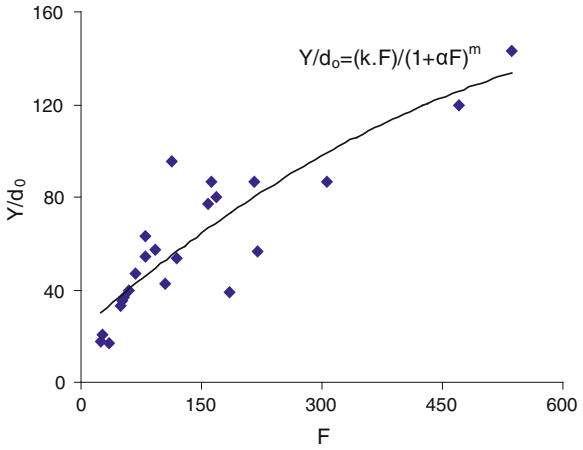

Fig. 19.5 Normalized maximum jet centerline level as a function of (F) for an initial jet angle of 30°

least-square fitting of Eq. 19.10 against the data for the maximum jet centerline level (Y) and an initial jet angle of 30°, where the optimum values of k, α, and m were determined as 1.35, 0.008, and 0.8, respectively.

19.4.3 Bottom Slope Effects

The electrical conductivity ratio and the lateral spreading were compared with and without bottom slope at three horizontal distances 20, 40 and 60 cm, that results in small variations between flow on a horizontal bed and a slope. The correlations between the two cases are in the range 86–89 %, which means the sloping bottom does not affect the flow regime. For the lateral spreading, it was also shown that the correlation is 88–91 %, much better than for the electrical conductivity.

Normalized lateral spreading (b/d_0) and thickness of the dense layer (z/d_0) are compared for four cases at horizontal distances 20, 40 and 60 cm along the x-axis with respect to the inclined angle (θ) and bottom slope (S_b). Different comparisons were made between measured parameters to see the effects of the initial angle and bottom slope. First we compared the normalized lateral spreading at three different positions, inclined angle (θ = 0°) and bottom slope (Sb = 0°) versus (θ = 30, Sb = 0); (θ = 0, Sb = 16); (θ = 30, Sb = 16). For the lateral spreading the trend line showed good correlation above 80 %, except for one of them.

Figure 19.6 presents the experimental results for the concentration (in percentage) that were measured at three distances along the flow, comparing with and without bottom slope for densimetric Froude numbers smaller and larger than 40. The concentration along the flow was improved by about 10 % with the bottom

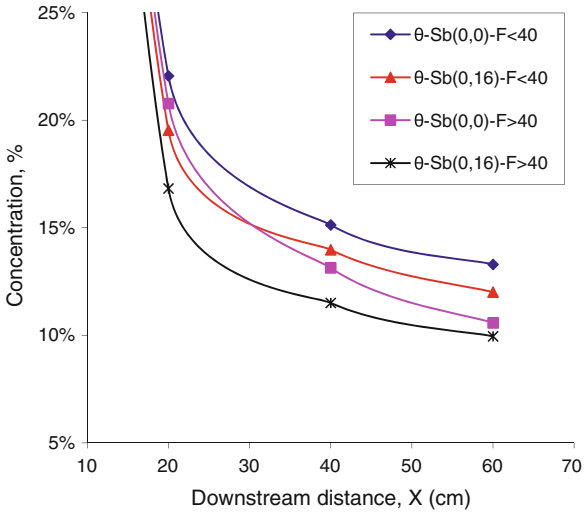

Fig. 19.6 Concentration in percentage along the flow with and without bottom slope

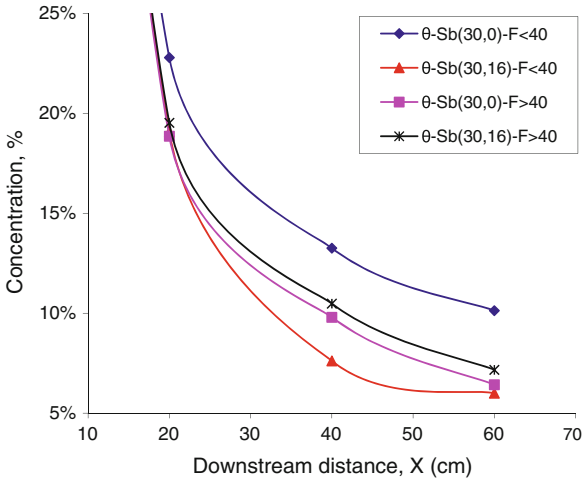

Fig. 19.7 Concentration in percentage along the flow with and without bottom slope (with 30° inclination)

slope for Froude number smaller than 40 which can be used for real discharge cases. Thus, this type of improvement can be used for brine discharge outlet to the recipients to minimize the concentration and let it dilute faster and go farther. Another comparison is presented in Fig. 19.7, also with and without bottom slope,

but this time including jet inclination angle of 30°. It also shows improvement in the concentration reduction of about 40 % with bottom slope and inclination for Froude numbers smaller than 40, but small differences for Froude numbers larger than 40.

19.5 Conclusions

The purpose of this study was originally to be able to determine the properties of different jet discharges with regard to bottom slope in the recipient and varying initial jet inclination angle. Desalination brine is the practical case to consider when studying environmental impact and assessment in connection with new projects. In reality, most of the recipients, e.g., marginal seas and oceans, naturally have a bottom slope, and it varies from one place to another. Two sets of laboratory experiments were conducted to investigate the behavior of negatively buoyant jets discharged at an angle to the horizontal into a quiescent body of water that may have a sloping bottom.

Several of the geometric jet quantities showed strong correlation and regression relationships could be developed where one quantity could be predicted from another. If maximum levels were correlated with the corresponding horizontal distances, the angle must be taken into account when developing predictive relationships in real life projects. It is believed that the empirical relationships developed in this study have a potential for use in practical design where the trajectory of brine jets needs to be estimated. Equations were proposed to relate levels and horizontal distances to each other.

Based on the findings in this study in the near- and intermediate regions the flow geometry depends on the angle of inclination and the rate of supply of the dense fluid. After an initial spreading, the flow geometry becomes relatively constant with the horizontal distance down the slope. For a given buoyancy flux, the normal layer width seems to weakly depend on slope. Lowering of the concentration (through mixing) was improved with the bottom slope by 10 % compared to the horizontal bottoms and improved by about 40 % with bottom slope together with an inclination of 30°. A suggestion in practical applications concerning desalination brines and similar discharge of heavy wastes is to have an inclination and a bottom slope together. This study is based on limited experiments for only 16 % bottom slope and 30° inclination; thus, further experimental work is needed.

References

Abraham, G. (1967). Jets with negative buoyancy in homogeneous fluids. *Journal of Hydraulic Research, 5*, 236–248.

Akiyama, J., & Stefan, H. G. (1984). Plunging flow into a reservoir: Theory. *Journal of Hydraulic Engineering, ASCE, 110*(4), 484–499.

Alavian, V. (1986). Behavior of density currents on an incline. *Journal of Fluid and Mechanics, ASCE, 112*(1), 27–42.

Bashitialshaaer, R., & Persson, K. M. (2012). Near and intermediate field Evolution of a negatively buoyant jet. *Journal of Basic and Applied Sciences, 8*(2), 513–527.

Bashitialshaaer, R., Larson, M., & Persson, K. M. (2012). An experimental investigation on inclined negatively buoyant jets. *Water: Advances in Water Desalination, 4*(3), 720–738. doi:10.3390/w4030720.

Bashitialshaaer, R., Larson, M., & Persson, K. M. (2013). An Experimental study to improve the design of brine discharge from desalination plants. *American Journal of Environmental Protection, 2*(6), 176–182.

Benjamin, T. B. (1968). Gravity currents and related phnonmena. *Journal of Fluid Mechanics, 31* (2), 209–248.

Bloomfield, L.J., & Kerr, R.C. (2000). A theoretical model of a turbulent fountain, *Journal of Fluid Mechanics*, *424*, 197–216.

Britter, R. E., & Linden, P. E. (1980). The motion of the front of a gravity current travelling down an incline. *Journal of Fluid and Mechanics, 99*(3), 531–543.

Burattini, P., Antonia, R. A., Rajagopalan, S., & Stephens, M. (2004). Effect of initial conditions on the near-field development of a round jet. *Experiments in Fluids, 37*, 56–64.

Christodoulou, G. C. (1991). Dilution of dense effluents on a sloping bottom. *Journal of Hydraulic Research, 29*(3), 329–339.

Christodoulou, G. C., & Papakonstantis, I. G. (2010). Simplified estimates of trajectory of inclined negatively buoyant jets. In *Environmental hydraulics* (pp. 165–170). London, UK: Taylor & Francis.

Christopher, G. B., & Andrew, P. A. (2007). *Review of experimental and computational studies of flow from the round jet.* Queen's University, Kingston, Ontario, Canada, INTERNAL REPORT No. 1, CEFDL., 2007/01.

Cipollina, A., Brucato, A., Grisafi, F., & Nicosia, S. (2005). Bench scale investigation of inclined dense jets. *Journal of Hydraulic Engineering Division of the American Society of Civil Engineers, 131*, 1017–1022.

Dimotakis, P. E. (2000). The mixing transition in turbulent flows. *Journal of Fluid Mechanics, 409*, 69–98.

Dimotakis, P. E., Miake-Lye, R. C., & Papantoniou, D. A. (1983). Structure and dynamics of round turbulent jets. *Physics of Fluids, 26*, 3185–3192.

Demetriou, J.D. (1978). Turbulent diffusion of vertical water jets with negative buoyancy (In Greek), Ph.D. Thesis, Greece: National Technical University of Athens.

Ellison, T. H., & Turner, J. S. (1959). Turbulent entrainment in stratified flows. *Journal of Fluid Mechanics, 9*, 423–448.

Ferrari, S., & Querzoli, G. (2010). Mixing and re-entrainment in a negatively buoyant jet. *Journal of Hydraulic Research, 48*, 632–640.

Fischer, H. B., List, E. J., Koh, R. C. Y., Imberger, J., & Brooks, N. H. (1979). *Mixing in inland and coastal waters*. New York, NY, USA: Academic Press.

Hauenstein, W., & Dracos, T. H. (1984). Investigation of plume density currents generated by inflows in lakes. *Journal of Hydraulic Research, 22*(3), 157–179.

Jirka, G.H., Doneker, R.L., & Steven, W.H. (1996). *User's manual for CORMIX: A hydrodynamic mixing zone model and decision support system for pollutant discharges into surface waters*. DeFrees Hydraulics Laboratory School of Civil and Environmental Engineering, Cornell University

Jirka, G.H. (2004). Integral model for turbulent buoyant jets in unbounded stratified flows, Part 1: The single round jet. *Environmental Fluid Mechanics*, *4*, 1–56.

Jirka, G. H. (2006). Integral model for turbulent buoyant jets in unbounded stratified flows. Part 2: Plane jet dynamics resulting from multiport diffuser jets. *Environmental Fluid Mechanics, 6*, 43–100.

Jirka, G. H. (2008). Improved discharge configuration for brine effluents from desalination plants. *Journal of Hydraulic Engineering, 134*, 116–120.

Kikkert, G. A., Davidson, M. J., & Nokes, R. I. (2007). Inclined negatively buoyant discharges. *Journal of Hydraulic Engineering Division of the American Society of Civil Engineers, 133*, 545–554.

Lindberg, W.R. (1994). Experiments on negatively buoyant jets, with and without cross-flow. In P.A. Davies & M.J. Valente Neves (Eds.), *Recent research advances in the fluid mechanics of turbulent jets and plumes, NATO, series E: Applied sciences* (vol. 255, pp. 131–145). Kluwer Academic Publishers

Matsuda, T., & Sakakibara, J. (2005). In the vortical structure in a round jet. *Physics of Fluids, 17*, 1–11.

Pantzlaff, L., & Lueptow, R.M. (1999). Transient positively and negatively buoyant turbulent round jets. *Experimental in Fluids*, *27*, 117–125.

Papakonstantis, I. G., Christodoulou, G. C., & Papanicolaou, P. N. (2011). Inclined negatively buoyant jets 1: Geometrical characteristics. *Journal of Hydraulic Research, 49*, 3–12.

Papanicolaou, P.N., & Kokkalis, T.J. (2008). Vertical buoyancy preserving and non-preserving fountains, in a homogeneous calm ambient. *International Journal of Heat and Mass Transfer*, *51*, 4109–4120

Pincince, A. B., & List, E. J. (1973). Disposal of brine into an estuary. *Journal of Water Pollution Control Federation, 45*, 2335–2344.

Roberts, P. J. W., Ferrier, A., & Daviero, G. (1997). Mixing in inclined dense jets. *Journal of Hydraulic Engineering Division of the American Society of Civil Engineers, 123*, 693–699.

Roberts, P. J. W., & Toms, G. (1987). Inclined dense jets inflowing current. *Journal of Hydraulic Engineering, ASCE, 113*(3), 323–341.

Shao, D., & Law W.-K. A. (2010). Mixing and boundary interactions of 30° and 45° inclined dense jets. *Environmental Fluid Mechanics*, *10*(5), 521–553.

Simpson, J. E. (1987). *Density Currents: In the environment and the laboratory*. Chichester, U.K.: Ellis Horwood Ltd.

Suresh, P. R., Srinivasan, K., Sundararajan, T., & Sarit, D. K. (2008). Reynolds number dependence of plane jet development in the transitional regime. *Physics of Fluids, 20*, 1–12.

Tsihrintzisand, V.A., & Alavian, V. (1986). Mathematical modeling of boundary attached gravity plumes. In *Proceedings International Symposium on Buoyant Flows* (pp. 289–300), Athens, Greece.

Turner, J. S. (1966). Jets and plumes with negative or reversing buoyancy. *Journal of Fluid Mechanics, 26*(1966), 779–792.

Zeitoun, M. A., Reid, R. O., McHilhenny, W. F., & Mitchell, T. M. (1972). *Model studies of outfall systems for desalination plants*. Research and Development Progress Report No. 804, Office of Saline Water, U.S. Department of the Interior, Washington, DC, USA.

Zeitoun, M. A., McHilhenny, W. F., & Reid, R. O. (1970). *Conceptual designs of outfall systems for desalination plants*. Research and Development Progress Report No. 550, Office of Saline Water, U.S. Department of the Interior, Washington, DC, USA.

Zhang, H., & Baddour, R.E. (1998). Maximum penetration of vertical round dense jets at small and large Froude numbers, Technical Note No. 12147. *Journal of Hydraulic Engineering*, *ASCE 124*(5), 550–553.

Chapter 20
Concentrated Brine and Heat Dispersion into Shallow Coastal Waters of the Arabian Gulf

Sami Al-Sanea and Jamel Orfi

Abstract The main goal of this work is to assess the possible impacts of an existing desalination plant on the marine environment under various discharge conditions. Assessment is made through the determination, by using mathematical modeling, of the excess salinity and temperature distributions over the nominal seawater values as caused by the desalination plant effluent discharge. This chapter presents first a review of brine discharge models and studies followed by a rigorous numerical analysis study of a typical discharge problem into the Arabian Gulf. The mathematical formulation centers on the concept of shallow water equations in which the 3-D problem is reduced to an equivalent 2-D one by integrating the governing equations over the depth of flow. Appropriate boundary conditions, seabed friction, wind stress, and heat transfer correlations for thermal exchange at water-air interface are used. After validating the numerical model, it is applied to determine the salinity and temperature distributions in shallow coastal waters resulting from effluent discharge from an existing desalination plant situated on the Arabian Gulf. Parametric studies of the effects of a number of influential conditions are carried out by using the actual seabed topography and plant discharge and intake port locations. Effects of sea current magnitude and direction and plant discharge flow rate are in particular presented and analyzed. Possible plant discharge-intake port interactions were predicted with varying degrees of influence. The results presented indicated such interactions and quantified values of salinity and temperature at the plant intake port.

S. Al-Sanea (✉) · J. Orfi
Mechanical Engineering Department, King Saud University, Riyadh, Saudi Arabia
e-mail: sanea@KSU.EDU.SA

J. Orfi
e-mail: orfij@ksu.edu.sa

T.M. Missimer et al. (eds.), *Intakes and Outfalls for Seawater Reverse-Osmosis Desalination Facilities*, Environmental Science and Engineering,
DOI 10.1007/978-3-319-13203-7_20

20.1 Introduction

20.1.1 Background

The Kingdom of Saudi Arabia is undergoing rapid and massive development in all aspects including the industrial, power-generating, and desalination sectors. The existing desalination and power plants, in addition to those under construction and those planned for the future, need to be assessed with regard to their adverse impact on the natural environment, especially in shallow coastal regions. Analyzing existing and potential environmental problems and finding means to mitigate possible impacts are crucially important to the marine ecosystem as well as to the operating thermal efficiency of the desalination plants. Mathematical models provide an essential tool for predicting and analyzing impacts to help preclude possible design and implementation problems associated with outfalls.

Desalination plants consume huge amounts of energy to produce fresh water from seawater and return large quantities of warm, concentrated brine to the marine environment. The natural marine ecosystem may be adversely affected by possible increase in salinity and temperature, especially in shallow coastal regions.

In addition to the possible adverse impact a desalination plant discharge can have on the natural environment (particularly when discharged into shallow coastal waters), energy consumption and operating thermal efficiency of the plant can also be affected adversely. These problems are mainly related to:

- the energy needed for separating freshwater from seawater increases with increasing seawater salinity
- the fact that the efficiency of the plant cooling system deteriorates with increasing cooling water temperature.

The aforementioned problems may occur from possible recirculation of the heated and more concentrated brine effluents back into the intake port of the plant. In such a case, the plant would withdraw water from the sea at a salinity and temperature higher than the ambient seawater values. An increase in feed-water salinity from 4 to 5 %, for example, would require about 25 % more energy for seawater desalination.

It is therefore essential that the intake port of the desalination plant should withdraw seawater at the ambient salinity and temperature of the sea. Discharge-intake port interaction must, accordingly, be minimized. To achieve this, detailed information is required about the salinity and temperature distributions resulting from the plant discharge into the shallow coastal waters, and particularly in the vicinity of the plant. In addition, quite a few factors need to be considered and their corresponding effects be assessed through regulatory requirements and compliance. Such factors include: plant desalting capacity, plant site (coastline details and seabed topography), location of discharge and intake ports (separation distance and presence of natural or manmade barriers), sea-current speed and direction, and wind speed and direction.

20.1.2 Brine Discharge Models and Studies

Existing, operational desalination and power plants provide an indication of the types of environmental impact that need to be addressed. These impacts can be classified into several aspects such as liquid waste (concentrate), solid waste, gas emissions (CO_2), etc. The magnitude of impact from these sources of pollution will depend on the mode of desalination, or type of power generation plant, the type of fuel burned to generate the energy required for desalination, the geographical location of the facility, and the characteristics of the receiving waters.

Lattemann (2009) discussed the key concerns of desalination plant impacts on the marine environment in three regions, the Arabian Gulf, the Red Sea and the Mediterranean Sea. The author presented first an overview on the desalination capacities in these regions and focused on important factors affecting brine discharge problems such as intake and outfall structures and reject streams. The author described bio-fouling, scaling and corrosion and discussed methods for their respective control.

Bleninger and Jirka (2010) reviewed environmental impacts that can result from brine discharges. They reported results from available monitoring and laboratory studies and noted that the majority of studies focused on a limited number of species over a short period of time with no baseline data. The need for a more uniform assessment and monitoring approach was underlined. The socio-economic aspects related to brine discharge problems in several regions were also reviewed. The authors presented environmental standards for temperature, salinity, and residual chemicals as well as regulations on mixing zones. The results show that brine flow rates discharged into the sea are a large percentage of the intake rate; generally up to 40 % (Reverse Osmosis, RO) and up to 90 % (Multi Stage Flash, MSF, including cooling water). The brine flow rate is 4–5 times higher for thermal desalination than for RO processes relative to the amount of produced fresh water.

Table 20.1 gives the effluent salinity and temperature for the main desalination processes. One can see that the brine discharged salinity in RO can be as high as 85 g/kg for sea water desalination while in thermal processes, the salinity of the rejected brine should not exceed a certain allowable design value set by the $CaSO_4$ (Calcium Sulfate) solubility. This is in order to limit the risk of corrosion and scaling of the components of the desalination plant.

In addition, the effluent contains additives such as chemicals used for bio-fouling control and anti-scalants as well as corrosion products. Several studies analyzed the chemical aspects of brine discharge and impacts on the marine environment [see for example Ahmed et al. (2000) and Danoun (2007)]. Al Mutaz (1991) and Abdul Azis, et al. (2000) discussed impact of effluents from Saudi desalination plants in Jeddah (Red Sea) and Al-Jubail (Arabian Gulf) desalination plants, respectively.

Desalination specific environmental impact assessment (EIA) procedures were proposed by Hoepner (1999), while Alameddine and El-Fadel (2007) adopted discharge assessment methodology consisting of six phases. Munoz and Fernandez-Alba (2008) presented a life-cycle assessment methodology and showed that

Table 20.1 Effluent salinity and temperature for RO, MSF, and MED processes (adapted from Lattemann et al. 2009)

Brine property	Process		
	Reverse osmosis (RO)	Multi stage flash (MSF)	Multiple effect distillation (MED)
Brine concentration	65–85 g/kg (SWRO)	60–70 g/kg (brine)	60–70 g/kg (brine)
		Ambient salinity (cooling water)	Ambient salinity (cooling water)
	1–25 g/kg (BWRO)	45–50 g/kg (combined)	50–60 g/kg (combined)
Brine temperature (above ambient temperature)	Close to ambient temperature	3–5 °C (brine)	5–25 °C (brine)
		8–12 °C (cooling water)	8–12 °C or more (cooling water)
		5–10 °C (combined)	10–20 °C (combined)

RO Reverse Osmosis, *MED* Multiple Effect Distillation, *MSF* Multi Stage Flash

reverse osmosis desalination could significantly reduce its environmental impact if, instead of seawater resources, brackish groundwater resources were used.

Methods for brine rejection can be divided into two classes depending on whether the desalination plants are inland (evaporation pond method) or coastal (surface water discharge method). Alameddine and El-Fadel (2007) compared the advantages and disadvantages of various brine disposal options and proposed design recommendations for brine discharge. Bleninger and Jirka (2010) and Bleninger (2006) discussed the "zero liquid discharge" (ZLD) method which has the potential to provide freshwater without any brine discharges and impacts on the marine environment.

A desalination process separates the feed saline water, which can be brackish water or seawater, into product water with low salinity and concentrated brine wastes. The energy input required for a separation process is a function of several parameters including the separation process itself, the salinity, and the temperature of the incoming saline water. The minimization of this required energy is very important since it reduces the cost of producing fresh water and decreases the generation of greenhouse gases as well as decreases the disposal of various pollution products into the sea or atmosphere.

Several studies developed general relations for the minimum work input required for desalination processes using the second law of thermodynamics (Sharqawy et al. 2011; AlZahrani 2013). These relations determine the minimum work input per unit mass of fresh water produced for various feed saline water and fresh water salinities.

For practical situations, the energy required for desalination is much higher than that computed for the reversible separation due to the irreversibility occurring in each component (i.e. pump, evaporation chamber, membrane, valve, etc.) of each desalination process (MSF, MED, RO, etc.). In fact, current desalination processes require large amounts of electrical energy to operate different types of pumps (high pressure pumps, pumps to transport liquid streams, etc.) for the RO process or to heat steam for the evaporation process in thermal desalination plants such as MED and MSF.

Table 20.2 Energy consumption and gain output ratio (GOR, kg of product per kg of required steam) for the main industrial sea water desalination processes (Zhao et al. 2011)

Process	Temperature of heating steam (°C)	Top Temp. (°C)	GOR, kg/kg	Energy consumption	
				Thermal energy kJ/kg	Power kWh/m^3
MSF	130	120	10–12	185–227	2.5–4
	100	90	7–9	252–328	2.5–4
	80	70	4–5	462–567	2.5–4
MED-TVC	150	70	12–15	151–189	1.2–1.8
	120	70	10–12	189–231	1.2–1.8
LT-MED	90	80	10–13	177–231	1.2–1.8
	80	70	8–10	235–294	1.2–1.8
	70	60	6–8	294–395	1.2–1.8
VC					8–16
RO with energy recovery					5–6
RO without energy recovery					7–8

RO Reverse Osmosis, *MED* Multiple Effect Distillation, *MSF* Multi Stage Flash, *TVC* Thermal vapor compression, *LT* Low temperature

Table 20.2 gives the gain output ratio (GOR, defined as ratio of mass flow rate of permeate to mass flow rate of required steam) and energy consumption for the main industrial desalination processes at different conditions (Zhao et al. 2011). It shows in particular the MED-TVC (Thermal Vapor Compression) offers a higher performance in terms of GOR and energy consumption than the other thermal processes. Besides, the energy consumption for RO with recovery device is the lowest one.

The physical phenomena that act on the brine discharged into surface water bodies, such as a coastal sea, include advection, diffusion, convection, and buoyancy. The discharge process can be divided into the near field region nearest to the outfall discharge before boundary interaction (controlled by the source/discharge characteristics), and the far field region, where ambient transport mechanisms including ambient diffusion and advection dominate (Kuipers and Vreugdenhil 1973; Spalding 1975). An intermediate field separating the near and far fields can also be considered.

Representative studies on brine and heat dispersion in receiving water bodies are reviewed here with emphasis on those most relevant to the present work. Among the classical and pioneering studies in which the mathematical modeling of free surface flows has been explained comprehensively are those of Kuipers and Vreugdenhil (1973), Spalding (1975) and Rodi (1978). Kuipers and Vreugdenhil (1973) presented a detailed account on the nature of shallow water flows and the derivation of the depth-averaged equations.

Al-Sanea (1982) developed a finite-volume numerical procedure for the calculation of two-dimensional depth-integrated shallow-water flows. The procedure was based on depth correction analogous to the pressure correction procedure on which

the very well-known SIMPLE algorithm of Patankar and Spalding (1972) was based; see also Patankar (1980). Subsequently, Al-Sanea (1993) developed a model based on the computer program 2/E/FIX of Pun and Spalding (1977) (Al-Sanea et al. 1980) for calculating the flow and salinity distribution resulting from desalination plant discharges into shallow waters. The model accounted for the physical features that affect the concentrated brine dispersion process including convective and diffusive transport, wind stresses, seabed friction, and variable seabed elevation. Results of a parametric study for a hypothetical desalination plant effluent discharge under a range of meteorological, hydrological, topographical, and plant operating conditions, demonstrated the importance of the various factors that act on brine dispersion. Salinity contours have shown possible scenarios in which plant discharge can affect intake under different conditions. Heat transfer was, however, not included in the model.

More recent studies include those of Purnama et al. (2003) who used an analytical model to solve the transient salinity diffusion-advection equation in order to investigate dispersion of brine waste discharges into sea. A sloping sandy beach was considered in which the seabed depth increased until reaching a constant depth. Contours of salt concentration were presented. Employing the same model, Purnama and Al-Barwani (2005) studied means to minimize shoreline salinity levels without building a longer sea outfall. Such means consisted of creating a jump discontinuity on a seabed depth profile as well as keeping outfall location in the deeper region. A similar analytical model was used by Shao et al. (2008) to study effects of oscillatory tidal currents on brine discharge characteristics into shallow coastal water with a flat seabed. Results presented showed increase of salinity in coastal waters in vicinity of outfall and along shoreline due to continuous brine discharges.

Purnama and Al-Barwani (2006) solved the 2-D advection-diffusion equation for salt concentration to investigate effect of a tidally oscillating flow in dispersing brine waste discharge into sea. The geometry was simplified by using a straight coast with a constant water depth. The diffusive process was represented by dispersion coefficients and the brine waste was discharged at a constant rate. The plume was assumed to be vertically well mixed over the water depth. Results showed that, due to flow oscillation, the plumes also spread towards the upstream side of the outfall. However, by simulating a longer outfall, the potential impact of brine discharges into the sea could be reduced.

Al-Barwani and Purnama (2007) studied the effect of beach erosion on dispersing the brine waste discharged into sea. The authors used the same model used in Prunama and Al-Barwani (2006) but under steady-state conditions and allowing the seabed depth to vary as a power function of distance from the beach and neglecting the dispersion term in the longitudinal direction along the beach. The study is relevant to a plant that is built and operated with an outfall to satisfy imposed site environmental regulation compliance but the beach is subsequently being eroded.

A number of studies have used the Cornel Mixing Zone Expert System CORMIX developed by Jirka and co-authors (Doneker and Jirka 2001). This tool combines a series of software systems for analysis, prediction, and design of aqueous discharges into watercourses. The system provides comprehensive

approach to mixing zone analysis, regulatory assessment, and outfall design (Donecker and Jirka 2001). The CORMIX methodology is based on the role of boundary interaction on mixing and uses several hydrodynamic criteria and physical concepts such as the length scale, jet to plume transition, jet to cross flow length scale concept.

Alameddine and El-Fadel (2007) used CORMIX to simulate dispersion of a brine plume in a marine environment by considering the discharge of heated effluent from a desalination-power plant into the Arabian Gulf. The authors compared the mixing behavior and efficiency of surface, submerged single-port, and submerged multi-port outfalls. Results revealed the inadequacy of using surface discharge outfalls for brine disposal. A multi-port discharge proved to be adequate to enhance dilution rates, whereby a tenfold dilution rate was achieved within a 300 m mixing zone. The authors highlighted several limitations of the CORMIX model including its limited capability for simulating the discharge of large flow volumes into shallow areas.

Malcangio and Petrillo (2010) used a 3-D model to simulate brine discharge from desalination plants into a coastal region in southern Italy characterized by presence of protected vegetation species. The Reynolds Averaged Navier-Stokes equations (RANS) were considered and data on topography of target area and climatic conditions were introduced in the model. Results in terms of excess salinity were analyzed and the most suitable location for the brine outfall was determined.

Palomar and Losada (2011) discussed three basic approaches for modeling impact of brine discharge on the marine environment. These are: (i) models based on a dimensional analysis of the phenomenon, (ii) models based on integration of differential equations along the cross section of flow, and (iii) hydrodynamic models. The first and second types of models are based on several assumptions and restrictions reducing in general their accuracy and reliability. The hydrodynamic models solve the conservation equations of mass, momentum, and constituents. The energy equation is not solved in general. Compared to the other types of models, the hydrodynamic models are more rigorous, capable of modeling coupled, complex phenomena, and simulation of different configurations of discharge, intake, and ambient conditions. However, these models present two major limitations; firstly, coupling between near field and far field is difficult due to different spatial and time scales and, secondly, long computational time is required.

Palomar et al. (2012) examined modeling of near field brine discharge and analyzed assumptions, capability, limitations, and reliability of steady-state models used. These models were either based on dimensional analysis such as CORMIX or based on integration of differential equations such as CORJET, VISUAL PLUMES, and VISJET. The authors noted that the lack of validation studies of negatively buoyant jets was a common shortcoming in these commercial models. Significant errors were detected in the sensitivity analyses carried out. Palomar et al. (2012) focused on the validation of these models via performing many tests simulating different cases and using available published experimental data. The authors outlined limitations of each tool and detected errors and discrepancies that could result in the underestimation of dilution by as much as 60–90 %.

A simple model for simulating behavior of dense jets was developed by Cipollina et al. (2004). Cipollina's model considered four basic jet parameters, namely, flow rate, density, inclination, and diameter. The velocity and concentration distributions around the jet axis were assumed to be Gaussian and the entrainment velocity was supposed to be proportional to local jet velocity. Results included information on trajectory, spreading, and dilution of inclined dense jets. Abou-Elhaggag et al. (2011) investigated jet trajectory and dilution of submerged negatively-buoyant jet discharging vertically over a flat bottom in a calm ambient environment. Experimental observations made for terminal height of rise of dense jets and for concentration profiles along jet trajectory were used to validate a numerical model by using the FLUENT package. Various port diameters and concentration of effluent salinities were investigated and a new model for the terminal height of rise of dense jets was proposed.

Fernadez et al. (2012) studied the accuracy of four mixing zone models by conducting a comparative study with brine discharge measurements from a reverse osmosis desalination plant in Spain. The authors concluded that each model was conservative in its results except one model whose predictions were very close to measured data. Very recently, Oliver et al. (2013) developed an integral model to predict the near field behavior of negatively buoyant discharges in quiescent ambient fluid. The model included influences of additional mixing associated with buoyancy induced instabilities. Comparisons were carried out with predictive models and experimental data.

20.1.3 Current Status and Objectives of Present Work

The previous section has reviewed studies and considered a number of important issues related to brine discharges from desalination/power plants. It is clear that there is a continuing need for assessment of environmental impact of brine discharges from desalination plants as well as assessment of likely flow interaction between plant discharge and intake ports. While the former assessment concerns environment protection, the latter assessment concerns thermal efficiency of the plant and the energy required for desalination. These assessments can only be made by knowledge of detailed temperature, chemical pollutants, and brine distributions in bodies of water resulting from plant effluent discharges. The main concluding remarks of this review can be summarized as follows:

- Bodies of water where concentrated brine and heat are discharged can broadly be classified as shallow waters and deep waters. For each class, different mathematical models apply with specific features.
- The problem of desalination plant discharge-intake port interaction has in large been overlooked despite its possible effect on increasing feed water salinity and hence a likely increase in energy required for salt separation as part of the desalination process.

- Reducing energy consumption for desalination is crucial. Efforts should focus to improve plant performance, minimize discharge-intake port interaction, and reduce environmental impact.
- Few studies have considered thermal analysis. Thus, the energy equation was typically not included in previous models of brine disposal from desalination plants.
- More emphasis was given to the near field analysis, while only a small number of studies investigated the far field. Coupling between near and far fields is important and Computational Fluid Dynamics (CFD) models are potentially capable for such coupling and analysis.
- The majority of brine and heat dispersion studies, particularly those based on analytical tools, have adopted simplified mathematical models with various limiting assumptions. Few studies have used rigorous mathematical models.

The purpose of this work is to present and validate a numerical model for predicting brine and heat dispersion into shallow coastal waters. The mathematical formulation centers on the concept of shallow water equations in which the 3-D problem is reduced to an equivalent 2-D one by integrating the governing equations over the depth of flow.

After validating the numerical model, it is applied after appropriate modifications to determine the salinity and temperature distributions in shallow coastal waters resulting from effluent discharge from an existing desalination/power plant situated on the Arabian Gulf. Parametric studies of the effects of a number of influential conditions are carried out by using the actual seabed topography and plant discharge and intake port locations. Brief information on all of these aspects as well as the discharged mass flow rate and variable water depth are given later. Next, the mathematical formulation and numerical solution procedure are presented.

20.2 Mathematical Formulation

20.2.1 Shallow Water Approximations

The final form of the mathematical model to be employed in the study is based on the shallow-water approximations. Therefore, the governing equations are depth-averaged (integrated) by assuming negligible variations of velocity and temperature over the depth and by neglecting the vertical velocity component, thus rendering the three-dimensional problem to be two-dimensional. Further, the eddy viscosity and diffusivity coefficients are assumed constant. These assumptions are in harmony with the free-surface-flow approximations in shallow and wide stretches of water (Kuipers and Vreugdenhil 1973; Spalding 1975; Al-Sanea 1982, 2010; Al-Sanea and Orfi 2013).

Figure 20.1 shows a schematic of the modeled flow domain. The flow is bounded below by a rigid, fixed surface $z = z_b$ (x, y) and by a free surface $z = z_b$ (x, y) + h (x, y, t) above a horizontal datum-plane and subjected to atmospheric

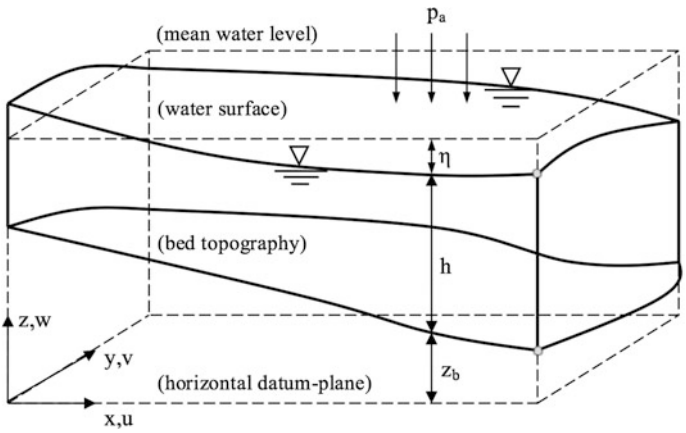

Fig. 20.1 Definition of bottom height, depth, mean water level, and water surface (Al-Sanea 1982)

pressure (p_a), where h is the local water depth. The integration is carried out from the bottom to the surface, i.e. from z_b to $z_b + h$. The depth-averaged quantities are defined by the following relations:

$$\bar{u} = \frac{1}{h}\int_{z_b}^{z_b+h} u\, dz, \quad \bar{v} = \frac{1}{h}\int_{z_b}^{z_b+h} v\, dz, \quad \text{and} \quad \bar{\tau} = \frac{1}{h}\int_{z_b}^{z_b+h} \tau\, dz \tag{20.1}$$

On integrating the equation system, making use of Leibnitz's rule and the kinematic boundary conditions at the surface and bottom (see Al-Sanea 1982 for details), one obtains the depth-averaged conservation equations.

20.2.2 The Governing Differential Equations Solved

20.2.2.1 Further Basic Assumptions

So far, the only approximations made to the three-dimensional Navier-Stokes equations, in deriving the general shallow-water equations, are:

1. The assumption of a hydrostatic pressure distribution.
2. The fluid is assumed to be incompressible and homogenous.
3. Gain or loss of mass from surface (rain, evaporation) and bottom (seepage) are not considered.
4. The vertical velocity profiles are approximated to be nearly uniform; hence depth-averaged values are used.
5. The wind and bottom stresses are related to the square of the depth-averaged velocities (Al-Sanea 1982).

6. The fluid stresses are expressed by a constant laminar- or eddy-viscosity coefficient multiplying the depth-averaged velocity gradients (Al-Sanea 1982).

In the present formulation, it is further assumed that (Spalding 1975):

7. The flow is steady.
8. The "rigid-lid" approximation is valid; however, the bed topography can vary.
9. Flow over small stretches of water; hence, negligible atmospheric-pressure variation.

20.2.2.2 The Resulting Governing Equations

Subject to the above assumptions the system of equations reduces to:

Conservation of mass

$$\frac{\partial}{\partial x}(h\,\bar{u}) + \frac{\partial}{\partial y}(h\,\bar{v}) = 0 \tag{20.2}$$

where $\bar{u}$ and $\bar{v}$ are the depth-averaged velocity components in the x- and y-directions, respectively, and h is the local depth of flow.

Conservation of u-momentum

$$\frac{\partial}{\partial x}(h\,\bar{u}^2) + \frac{\partial}{\partial y}(h\,\bar{u}\,\bar{v}) - \frac{1}{\rho}\frac{\partial}{\partial x}\left(h\,\bar{\mu}_{eff}\frac{\partial \bar{u}}{\partial x}\right) - \frac{1}{\rho}\frac{\partial}{\partial y}\left(h\,\bar{\mu}_{eff}\frac{\partial \bar{u}}{\partial y}\right) = S_u \tag{20.3a}$$

where ρ is the water density, $\bar{\mu}_{eff}$ is the effective viscosity and S_u is the source term for u and is given by:

$$S_u = -\frac{h}{\rho}\frac{\partial p}{\partial x} + h f\,\bar{v} - C_f \bar{u}(\bar{u}^2 + \bar{v}^2)^{1/2} + C_s\frac{\rho_{air}}{\rho}U_o(U_o^2 + V_o^2)^{1/2} \tag{20.3b}$$

where p is the static pressure, f is the Coriolis parameter, C_f is the seabed friction factor, C_s is the wind force friction factor, ρ_{air} is the air density, U_o and V_o are the wind relative velocities with respect to the water velocity in the x- and y-directions, respectively.

Conservation of v-momentum

$$\frac{\partial}{\partial x}(h\,\bar{u}\,\bar{v}) + \frac{\partial}{\partial y}(h\,\bar{v}^2) - \frac{1}{\rho}\frac{\partial}{\partial x}\left(h\,\bar{\mu}_{eff}\frac{\partial \bar{v}}{\partial x}\right) - \frac{1}{\rho}\frac{\partial}{\partial y}\left(h\,\bar{\mu}_{eff}\frac{\partial \bar{v}}{\partial y}\right) = S_v \tag{20.4a}$$

where S_v is the source term for v and is given by:

$$S_v = -\frac{h}{\rho}\frac{\partial p}{\partial y} - h f\ \bar{u} - C_f \bar{v}(\bar{u}^2 + \bar{v}^2)^{1/2} + C_s \frac{\rho_{air}}{\rho} V_o (U_o^2 + V_o^2)^{1/2} \qquad (20.4b)$$

Conservation of energy

$$\frac{\partial}{\partial x}(h\ \bar{u}\ \bar{T}) + \frac{\partial}{\partial y}(h\ \bar{v}\ \bar{T}) - \frac{1}{\rho}\frac{\partial}{\partial x}\left(h\ \frac{\bar{\mu}_{eff}}{\sigma_T}\frac{\partial \bar{T}}{\partial x}\right) - \frac{1}{\rho}\frac{\partial}{\partial y}\left(h\ \frac{\bar{\mu}_{eff}}{\sigma_T}\frac{\partial \bar{T}}{\partial y}\right) = \frac{S_T}{c_p} \qquad (20.5)$$

where $\bar{T}$ is the depth-averaged temperature, σ_T is the turbulent Prandtl number, c_p is the specific heat, and S_T is the source (or sink) term for T and represents energy interaction at the air-water interface. Convection heat transfer and evaporation effects may be accounted for in the energy equation through this S_T term.

Conservation of chemical species

$$\frac{\partial}{\partial x}(h\bar{u}\,\bar{c}) + \frac{\partial}{\partial y}(h\bar{v}\,\bar{c}) - \frac{1}{\rho}\frac{\partial}{\partial x}\left(h\frac{\bar{\mu}_{eff}}{\sigma_c}\frac{\partial \bar{c}}{\partial x}\right) - \frac{1}{\rho}\frac{\partial}{\partial y}\left(h\frac{\bar{\mu}_{eff}}{\sigma_c}\frac{\partial \bar{c}}{\partial y}\right) = S_c \qquad (20.6)$$

where $\bar{c}$ is the depth-averaged concentration of a chemical species in the solution, e.g. salt or salinity (Al-Sanea 1993), σ_c is the turbulent Schmidt number, and S_c is the source (or sink) term for c which is normally zero.

20.2.2.3 The Common Form of Transport Equation

All the above governing equations can be recast in the common form of a single general transport equation given below, enabling one solution procedure for all equations.

$$\frac{\partial}{\partial x}(h\bar{u}\,\bar{\phi}) + \frac{\partial}{\partial y}(h\bar{v}\,\bar{\phi}) - \frac{1}{\rho}\frac{\partial}{\partial x}\left(h\,\bar{\Gamma}_{eff,\phi}\frac{\partial \bar{\phi}}{\partial x}\right) - \frac{1}{\rho}\frac{\partial}{\partial y}\left(h\,\bar{\Gamma}_{eff,\phi}\frac{\partial \bar{\phi}}{\partial y}\right) = S_\phi \qquad (20.7)$$

where $\bar{\phi}$ is the general depth-averaged variable and stands for 1, $\bar{u}$, $\bar{v}$, $\bar{T}$, and $\bar{c}$ in Eqs. (20.2) through (20.6), respectively; $\bar{\Gamma}_{eff,\phi}$ is the effective exchange (diffusion) coefficient and stands for 0, $\bar{\mu}_{eff}$, $\bar{\mu}_{eff}$, $\bar{\mu}_{eff}/\sigma_T$, and $\bar{\mu}_{eff}/\sigma_c$ in Eqs. (20.2) through (20.6), respectively; and S_ϕ is the appropriate source and/or sink of the variable concerned ($\bar{\phi}$) which takes various expressions or be equal to zero.

20.2.2.4 Boundary Conditions

Solid Boundaries

The velocity components at solid boundaries are set to zero. The gradient of temperature and salinity in the direction normal to the solid boundaries is also set to zero.

Discharge Port

The velocity at the discharge port is fixed according to the discharge port area and the total mass flow rate of the effluent discharged to the sea. The temperature and salinity at the discharge port equal those of the heated and saline water coming out of the plant.

Intake Port

The velocity at the intake port is fixed according to the intake port area and the total mass flow rate withdrawn from the sea to the plant. However, the temperature and salinity at the intake port are unknown and calculated by the iterative solution procedure as an output from the computer model.

Sea Inlet and Sea Free Stream Boundaries

The velocity components are prescribed values as relevant to sea current with salinity and temperature values corresponding to ambient sea values. The sea current speed and direction are assumed nominal values and are also varied through a parametric study.

Sea Outlet Boundary

The velocity, salinity, and temperature gradients normal to this boundary are set to zero.

Thermal Interchange at Water-Air Interface

The heat rejected from the plant disperses into the sea water and is ultimately exchanged with the atmosphere from the water surface. Details of energy balance giving the net thermal interchange at the water-air interface are given in Spalding (1975), Al-Sanea (2010) and Al-Sanea and Orfi (2013). The equilibrium seawater

temperature is calculated in the absence of external thermal load, due to plant discharge, and used in the energy balance, see Al-Sanea and Orfi (2013).

Wind Stress and Seabed Friction

These are accounted for through appropriate correlations and introduced by the source terms in the momentum equations, see Eqs. (20.3b and 20.4b).

20.3 Numerical Solution Procedure and Model Validation

Due to space limitation, the numerical solution procedure and numerical model validation are briefly described in this section. More details can be found in Al-Sanea (2010) and Al-Sanea and Orfi (2013). It suffices to mention here that the stage of model validation is conducted prior to computer model application to a case study. The latter involves determining the salinity and temperature distributions in shallow coastal waters resulting from effluent discharge from an existing desalination plant situated on the Arabian Gulf.

20.3.1 Numerical Solution Procedure

The computer model used in this study is developed in-house by the first author and is an extension of that originally developed by Al-Sanea (1993) based on the 2/E/FIX CFD computer code of Pun and Spalding (1977) (Al-Sanea et al. 1980). The numerical solution procedure used employs the control-volume finite-difference method for the discretization of the depth-integrated conservation equations appropriate to shallow free-surface water flows. This computer code employs the well-known SIMPLE algorithm of Patankar and Spalding (1972) and Patankar (1980).

20.3.2 Numerical Model Validation

Numerical model validation was conducted in two stages which required appropriate model modifications. A preliminary stage was conducted by comparing numerical results with closed-form analytical solutions derived for 1-D channel flows with heat transfer. Results showed that the agreement between numerical model predictions and analytical results was excellent, see Al-Sanea and Orfi (2013) for details. The second stage of model validation considered a more

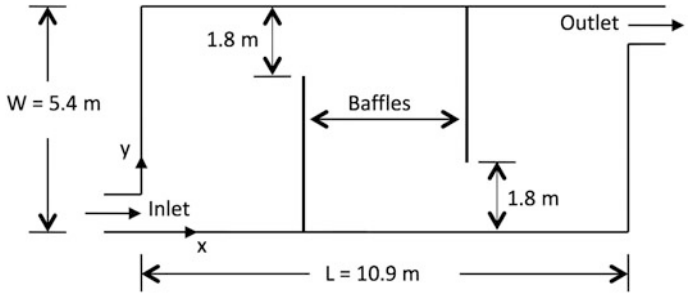

Fig. 20.2 *Top view* of the geometrical configuration of the experimental cooling pond of Cerco (1977) used to validate the present numerical model

challenging problem by comparing numerical results with 2-D flow and heat transfer in shallow cooling ponds in which temperature measurements were available under controlled laboratory conditions. Cerco (1977) used laboratory measurements to provide detailed data for the design of shallow experimental cooling ponds. He used various designs and baffle arrangements for the pond and evaluated performance for different flow rates.

Figure 20.2 describes a geometrical configuration of the experimental cooling pond used for validation of the present numerical model. Figure 20.3a through d presents dimensionless temperature profiles at the middle of the pond (X = 0.5) and across its width Y showing comparisons between present numerical predictions and experimental data of Cerco (1977) for four different cases. These cases involve different mass flow rates in the presence or absence of baffles. It is concluded that the agreement between predictions and measurements is, in general, quite good, see Al-Sanea and Orfi (2013) for details.

Besides, a grid independence study was conducted in which different sizes of the finite-volume grid were employed and their effects on the results were investigated accordingly. A grid of 40 × 33 (40 nodes in the x direction) was selected for use in all production runs.

20.4 Application to a Desalination Plant Discharge

After validating the mathematical model as briefly described in the previous section, the present section concerns model application to a case study. The case study involves the determination of salinity and temperature distributions in shallow coastal waters resulting from effluent discharge from an existing desalination plant situated on the Arabian Gulf. Parametric studies of the effects of a number of influential conditions are also carried out.

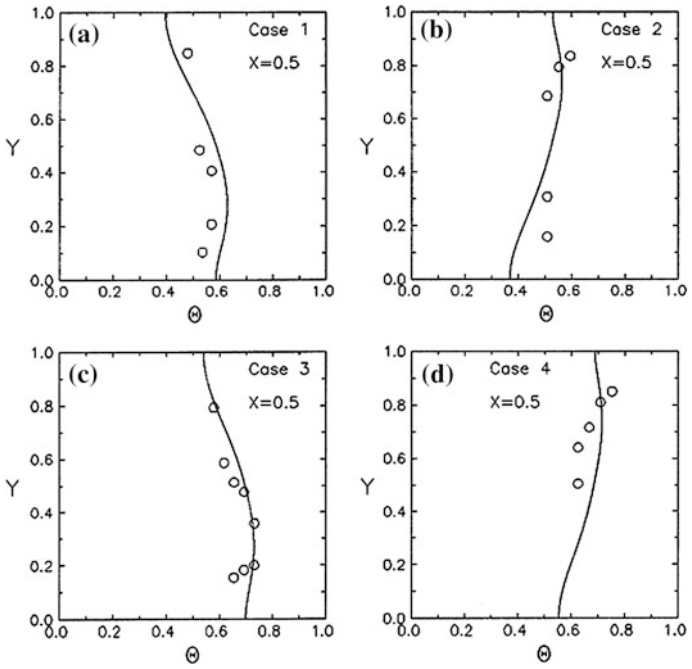

Fig. 20.3 Dimensionless temperature profiles at middle of pond (X = 0.5) for Cases 1 through 4 showing comparison between present numerical predictions (*lines*) and measurements (*circles*, Cerco 1977)

20.4.1 Seabed topography, computational domain, and parameters varied

The seabed topography of the coastal region in the vicinity of the desalination/power plant considered in the present investigation is depicted in Fig. 20.4. The depth contours are shown with values of depth given relative to a datum level which is 3 m above the mean water level. It is noted that very close to the coast, the depth contours are nearly parallel to the shoreline. This indicates that the water depth increases nearly linearly with distance away from the coastline. The first contour shown closest to the shoreline is the contour with a water depth of 6 m, relative to the datum used, and is about 50–100 m away from the shoreline. In general and as shown, the water depth increases from about 6 to 10 m, relative to the datum, in the next 100–200 m distance away from the shoreline. A large coastal region of nearly uniform water depth then persists till a distance of about 1000–1500 m away from the shoreline with a water depth of about 10–11 m, relative to the datum. This region is characterized by a coarse concentration of contour lines where the distance between consecutive contour lines is relatively wider. Beyond this region, the water depth increases continuously to over 20 m, relative to the datum, as seen at the bottom right of Fig. 20.4. Also, a reef can be noticed near the bottom left of the

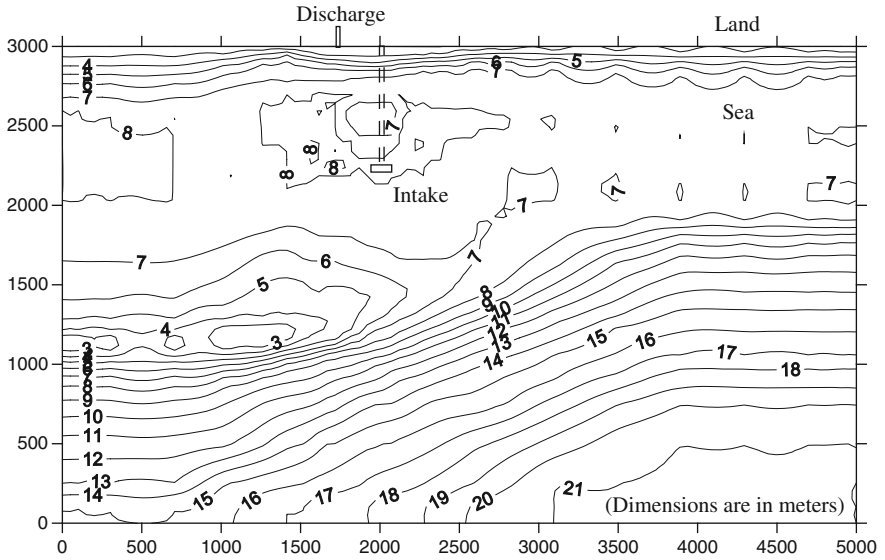

Fig. 20.4 Seabed topography in the vicinity of the desalination/power plant with water depth contour values relative to a datum level which is 3 m above the mean water level

figure where there is a concentration of contours in which the water depth gets relatively much shallower with a value of less than 5 m, relative to the datum used.

The above description of the seabed topography is accounted for in the computer model by feeding in the local values of the water depth into the finite-volume equations. As mentioned before, the local depth of flow (h) is introduced into the depth-integrated governing conservation differential equations and into their finite-volume counterparts by modifying the finite-volume areas and volume of every nodal point in the grid.

Figure 20.5 shows the calculation domain selected to encompass the coastal region in the vicinity of the plant with the dimensions, shown not to scale, extending over 5 km by 3 km along the shoreline and offshore, respectively.

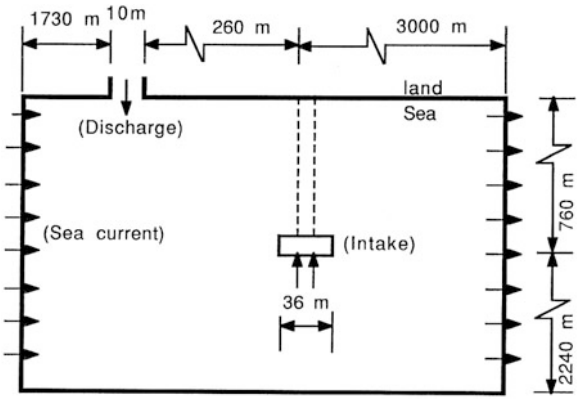

Fig. 20.5 Computational domain encompassing coastal region in vicinity of the desalination/power plant showing discharge and intake port locations and dimensions (not to scale)

Parametric studies of the effects of a number of influential conditions were carried out in order to investigate the dispersion of the heated and concentrated brine discharged into the coastal waters. This was done by using the actual seabed topography and the plant discharge and intake port locations. The parametric studies involve investigating the effects of varying: (i) sea current magnitude and direction, (ii) wind speed magnitude and direction, (iii) seawater depth in vicinity of plant, and (iv) plant discharge flow rate. Only results on the effect of sea current magnitude and direction and plant discharge flow rate are considered in the present study.

For a produced desalinated water rate of 3 m^3/s, the nominal value of the discharged mass flow rate is 55 m^3/s. In other words, 58 m^3/s of seawater, representing the feed water and the cooling water amounts, is withdrawn from the sea through the intake port, 3 m^3/s is the rate of fresh water produced, while 55 m^3/s of heated water with a higher salinity is discharged to the sea through the exit port of the plant.

The nominal values of the parameters used are summarized in Table 20.3 along with their ranges.

Detailed contours are presented, with dimensionless values of salinity and temperature in excess of nominal (ambient) seawater values, in order to determine the extent of coastal area affected by the discharged effluent. The dimensionless salinity (C) and dimensionless temperature (θ) are defined as follows:

$$C = \frac{c - c_{sea}}{c_{dis} - c_{sea}} \quad \text{and} \quad \theta = \frac{T - T_{sea}}{T_{dis} - T_{sea}} \tag{20.8}$$

where c_{sea} and T_{sea} are the nominal values far away from the discharge and intake port locations and c_{dis} and T_{dis} are, respectively, the concentration and temperature of the effluent water as discharged from the plant.

The value of c_{sea} is the nominal value of seawater salinity which is taken equal to 0.05. The value of c_{dis} is set as:

$$c_{dis} = c_{sea} + 0.01 \tag{20.9}$$

Table 20.3 The parameters varied, their nominal values and ranges

Parameter	u_{sea} (m/s)	v_{sea} (m/s)	u_{wind} (m/s)	v_{wind} (m/s)	Relative mean water level (m)	Plant desalting capacity[a] (%)
Nominal value	0.2	0.0	0.0	0.0	0.0	100
Range	0.05–0.35	−0.05–0.01	−10–2	−10–2	−1–1	75–250

[a]Plant desalting capacity relative to nominal capacity

The value of T_{sea} is set equal to the seawater equilibrium temperature (T_{eq}). The value of T_{dis} is set as:

$$T_{dis} = T_{sea} + 10 \tag{20.10}$$

It is noted that the dimensionless values of salinity (C) and temperature (θ) according to Eq. (20.8) range from 0 to 1. The value of zero corresponds to the ambient seawater value and the value of one corresponds to the value at the discharge port.

The seawater equilibrium temperature (T_{eq}) is calculated separately and independently of the plant discharge conditions. Being affected by environmental conditions, it is determined iteratively by the same computer model in the absence of interaction with the discharge and intake ports of the plant. In the present calculations, T_{eq} is calculated under the following conditions: ambient air temperature (T_{air}) of 20 °C, relative humidity (ϕ) of 60 %, and a daily-averaged solar flux absorbed of 250 W/m^2. A seawater equilibrium temperature (T_{eq}) equals to 20.9 °C is obtained and used in the simulations (Al-Sanea and Orfi 2013).

20.4.2 *Effect of Sea Current Velocity-Component Parallel to Shoreline*

The sea current is a vector quantity that has both direction and magnitude. The sea current velocity is analyzed into two components; one component is parallel to the shoreline the magnitude of which is investigated in the present section, while the other component is normal to the shoreline the magnitude of which is investigated in the next section.

The sea current velocity is one of the most important parameters expected to influence the dispersion process of the heated saline discharge in shallow coastal waters. Therefore, the salinity and temperature distributions are expected to be affected largely by the sea current velocity for two main reasons. The first reason is that the sea current determines the amount (rate) of seawater available for mixing with that amount (rate) of the discharged effluent and hence affects the dilution process. The second reason is that the sea current direction and magnitude can have determinant effect on the direction of movement of the effluent as it discharges into the sea. Certain conditions can also lead to discharge-intake port interaction causing an adverse impact on the plant operation. As mentioned above, the effect of sea current velocity component parallel to shoreline is investigated first. This is done while the sea current velocity component normal to shoreline is kept at its nominal value of zero. All other parameters are also kept at their nominal values (summarized in Table 20.3).

The sea current velocity component parallel to shoreline is varied in the range $0.05 \leq u_{sea} \leq 0.35$ m/s with an increment of 0.05 m/s. With reference to Fig. 20.4,

this direction is from left to right (i.e. from southwest direction to north east direction, which is parallel to the coastline). This is the worst case scenario under these conditions since the intake to the plant is situated at location downstream relative of the discharge from the plant. Therefore, discharge-intake interaction could be possible. Representative salinity contours with dimensionless values are shown in Fig. 20.6, for u_{sea} = 0.1, 0.15, and 0.2 m/s, respectively. These values are chosen, with u_{sea} = 0.2 m/s as the characteristic value. As will be shown, these are the most interesting among the other values over the range that u_{sea} is varied (see Table 20.3). Contour values are selected to have common presence in all figures in

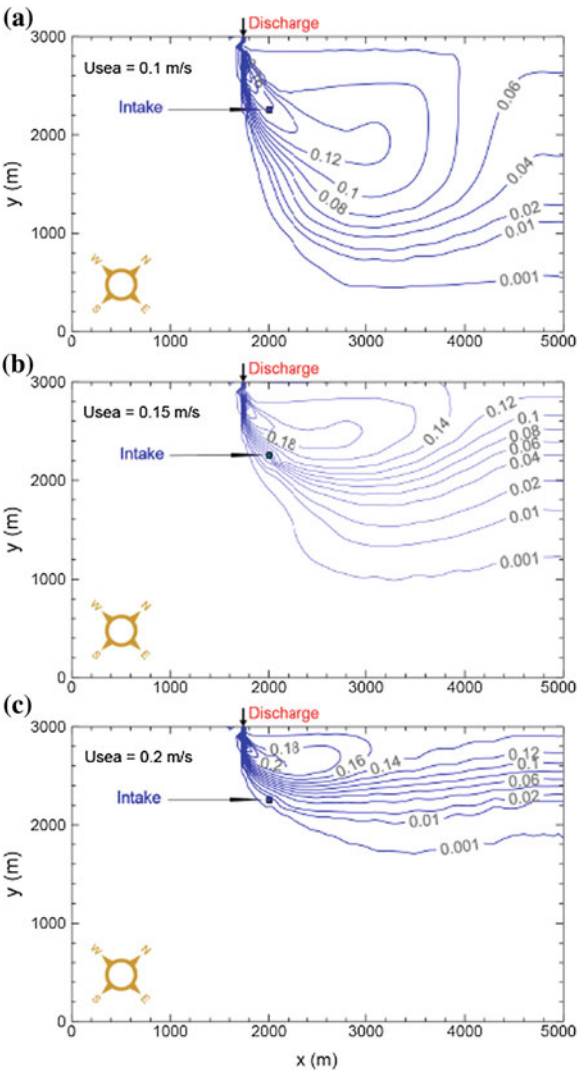

Fig. 20.6 Dimensionless salinity contours showing effect of sea current velocity component parallel to shoreline (u_{sea}); **a** u_{sea} = 0.1 m/s, **b** u_{sea} = 0.15 m/s, **c** u_{sea} = 0.2 m/s

order to facilitate comparisons and ease of interpretation. In general, the following dimensionless contour values are selected: 0.001, 0.01, 0.02, 0.04, 0.06, 0.08, 0.1, etc. generally with an interval of 0.02. The first contour value of 0.001 is considered to have effectively the ambient seawater concentration, i.e. salinities along this contour are considered to be practically unaffected by the discharge from the plant.

With reference to Fig. 20.6a where u_{sea} = 0.1 m/s, it can be seen that the sea current along the shoreline deflects the effluent discharging from the exit port of the plant in the downstream direction. Accordingly, the region far away from the coastline and the upstream region have salinities equal to the ambient sea salinity. The predictions show that the salinity increases nearer to the discharge port. Of course, at the discharge port salinity is equal to the discharge salinity from the plant having a dimensionless value of 1. The salinity at the plant intake is perhaps the most important salinity value. This location, indicated on the figure, appears to be strongly affected by the discharge conditions. The contours reveal a relative salinity at intake of about 0.16. This value results from the center of the discharged effluent passing directly over the intake under these conditions.

As u_{sea} increases to 0.15 m/s, the stronger current deflects the effluent toward the coastline, as shown in Fig. 20.6b. The contour lines compress and the coastal area affected by the discharge shrinks. However, although the affected coastline area decreases, higher salinity occurs in the region nearer to the coastline. Nevertheless, the plant intake port lies outside of the core of the plume and now has a relative salinity of 0.08, in contrast to the results shown in Fig. 20.6a. Increasing u_{sea} to 0.2 m/s, shown in Fig. 20.6c, collapses the discharged effluent onto the coast where salinity contours becoming parallel with the coastline at far downstream locations. The effluent area is now smaller, but the salinity is higher closer to coastline. Under these conditions, the intake port experiences very little of the discharged effluent. The discharged effluent lies away from the intake port, closer to the coastline, and the relative salinity near the intake port is less than 0.01.

The corresponding results for the effect of sea current velocity component parallel to shoreline on the temperature distributions are presented in Fig. 20.7. The striking feature is that the trends of variation of these contours are very similar to those of the salinity contours shown earlier in Fig. 20.6. However, by closer examination of the results, it becomes clear that there are slight differences in the absolute values of the contours. For a given location, the dimensionless temperature is slightly less than the corresponding dimensionless salinity. As a consequence, the area enclosed by a certain value of dimensionless temperature is slightly smaller than that enclosed by the same value of dimensionless salinity. This small difference between the temperature and salinity results can be attributed to the effect of heat transfer at the sea surface. By comparing the energy and concentration conservation equations (Eqs. 20.5 and 20.6, respectively) and by imposing similar boundary conditions, one might expect such an outcome by casting the results in a dimensionless form.

The close values between the dimensionless temperature and salinity, with temperature values being slightly smaller, indicate that there is a net heat loss at the water-air interface, as to be expected. However, as it turned out to be, this thermal loss is less effective, compared to the process of mixing (dispersion) between the

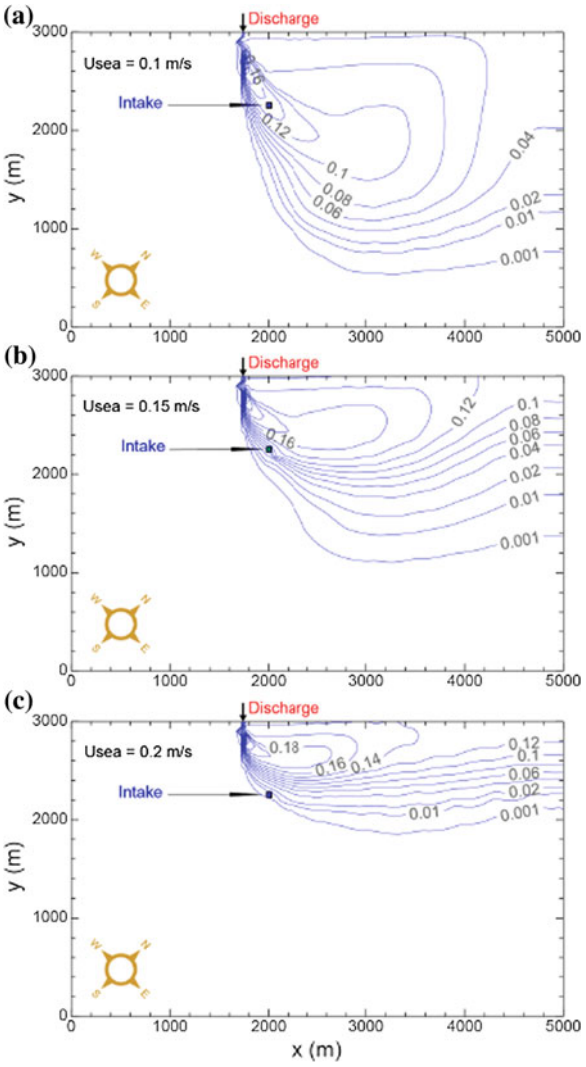

Fig. 20.7 Dimensionless temperature contours showing effect of sea current velocity component parallel to shoreline (u_{sea}); **a** u_{sea} = 0.1 m/s, **b** u_{sea} = 0.15 m/s, **c** u_{sea} = 0.2 m/s

heated discharged effluent and the cooler receiving seawater body, in altering the discharged effluent temperature. In other words, the discharged heated effluent has been cooled down dominantly by mixing with the cooler seawater than by the net heat loss from the surface under the present conditions. With regard to the salinity of the discharged effluent, this has been reduced solely by mixing with the seawater that is less saline. By suppressing the sources and sinks of heat at the water-air interface, the dimensionless temperature results should have been identical to the dimensionless salinity results.

Figure 20.8 shows the variations of the dimensionless salinity and temperature at plant intake (C_{in} and θ_{in}, respectively) with the sea current velocity-component

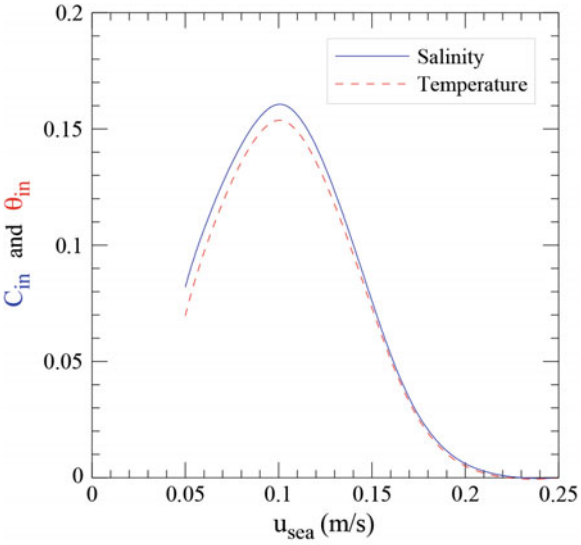

Fig. 20.8 Dimensionless salinity and temperature at plant intake port versus sea current velocity component parallel to shoreline

parallel to shoreline (u_{sea}). All other parameters are kept constant at their nominal values. The results show that the worst conditions take place at u_{sea} = 0.1 m/s at which C_{in} and θ_{in} assume their highest values as far as this parameter is concerned. Under such conditions, the location of the intake port of the plant coincides with the center of the effluent expelled from the plant discharge port. At values of u_{sea} smaller or higher than u_{sea} = 0.1 m/s, the intake port falls on the edges of the discharged effluent. At u_{sea} > 0.2 m/s, the intake port almost completely escapes the influence of the effluent. The contour plots shown previously in Figs. 20.6 and 20.7, for salinity and temperature, respectively, help clarify and further explain the present results. It is interesting to note that, for a given u_{sea}, values of the dimensionless temperature are always smaller than values of dimensionless salinity. This relative reduction in temperature is attributed to net heat loss from the water surface due to temperatures elevated above the equilibrium temperature.

Table 20.4 summarizes values of dimensionless and dimensional salinity (C_{in} and c_{in}) as well as dimensionless and dimensional temperature (θ_{in} and T_{in}) at plant intake

Table 20.4 Dimensionless and dimensional salinities (C_{in} and c_{in}) and temperatures (θ_{in} and T_{in}) at plant intake for different sea current velocity-component parallel to shoreline (u_{sea})

	u_{sea} (m/s)						
	0.05	0.1	0.15	**(0.2)**	0.25	0.3	0.35
C_{in} × 100	8.197	16.06	7.6	0.6034	0.0	0.0	0.0
c_{in} × 100	5.082	5.161	5.076	5.006	5.000	5.000	5.000
θ_{in} × 100	6.954	15.37	7.299	0.5003	0.0	0.0	0.0
T_{in} (°C)	21.60	22.44	21.63	20.95	20.90	20.90	20.90

for different sea current velocity-component parallel to shoreline (u_{sea}). All other parameters are kept constant at their nominal values. The number in parenthesis and bold in the table is the nominal value of the parameter under consideration.

20.4.3 *Effect of Sea Current Velocity-Component Normal to Shoreline*

The effect of sea current velocity-component normal to shoreline (v_{sea}) is investigated while keeping the parallel component constant at the nominal value of $u_{sea} = 0.2$ m/s. All other parameters are kept at their nominal (representative) values. The values of v_{sea} investigated are:−0.05, −0.04, −0.03, −0.02, −0.01, 0.0, and 0.01 m/s. The negative value is in the direction away from the shoreline, the positive value is toward the shoreline, while the zero is the nominal value of this parameter. Representative salinity contours are presented in Fig. 20.9 for $v_{sea} = -0.04$, −0.02, and 0.01 m/s, respectively.

As clearly seen from Fig. 20.9a, with $v_{sea} = -0.04$ m/s, away from shoreline, the effluent spreads far into the sea covering a relatively large area. As a result, the intake port is significantly affected with the relative salinity at the intake of about 0.08. As v_{sea} is decreased to −0.02 m/s (Fig. 20.9b) the seaward effluent spread is reduced and the affected area becomes smaller. However, this takes place at the expense of increasing salinity close to the shoreline. The salinity at the intake port is reduced now to about 0.04 (half of the previous value) as a result of a relatively larger effluent deflection toward the shoreline. This salinity at the intake port is further reduced to about 0.001 as shown in Fig. 20.9c, for $v_{sea} = 0.01$ m/s. Under the present conditions, sea current velocity component toward the shoreline acts to reduce the effluent spread. The area of spread is now much smaller and is confined closer to the shoreline but with, of course, much higher salinity concentration. An intermediate stage between the results in Fig. 20.9b and c is that for $v_{sea} = 0.0$ with results already presented in Fig. 20.6c. Plots and tabulated values of salinity at plant intake as affected by v_{sea} are presented later.

The corresponding temperature distributions are presented in Fig. 20.10 showing the effect of v_{sea}. As mentioned earlier, these distributions resemble those of the salinity distributions but with dimensionless values that are slightly smaller.

Figure 20.11 shows the dependence of the dimensionless salinity and temperature at plant intake (C_{in} and θ_{in}, respectively) on the sea current velocity-component normal to shoreline (v_{sea}). Of course, all other parameters are kept constant at their nominal values including the resetting of u_{sea} to its nominal value of $u_{sea} = 0.2$ m/s. The −ve values of v_{sea} designate the direction away from the shoreline; such a direction for v_{sea} increases the possibility of discharge-intake port interaction. Indeed, the results show that C_{in} and θ_{in} increase with increasing v_{sea}, in this negative direction, as the intake port location becomes closer to the center of the discharged effluent. On the other side, as $v_{sea} = 0$ (the default value) or becomes

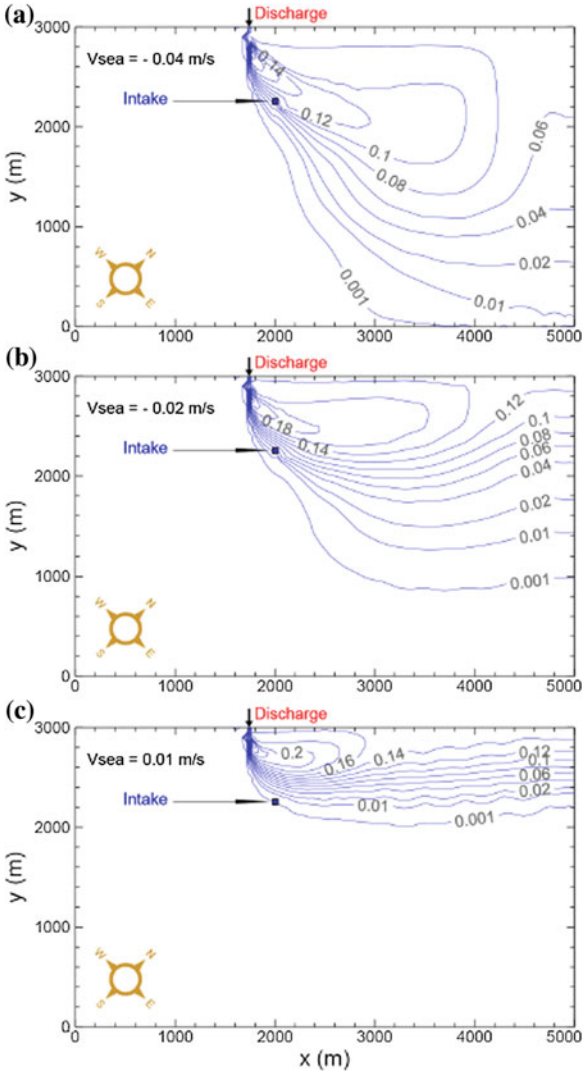

Fig. 20.9 Dimensionless salinity contours showing effect of sea current velocity component normal to shoreline (v_{sea}); **a** $v_{sea} = -0.04$ m/s, **b** $v_{sea} = -0.02$ m/s, **c** $v_{sea} = 0.01$ m/s (−ve is away from shoreline and +ve is toward shoreline)

+ve, the values of C_{in} and θ_{in} become extremely small indicating practically no discharge influence on the intake conditions.

Table 20.5 summarizes values of dimensionless and dimensional salinity (C_{in} and c_{in}) as well as dimensionless and dimensional temperature (θ_{in} and T_{in}) at plant intake for different sea current velocity-component normal to shoreline (v_{sea}). The value written in parenthesis and bold in the table is the nominal value of the parameter under consideration.

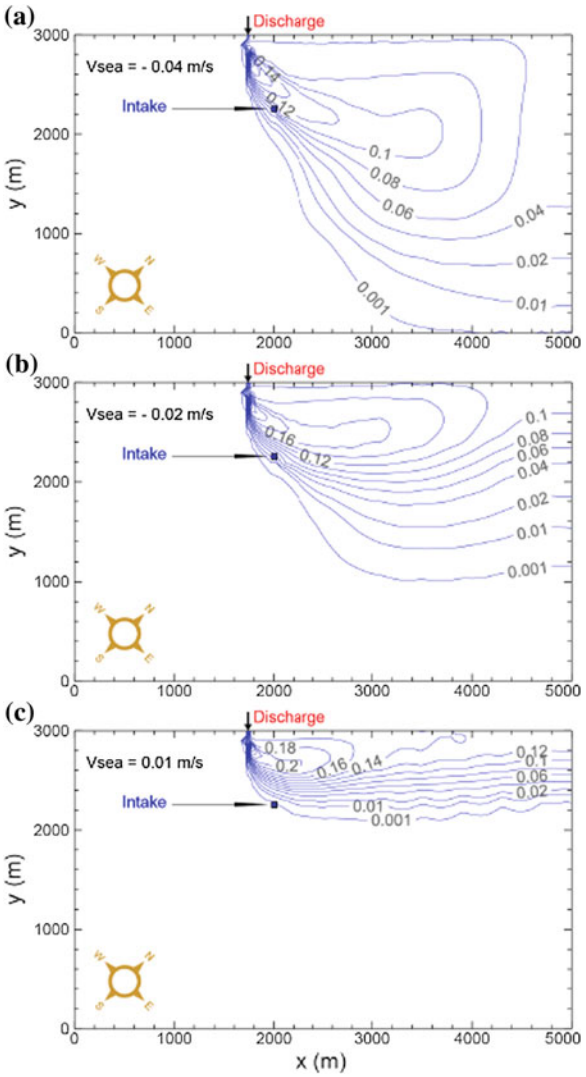

Fig. 20.10 Dimensionless temperature contours showing effect of sea current velocity component normal to shoreline (v_{sea}); **a** $v_{sea} = -0.04$ m/s, **b** $v_{sea} = -0.02$ m/s, **c** $v_{sea} = 0.01$ m/s (−ve is away from shoreline and +ve is toward shoreline)

20.4.4 Effect of Plant Desalting Capacity

The effect of varying mass flow rate of the effluent discharged from the exit port of the power/desalination plant is presented and analyzed in this section. This mass flow rate is taken to be proportional to the desalting capacity of the plant. The nominal value of the discharged mass flow rate, for a 3000 kg/s of produced desalinated water, is 55,000 kg/s.

The scenario of investigating the effect of varying plant desalting capacity is not really hypothetical since it involves possible upgrading of the current existing plant,

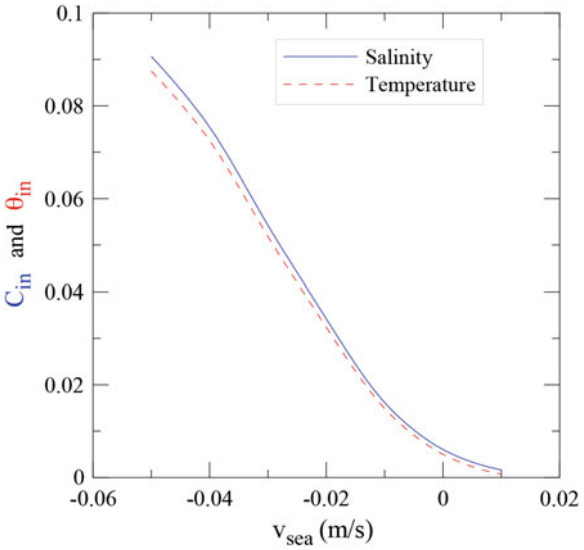

Fig. 20.11 Dimensionless salinity and temperature at plant intake port versus sea current velocity component normal to shoreline (−ve v_{sea} is in direction away from shoreline and +ve is toward shoreline)

Table 20.5 Dimensionless and dimensional salinities (C_{in} and c_{in}) and temperatures (θ_{in} and T_{in}) at plant intake for different sea current velocity-component normal to shoreline (v_{sea})

	v_{sea} (m/s)						
	−0.05	−0.04	−0.03	−0.02	−0.01	**(0.0)**	0.01
$C_{in} \times 100$	9.062	7.539	5.422	3.421	1.616	0.6034	0.1652
$c_{in} \times 100$	5.091	5.075	5.054	5.034	5.016	5.006	5.002
$\theta_{in} \times 100$	8.748	7.249	5.180	3.238	1.488	0.5003	0.0712
T_{in} (°C)	21.77	21.62	21.42	21.22	21.05	20.95	20.91

building a new plant, or working with less than full plant capacity. Therefore, the following percentages of plant desalting capacity are considered relative to the nominal capacity: 75, 100 % (the nominal case), 125, 150, 200, and 250 %. For this study, the intake and discharge flow rates were proportionally altered.

Representative temperature contours are shown in Fig. 20.12, for plant desalting capacity of 75, 125, and 200 %, respectively, with the nominal results already presented in Fig. 20.6c. The results show that with increasing plant discharge flow rate, the effluent spreads further into the sea covering a wider area. In doing so, the temperature increases in the region far away from the shoreline and decreases in the region close to the shoreline. This is attributed to increasing amount of hot discharge and increasing momentum of the issuing effluent with increasing plant desalting capacity. The increase in momentum, results in smaller deflection of effluent by the sea current and hence smaller temperature gradients in the region close to the shoreline. As seen, the intake port gets exposed to the discharged effluent with increasing plant desalting capacity. While the intake port almost

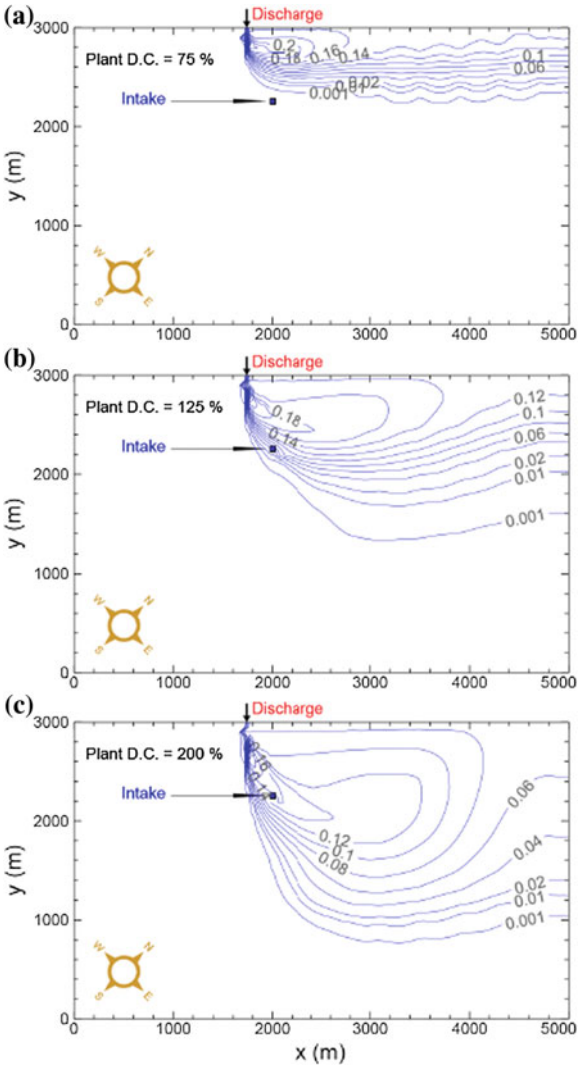

Fig. 20.12 Dimensionless temperature contours showing effect of plant desalting capacity (PDC) as a percentage of nominal capacity; **a** PDC = 75 %, **b** PDC = 125 %, **c** PDC = 200 %

completely experiences little influence from the discharge plume under the conditions in Fig. 20.12a, in Fig. 20.12c it lies directly in the path of the core of the plume under the conditions shown in Fig. 20.12c. The corresponding salinity contours, not presented here, show similar distributions to the isotherms.

Table 20.6 summarizes values of dimensional salinity (c_{in}) as well as dimensional temperature (T_{in}) at plant intake for different plant desalting capacities relative to nominal capacity. The plant desalting capacity is measured as a percentage of the plant nominal capacity (the nominal capacity being 100 %). All other parameters are kept constant at their nominal values. The value written in parenthesis and bold in

Table 20.6 Dimensional salinity (c_{in}) and temperature (T_{in}) at plant intake for different plant desalting capacities relative to nominal capacity

	Plant desalting capacity relative to nominal capacity (%)					
	75	**(100)**	125	150	200	250
$c_{in} \times 100$	5.000	5.006	5.049	5.103	5.159	5.162
T_{in} (°C)	20.9	20.95	21.37	21.90	22.45	22.47

Table 20.6 is the nominal value for the plant desalting capacity. As shown, salinity and temperature at the intake were nearly unaffected by the discharge for a plant desalting capacity <100 %, i.e. there is no noticeable discharge-intake port interaction. However, c_{in} and T_{in} increased continuously with increasing plant capacity and reached their highest values (the worst conditions) at a plant capacity of about 200 %. At the latter value, the center of the discharged effluent passes through the intake port. The contour plots for temperature shown previously in Fig. 20.12 give further clarification of the present results.

20.5 Conclusions

The present chapter presented and discussed results obtained from a numerical model for the dispersion of concentrated, heated brine in a shallow coastal region. The mathematical model was based on the shallow-water approximations in which the governing equations were depth averaged by assuming negligible variations of velocity, temperature, and salinity over the depth and by neglecting the vertical velocity component, thus rendering the problem to be two-dimensional. Appropriate boundary conditions were used.

The application was made for a desalination/power plant situated on the Arabian Gulf in KSA. The seabed topography of the coastal area in the vicinity of the plant was used in the study.

Parametric studies evaluated the effects of varying sea current magnitude and direction and plant discharge flow rates. The results were presented, for generalization, in the form of dimensionless salinity (C) and dimensionless temperature (θ). This was done by normalizing the salinity (c) and temperature (T) by reference values for the nominal seawater far away from the plant (c_{sea} and T_{sea}) and by reference values for nominal salinity and temperature at the plant discharge port (c_{dis} and T_{dis}). Contours were presented, with values of salinity and temperature in excess of nominal seawater values, which could be used to determine the extent of coastal area affected by the discharged effluent.

Possible plant discharge-intake port interactions were predicted with varying degrees of strength depending upon the various conditions. The results presented indicate such interactions and quantified values of salinity and temperature at the plant intake port (C_{in} and θ_{in}) for different scenarios. For a given set of conditions,

salinity contour shapes were shown to be very similar to those of temperature, and dimensionless salinity and temperature values were predicted to be close to each other. This indicated that the heat and mass transfer analogy was approximately valid under the present conditions. For the range of parameters considered, the following results could be summarized:

- C_{in} and θ_{in} increased from 0 (negligible discharge-intake port interaction) to 0.16 as a result of varying sea current magnitude and direction.
- C_{in} and θ_{in} increased from 0 to 0.16 as a result of increasing plant discharge flow rate.

The above values of C_{in} and θ_{in} in excess of zero, which took place under certain conditions, indicated discharge-intake port interaction, in which the plant would withdraw seawater with salinity and temperature higher than the nominal seawater values. As a result, plant thermal efficiency would decrease and energy required for desalination increase. Possible remedies include increasing distance between intake and discharge ports and/or constructing artificial partitions, to reduce short-circuiting, both of which could require substantial capital cost.

Acknowledgments This project was supported by NSTIP strategic technologies program number (08-ENV405-2) in the Kingdom of Saudi Arabia.

References

Abdul Azis, P. K., Al-Tisan, I., Al-Daili, M., Green, T. N., Ghani, A., Dalvi, I., & Javeed, M. A. (2000). Effects of environment on source water for desalination plants on the eastern coast of Saudi Arabia. *Desalination, 132*, 29–40.

Abou-Elhaggag, M. E., El-Gamal, M. H., & Farouk, M. I. (2011). Experimental and numerical investigation of desalination plant outfalls in limited disposal areas. *Journal of Environmental Protection, 2*, 828–839.

Ahmed, M., Shayya, W. H., Hoey, D., Mahendran, A., Morris, R., & Al-Handaly, J. (2000). Use of evaporation ponds for brine disposal in desalination plants. *Desalination, 130*, 155–168.

Alameddine, I., & El-Fadel, M. (2007). Brine discharge from desalination plants: A modelling approach to an optimized outfall design. *Desalination, 214*, 241–260.

Al-Barwani, H. H., & Purnama, A. (2007). Re-assessing the impact of desalination plants brine discharges on eroding beaches. *Desalination, 204*, 94–101.

Al Mutaz, I. (1991). Environmental impact of seawater desalination plants. *Environmental Monitoring and Assessment, 16*, 75–84.

Al-Sanea, S. A., Pun, W. M., & Spalding, D. B. (1980). Computation of two-dimensional elliptic flows, including heat transfer. In K. Morgan, C. Taylor, & C. A. Brebbia (Eds.), *Computer Methods in Fluids* (pp. 217–256). London: Pentech Press.

Al-Sanea, S. A. (1982). *Numerical modeling of two-dimensional shallow-water flows*. Ph.D. thesis, Department of Mechanical Engineering, Imperial College of Science and Technology, London, UK.

Al-Sanea, S. A. (1993). Computation of the flow and salinity distribution in the vicinity of discharge and intake ports of a desalination plant. Journal of King Saud University, *5*, Engineering Science, *1*, 123–140.

Al-Sanea, S. A. (2010). Computational fluid dynamics applied to free-surface flows. Lecture 4 in Course ME 596: Selected Topics in Thermo-fluids (Part 1), Department of Mechanical Engineering, King Saud University, Riyadh.

Al-Sanea, S., & Orfi, J. (2013). Environmental impact and solutions for desalination plant discharge into shallow coastal regions (215 p). Final Report, NPST-KSU, Project: 08-ENV405–2, Riyadh, KSA.

AlZahrani, A. (2013). *Energy and exergy analysis of desalination and dual purpose plants*. MSC thesis, Department of mechanical engineering, King Saud University, KSA.

Bleninger, T. (2006). Coupled 3D hydrodynamic models for submarine outfalls. In *Environmental Hydraulic Design and Control of Multiport Diffusers.* Germany: University of Karlsruhe.

Bleninger, T., & Jirka, G. H. (2010). Environmental planning, prediction and management of brine discharges from desalination plants (237 p). Final report, Middle East Desalination Research Center, MEDRC Project: 07-AS-003, Muscat, Oman.

Cerco, C. F. (1977). *Experimental and analytical study of the design of shallow cooling ponds*. MS thesis, Department of Civil Engineering, MIT, Cambridge, Massachusetts.

Cipollina, A., Bonfiglio, A., Micale, G., & Brucato, A. (2004). Dense jet modelling applied to the design of dense effluent diffusers. *Desalination, 167*, 459–468.

Danoun, R. (2007). Desalination plants: Potential impacts of brine discharge on marine life (55 p). Final Project Report, University of Sydney.

Doneker, R. L., & Jirka, G. H. (2001). CORMIX-GI systems for mixing zone analysis of brine wastewater disposal. *Desalination, 139*(1–3), 263–274. doi:10.1016/S0011-9164(01)00318-6.

Fernadez, A. L., Ferrero-Vicente, L. M., Marco-Mendez, C., Martinez- Garcia, E., Zubcoff, J., & Sanchez-Lizaso, J. L. (2012). Comparing four mixing zone models with brine discharge measurements from a reverse osmosis desalination plant in Spain. *Desalination, 286*, 217–224.

Hoepner, T. (1999). A procedure for environmental impact assessments (EIA) for seawater desalination plants. *Desalination, 124*, 1–12.

Kuipers, J, & Vreugdenhil, C. B. (1973). Calculations of two-dimensional horizontal flow. Report S 163, Part I, Delft Hydraulics Lab, Netherlands.

Lattemann, S. (2009). Protecting the marine environment. In A. Cipollina, G. Micale, & L. Rizzuti (Eds.), *Sea Water Desalination* (pp. 273–299). Berlin: Springer.

Lattemann, S., Kennedy, M., Schippers, J., & Amy, G. (2009). Global desalination situation. In I. Escobar & A. Schäfer (Eds.), *Sustainable Water for the Future* (pp. 7–39). The Netherlands: Elsevier.

Malcangio, D., & Petrillo, A. F. (2010). Modeling of brine outfall at the planning stage of desalination plants. *Desalination, 254*, 114–125.

Munoz, I., & Fernandez-Alba, A. R. (2008). Reducing the environmental impacts of reverse osmosis desalination by using brackish groundwater resources. *Water Research, 42*, 801–811.

Oliver, C. J., Davidson, M. J., & Nokes, R. I. (2013). Predicting the near field of desalination discharges in a stationary environment. *Desalination, 309*, 148–155.

Palomar, P., & Losada, I. (2011). Impacts of brine discharge on the marine environment. modelling as a predictive tool, Chapter 3. In: *Desalination, Trends and Technologies* (pp. 279–310) www.intechopen.com.

Palomar, P., Lara, J. L., & Losada, I. J. (2012a). Near field brine discharge modeling part 2: Validation of commercial tools. *Desalination, 290*, 28–42.

Palomar, P., Lara, J. L., Losada, I. J., Rodrigo, M., & Alvárez, A. (2012b). Near field brine discharge modeling part 1: Analysis of commercial tools. *Desalination, 290*, 14–27.

Patankar, S. V., & Spalding, D. B. (1972). A calculation procedure for heat, mass and momentum transfer in three-dimensional parabolic flows. *International Journal of Heat and Mass Transfer, 15*, 1787–1806.

Patankar, S. V. (1980). *Numerical Heat Transfer and Fluid Flow*. Washington, DC: Hemisphere Publishing Corporation.

Pun, W. M., & Spalding, D. B. (1977). *A general computer program for two-dimensional elliptic flows*. Report no. HTS/76/2, Department of Mechanical Engineering, Imperial College of Science and Technology, London, UK.

Purnama, A., Al-Barwani, H. H., & Al-Lawatia, M. (2003). Modeling dispersion of brine waste discharges from a coastal desalination plant. *Desalination, 155*, 41–47.

Purnama, A., & Al-Barwani, A. A. (2005). Some criteria to minimize the impact of brine discharge into the sea. *Desalination, 171*, 167–172.

Purnama, A., & Al-Barwani, H. H. (2006). Spreading of brine waste discharges into the Gulf of Oman. *Desalination, 195*, 26–31.

Rodi, W. (1978). *Turbulence models and their application in hydraulics—a state of the art review*. Report no. SFB 80/T/127, University of Karlsruhe, Germany.

Shao, D. D., Law, A. W. K., & Li, H. Y. (2008). Brine discharges into shallow coastal waters with mean and oscillatory tidal currents. *Journal of Hydro-environment Research, 2*, 91–97.

Sharqawy, M. H., Lienhard V, J. H., & Zubair, S. M. (2011). On exergy calculations of seawater with applications in desalination systems. *International Journal of Thermal Sciences, 50*, 187–196.

Spalding, D. B. (1975). Transfer of heat in rivers, bays, lakes and estuaries. THIRBLE, Report No. HTS/75/4, Department of Mechanical Engineering, Imperial College of Science and Technology, London, UK.

Zhao, D., Xue, J., Li, S., Sun, H., & Zhang, D. Q. (2011). Theoretical analyses of thermal and economical aspects of multi-effect distillation desalination dealing with high-salinity wastewater. *Desalination, 273*, 292–298.

Chapter 21
Far-Field Ocean Conditions and Concentrate Discharges Modeling Along the Saudi Coast of the Red Sea

Peng Zhan, Fengchao Yao, Aditya R. Kartadikaria, Yesubabu Viswanadhapalli, Ganesh Gopalakrishnan and Ibrahim Hoteit

Abstract An integrated modeling system is developed to simulate the far-field dispersions of concentrate discharges along the Saudi coast of the Red Sea. It comprises the Weather Research and Forecast (WRF) model for simulating the atmospheric circulations, the MIT general circulation model (MITgcm) for simulating the large-scale ocean conditions, and the Connectivity Modeling System (CMS) for tracking particle pathways. We use the system outputs and remote sensing altimetry data to study and analyze the atmospheric and oceanic conditions along the Saudi coast of the Red Sea and to conduct particle tracking experiments. The model simulations show distinctive patterns of seasonal variations in both the atmospheric conditions and the large-scale ocean circulation in the Red Sea, which are also reflected in the salinity and temperature distributions along the Saudi coast.

P. Zhan (✉) · F. Yao · A.R. Kartadikaria · Y. Viswanadhapalli · I. Hoteit
Division of Physical Sciences and Engineering, King Abdullah University of Science and Technology, Thuwal, Saudi Arabia
e-mail: peng.zhan@kaust.edu.sa

F. Yao
e-mail: fengchao.yao@kaust.edu.sa

A.R. Kartadikaria
e-mail: aditya.kartadikaria@kaust.edu.sa

Y. Viswanadhapalli
e-mail: y.viswanadhapalli@kaust.edu.sa

I. Hoteit
e-mail: Ibrahim.hoteit@kaust.edu.sa

G. Gopalakrishnan
Scripps Institution of Oceanography, University of California San Diego, San Diego, California
e-mail: ggopalak@ucsd.edu

T.M. Missimer et al. (eds.), *Intakes and Outfalls for Seawater Reverse-Osmosis Desalination Facilities*, Environmental Science and Engineering,
DOI 10.1007/978-3-319-13203-7_21

The impact of this seasonality on the far-field dispersion of concentrate discharges are illustrated in seasonal dispersion scenarios with discharging outfalls located at the northern, central and southern Saudi coasts of the Red Sea.

21.1 Introduction

The Red Sea is a marginal sea located between the Arabian Peninsula and the African continent. This long and narrow basin spans over 2000 km and connects to the Gulf of Aden through the Strait of Bab el Mandeb. The basin bifurcates into the Gulf of Aqaba and the Gulf of Suez at the northern end (Fig. 21.1). The latter connects to the Mediterranean Sea through the Suez Canal with a negligible water exchange (Sofianos et al. 2002).

The Kingdom of Saudi Arabia occupies the largest portion of coast along the Red Sea in the west of the Arabian Peninsula. Not surprisingly, the conditions of the Red Sea profoundly affect people's social and economic lives in the kingdom. In addition, isolated from the world ocean, the Red Sea serves as a sanctuary for a unique marine ecosystem and an ideal habitat for the coral reef community (Berumen et al. 2013). However, the Saudi coast is experiencing large industrial and population expansions including constructions of new cities, massive desalination plants, oil refineries and aquaculture farms. For instance, desalination of seawater, serving as a reliable and drought-proof source of local water supply, is becoming increasingly important for the Kingdom. The released brine and chemical discharges should be effectively diluted and transported into the far-field sea, otherwise, effluent discharges of wastewater or brines would adversely affect the local marine ecosystem and aquatic resources in the inshore coastal areas. It is, therefore, crucial to study and evaluate the environmental influence of such human activities on the Red Sea in order to mitigate their impacts and to optimally utilize the coastal resources.

As in any other sea, dispersion of outfall concentrate discharges in the Red Sea is controlled by two different dynamical stages. In the first stage near the outfall, the concentrate usually possesses highly negative buoyancy compared with the ambient seawater and, as a result, undergoes significant mixing and diluting. In the second stage, when the concentrate reaches a neutral buoyancy condition with the ambient seawater, the dispersion is primarily controlled by the advection and diffusion of the large-scale circulation in the Red Sea. While the dynamical modeling of the first stage calls for near-field non-hydrostatic hydrodynamic models with fine resolutions in both horizontal (in the order of tens of meters) and vertical (in the order of meters) directions, the far-field modeling of the dispersion occurring in the second stage often involves hydrostatic ocean general circulation models with relatively lower resolution (few kilometers). Because the initial dilution in the first stage also depends on the vertical stratification and currents in the ambient seawater, the large-scale circulation in the Red Sea is important for both the near-field and far-field modeling.

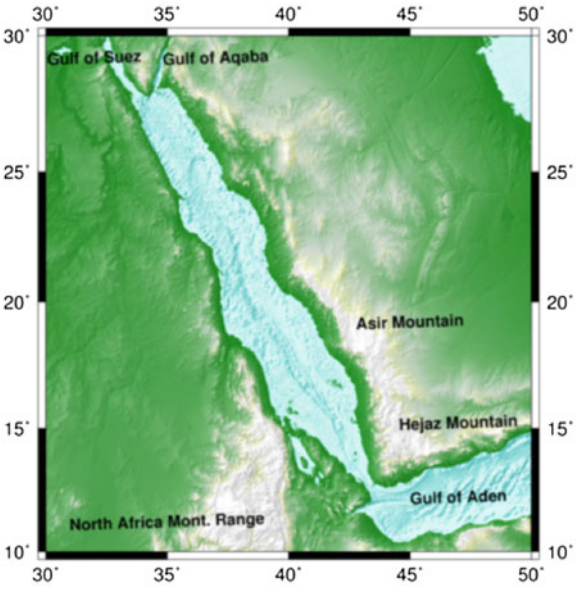

Fig. 21.1 Map of the Red Sea topography and model domain for the Red Sea MITgcm

The large-scale ocean circulation in the Red Sea is a coupled response to the atmospheric forcing and the water exchanges with the Indian Ocean through the Strait of Bab el Mandeb (Sofianos and Johns 2002). The atmospheric forcing includes surface heat flux, excessive freshwater loss due to evaporation, and wind stress. All the components of the atmospheric forcing show strong seasonal variations, driving a seasonally reversing overturning circulation in the Red Sea (Yao et al. 2014b). During winter, cold and high-salinity water is formed in the northern Red Sea due to heat loss and evaporation and is exported to the Gulf of Aden as a deep outflow, compensated by a surface inflow from the Gulf of Aden (Yao et al. 2014a). In response to the reversal of the surface winds in the Red Sea and the Arabian Sea during the summer Indian monsoon, the summer overturning circulation is strikingly reversed from the winter overturning circulation, and is composed of a surface outflow, a subsurface intrusion from the Gulf of Aden and a greatly reduced deep outflow. Despite the narrowness of the basin, the circulation in the Red Sea also exhibits strong lateral variability associated with boundary currents and meso-scale eddies throughout the year as suggested by modeling studies and satellite sea level anomaly data (Yao et al. 2014b; Zhai and Bower 2013; Zhan et al. 2014).

In this chapter, we first analyze remote sensing altimetry data to examine the large-scale background flow and the seasonal variation of sea level in the Red Sea. This would provide the basic information about the general circulation occurring in this region. We then present the development of an integrated modeling system to simulate the atmospheric conditions, the general ocean circulation, and particle dispersion, based on the atmospheric and oceanic conditions as well as their seasonalities over the Red Sea region, especially along the Saudi coast, are

described and analyzed. Using these model outputs, we conduct particles releasing experiments to illustrate the far-field dispersion of concentrate discharges under different seasonal scenarios along the Saudi coast of the Red Sea.

The remaining part of the chapter is organized as follows. Section 21.2 analyzes the sea level anomalies and absolute dynamic topography remote sensing data. Section 21.3 introduces the integrated modeling system. The simulated atmospheric and oceanic conditions are described in Sect. 21.4. Section 21.5 presents the results of far-field concentrate discharges experiments released along the Saudi coast. Section 21.6 concludes with a summary and a discussion of future work.

21.2 Sea Level Variations

The currents in the meso- and large-scale ocean circulation are reflected by the sea level through the geostrophic relationship. In this section, we analyze the Archiving Validation and Interpretation of Satellite Data in Oceanography (AVISO) altimetry and discuss the seasonal variations of sea level in the Red Sea, focusing on the Saudi coast.

Sea level anomalies (SLA) represent the variations of the sea surface height relative to the mean sea surface (MSS). We use the AVISO merged product of TOPEX/POSEIDON, Jason-1, Envisat and European Research Satellite (ERS) (Dibarboure et al. 2008), computed with the MSS CNES-CLS-2011 referenced to a 20-year period from 1993 to 2012, available at ftp://ftp.aviso.altimetry.fr/global/delayed-time/grids/. AVISO also provides the absolute dynamic topography (ADT), from which the mean dynamic topography (MDT) which can be obtained as MDT = ADT − SLA. Serving as the reference surface to ADT, the MDT represents the sea level variation associated with the stationary components (long-term mean currents) of ocean dynamics. Our analyses are based on monthly data with a resolution of 1/4° from January 1993 to December 2012.

In the Red Sea, the MDT increases northward from the Strait of Bab el Mandeb up to ∼18°N, before gradually decreasing all the way to the north as shown in Figs. 21.2 and 21.3. The sea level bulge in the central Red Sea was attributed to the surface winds pattern by Sofianos and Johns (2001). The different slope of MDT between the southern and northern Red Sea indicates opposite geostrophic currents flowing westward south of ∼18°N and eastward in the central and northern Red Sea. In the central basin between ∼18°N and ∼24°N, where the slope is relatively steep, the flow exhibits a larger geostrophic velocity, up to 0.2 m/s. This mean stationary eastward geostrophic current in the northern and central Red Sea transports considerable water eastward across the basin to the Saudi coast.

Superimposed on the background flow, eddies and boundary currents also play a key role in transporting kinetic energy, heat, and biogeochemical particles within the basin of the Red Sea. These time-varying dynamics are generally more energetic than the background flow and they may even dominate the structure of the circulation. Information about their features cannot be derived from MDT, but from SLA.

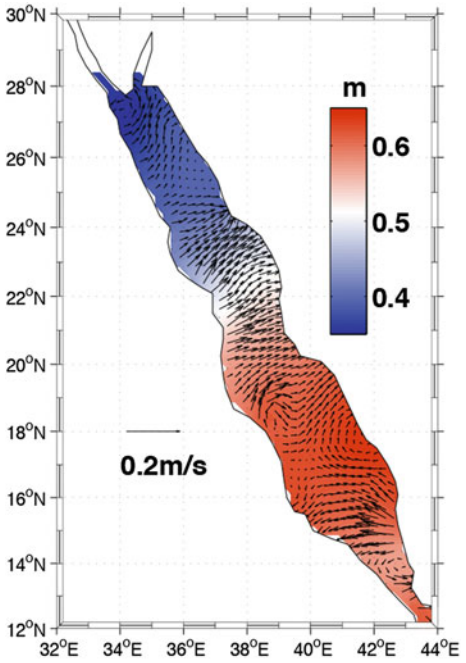

Fig. 21.2 The MDT and the associated geostrophic current

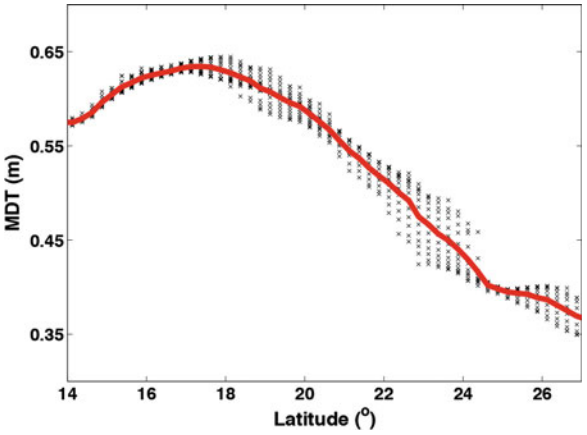

Fig. 21.3 The scatter plot of MDT as a function of latitude (*black cross*) and its zonal mean (*red solid curve*)

To study both the temporal and the spatial patterns of the SLA in the Red Sea, the 20-year monthly mean AVISO SLA data are analyzed using an Empirical Orthogonal Functions (EOF) analysis. The EOF analysis extracts the dominant modes from a spatio-temporal dataset according to their overall variance contributions (Emery and Thomson 2001). The EOF modes can be used to analyze the spatial variability of SLA, while the time series of their principal components (PCs) quantify their evolution over time.

The EOF analysis of SLA in the Red Sea shows that the first mode accounts for 89 % of the total variance, indicating the absolute dominance of the leading mode. As shown Fig. 21.4a, the first EOF mode of the monthly SLA is positive throughout the entire Red Sea basin. The uniform sign suggests that the SLA would rise and fall in phase over the entire basin of the Red Sea, with remarkable eddy variability in the central and northern Red Sea. Figure 21.4b suggests that the climatological mean PC time series of the first EOF mode exhibits a prominent seasonal cycle, with a peak in January and a trough in August. The sign shifts that occur in May-June (from positive to negative) and in October–November (from negative to positive) mark the shift of anomaly relative to the MDT. Given that the first EOF mode is positive across the basin, the SLA is predominantly higher/lower than the MDT during winter/summer over the entire Red Sea. Larger variability of SLA is observed along the Saudi coast than along the African coast, with the largest annual variation of $\sim$0.4 m appearing in the central basin at about 19°N. This seasonal reversal of the tilting of SLA implies that the associated geostrophic current is generally northward during winter and southward during summer.

The variations of SLA in the Red Sea can be largely attributed to the seasonal differences in the atmosphere. The Red Sea basin is indeed separated into two parts according to the wind seasonal regimes (Jiang et al. 2009). In the northern part of the basin the wind blows from the northwest all around the year. However, the northeast Indian Monsoon controls the surface wind distinctively over the basin south of $\sim$19°N, reversing from northwesterly during summer (June–October) to southeasterly during winter (November–May). The variation of SLA in the southern

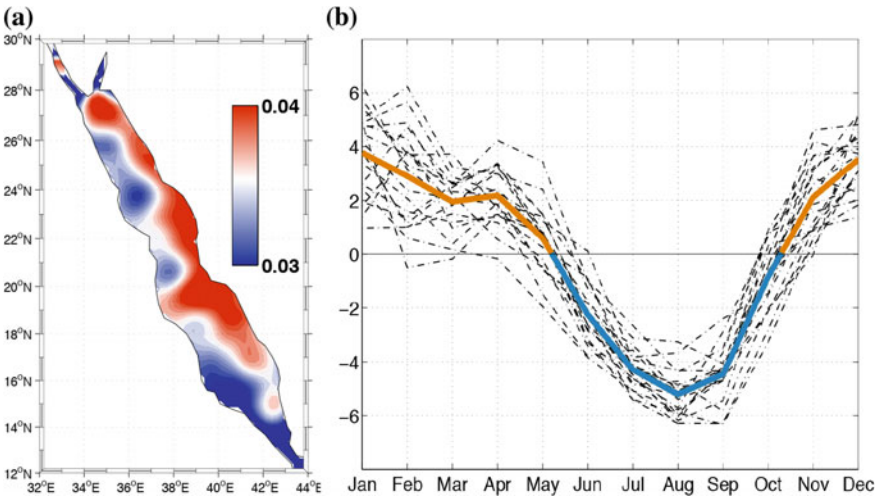

Fig. 21.4 **a** The first EOF mode of the monthly SLA. **b** Monthly standard deviations of the PC time series associated with first EOF mode. The *black dot curves* represent the time series in each year from 1993 to 2012, and the *solid colored curve* represents the climatological mean during that period, where the *yellow*, *blue parts* show the positive, negative period, respectively

Red Sea could partly be explained by the Ekman transport associated with the seasonally reversing winds. The southeasterly winds during winter (northwesterly during summer) transports water to the east (west) and cause a higher SLA along the Saudi (African) coast. The alternation of wind patterns over the southern basin agrees remarkably well with the first PC of SLA. Similarly, in the northern Red Sea, the northwesterly winds during summer leads to a western transport causing a higher SLA along the African coast. Nevertheless, the higher SLA along the Saudi coast during winter cannot be easily explained as it contradicts with the westward Ekman transport associated with the northwesterly winds. One can therefore expect a northward compensation boundary current along the Saudi coast during winter, which is reported by Yao et al. (2014a) from a model point of view.

21.3 Modeling System

This section describes the integrated modeling system that has been developed to simulate the atmospheric and oceanic conditions, and the resulting concentrate discharges in the Red Sea. The system consists of the Weather Research and Forecasting (WRF) model (Michalakes et al. 2005), the regional nested MIT general circulation model (MITgcm) (Marshall et al. 1997a, b), and the Connectivity Modeling System (CMS) (Paris et al. 2013).

21.3.1 Atmospheric Model—WRF

The atmospheric conditions are simulated using the Advanced Research WRF (ARW) (Skamarock et al. 2008). The model is configured over the Red Sea and is nested within a larger domain covering the central Middle East and North Africa. The horizontal resolution is 30 km for the coarse resolution model and 10 km for the finer resolution model, both configured with 35 vertical levels. Initial and boundary conditions for WRF are obtained from the National Center for Environmental Prediction (NCEP) Final Analysis (FNL) product. Observations available from the Atmospheric Data Project (ADP) are assimilated into WRF using a 3-Dimensional Variational (3DVAR) data assimilation technique. An atmospheric reanalysis product is generated for the Red Sea using this assimilative WRF by daily initializing the model at 12 UTC using the consecutive integration method (Langodan et al. 2014; Lo et al. 2008). The ADP observations are assimilated every 6-h for a period of 36 h using the respective WRF forecast as background in the next assimilation cycle. The first 12-h simulation serves as the model spinning-up period, and is thus neglected. For better representation of land-sea contrast in WRF over coastal regions, we modified the lower boundary conditions by replacing the

coarse-resolution SST from FNL with high-resolution SST from the Real-Time Global High-Resolution (RTG-HR). The model physics adopted in WRF are the same as those in Jiang et al. (2009).

21.3.2 Ocean Model—MITgcm

The large-scale circulation in the Red Sea is simulated using the MITgcm. The MITgcm is a primitive-equation oceanic general circulation model solving the Navier-Stokes equations under the Boussinesq approximation. The model equations are discretized in z coordinates in the vertical direction and, for each level, are configured in a staggered Arakawa C-grid. The MITgcm includes both non-hydrostatic and hydrostatic formulations. It is implemented here in hydrostatic mode with an implicit free surface. The model domain extends from 10°N to 30°N and from 30°E to 50°E (Fig. 21.1), covering the entire Red Sea basin, the Gulf of Aqaba and the Gulf of Suez in the north end, as well as the Gulf of Aden, where the only (eastern) open boundary is located. The model has a horizontal resolution of 4 km and 50 vertical layers with thicknesses ranging between 4 m at the sea surface up to 300 m at the sea bottom. The model topography is generated from the General Bathymetric Chart of the Ocean (Ioc 2003). The model is integrated from January 2000 to December 2010, forced with the 3-hourly Red Sea WRF atmospheric fields, including momentum, heat and fresh water fluxes. The eastern boundary is nested within a large-domain coarser MITgcm configured for the Arabian Peninsula including the Arabian Sea. The results between 2009 and 2010 are presented in this study.

21.3.3 Connectivity Model—CMS

Forward simulation of passive particles is widely used to estimate a range of likely water concentrate discharges in the ocean (Haza et al. 2007; Piterbarg 2001; Veneziani et al. 2004, 2005). This is a challenging problem for the Red Sea because of the seasonally varying wind and current conditions. In this study, the trajectories of individual-based particles from pre-specified point source regions are simulated using the CMS. CMS is a multi-scale probabilistic model of particle dispersal based on a stochastic Lagrangian framework. The Lagrangian formulation for particle dispersion is a powerful tool to study and analyze the hydrodynamic behavior of fluids (Hegarty et al. 2013; Stohl et al. 2005). Given a velocity field, often resulting from a general circulation model, the CMS calculates particle locations and keeps track of their pathways following a multiple and multi-grid approach.

CMS can be used to simulate phenomena such as advection, dispersion and retention. It could be configured to distinguish the particles that either settle on the topography or swim away, and therefore may be beneficial for a broad range of

applications, ranging from the dispersion of contaminant plumes from discharges and deep-water ventilation, to larval migrations and probability of population connectivity. In this study, the trajectories of passive particles are calculated with CMS based on daily averaged 3-Dimensional velocity fields as simulated by the Red Sea MITgcm.

21.4 Simulated Atmospheric and Oceanic Conditions

This section first describes the key features of the atmospheric conditions along the Saudi coast based on the WRF simulation results. This is followed by an analysis of the large-scale ocean circulation and hydrographic properties in different seasons in the Red Sea as simulated by the MITgcm.

21.4.1 Atmospheric Conditions

To describe the seasonal variability of the general atmospheric conditions over the Red Sea, especially along the Saudi coast, Hovmoller diagrams of the surface winds and surface air temperature are plotted based on the WRF outputs.

As shown in Fig. 21.5, the wind field over the Saudi coast exhibits considerable seasonality. In summer (from June to October), northwesterly winds originated from the Mediterranean region persist along the Saudi coast. In winter (from November to April), the region north of ~20°N is dominated by northwesterly winds, forming a convergence zone at about 19°N with the topographically diverted southeasterly winds blowing from through the Gulf of Aden. These converging winds funnel out through the Tokar gap. It is reported that the strength of the wind

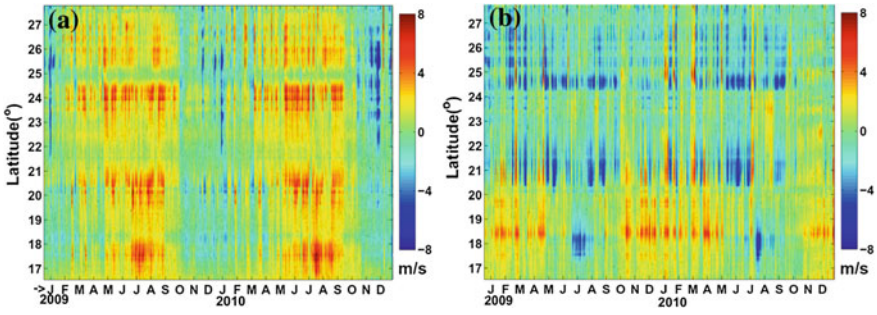

Fig. 21.5 **a** The Hovmoller diagram of the zonal surface winds along the Saudi coast of the Red Sea. **b** The hovmoller diagram of the meridional surface winds along the Saudi coast of the Red Sea

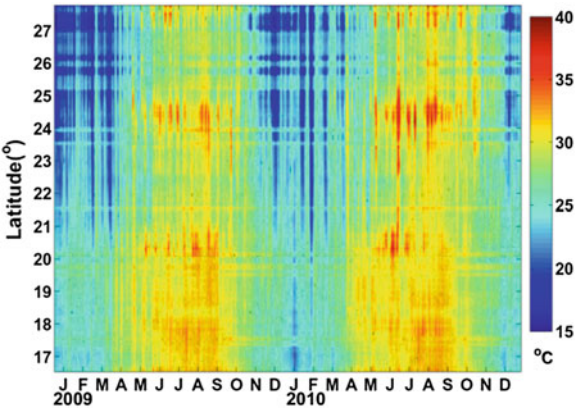

Fig. 21.6 The Hovmoller diagram of the surface air temperature along the Saudi coast of the Red Sea

and its direction depends on the seasonal movement of the Inter Tropical Convergence Zone (ITCZ) (Jiang et al. 2009).

The orography has a profound influence on the local dominant wind regimes (Jiang et al. 2009; Ralston et al. 2013). The Red Sea is indeed surrounded by high mountain ranges that constrain the winds to blow along the axis of the basin, except for some gaps where valleys cutting across the mountain ridges generate unique local wind flows. Intense across-basin winds (Fig. 21.5) are associated with mountain gaps located at latitudes 23.5–24.5°N, 20–21°N and 17–18°N. These wind jets could reach up to 15 m/s, and transport a large amount of dust towards the Arabian Peninsula during summer and bring moist subtropical air towards the Southern Sudan region during winter.

Figure 21.6 shows that the surface air temperature also exhibits an obvious seasonal cycle along the Saudi coastline of the Red Sea. The air temperature between November and April exhibits cooler patterns than the summer months throughout the whole coastline, with generally a northward decreasing trend. Apart for the latitudinal variation of heat flux, the tropical monsoonal air transported by the southeasterly winds could be also responsible for the warm features along the southern Saudi coast during the winter. The temperature in summer exhibits multiple peaks (≥36 °C) at 17–18°N, 20–21°N, and 24–25°N. These locations correspond remarkably well with the mountain gaps, through which across-basin African and Arabian hot wind jets blow. Overall, Figs. 21.5 and 21. 6 reveal that local wind circulation has a significant influence on the surface temperature distribution.

21.4.2 General Circulation in the Red Sea

Overall, the large-scale circulation and vertical structure in the Red Sea manifest a complex pattern that varies seasonally, latitudinally and longitudinally. This subsection describes the typical winter and summer surface circulations along three

zonal sections located in the northern, central and southern Red Sea as simulated by the MITgcm. This provides relevant information for the far-field modeling of concentrate discharges along the Saudi coast.

The winter surface circulation for February 2009 is displayed in Figs. 21.7a, b, and the vertical sections at latitudes 27° 20′N, 21° 30′N, and 16° 50′N are depicted in Fig. 21.8. As the upper branch of the overturning circulation, the winter surface current field in the Red Sea is characterized by an intruding low-salinity inflow from the Gulf of Aden. The inflow initially appears as a western boundary current but is unidentifiable north of 20°N, where a chain of alternating meso-scale eddies dominate. Saline (∼40 psu) and cold (∼22 °C) water is found in the northern basin, where the sinking in the winter overturning circulation occurs as shown in the climatological results in Yao et al. (2014b). As the surface density gradually increases towards the north, the vertical structures across the basin show a general trend of decrease in stratification, with an almost uniform vertical structure in salinity and temperature appearing in the northern section. In each vertical section, the stratification around the Saudi coast is weak as suggested by the almost vertical isopycnals, but the stratification becomes more evident along the African coast, particularly in the southern Red Sea, where the isopycnals tilt upward to the west.

As the surface heat flux changes from cooling to warming and the summer Indian monsoon is established in the region, the surface circulation and vertical structure in the Red Sea from June to September differ drastically from the winter

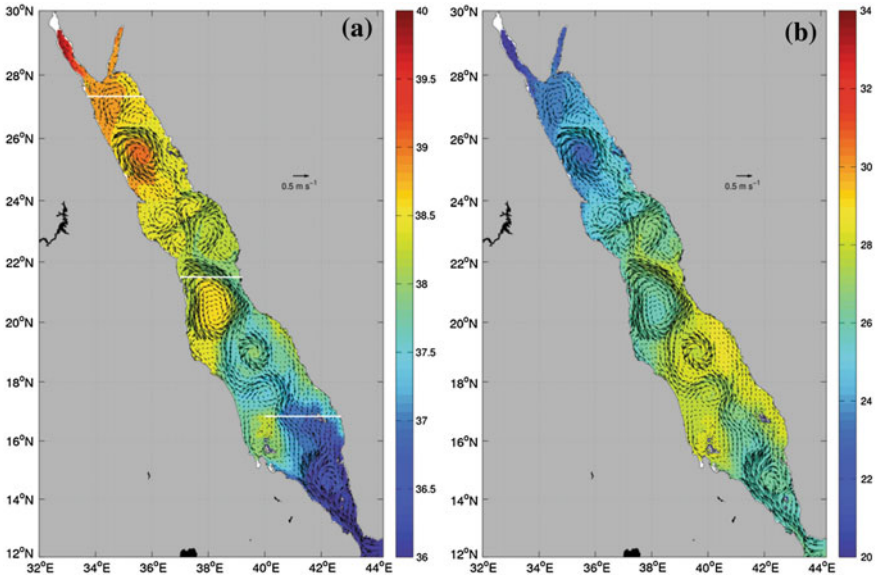

Fig. 21.7 **a** Surface current and salinity fields for the February 2009 MITgcm model results. The *white lines* denote the locations of the vertical sections across the basin. **b** Surface current and temperature fields for the February 2009 MITgcm model results

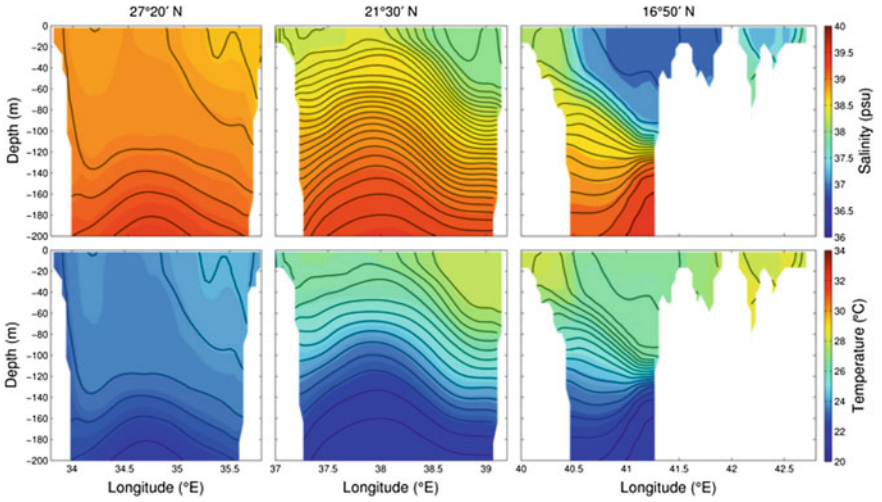

Fig. 21.8 Vertical sections of salinity and temperature in the northern, central and southern Red Sea for the February 2009 MITgcm results. Also plotted are the contours of potential density with a interval of 0.2 kg m^{-3}. The contour intervals of the locations of each section are donated in Fig. 21.7a

condition (Figs. 21.9a, b and 21.10). The surface currents in the Red Sea reverse to a southward outflow that increases the surface salinity in the southern basin. The surface water is greatly warmed up in the entire basin, with a maximum temperature of about 34 °C. The meso-scale eddies in the Red Sea appear more organized than in winter, and a strong anti-cyclonic eddy emerges around 18°N as a result of the Tokar Jet blowing from the African coast (Zhai and Bower 2013). In contrast to the winter season, the surface heating during summer re-establishes or enhances the vertical stratification in the Red Sea, and the isopyncals at the central and southern section tend to tilt upward to the east. This structure is associated with coastal upwelling driven by the northwesterly surface winds during summer (Fig. 21.9). In the southern section, the subsurface intrusion is manifested as fresh and cold water along the Saudi coast at a depth of about 100 m.

Complete seasonal cycles of the surface hydrographic properties along the Saudi coast are shown in Fig. 21.11. The seasonal cycle of the surface salinity closely corresponds to the seasonal reversal of the surface circulation. From October to May, the surface salinity along the Saudi coast is gradually freshened by the surface inflow with the salinity front retreating to the north. From June to September, the high-salinity water in the north is advected towards the south, causing a substantial salinity increase along the Saudi coast. In contrast, the seasonal pattern of the surface temperature is more of a response to the seasonal heat flux over the surface of the Red Sea, and two contrasting seasonal regimes can be recognized, with the coldest surface temperature reached in February in the northern end and the warmest in September between 14 and 18°N.

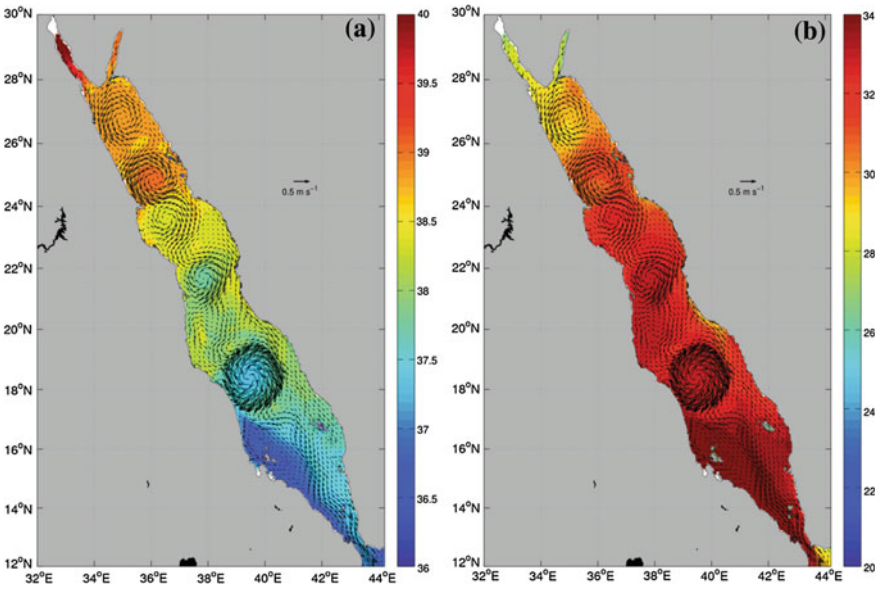

Fig. 21.9 **a** Surface current and salinity fields for the August 2009 MITgcm model results. **b** Surface current and temperature fields for the August 2009 MITgcm model results

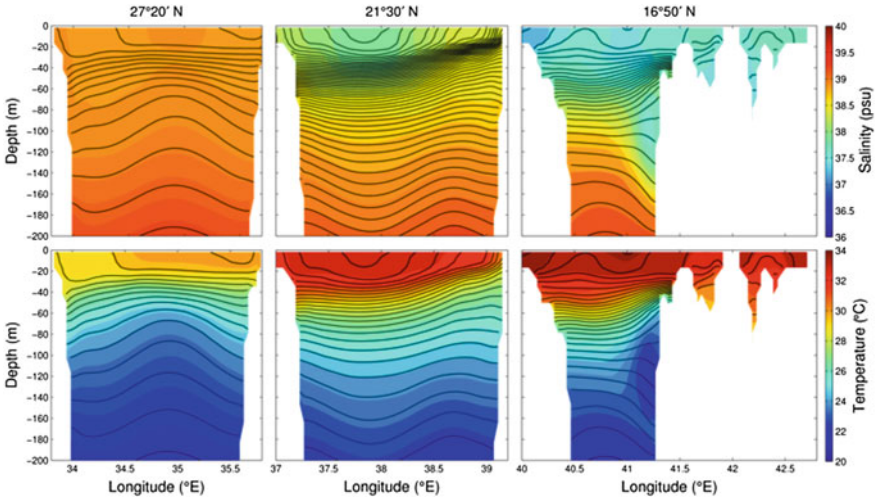

Fig. 21.10 Same as in Fig. 21.8, except for the results in August 2009

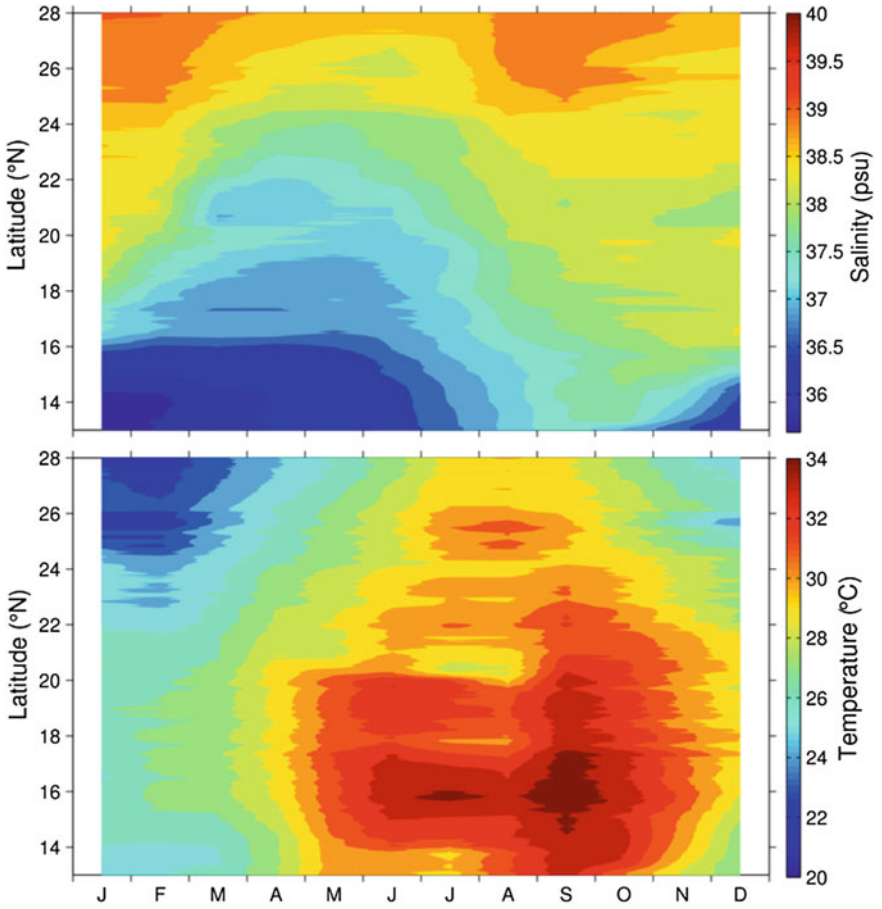

Fig. 21.11 Seasonal cycles of salinity (*top*) and temperature (*bottom*) distributions along the Saudi coast in the 2009 MITgcm results

21.5 Dispersion Experiments and Results

To evaluate the water concentrate discharges situation in the far-field under the Red Sea seasonal conditions, the CMS is implemented based on the 3-dimensional velocity fields obtained from the 4-km Red Sea MITgcm, and the results from 2009 to 2010 are presented. The particles are released as ensembles from polygons offshore of three main Saudi industrial cities along the Red Sea coast: Duba (27.3439°N, 35.6931°E), Jeddah (21.3231°N, 39.0985°E) and Jizan (16.8625°N, 42.5463°E), on June 5th 2009 for the summer scenario and on December 5th 2009 for the winter scenario. Each simulation was run offline for 150 days with daily averaged outputs from MITgcm.

As can be seen from Figs. 21.12 and 21.13, the particles released offshore of Duba in summer are trapped by a cyclonic eddy that flows counterclockwise in the northern end of the Red Sea. It takes about one month for the particles to move from Duba to the western side. The particle trajectories exhibit weak dispersion during the first two months after being released then gradually expand while sinking down from the African coast to the interior of the northern basin. In winter, the particles released offshore of Duba are transported counterclockwise along the northern coast. Some particles enter the Gulf of Aqaba and the Gulf of Suez, but the majorities are transported to the west and move southward along the African coast with rapid sinking reaching depths over 200 m or more. This area was also reported as the region where the major water sinking in the Red Sea overturning circulation occurs (Yao et al. 2014b).

Figure 21.14 suggests that some particles released offshore of Jeddah in summer meander towards the northern end of the basin where they sink down into depths over 120 m. Other particles are trapped into an eddy in the central basin and circulate locally while sinking to the deep layers. These results suggest the possibility of substantial long-distance advection for the particles released in the summer from Jeddah. According to Fig. 21.15, the particles released offshore of Jeddah in winter remain in the shallow water and flow northward following a narrow pathway until ~26°N, where they get trapped in a complex eddy system that amplifies the diffusion of particles. This reinforces mounting evidences that eddies play a crucial role in transporting concentrate discharges in the Red Sea.

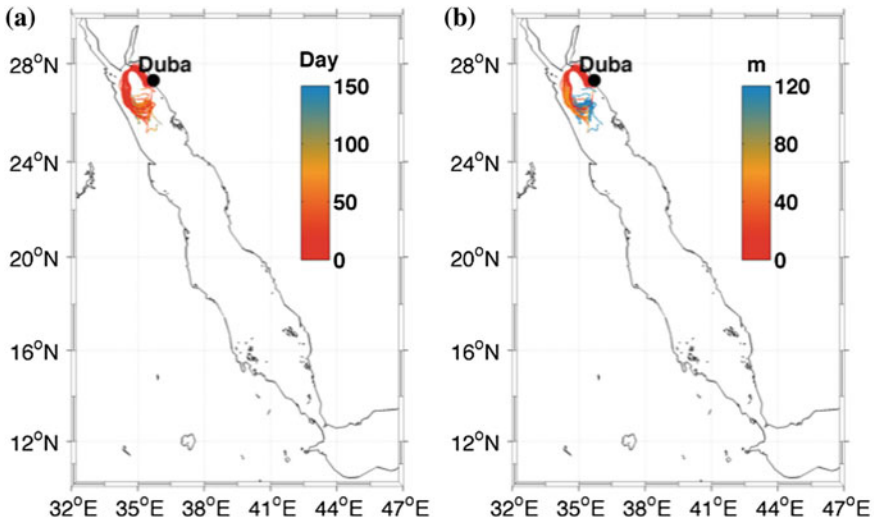

Fig. 21.12 The trajectories of particles released offshore of Duba on June 5th 2009. The *black dot* shows the releasing location and the lines depict particle trajectories with color representing **a** number of days after releasing and **b** depth, respectively

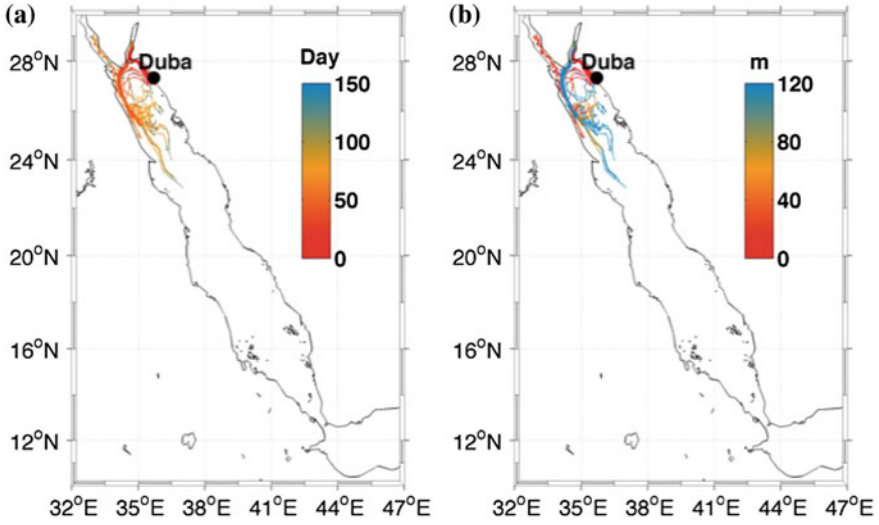

Fig. 21.13 Same as in Fig. 21.12, except for the trajectories of particles released offshore of Duba on December 5th 2009

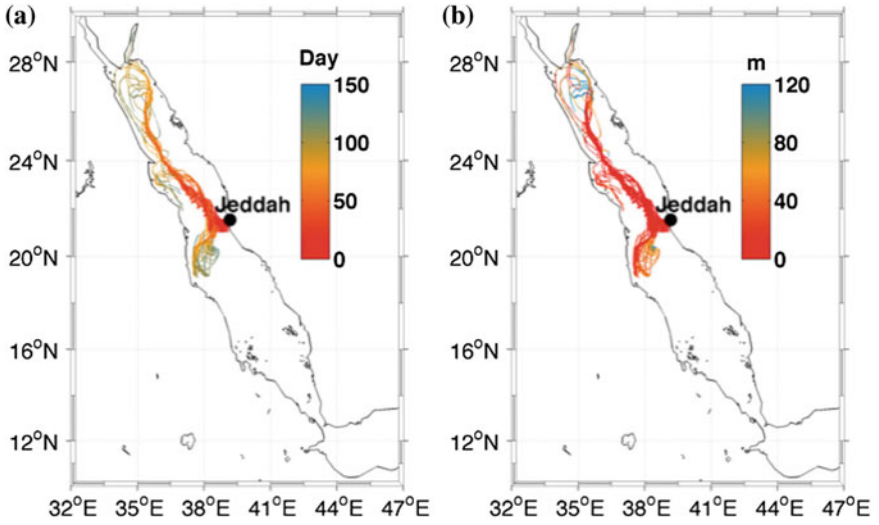

Fig. 21.14 Same as in Fig. 21.12, except for the trajectories of particles released offshore of Jeddah on June 5th 2009

The particles released in the Red Sea may even affect regions outside the basin. As can be seen from Fig. 21.16, the particles released offshore of Jizan in summer remain clustered and flow with the southward current along the Yemeni coast. After they reach the Gulf of Aden, some of the particles flow eastwardly along the

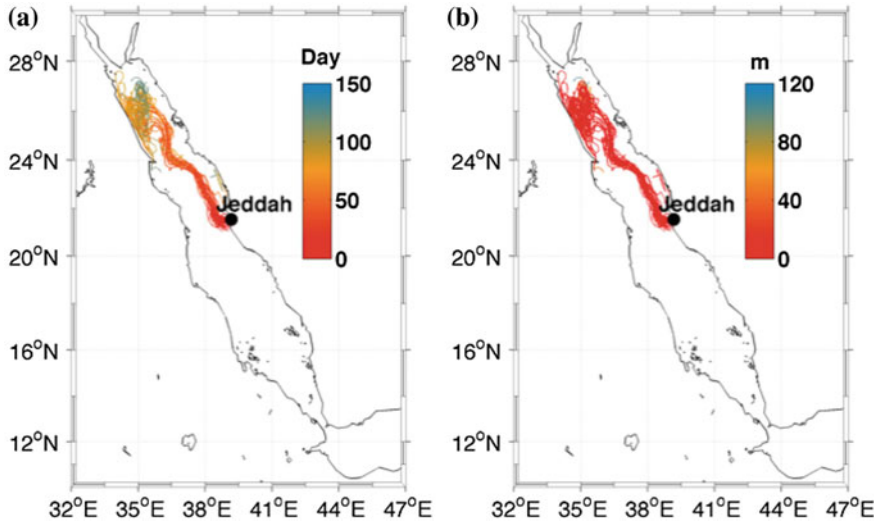

Fig. 21.15 Same as in Fig. 21.12, except for the trajectories of particles released offshore of Jeddah on December 5th 2009

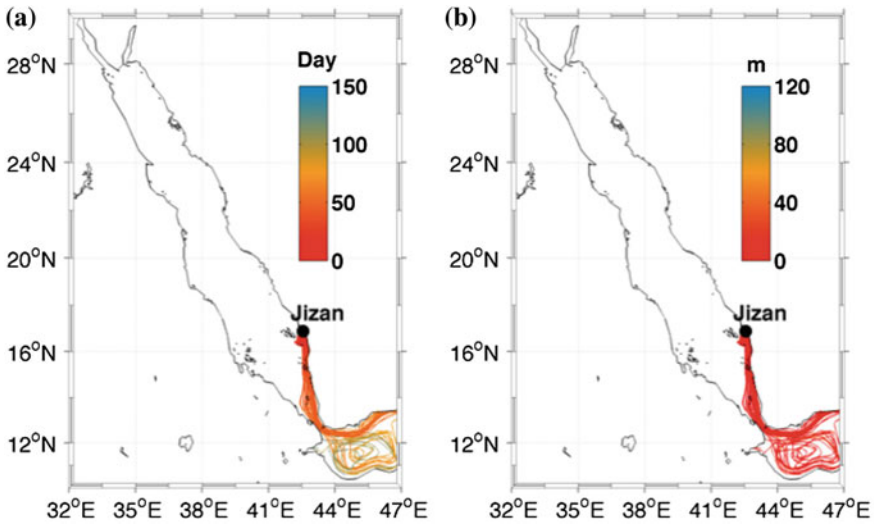

Fig. 21.16 Same as in Fig. 21.12, except for the trajectories of particles released offshore of Jizan on June 5th 2009

southern Yemeni coast, and others are trapped in a cyclonic eddy located right outside the Strait of Bab el Mandeb. No obvious sinking is occurring for these particles. In contrast, the particles released offshore of Jizan in winter (Fig. 21.17) move northward along the Saudi coast before they get trapped by an eddy located at

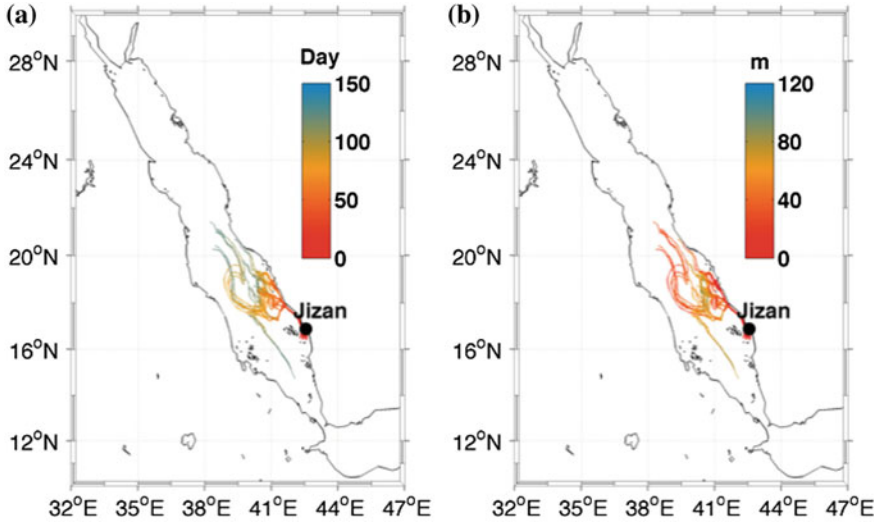

Fig. 21.17 Same as in Fig. 21.12, except for the trajectories of particles released offshore of Jizan on December 5th 2009

$\sim$18°N, where a small portion sinks down to a depth of about 50 m and then are advected to the south. The remaining particles in the upper layers meander towards the north, and then gradually spread over the central basin.

21.6 Summary and Discussion

This chapter examined the dispersion of concentrate discharges along the Saudi coast under the complex seasonal atmospheric and oceanic conditions in the Red Sea. The analysis of remote sensing altimetry data revealed a dominant eastward stationary background flow in the Red Sea basin. The sea level exhibits a significant seasonal cycle, with the Saudi coast subject to a larger sea level variation than the African coast. In addition to the observations, we have presented an integrated modeling system for the Red Sea to study the atmospheric and oceanic circulations, focusing on the Saudi coast, and to simulate particles discharges under different seasonal scenarios. The general near-surface winds over the Red Sea are orographically steered to flow along the main axis of the basin due to the high mountain ranges surrounding the basin, with significant seasonal variations. The seasonal variations of atmospheric forcing and water exchanges with the Gulf of Aden determine the seasonal hydrodynamics features of the Red Sea, including pronounced eddy variability, stratification distribution, and overturning circulation. The patterns of the particle trajectories significantly vary with seasons due to the reversal of the seasonal circulation. The far-field simulations of particle trajectories

suggest that boundary currents and eddies play a crucial role in spreading the concentrate discharges from the Saudi coastal regions into the open sea. Our results suggest that eddies and boundary currents may have a great influence on transporting kinetic energy, heat, and biogeochemical particles in this long and narrow basin. Moreover, the distinct seasonal overturning circulation may also affect the coastal mixing and marine productivity. These important factors will be investigated in future studies.

An extension of this modeling system is to couple both near-field and far-field simulations. To achieve the near-field first-stage simulation, the modeling system needs to be configured with the non-hydrostatic mode and much finer resolution to accurately evaluate the dispersal distances of particulate and concentrate discharges, and to provide a framework for evaluating what aspects of the circulations influence the most the distribution and transport of the particles. Aside from tracking the particles trajectories, monitoring the evolution of tracers and concentrations distributions is also of great importance. We will extend the capabilities of our modeling system to simulate and investigate more aspects of potential discharges impacts on the coastal ecosystem of the Red Sea.

Acknowledgments The research reported in this publication was supported by the King Abdullah University of Science and Technology (KAUST).

References

Berumen, M. L., et al. (2013). The status of coral reef ecology research in the Red Sea. *Coral Reefs, 32*(3), 737–748. doi:10.1007/S00338-013-1055-8.

Dibarboure, G., Lauret, O., Mertz, F., Rosmorduc, V., & Maheu, C. (2008). SSALTO/DUACS user handbook:(M) SLA and (M) ADT near-real time and delayed time products. *Rep. CLS-DOS-NT, 6*, 39.

Emery, W. J., & Thomson, R. E. (2001). *Data analysis methods in physical oceanography* (2nd ed.). Amsterdam: Elsevier.

Haza, A. C., Piterbarg, L. I., Martin, P., Ozgokmen, T. M., & Griffa, A. (2007). A Lagrangian subgridscale model for particle transport improvement and application in the Adriatic Sea using the Navy Coastal Ocean Model. *Ocean Modelling, 17*(1), 68–91. doi:10.1016/J.Ocemod.2006.10.004.

Hegarty, J., Draxler, R. R., Stein, A. F., Brioude, J., Mountain, M., Eluszkiewicz, J., et al. (2013). Evaluation of Lagrangian particle dispersion models with measurements from controlled tracer releases. *Journal of Applied Meteorology and Climatology, 52*(12), 2623–2637. doi:10.1175/Jamc-D-13-0125.1.

Ioc, I. (2003). *BODC, 2003. Centenary edition of the GEBCO Digital Atlas, published on CD-ROM on behalf of the Intergovernmental Oceanographic Commission and the International Hydrographic Organization as part of the general bathymetric chart of the oceans*. Liverpool, United Kingdom: British Oceanographic Data Centre.

Jiang, H., Farrar, J. T., Beardsley, R. C., Chen, R., & Chen, C. (2009). Zonal surface wind jets across the Red Sea due to mountain gap forcing along both sides of the Red Sea. *Geophysical Research Letters, 36*(19), L19605. doi:10.1029/2009GL040008.

Langodan, S., Cavaleri, L., Viswanadhapalli, Y., & Hoteit, I. (2014). The Red Sea: A natural laboratory for wind and wave modeling. *Journal of Physical Oceanography*. Accepted with ref no: JPO-D-13-0242.

Lo, J. C. F., Yang, Z. L., & Pielke, R. A. (2008). Assessment of three dynamical climate downscaling methods using the weather research and forecasting (WRF) model. *Journal of Geophysical Research*: *Atmospheres*, *113*(D9).

Marshall, J., Adcroft, A., Hill, C., Perelman, L., & Heisey, C. (1997a). A finite-volume, incompressible Navier Stokes model for studies of the ocean on parallel computers. *Journal of Geophysical Research: Oceans, 102*(C3), 5753–5766. doi:10.1029/96jc02775.

Marshall, J., Hill, C., Perelman, L., & Adcroft, A. (1997b). Hydrostatic, quasi-hydrostatic, and nonhydrostatic ocean modeling. *Journal of Geophysical Research: Oceans, 102*(C3), 5733–5752. doi:10.1029/96jc02776.

Michalakes, J., Dudhia, J., Gill, D., Henderson, T., Klemp, J., Skamarock, W., et al. (2005). The weather research and forecast model: Software architecture and performance. *Use of High Performance Computing in Meteorology*. 156–168, doi:10.1142/9789812701831_0012.

Paris, C. B., Helgers, J., Van Sebille, E., & Srinivasan, A. (2013). Connectivity modeling system: A probabilistic modeling tool for the multi-scale tracking of biotic and abiotic variability in the ocean. *Environmental Modelling and Software, 42*, 47–54.

Piterbarg, L. I. (2001). Short-term prediction of Lagrangian trajectories. *Journal of Atmospheric and Oceanic Technology, 18*(8), 1398–1410. doi:10.1175/1520-0426(2001)018<1398:Stpolt>2.0.Co;2.

Ralston, D. K., Jiang, H. S., & Farrar, J. T. (2013). Waves in the Red Sea: Response to monsoonal and mountain gap winds. *Continental Shelf Research, 65*, 1–13. doi:10.1016/J.Csr.2013.05.017.

Skamarock, W., Klemp, J., Dudhia, J., Gill, D., Barker, D., Dudha, M., et al. (2008). A description of the advanced research WRF ver 30. Technical Note. NCAR/TN-475+STR. 113.

Sofianos, S. S., & Johns, W. E. (2001). Wind induced sea level variability in the Red Sea. *Geophysical Reseach Letters, 28*(16), 3175–3178. doi:10.1029/2000gl012442.

Sofianos, S. S., & Johns, W. E. (2002). An oceanic general circulation model (OGCM) investigation of the Red Sea circulation, 1. Exchange between the Red Sea and the Indian Ocean. *Journal of Geophysical Research*: *Oceans*, *107*(C11), doi:Artn 3196, doi:10.1029/2001jc001184.

Sofianos, S. S., Johns, W. E., & Murray, S. P. (2002). Heat and freshwater budgets in the Red Sea from direct observations at Bab el Mandeb. *Deep-Sea Research Part II, 49*(7–8), 1323–1340. doi:10.1016/S0967-0645(01)00164-3. (Pii S0967-0645(01)00164-3).

Stohl, A., Forster, C., Frank, A., Seibert, P., & Wotawa, G. (2005). Technical note: The Lagrangian particle dispersion model FLEXPART version 6.2. *Atmospheric Chemistry and Physics, 5*, 2461–2474.

Veneziani, M., Griffa, A., Garraffo, Z. D., & Chassignet, E. P. (2005). Lagrangian spin parameter and coherent structures from trajectories released in a high-resolution ocean model. *Journal of Marine Research, 63*(4), 753–788. doi:10.1357/0022240054663187.

Veneziani, M., Griffa, A., Reynolds, A. M., & Mariano, A. J. (2004). Oceanic turbulence and stochastic models from subsurface Lagrangian data for the northwest Atlantic Ocean. *Journal of Physical Oceanography, 34*(8), 1884–1906. doi:10.1175/1520-0485(2004)034<1884:Otasmf>2.0.Co;2.

Yao, F., Hoteit, I., Pratt, L. J., Bower, A. S., Köhl, A., Gopalakrishnan, G., & Rivas, D. (2014a). Seasonal overturning circulation in the Red Sea: 2. Winter circulation. *Journal of Geophysical Research: Oceans, 119*(4), 2263–2289. doi:10.1002/2013JC009331.

Yao, F., Hoteit, I., Pratt, L. J., Bower, A. S., Zhai, P., Köhl, A., & Gopalakrishnan, G. (2014b). Seasonal overturning circulation in the Red Sea: 1. Model validation and summer circulation. *Journal of Geophysical Research: Oceans, 119*(4), 2238–2262. doi:10.1002/2013JC009004.

Zhai, P., & Bower, A. (2013). The response of the Red Sea to a strong wind jet near the Tokar Gap in summer. *Journal of Geophysical Research: Oceans, 118*(1), 422–434. doi:10.1029/2012jc008444.

Zhan, P., Subramanian, A. C., Yao, F., & Hoteit, I. (2014). Eddies in the Red Sea: A statistical and dynamical study. *Journal of Geophysical Research*: *Oceans*, *119*(6), 3909–3925, doi:10.1002/2013JC009563.

Chapter 22
Observing, Monitoring and Evaluating the Effects of Discharge Plumes in Coastal Regions

Burton Jones, Elizabeth Teel, Bridget Seegers and Matthew Ragan

Abstract Our ability to predict, observe, and monitor the performance of ocean outfall discharges is rapidly transforming through advances in numerical modeling, remote sensing and underwater vehicle technology. The rapid implementation of sensor and AUV technology has transformed our ability to monitor effluent plumes from coastal discharges of both brine and wastewater. Advances in remote sensing technology provide new views of anthropogenic discharges into coastal seas and oceans. Improved spatial and temporal resolution of coastal models provides more comprehensive dispersion estimates from these discharges. The combined capabilities now provide more detailed observations of the oceanographic processes affecting the dispersion of these discharges and produce statistical maps of the dispersion of properties related to the effluents. These results will contribute to management and design of ocean outfalls and enable better interpretation of discharge effects on coastal ocean ecosystems.

22.1 Introduction

The disproportionate growth of coastal populations globally places increased stresses on the coastal environment (Turner et al. 1996). The increase in population often outpaces the increase in infrastructure resulting in increased loads of terrestrially derived contaminants into coastal oceans and seas. The effects of these discharges can endanger both human health and coastal ecological health, including coastal fisheries (Islam and Tanaka 2004).

Effective wastewater treatment coupled with appropriately designed wastewater discharges provides one mechanism for reducing the effects of coastal contamination

B. Jones (✉) · E. Teel · B. Seegers · M. Ragan
Department of Biological Sciences, University of Southern California, Los Angeles, CA, USA
e-mail: burt.jones@kaust.edu.sa

T.M. Missimer et al. (eds.), *Intakes and Outfalls for Seawater Reverse-Osmosis Desalination Facilities*, Environmental Science and Engineering,
DOI 10.1007/978-3-319-13203-7_22

from populated areas. However, both the design of discharges and appropriate evaluation of the effectiveness of these discharge systems requires sampling and observational capabilities that have only come into maturity within the last few years (Rogowski et al. 2013; Smith et al. 2011).

In order to detect and map ocean discharge effluent dispersion sensors are required that can unambiguously differentiate the characteristic signatures from the discharge affected water from the variations that occur in natural ambient water. It has taken time and innovation to develop appropriate sensors. Even now, with recent sensor progress, not all relevant variables such as bacteria, viruses and specific chemical contaminants of interest can be detected. Therefore, inference of the concentrations and dispersion of contaminants depends on significant correlations between variables that can be easily measured in situ and variables that are elusive or can only be measured in the laboratory.

Public health concerns in the coastal environment usually relate to microbial contamination, especially human pathogens (California Environmental Protection Agency 2012), and to toxins that derive from algal blooms and are often communicated to humans through seafood consumption. The connectivity between human health and human pathogen contaminated coastal waters has been clearly documented (Haile et al. 1999). Sewage outfall discharges are an obvious source of human pathogens to the coastal ocean and the bacteria within these discharge plumes may remain active for several days following discharge (Paul et al. 1997). Toxic or harmful algal blooms are often associated with significant anthropogenic nutrient inputs (Anderson et al. 2008). Sometimes this linkage is less than clear in that it has been shown that in the coastal region of Southern California that the wastewater outfalls contribute a significant amount of inorganic nitrogen into the upper layer of the ocean (Howard et al. 2012).

Detection of change in coastal ecosystems due to chronic contaminant loading often requires more time to establish than is required to detect public health issues. Often, by the time the environmental response to anthropogenic discharge is discovered, the overall effect on the ecosystem may be irreversible. Anthropogenic nutrients that come from sewage effluent, river discharge or groundwater pathways have been suggested to be responsible for the decline of coral reef ecosystems in many locations around the world.

22.2 Approach

Recent advances in sensors, vehicles and modeling techniques have transformed our ability to predict, map and monitor the ocean outfall discharge plumes. These capabilities have resulted in the ability to create more comprehensive statistical products from both modeling and observations that can assist planning, design and implementation of future ocean outfall infrastructure.

22.2.1 Sensors

Beginning in the late 1970s and 1980s sensors began to become available that facilitated the transition in our ability to readily detect outfall plumes in the ocean. Prior to that sampling of ocean plumes required the obtaining of water samples for laboratory analyses of inorganic nutrients, microbial indicator organisms and other relevant constituents that could be measured. Currently there are many sampling technologies available and the proper approach to monitoring and tracking the discharge plumes depends upon the type of discharge (cooling water, desalination brine, or wastewater effluent) and the level of treatment prior to discharge. We use wastewater as a primary example of the capabilities.

Early efforts using CTDs, transmissometers and fluorometers provided the capability to begin to discriminate between effluent plumes in situ and in real time based on the simple partitioning of particles between chlorophyll fluorescent phytoplankton particles and non-phytoplankton particles (Wu et al. 1994). While this analysis was useful, the results were sometimes ambiguous because there can be alternative sources of lower salinity water and suspended particles in the coastal ocean. Subsequent efforts used more sophisticated optical instrumentation that included in situ spectrophotometers and multi-wavelength fluorometers to demonstrate that certain fluorescent signals coming from the dissolved organic constituents of effluent plumes may provide a more specific unique identification of effluent plumes (Petrenko et al. 1997). Following on the multi-spectral fluorescence results, fluorometers that measure colored dissolved organic matter (CDOM) have been adopted for effectively mapping effluent plumes off of Southern California (Rogowski et al. 2013). Although surface runoff may be an additional source of CDOM in the coastal system (Reifel et al. 2009), that runoff is generally constrained to the surface layer of the ocean and can readily be differentiated from the submerged sewage effluent plume via a multidimensional analysis of temperature, salinity, depth and CDOM.

Sensors continue to evolve. Recent developments include a sensor to detect nitrate concentration in the ocean (Johnson and Coletti 2002). While this sensor provides an additional resource in the ocean observing tool box, most often the primary form of nitrogen in wastewater outfalls is ammonium (Jones et al. 1990). At present there is not a rapid, in situ methodology for detection of ammonium in seawater that can resolve ammonium concentrations consistent with physical and optical sensors. Other new technologies include the development of in situ samplers and sensors that have telemetering capabilities. The MBARI Environmental Sample Processor (ESP) enables in situ water sample processing and processing including taxonomic identification of harmful algal species, human pathogens, and detection of toxins such as domoic acid (Scholin et al. 2006, 2009). Under water mass spectrometers have been developed that are capable of resolving gases, volatile organic carbon compounds, and semi-volatile compounds and can be deployed on larger autonomous vehicles (Camilli and Duryea 2009; Camilli et al. 2010; Short et al. 2001; Wenner et al. 2004).

New remote sensing technology provides additional capabilities beyond the early ocean color observations. Ocean color measurements, synthetic aperture radar (SAR), and thermal sensors are capable of detecting signatures from various types of discharges, particularly surfacing discharges. Ocean color measurements provide a unique tool for detecting the ocean color signature from surfacing effluent plumes and from coastal freshwater discharges. Similar to in situ sensing, the signatures of effluent and coastal freshwater plumes, dissolved organic matter absorption and suspended particulate matter are readily detected by ocean color measurements [e.g. Kratzer et al. 2008; Coble 2007; Svejkovsky et al. 2010; D'Sa and Miller 2003]. Spatial resolution of the major ocean color satellites may be too coarse for detection of some discharges, but airborne imagers such as the AVIRIS or PRISM sensors (Lee et al. 1994), and the HICO imager (Corson et al. 2008) on the International Space Station provide a combination of better spectral resolution and spatial resolution. However, both of these hyperspectral, high spatial resolution sensors lack the ability to routinely monitor a given region for extended periods of time. The Korean GOCI satellite has demonstrated the capability of a geostationary instrument for tracking the dispersion of an effluent field discharged from a ship (Hong et al. 2012). GOCI can obtain up to 8 images per day with spatial resolution of 500 × 500 m, better than the resolution of MODIS' color bands. But GOCI's coverage area is limited to the region surrounding the Korean peninsula bounded by the East/Japan Sea, Tsushima Strait and Yellow Sea. Additional geostationary satellites in different regions will facilitate the capabilities in other areas where there are significant stressors to the coastal ocean.

22.2.2 Vehicles

Through the last few years autonomous vehicles have gained sufficient reliability and endurance to be used for a range of time and space scales and have greatly influenced research approaches. Prior to the development of these vehicles, the field was dependent on the use of traditional station sampling and towed platforms requiring the use of research vessels and significant personnel activity at sea. Autonomous vehicles modify the role of personnel from those needed for the physical acquisition of samples and data to primarily preparation, planning and data analysis.

The simultaneous development of low energy, rapid-sampling sensors and autonomous vehicles has facilitated a dramatic shift in our ability to map and monitor submerged brine discharge and wastewater effluent. Two major types of vehicles provide similar, but complementary types of observations discharge plumes (Fig.22.1). Propelled vehicles, such as the Hydroid Remus, Isurus, or Mares, provide relatively synoptic surveys discharge plumes (Rogowski et al. 2012, 2013; Ramos and Neves 2008). Buoyancy propelled ocean gliders, while not synoptic over their entire survey, can provide a longer term monitoring tool that is capable of weeks to months of sustained monitoring (Todd et al. 2009; Seegers et al. 2014). Depending on the sensor payload, both propelled and glider vehicles can provide characterization

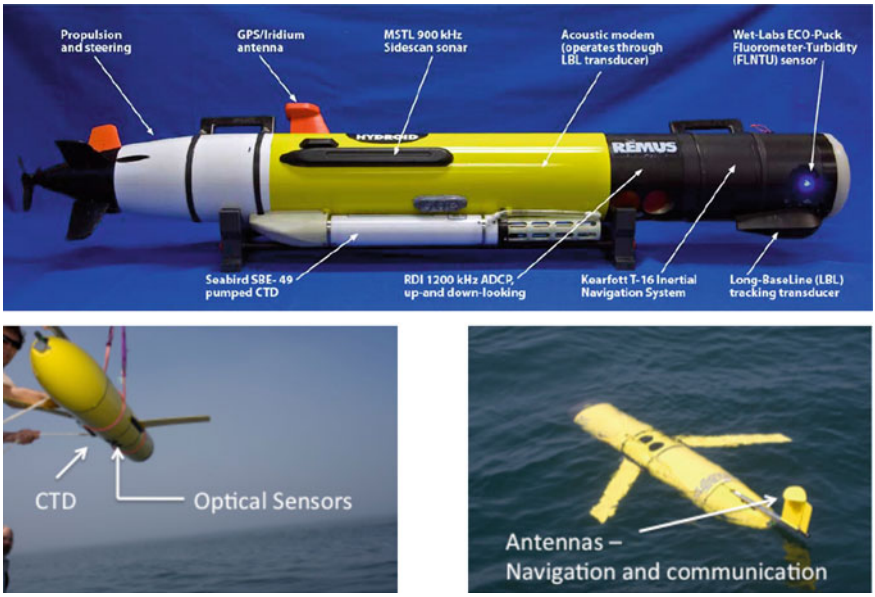

Fig. 22.1 Two types of vehicles that have been used for mapping of wastewater outfall plumes. The *top panel* shows a Kongsberg Remus-100 propelled vehicle equipped with sensors and can provide relatively synoptic maps of a effluent plume. The two *lower panels* shows a Webb Research Slocum glider equipped with a CTD, multi-channel fluorometer, and multi-wavelength backscatter sensor that can be used for long term characterization of effluent plumes

and mapping not only of the discharge plume, but of related environmental variables including temperature, salinity, density, suspended particles, phytoplankton chlorophyll, nitrate nitrogen, ambient light field (radiometry), etc. (Rudnick and Perry 2003). Gilders, in particular, can also provide a near real-time, spatial-temporal data stream of physical data than provide input into data-assimilating four-dimensional coastal physical and ecosystem models that can provide both nowcasts and forecasts of environmental processes in the coastal ocean (Chao et al. 2008).

In the example that is discussed below, the Teledyne-Webb Slocum glider carried a Seabird CTD and two WETLabs EcoTriplet pucks. One puck was configured with three fluorometers (chlorophyll, colored dissolved organic matter (CDOM), and phycoerythrin (PE). The PE fluorometer can be used for tracer studies using Rhodamine WT because the wavelengths on the PE fluorometer fit the absorption and fluorescence wavelengths for Rhodamine WT, which is a dye that is commonly used in short-term coastal wastewater tracer studies (Bogucki et al. 2005). A second Eco Triplet was fitted with 3 optical backscatter channels selected for 532, 660, and 880 nm. These particular wavelengths were chosen because they are wavelengths where there is minimal absorption by phytoplankton and organic matter. These gliders can also be equipped with dissolved oxygen optodes and nitrate sensors.

22.2.3 Models

Until recently, modeling plumes from various types (thermal, wastewater, desalination brines) of discharges was divided into more empirical near-field models that provided fundamental characteristics of the near-field plume (Roberts et al. 2011) and larger scale ocean circulation models that could provide the far field dispersion, but not the smaller scale entrainment and/or nearshore interactions (Blumberg and Connolly 1996). Improvements to the resolution and parameterization of ocean circulation models has led to the ability to model discharge plumes in the coastal ocean at the scale near to the scale of the larger outfall diffusers (Uchiyama et al. 2014). Uchiyama et al. (2014) created a nested Regional Ocean Modeling System (ROMS) that provided coupling between large scale ocean processes and small scale, 75 m horizontal resolution. The problem that now arises is that the models are capable of providing results at resolutions that exceed our observational capabilities. Nevertheless, these small-scale models now provide a source for meaningful statistics that can be used in the design and management of coastal discharges with relevant forcing from local to large scale ocean processes.

22.3 Examples from Modeling and Observation Efforts

Coastal models with increased spatial and temporal resolution are providing significant insights into dispersion processes in the coastal seas. The results shown by Uchiyama et al. (2014) provide an example of results from an extended model run that includes large scale forcing and local winds. Figure 22.2 shows three examples of dispersion from two large outfalls in the Los Angeles/Orange County region of the Southern California Bight. A number of features are evident in these examples. Three example snapshots from the Orange County Sanitation District's (OCSD) offshore outfall diffuser, located at about 60 m water depth, are shown in the left hand panels and three snapshots from the City of Los Angeles' Hyperion Treatment Plant (HTP) outfall are shown in the right-hand 3 panels. Several conclusions come from these results. Initial dispersion from the outfalls tends to be alongshore in either direction, depending on the prevailing currents and the associated tidal modulation of the mean currents. At times the dispersion can appear quite simple in the alongshore direction as in the example from the OCSD outfall on September 22, 2006. What is not readily apparent in the figure is that there is an additional outfall from the Los Angeles County Sanitation District that discharges 300–400 million gallons per day ($1.1–1.5 \times 10^6$ m^3/day) of treated wastewater. The outfall is located on the left side of the map where the OCSD plume passes over the Palos Verdes shelf. Thus in a region where there are multiple large outfalls along the coast, the

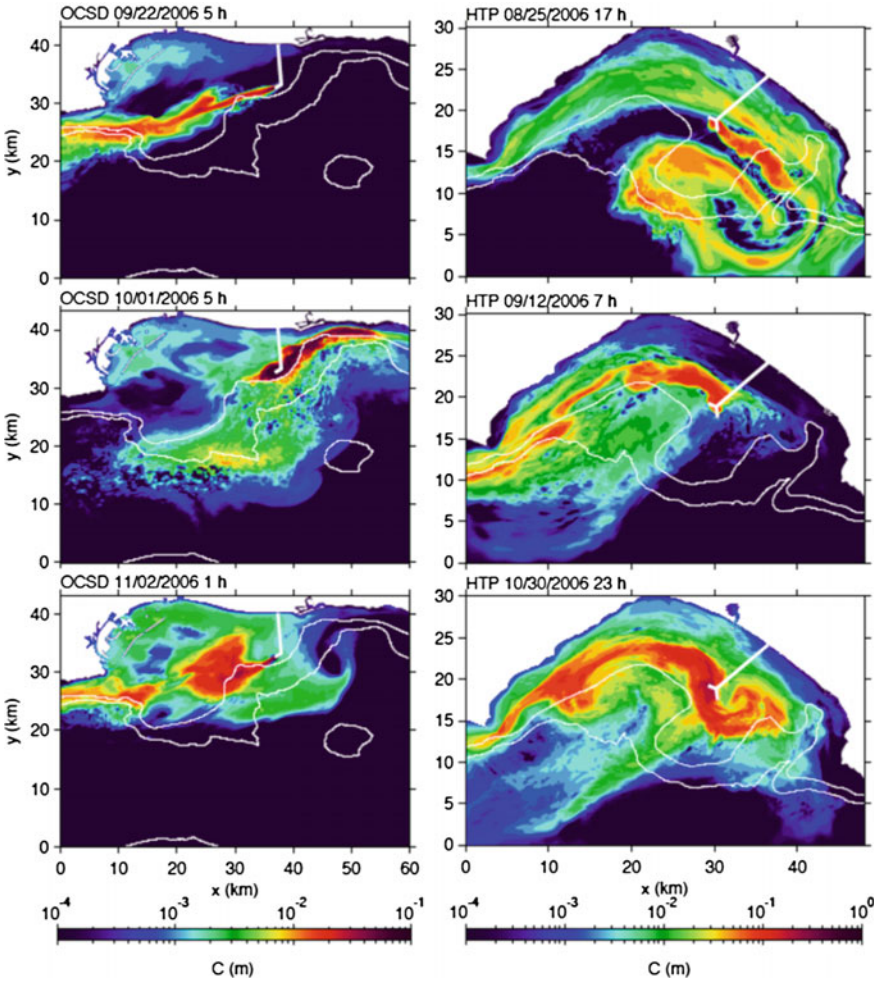

Fig. 22.2 Images of the instantaneous distribution of effluent from two submerged coastal outfalls based on a high resolution ROMS model developed at UCLA (Uchiyama et al. 2014). The three *left hand panels* show dispersion from the Orange County Sanitation District's offshore outfall located in about 60 m water depth. Each panel shows a different distribution taken from different times in the model run. The times are indicated above each panel. The set of images on the *right* are snapshots based on the model of dispersion from the City of Los Angeles' Hyperion Treatment Plant outfall, also located in about 60 m water depth. Again, the 3 snapshots provide distinct dispersal patterns from different times in the model run

plumes may occasionally overlap with one another, and possibly mix with each other. At other times the pattern of dispersion is more complex as the result of the varying currents and associated stratification in the region. The effect of stirring and stretching of these plumes due to current variations is especially evident in examples

from the HTP discharge in Santa Monica Bay. Finally, it is clear that the dispersion processes can transport the effluent plumes for distances that extend for tens of kilometers. It is difficult to map these types of distributions with traditional ship-based sampling. Towed undulating vehicles provide an alternative method for rapid detection of these plumes, but to capture the many patterns of the plume would require extensive days at sea for the ship and its associated vehicle.

22.3.1 AUV Mapping

As previously mentioned, propelled autonomous underwater vehicles (AUVs) provide a means for rapid, synoptic mapping of effluent plumes. Rogowski et al. (2011) used the Remus-100 vehicle equipped with a CTD and fluorometers to map out the discharge from San Diego's Point Loma ocean outfall where the discharge depth is about 93–95 m. Rogowski et al. (2012) showed that effluent dilution could be computed from the CDOM concentration and created dilution cross-sections from the CDOM maps obtained with the resulting maps obtained with the AUV. An example of a CDOM map obtained over the course of several hours is shown in Fig. 22.3.

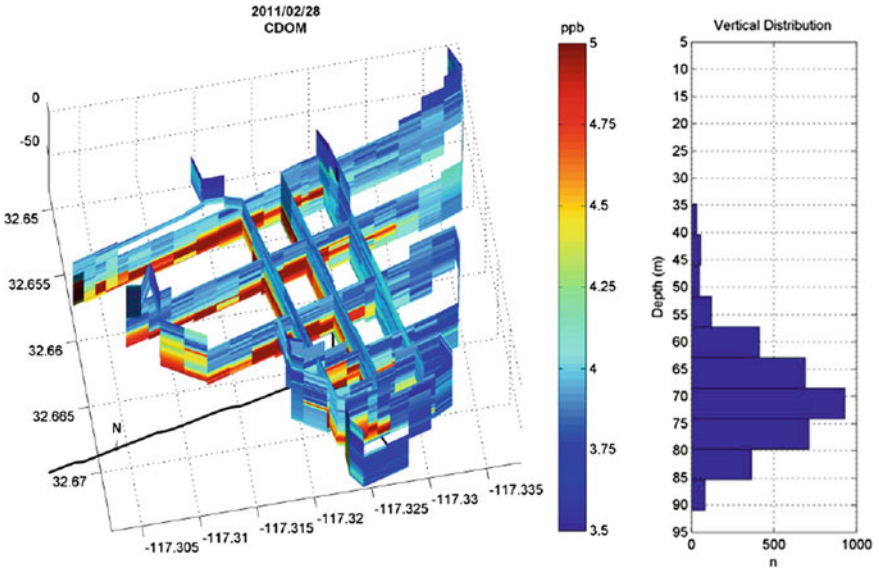

Fig. 22.3 Three-dimensional curtain plot of the distribution of CDOM, a tracer for wastewater effluent, from the San Diego Point Loma outfall. The data was obtained with a Remus AUV equipped with a CDOM fluorometer and other sensors (Rogowski et al. 2012)

22.3.2 Resolving Plumes Dispersion with Autonomous Gliders

Gliders provide another AUV tool for maintaining persistent observations of a coastal region where an outfall diffuser or other type of discharge might be located. While gliders do not have the speed of the propelled vehicles, they have the ability to maintain a multi-week to multi-month deployment with horizontal speeds of about 1 km per hour. Webb gliders have been used actively since 2009 to provide monitoring of the region offshore from the Orange County Sanitation District's Wastewater Treatment Plant discharging into San Pedro Bay south of Los Angeles, California, USA (Fig. 22.4). The basic pattern was a zigzag through the area that required 3–4 days to complete. While the overall pattern was not synoptic, individual transects or portions thereof within the overall pattern provide some synopticity. Overall, the observations provide an extended time series that can be used to provide statistics of the distributions of both water quality measures (temperature, salinity, density, chlorophyll concentration, suspended particulate distributions via optical backscatter) and specific effluent tracers such as CDOM.

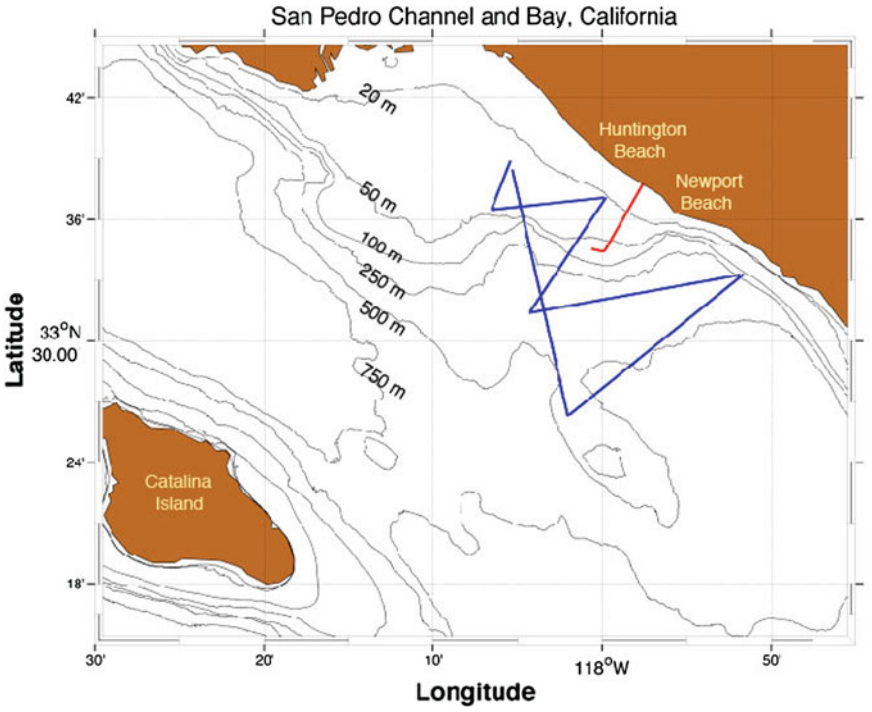

Fig. 22.4 Map of San Pedro Channel/San Pedro Bay region offshore from the cities of Huntington Beach and Newport Beach. The *red line* is the Orange County Sanitation District's offshore outfall discharging at approximately 57 m depth beneath the surface. The *blue line* is the programmed track for the glider AUV that was used to map the region between March and June 2010

A single traverse of the pattern provides a 3-dimensional snapshot of the plume over the course of the survey. In one survey from April 7 to 9, 2009, the effluent plume, indicated by the distribution of CDOM, can be observed 10–20 km away from the discharge source, as shown in Fig. 22.5. The figure shows four variables

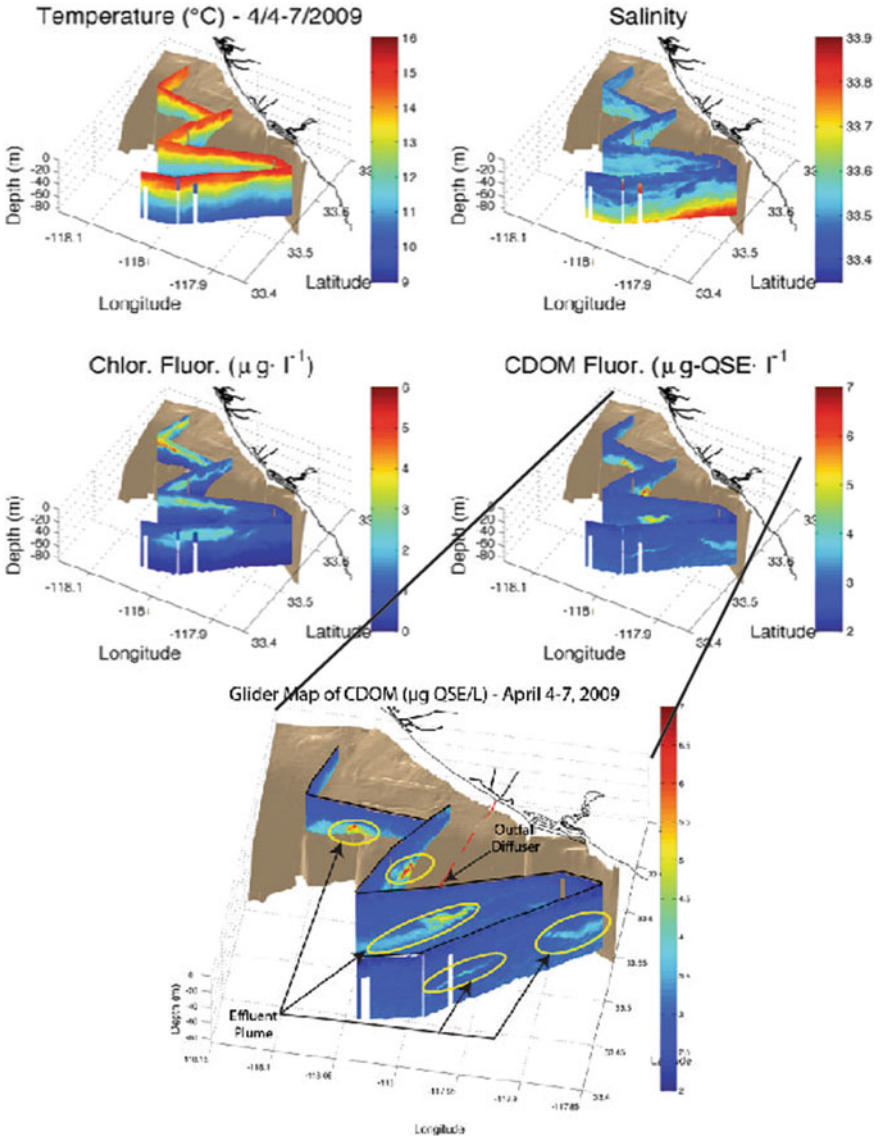

Fig. 22.5 A glider map following the pattern in Fig. 22.4 for the period of April 4–7, 2009. The plot is a 3-dimensional projection of the data where the *tan area* represents the bottom topography and the *black lines* represent the coastline. The outfall location is indicated by the *red line* along the sea bottom in the bottom CDOM panel

that are measured by the USC glider. The CDOM distribution indicates that away from the outfall the plume CDOM concentration decreased presumably due to farfield ambient mixing processes. The plume, in this case, was distributed as several thin patches having cross-shelf spatial extents of several kilometers. These patches were located beneath the pycnocline, satisfying the design specifications that the plume be submerged beneath the pycnocline for a significant fraction of the year. As Rogowski et al. (2012) have demonstrated, dilution maps can be created from the CDOM concentration, provided that calibrations are carried out with the source effluent. These types of results become important for the operators of wastewater treatment plants that discharge into the coastal ocean. The resulting dilution field can help to validate the performance of their outfall diffusers and therefore, establishing compliance with their discharge permits.

An individual cross-shelf transect near the outfall provides an example of the detail that can be resolved from the glider survey (Fig. 22.6). The length of a glider's dive cycle is approximately three times the dive depth. So a dive to 40 m has a horizontal resolution of about 120 and 100 m dive has a nominal horizontal

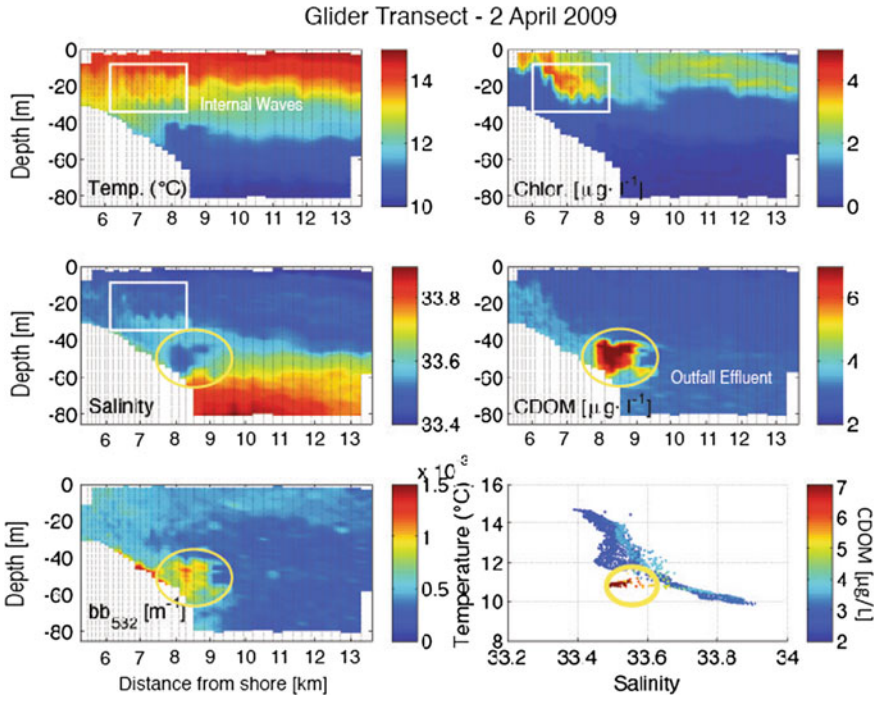

Fig. 22.6 A single cross-shelf section from the glider monitoring of the San Pedro region nearest the OCSD outfall. The continental shelf is indicated by the *white area* in the *lower left hand portion* of each panel. The *white box* outlines an area where internal waves are evident. The *yellow oval* outlines the nearfield region of the outfall plume nearest the outfall diffuser

resolution of 300 m at either surface or bottom of the dive and 150 m at mid-depth. Because the glider passed near the northwest end of the outfall diffuser, the effluent plume is clearly evident in the section (indicated by the yellow oval in Fig. 22.5). The plume is characterized by lower salinity, elevated CDOM concentrations, elevated suspended particle concentration as indicated by the optical backscatter (b_b532), and lower chlorophyll concentration. The lower concentration of chlorophyll results from entrainment of ambient water from the discharge depth that is below the region of high chlorophyll. The CDOM concentration of the plume is higher than the CDOM concentrations offshore between the surface and 85 m. A region of elevated CDOM extends from the shelf break toward the coast within about 10 m of the bottom. Although there are not supporting current meter observations for this period, the CDOM pattern suggests shoreward transport of the effluent plume near the bottom. This type of transport is consistent with near bottom transport driven by internal tides that are frequently observed on the San Pedro continental shelf (Noble et al. 2009). As this feature advects shoreward it rises in elevation above the sea bottom to within 10 m from the surface, as can be seen in the portion of the section nearest the coast (left hand side of sections in Fig. 22.6).

An additional process that is resolved in this section is the presence of internal waves in the thermocline. The internal waves are apparent in several of the measured properties including temperature, chlorophyll, salinity, density (not shown), and subtly in optical backscatter (b_b532) (Fig. 22.6, indicated by white rectangle). The waves first appear just shoreward of the shelf break to about the 30 m isobath where the water column appears to become more mixed, perhaps due to the breaking of the internal waves. The vertical amplitude of these waves is about 5–6 m.

22.3.3 Providing Regional Statistics

By sustaining measurements over extended periods of time (weeks–months), it becomes possible to statistically characterize the environment where the discharge is occurring and when the discharge is present to create statistical maps of the presence or impact of the discharge plume. An example in Fig. 22.7 of a statistical analysis of glider observations is from a 3 months deployment between March and June 2010. The region of sampling is the same region that was described above in San Pedro Bay, California.

A three-dimensional projection of the statistical mean and standard deviation fields is shown in Fig. 22.7. The view in this panel is looking toward the coast from the west. Density (left hand panels) and CDOM concentration (right hand panels) are shown in this example. The bottom panels show the number of glider passes that were obtained. The mean and standard deviation panels only display the areas where 10 or more passes are included in the statistics.

Density distribution was relatively uniform over the area during this period. The variability of density is highest in the surface layer and over the shelf. An area of secondary variability occurred in the subsurface region of the pycnocline offshore

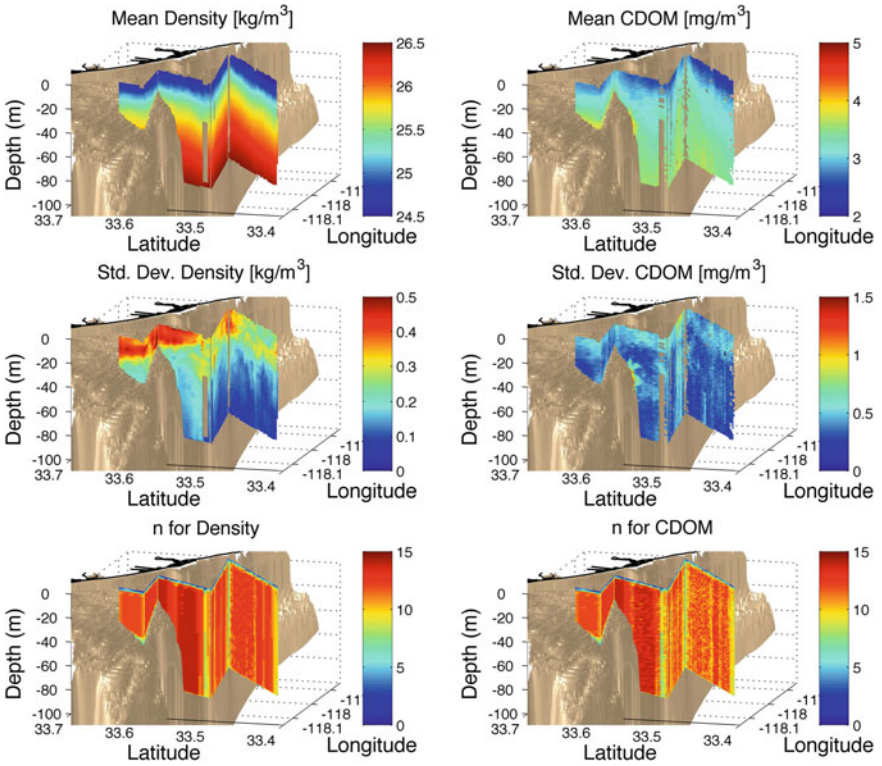

Fig. 22.7 An example of the curtain plot of mean and standard deviation from a total of 15 glider traverses of the overall pattern in Fig. 22.4. The number of occurrences for each gridded data point used in the statistics is indicated in the *bottom panels* where n is the number of occurrences for each grid point. The gridded mean and standard deviation panels only display data where n is equal to or greater than 10

from the shelf break. Pycnocline location and variability is important to the vertical dispersion of a buoyant discharge and the location of pycnocline variability is important to the effluent dispersion. CDOM also generally shows a stratified distribution with low levels in the upper layer and increasing with depth. This type of distribution is typical in the ocean where near surface organic matter is oxidized by the incoming solar radiation. Higher concentrations are evident near the outfall and close to the coast in either direction from the outfall. The standard deviation indicates where regions of higher variability occur. Again, the area near the outfall is highly variable, and there is a subsurface region to the south (to the right in the image) where high variability is observed near the coast.

Similar to the snapshots shown in Fig. 22.5, an individual transect can be examined for its statistical structure. Using the same transect location that was shown in Figs. 22.4, 22.5 and 22.6, closer inspection of binned data along a single transect line detail can be looked at statistically over time. Figure 22.8 shows the sections of

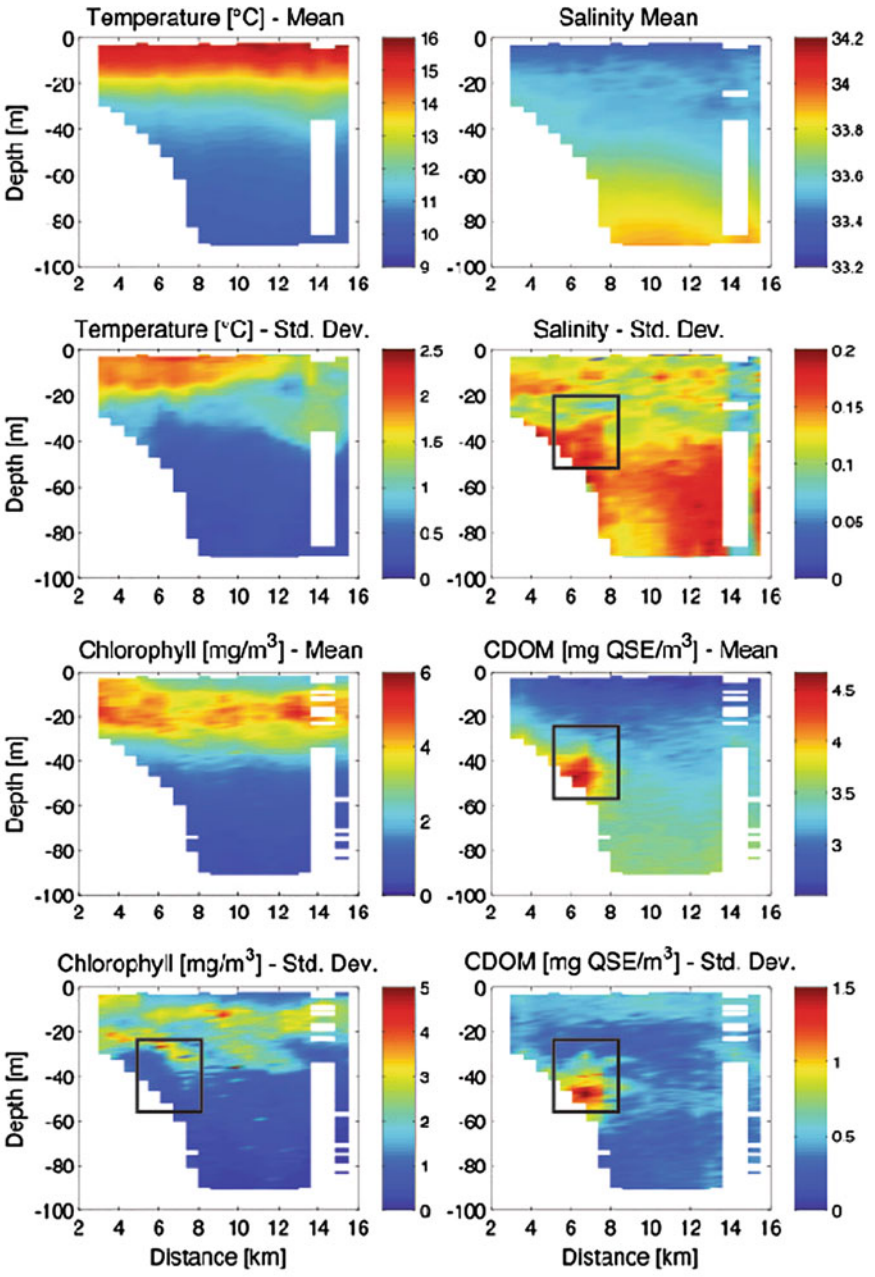

Fig. 22.8 These panels are the statistical distributions for the transect nearest the outfall diffuser. As in Fig. 22.7, only grid points where n ≥ 10 are shown. The *black box* outlines the area most directly affected by the wastewater discharge

the three-month mean and standard deviation for the variables of temperature salinity, chlorophyll, and CDOM. The mean fields of temperature and salinity do not provide a strong signature from the discharge plume, while the mean CDOM pattern clearly shows high values near the outfall diffuser over the outer shelf. Both the mean and variability are high in this region. The extension of an elevated standard deviation offshore from the outfall, suggest that the plume often extends seaward from the discharge remaining at an equilibrium depth. The shoreward extension of the standard deviation also suggests that this is a recurrent process. Interestingly, the low standard deviation of chlorophyll near the discharge and extending shoreward a bit may indicate that discharge entrainment of the deeper ambient seawater is influencing the chlorophyll concentration in this area. Because it is difficult to match individual snapshots between observations and model runs, the statistics of both may provide a more accurate characterization of the similarity between model and data, as Uchiyama et al. (2014) have described.

22.4 Discussion

Modern observation and modeling tools are providing an unprecedented level of resolution, monitoring, and analysis of dispersion of various anthropogenic discharges into the coastal ocean. Increased resolution of coastal numerical models provides detailed information on the response of these discharges to the spectrum of processes that influence coastal oceans and seas. As mentioned, numerical models are now of sufficient resolution that it is difficult to provide synoptic observations on the same time and space scales to validate the complexity of dispersion that the models provide. The models are also approaching the scale where they may soon be able to account for the nearfield performance of the discharge plumes.

Autonomous vehicles can provide sustained monitoring of ocean outfall discharges, whether wastewater or desalination brine discharges, for periods from months to years. The combined capabilities of numerical models and vehicles provide data sets that allow for unprecedented statistical evaluation of the influence of these discharges on the coastal ocean. Propelled vehicles such as the Remus-100 (Rogowski et al. 2013; Van der Merwe 2014) or Mares (Ramos 2013) can provide unparalleled synoptic resolution of the nearfield plumes from these discharges. Autonomous gliders, while less synoptic, can be deployed for weeks to months providing an extensive temporal and spatial mapping of effluent dispersion. As demonstrated in Fig. 22.5, gliders can also capture snapshots of key oceanographic phenomena that affect discharge plumes, but whose detection may elude more traditional boat sampling. The incorporation of modern optical sensors now provides unambiguous detection and resolution of wastewater plumes and existing temperature and conductivity sensors provide the capability for resolving brine discharges. Mass spectrometers are being deployed on autonomous vehicles (Camilli et al. 2010) for other applications and should prove beneficial for examining discharge plumes. Combining the types of tools used such as autonomous vehicles,

in situ multi-variable sampler such as the ESP, and new remote sensing tools including geostationary (Hong et al. 2012) and hyperspectral imagers such as HICO can provide a high degree of plume resolution and monitoring (Corson et al. 2008). Such extensive temporal and spatial data sets are amenable to statistical analyses for characterization of the ambient conditions and effluent dispersion of the discharge effluent within the often-complex coastal ocean.

Acknowledgments The activities supporting the observations presented took place between 2009 and 2012. Those whose efforts contributed to the success of the observations include Ivona Cetinic, Carl Oberg, Arvind Pereira, the Orange County Sanitation District Environmental Monitoring Division, and Ray Arntz and Kayaa Heller from Sundiver for their operational support that was essential to the success of these efforts. Financial support for the research was provided by USC Sea Grant, Orange County Sanitation District, the National Oceanographic and Atmospheric Administration's ECOHAB and MERHAB programs, the Southern California Coastal Ocean Observation System (part of NOAA IOOS), and King Abdullah University of Science and Technology.

References

Anderson, D. M., Burkholder, J. M., Cochlan, W. P., Glibert, P. M., Gobler, C. J., Heil, C. A., et al. (2008). Harmful algal blooms and eutrophication: Examining linkages from selected coastal regions of the United States. *Harmful Algae, 8*, 39–53.

Blumberg, A. F., & Connolly, J. P. (1996). *Modeling fate and transport of pathogenic organisms in Mamala Bay*. Hawaii, USA: Honolulu.

Bogucki, D. J., Jones, B. H., & Carr, M. E. (2005). Remote measurements of horizontal eddy diffusivity. *Journal of Atmospheric and Oceanic Technology, 22*, 1373–1380.

California Environmental Protection Agency, S. W. R. C. B. (2012). Water quality control plan: Ocean waters of California. In C. E. P. A. (Ed.), *State water resources control board*. Sacramento, California: State Water Resources Control Board.

Camilli, R., & Duryea, A. N. (2009). Characterizing spatial and temporal variability of dissolved gases in aquatic environments with in situ mass spectrometry. *Environmental Science and Technology, 43*, 5014–5021.

Camilli, R., Reddy, C. M., Yoerger, D. R., Van Mooy, B. A. S., Jakuba, M. V., Kinsey, J. C., et al. (2010). Tracking hydrocarbon plume transport and biodegradation at deepwater horizon. *Science, 330*, 201–204.

Chao, Y., LiIZ, J., Farrara, J. D., Moline, M. A., Schofield, O. M. E., & Majumdar, S. J. (2008). Synergistic applications of autonomous underwater vehicles and regional ocean modeling system in coastal ocean forecasting. *Limnology and Oceanography, 53*, 2251–2263.

Coble, P. G. (2007). Marine optical biogeochemistry: The chemistry of ocean color. *Chemical Reviews, 107*, 402–418.

Corson, M. R., Korwan, D. R., Lucke, R. L., Snyder, W. A., & Davis, C. O. (2008). The hyperspectral imager for the Coastal Ocean (HICO) on the international space station. In *IEEE International Geoscience and Remote Sensing Symposium*, *IGARSS 2008* (pp. 101–104). Piscataway: IEEE.

D'sa, E. J., & Miller, R. L. (2003). Bio-optical properties in waters influenced by the Mississippi River during low flow conditions. *Remote Sensing of Environment, 84*, 538–549.

Haile, R. W., Witte, J. S., Gold, M., Cressy, R., McGee, C., Millikan, R. C., et al. (1999). The health effects of swimming in ocean water contaminated by storm drain runoff. *Epidemiology, 10*, 355–363.

Hong, G. H., Yang, D. B., Lee, H. M., Yang, S. R., Chung, H. W., Kim, C. J., et al. (2012). Surveillance of waste disposal activity at sea using satellite ocean color imagers: GOCI and MODIS. *Ocean Science Journal, 47*, 387–394.

Howard, M. D., Sutula, M., Caron, D., Chao, Y., Farrara, J., Frenzel, H., et al. (2012). Comparison of natural and anthropogenic nutrient sources in the Southern California Bight. In K. Schift (Ed.), *Southern California coastal water research project—Annual report*. Costa Mesa, California, USA: Southern California Coastal Water Research Project.

Islam, M. S., & Tanaka, M. (2004). Impacts of pollution on coastal and marine ecosystems including coastal and marine fisheries and approach for management: A review and synthesis. *Marine Pollution Bulletin, 48*, 624–649.

Johnson, K. S., & Coletti, L. J. (2002). In situ ultraviolet spectrophotometry for high resolution and long-term monitoring of nitrate, bromide and bisulfide in the ocean. *Deep-Sea Research Part I-Oceanographic Research Papers, 49*, 1291–1305.

Jones, B. H., Bratovich, A., Dickey, T. D., Kleppel, G., Steele, A., Iturriaga, R., & Haydock, I. (1990). Variability of physical, chemical, and biological parameters in the vicinity of an ocean outfall plume. In E. J. List & G. H. JirkaI (Eds.), *3rd International Conference on Stratified Flows, 1987 Pasadena* (pp. 877–890). CA: American Society of Civil Engineers.

Kratzer, S., Brockmann, C., & Moore, G. (2008). Using MERIS full resolution data to monitor coastal waters—A case study from Himmerfjarden, a fjord-like bay in the northwestern Baltic Sea. *Remote Sensing of Environment, 112*, 2284–2300.

Lee, Z. P., Carder, K. L., Hawes, S. K., Steward, R. G., Peacock, T. G., & Davis, C. O. (1994). Model for the interpretation of hyperspectral remote-sensing reflectance. *Applied Optics, 33*, 5721–5732.

Noble, M., Jones, B., Hamilton, P., Xu, J., Robertson, G., Rosenfeld, L., & Largier, J. (2009). Cross-shelf transport into nearshore waters due to shoaling internal tides in San Pedro Bay, CA. *Continental Shelf Research, 29*, 1768–1785.

Paul, J. H., Rose, J. B., Jiang, S. C., London, P., Xhou, X. T., & Kellogg, C. (1997). Coliphage and indigenous phage in Mamala Bay, Oahu, Hawaii. *Applied and Environmental Microbiology, 63*, 133–138.

Petrenko, A. A., Jones, B. H., Dickey, T. D., Lenaitre, M., & Moore, C. (1997). Effects of a sewage plume on the biology, optical characteristics, and particle size distributions of coastal waters. *Journal of Geophysical Research-Oceans, 102*, 25061–25071.

Ramos, P. A. G. (2013). Geostatistical prediction of ocean outfall plume characteristics based on an autonomous underwater vehicle regular paper. *International Journal of Advanced Robotic Systems, 10*, 289. doi:10.5772/56644.

Ramos, P., & Neves, M. V. (2008). Environmental impact assessment and management of sewage outfall discharges using AUV'S. In A. V. Inzartsev (Ed.), *Underwater vehicles*. Vienna, Austria: I-Tech.

Reifel, K. M., Johnson, S. C., Digacomo, P. M., Mengel, M. J., Nezlin, N. P., Warrick, J. A., & Jones, B. H. (2009). Impacts of stormwater runoff contaminants in the Southern California Bight: Relationships among plume constituents. *Continental Shelf Research, 29*, 1821–1835.

Roberts, P. J. W., Hunt, C. D., Mickelson, M. J., & Tian, X. D. (2011). Field and model studies of the Boston outfall. *Journal of Hydraulic Engineering-Asce, 137*, 1415–1425.

Rogowski, P., Terrill, E., Otero, M., Hazard, L., & Middleton, W. (Eds.). (2011). Mapping ocean outfall plumes and their mixing using autonomous underwater vehicles, in international symposium on outfall systems, Mar del Plata: Argentina.

Rogowski, P., Terrill, E., Otero, M., Hazard, L., & Middleton, W. (2012). Mapping ocean outfall plumes and their mixing using autonomous underwater vehicles. *Journal of Geophysical Research-Oceans, 117*, Doi: 10.1029/2011gc7804.

Rogowski, P., Terrill, E., Otero, M., Hazard, L., & Middleton, W. (2013). Ocean outfall plume characterization using an autonomous underwater vehicle. *Water Science and Technology, 67*, 925–933.

Rudnick, D. L., & Perry, M. J. (2003). *ALPS: Autonomous and Lagrangian Platforms and Sensors,* p. 64. Workshop Report. http://www.geo-prose.com/ALPS.

Scholin, C., Jensen, S., Roman, B., Massion, E., Marin, R., Preston, C., et al. (2006). The environmental sample processor (ESP)—An autonomous robotic device for detecting microorganisms remotely using molecular probe technology. *Oceans, 2006*(1–4), 1179–1182.

Scholin, C., Doucette, G., Jensen, S., Roman, B., Pargett, D., Marin, R., et al. (2009). Remote detection of marine microbes, small invertebrates, harmful algae, and biotoxins using the environmental sample processor (Esp). *Oceanography, 22*, 158–167.

Seegers, B. N., Birch, J. M., Marin, R., Scholin, C. A., Caron, D. A., Seubert, E. L., Howard, M. D. A., Robertson, G. L., & Jones, B. H. (2014). Subsurface seeding of surface harmful algal blooms observed through the integration of autonomous gliders, moored environmental sample processors, and satellite remote sensing in Southern California. *Limnology and Oceanography* (in review).

Short, R. T., Fries, D. P., Kerr, M. L., Lembke, C. E., Toler, S. K., Wenner, P. G., & Byrne, R. H. (2001). Underwater mass spectrometers for in situ chemical analysis of the hydrosphere. *Journal of the American Society for Mass Spectrometry, 12*, 676–682.

Smith, R. N., Schwager, M., Smith, S. L., Jones, B. H., Rus, D., & Sukhatme, G. S. (2011). Persistent ocean monitoring with underwater gliders: Adapting sampling resolution. *Journal of Field Robotics, 28*, 714–741.

Svejkovsky, J., Nezlin, N. P., Mustain, N. M., & Kum, J. B. (2010). Tracking stormwater discharge plumes and water quality of the Tijuana River with multispectral aerial imagery. *Estuarine, Coastal and Shelf Science, 87*, 387–398.

Todd, R. E., Rudnick, D. L., & Davis, R. E. (2009). Monitoring the greater San Pedro Bay region using autonomous underwater gliders during fall of 2006. *Journal of Geophysical Research-Oceans, 114*. Artn C06001, Doi:10.1029/2008jc005086.

Turner, R. K., Subak, S., & Adger, W. N. (1996). Pressures, trends, and impacts in coastal zones: Interactions between socioeconomic and natural systems. *Environmental Management, 20*, 159–173.

Uchiyama, Y., Idica, E. Y., McWilliams, J. C., & Stolzenbach, K. D. (2014). Wastewater effluent dispersal in Southern California Bays. *Continental Shelf Research, 76*(1), 36–52. doi:10.1016/j.csr.2014.01.002.

Van der Merwe, R. (2014). *Marine monitoring and environmental management of SWRO concentrate discharge: A case study of the KAUST SWRO plant*. Thuwal: King Abdullah University of Science and Technology.

Wenner, P. G., Bell, R. J., Van Amerom, F. H. W., Toler, S. K., Edkins, J. E., Hall, M. L., et al. (2004). Environmental chemical mapping using an underwater mass spectrometer. *Trac-Trends in Analytical Chemistry, 23*, 288–295.

Wu, Y. C., Washburn, L., & Jones, B. H. (1994). Buoyant plume dispersion in a coastal environment—Evolving plume structure and dynamics. *Continental Shelf Research, 14*, 1001–1023.

Chapter 23
Innovations in Design and Monitoring of Desalination Discharges

Burton Jones

Abstract Seawater reverse osmosis desalination systems produce brine (concentrate) that normally must be discharged back to the sea. The concentrate can have up to twice the salinity of the feedwater and can cause environmental impacts to the marine environment. Innovation in the design and evaluation of diffuser systems has led to reductions in potential environmental impacts by causing rapid dispersion of the high salinity plume. The nearfield and farfield models used to assess potential environmental impacts of the dense water discharge have also been improved to allow assessment of impacts and to make design changes that lessen them. The selection of discharge sites has been improved by the ability of obtaining rapid and accurate bathymetric and water quality data that can be used in models to assess circulation and other aspects of outfall design and to monitor and assess potential discharge impacts.

23.1 Introduction

Continued population growth and insufficient natural freshwater supplies in arid and semi-arid regions press the need for increased use of seawater desalination as a new freshwater supply source. These needs often conflict with the desires and regulations of the regions that demand preservation of environmental quality to maintain healthy natural ecosystems. The environmental impacts from desalination plants lay both on the intake and discharge sides of the operation. The desalination reject water consists of not only of the brine and other components concentrated through the desalination process, but also includes antifouling agents, antiscalants, coagulants, anti-foaming agents and cleaning chemicals added to the water to maintain efficient operation of the facility (Lattemann and Höpner 2008).

B. Jones (✉)
Red Sea Research Center, King Abdullah University of Science and Technology, Thuwal, Saudi Arabia
e-mail: burt.jones@kaust.edu.sa

T.M. Missimer et al. (eds.), *Intakes and Outfalls for Seawater Reverse-Osmosis Desalination Facilities*, Environmental Science and Engineering,
DOI 10.1007/978-3-319-13203-7_23

Thus, implementation of desalination facilities that minimize impacts on the coastal environment requires mechanisms to offset the characteristics of the discharged effluents. Discharge outfalls that create adequate dilution continue to be a primary tool for reducing the alteration of the ambient environment near the discharge. Effective dilution is accomplished through the design of outfalls with diffusers that facilitate the dilution of the effluent within the ambient environment. The design and evaluation of these outfalls is most often accomplished with laboratory fluid modeling where a range of flow and stratification conditions can be readily tested. Numerical modeling is much more effective. The effectiveness of these approaches can be evaluated in the planning stages with modeling and once in place, continued modeling and monitoring efforts provide a evaluation of the desired performance and environmental impacts on the local system.

23.2 Innovations in Outfall and Diffuser Design and Evaluation

Recent advances in laboratory fluid modeling and imaging along with the dimensional analysis that is common practice in environmental fluid mechanics have provided insights into the complexities of the initial mixing processes. These techniques provide analysis of individual port configurations (such as single port, multiport, rosette style diffusers, etc.) and in the process provide 3-dimensional resolution of the flow and turbulence within the resulting effluent flows (Chaps. 17, 18 and 19). These experiments have led to optimization of port design in terms of port angle, alternating port directions and alignment angle of the ports for rosette diffusers. The complexity of the fluid dynamic processes, such as Coanda dynamical interaction, is often difficult for numerical modeling to simulate. But scaled laboratory models provide sufficient resolution of these processes that they can be transferred to inputs for far-field models.

The results from the nearfield modeling and parameterization of nearfield processes can then be incorporated into a tiered approach to planning, design and implementation of new effluent discharges. These tiered approaches utilize the capabilities of the nearfield models along with evaluation of the environment of the receiving waters, and environmental regulations to evaluate optimal locations, diffuser and outfall design and desired performance objectives for the design and construction of the outfall. Following the initiation of the operation of the outfall, the tiered approach can be applied to performance evaluation and environmental monitoring to validate the performance of the models and predictions.

The nearfield models provide input into the farfield models that are used to evaluate the larger scale effects and dispersion of coastal effluent plumes. Some of these results are useful at the scale of the facility itself where the desire is to minimize the interaction between the discharge effluent and the seawater intake for the

desalination plant (e.g., Chap. 21). The farfield models provide innovation at the much larger spatial scales that have relevance to regional and extended temporal impacts from the discharge.

23.3 Innovations in Nearfield and Farfield Modeling

A variety of approaches are taken for farfield modeling of effluent plumes. As there are various numerical approaches to the farfield modeling, the approach taken will depend on the environment and scale where the model is to be applied. Often 2-dimensional approximations can be quite effective in shallow coastal regions where a combination of tidal currents and/or wind mixing are likely to create a well-mixed water column that can be treated with two-dimensional solutions. These techniques can be applied to all types of effluent discharges, and as is happening more frequently, outfalls may combine discharges from thermal, waster water, and/or desalination discharges (Chaps. 18 and 20). In many coastal situations where stratification is important, and the accompanying stratification complex with vertical and horizontal current variability, more sophisticated three-dimensional modeling will be needed (Chap. 21; Uchiyama et al. 2014). The models often used for the farfield coastal modeling come from both commercial software systems such as Delft-3D (Chap. 18) and from various community tools such as the Regional Ocean Modeling System (ROMS), or the MIT Global Circulation Model (MITgcm). While these models may differ in the specific details of how they handle the numerical details of the model, they are usually similar in that they solve the Navier-Stokes equations with the Boussinesq approximation. However, the ability of these models to provide detailed, accurate representations of the farfield dispersion processes is improving at least as rapidly as the sophistication of our computing resources, with new, larger multi-core supercomputing resources providing ability to run models at finer spatial scales and, if needed, time steps.

These advances enable high resolution coastal models that are nested within larger ocean schemes that provide realistic open-ocean forcing and coupling with global processes (Chap. 22; Chao et al. 2009; Uchiyama et al. 2014). These models have the capability to function in real-time providing both nowcasts and forecasts of the region and the relevant discharge plumes through the assimilation of the more comprehensive data streams that are becoming available through coastal ocean observatories (e.g. Chao et al. 2009; Hoteit et al. 2008; Korres et al. 2012). Retrospectively, these models provide the ability to estimate detailed statistical analysis of plume dispersion over a wide range of realistic oceanographic conditions. Ultimately, as these techniques improve these modeling efforts will include full characterization or the wave field and wave-induced nearshore circulation. While not likely to attain the resolution down to the jet scale, the models are already approaching the resolution of the nearfield (tens of meters) required to resolve the entrainment into the coastal circulation.

23.4 Innovations in Environmental Monitoring

As with design and modeling of outfalls, techniques for monitoring of ocean outfalls are also rapidly evolving. From the early days of outfall monitoring where positioning a boat that could obtain water or benthic samples over some sort of sampling grid agreed upon with the regulators, to the modern ocean observatories, sensor and observing platforms and resources have changed dramatically.

Tracer techniques have been routinely used to evaluate the actual performance of ocean outfalls once the outfalls are activated. Monitoring of outfalls off the coast of New South Wales, Australia have utilized dye studies to measure the initial dilution and dispersion from a desalination brine discharge. Dyes are often introduced when unambiguous indicators from a discharge source are required (Percly and Roldao 2013). With wastewater outfalls, there is often sufficient dissolved organic matter in the wastewater, that it provides a signal well above ambient concentrations that also provides an unambiguous tracer for the discharge (e.g. Petrenko et al. 1997; Rogowski et al. 2013; Chap. 22).

Because brine discharges, especially from RO plants, are dense plumes, they spread horizontally near the bottom and therefore are most likely to affect epibenthic and benthic assemblages of organisms. The impacts of these discharges on the local benthic communities are a large concern for the long-term operation of desalination facilities. Examining both the existing population and the recruitment to the area are required to evaluate the effect of the discharge on the environmental health (Natural Solutions 2006; Natural Solutions and SKM 2006). Examples from New South Wales indicate that significant effects are constrained within the zone of initial dilution and that the natural annual variability of species abundance and community structure is greater than the differences that appear between the near-field community and the reference communities. Although not discussed within this book, modern molecular biology techniques may provide more sensitive measurements of organismal response to environmental stress. Genomic and transcriptomic methods may provide sensitive indices of environmental stress that may not be immediately evident in the more traditional environmental impact assessment methods where community structure is often used to evaluate differential effects of a discharge.

The rapid development of more sophisticated in situ sensors and autonomous vehicles has transformed our ability to observe discharge plumes in the environment. Modern chemical and optical sensors combined with both propelled and buoyancy driven vehicles enable rapid and sustained (respectively) monitoring of these discharge plumes. Propelled vehicles such as the Hydroid Remus vehicle are capable of terrain following with precise navigation so that a dense brine plume can be more easily traced (van der Merwe et al. 2014; Rogowski et al. 2013). An additional advantage of the propelled vehicles is their ability to cover a relatively large area rapidly, traveling at 3–4 knots (5.5–7.4 km/h).

Buoyancy driven gliders, while lacking the speed of the propelled vehicles, have the ability to sustain continued observations over periods up to several months

(Chap. 22). An example of deploying a glider equipped with physical and optical sensors near a wastewater outfall demonstrates that the sustained observations provide snapshots of the plume over time and these observations can be transformed into statistical products that are useful for comparison with the statistics from model simulations (e.g. Uchiyama et al. 2014). These tools also provide inputs of temperature, salinity, and density that can be transmitted in near real-time for assimilation into real-time operational nowcast/forecast models, thus improving model estimates in real-time.

23.5 Discussion and Conclusions

The combined capabilities of laboratory and numerical models for design and implementation, improved monitoring techniques for the coastal environment, with real-time observations and modeling enable us to better understand, manage, and predict the impacts of placing desalination facilities in strategic areas of freshwater need. Bleninger and Morelissen (Chap. 18) have outlined a tiered approach to analysis and design of new discharges from various types of discharges. Lattemann and Höpner (2008) have indicated that an integrated, methodological approach to design, placement and monitoring of desalination facilities is required. Modeling tools from the initial dilution and nearfield (Chaps. 17, 18, 19 and 22) to the farfield (Chaps. 21 and 22) are now available for evaluation of plume processes at all relevant scales. Monitoring approaches and the required tools have evolved rapidly (Chap. 22), but it is expected that these capabilities will continue to evolve and improve.

References

Chao, Y., Li, Z. J., Farrara, J., McWilliams, J. C., Bellingham, J., et al. (2009). Development, implementation and evaluation of a data-assimilative ocean forecasting system off the central California coast. *Deep-Sea Research Part II: Topical Studies in Oceanography, 56*, 100–126.

Hoteit, I., Pham, D. T., Triantafyllou, G., & Korres, G. (2008). A new approximate solution of the optimal nonlinear filter for data assimilation in meteorology and oceanography. *Monthly Weather Review, 136*, 317–334.

Korres, G., Triantafyllou, G., Petihakis, G., Raitsos, D. E., Hoteit, I., et al. (2012). A data assimilation tool for the Pagasitikos Gulf ecosystem dynamics: Methods and benefits. *Journal of Marine Systems, 94*, S102–S117.

Lattemann, S., & Höpner, T. (2008). Environmental impact and impact assessment of seawater desalination. *Desalination, 220*, 1–15.

Natural Solutions and SKM. (2006). Baseline water quality and marine ecology monitoring program.

Natural Solutions. (2006). Environmental impact assessment for the gold coast desalination project.

Percly, J. O. G., & Roldao, J. S. F. (2013). Dye tracers as a tool for outfall studies: Dilution measurement approach. *Water Science and Technology, 67*, 1564–1573.

Petrenko, A. A., Jones, B. H., Dickey, T. D., LeHaitre, M., & Moore, C. (1997). Effects of a sewage plume on the biology, optical characteristics, and particle size distributions of coastal waters. *Journal of Geophysical Research-Oceans, 102*, 25061–25071.

Rogowski, P., Terrill, E., Otero, M., Hazard, L., & Middleton, W. (2013). Ocean outfall plume characterization using an autonomous underwater vehicle. *Water Science and Technology, 67*, 925–933.

Uchiyama, Y., Idica, E. Y., McWilliams, J. C., & Stolzenbach, K. D. (2014). Wastewater effluent dispersal in Southern California bays. *Continental Shelf Research, 76*, 36–52.

van der Merwe, R., Bleninger, T., Acevedo-Feliz, D., Latteman, S., & Amy, G. (2014). In-situ monitoring and assessment of SWRO concentrate discharge. *Journal of Applied Water Engineering and Research* (in press).